# Underwater Sound Field Verification

## Vineyard Wind 1 Final Report

21 April 2024

Submitted to:

DEME Group

Authors:

Elizabeth T. Küsel
Cristian Graupe
Thomas J. Stephen
Carmen Lawrence
Mark P. Cotter
David G. Zeddies

P001705-001
Document 03233
Version 1.0

Suggested citation:

Küsel, E.T., C. Graupe, T. J. Stephen, C. Lawrence, M. P. Cotter, and D.G. Zeddies. 2024. Underwater Sound Field Verification: Vineyard Wind 1 Final Report. **Document 03233**, **Version 1.0**. Technical report by JASCO Applied Sciences for **DEME Group**.

# Contents

# Figures

# Tables

# 1. Introduction

## 1.1. Pile Driving for Offshore Wind Farms

Vineyard Wind, LLC is building an 806 MW offshore wind farm (OWF) located in the Bureau of Ocean Energy Management (BOEM) Lease Area OCS-A 0501. The Lease Area is located on the Northeast Atlantic continental shelf within the Massachusetts Wind Energy Area (MA WEA), in water depths ranging from approximately 37–49 m (121–161 ft). At its closest points, the 675.4 square kilometer ($km^2$) (166,886 acres) Lease Area is approximately 22.5 km (15 mi) from the southeast corner of Martha's Vineyard and a similar distance from the southwest side of Nantucket (Figure 1).

The Vineyard Wind 1 Wind Farm (VW1) includes a total of 62 wind turbine generators (WTG), each supported by a monopile foundation, and an offshore substation/electrical service platform (ESP) supported by a four-leg jacket foundation. All WTG monopiles for the VW1 have a diameter of 9.6 m, while the pin piles for the jacket foundation had a diameter of 2.45 m. Installation of each monopile and the jacket foundation required the use of impact pile driving. Impact pile driving of the WTG and ESP foundations commenced on 6 Jun 2023 and acoustic monitoring for sound field verification took place until 7 Sep 2023 with the installation of the 12$^{th}$ monopile, for a total of 13 foundations (12 monopiles and 1 jacket foundation) monitored (Figure 1).

Permitting conditions, reflected in the approved Sound Field Verification plan (11 May 2023), required Vineyard Wind to perform acoustic monitoring of impact pile driving during the first (representative) installation of each foundation type (1 monopile and 1 jacket). Vineyard Wind committed to monitoring the first two monopiles and the jacket foundation installation (Sound Field Verification Plan, 11 May 2023). On behalf of Vineyard Wind, JASCO Applied Sciences (JASCO) was contracted by DEME Offshore US (DEME) to perform acoustic verification measurements of pile driving and regional ambient noise characteristics during the installation. Measurements performed by JASCO found the received levels of the first piles exceeded the predicted levels. For this reason, and noting the provision in Vineyard Wind's approvals allowed for a request to reduce clearance and shutdown zones if at least three piles supported the reduction, 12 monopiles and 1 jacket foundation (Section 1.3) were measured, with the last five monopiles representing noise attenuation configuration and maintenance procedures to be used for the remainder of the project.

Four Autonomous Multichannel Acoustic Recorders (AMARs) were deployed by JASCO on behalf of Vineyard Wind to measure sound levels at ranges of 750, 2000, 4000, and 8000 m along the 225° azimuth radial from the north, or to the southwest of the pile. This direction was chosen because depths along the radial gradually sloped towards deeper water away from the pile, where sound propagation was expected to be greatest. A fifth AMAR was also deployed at 750 m from the pile and offset by 90° from the measurement radial. Figure 2 shows an overview of the station locations with respect to the first monopile installed for illustrative purposes. The offshore pile installation vessel's (Orion) orientation could vary from pile to pile, but the mooring orientation was always the same. JASCO's impulse detector was used to detect single strike events and acoustic metrics were calculated for each detection. Cumulative metrics were computed over the total duration of impact pile driving for each pile. Summary of acoustic results per pile, estimated acoustic ranges to regulatory thresholds for potential marine mammal injury and behavioral disturbances, as well as background sound levels prior to the start of pile driving are presented in this report. Modeled distances to permanent threshold shift (PTS) and behavioral disturbance thresholds are also presented along side distances estimated from the sound measurements.

The objective of this document is to summarize the measured sound levels during impact pile driving of the first thirteen VW1 foundations that were installed between June and September 2023. The summary includes the ranges to acoustic thresholds that may result in injury (Level A (cetaceans), (NMFS 2018)) or behavioral disruption (Level B (cetaceans), NMFS 2018, (McCauley et al. 2000a), (Finneran et al. 2017), https://www.fisheries.noaa.gov/s3/2023-02/MMAcousticThresholds_secureFEB2023_OPR1.pdf) of cetaceans, sea turtles, and fish near the construction areas. Ranges to acoustic thresholds derived from measurements are compared to predicted (modeled) ranges.

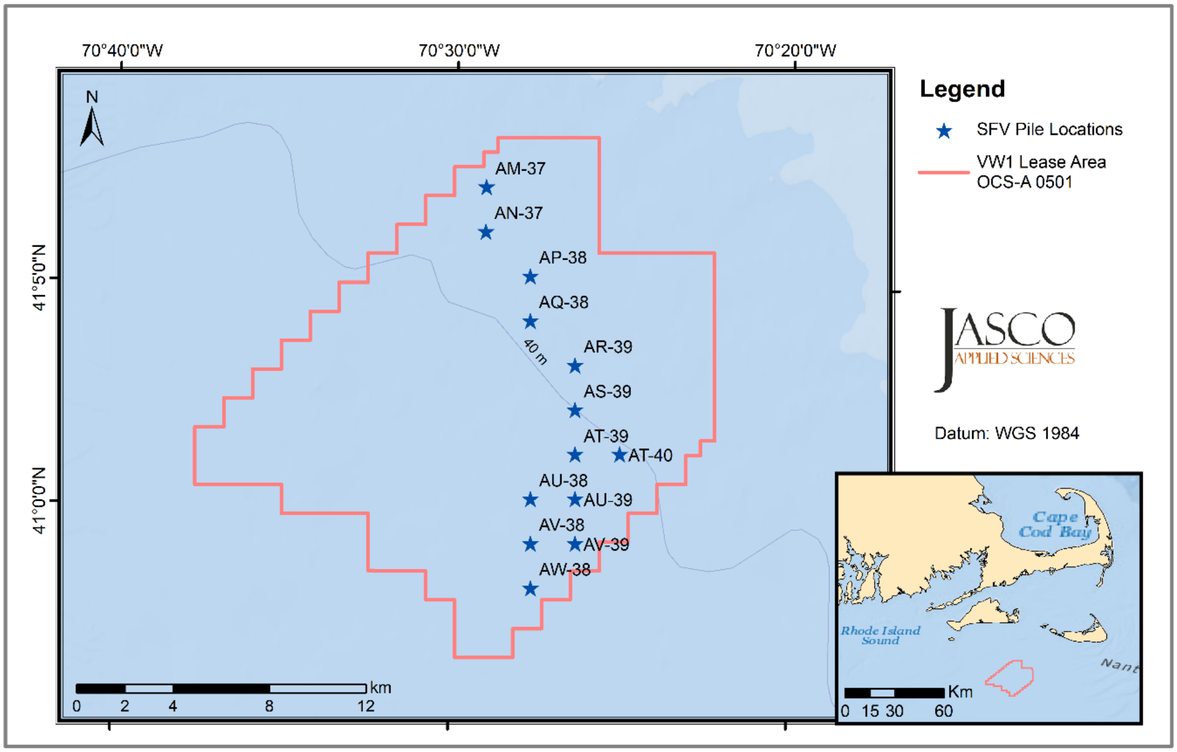


Figure 1. Map showing VW1 Lease Area, OCS-A 0501 and the location of the piles monitored during the sound field verification.

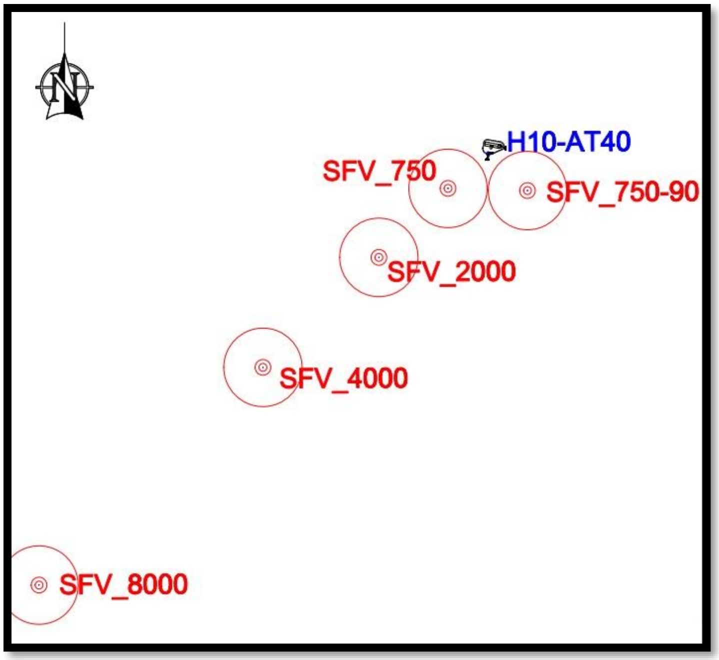


Figure 2. Drawing schematics provided by DEME, of the locations of the sound field verification moorings with respect to the piling vessel for the installation of pile AT-40.

## 1.2. Effects Assessment Criteria

The Marine Mammal Protection Act (MMPA) prohibits the take of marine mammals. The term "take" is defined as: to harass, hunt, capture, or kill, or attempt to harass, hunt, capture, or kill any marine mammal. MMPA regulations define harassment in two categories relevant to Vineyard Wind 1 construction and operations. These are:

- **Level A**: Any act of pursuit, torment, or annoyance that has the potential to injure a marine mammal or marine mammal stock in the wild, and
- **Level B**: Any act of pursuit, torment or annoyance that has the potential to disturb a marine mammal or marine mammal stock in the wild by disrupting behavioral patterns, including, but not limited to, migrating, breathing, nursing, breeding, feeding, or sheltering but that does not have the potential to injure a marine mammal or marine mammal stock in the wild (16 U.S.C. 1362).

The assessment criteria applied during the sound field verification stage of VW1 construction activities are the acoustic exposure criteria used by United States regulators to estimate marine mammal takes. In 2016, the National Oceanographic and Atmospheric Administration (NOAA) Fisheries issued a Technical Guidance document that provides acoustic thresholds for onset of permanent threshold shift (PTS), or auditory injury, in marine mammal hearing for most sound sources, which was updated in 2018 (NMFS 2016, 2018).

NMFS also provided guidance on using weighting functions when applying Level A harassment criteria. The Guidance recommends using a dual criterion for assessing Level A exposures, including a PK (unweighted/flat) sound level metric and a cumulative SEL metric with frequency weighting. Both acoustic criteria and weighting function application are divided into functional hearing groups (low-, mid-, and high-frequency cetaceans and phocid pinnipeds) that species are assigned to, based on their respective hearing frequency ranges. This report applies the most recent sound exposure criteria used by NMFS to estimate acoustic injury (NMFS 2018).

The Level B criteria is based on sound levels thought to elicit disruptive behavioral responses from observations of mysticetes (Malme et al. 1983, 1984, Richardson et al. 1986, 1990), and are described using the SPL metric (NOAA 2005). NMFS currently uses behavioral response thresholds of SPL 160 dB re 1 μPa$^2$ for marine mammals exposed to non-explosive intermittent sounds, like impact pile driving (NMFS 2022).

### 1.2.1. Marine Mammal Hearing groups

Current data and predictions show that marine mammal species differ in their hearing capabilities, in absolute hearing sensitivity as well as frequency band of hearing (Richardson et al. 1995, Wartzok and Ketten 1999, Southall et al. 2007, Au and Hastings 2008). While hearing measurements are available for a small number of species based on captive animal studies, there are no direct measurements of many odontocetes or any mysticetes. As a result, hearing distances for many odontocetes are grouped with similar species, and predictions for mysticetes are based on other methods including: anatomical studies and modeling (Houser et al. 2001, Parks et al. 2007, Tubelli et al. 2012, Cranford and Krysl 2015); vocalizations (see reviews in Richardson et al. 1995, Wartzok and Ketten 1999, Au and Hastings 2008); taxonomy; and behavioral responses to sound (Dahlheim and Ljungblad 1990, see review in Reichmuth et al. 2007). In 2007, Southall et al. proposed that marine mammals be divided into hearing groups. This division was updated in 2016 and 2018 by NOAA Fisheries using more recent best available science (Table 1).

Southall et al. (2019) published an updated set of Level A sound exposure criteria (including PTS in marine mammals). While the authors propose a new nomenclature and classification for the marine mammal functional hearing groups, the proposed thresholds and weighting functions do not differ in effect from those proposed by NOAA Fisheries (2018). The new hearing groups proposed by Southall et al. (2019) have not yet been adopted by NOAA. The NOAA Fisheries (NMFS 2018) hearing groups presented in Table 1 were used in this analysis.

Table 1. Marine mammal hearing groups (Sills et al. 2014, NMFS 2018).

| Hearing group | Generalized hearing range [a] |
|---|---|
| Low-frequency cetaceans (LFC) (mysticetes or baleen whales) | 7 Hz to 35 kHz |
| Mid-frequency cetaceans (MFC) (odontocetes: delphinids, beaked whales) | 150 Hz to 160 kHz |
| High-frequency cetaceans (HFC) (other odontocetes) | 275 Hz to 160 kHz |
| Phocid pinnipeds in water (PW)[b] | 50 Hz to 86 kHz |

[a] The generalized hearing distance is for all species within a group. Individual hearing will vary.

[b] Sound from piling will not reach NOAA Fisheries thresholds for behavioral disturbance of seals in air (90 dB [rms] re 20 μPa$^2$ for harbor seals and 100 dB [rms] re 20 μPa$^2$ for all other seal species) at the closest land-based sites where seals may spend time out of the water. Thus in-air hearing is not considered further.

## 1.2.2. Marine Mammal Auditory Weighting Functions and Injury Exposure Criteria

The potential for anthropogenic sound to impact marine mammals is largely dependent on whether the sound occurs at frequencies that an animal can hear well unless the sound pressure level is so high that it can cause physical tissue damage regardless of frequency. Auditory (frequency) weighting functions are based on composite audiograms and temporary threshold shift (TTS) data and reflect an animal's susceptibility to noise-induced hearing loss (Nedwell and Turnpenny 1998, Nedwell et al. 2007). Auditory weighting functions have been proposed for marine mammals, specifically associated with PTS thresholds expressed in metrics that consider what is known about marine mammal hearing (e.g., SEL) (Southall et al. 2007, Erbe et al. 2016, Finneran 2016). Marine mammal auditory weighting functions for all hearing groups (see Table 1) published by Finneran (2016) are included in the NMFS (2018) Technical Guidance for use in conjunction with corresponding permanent threshold shift (PTS [Level A] onset acoustic criteria; Table 2). See Appendix F.3 for a detailed description of the weighting functions.

The application of marine mammal auditory weighting functions emphasizes the importance of taking measurements and characterizing sound sources in terms of their overlap with biologically important frequencies (e.g., frequencies used for environmental awareness, communication, and the detection of predators or prey), and not only the frequencies that are relevant to achieving the objectives of the sound producing activity (i.e., context of sound source; NMFS 2018).

Injury to the hearing apparatus of a marine mammal may result from brief exposure to an intense sound or from longer fatiguing sound exposures. Damage to hearing from brief exposure to intense sounds is independent of the duration of the signal, and the PK metric is used to assess the potential risk for injury. For longer-duration exposures, a measure of the total received sound energy is needed. The SEL metric is proportional to sound energy and is calculated by summing over the duration of the received signal. The NMFS (2018) criteria incorporate the best available science to estimate PTS onset in marine mammals from instantaneous peak (PK) sound pressure levels and sound energy accumulated over 24 h (SEL; $L_E$) (Table 2).

Table 2. Summary of relevant permanent threshold shift (PTS) onset acoustic thresholds for marine mammal hearing groups (NMFS 2018).

| Faunal group | Impulsive signals [a] | |
|---|---|---|
| | Unweighted $L_{pk}$ (dB re 1 µPa) | Frequency-weighted $L_{E,24h}$ (dB re 1 µPa$^2$·s) |
| Low-frequency cetaceans (LFC) | 219 | 183 |
| Mid-frequency cetaceans (MFC) | 230 | 185 |
| High-frequency cetaceans (HFC) | 202 | 155 |
| Phocid seals in water (PW) | 218 | 185 |

[a] Dual-metric acoustic thresholds for impulsive sounds: Of these two metrics, the one with the larger acoustic isopleth or the larger exposure effect is used to assess PTS onset. If a non-impulsive sound has the potential of exceeding the peak sound pressure level thresholds associated with impulsive sounds, these thresholds are also considered.

## 1.2.3. Marine Mammal Behavioral Response Exposure Criteria

Numerous studies on marine mammal behavioral responses to sound exposure have not resulted in consensus in the scientific community regarding the appropriate metric for assessing behavioral reactions. It is recognized that the context in which the sound is received affects the nature and extent of responses to a stimulus (Southall et al. 2007, Ellison et al. 2012). Due to the complexity and variability of marine mammal behavioral responses to acoustic exposure, NMFS has not yet released updated technical guidance for determining potential behavioral responses of marine mammals exposed to sounds (NMFS 2018)(NMFS 2018)(NMFS 2018)(NMFS 2018)(NMFS 2018)(NMFS 2018)(NMFS 2018) and currently uses a step function to assess behavioral impact (NOAA 2005). An SPL of 120 dB re 1 μPa$^2$ was set as the behavioral disruption threshold for migrating mysticetes (NOAA 2005), which was based on the responses of migrating mysticete whales to airgun sounds (intermittent sound) (Malme et al. 1983, 1984). The HESS team recognized that behavioral responses to sound may occur at lower levels, but substantial responses were only likely to occur above an SPL of 140 dB re 1 μPa$^2$. NMFS currently uses behavioral response thresholds of SPL 160 dB re 1 μPa$^2$ for non-explosive, intermittent sounds, such as impact pile driving, for all marine mammal species (NMFS 2022).

## 1.2.4. Acoustic Criteria – Sea Turtles and Fish

In a cooperative effort between Federal and State transportation and resource agencies, interim criteria were developed to assess the potential for injury to fish exposed to impact pile driving sounds (Stadler and Woodbury 2009) and described by the Fisheries Hydroacoustic Working Group (FHWG 2008). The injury and behavioral response levels for fish were compiled and listed in NMFS ESA Acoustic Thresholds (noaa.gov) for assessing the potential effects to ESA-listed fish exposed to elevated levels of underwater sound from pile driving.

A technical report by an American National Standards Institute (ANSI) registered committee (Popper et al. 2014) reviewed available data and suggested metrics and methods for estimating acoustic impacts for fish. Their report includes thresholds for potential injury but does not define sound levels that may result in behavioral response, though it does indicate a high likelihood of response near impact pile driving (tens of meters), a moderate response at intermediate distances (hundreds of meters), and a low response far (thousands of meters) from the pile (Popper et al. 2014). Criteria for impulsive sources used in the monitoring is listed in Table 3.

Injury, impairment, and behavioral thresholds for sea turtles were developed for use by the US Navy (Finneran et al. 2017) based on exposure studies (e.g., McCauley et al. 2000b). Dual criteria (PK and SEL) have been suggested for PTS and TTS, along with auditory weighting functions published by Finneran et al. (2017) used in conjunction with SEL thresholds for PTS and TTS. The recommended behavioral threshold is an SPL of 175 dB re 1 μPa$^2$ (McCauley et al. 2000b, Finneran et al. 2017) (Table 3).

Table 3. Acoustic metrics and thresholds for fish and sea turtles currently used by National Marine Fisheries Service (NMFS) for impact pile driving.

| Faunal group | Injury | | Behavior |
|---|---|---|---|
| | $L_{pk}$ | $L_E$ | $L_p$ |
| Fish ≥ 2 g [a] | 206 | 187 | 150 |
| Fish < 2 g [a] | | 183 | |
| Sea turtles [b, c] | 232 | 204 | 175 |

$L_{pk}$ – peak sound pressure (dB re 1 µPa); $L_E$ – sound exposure level (dB re 1 µPa$^2$·s), $L_p$ – root mean square sound pressure level (dB re 1 µPa$^2$).

[a] NMFS recommended criteria adopted from the Fisheries Hydroacoustic Working Group (FHWG 2008).

[b] Finneran et al. (2017).

[c] McCauley et al. (2000b).

## 1.3. Monitored Piles

Information presented in Table 4 was retrieved from pile driving logs provided to JASCO by DEME after completion of each pile installation. Table 5 shows summary piling data from all of the piles.

Table 4. Geographic (WGS 84) and UTM (NAD83 (2011) zone 19 N ) coordinate locations, and bottom depth for each foundation monitored during the sound field verification (Figure 1).

| Foundation Type | Foundation ID | Easting (m) | Northing (m) | Latitude (N) | Longitude (W) | Bottom Depth (m) |
|---|---|---|---|---|---|---|
| Monopile | AT-40 | 380842 | 4542036 | 41° 1.2494' | 70° 25.0357' | 41.2 |
| Monopile | AU-39 | 378990 | 4540184 | 41° 0.2323' | 70° 26.3351' | 42.1 |
| Monopile | AP-38 | 377138 | 4549444 | 41° 5.2190' | 70° 27.7668' | 39.5 |
| Monopile | AV-39 | 378990 | 4538332 | 40° 59.2317' | 70° 26.3134' | 42.8 |
| Monopile | AR-39 | 378990 | 4545740 | 41° 3.2344' | 70° 26.4005' | 41.4 |
| Monopile | AW-38 | 377138 | 4536480 | 40° 58.2144' | 70° 27.6119' | 43.7 |
| Monopile | AQ-38 | 377138 | 4547592 | 41° 4.2184' | 70° 27.7446' | 41.4 |
| Monopile | AT-39 | 378990 | 4542036 | 41° 1.2330' | 70° 26.3569' | 41.9 |
| Monopile | AS-39 | 378990 | 4543888 | 41° 2.2337' | 70° 26.3787' | 39.7 |
| Monopile | AV-38 | 377138 | 4538332 | 40° 59.2150' | 70° 27.6340' | 43.1 |
| Monopile | AN-37 | 375286 | 4551296 | 41° 6.2027' | 70° 29.1119' | 40.5 |
| Monopile | AU-38 | 377138 | 4540184 | 41° 0.2157' | 70° 27.6560' | 42.9 |
| Jacket | AM-37 | 375320 | 4553148 | 41° 7.2037' | 70° 29.1101' | 38.6 |

Table 5. Summary of pile driving activities for all 13 piles monitored.

| Date | 2023-06-06 | 2023-06-09 | 2023-06-17 | 2023-06-26 | 2023-07-03 | 2023-07-09 | 2023-07-15/22 |
|---|---|---|---|---|---|---|---|
| **Pile-Driving Activity** | | | | | | | |
| Pile identifier | AT-40 | AU-39 | AP-38 | AV-39 | AR-39 | AW-38 | AM-37[a] |
| Pile diameter (m) | 9.6 | 9.6 | 9.6 | 9.6 | 9.6 | 9.6 | 2.45 |
| Pile length (m) | 74.93 | 75.34 | 72.80 | 78.3 | 74.6 | 79.3 | 81.83 |
| Bottom depth (m) | 41.2 | 42.1 | 39.5 | 42.8 | 41.4 | 43.7 | 38.6 |
| Hammer type | IHC S-4000 | IHC S-4000 | IHC S-4000 | IHC S-4000 | IHC S-4000 | IHC S-4000 | IHC S-2000 |
| Total hammer strikes | 4329 | 3182 | 3511 | 4007 | 3895 | 3419 | A2: 7572, C4: 6782, A4: 6774, C2: 7198 |
| Total penetration (m) | 29.41 | 28.94 | 28.90 | 31.15 | 28.98 | 31.29 | 66.00 |
| Pile Driving Start Time (hh:mm:ss) UTC | 10:37:36 | 17:57:05 | 22:34:38 (17 Jun) | 21:47:30 (26 Jun) | 18:51:12 | 15:28:44 | 12:14:48 (15 Jul) |
| Pile Driving End Time (hh:mm:ss) UTC | 14:05:38 | 19:34:22 | 01:04:42 (18 Jun) | 01:39:53 (27 Jun) | 21:24:06 | 17:09:55 | 19:03:25 (22 Jul) |
| Net duration of pile driving (hh:mm:ss) | 01:55:19 | 01:19:41 | 01:31:59 | 01:42:11 | 01:45:06 | 01:21:50 | 10:46:46 |
| Maximum single strike energy (kJ) | 2488 | 4091 | 3632 | 3343 | 4079 | 3057 | 1216 |
| Total energy transferred (kJ) | 5338287 | 6459536 | 8718298 | 9028159 | 9129029 | 7930892 | 16780261 |
| **Noise Attenuation Systems (NAS)** | | | | | | | |
| Hydro Sound Damper (HSD) | yes | yes | yes | yes | yes | yes | yes |
| FAD*: BBC (730 m length) | 485 $m^3$/min | 485 $m^3$/min | 483 $m^3$/min | 448.5 $m^3$/min | 448.5 $m^3$/min | 483 $m^3$/min | 448 $m^3$/min |
| FAD*: BBC (960 m length) | N/A | N/A | N/A | 414 $m^3$/min | 393.6 $m^3$/min | 414 $m^3$/min | 393.6 $m^3$/min |

[a] Pile AM-37 refers to pin piles of the jacket foundation composed of 4 legs: A2, A4, C2, and C4.

| Date | 2023-08-05/06 | 2023-08-07 | 2023-08-14 | 2023-09-03 | 2023-09-05 | 2023-09-07 |
|---|---|---|---|---|---|---|
| **Pile-Driving Activity** | | | | | | |
| Pile identifier | AQ-38 | AT-39 | AS-39 | AV-38 | AN-37 | AU-38 |
| Pile diameter (m) | 9.6 | 9.6 | 9.6 | 9.6 | 9.6 | 9.6 |
| Bottom depth (m) | 41.4 | 41.9 | 39.7 | 43.1 | 40.5 | 42.9 |
| Pile length (m) | 76.00 | 75.86 | 73.49 | 78.98 | 74.97 | 76.10 |
| Hammer type | IHC S-4000 | IHC S-4000 | IHC S-4000 | IHC S-4000 | IHC S-4000 | IHC S-4000 |
| Total hammer strikes | 3023 | 3159 | 2995 | 3470 | 3682 | 2884 |
| Total penetration (m) | 30.28 | 29.74 | 29.53 | 31.75 | 30.24 | 28.80 |
| Pile Driving Start Time (hh:mm:ss) UTC | 11:45:04 (5 Aug) | 16:11:33 | 19:33:46 | 17:55:27 | 21:51:07 | 20:07:13 |
| Pile Driving End Time (hh:mm:ss) UTC | 13:29:58 (6 Aug) | 18:06:14 | 21:12:07 | 19:38:12 | 00:01:50 | 22:41:30 |
| Net duration of pile driving (hh:mm:ss) | 01:44:15 | 01:26:38 | 01:17:18 | 01:22:33 | 01:32:27 | 01:15:38 |
| Maximum single strike energy (kJ) | 3227 | 3831 | 3126 | 3519 | 3748 | 3825 |
| Total energy transferred (kJ) | 6724399 | 7479056 | 6663389 | 7955883 | 9411583 | 6586442 |
| **Noise Attenuation** | | | | | | |
| Hydro Sound Damper (HSD) | yes | yes | yes | yes | yes | yes |
| FAD*: BBC (730 m length) | 448.5 $m^3$/min | 448.5 $m^3$/min | 483 $m^3$/min | 448.5 $m^3$/min | 448.5 $m^3$/min | 448.5 $m^3$/min |
| FAD*: BBC (960 m length) | 448.5 $m^3$/min | 414 $m^3$/min | N/A | 448.5 $m^3$/min | 448.5 $m^3$/min | 448.5 $m^3$/min |

* FAD = free air delivery

## 1.4. Noise Mitigation Measures

A Hydrosound Damper System (HSD) and either a single or double big bubble curtain (BBC) were deployed for all marine impact piling as noise mitigation measures. Two sets of hoses were used for the inner and outer bubble curtains and were used alternately from pile to pile. Table 6 gives a summary of the bubble curtain hoses and shapes for each monitored pile.

BBC improvement procedures were implemented for the installation of foundation AQ-38 and adopted for all subsequent monopiles. The improved protocol consisted in re-drilling of the bubble curtain hoses during each hose retrieval and prior to the redeployment of the BBC hoses to ensure all sections were cleared and free of sediments for optimal BBC performance.

Table 6. Summary of bubble curtain hoses used for each monitored pile.

| Pile ID | Inner Bubble Curtain # of compressors | Hose Set | Outer Bubble Curtain # of compressors | Hose Set | Shape |
|---|---|---|---|---|---|
| AT-40 | 13 | 1 | N/A | N/A | Irregular |
| AU-39 | 13 | 2 | N/A | N/A | Irregular |
| AP-38 | 14 | 1 | N/A | N/A | Circular |
| AV-39 | 13 | 2 | 12 | 1 | Circular |
| AR-39 | 13 | 1 | 13 | 2 | Circular |
| AW-38 | 14 | 2 | 12 | 1 | Circular |
| AM-37 | 13 | 1 | 12 | 2 | Circular |
| AQ-38 | 14 | 2 | 13 | 1 | Circular |
| AT-39 | 14 | 1 | 12 | 2 | Circular |
| AS-39 | 14 | 2 | N/A | N/A | Circular |
| AV-38 | 13 | 1 | 13 | 2 | Circular |
| AN-37 | 13 | 2 | 13 | 1 | Circular |
| AU-38 | 13 | 1 | 13 | 2 | Circular |

N/A = not applicable

## 1.5. Environmental Conditions

### 1.5.1. Bottom Type

VW1 lease area is located on the Southern New England sub-region (Cook and Auster 2007) of the Northeast Atlantic continental shelf, which has a gentle slope (0.03–0.05 degrees) towards the shelf edge. The lease area has very homogeneous seafloor conditions and is dominated by fine sand and silt. Sediments are coarser on the northwest corner becoming increasingly muddy towards the southeast end of the lease area (Guida et al. 2017).

## 1.5.2. Ambient noise

The ambient, or background, sound levels that create the ocean soundscape consist of many natural and anthropogenic sources (Figure 3). In the lease area, the main environmental sources of sound are likely wind and precipitation. Wind-generated sea states and precipitation are well-described sources of sound in the ocean, with contributions typically above ~100 Hz for wind noise and 500 Hz for precipitation (e.g., Wenz 1962, Ross 1976). At lower frequencies (<100 Hz), earthquakes and other geological events contribute to the soundscape but anthropogenic sounds tend to dominate this frequency band. A recent study by Van Parijs et al. (2023) in the southern New England wind farm development area, reported broadband SPLs between 105 to 112 dB (re 1 µPa$^2$) measured from all data at each of the seven recording sites. Decidecade levels generally showed higher amplitudes at the lower frequencies, with sources above ambient background noise usually below 1 kHz. Their study and data set provides a comparison for the baseline measurements recorded during this study.

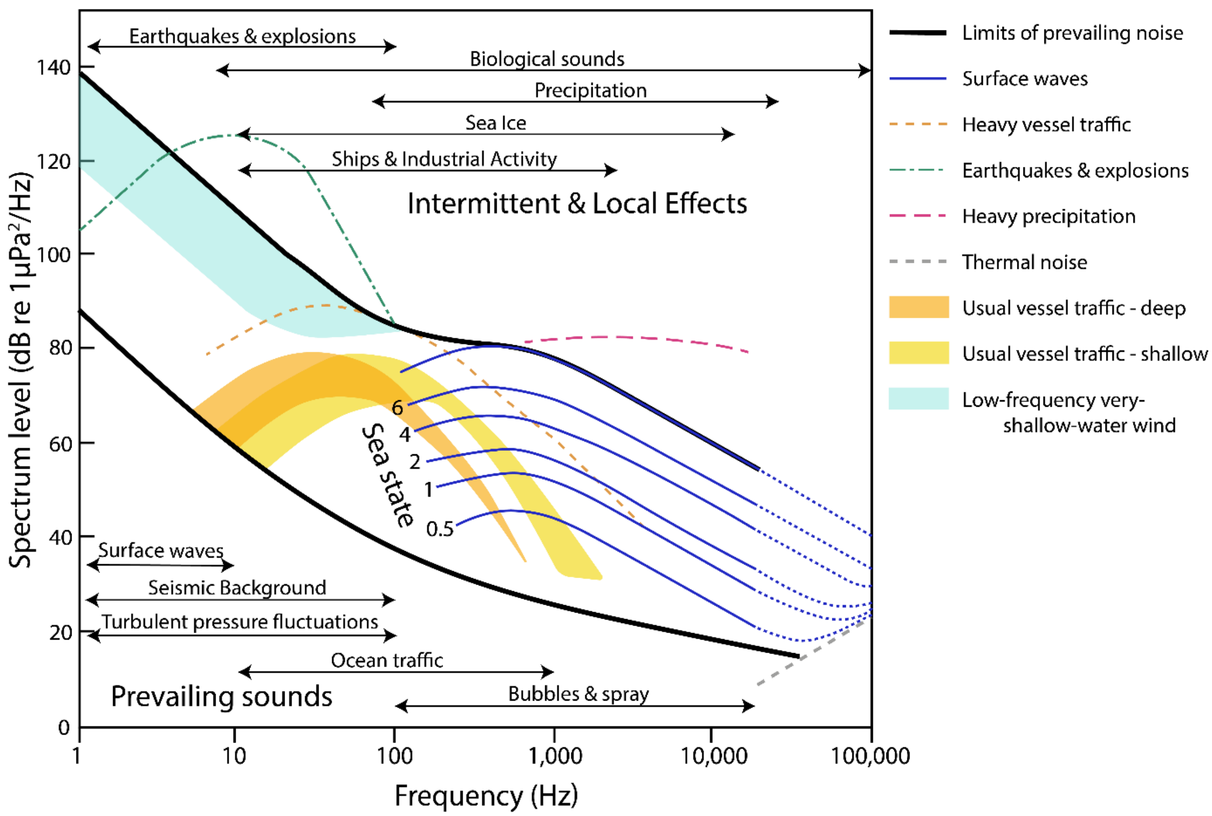


Figure 3. Wenz curves describing pressure spectral density levels of marine ambient sound from weather, wind, geologic activity, and commercial shipping (adapted from NRC 2003, based on Wenz 1962). Thick lines indicate limits of prevailing ambient sound.

## 1.5.3. Weather

Parameters describing weather conditions during each day when a monitored pile was installed is presented on Table 7.

Table 7. Weather conditions during each monitored pile driving event.

| Pile ID | Date | Wind 10 m above the water | | | Total Wave | | Air Temperature (°C) | Min Cloud Base (ft) | Visibility (nm) |
|---|---|---|---|---|---|---|---|---|---|
| | | Direction | Speed (m/s) | Max gusts (m/s) | Significant Height (m) | Direction | | | |
| AT-40 | 6 Jun | NW to SW | 4-7 | 11 | 0.3-0.7 | SSE to SSW | 14-17 | nlc | 5 |
| AU-39 | 9 Jun | SW to SSE | 2-3 | 5 | 0.4-0.5 | S | 14-16 | nlc | 4-5 |
| AP-38 | 17 Jun | SSE to WSE | 5-9 | 11 | 0.8-1.1 | S to SSE | 16-18 | 500 | 3-5 |
| AV-39 | 26 Jun | S to SSW | 2-6 | 10 | 0.7-1.1 | SSE | 18-21 | 100 | 1-5 |
| | 27 Jun | S | 7–10 | 14 | 1.6–1.9 | NW to ENE | 19-20 | 1000 | 5 |
| AR-39 | 3 Jul | S to SSW | 7-9 | 13 | 1.4-1.8 | S to SSE | 19 | 2000 | 4-5 |
| AW-38 | 9 Jul | N to NE | 3-5 | 7 | 0.8-1.0 | SE | 17-18 | 100 | 1-3 |
| AM-37 | 15 Jul | S to SSW | 5–7 | 10 | 0.9–1.1 | E to SSW | 22–24 | 1000 | 4–5 |
| | 16 Jul | S to SSE | 7–10 | 13 | 1.1–1.4 | E to WSW | 22–23 | 500 | 4–5 |
| | 17 Jul | S to SSW | 7-9 | 13 | 1.9-2.1 | S | 21 | 2000 | 3-5 |
| | 21 Jul | E to SSE | 1–5 | 6 | 0.5–0.6 | S to SSE | 20–22 | 100 | 1–5 |
| | 22 Jul | NW to SW | 2–5 | 5 | 0.4–0.5 | S to SSE | 21–23 | nlc | 3–5 |
| AQ-38 | 5 Aug | W to SSW | 3-8 | 11 | 1.1-1.3 | ESE to SSE | 18-20 | 1000 | 1-5 |
| | 6 Aug | WNW to SW | 1-5 | 6 | 0.6-0.7 | S | 21-23 | 3500 | 4-5 |
| AT-39 | 7 Aug | SW to SSE | 2-8 | 10 | 0.5-1.0 | S to SSE | 21-22 | 3500 | 3-5 |
| AS-39 | 14 Aug | WNW to SSW | 3-6 | 8 | 0.6-0.9 | SSW to S | 21-23 | 1000 | 5 |
| AV-38 | 3 Sep | SW to SSW | 4-6 | 8 | 0.9-1.2 | E to ESE | 18-20 | 2000 | 5 |
| AN-37 | 5 Sep | N to NW | 2-7 | 9 | 1.4-1.7 | E | 18-19 | nlc | 5 |
| AU-38 | 7 Sep | WSW to SSW | 4-6 | 8 | 0.9-1.5 | ENE | 19-20 | 100 | 2-5 |

nlc = Noctilucent Clouds

# 2. Methods

## 2.1. Acoustic Data Acquisition

Acoustic and water column data were collected for this project. Acoustic data were collected using Autonomous Multichannel Acoustic Recorders (AMARs, manufactured by JASCO). All acoustic recording systems were calibrated using a GRAS 42AC pistonphone precision sound source (Appendix 5.E.1.1). The pressure sensitivity obtained from the pistonphone calibration was used in the subsequent data analysis. A conductivity-temperature-depth (CTD) logger was used to collect temperature and salinity profiles, from which sound speed was calculated, to supplement the acoustic data.

The AMAR stations were named according to their nominal distance from the piling area. The following subsections describe each type of equipment in detail and how it was used to collect data for the Project.

### 2.1.1. Underwater Acoustic Recorders

Underwater sound was recorded over thirteen deployments with AMARs G4 deployed at five stations, nominally 750, 750 at 90°, 2000, 4000, and 8000 m from each monitored pile (Figure 1; Table 1). Each AMAR was fitted with two GeoSpectrum M36 hydrophones configured to sample at 256 ksps (128 kHz recording bandwidth) with 24-bit resolution. Table 8 lists each station and corresponding AMAR IDs, and hydrophone models, sensitivities and depths for each monitored pile.

Table 8. Automonous monitoring equipment for each monitored pile during the sound field verification.

| Station | AMAR ID | Channel | Height from Bottom (m) | Model | Sensitivity dB re 1 V/µPa |
|---|---|---|---|---|---|
| **Foundation AT-40** | | | | | |
| AT40-750 | 863 | 1 | 3 | M36-V00-900 | -209.7 |
| AT40-750 | 863 | 2 | 20 | M36-V00-902 | -200.6 |
| AT40-2000 | 855 | 1 | 3 | M36-V00-900 | –200.2 |
| AT40-2000 | 855 | 2 | 20 | M36-V00-900 | -200.5 |
| AT40-4000 | 860 | 1 | 3 | M36-V00-900 | -200.3 |
| AT40-4000 | 860 | 2 | 20 | M36-V00-900 | -200.5 |
| AT40-8000 | 864 | 1 | 3 | M36-V35-900 | -163.9 |
| AT40-8000 | 864 | 2 | 20 | M36-V00-900 | -200.4 |
| AT40-75090 | 865 | 1 | 3 | M36-V00-900 | -200.8 |
| AT40-75090 | 865 | 2 | 20 | M36-V00-902 | -209.1 |
| **Foundation AU-39** | | | | | |
| AU39-750 | 863 | 1 | 3 | M36-V00-900 | -209.7 |
| AU39-750 | 863 | 2 | 20 | M36-V00-902 | -200.6 |
| AU39-2000 | 855 | 1 | 3 | M36-V00-900 | –200.2 |
| AU39-2000 | 855 | 2 | 20 | M36-V00-900 | -200.5 |
| AU39-4000 | 860 | 1 | 3 | M36-V00-900 | -200.3 |
| AU39-4000 | 860 | 2 | 20 | M36-V00-900 | -200.5 |
| AU39-8000 | 864 | 1 | 3 | M36-V35-900 | -163.9 |
| AU39-8000 | 864 | 2 | 20 | M36-V00-900 | -200.4 |
| AU39-75090 | 865 | 1 | 3 | M36-V00-900 | -200.8 |
| AU39-75090 | 865 | 2 | 20 | M36-V00-902 | -209.1 |
| **Foundation AP-38** | | | | | |
| AP38-750 | 863 | 1 | 3 | M36-V00-900 | -209.7 |
| AP38-750 | 863 | 2 | 20 | M36-V00-902 | -200.6 |
| AP38-2000 | 855 | 1 | 3 | M36-V00-900 | –200.2 |
| AP38-2000 | 855 | 2 | 20 | M36-V00-900 | -200.5 |
| AP38-4000 | 860 | 1 | 3 | M36-V00-900 | -200.3 |
| AP38-4000 | 860 | 2 | 20 | M36-V00-900 | -200.5 |
| AP38-9000 | 864 | 1 | 3 | M36-V35-900 | -163.9 |
| AP38-9000 | 864 | 2 | 20 | M36-V00-900 | -200.4 |
| AP38-75090 | 865 | 1 | 3 | M36-V00-900 | -200.8 |
| AP38-75090 | 865 | 2 | 20 | M36-V00-902 | -209.1 |
| **Foundation AV-39** | | | | | |
| AV39-750 | 863 | 1 | 3 | M36-V00-900 | -200.4 |
| AV39-750 | 863 | 2 | 20 | M36-V00-902 | -209.6 |
| AV39-2000 | 855 | 1 | 3 | M36-V00-900 | -200.3 |

| Station | AMAR ID | Channel | Height from Bottom (m) | Model | Sensitivity dB re 1 V/µPa |
|---|---|---|---|---|---|
| AV39-2000 | 855 | 2 | 20 | M36-V00-900 | -200.4 |
| AV39-4000 | 860 | 1 | 3 | M36-V00-900 | -199.8 |
| AV39-4000 | 860 | 2 | 20 | M36-V00-900 | -200.1 |
| AV39-8000 | 864 | 1 | 3 | M36-V00-900 | -200.3 |
| AV39-8000 | 864 | 2 | 20 | M36-V00-900 | -200.2 |
| AV39-75090 | 865 | 1 | 3 | M36-V00-900 | -200.2 |
| AV39-75090 | 865 | 2 | 20 | M36-V00-902 | -209.4 |
| **Foundation AR-39** | | | | | |
| AR39-750 | 863 | 1 | 3 | M36-V00-900 | -208.5 |
| AR39-750 | 863 | 2 | 20 | M36-V00-902 | -199.6 |
| AR39-2000 | 855 | 1 | 3 | M36-V00-900 | –199.6 |
| AR39-2000 | 855 | 2 | 20 | M36-V00-900 | -199.9 |
| AR39-6000 | 864 | 1 | 3 | M36-V00-900 | -199.8 |
| AR39-6000 | 864 | 2 | 20 | M36-V00-900 | -199.4 |
| AR39-75090 | 865 | 1 | 3 | M36-V00-900 | -199.5 |
| AR39-75090 | 865 | 2 | 20 | M36-V00-902 | -208.3 |
| **Foundation AW-38** | | | | | |
| AW38-750 | 863 | 1 | 3 | M36-V00-900 | -200.5 |
| AW38-750 | 863 | 2 | 20 | M36-V00-902 | -209.4 |
| AW38-2000 | 855 | 1 | 3 | M36-V00-900 | -200.5 |
| AW38-2000 | 855 | 2 | 20 | M36-V00-900 | -200.8 |
| AW38-4000 | 860 | 1 | 3 | M36-V00-900 | -200.3 |
| AW38-4000 | 860 | 2 | 20 | M36-V00-900 | -200.4 |
| AW38-8000 | 864 | 1 | 3 | M36-V00-900 | -200.7 |
| AW38-8000 | 864 | 2 | 20 | M36-V00-900 | -200.3 |
| AW38-75090 | 865 | 1 | 3 | M36-V00-900 | -200.4 |
| AW38-75090 | 865 | 2 | 20 | M36-V00-902 | -209.2 |
| **Foundation AM-37** | | | | | |
| AM37-750 | 863 | 1 | 3 | M36-V00-900 | -208.9 |
| AM37-750 | 863 | 2 | 20 | M36-V00-902 | -208.8 |
| AM37-2000 | 855 | 1 | 3 | M36-V00-900 | -199.3 |
| AM37-2000 | 855 | 2 | 20 | M36-V00-900 | -200.0 |
| AM37-4000 | 860 | 1 | 3 | M36-V00-900 | -199.7 |
| AM37-4000 | 860 | 2 | 20 | M36-V00-900 | -200.0 |
| AM37-8000 | 864 | 1 | 3 | M36-V00-900 | -199.8 |
| AM37-8000 | 864 | 2 | 20 | M36-V00-900 | -199.5 |
| AM37-75090 | 865 | 1 | 3 | M36-V00-900 | -199.3 |
| AM37-75090 | 865 | 2 | 20 | M36-V00-902 | -208.9 |

| Station | AMAR ID | Channel | Height from Bottom (m) | Model | Sensitivity dB re 1 V/μPa |
|---|---|---|---|---|---|
| **Foundation AQ-38** | | | | | |
| AQ38-750 | 863 | 2 | 20 | M36-V00-902 | -209.7 |
| AQ38-2000 | 855 | 1 | 3 | M36-V00-900 | -200.5 |
| AQ38-2000 | 855 | 2 | 20 | M36-V00-900 | -200.8 |
| AQ38-4000 | 860 | 1 | 3 | M36-V00-900 | -200.3 |
| AQ38-4000 | 860 | 2 | 20 | M36-V00-900 | -200.4 |
| AQ38-8000 | 864 | 1 | 3 | M36-V00-900 | -200.4 |
| AQ38-8000 | 864 | 2 | 20 | M36-V00-900 | -200.3 |
| AQ38-75090 | 865 | 1 | 3 | M36-V00-900 | -200.4 |
| AQ38-75090 | 865 | 2 | 20 | M36-V00-902 | -209.2 |
| **Foundation AT-39** | | | | | |
| AT39-750 | 863 | 2 | 20 | M36-V00-902 | -209.3 |
| AT39-2000 | 855 | 1 | 3 | M36-V00-900 | -200.3 |
| AT39-2000 | 855 | 2 | 20 | M36-V00-900 | -200.7 |
| AT39-8000 | 864 | 2 | 20 | M36-V00-900 | -200.1 |
| AT39-75090 | 865 | 1 | 3 | M36-V00-900 | -200.6 |
| AT39-75090 | 865 | 2 | 20 | M36-V00-902 | -209.0 |
| **Foundation AS-39** | | | | | |
| AS39-750 | 863 | 2 | 20 | M36-V00-902 | -209.3 |
| AS39-2000 | 855 | 1 | 3 | M36-V00-900 | -200.3 |
| AS39-2000 | 855 | 2 | 20 | M36-V00-900 | -200.7 |
| AS39-4000 | 860 | 1 | 3 | M36-V00-900 | -200.3 |
| AS39-4000 | 860 | 2 | 20 | M36-V00-900 | -200.4 |
| AS39-75090 | 865 | 1 | 3 | M36-V00-900 | -200.6 |
| AS39-75090 | 865 | 2 | 20 | M36-V00-902 | -209.0 |
| **Foundation AV-38** | | | | | |
| AV38-750 | 863 | 2 | 20 | M36-V00-902 | -209.7 |
| AV38-2000 | 855 | 1 | 3 | M36-V00-900 | -200.4 |
| AV38-2000 | 855 | 2 | 20 | M36-V00-900 | -200.8 |
| AV38-4000 | 860 | 1 | 3 | M36-V00-900 | -200.3 |
| AV38-4000 | 860 | 2 | 20 | M36-V00-900 | -200.6 |
| AV38-8000 | 603 | 2 | 20 | M36-V00-900 | -200.3 |
| AV38-75090 | 865 | 1 | 3 | M36-V00-900 | -201.2 |
| AV38-75090 | 865 | 2 | 20 | M36-V00-902 | -209.2 |
| **Foundation AN-37** | | | | | |
| AN37-750 | 863 | 2 | 20 | M36-V00-902 | -209.8 |
| AN37-2000 | 855 | 1 | 3 | M36-V00-900 | -200.3 |
| AN37-2000 | 855 | 2 | 20 | M36-V00-900 | -200.6 |

| Station | AMAR ID | Channel | Height from Bottom (m) | Model | Sensitivity dB re 1 V/µPa |
|---|---|---|---|---|---|
| AN37-4000 | 860 | 1 | 3 | M36-V00-900 | -200.3 |
| AN37-4000 | 860 | 2 | 20 | M36-V00-900 | -201.1 |
| AN37-8000 | 603 | 2 | 20 | M36-V00-900 | -200.4 |
| AN37-75090 | 865 | 1 | 3 | M36-V00-900 | -201.0 |
| AN37-75090 | 865 | 2 | 20 | M36-V00-902 | -209.4 |
| **Foundation AU-38** | | | | | |
| AU38-750 | 863 | 2 | 20 | M36-V00-902 | -209.8 |
| AU38-2000 | 855 | 1 | 3 | M36-V00-900 | -200.3 |
| AU38-2000 | 855 | 2 | 20 | M36-V00-900 | -200.6 |
| AU38-4000 | 860 | 1 | 3 | M36-V00-900 | -200.3 |
| AU38-4000 | 860 | 2 | 20 | M36-V00-900 | -201.1 |
| AU38-8000 | 603 | 2 | 20 | M36-V00-900 | -200.4 |
| AU38-75090 | 865 | 1 | 3 | M36-V00-900 | -201.0 |
| AU38-75090 | 865 | 2 | 20 | M36-V00-902 | -209.4 |

### 2.1.2. Deployment Locations

All stations where AMARs were deployed during the sound field verification with corresponding AMAR IDs, geographic coordinates, depth at the bottom and the distance from the source pile driving are listed in Table 9.

Table 9. Location (WGS84) of stations for each monitored pile during the sound field verification.

| Station (m) | Recorder ID | Latitude (N) | Longitude (W) | Water depth (m) | Distance to pile (m) |
|---|---|---|---|---|---|
| **Foundation AT-40** | | | | | |
| 750 | AMAR-863 | 41° 0.966' | 70° 25.422' | 43 | 753 |
| 750-90° | AMAR-865 | 41° 0.960' | 70° 24.697' | 40.2 | 715 |
| 2,000 | AMAR-855 | 41° 0.483' | 70° 26.042' | 43.9 | 1999 |
| 4,000 | AMAR-860 | 40° 59.712' | 70° 27.082' | 44.8 | 4038 |
| 8,000 | AMAR-864 | 40° 58.186' | 70° 29.089' | 45 | 8023 |
| **Foundation AU-39** | | | | | |
| 750 | AMAR-863 | 40° 59.954' | 70° 25.969' | 44.4 | 740 |
| 750-90° | AMAR-865 | 40° 59.965' | 70° 25.969' | 44.4 | 712 |
| 2,000 | AMAR-855 | 40° 59.472' | 70° 27.362' | 45.0 | 2012 |
| 4,000 | AMAR-860 | 40° 58.712' | 70° 28.364' | 45.3 | 3999 |
| 8,000 | AMAR-864 | 40° 57.159' | 70° 30.373' | 47.2 | 8022 |
| **Foundation AP-38** | | | | | |

| Station (m) | Recorder ID | Latitude (°N) | Longitude (°W) | Water depth (m) | Distance to pile (m) |
|---|---|---|---|---|---|
| 750 | AMAR-863 | 41° 4.963' | 70° 28.153' | 42.1 | 748 |
| 750-90° | AMAR-865 | 41° 4.982' | 70° 27.373' | 43.3 | 704 |
| 2,000 | AMAR-855 | 41° 4.501' | 70° 28.761' | 43.0 | 1923 |
| 4,000 | AMAR-860 | 41° 3.728' | 70° 29.777' | 46.1 | 3940 |
| 9,000 | AMAR-864 | 41° 1.804' | 70° 32.311' | 47.0 | 8965 |
| **Foundation AV-39** | | | | | |
| 750 | AMAR-863 | 40° 58.938’ | 70° 26.694’ | 45.0 | 761 |
| 750-90° | AMAR-865 | 40° 58.953’ | 70° 25.942’ | 45.0 | 732 |
| 2,000 | AMAR-855 | 40° 58.4682’ | 70° 27.318’ | 45.2 | 1992 |
| 4,000 | AMAR-860 | 40° 57.7152’ | 70° 28.332’ | 46.6 | 3987 |
| 8,000 | AMAR-864 | 40° 56.1828’ | 70° 30.396’ | 49.3 | 8032 |
| **Foundation AR-39** | | | | | |
| 750 | AMAR-863 | 41° 2.947' | 70° 26.780' | 42.1 | 752 |
| 750-90° | AMAR-865 | 41° 2.950' | 70° 25.996' | 43.3 | 773 |
| 2,000 | AMAR-855 | 41° 2.498' | 70° 27.378' | 43.0 | 1931 |
| 6,000 | AMAR-864 | 41° 0.953' | 70° 29.414' | 47.0 | 5964 |
| **Foundation AW-38** | | | | | |
| 750 | AMAR-863 | 40° 57.974' | 70° 28.051' | 46 | 759 |
| 750-90° | AMAR-865 | 40° 57.935' | 70° 27.212' | 46 | 762 |
| 2,000 | AMAR-855 | 40° 57.464' | 70° 28.640' | 47 | 2001 |
| 4,000 | AMAR-860 | 40° 56.715' | 70° 29.608' | 47 | 3941 |
| 8,000 | AMAR-864 | 40° 55.163' | 70° 31.661' | 51 | 8007 |
| **Foundation AM-37** | | | | | |
| 750 | AMAR-863 | 41° 6.891' | 70° 29.529' | 39 | 823 |
| 750-90° | AMAR-865 | 41° 6.882' | 70° 28.717' | 40 | 810 |
| 2,000 | AMAR-855 | 41° 6.413' | 70° 30.149' | 40 | 2062 |
| 4,000 | AMAR-860 | 41° 5.620' | 70° 31.130' | 41 | 4070 |
| 8,000 | AMAR-864 | 41° 4.108' | 70° 33.123' | 42 | 8020 |
| **Foundation AQ-38** | | | | | |
| 750 | AMAR-863 | 41° 3.931' | 70° 28.140' | 43.2 | 767 |
| 750-90° | AMAR-865 | 41° 3.935' | 70° 27.383' | 41.0 | 729 |
| 2,000 | AMAR-855 | 41° 3.463' | 70° 28.766' | 47.0 | 1998 |
| 4,000 | AMAR-860 | 41° 2.692' | 70° 29.786' | 46.3 | 4017 |
| 8,000 | AMAR-864 | 41° 1.148' | 70° 31.802' | 47.5 | 8033 |
| **Foundation AT-39** | | | | | |

| Station (m) | Recorder ID | Latitude (°N) | Longitude (°W) | Water depth (m) | Distance to pile (m) |
|---|---|---|---|---|---|
| 750 | AMAR-863 | 41° 0.943' | 70° 26.751' | 42.6 | 770 |
| 750-90° | AMAR-865 | 41° 0.942' | 70° 25.969' | 42.8 | 766 |
| 2,000 | AMAR-855 | 41° 0.452' | 70° 27.369' | 42.6 | 2024 |
| 8,000 | AMAR-864 | 40° 58.171' | 70° 30.420' | 43.5 | 8031 |
| **Foundation AS-39** | | | | | |
| 750 | AMAR-863 | 41° 1.956' | 70° 26.764' | 42.2 | 744 |
| 750-90° | AMAR-865 | 41° 1.948' | 70° 25.998' | 43.0 | 751 |
| 2,000 | AMAR-855 | 41° 1.476' | 70° 27.389' | 43.7 | 1991 |
| 4,000 | AMAR-860 | 41° 0.739' | 70° 28.368' | 43.9 | 3925 |
| **Foundation AV-38** | | | | | |
| 750 | AMAR-863 | 40° 58.923' | 70° 28.056' | 46.1 | 801 |
| 750-90° | AMAR-865 | 40° 58.922' | 70° 27.372' | 45.0 | 655 |
| 2,000 | AMAR-855 | 40° 58.481' | 70° 28.726' | 46.1 | 2046 |
| 4,000 | AMAR-860 | 40° 57.702' | 70° 29.714' | 48.3 | 4041 |
| 8,000 | AMAR-603 | 40° 56.140' | 70° 31.723' | 50.1 | 8076 |
| **Foundation AN-37** | | | | | |
| 750 | AMAR-863 | 41° 5.886' | 70° 29.505' | 42.6 | 807 |
| 750-90° | AMAR-865 | 41° 5.934' | 70° 28.692' | 41.0 | 769 |
| 2,000 | AMAR-855 | 41° 5.4' | 70° 30.11' | 43.3 | 2037 |
| 4,000 | AMAR-860 | 41° 4.536' | 70° 30.945' | 42.8 | 4015 |
| 8,000 | AMAR-603 | 41° 2.878' | 70° 32.789' | 48.6 | 8023 |
| **Foundation AU-38** | | | | | |
| 750 | AMAR-863 | 40° 59.931' | 70° 28.0236' | 44.8 | 737 |
| 750-90° | AMAR-865 | 40° 59.899' | 70° 27.243' | 44.4 | 822 |
| 2,000 | AMAR-855 | 40° 59.448' | 70° 28.6728' | 46.1 | 2012 |
| 4,000 | AMAR-860 | 40° 58.663' | 70° 29.659' | 46.1 | 4016 |
| 8,000 | AMAR-603 | 40° 57.011' | 70° 31.891' | 50.1 | 8390 |

### 2.1.3. CTD Casts

The conductivity, temperature, and depth (CTD) of the water column were measured with a Minos-X CTD (manufactured by AML Oceanographic; Figure 4) at SFV stations either after deployment or retrieval of the base plates, while the vessel was stationary and holding position. At each location, CTD profiles were measured by lowering the CTD to the ocean bottom and back up to the surface, creating a downcast and upcast profile. For each measurement, the sound speed profile of the water column was calculated from the CTD data. Appendix G shows the CTD measurements collected for this study.


Figure 4. Minos-X CTD (AML Oceanographic) used to collect sound speed data during the Project.

## 2.2. Automated Data Analysis

### 2.2.1. Pile Driving Event Detection

The Automated Impulse Detector is based on a Teager-Kaiser energy detector. First, the pressure time series was high-pass filtered at 10 Hz. The high-pass filter used was a Finite Impulse Response (FIR) filter with frequency response shown in Figure 5. The filtered time-series were squared, summed over a 25 milliseconds (ms) window, divided by the number of samples in the 25 ms window, and then the square-root was taken. Finally, the 25 ms 'time-series' was divided by its mean value for each 5 s buffer of data that is passed to the Teager-Kaiser operator (Kaiser 1990, Kandia and Stylianou 2006). Normalizing the 5 s buffer by its mean value allows us to use a fixed threshold that is independent of the absolute magnitude of the raw time-series data. When the TK operator exceeded the detector threshold, manually set empirically between 20 to 90 depending on the monitoring station and its noise content, a pile strike was detected. The processing then selected a 0.5 s window from the original time series centered on the impulse detection time. The detector was configured with a "lock-out" of 0.75 s after a strike was identified to minimize false detections on multipath arrivals.

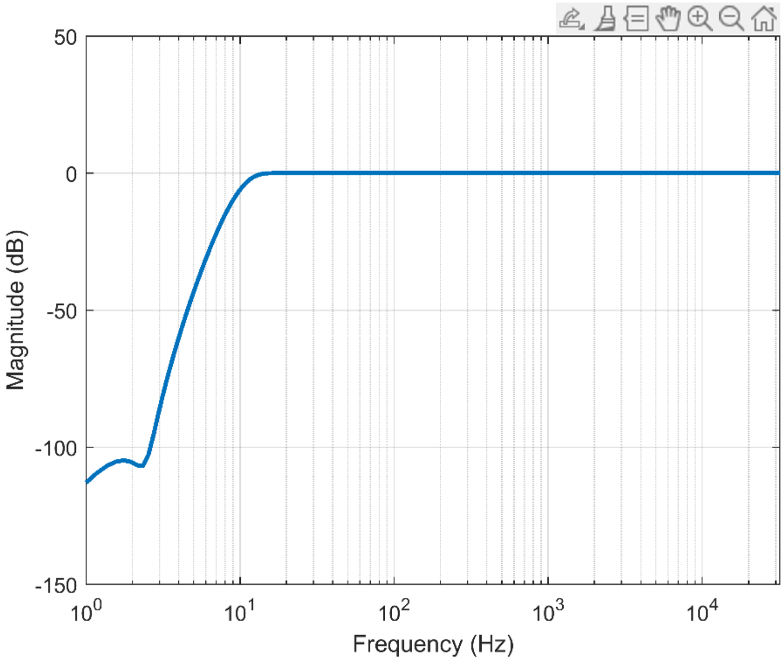


Figure 5. Frequency response of high-pass filter used in the data analysis.

### 2.2.2. Ambient Data Analysis

In this report, we define ambient data as the background sound levels just prior to the start of hammer strikes for each pile monitored. The data available for this analysis consisted of 2 to 10 minutes of recorded data collected prior to piling. Computed rms sound pressure level (SPL) for each minute of data available was averaged and plotted as a function of decidecade frequency bands. Broadband ambient levels were also computed per station and channel for each pile (Section 3.2).

## 2.3. Data Analysis

### 2.3.1. Pile Driving Sound Levels

Once the pile installation via impact piling was complete, acoustic data were downloaded from the AMARs and analyzed using the Teager-Kaiser impulse detector built into JASCO's specialized software PAMlab. Analysis consisted of calculating peak pressure level (PK), 90% sound pressure level (rms SPL), and (unweighted) sound exposure level (SEL) (see Appendix F.1) of all pile driving impulses recorded through the pile installation and summary statistics, including: total number of strikes (impulses), and maximum SPL. Per-strike acoustic metrics such as PK, SPL, SEL were plotted versus time along with the cumulative SEL. Decidecade band level box plots, and per-pile maximum and mean acoustic metrics and exceedance levels at $L_{95}$, $L_{75}$, $L_{50}$ (median), $L_{25}$, and $L_{5}$ (see Appendix F.1 for definitions), are reported for all thirteen foundations at the nominal locations of 750, 2,000, 4,000, and 8,000 m as well as an additional station at 750 m at 90° from the measurement radial from the source. The sound level statistics quantify the observed distribution of recorded sound levels. Following standard acoustical practice, the nth percentile level ($L_n$) is the SPL or SEL exceeded by n% of the data. $L_{max}$ is the maximum recorded sound level. $L_{mean}$ is the linear arithmetic mean of the sound power, which can be significantly different from the median sound level ($L_{50}$).

A 10 Hz high-pass filter was applied to all AMAR measurements to remove mooring and environmental noise.

## 2.3.2. Cumulative Sound Exposure Levels

The cumulative SEL (cSEL) were estimated at each recorder by summing the single-strike SEL (SELss) in linear space for each detection. The final value corresponding to all detections from each recorder, represented the total energy at the end of pile driving (full installation). Unweighted cSEL was reported for each foundation monitored, noting that cSEL for the jacket foundation corresponded to summing the SELss for the four installed pin piles. The unweighted cSEL was used to estimate ranges to injury thresholds for sturgeon.

Marine mammal frequency-weighted cSEL were computed for the impact piling impulses recorded at each AMAR for low-, mid-, and high-frequency cetaceans (LF, MF, and HF cetaceans, respectively) and pinnipeds in water (PW). Frequency-weighting was also applied to SELss and used to obtain the frequency weighted cSEL for sea turtles underwater (TU). Frequency-weighted cSEL were then used to calculate ranges to physical injury (PTS) thresholds.

## 2.3.3. Range estimation

Approximate ranges to acoustic thresholds for potential animal injury or behavioral response were obtained by fitting the $L_5$ exceedance levels (see Appendix F.1 for definitions) of cumulative SEL (cSEL), PK, and rms SPL measured at range *r* from the pile to the following equation:

$$RL = SL + A\log_{10} r + \alpha r \quad (1)$$

where *RL* is the received level, *SL* is the intercept term, representing a far-field source level estimate, *A* is the geometric spreading loss coefficient, and $\alpha$ is the intrinsic attenuation coefficient (in dB/m). It is noted that $\alpha$ refers to energy loss, primarily due to multiple seabed interactions occurring in a shallow water environment. For convenience and comparison to previously published results, $\alpha$ is reported in dB/km (equivalent to $\alpha \cdot 10^{-3}$ dB/m).

The acoustic range to a given threshold is found by fitting *RL* measured at stations with known ranges to Equation 1. When the propagation loss is assumed to be log-linear with range, then $\alpha = 0$ (no attenuation).

An analytical derivation of damped cylindrical spreading loss in single-strike SEL from pile driving is provided by Lippert et al. (2018) in which the DCS model is (Zampolli et al. 2013):

$$L_E(r) = L_E(r_1) - 10 \cdot \log_{10}\frac{r}{r_1}\, dB - \alpha(r - r_1), \quad (2)$$

with $r_1$ being the reference range, $\alpha$ being the decay factor or intrinsic attenuation, and $L_E$ being the sound exposure level representing a depth-averaged quantity. As noted by Lippert et al. (2018), uncertainties arise in this derivation due to several factors including the choice of the reference range and the comparison of single-depth measurements to the depth-averaged assumption.

While Zampolli et al. (2013) had shown that the DCS model is valid up to the pile wall for depth-averaged measurements, Dahl et al. (2012) found that the lower limit on $r_1$ for a single depth measurement is about three water depths. Ainslie et al. (2020) further studied the application of DCS models to measured pile driving data and notes that the exact limit on $r_1$ depends on both water depth and bottom geoacoustic properties.

At the time of this report, analytical studies for fitting DCS models to *M-weighted* (frequency-weighted) metrics including cumulative SEL have not been conducted to the authors' knowledge.

# 3. Results

## 3.1. Pile Driving Sound Levels

Received levels of detected impulses for each monitored pile are shown in 5.Appendix A, presented in the order of pile installation. Measured sounds (PK, SPL, and cSEL), sound levels per station, ranges to acoustic thresholds, and results from the regression analysis are presented, where cumulative SEL (cSEL) represents the total sound energy at the end of pile driving.

Collected data from the installation of the first six foundations (AT-40, AU-39, AP-38, AV-39, AR-39, and AW-38) were reanalyzed to follow the same optimized procedure adopted for the remainder of the monitored piles. The procedure involved re-running the impulse detector after using a high pass filter to remove noise below 10 Hz that was not associated with pile driving activities. Consequently, the number of detections and the overall results for these piles may differ from the original interim reports. (Notably, received levels from the mid-water column hydrophone at 4,000 m from AP-38 were reduced after removing signal energy below 10 Hz; resulting in shorter range estimates than in the interim report.)

For each monitored pile, regression curves were fitted to the data from all available stations either with or without an attenuation coefficient term. Without intrinsic attenuation, regression fits used equations of the form A*log(r), where A is the geometric spreading loss coefficient and r is the range. With intrinsic attenuation, regression fits used the equations of the form A*log(r) + αr, where A is the geometric spreading loss coefficient, r is the range, and α is the intrinsic attenuation coefficient (in dB/m).

Tables 10–15 present a summary of the relevant results in terms of distances to regulatory thresholds for all monopiles monitored. Similar results for the installation of the jacket foundation are presented in Appendix A.7 (Tables A-60 and A-61). Distances for each species group to PTS (cSEL) threshold for $L_5$ received levels for each monopile are shown in Table 10, without attenuation coefficient, and Table 11, with an attenuation coefficient. A similar summary for PTS (cSEL) for the jacket foundation is shown in Table 12, without an attenuation coefficient and with an attenuation coefficient. Ranges to behavioral thresholds (SPL) for monopile installation is shown in Table 12 without an attenuation coefficient, and Table 14 with an attenuation coefficient. Ranges to behavioral threshold for the jacket foundation with and without an attenuation coefficient are shown in Table 15. Predicted ranges are the modeled ranges with 6-dB attenuation from Table 5 in the IHA, Tables 7.1.20 and 7.1.25 of BiOp; and Table 6 in the IHA, Table 7.1.20 of BiOp (Pyć et al. 2018). Ranges to updated sea turtle thresholds with weighting and fish thresholds were obtained from the original modeling.

Table 10. Summary of isopleth distances (in meters) to NMFS cSEL physiological thresholds without intrinsic attenuation for impact driving installation of all 12 monopiles monitored.

| Group | Injury: cSEL (dB re 1 μPa²·s) | Predicted (m) | AT-40 | AU-39 | AP-38 | AV-39 | AR-39 | AW-38 | AQ-38 | AT-39 | AS-39 | AV-38 | AN-37 | AU-38 |
|---|---|---|---|---|---|---|---|---|---|---|---|---|---|---|
| LFC | 183 | 3,191 | 2,700 | 2,890 | 2,500 | 1,830 | 1,700 | 3,050 | 900 | 1,810 | 2,270 | 2,110 | 1,500 | 1,630 |
| MFC | 185 | 43 | 10 | 10 | 10 | 10 | 10 | 10 | 10 | 10 | 10 | 10 | 10 | 10 |
| HFC | 155 | 71 | 480 | 90 | 450 | 110 | 30 | 150 | 40 | 90 | 720 | 90 | 80 | 50 |
| PW | 185 | 153 | 160 | 100 | 90 | 140 | 100 | 140 | 40 | 120 | 110 | 130 | 90 | 90 |
| ST | 204 | 161 | 270 | 190 | 180 | 240 | 180 | 280 | 70 | 220 | 200 | 230 | 160 | 160 |
| AS | 187 | 6,894 | 5,110 | 6,240 | 5,820 | 3,950 | 4,460 | 6,580 | 2,300 | 4,000 | 6,080 | 4,460 | 3,490 | 4,090 |

Table 11. Summary of isopleth distances (in meters) to NMFS cSEL physiological thresholds with intrinsic attenuation for impact driving installation of all 12 monopiles monitored.

| Group | Injury: cSEL (dB re 1 μPa²·s) | Predicted (m) | AT-40 | AU-39 | AP-38 | AV-39 | AR-39 | AW-38 | AQ-38 | AT-39 | AS-39 | AV-38 | AN-37 | AU-38 |
|---|---|---|---|---|---|---|---|---|---|---|---|---|---|---|
| LFC | 183 | 3,191 | 2,800 | 3,640 | 3,220 | 1,850 | 1,750 | 3,190 | 880 | 1,890 | 2,330 | 2,370 | 1,820 | 1,860 |
| MFC | 185 | 43 | 20 | 10 | 10 | 10 | 10 | 10 | 10 | 10 | 10 | 10 | 10 | 10 |
| HFC | 155 | 71 | 520 | 40 | 300 | 160 | <100 | 190 | 10 | 60 | 610 | 60 | 200 | 70 |
| PW | 185 | 153 | 140 | 10 | 10 | 140 | 90 | 120 | 10 | 100 | 70 | 80 | 10 | 40 |
| ST | 204 | 161 | 250 | 20 | 30 | 230 | 140 | 240 | 10 | 180 | 160 | 140 | 10 | 50 |
| AS | 187 | 6,894 | 5,210 | 6,200 | 6,250 | 4,130 | 4,670 | 6,500 | 3,140 | 4,430 | 5,250 | 4,860 | 4,340 | 4,710 |

Table 12. Summary of isopleth distances (in meters) to NMFS cSEL physiological thresholds with and without intrinsic attenuation for impact driving installation of the jacket foundation AM-37, which includes piling of 4 pin piles.

| Group | Injury: cSEL (dB re 1 μPa²·s) | Predicted (m) | Without intrinsic attenuation | With intrinsic attenuation |
|---|---|---|---|---|
| LFC | 183 | 7,253 | 2,610 | 2,810 |
| MFC | 185 | 71 | 10 | 10 |
| HFC | 155 | 564 | 220 | 280 |
| PW | 185 | 977 | 180 | 120 |
| ST | 204 | 381 | 260 | 200 |
| AS | 187 | 7,803 | 4,060 | 4,410 |

Table 13. Summary of isopleth distances (in meters) for the NMFS behavioral thresholds without intrinsic attenuation for impact driving installation of all 12 monopiles monitored.

| Group | Behavior: SPL (dB re 1μPa²) | Predicted (m) | AT-40 | AU-39 | AP-38 | AV-39 | AR-39 | AW-38 | AQ-38 | AT-39 | AS-39 | AV-38 | AN-37 | AU-38 |
|---|---|---|---|---|---|---|---|---|---|---|---|---|---|---|
| MM | 160 | 4,121 | 4,610 | 5,690 | 5,410 | 3,710 | 4,390 | 6,300 | 3,060 | 4,030 | 5,740 | 4,630 | 3,220 | 5,310 |
| ST | 175 | 1,400 | 540 | 610 | 620 | 460 | 420 | 640 | 300 | 530 | 570 | 530 | 390 | 560 |
| AS | 150 | 9,229 | 19,270 | 25,260 | 22,960 | 14,950 | 20,850 | 29,120 | 14,280 | 15,620 | 26,830 | 19,640 | 13,080 | 23,750 |

Table 14. Summary of isopleth distances (in meters) for the NMFS behavioral thresholds with intrinsic attenuation for impact driving installation of all 12 monopiles monitored.

| Group | Behavior: SPL (dB re 1µPa$^2$) | Predicted (m) | AT-40 | AU-39 | AP-38 | AV-39 | AR-39 | AW-38 | AQ-38 | AT-39 | AS-39 | AV-38 | AN-37 | AU-38 |
|---|---|---|---|---|---|---|---|---|---|---|---|---|---|---|
| MM | 160 | 4,121 | 4,820 | 5,830 | 5,740 | 3,790 | 4,450 | 6,290 | 3,290 | 4,260 | 6,870 | 5,000 | 4,000 | 5,720 |
| ST | 175 | 1,400 | 490 | 510 | 550 | 440 | 400 | 620 | 250 | 480 | 590 | 440 | 130 | 370 |
| AS | 150 | 9,229 | 13,520 | 12,760 | 13,970 | 13,410 | 15,760 | 20,720 | 11,440 | 12,130 | 14,030 | 11,880 | 8,920 | 11,900 |

Table 15. Summary of isopleth distances (in meters) for the NMFS behavioral thresholds with and without intrinsic attenuation for impact driving installation of the jacket foundation AM-37, which includes piling of 4 pin piles.

| Group | Behavior: SPL (dB re 1µPa$^2$) | Predicted (m) | Without intrinsic attenuation | With intrinsic attenuation |
|---|---|---|---|---|
| MM | 160 | 3,330 | 1,180 | 1,180 |
| ST | 175 | 727 | 180 | 180 |
| AS | 150 | 4,220 | 4,220 | 4,200 |

## 3.2. Ambient Sound Levels

AMARs were deployed at least a few hours prior to the commencement of pile driving, and recovered soon after operations ended, and the pile was completely installed. Hence, the recorders were fixed prior to pile driving until their recovery for data analysis. Table 16 shows the broadband ambient sound levels immediately before the start of impact pile driving for the monitored piles, station, and hydrophone channels. The grey cells correspond to the channels that were not functioning properly and were left out of the analysis. Cells with asterisks correspond to channels where not enough data was available prior to the commencement of pile driving for the calculation of ambient levels. At least 2 minutes and at most 10 minutes were used to estimate average rms SPL sound levels prior to piling. The double asterisks on station AR39-4000 is to indicate that, the range of measurements was actually taken at a nominal distance of 6000 m. The triple asterisks on station AP38-8000 is to indicate that, the range of measurements was actually taken at a nominal distance of 9000 m. Figure 6 shows a scatter plot of the broadband ambient noise levels for all data and grouped by recording station. The spectra of ambient sound prior to pile driving of each foundation are presented in Appendix D.

Table 16. Average broadband ambient noise levels (rms SPL) prior to the commencement of piling, recorded at each station for all monitored piles.

| Pile ID | Channel | Ambient noise levels (dB re 1 µPa²) | | | | |
|---|---|---|---|---|---|---|
| | | 750 m | 750-90 m | 2000 m | 4000 m | 8000 m |
| AT-40 | 1 | 162.7 | 137.4 | | 143.7 | |
| | 2 | 142.0 | 137.7 | 137.3 | 131.8 | 139.8 |
| AU-39 | 1 | 144.2 | 133.8 | | 127.8 | |
| | 2 | 135.1 | 131.9 | 130.2 | 126.9 | 123.1 |
| AP-38 | 1 | 131.9 | * | 125.6 | 119.7 | |
| | 2 | 130.5 | 123.0 | 126.9 | 127.1 | 116.5 *** |
| AV-39 | 1 | 131.8 | * | 125.8 | 122.5 | 116.4 |
| | 2 | 132.0 | * | 125.5 | 122.5 | 117.5 |
| AR-39 | 1 | | 131.0 | 126.3 | 112.9 ** | |
| | 2 | 126.9 | 133.9 | 125.1 | 114.2 ** | |
| AW-38 | 1 | | 132.3 | 130.5 | 125.6 | 122.5 |
| | 2 | 132.4 | 131.7 | 125.9 | 124.2 | 123.1 |
| AM-37 | 1 | | 129.4 | 129.0 | 125.0 | 119.4 |
| | 2 | 130.6 | 133.4 | 130.3 | 132.6 | 119.1 |
| AQ-38 | 1 | | 159.0 | 152.6 | 129.0 | 135.3 |
| | 2 | 138.3 | 144.9 | 137.7 | 129.6 | 126.4 |
| AT-39 | 1 | | 134.3 | 128.9 | | |
| | 2 | 130.2 | 131.5 | 131.4 | 138.7 | 121.6 |
| AS-39 | 1 | | 136.9 | 131.0 | 121.4 | |
| | 2 | 133.2 | 135.9 | 125.7 | 122.6 | |
| AV-38 | 1 | | * | 142.0 | * | * |
| | 2 | * | * | 123.8 | * | 122.7 |
| AN-37 | 1 | | 137.0 | 132.0 | 125.0 | |
| | 2 | 133.5 | 135.4 | 135.1 | 124.1 | 123.6 |
| AU-38 | 1 | | 137.7 | 131.9 | 133.5 | |
| | 2 | 137.0 | 137.4 | 132.0 | 128.7 | 123.5 |

* insufficient data reviewed for ambient calculation
** measured at 6000 m at nominal 4000 m station
*** measured at 9000 m at nominal 8000 m station

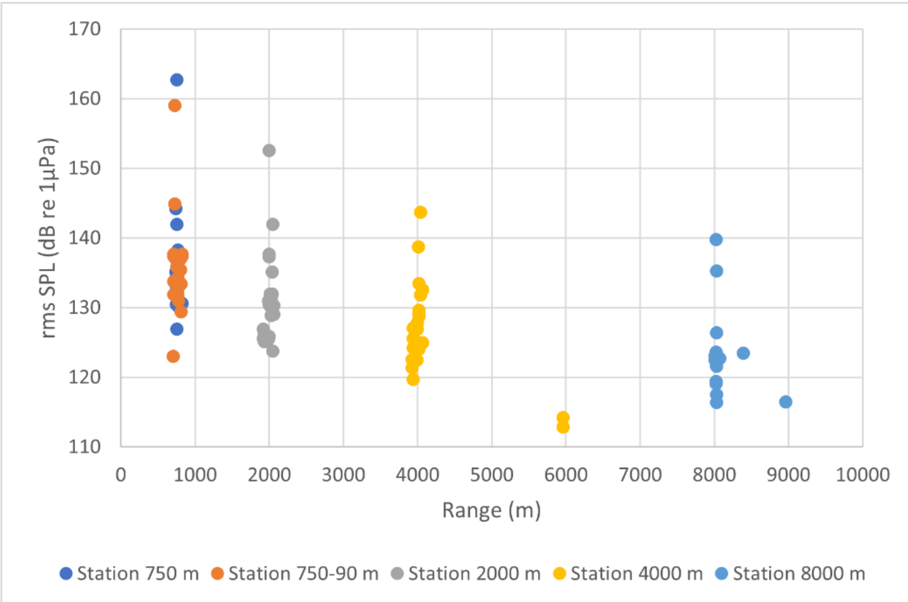


Figure 6. Broadband ambient noise level (rms SPL) scatter plot prior to the commencement of piling. Different colors correspond to the different SFV stations.

## 3.3. Analysis of Five Piles with Same Double Bubble Curtain Maintenance

The maintenance schedule of the double bubble curtain was optimized starting from the installation of foundation AQ-38 onwards to maximize performance given the fine sediments encountered in the lease area. Five monopiles (AQ-38, AT-39, AV-38, AN-37, and AU-38) were installed following this optimized maintenance schedule for the double big bubble curtain (DBBC, 730 m and 960 m), which was serviced and maintained by re-drilling the hose holes upon every hose retrieval and prior to redeployment in the field. Here we analyze measured data from these five piles as they represent installation with the same noise mitigation system, i.e. using a Hydrosound Damper System (HSD) and the optimized DBBC.

With the optimized maintenance routine, the resulting ranges to injury thresholds were within the predicted distances, e.g., low-frequency cetacean cSEL was <3,191 m for all five piles, with the exception that high-frequency cetaceans occasionally exceeded the predicted 71 m range, but this is likely due to noise when extrapolating to short distances from fittings collected farther away. Measurement variance and non-piling noise contribute to error at extrapolated distances.

Level B ranges to SPL thresholds were often close to or could exceed the predicted range of 4,121 m for low-frequency marine mammals, ranging from 3,000 m to over 5,000 m. The ranges to SPL 150 dB re 1 $\mu Pa^2$ for sturgeon exceeded the predicted distance of 9,229 m in most cases (9 km to 23 km). For the five foundations installed using this noise attenuation configuration and maintenance routine, the expected distance to SPL thresholds were determined by fitting the combined (pooled) received levels from all the stations for each of the installed piles. The maximum hammer energy, number of strikes, and water depth were similar for each pile (Table 17) so no normalization with respect to these parameters was performed.

Table 17. Comparison of maximum energy (kJ), number of strikes, water depth (m), and ranges to SPL 160 and 150 dB re 1µPa$^2$ for five consecutive piles with double bubble curtain.

| Pile ID | Max Energy (kJ) | Number Strikes | Water Depth (m) | R (m) to 160 SPL | R (m) to 150 SPL |
|---|---|---|---|---|---|
| AQ-38 | 3227 | 3023 | 41.4 | 3,060 | 14,280 |
| AT-39 | 3831 | 3159 | 41.98 | 4,030 | 14,410 |
| AV-38 | 3519 | 3470 | 43.1 | 4,630 | 19,640 |
| AN-37 | 3748 | 3682 | 40.45 | 3,220 | 13,080 |
| AU-38 | 3825 | 2884 | 42.95 | 5,310 | 23,750 |

Pooling the $L_5$ received levels at each station and fitting without and with attenuation coefficient (Figure 7 and Figure 8, respectively), result in coefficients that are near expected values – the fit without attenuation coefficient is close to practical spreading loss while the fit with attenuation coefficient is close to damped cylindrical spreading loss. The ranges to SPL 160 and 150 dB re 1µPa$^2$ without attenuation coefficient are 3,750 m and 15,500 m, respectively. With attenuation coefficient, the ranges to SPL 160 and 150 dB re 1µPa$^2$ are 4,000 m and 11,000 m.

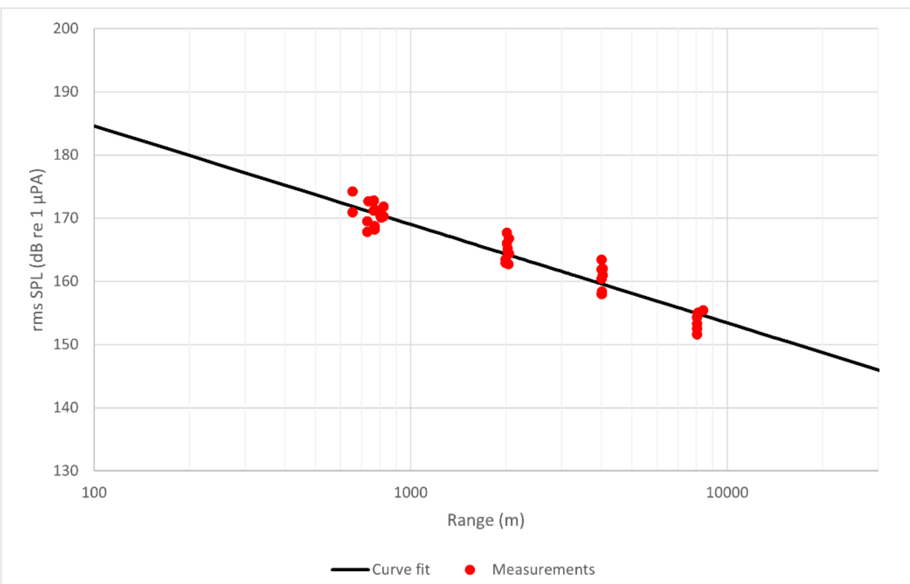


Figure 7. $L_5$ received levels at each station fitted using A*log(r) (no attenuation factor), where the fitting parameter A = -15.6.

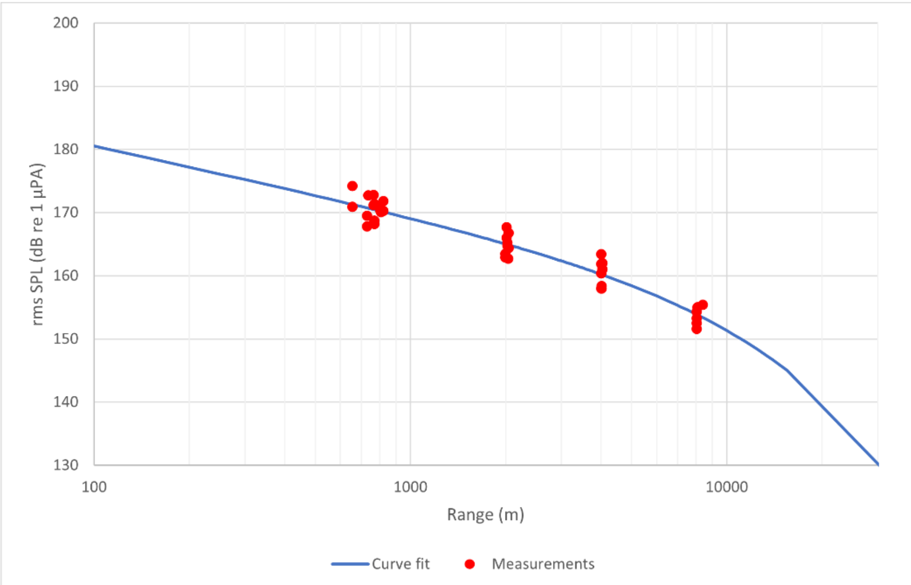


Figure 8. $L_5$ received levels at each station fitted using A*log(r) - $\alpha$r (with attenuation factor), where the coefficient parameter A = -10.8 and $\alpha$ = -0.000771.

# 4. Discussion

## 4.1. Ranges to thresholds

Sound field verification measurements were performed during the installation of thirteen foundations, twelve monopiles and one jacket foundation. A Hydro Sound Damper (HSD) system was employed as a near-field attenuation device close the monopiles and either a single or double big bubble curtain (BBC) at greater distance surrounding the monopile. The first three monopiles (AT-40, AU-39, and AP-38) were installed with a single BBC at ~115 m around the pile (though for the first two piles the curtain was not circular). The length of this bubble curtain is 730 m and typical free air delivery (FAD) was ~448 m³/min. After finding that the distances to predicted marine mammal thresholds were exceeded with this configuration (Table 10 and Table 11), a second big bubble curtain was included for subsequent piles, such that the complete attenuation system consisted of the HSD and a double big bubble curtain (DBBC). The second bubble curtain was ~150 m radius from the pile. Its length was 960 m and typical free air delivery was also ~448 m³/min. The distance to thresholds for monopiles four (AV-39) and five (AR-39) were substantially less than the first three monopiles and did not exceed the predicted ranges to threshold (although the marine mammal Level B range was slightly longer than the predicted for AR-39), indicating that addition of the second big bubble curtain was effective in reducing sound energy in the water. The distances to thresholds for the sixth monopile (AW-38), however, were again similar to the first three piles despite the DBBC. It was determined that the maintenance schedule and improvement / optimization procedures of the bubble curtains would be revised such that the holes were re-drilled prior to each deployment of the hoses. This enhanced BBC maintenance protocol, implemented from the installation of foundation AQ-38 onwards, is an adjustment from typical bubble curtain operations in the North Sea where hoses are usually drilled after every third deployment but was done here to maximize performance considering siltier sediments in the lease area. The seventh foundation (AM-37) installed was the jacket foundation, and distances to marine mammal, sea turtle, and Atlantic sturgeon thresholds were less than predicted distances. Foundations eight and nine (AQ-38 and AT-39), eleven through thirteen (AV-38, AN-37, and AU-38) were monopiles driven using the HSD and DBBC maintained by the enhanced BBC maintenance protocol before each deployment. Foundation nine (monopile AS-39) was driven with the HSD and a single BBC due to a mechanical failure on the second bubble curtain vessel. The five monopile foundations (AQ-38, AT-39, AV-38, AN-37, and AU-38) driven using the HSD and DBBC with enhanced maintenance protocol represent the NAS configuration, maintenance schedule and optimization procedures to be used for the remaining foundations and were analyzed in greater detail here.

Distances to injury SEL thresholds for foundations eight and nine, and eleven through thirteen were less than the predicted distances for low-frequency cetaceans, mid-frequency cetaceans, and pinnipeds (Table 10 and Table 11). For high-frequency cetaceans the distances to thresholds could exceed the predicted range of 71 m, with an extrapolated distance from measurements of up to 90 m without attenuation coefficient (AT-39 and AV-39, Table 10) and 200 m with attenuation coefficient (AN-37, Table 11). This exceedance is probably not meaningful because 90 m is within both bubble curtains and 200 m and is, at least in part, due to noise in the extrapolation process exaggerated by the attenuation coefficient term because without attenuation the range for pile AN-37 was 80 m. Additionally, there is substantial higher-frequency noise produced by dynamic positioning thrusters rather than pile driving that disproportionately affects calculation of the high-frequency cetacean range. For sea turtles the predicted range was 161 m but distances ~200 m were measured. The closest measurements were made at 750 m, so it is difficult to determine if this is an actual exceedance or just the result of extrapolation in the fitting process and thruster noise. The predicted range for sturgeon was 6,894 m, but ~4,000 m (up to 4,460 m) was measured. While the modeling used to obtain the predicted ranges differed from the actual installation, it is noted that the measured distances for cetacean and pinniped Level A SEL were less than the predicted ranges.

For the five piles driven with the HSD and DBBC, the predicted distances to behavioral and harassment SPL thresholds were not exceeded for sea turtles but were for marine mammals and sturgeon. For two piles, AV-38 and AU-38, the predicted distance of 4,121 m to the marine mammal threshold of SPL 160 dB re 1 μPa$^2$ was exceeded (4,630 and 5,310 without attenuation coefficient, respectively). And, for almost all piles the measured distance to the sturgeon behavioral threshold of SPL 150 dB re 1 μPa$^2$ exceeded the predicted distance of 9229 m, with extrapolated distances >20 km.

With the five piles installed using the HSD and DBBC with the accelerated maintenance schedule, the (SPL) data were pooled and analyzed to better understand the expected sound fields for the remainder of the project. The received levels from all piles were pooled before the fitting process (Section 3.3). Because the maximum hammer energy, number of strikes, and water depth were similar for each pile (Table 5), no normalization with respect to these parameters was performed. The resulting received levels were less than, but close to, the predicted range of 4,121 m to SPL 160 dB re 1μPa$^2$ for marine mammal Level B threshold, at 3,750 m (fitted combined data without attenuation coefficient), and 4,000 m (fitted combined data with attenuation coefficient). The expected distance to 150 dB re 1μPa$^2$ harassment threshold for sturgeon is greater than the predicted distance of 9,229 m. Fitted distances results in an expected distances of 15,500 without attenuation coefficient and 11,000 m with attenuation coefficient. Pooling the measured data before fitting makes for a more robust data set where noise is averaged at the stations. The resulting fitting with attenuation coefficient matches expectations of damped cylindrical spreading loss (Section 3.3) and argues for its use here as estimates for the expected range to these SPL thresholds.

## 4.2. Ambient Sound Levels

A study in the southern New England wind farm development area found the mean ambient broadband sound pressure in the area to be between SPL 105  and 112 dB re 1 $\mu Pa^2$ (Van Parijs et al. (2023). Ambient SPL recorded on the SFV equipment just before pile driving began (Section 3.2) found higher levels (often SPL >130 dB re 1 $\mu Pa^2$) than reported by Van Parijs et al. (2023). While the Van Parijs et al. (2023) measurements do include typical vessel traffic for the area, the levels recorded on the SFV equipment also include the vessels associated with pile installation (e.g., the installation vessel, and two bubble curtain vessels). The installation vessel and bubble curtain vessels used multiple generators and dynamic positioning thrusters which can be heard in the recordings and account for the higher ambient levels just before pile driving commences. The contribution of the thrusters to the ambient levels is evident in that recording stations closer to the pile (750 m) tended to have higher broadband levels than farther stations (Table 16). The positioning of the vessels relative to the recording stations, the operation of the bubble curtains, which would attenuate sounds from the vessels, and noise generated from the bubble curtains themselves affect the received levels at the stations.

# 5. Conclusion

Ambient sound levels directly before pile driving were high in this area with clear contributions from vessels, including dynamic positioning thrusters. High ambient levels likely extended some measured ranges, especially ranges determined for unweighted broadband metrics (notably fish harassment and cetacean Level B). Pooling data from the five piles using the HSD and DBBC maintained by re-drilling hoses before each deployment and fitting with attenuation coefficient offers the most representative understanding of piling effects for the remainder of the foundation installation. It is seen in the pooled data that injury thresholds are unlikely to be exceeded for any of the species. Level A (injury) was not exceeded for LF cetaceans, MF cetaceans, or pinnipeds. And, while there were measured exceedance for HF cetaceans, the range was within the bubble curtains and likely was an artefact of non-piling noise and the fitting process. For sturgeon, the injury threshold range (~4000 m) was below the predicted range (6,894 m). Level B ranges for marine mammals were close to (between 3,290 and 5,720 m) the predicted range (4,120 m), while ranges to harassment for sturgeon exceeded the predicted range (11,000+ m versus the expected distance of 9,229 m). As was observed with injury ranges for sturgeon, the ambient levels in the area were high and the range calculation is based on unweighted broadband levels – meaning sound energy due to other sources than pile driving and sound energy outside of the animal's hearing range was included, potentially overestimating the distance to behavioral and harassment thresholds from piling.

# Literature Cited

[FHWG] Fisheries Hydroacoustic Working Group. 2008. *Agreement in Principle for Interim Criteria for Injury to Fish from Pile Driving Activities*. 12 Jun 2008 edition. https://dot.ca.gov/-/media/dot-media/programs/environmental-analysis/documents/ser/bio-fhwg-criteria-agree-a11y.pdf.

[GARFO] Greater Atlantic Regional Fisheries Office. 2019. *GARFO Acoustics Tool: Analyzing the effects of pile driving on ESA-listed species in the Greater Atlantic Region National Marine Fisheries Service* (web page), 8 Aug 2019. http://www.greateratlantic.fisheries.noaa.gov/protected/section7/guidance/consultation/index.html.

[HESS] High Energy Seismic Survey. 1999. *High Energy Seismic Survey Review Process and Interim Operational Guidelines for Marine Surveys Offshore Southern California*. Prepared for the California State Lands Commission and the United States Minerals Management Service Pacific Outer Continental Shelf Region by the High Energy Seismic Survey Team, Camarillo, CA, USA. 98 p. https://ntrl.ntis.gov/NTRL/dashboard/searchResults/titleDetail/PB2001100103.xhtml.

[ISO] International Organization for Standardization. 1996. *ISO 2923:1996 Acoustics — Measurement of noise on board vessels*. Geneva. https://www.iso.org/obp/ui#iso:std:iso:2923:ed-2:v1:en.

[NMFS] National Marine Fisheries Service (US) and [NOAA] National Oceanic and Atmospheric Administration (US). 2005. Endangered fish and wildlife: Notice of intent to prepare an environmental impact statement. *Federal Register* 70(7): 1871-1875. http://www.nmfs.noaa.gov/pr/pdfs/fr/fr70-1871.pdf.

[NMFS] National Marine Fisheries Service (US). 2016. *Technical Guidance for Assessing the Effects of Anthropogenic Sound on Marine Mammal Hearing: Underwater Acoustic Thresholds for Onset of Permanent and Temporary Threshold Shifts*. US Department of Commerce, NOAA. NOAA Technical Memorandum NMFS-OPR-55. 178 p.

[NMFS] National Marine Fisheries Service (US). 2018. *2018 Revision to: Technical Guidance for Assessing the Effects of Anthropogenic Sound on Marine Mammal Hearing (Version 2.0): Underwater Thresholds for Onset of Permanent and Temporary Threshold Shifts*. US Department of Commerce, NOAA. NOAA Technical Memorandum NMFS-OPR-59. 167 p. https://media.fisheries.noaa.gov/dam-migration/tech_memo_acoustic_guidance_(20)_(pdf)_508.pdf.

[NMFS] National Marine Fisheries Service (US). 2022. *Summary of Marine Mammal Protection Act Acoustic Thresholds*. 7 p. https://media.fisheries.noaa.gov/2022-05/MM%20Acoustic%20Thresholds%20%28508%29_secure%20%28May%202022%29.pdf.

[NRC] National Research Council (US). 2003. *Ocean Noise and Marine Mammals*. National Research Council (US), Ocean Studies Board, Committee on Potential Impacts of Ambient Noise in the Ocean on Marine Mammals. The National Academies Press, Washington, DC, USA. https://doi.org/10.17226/10564.

Au, W.W.L. and M.C. Hastings. 2008. *Principles of Marine Bioacoustics*. Modern Acoustics and Signal Processing. Springer, New York. 510 p. https://doi.org/10.1007/978-0-387-78365-9.

Collins, M.D. 1993. A split-step Padé solution for the parabolic equation method. *Journal of the Acoustical Society of America* 93(4): 1736-1742. https://doi.org/10.1121/1.406739.

Cook, R.R. and P.J. Auster. 2007. A bioregional classification of the continental shelf of northeastern North America for conservation analysis and planning based on representation.

Cranford, T.W. and P. Krysl. 2015. Fin whale sound reception mechanisms: Skull vibration enables low-frequency hearing. *PLOS ONE* 10(1). https://doi.org/10.1371/journal.pone.0116222.

Dahlheim, M.E. and D.K. Ljungblad. 1990. Preliminary Hearing Study on Gray Whales (*Eschrichtius Robustus*) in the Field. *In* Thomas, J.A. and R.A. Kastelein (eds.). *Sensory abilities of Cetaceans*. Volume 196. Springer Science+Business Media, Boston. pp. 335-346. https://doi.org/10.1007/978-1-4899-0858-2_22.

Dekeling, R.P.A., M.L. Tasker, M.A. Ainslie, M. Andersson, M. André, M. Castellote, J.F. Borsani, J. Dalen, T. Folegot, et al. 2014. *Monitoring Guidance for Underwater Noise in European Seas, Part III: Background Information and Annexes*. Publications Office of the European Union, JRC Scientific and Policy Report EUR 26556 EN, Luxembourg. http://publications.jrc.ec.europa.eu/repository/handle/JRC88885.

Ellison, W.T., B.L. Southall, C.W. Clark, and A.S. Frankel. 2012. A New Context-Based Approach to Assess Marine Mammal Behavioral Responses to Anthropogenic Sounds. *Conservation Biology* 26(1): 21-28. https://doi.org/10.1111/j.1523-1739.2011.01803.x.

Erbe, C., R.D. McCauley, and A. Gavrilov. 2016. Characterizing marine soundscapes. *In* Popper, A.N. and A.D. Hawkins (eds.). *The Effects of Noise on Aquatic Life II*. Volume 875. Springer, New York. pp. 265-271. https://doi.org/10.1007/978-1-4939-2981-8_31.

Finneran, J.J. 2015. *Auditory weighting functions and TTS/PTS exposure functions for cetaceans and marine carnivores*. Technical report by SSC Pacific, San Diego, CA, USA.

Finneran, J.J. 2016. *Auditory weighting functions and TTS/PTS exposure functions for marine mammals exposed to underwater noise*. Technical Report for Space and Naval Warfare Systems Center Pacific, San Diego, CA, USA. 49 p. https://apps.dtic.mil/dtic/tr/fulltext/u2/1026445.pdf.

Finneran, J.J., E.E. Henderson, D.S. Houser, K. Jenkins, S. Kotecki, and J. Mulsow. 2017. *Criteria and Thresholds for U.S. Navy Acoustic and Explosive Effects Analysis (Phase III)*. Technical report by Space and Naval Warfare Systems Center Pacific (SSC Pacific). 183 p. https://nwtteis.com/portals/nwtteis/files/technical_reports/Criteria_and_Thresholds_for_U.S._Navy_Acoustic_and_Explosive_Effects_Analysis_June2017.pdf.

Guida, V., A. Drohan, H. Welch, J. McHenry, D. Johnson, V. Kentner, J. Brink, D. Timmons, and E. Estela-Gomez. 2017. Habitat mapping and assessment of northeast wind energy areas. *OCS Study BOEM* 88: 312.

Houser, D.S., D.A. Helweg, and P.W.B. Moore. 2001. A bandpass filter-bank model of auditory sensitivity in the humpback whale. *Aquatic Mammals* 27(2): 82-91. https://www.aquaticmammalsjournal.org/share/AquaticMammalsIssueArchives/2001/AquaticMammals_27-02/27-02_Houser.PDF.

Kaiser, J.F. 1990. On a simple algorithm to calculate the 'energy' of a signal. *IEEE International Conference on Acoustics, Speech, and Signal Processing*. 3-6 Apr 1990, Albuquerque, NM, USA. pp. 381-384. https://doi.org/10.1109/ICASSP.1990.115702.

Kandia, V. and Y. Stylianou. 2006. Detection of sperm whale clicks based on the Teager-Kaiser energy operator. *Applied Acoustics* 67: 1144-1163. https://doi.org/10.1016/j.apacoust.2006.05.007.

Malme, C.I., P.R. Miles, C.W. Clark, P.L. Tyack, and J.E. Bird. 1983. *Investigations of the Potential Effects of Underwater Noise from Petroleum Industry Activities on Migrating Gray Whale Behavior. Final Report for the Period of 7 June 1982 - 31 July 1983*. Report 5366. Report by Bolt Beranek and Newman Inc. for US Department of the Interior, Minerals Management Service, Alaska OCS Office, Cambridge, MA, USA. https://www.boem.gov/sites/default/files/boem-newsroom/Library/Publications/1983/rpt5366.pdf.

Malme, C.I., P.R. Miles, C.W. Clark, P.L. Tyack, and J.E. Bird. 1984. *Investigations of the Potential Effects of Underwater Noise from Petroleum Industry Activities on Migrating Gray Whale Behavior. Phase II: January 1984 Migration*. Report 5586. Report by Bolt Beranek and Newman Inc. for the US Department of the Interior, Minerals Management Service, Cambridge, MA, USA. https://www.boem.gov/sites/default/files/boem-newsroom/Library/Publications/1983/rpt5586.pdf.

Martin, S.B. and D.R. Barclay. 2019. Determining the dependence of marine pile driving sound levels on strike energy, pile penetration, and propagation effects using a linear mixed model based on damped cylindrical spreading. *Journal of the Acoustical Society of America* 146(1): 109-121. https://doi.org/10.1121/1.5114797.

Martin, S.B., K. Lucke, and D.R. Barclay. 2020. Techniques for distinguishing between impulsive and non-impulsive sound in the context of regulating sound exposure for marine mammals. *Journal of the Acoustical Society of America* 147(4): 2159-2176. https://doi.org/10.1121/10.0000971.

McCauley, R.D., J. Fewtrell, A.J. Duncan, C. Jenner, M.-N. Jenner, J.D. Penrose, R.I.T. Prince, A. Adhitya, J. Murdoch, et al. 2000a. *Marine seismic surveys: Analysis and propagation of air-gun signals; and effects of air-gun exposure on humpback whales, sea turtles, fishes and squid*. Report R99-15. Prepared for Australian Petroleum Production Exploration Association by Centre for Maine Science and Technology, Western Australia. 198 p. https://cmst.curtin.edu.au/wp-content/uploads/sites/4/2016/05/McCauley-et-al-Seismic-effects-2000.pdf.

McCauley, R.D., J. Fewtrell, A.J. Duncan, C. Jenner, M.-N. Jenner, J.D. Penrose, R.I.T. Prince, A. Adhitya, J. Murdoch, et al. 2000b. Marine seismic surveys: A study of environmental implications. *Australian Petroleum Production Exploration Association (APPEA) Journal* 40(1): 692-708. https://doi.org/10.1071/AJ99048.

Nedwell, J.R. and A.W. Turnpenny. 1998. The use of a generic frequency weighting scale in estimating environmental effect. *Workshop on Seismics and Marine Mammals*. 23–25 Jun 1998, London, UK.

Nedwell, J.R., A.W. Turnpenny, J. Lovell, S.J. Parvin, R. Workman, J.A.L. Spinks, and D. Howell. 2007. *A validation of the $dB_{ht}$ as a measure of the behavioural and auditory effects of underwater noise*. Document 534R1231 Report by Subacoustech Ltd. for Chevron Ltd, TotalFinaElf Exploration UK PLC, Department of Business, Enterprise and Regulatory Reform, Shell UK Exploration and Production Ltd, The Industry Technology Facilitator, Joint Nature Conservation Committee, and The UK Ministry of Defence. 74 p. https://tethys.pnnl.gov/sites/default/files/publications/Nedwell-et-al-2007.pdf.

Parks, S.E., C.W. Clark, and P.L. Tyack. 2007. Short-and long-term changes in right whale calling behavior: The potential effects of noise on acoustic communication. *Journal of the Acoustical Society of America* 122(6): 3725-3731. https://doi.org/10.1121/1.2799904.

Popper, A.N., A.D. Hawkins, R.R. Fay, D.A. Mann, S. Bartol, T.J. Carlson, S. Coombs, W.T. Ellison, R.L. Gentry, et al. 2014. *Sound Exposure Guidelines for Fishes and Sea Turtles: A Technical Report prepared by ANSI-Accredited Standards Committee S3/SC1 and registered with ANSI*. ASA S3/SC1.4 TR-2014. SpringerBriefs in Oceanography. ASA Press and Springer. https://doi.org/10.1007/978-3-319-06659-2.

Pyć, C.D., D.G. Zeddies, S.L. Denes, and M.J. Weirathmueller. 2018. *Appendix III-M: REVISED DRAFT - Supplemental Information for the Assessment of Potential Acoustic and Non-acoustic Impact Producing Factors on Marine Fauna during Construction of the Vineyard Wind Project*. Document 001639, Version 3.1. Technical report by JASCO Applied Sciences (USA) Inc. for Vineyard Wind. https://www.boem.gov/sites/default/files/renewable-energy-program/State-Activities/MA/Vineyard-Wind/Vineyard-Wind-COP-Volume-III-Appendix-III-M.pdf.

Reichmuth, C., J. Mulsow, J.J. Finneran, D.S. Houser, and A.Y. Supin. 2007. Measurement and Response Characteristics of Auditory Brainstem Responses in Pinnipeds. *Aquatic Mammals* 33(1): 132-150. https://doi.org/10.1578/AM.33.1.2007.132.

Richardson, W.J., B. Würsig, and C.R. Greene, Jr. 1986. Reactions of bowhead whales, *Balaena mysticetus*, to seismic exploration in the Canadian Beaufort Sea. *Journal of the Acoustical Society of America* 79(4): 1117-1128. https://doi.org/10.1121/1.393384.

Richardson, W.J., B. Würsig, and C.R. Greene, Jr. 1990. Reactions of bowhead whales, *Balaena mysticetus*, to drilling and dredging noise in the Canadian Beaufort Sea. *Marine Environmental Research* 29(2): 135-160. https://doi.org/10.1016/0141-1136(90)90032-J.

Richardson, W.J., C.R. Greene, Jr., C.I. Malme, and D.H. Thomson. 1995. *Marine Mammals and Noise*. Academic Press, San Diego, CA, USA. 576 p. https://doi.org/10.1016/C2009-0-02253-3.

Ross, D. 1976. *Mechanics of Underwater Noise*. Pergamon Press, NY, USA.

Sills, J.M., B.L. Southall, and C. Reichmuth. 2014. Amphibious hearing in spotted seals (*Phoca largha*): Underwater audiograms, aerial audiograms and critical ratio measurements. *Journal of Experimental Biology* 217(5): 726-734. https://doi.org/10.1242/jeb.097469.

Southall, B.L., A.E. Bowles, W.T. Ellison, J.J. Finneran, R.L. Gentry, C.R. Greene, Jr., D. Kastak, D.R. Ketten, J.H. Miller, et al. 2007. Marine Mammal Noise Exposure Criteria: Initial Scientific Recommendations. *Aquatic Mammals* 33(4): 411-521. https://doi.org/10.1578/AM.33.4.2007.411.

Southall, B.L., J.J. Finneran, C.J. Reichmuth, P.E. Nachtigall, D.R. Ketten, A.E. Bowles, W.T. Ellison, D.P. Nowacek, and P.L. Tyack. 2019. Marine Mammal Noise Exposure Criteria: Updated Scientific Recommendations for Residual Hearing Effects. *Aquatic Mammals* 45(2): 125-232. https://doi.org/10.1578/AM.45.2.2019.125.

Tubelli, A.A., A. Zosuls, D.R. Ketten, and D.C. Mountain. 2012. Prediction of a mysticete audiogram via finite element analysis of the middle ear. *In* Popper, A.N. and A.D. Hawkins (eds.). *The Effects of Noise on Aquatic Life*. Volume 730. Springer, New York. pp. 57-59. https://doi.org/10.1007/978-1-4419-7311-5_12.

Van Parijs, S.M., A.I. DeAngelis, T. Aldrich, R. Gordon, A. Holdman, J.A. McCordic, X. Mouy, T.J. Rowell, S. Tennant, et al. 2023. Establishing baselines for predicting change in ambient sound metrics, marine mammal, and vessel occurrence within a US offshore wind energy area. *ICES Journal of Marine Science*: fsad148 %@ 1054-3139.

Wartzok, D. and D.R. Ketten. 1999. Marine Mammal Sensory Systems. (Chapter 4) *In* Reynolds, J. and S. Rommel (eds.). *Biology of Marine Mammals*. Smithsonian Institution Press, Washington, DC. pp. 117-175.

Wenz, G.M. 1962. Acoustic Ambient Noise in the Ocean: Spectra and Sources. *Journal of the Acoustical Society of America* 34(12): 1936-1956. https://doi.org/10.1121/1.1909155.

# Acknowledgements

We acknowledge and thank other members of JASCO who contributed to this report. Jonathan Barrows, Bailey Jenkins, Courtney Dreyfus, and Robert Mills participated in the cruises to deploy, recover, and service the instruments used in the sound field verification, and were also responsible for the many data downloads and transferring. Dara Carr and Karen Scanlon edited and formatted this report. We also acknowledge the crew of the FV Beth Anne for their support during the field trips to deploy and recover the SFV moorings.

# Appendix A. Acoustic Results Per Foundation

Acoustic results for each measured foundation are shown in the following sections. Results include recording system information and measurement locations, along with impulses detected (total number of strikes produced are listed Appendix C hammer logs), received levels, and spectra at each station.

## A.1. Foundation AT-40

Summary of measurements are shown in Table A-1. Channel 1 (bottom hydrophone) at station AT40-2000 was not functioning properly and was excluded from the analysis. Channel 1 at station AT40-8000 had a hydrophone with a higher sensitivity, of approximately -165 dB, which resulted in clipping as sound peak levels (PK) at this distance were also near 165 dB. Therefore, data from AT40-8000 channel 1 were also excluded from this analysis.

### A.1.1. Summary of Measured Sound Levels

Table A-1. Summary of Autonomous Multichannel Acoustic Recorder (AMAR) locations and measured sound levels for pile AT-40. Computed PK and SPL levels are shown for the $L_{max}$.

| Location (nominal) | Recorder ID | Distance (m) | Water depth (m) | Channel | Impulses detected* (clipped) | PK (dB re 1 µPa) | SPL (dB re 1 µPa$^2$) | cSEL (dB re 1 µPa$^2$·s) |
|---|---|---|---|---|---|---|---|---|
| 750 | AMAR-863 | 753 | 43.0 | 1 | 3591 | 183.5 | 173.6 | 199.2 |
| | | | | 2 | 4303 | 185.5 | 173.7 | 197.7 |
| 750 @ 90° | AMAR-865 | 715 | 40.2 | 1 | 4304 | 184.8 | 174.3 | 200.2 |
| | | | | 2 | 4307 | 184.0 | 173.4 | 198.7 |
| 2000 | AMAR-855 | 1999 | 43.9 | | | | | |
| | | | | 2 | 4256 | 177.6 | 167.6 | 193.3 |
| 4000 | AMAR-860 | 4038 | 44.8 | 1 | 4289 | 174.4 | 162.5 | 188.7 |
| | | | | 2 | 4305 | 172.6 | 163.0 | 188.9 |
| 8000 | AMAR-864 | 8023 | 45.0 | | | | | |
| | | | | 2 | 4283 | 168.1 | 157.0 | 183.6 |

* Number of strikes produced (from hammer log): 4329

### A.1.2. Sound Levels per Station

#### A.1.2.1. Station AT40-750

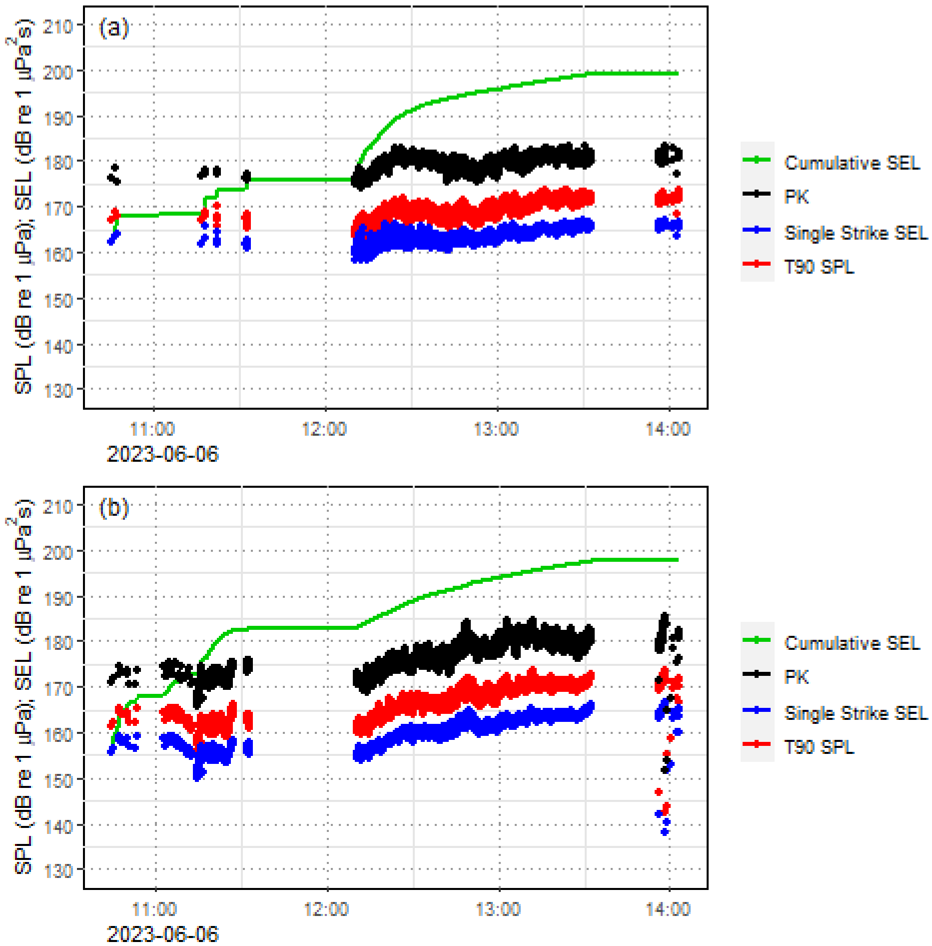


Figure A-1. Received levels for impact pile driving installation of AT-40 at monitoring station AT40-750 for channel 1 (a) and channel 2 (b). Peak SPL (PK, black), rms SPL (T90 SPL, red), single strike SEL (blue) and cumulative SEL (green) versus time (UTC). For periods during which there was no pile driving the cSEL is necessarily displayed as a constant value over time.

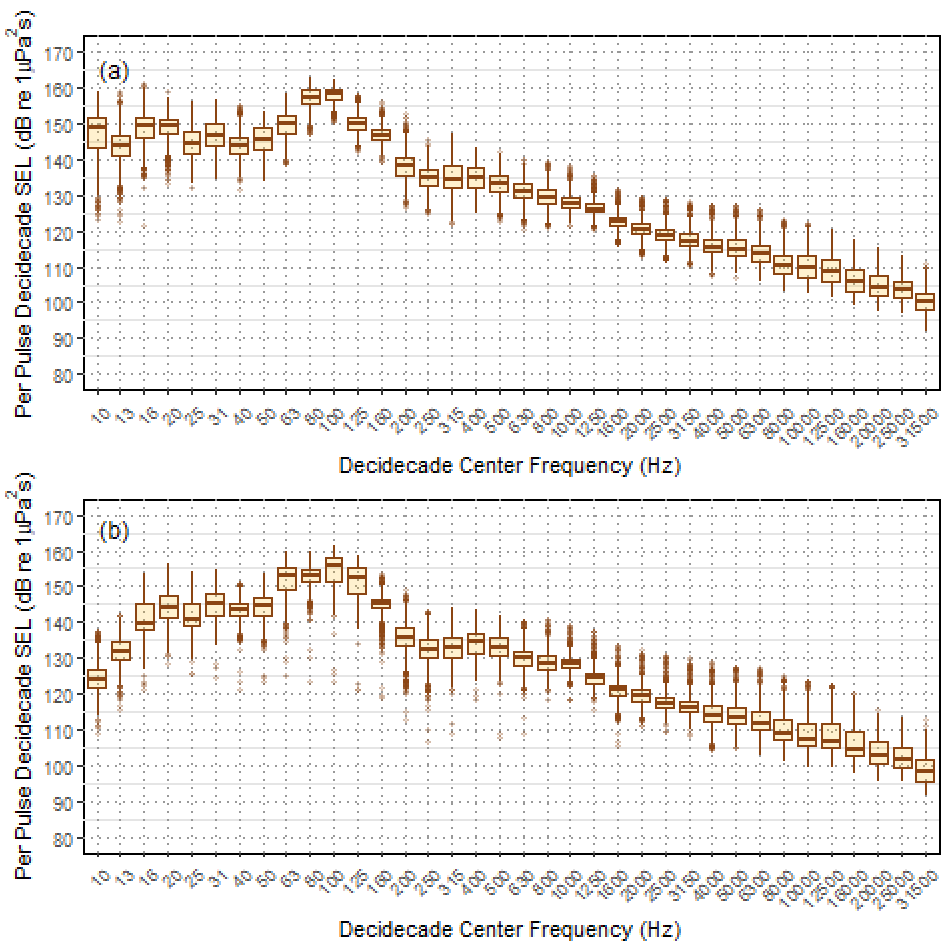


Figure A-2. Distribution of decidecade band level single strike SEL for pile driving installation of AT-40 at monitoring station AT40-750 for channel 1 (a) and channel 2 (b). Beige bars indicate the first, second, and third quartiles (*25^th^*, *50^th^*, and *75^th^*) or as exceedances $L_{75}$, $L_{50}$, and $L_{25}$. Upper error bars indicate the maximum levels ($L_{max}$). Lower error bars indicate the 5th percentile or $L_{95}$.

Table A-2. Received level statistics for pile driving installation of AT-40 at monitoring station AT40-750.

| Sound level statistic | PK (dB re 1 µPa) | rms SPL (dB re 1 µPa$^2$) | SELss (dB re 1 µPa$^2$·s) |
|---|---|---|---|
| **Channel 1 (bottom)** | | | |
| $L_{max}$ | 183.5 | 173.6 | 166.9 |
| $L_5$ | 181.8 | 172.3 | 165.9 |
| $L_{25}$ | 180.9 | 171.1 | 164.7 |
| $L_{50}$ | 180.0 | 169.3 | 163.4 |
| $L_{75}$ | 178.7 | 168.0 | 162.4 |
| $L_{95}$ | 176.7 | 165.9 | 160.8 |
| $L_{mean}$ | 179.9 | 169.8 | 163.7 |
| **Channel 2 (mid-water)** | | | |
| $L_{max}$ | 185.5 | 173.7 | 166.4 |
| $L_5$ | 182.0 | 171.4 | 164.4 |
| $L_{25}$ | 180.0 | 170.1 | 163.2 |
| $L_{50}$ | 177.6 | 167.5 | 160.8 |
| $L_{75}$ | 174.5 | 164.8 | 158.2 |
| $L_{95}$ | 171.1 | 160.8 | 154.9 |
| $L_{mean}$ | 178.4 | 168.2 | 161.4 |

### A.1.2.2. Station AT40-75090

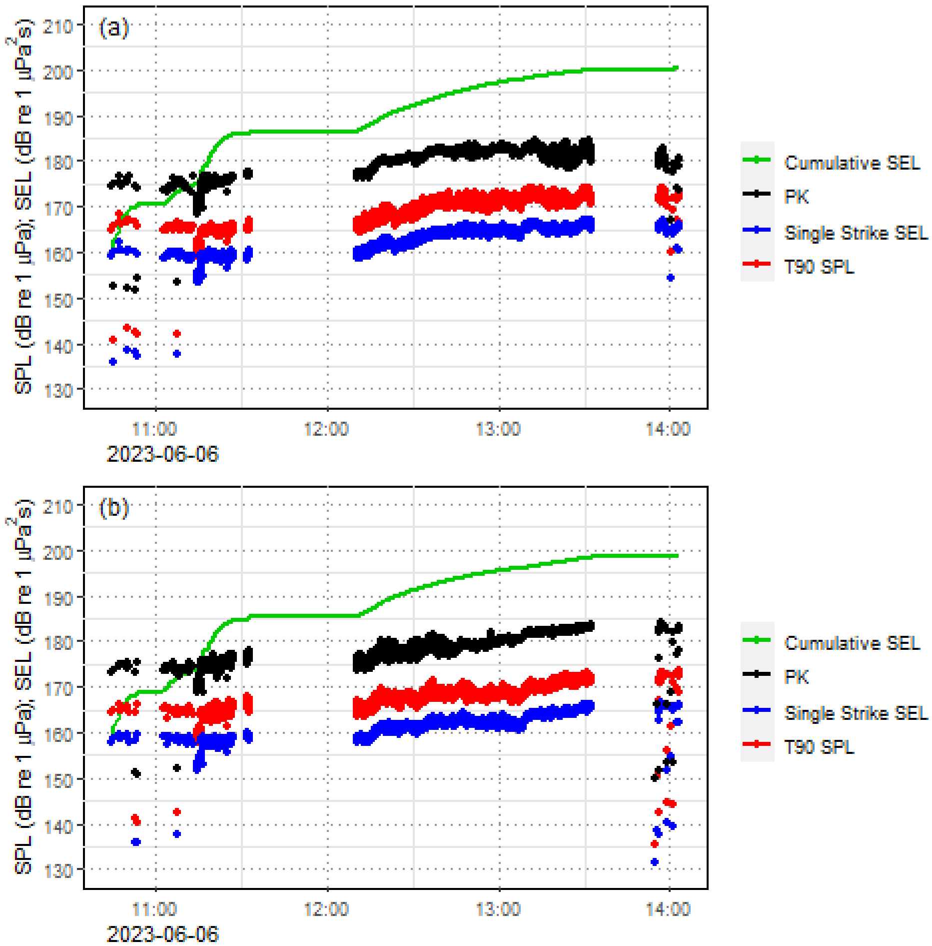


Figure A-3. Received levels for impact pile driving installation of AT-40 at monitoring station AT40-75090 for channel 1 (a) and channel 2 (b). Peak SPL (PK, black), rms SPL (T90 SPL, red), single strike SEL (blue) and cumulative SEL (green) versus time (UTC). For periods during which there was no pile driving the cSEL is necessarily displayed as a constant value over time.

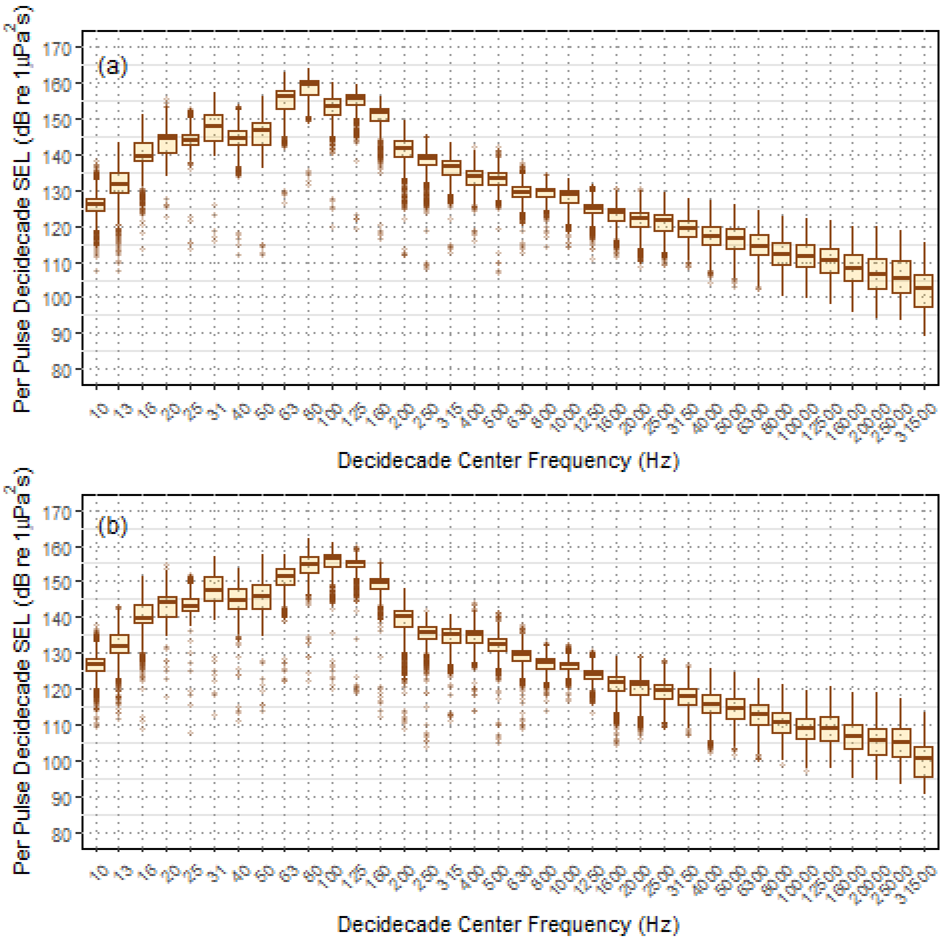


Figure A-4. Distribution of decidecade band level single strike SEL for pile driving installation of AT-40 at monitoring station AT40-75090 for channel 1 (a) and channel 2 (b). Beige bars indicate the first, second, and third quartiles (*25th*, *50th*, and *75th*) or as exceedances $L_{75}$, $L_{50}$, and $L_{25}$. Upper error bars indicate the maximum levels ($L_{max}$). Lower error bars indicate the 5th percentile or $L_{95}$.

Table A-3. Received level statistics for pile driving installation of AT-40 at monitoring station AT40-75090.

| Sound level statistic | PK (dB re 1 µPa) | rms SPL (dB re 1 µPa$^2$) | SELss (dB re 1 µPa$^2$·s) |
|---|---|---|---|
| **Channel 1 (bottom)** | | | |
| $L_{max}$ | 184.8 | 174.3 | 167.3 |
| $L_5$ | 183.1 | 173.0 | 166.2 |
| $L_{25}$ | 182.2 | 171.7 | 165.1 |
| $L_{50}$ | 181.3 | 170.6 | 164.2 |
| $L_{75}$ | 179.9 | 167.9 | 161.6 |
| $L_{95}$ | 175.1 | 164.4 | 159.0 |
| $L_{mean}$ | 181.0 | 170.4 | 163.8 |
| **Channel 2 (mid-water)** | | | |
| $L_{max}$ | 184.0 | 173.4 | 166.6 |
| $L_5$ | 182.8 | 171.7 | 165.2 |
| $L_{25}$ | 181.6 | 169.6 | 163.3 |
| $L_{50}$ | 179.0 | 168.2 | 162.0 |
| $L_{75}$ | 177.1 | 167.0 | 160.7 |
| $L_{95}$ | 174.5 | 164.1 | 157.8 |
| $L_{mean}$ | 179.7 | 168.7 | 162.3 |

## A.1.2.3. Station AT40-2000

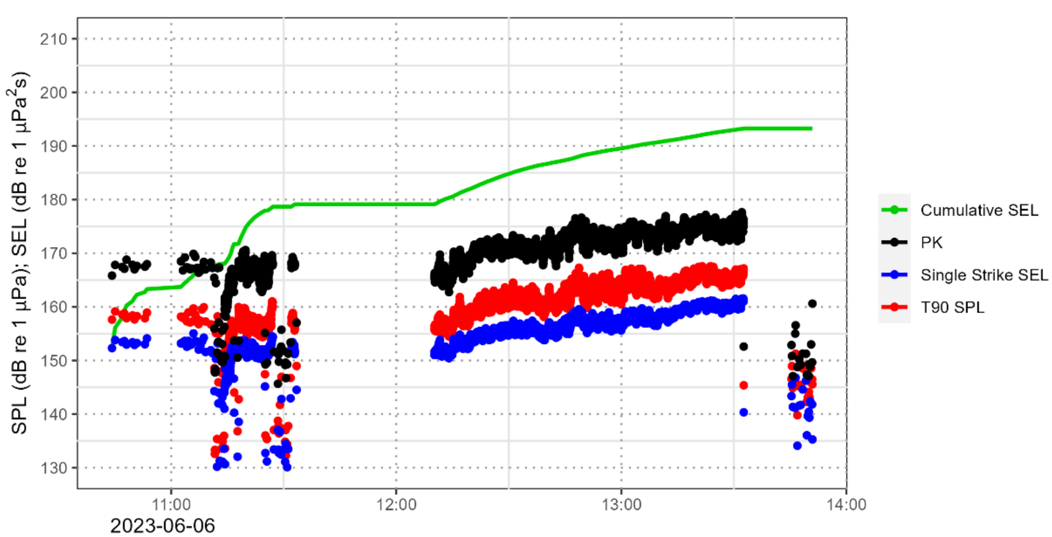


Figure A-5. Received levels for impact pile driving installation of AT-40 at monitoring station AT40-2000 for channel 2. Peak SPL (PK, black), rms SPL (T90 SPL, red), single strike SEL (blue) and cumulative SEL (green) versus time (UTC). For periods during which there was no pile driving the cSEL is necessarily displayed as a constant value over time.

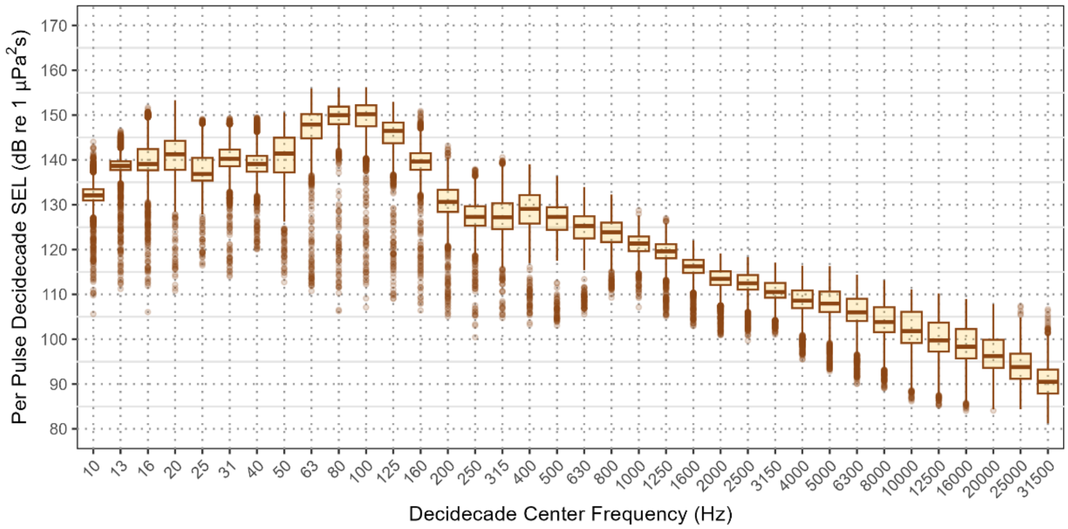


Figure A-6. Distribution of decidecade band level single strike SEL for pile driving installation of AT-40 at monitoring station AT40-2000 for channel 2. Beige bars indicate the first, second, and third quartiles (*25th*, *50th*, and *75th*) or as exceedances $L_{75}$, $L_{50}$, and $L_{25}$. Upper error bars indicate the maximum levels ($L_{max}$). Lower error bars indicate the 5th percentile or $L_{95}$.

Table A-4. Received level statistics for pile driving installation of AT-40 at monitoring station AT40-2000.

| Sound level statistic | PK (dB re 1 µPa) | rms SPL (dB re 1 µPa²) | SELss (dB re 1 µPa²·s) |
|---|---|---|---|
| **Channel 2 (mid-water)** | | | |
| $L_{max}$ | 177.6 | 167.6 | 161.6 |
| $L_5$ | 175.4 | 166.1 | 160.4 |
| $L_{25}$ | 173.8 | 164.5 | 158.4 |
| $L_{50}$ | 171.8 | 161.8 | 156.2 |
| $L_{75}$ | 169.3 | 159.2 | 154.1 |
| $L_{95}$ | 165.0 | 155.5 | 151.0 |
| $L_{mean}$ | 172.2 | 162.6 | 157.0 |

## A.1.2.4. Station AT40-4000

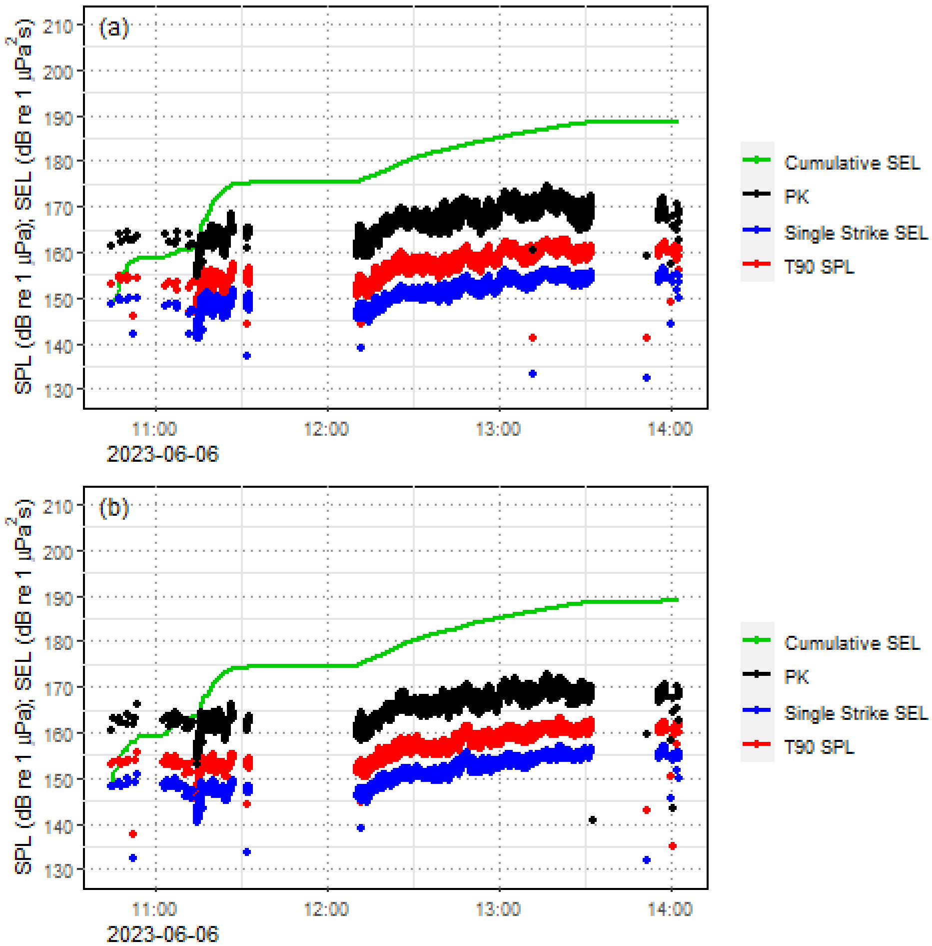


Figure A-7. Received levels for impact pile driving installation of AT-40 at monitoring station AT40-4000 for channel 1 (a) and channel 2 (b). Peak SPL (PK, black), rms SPL (T90 SPL, red), single strike SEL (blue) and cumulative SEL (green) versus time (UTC). For periods during which there is no pile driving the cSEL is necessarily displayed as a constant value over time.

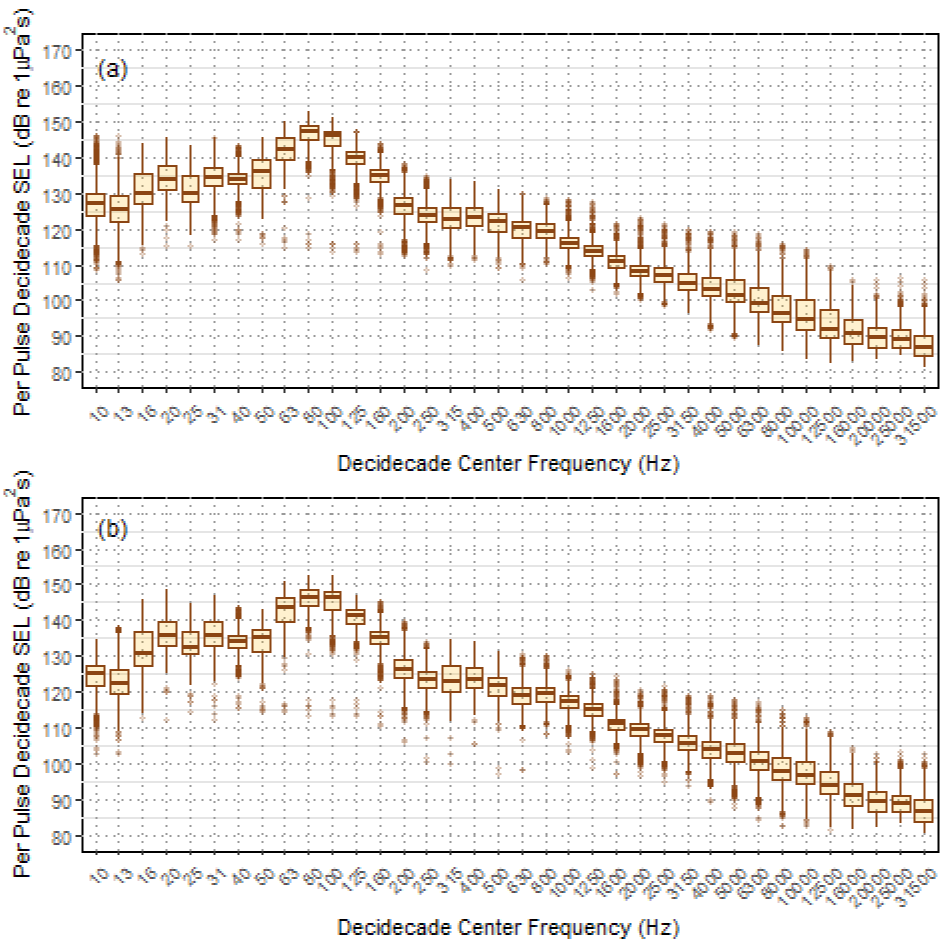


Figure A-8. Distribution of decidecade band level single strike SEL for pile driving installation of AT-40 at monitoring station AT40-4000 for channel 1 (a) and channel 2 (b). Beige bars indicate the first, second, and third quartiles (*25th*, *50th*, and *75th*) or as exceedances $L_{75}$, $L_{50}$, and $L_{25}$. Upper error bars indicate the maximum levels ($L_{max}$). Lower error bars indicate the 5th percentile or $L_{95}$.

Table A-5. Received level statistics for pile driving installation of AT-40 at monitoring station AT40-4000.

| Sound level statistic | PK (dB re 1 µPa) | rms SPL (dB re 1 µPa$^2$) | SELss (dB re 1 µPa$^2$·s) |
|---|---|---|---|
| **Channel 1 (bottom)** | | | |
| $L_{max}$ | 174.4 | 162.5 | 156.2 |
| $L_5$ | 172.0 | 161.6 | 155.3 |
| $L_{25}$ | 169.6 | 159.8 | 153.8 |
| $L_{50}$ | 167.6 | 158.0 | 151.7 |
| $L_{75}$ | 165.4 | 155.7 | 149.8 |
| $L_{95}$ | 161.5 | 152.1 | 146.6 |
| $L_{mean}$ | 168.3 | 158.4 | 152.3 |
| **Channel 2 (mid-water)** | | | |
| $L_{max}$ | 172.6 | 163.0 | 156.9 |
| $L_5$ | 170.5 | 161.4 | 155.6 |
| $L_{25}$ | 168.5 | 160.1 | 154.3 |
| $L_{50}$ | 166.7 | 157.9 | 152.1 |
| $L_{75}$ | 164.5 | 155.3 | 149.6 |
| $L_{95}$ | 160.6 | 151.9 | 146.4 |
| $L_{mean}$ | 167.2 | 158.4 | 152.6 |

## A.1.2.5. Station AT40-8000

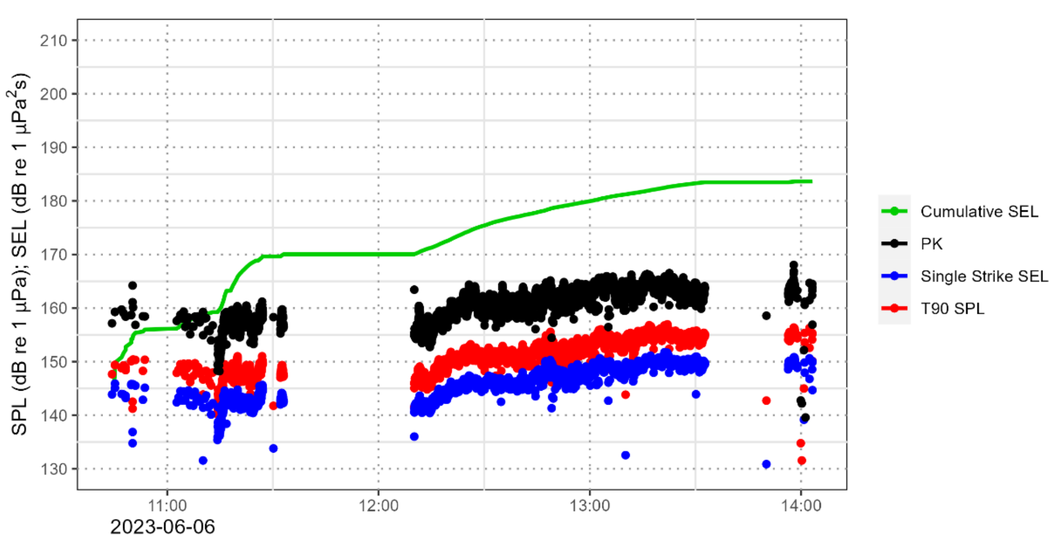


Figure A-9. Received levels for impact pile driving installation of AT-40 at monitoring station AT40-8000 for channel 2. Peak SPL (PK, black), rms SPL (T90 SPL, red), single strike SEL (blue) and cumulative SEL (green) versus time (UTC). For periods during which there is no pile driving the cSEL is necessarily displayed as a constant value over time.

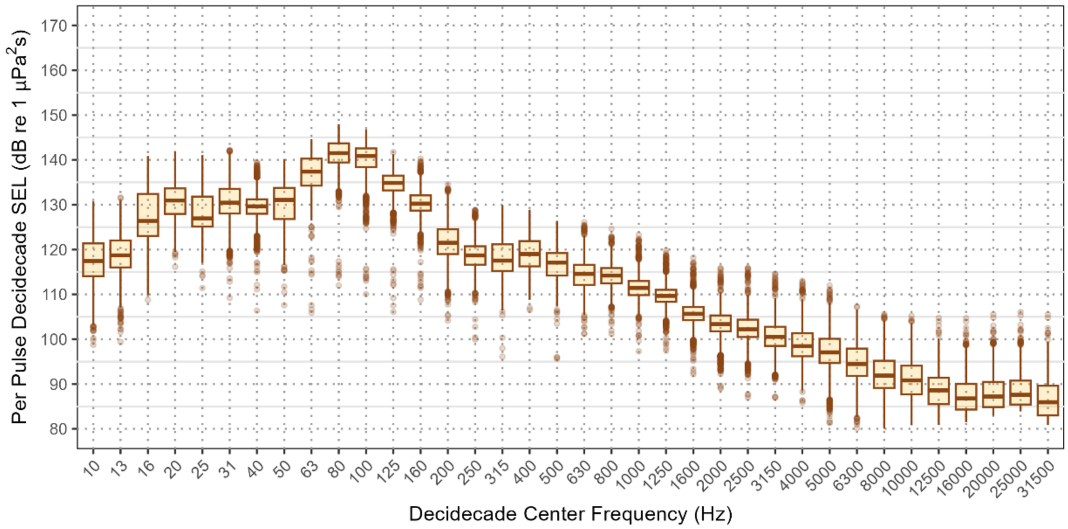


Figure A-10. Distribution of decidecade band level single strike SEL for pile driving installation of AT-40 at monitoring station AT40-8000 for channel 2. Beige bars indicate the first, second, and third quartiles (*25th*, *50th*, and *75th*) or as exceedances $L_{75}$, $L_{50}$, and $L_{25}$. Upper error bars indicate the maximum levels ($L_{max}$). Lower error bars indicate the 5th percentile or $L_{95}$.

Table A-6. Received level statistics for pile driving installation of AT-40 at monitoring station AT40-8000.

| Sound level statistic | PK (dB re 1 µPa) | rms SPL (dB re 1 µPa$^2$) | SELss (dB re 1 µPa$^2$·s) |
|---|---|---|---|
| **Channel 2 (mid-water)** | | | |
| $L_{max}$ | 168.1 | 157.0 | 151.8 |
| $L_5$ | 165.0 | 155.5 | 150.2 |
| $L_{25}$ | 163.2 | 154.0 | 149.0 |
| $L_{50}$ | 161.4 | 151.8 | 146.8 |
| $L_{75}$ | 159.2 | 149.9 | 144.8 |
| $L_{95}$ | 155.4 | 146.5 | 141.6 |
| $L_{mean}$ | 161.8 | 152.4 | 147.3 |

### A.1.3. Ranges to Acoustic Thresholds

Table A-7. Isopleth distances to NMFS physiological thresholds for impact driving installation of pile AT-40.

| Group | Injury: PK | | | | Injury: cSEL | | | |
|---|---|---|---|---|---|---|---|---|
| | Level (dB re 1µPa) | Predicted (m) | Measured (m) | Measured w/ attn. coeff. (m) | Level (dB re 1 µPa²·s) | Predicted (m) | Measured (m) | Measured w/ attn. coeff. (m) |
| LFC | 219 | 17 | 10 | 10 | 183 | 3,191 | 2,700 | 2,800 |
| MFC | 230 | 5 | 10 | 10 | 185 | 43 | 10 | 20 |
| HFC | 202 | 119 | 50 | 20 | 155 | 71 | 480 | 520 |
| PW | 218 | 19 | 10 | 10 | 185 | 153 | 160 | 140 |
| ST | 232 | 0 | 10 | 10 | 204 | 161 | 270 | 250 |
| AS | 206 | 78 | 30 | 10 | 187 | 6,894 | 5,110 | 5,210 |

Table A-8. Isopleth distances to NMFS behavioral thresholds for impact driving installation of pile AT-40.

| Group | Behavior: SPL | | | |
|---|---|---|---|---|
| | Level (dB re 1µPa²) | Predicted (m) | Measured (m) | Measured w/ attn. coeff. (m) |
| MM | 160 | 4,121 | 4,610 | 4,820 |
| ST | 175 | 1,400 | 540 | 490 |
| AS | 150 | 9,229 | 19,270 | 13,520 |

### A.1.4. Regression Analysis for Transmission Loss

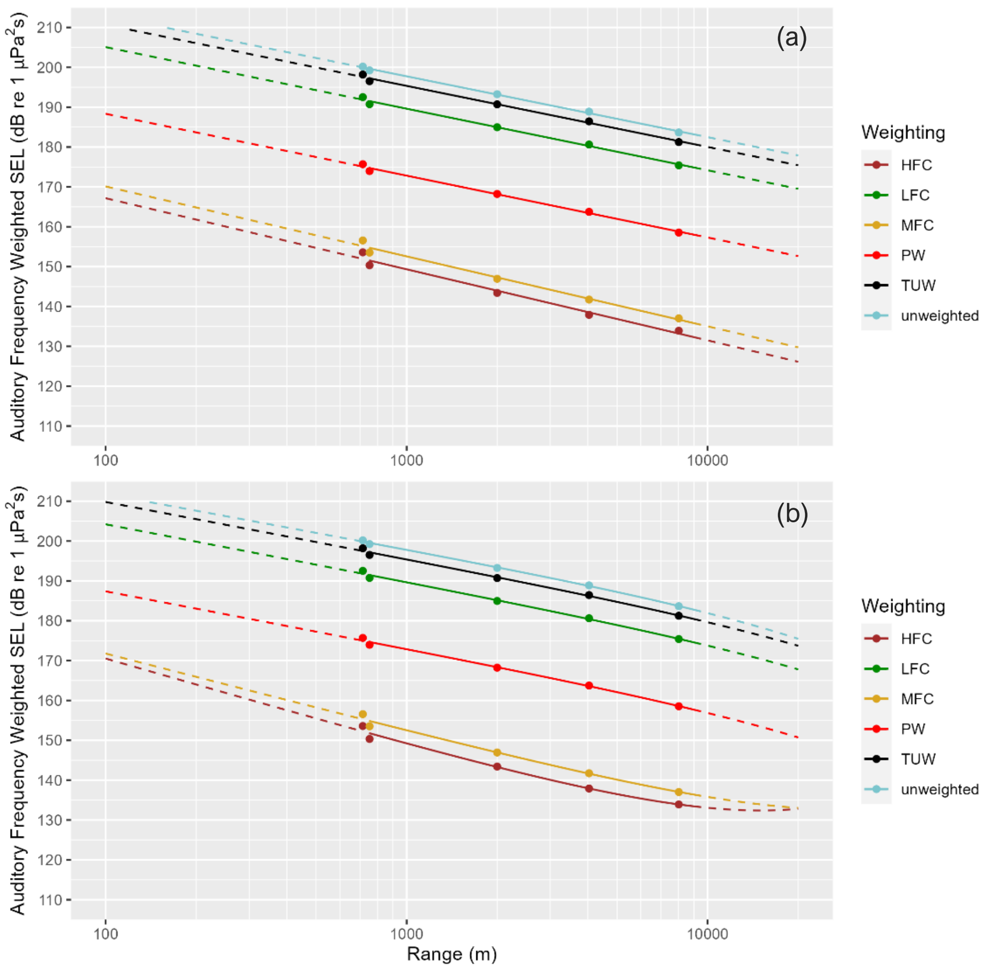


Figure A-11. Transmission loss determination based on regression analysis without (a) and with (b) intrinsic attenuation for the maximum received cumulative SEL (cSEL) at each recording station during installation of pile AT-40 on 6 Jun 2023.

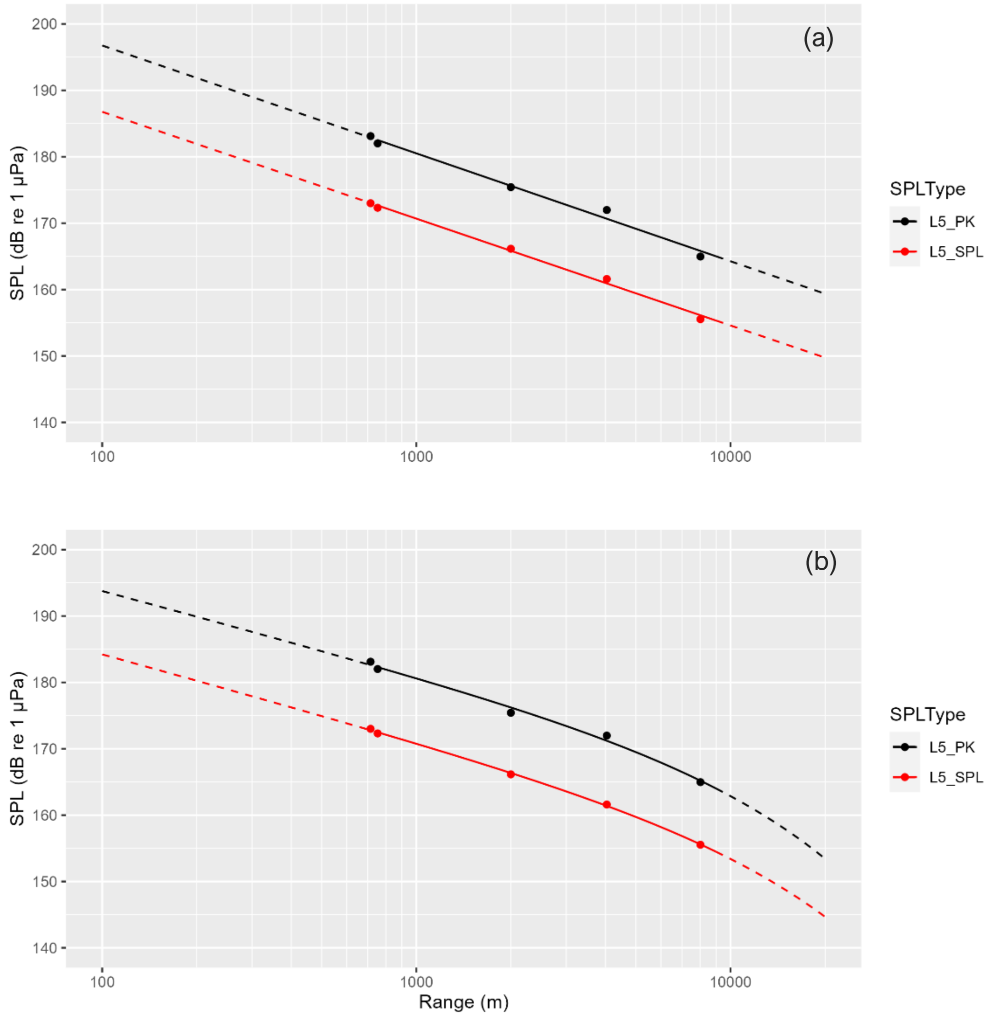


Figure A-12. Transmission loss determination based on regression analysis without (a) and with (b) intrinsic attenuation for $L_5$ PK and SPL maxima at each recording station during installation of pile AT-40 on 6 Jun 2023.

Table A-9. Regression analysis fitting coefficients for transmission loss with and without intrinsic attenuation for installation of pile AT-40 on 6 Jun 2023.

| Metric | A (dB/decade m) A*log(r) | A (dB/decade m) A*log(r) + αr/1000 | α (dB/ m) A*log(r) + αr/1000 |
|---|---|---|---|
| PK ($L_5$) (dB re 1 µPa) | -16.2 | -12.6 | -0.566 x $10^{-3}$ |
| rms SPL ($L_5$) (dB re 1 µPa$^2$) | -16.1 | -13.1 | -0.477 x $10^{-3}$ |
| cSEL (dB re 1 µPa$^2$·s) | -15.2 | -13.5 | -0.271 x $10^{-3}$ |
| cSEL, LF (dB re 1 µPa$^2$·s) | -15.4 | -14.1 | -0.201 x $10^{-3}$ |
| cSEL, MF (dB re 1 µPa$^2$·s) | -17.3 | -18.4 | 0.163 x $10^{-3}$ [a] |
| cSEL, HF (dB re 1 µPa$^2$·s) | -17.6 | -20.7 | 0.484 x $10^{-3}$ [a] |
| cSEL, PW (dB re 1 µPa$^2$·s) | -15.4 | -14.0 | -0.232 x $10^{-3}$ |
| cSEL, TU (dB re 1 µPa$^2$·s) | -15.3 | -14.0 | -0.196 x $10^{-3}$ |

[a] Positive attenuation coefficients could indicate ambient noise contamination and may not be valid.

## A.2. Foundation AU-39

Summary of measurements are shown in Table A-10. Channel 1 (bottom hydrophone) at station AU39-2000 was not functioning properly and was excluded from the analysis. Channel 1 at station AU39-8000 had a hydrophone with a higher sensitivity, of approximately -165 dB, which resulted in significant clipping as sound peak levels at this distance were also near 165 dB. Therefore, data from AU39-8000 channel 1 were also excluded from this analysis.

### A.2.1. Summary of Measured Sound Levels

Table A-10. Summary of Autonomous Multichannel Acoustic Recorder (AMAR) locations and measured sound levels for pile AU-39. Computed PK and SPL levels are shown for the $L_{max}$.

| Location (nominal) | Recorder ID | Distance (m) | Water depth (m) | Channel | Impulses Detected* (clipped) | PK (dB re 1 µPa) | SPL (dB re 1 µPa$^2$) | cSEL (dB re 1 µPa$^2$·s) |
|---|---|---|---|---|---|---|---|---|
| 750 | AMAR-863 | 740 | 44.4 | 1 | 3173 | 183.2 | 174.5 | 198.9 |
| | | | | 2 | 3233 | 183.1 | 173.7 | 198.6 |
| 750 @ 90° | AMAR-865 | 712 | 44.4 | 1 | 2796 | 185.7 | 175.3 | 197.3 |
| | | | | 2 | 2798 | 187.0 | 175.5 | 197.3 |
| 2000 | AMAR-855 | 2012 | 45.0 | | | | | |
| | | | | 2 | 3206 | 179.5 | 169.8 | 195.4 |
| 4000 | AMAR-860 | 3999 | 45.3 | 1 | 3240 | 172.7 | 163.0 | 188.5 |
| | | | | 2 | 3209 | 174.4 | 164.8 | 189.9 |
| 8000 | AMAR-603 | 8022 | 47.2 | | | | | |
| | | | | 2 | 3217 | 167.8 | 158.2 | 184.4 |

* Number of strikes produced (from hammer log): 3182

## A.2.2. Sound Levels per Station

### A.2.2.1. Station AU39-750

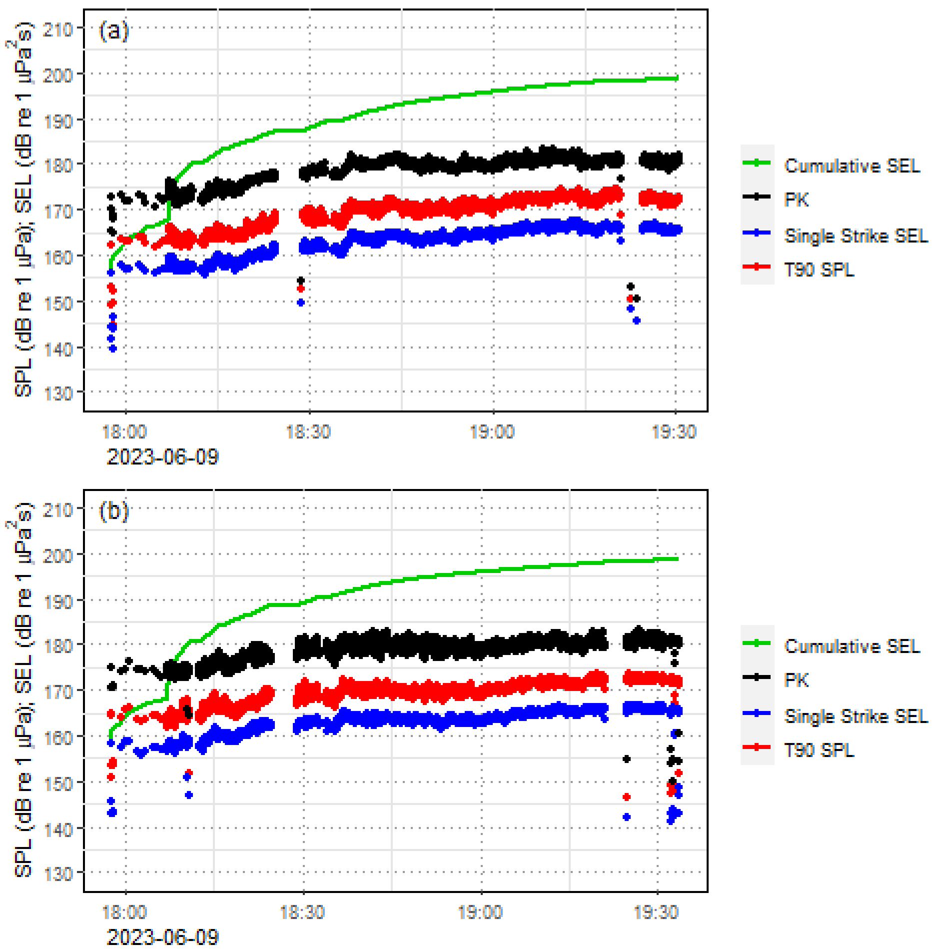


Figure A-13. Received levels for impact pile driving installation of AU-39 at monitoring station AU39-750 for channel 1 (a) and channel 2 (b). Peak SPL (PK, black), rms SPL (T90 SPL, red), single strike SEL (blue) and cumulative SEL (green) versus time (UTC). For periods during which there was no pile driving the cSEL is necessarily displayed as a constant value over time.

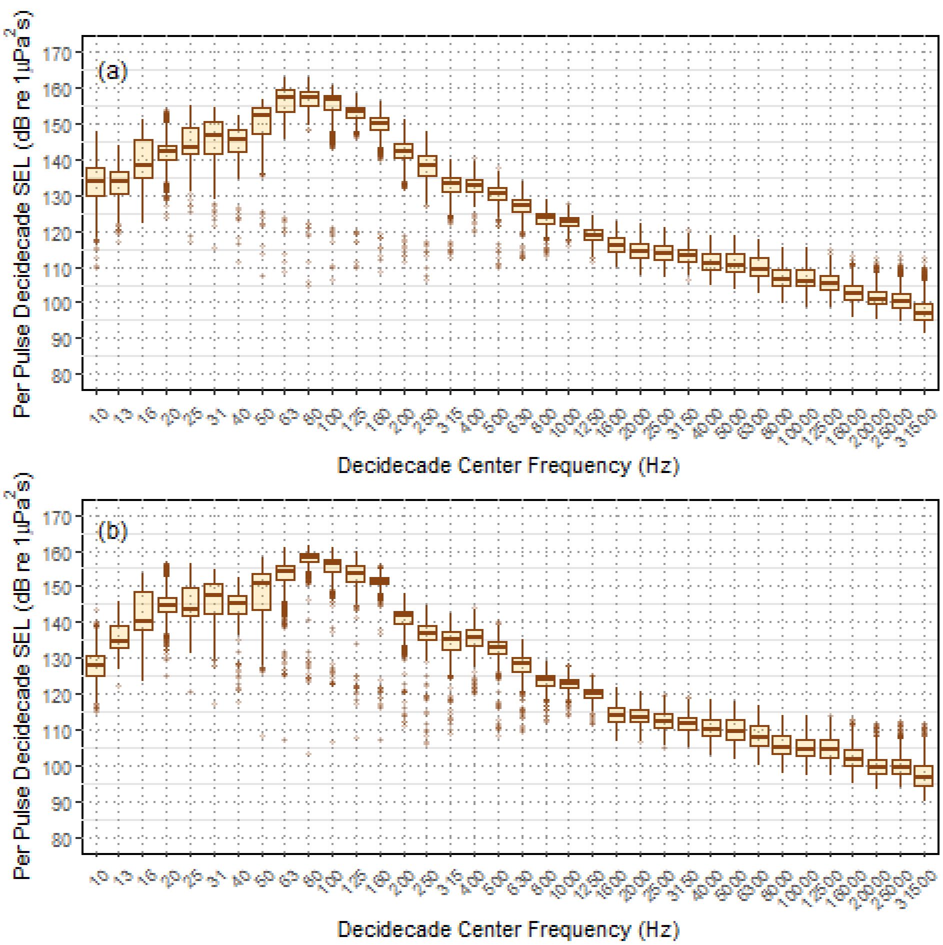


Figure A-14. Distribution of decidecade band level single strike SEL for pile driving installation of AU-39 at monitoring station AU39-750 for channel 1 (a) and channel 2 (b). Beige bars indicate the first, second, and third quartiles (*25th*, *50th*, and *75th*) or as exceedances $L_{75}$, $L_{50}$, and $L_{25}$. Upper error bars indicate the maximum levels ($L_{max}$). Lower error bars indicate the 5th percentile or $L_{95}$.

Table A-11. Received level statistics for pile driving installation of AU-39 at monitoring station AU39-750.

| Sound level statistic | PK (dB re 1 µPa) | rms SPL (dB re 1 µPa$^2$) | SELss (dB re 1 µPa$^2$·s) |
|---|---|---|---|
| Channel 1 (bottom) | | | |
| $L_{max}$ | 183.2 | 174.5 | 167.5 |
| $L_5$ | 181.6 | 173.1 | 166.4 |
| $L_{25}$ | 180.5 | 171.7 | 165.3 |
| $L_{50}$ | 179.7 | 170.4 | 163.9 |
| $L_{75}$ | 177.8 | 167.7 | 161.4 |
| $L_{95}$ | 173.1 | 163.6 | 157.4 |
| $L_{mean}$ | 179.4 | 170.3 | 163.9 |
| Channel 2 (mid-water) | | | |
| $L_{max}$ | 183.1 | 173.7 | 166.8 |
| $L_5$ | 181.6 | 172.4 | 166.0 |
| $L_{25}$ | 180.5 | 171.0 | 164.6 |
| $L_{50}$ | 179.4 | 169.8 | 163.5 |
| $L_{75}$ | 178.0 | 168.3 | 162.3 |
| $L_{95}$ | 174.3 | 164.5 | 158.2 |
| $L_{mean}$ | 179.4 | 169.9 | 163.6 |

### A.2.2.2. Station AU39-75090

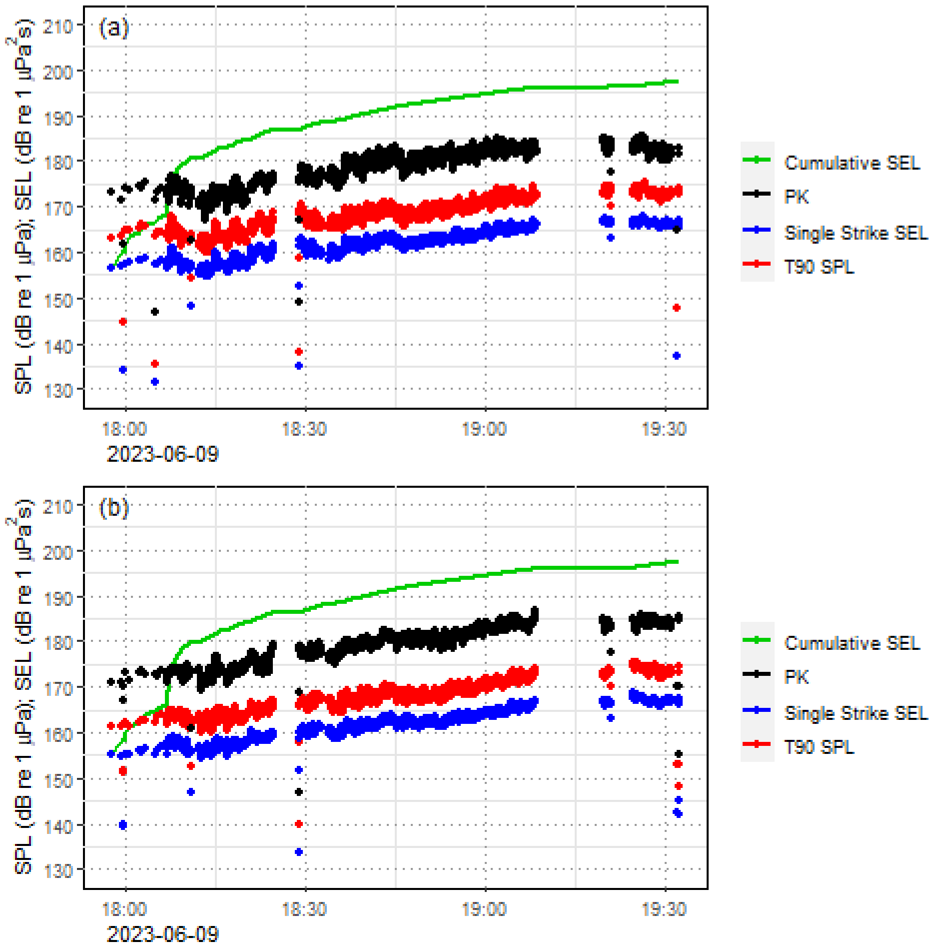


Figure A-15. Received levels for impact pile driving installation of AU-39 at monitoring station AU39-75090 for channel 1 (a) and channel 2 (b). Peak SPL (PK, black), rms SPL (T90 SPL, red), single strike SEL (blue) and cumulative SEL (green) versus time (UTC). For periods during which there was no pile driving the cSEL is necessarily displayed as a constant value over time.

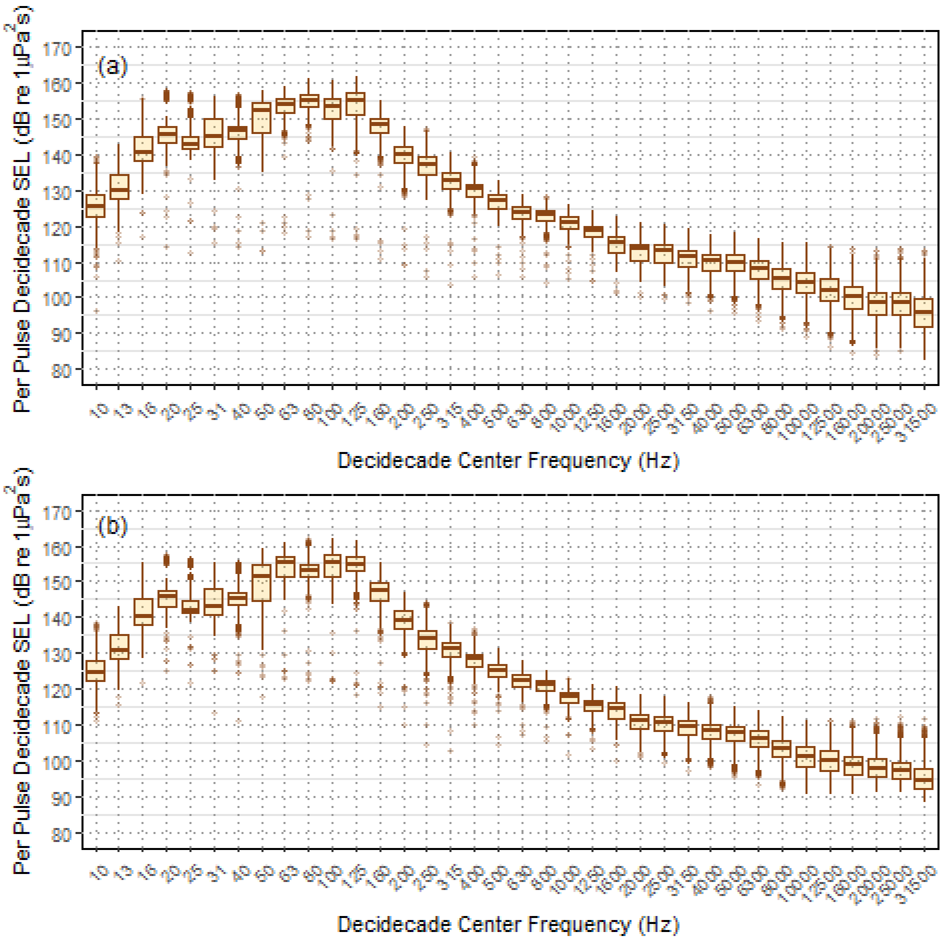


Figure A-16. Distribution of decidecade band level single strike SEL for pile driving installation of AU-39 at monitoring station AU39-75090 for channel 1 (a) and channel 2 (b). Beige bars indicate the first, second, and third quartiles (*25th*, *50th*, and *75th*) or as exceedances $L_{75}$, $L_{50}$, and $L_{25}$. Upper a bars indicate the maximum levels ($L_{max}$). Lower error bars indicate the 5th percentile or $L_{95}$.

Table A-12. Received level statistics for pile driving installation of AU-39 at monitoring station AU39-75090.

| Sound level statistic | PK (dB re 1 µPa) | rms SPL (dB re 1 µPa$^2$) | SELss (dB re 1 µPa$^2$·s) |
|---|---|---|---|
| **Channel 1 (bottom)** | | | |
| $L_{max}$ | 185.7 | 175.3 | 167.9 |
| $L_{5}$ | 183.6 | 173.3 | 166.5 |
| $L_{25}$ | 181.9 | 170.7 | 164.0 |
| $L_{50}$ | 179.6 | 168.5 | 162.2 |
| $L_{75}$ | 175.7 | 166.1 | 159.9 |
| $L_{95}$ | 171.6 | 162.8 | 156.7 |
| $L_{mean}$ | 180.1 | 169.4 | 162.8 |
| **Channel 2 (mid-water)** | | | |
| $L_{max}$ | 187.0 | 175.5 | 168.7 |
| $L_{5}$ | 184.5 | 173.5 | 166.9 |
| $L_{25}$ | 182.2 | 170.2 | 163.9 |
| $L_{50}$ | 179.9 | 167.9 | 161.9 |
| $L_{75}$ | 176.5 | 165.3 | 159.3 |
| $L_{95}$ | 172.5 | 162.2 | 156.2 |
| $L_{mean}$ | 180.7 | 169.2 | 162.8 |

## A.2.2.3. Station AU39-2000

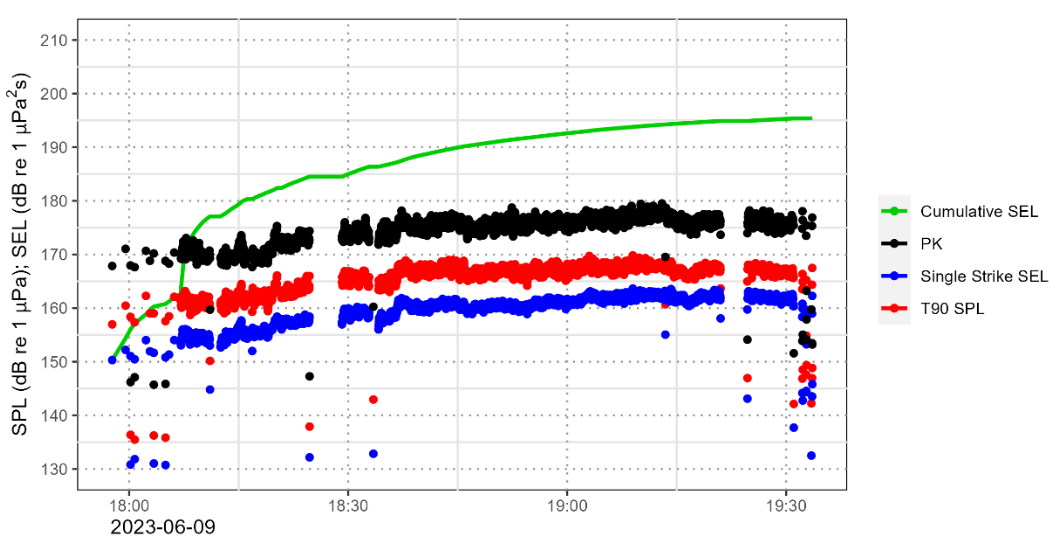


Figure A-17. Received levels for impact pile driving installation of AU-39 at monitoring station AU39-2000 for channel 2. Peak SPL (PK, black), rms SPL (T90 SPL, red), single strike SEL (blue) and cumulative SEL (green) versus time (UTC). For periods during which there was no pile driving the cSEL is necessarily displayed as a constant value over time.

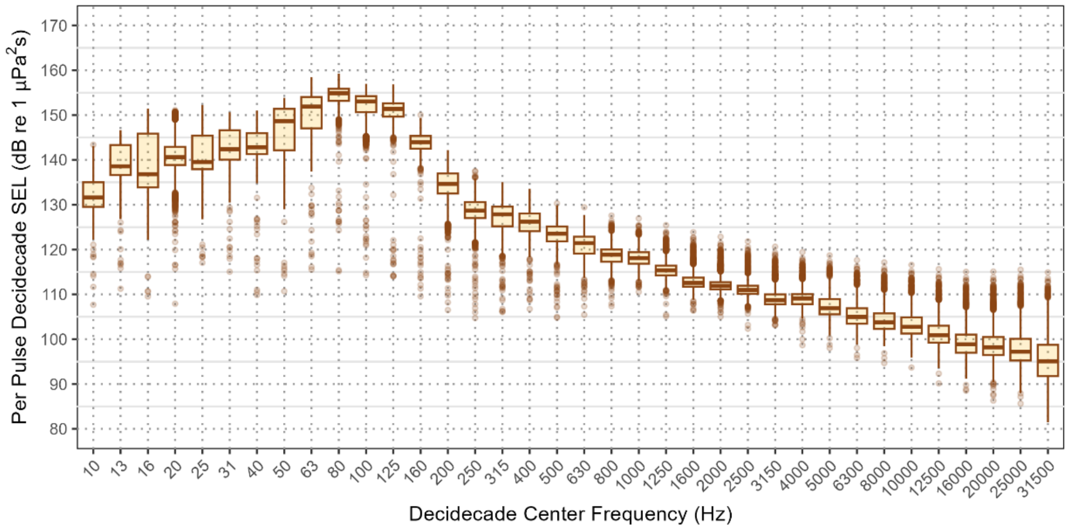


Figure A-18. Distribution of decidecade band level single strike SEL for pile driving installation of AU-39 at monitoring station AU39-2000 for channel 2. Beige bars indicate the first, second, and third quartiles (*25th*, *50th*, and *75th*) or as exceedances $L_{75}$, $L_{50}$, and $L_{25}$. Upper error bars indicate the maximum levels ($L_{max}$). Lower error bars indicate the 5th percentile or $L_{95}$.

Table A-13. Received level statistics for pile driving installation of AU-39 at monitoring station AU39-2000.

| Sound level statistic | PK (dB re 1 µPa) | rms SPL (dB re 1 µPa²) | SELss (dB re 1 µPa²·s) |
|---|---|---|---|
| **Channel 2 (mid-water)** | | | |
| $L_{max}$ | 179.5 | 169.8 | 163.7 |
| $L_5$ | 177.5 | 168.3 | 162.6 |
| $L_{25}$ | 176.3 | 167.3 | 161.6 |
| $L_{50}$ | 175.4 | 166.6 | 160.5 |
| $L_{75}$ | 173.5 | 164.8 | 158.4 |
| $L_{95}$ | 169.4 | 161.0 | 154.5 |
| $L_{mean}$ | 175.2 | 166.3 | 160.3 |

### A.2.2.4. Station AU39-4000

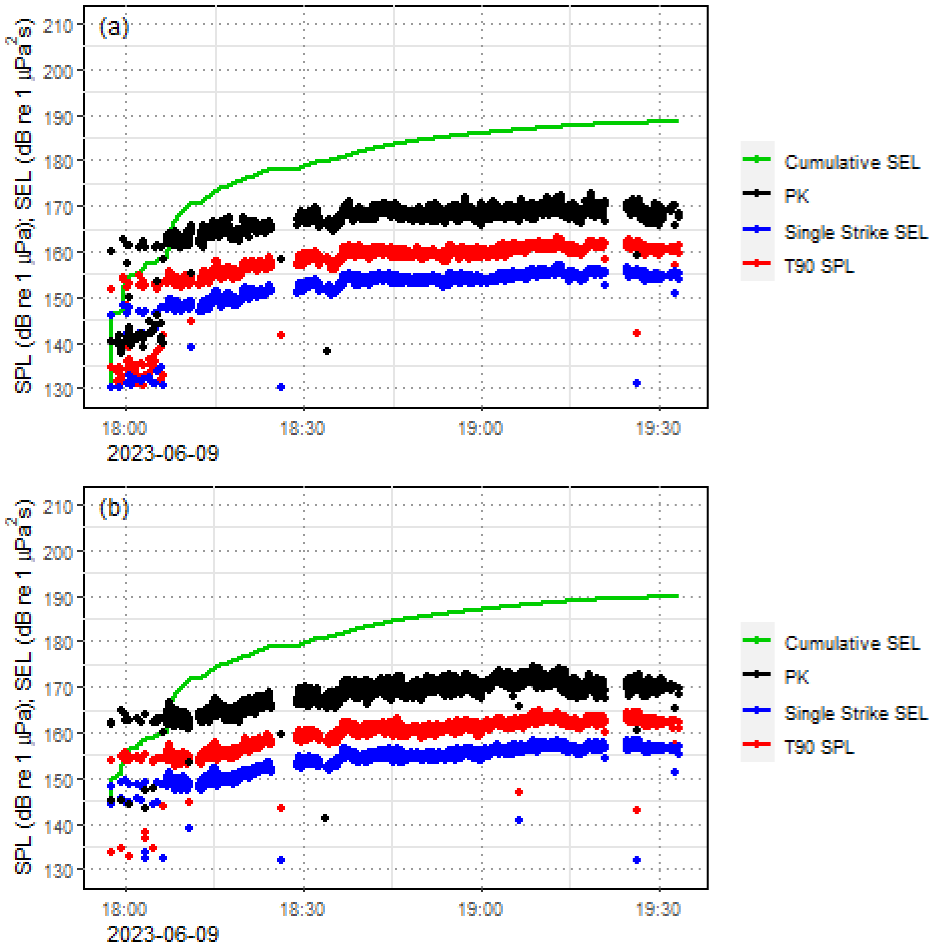


Figure A-19. Received levels for impact pile driving installation of AU-39 at monitoring station AU39-4000 for channel 1 (a) and channel 2 (b). Peak SPL (PK, black), rms SPL (T90 SPL, red), single strike SEL (blue) and cumulative SEL (green) versus time (UTC). For periods during which there is no pile driving the cSEL is necessarily displayed as a constant value over time.

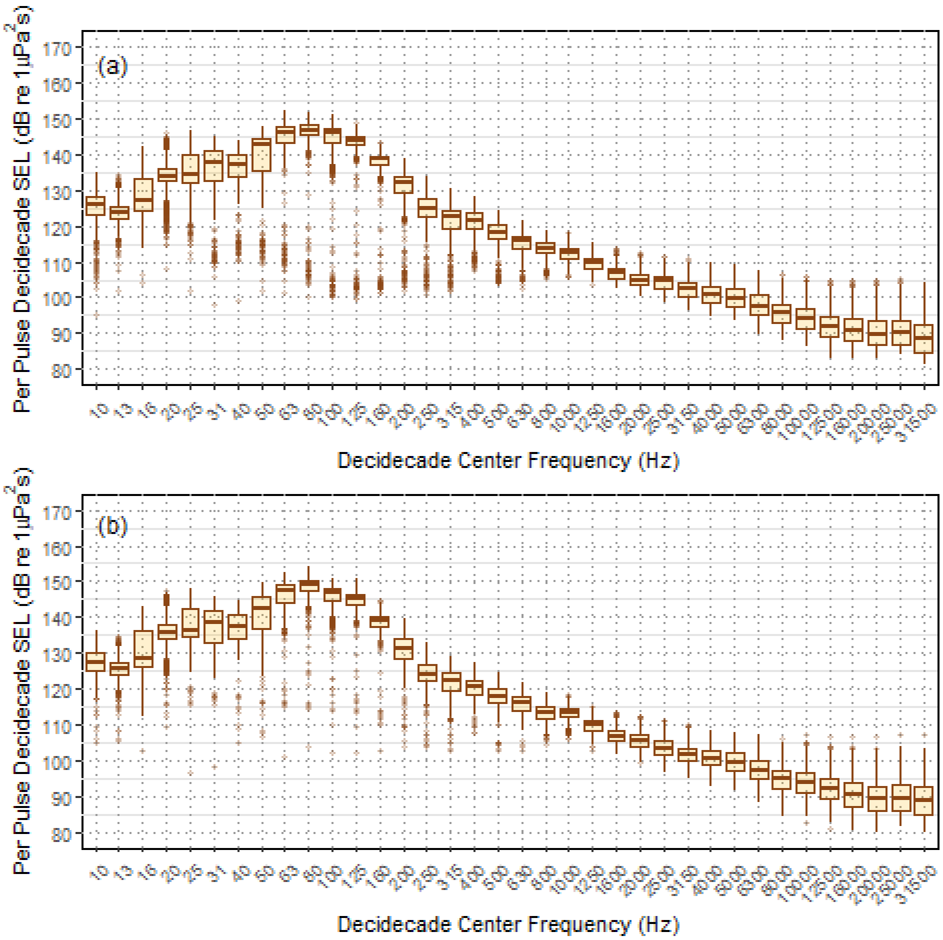


Figure A-20. Distribution of decidecade band level single strike SEL for pile driving installation of AU-39 at monitoring station AU39-4000 for channel 1 (a) and channel 2 (b). Beige bars indicate the first, second, and third quartiles (*25th*, *50th*, and *75th*) or as exceedances $L_{75}$, $L_{50}$, and $L_{25}$. Upper error bars indicate the maximum levels ($L_{max}$). Lower error bars indicate the 5th percentile or $L_{95}$.

Table A-14. Received level statistics for pile driving installation of AU-39 at monitoring station AU39-4000.

| Sound level statistic | PK (dB re 1 µPa) | rms SPL (dB re 1 µPa²) | SELss (dB re 1 µPa²·s) |
|---|---|---|---|
| **Channel 1 (bottom)** | | | |
| $L_{max}$ | 172.7 | 163.0 | 157.1 |
| $L_5$ | 170.1 | 161.6 | 155.6 |
| $L_{25}$ | 168.9 | 160.4 | 154.5 |
| $L_{50}$ | 168.0 | 159.6 | 153.7 |
| $L_{75}$ | 166.2 | 157.6 | 151.7 |
| $L_{95}$ | 162.6 | 153.6 | 148.0 |
| $L_{mean}$ | 167.9 | 159.3 | 153.4 |
| **Channel 2 (mid-water)** | | | |
| $L_{max}$ | 174.4 | 164.8 | 158.3 |
| $L_5$ | 172.2 | 163.1 | 157.2 |
| $L_{25}$ | 170.7 | 162.0 | 156.1 |
| $L_{50}$ | 169.5 | 160.7 | 154.9 |
| $L_{75}$ | 167.3 | 158.7 | 152.9 |
| $L_{95}$ | 163.3 | 154.6 | 149.0 |
| $L_{mean}$ | 169.5 | 160.6 | 154.8 |

## A.2.2.5. Station AU39-8000

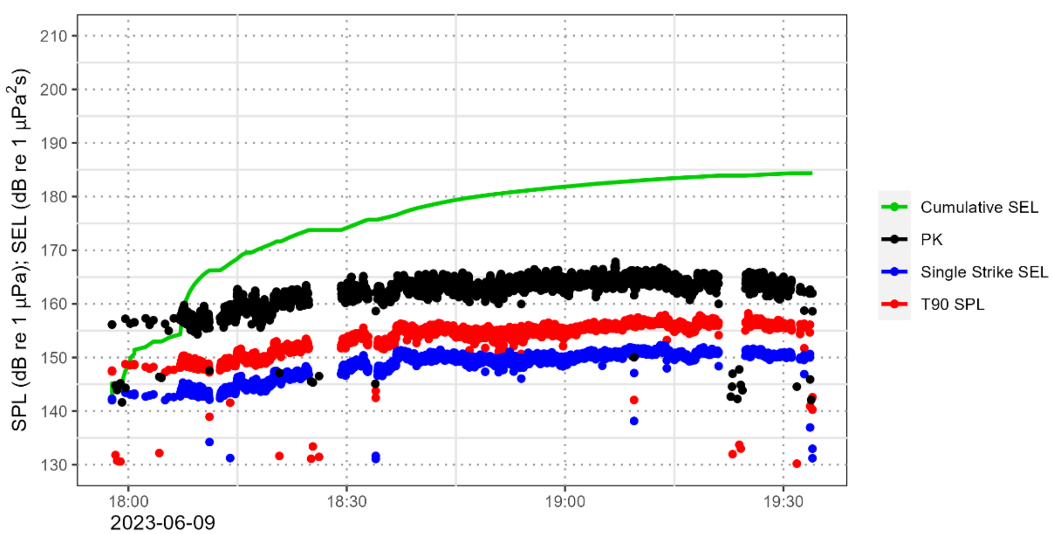


Figure A-21. Received levels for impact pile driving installation of AU-39 at monitoring station AU39-8000 for channel 2. Peak SPL (PK, black), rms SPL (T90 SPL, red), single strike SEL (blue) and cumulative SEL (green) versus time (UTC). For periods during which there is no pile driving the cSEL is necessarily displayed as a constant value over time.

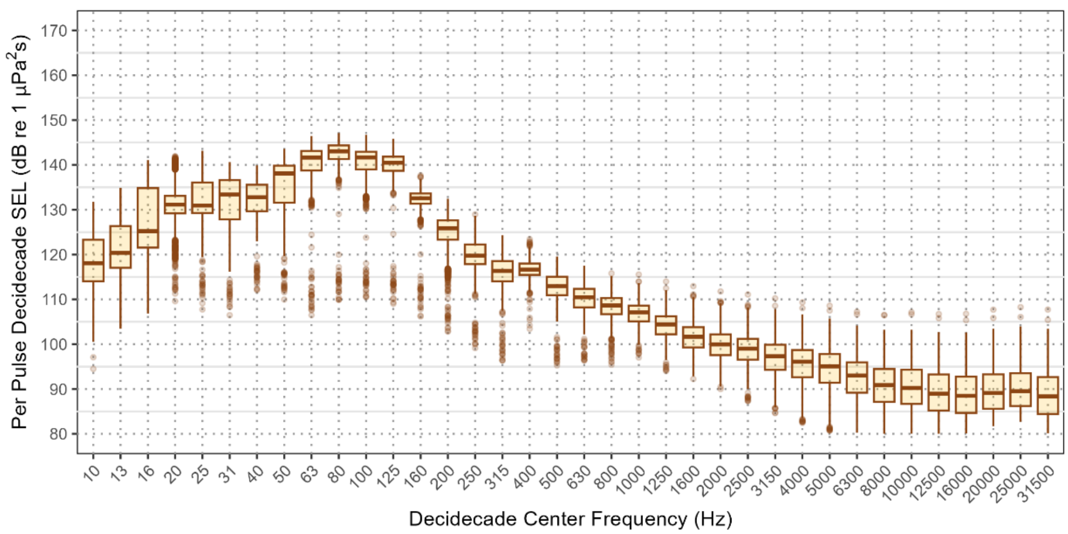


Figure A-22. Distribution of decidecade band level single strike SEL for pile driving installation of AU-39 at monitoring station AU39-8000 for channel 2. Beige bars indicate the first, second, and third quartiles (*25th*, *50th*, and *75th*) or as exceedances $L_{75}$, $L_{50}$, and $L_{25}$. Upper error bars indicate the maximum levels ($L_{max}$). Lower error bars indicate the 5th percentile or $L_{95}$.

Table A-15. Received level statistics for pile driving installation of AU-39 at monitoring station AU39-8000.

| Sound level statistic | PK (dB re 1 µPa) | rms SPL (dB re 1 µPa²) | SELss (dB re 1 µPa²·s) |
|---|---|---|---|
| **Channel 2 (mid-water)** | | | |
| $L_{max}$ | 167.8 | 158.2 | 152.3 |
| $L_5$ | 165.4 | 156.6 | 151.2 |
| $L_{25}$ | 164.2 | 155.7 | 150.4 |
| $L_{50}$ | 163.1 | 154.7 | 149.7 |
| $L_{75}$ | 161.6 | 152.6 | 147.7 |
| $L_{95}$ | 157.1 | 148.7 | 143.6 |
| $L_{mean}$ | 163.0 | 154.5 | 149.3 |

## A.2.3. Ranges to Acoustic Thresholds

Table A-16. Isopleth distances to NMFS physiological thresholds for impact driving installation of pile AU-39.

| Group | Injury: PK | | | | Injury: cSEL | | | |
|---|---|---|---|---|---|---|---|---|
| | Level (dB re 1µPa) | Predicted (m) | Measured (m) | Measured w/ attn. coeff. (m) | Level (dB re 1 µPa²·s) | Predicted (m) | Measured (m) | Measured w/ attn. coeff. (m) |
| LFC | 219 | 17 | 10 | 10 | 183 | 3,191 | 2,890 | 3,640 |
| MFC | 230 | 5 | 10 | 10 | 185 | 43 | 10 | 10 |
| HFC | 202 | 119 | 50 | 10 | 155 | 71 | 90 | 40 |
| PW | 218 | 19 | 10 | 10 | 185 | 153 | 100 | 10 |
| ST | 232 | 0 | 10 | 10 | 204 | 161 | 190 | 20 |
| AS | 206 | 78 | 30 | 10 | 187 | 6,894 | 6,240 | 6,200 |

Table A-17. Isopleth distances to NMFS behavioral thresholds for impact driving installation of pile AU-39.

| Group | Behavior: SPL | | | |
|---|---|---|---|---|
| | Level (dB re 1µPa²) | Predicted (m) | Measured (m) | Measured w/ attn. coeff. (m) |
| MM | 160 | 4,121 | 5,690 | 5,830 |
| ST | 175 | 1,400 | 610 | 510 |
| AS | 150 | 9,229 | 25,260 | 12,760 |

### A.2.4. Regression Analysis for Transmission Loss

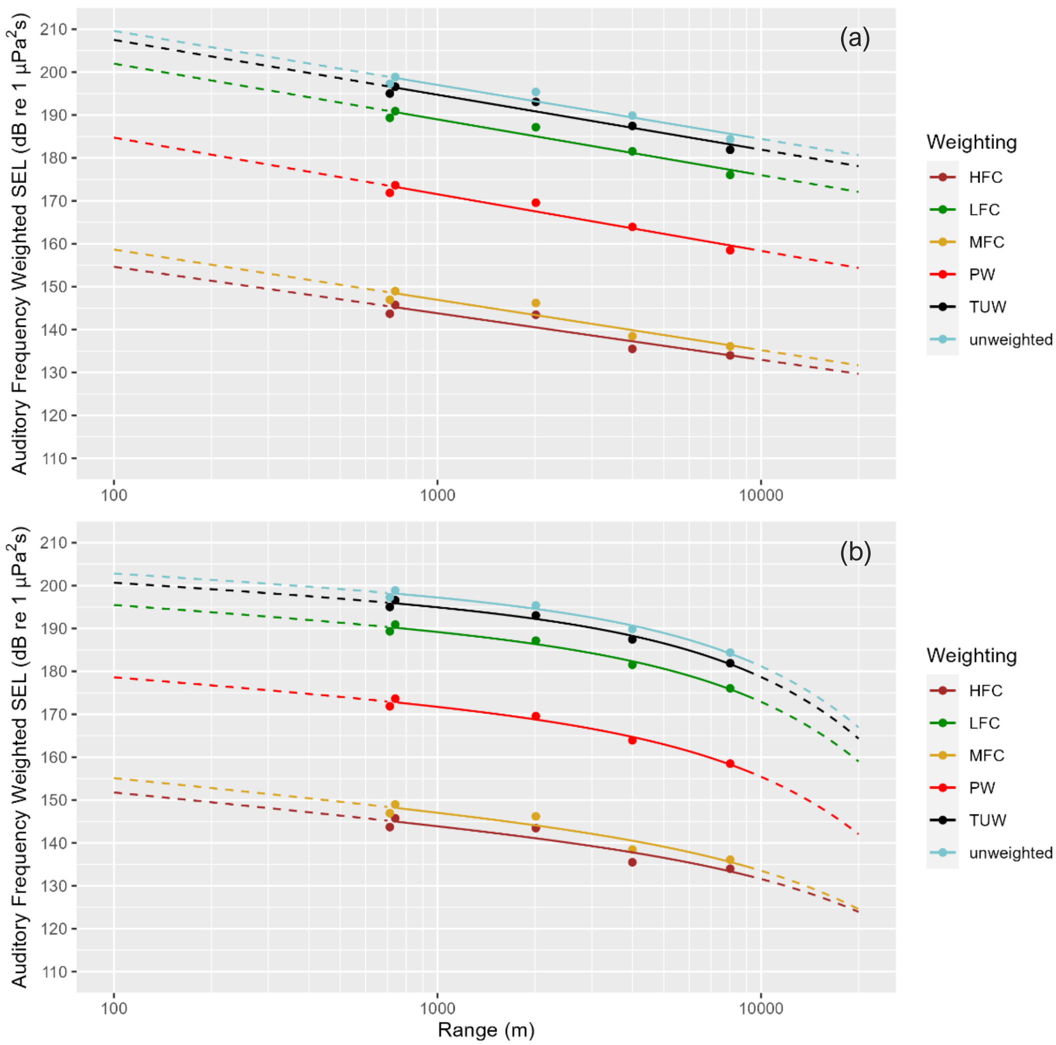


Figure A-23. Transmission loss determination based on regression analysis without (a) and with (b) intrinsic attenuation for the maximum received cumulative SEL (cSEL) at each recording station during installation of pile AU-39 on 9 Jun 2023.

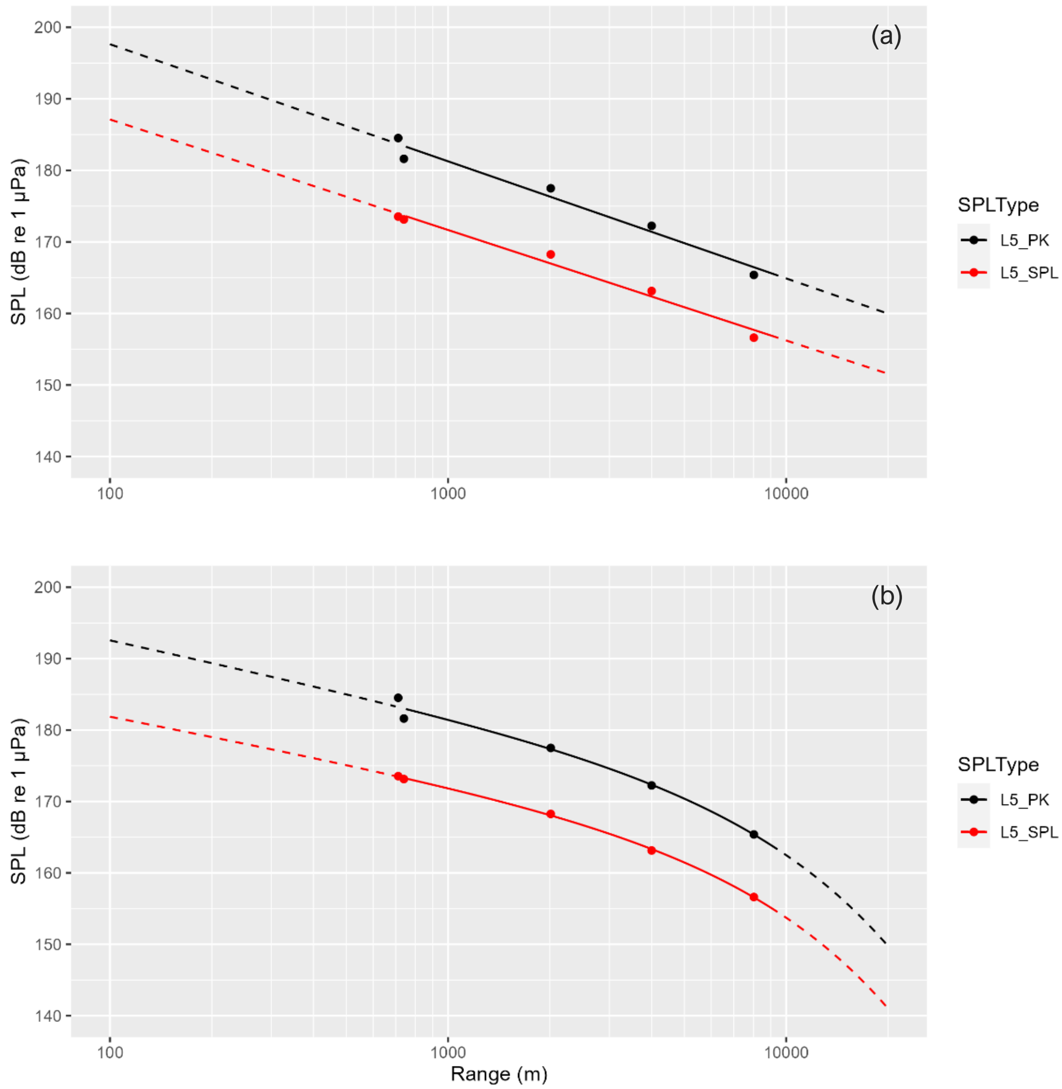


Figure A-24. Transmission loss determination based on regression analysis without (a) and with (b) intrinsic attenuation for $L_5$ PK and SPL maxima at each recording station during installation of pile AU-39 on 9 Jun 2023.

Table A-18. Regression analysis fitting coefficients for transmission loss with and without intrinsic attenuation for installation of pile AU-39 on 9 Jun 2023.

| Metric | A (dB/decade m) A*log(r) | A (dB/decade m) A*log(r) + αr/1000 | α (dB/ m) A*log(r) + αr/1000 |
|---|---|---|---|
| PK ($L_5$) (dB re 1 μPa) | -16.4 | -10.3 | $-0.963 \times 10^{-3}$ |
| rms SPL ($L_5$) (dB re 1 $μPa^2$) | -15.4 | -9.1 | $-0.995 \times 10^{-3}$ |
| cSEL (dB re 1 $μPa^2$·s) | -12.6 | -4.4 | $-1.291 \times 10^{-3}$ |
| cSEL, LF (dB re 1 $μPa^2$·s) | -13.0 | -5.2 | $-1.233 \times 10^{-3}$ |
| cSEL, MF (dB re 1 $μPa^2$·s) | -11.7 | -7.5 | $-0.671 \times 10^{-3}$ |
| cSEL, HF (dB re 1 $μPa^2$·s) | -10.8 | -7.4 | $-0.544 \times 10^{-3}$ |
| cSEL, PW (dB re 1 $μPa^2$·s) | -13.2 | -5.8 | $-1.162 \times 10^{-3}$ |
| cSEL, TU (dB re 1 $μPa^2$·s) | -12.8 | -4.6 | $-1.298 \times 10^{-3}$ |

# A.3. Foundation AP-38

Summary of measurements are shown in Table A-19. Channel 1 (bottom) at station AP38-75090 was not functioning properly and was excluded from the analysis. Channel 1 at station AP38-9000 had a hydrophone with a higher sensitivity, of approximately -165 dB, which resulted in significant clipping as sound peak levels at this distance were also near 165 dB. Therefore, data from AP38-9000 channel 1 were also excluded from this analysis.

## A.3.1. Summary of Measured Sound Levels

Table A-19. Summary of Autonomous Multichannel Acoustic Recorder (AMAR) locations and measured sound levels for pile AP-38. Computed PK and SPL levels are shown for the $L_{max}$.

| Location (nominal) | Recorder ID | Distance (m) | Water depth (m) | Channel | Impulses Detected* (clipped) | PK (dB re 1 μPa) | SPL (dB re 1 $μPa^2$) | cSEL (dB re 1 $μPa^2$·s) |
|---|---|---|---|---|---|---|---|---|
| 750 | AMAR-863 | 748 | 42.1 | 1 | 3057 | 183.4 | 173.2 | 197.2 |
| | | | | 2 | 3058 | 187.8 | 175.8 | 198.5 |
| 750 @ 90° | AMAR-865 | 704 | 43.3 | | | | | |
| | | | | 2 | 3527 | 184.3 | 174.6 | 197.3 |
| 2000 | AMAR-855 | 1923 | 43.0 | 1 | 3489 | 178.4 | 168.8 | 194.0 |
| | | | | 2 | 3481 | 178.9 | 169.2 | 195.0 |
| 4000 | AMAR-860 | 3940 | 46.1 | 1 | 3534 | 174.2 | 163.8 | 189.1 |
| | | | | 2 | 3416 | 173.5 | 164.8 | 190.3 |
| 9000 | AMAR-603 | 8965 | 47.0 | | | | | |
| | | | | 2 | 3361 | 167.5 | 157.4 | 183.1 |

* Number of strikes produced (from hammer log): 3511

## A.3.2. Sound Levels per Station

### A.3.2.1. Station AP38-750

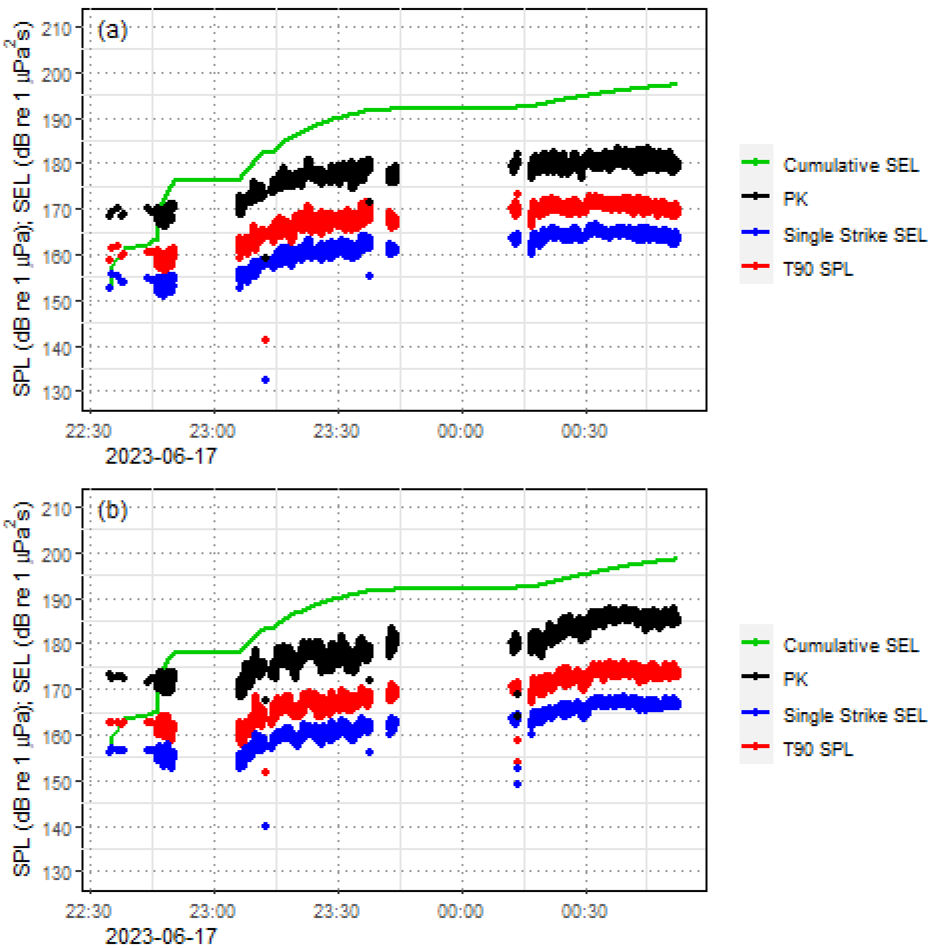


Figure A-25. Received levels for impact pile driving installation of AP-38 at monitoring station AP38-750 for channel 1 (a) and channel 2 (b). Peak SPL (PK, black), rms SPL (T90 SPL, red), single strike SEL (blue) and cumulative SEL (green) versus time (UTC). For periods during which there was no pile driving the cSEL is necessarily displayed as a constant value over time.

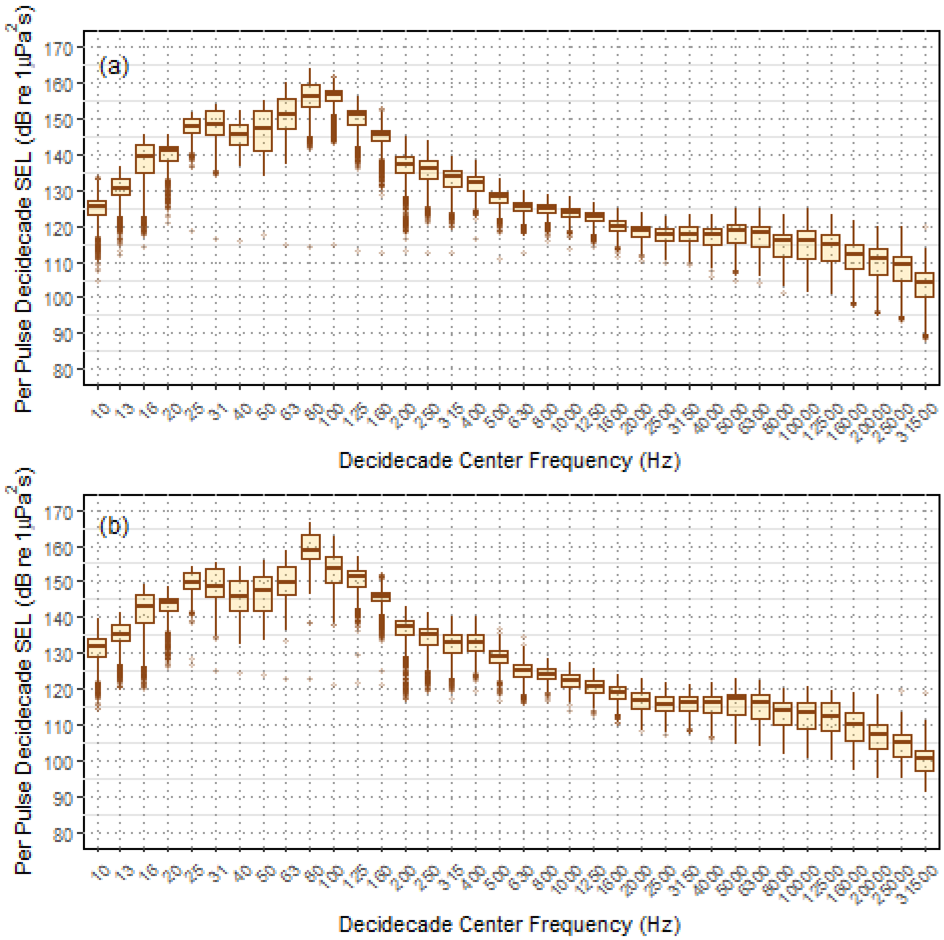


Figure A-26. Distribution of decidecade band level single strike SEL for pile driving installation of AP-38 at monitoring station AP38-750 for channel 1 (a) and channel 2 (b). Beige bars indicate the first, second, and third quartiles (*25th*, *50th*, and *75th*) or as exceedances $L_{75}$, $L_{50}$, and $L_{25}$. Upper error bars indicate the maximum levels ($L_{max}$). Lower error bars indicate the 5th percentile or $L_{95}$.

Table A-20. Received level statistics for pile driving installation of AP-38 at monitoring station AP38-750.

| Sound level statistic | PK (dB re 1 µPa) | rms SPL (dB re 1 µPa$^2$) | SELss (dB re 1 µPa$^2$·s) |
|---|---|---|---|
| **Channel 1 (bottom)** | | | |
| $L_{max}$ | 183.4 | 173.2 | 166.7 |
| $L_5$ | 181.4 | 171.3 | 165.1 |
| $L_{25}$ | 180.1 | 170.3 | 164.2 |
| $L_{50}$ | 178.4 | 168.5 | 162.0 |
| $L_{75}$ | 176.0 | 165.8 | 159.7 |
| $L_{95}$ | 169.8 | 160.1 | 154.3 |
| $L_{mean}$ | 178.5 | 168.6 | 162.4 |
| **Channel 2 (mid-water)** | | | |
| $L_{max}$ | 187.8 | 175.8 | 168.4 |
| $L_5$ | 186.5 | 174.5 | 167.3 |
| $L_{25}$ | 184.6 | 173.0 | 166.1 |
| $L_{50}$ | 179.0 | 168.4 | 161.9 |
| $L_{75}$ | 176.2 | 165.9 | 159.7 |
| $L_{95}$ | 171.7 | 160.9 | 155.1 |
| $L_{mean}$ | 182.0 | 170.6 | 163.7 |

## A.3.2.2. Station AP38-75090

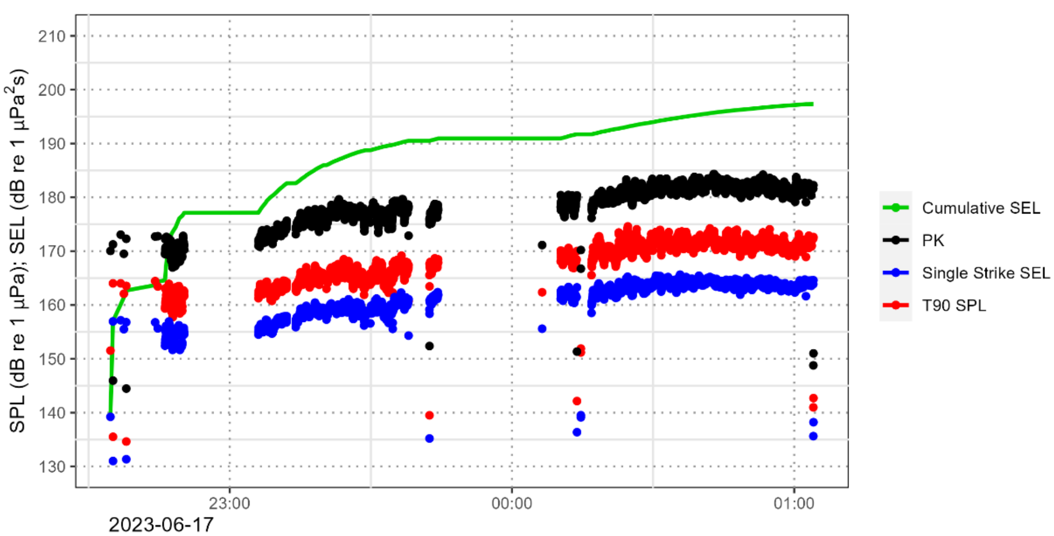


Figure A-27. Received levels for impact pile driving installation of AP-38 at monitoring station AP38-75090 for channel 1. Peak SPL (PK, black), rms SPL (T90 SPL, red), single strike SEL (blue) and cumulative SEL (green) versus time (UTC). For periods during which there was no pile driving the cSEL is necessarily displayed as a constant value over time.

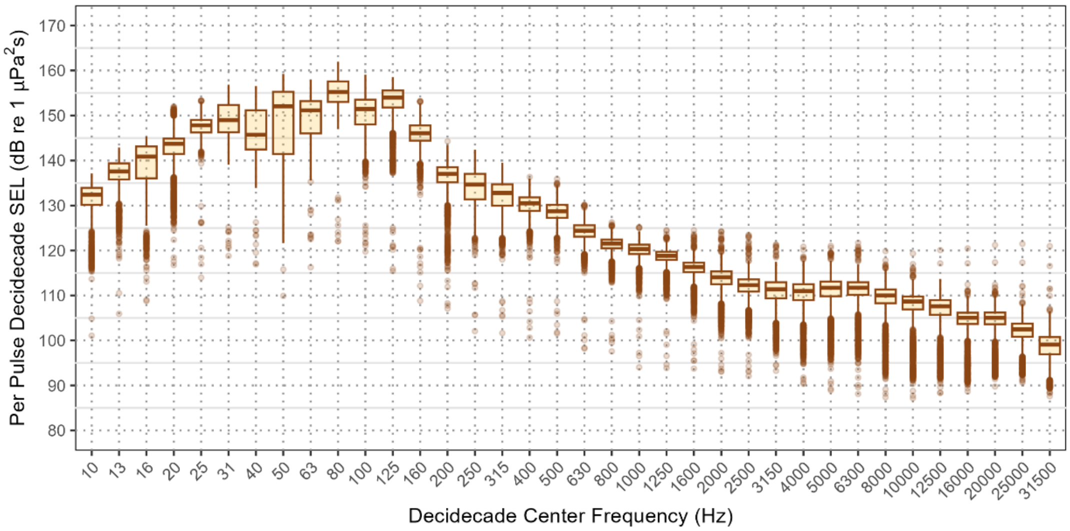


Figure A-28. Distribution of decidecade band level single strike SEL for pile driving installation of AP-38 at monitoring station AP38-75090 for channel 1. Beige bars indicate the first, second, and third quartiles (*25th*, *50th*, and *75th*) or as exceedances $L_{75}$, $L_{50}$, and $L_{25}$. Upper error bars indicate the maximum levels ($L_{max}$). Lower error bars indicate the 5th percentile or $L_{95}$.

Table A-21. Received level statistics for pile driving installation of AP-38 at monitoring station AP38-75090.

| Sound level statistic | PK (dB re 1 µPa) | rms SPL (dB re 1 µPa²) | SELss (dB re 1 µPa²·s) |
|---|---|---|---|
| **Channel 1 (bottom)** | | | |
| $L_{max}$ | 184.3 | 174.6 | 165.6 |
| $L_5$ | 182.8 | 172.6 | 164.6 |
| $L_{25}$ | 181.6 | 171.1 | 163.7 |
| $L_{50}$ | 178.9 | 168.4 | 161.6 |
| $L_{75}$ | 176.5 | 165.1 | 158.8 |
| $L_{95}$ | 171.5 | 162.1 | 155.3 |
| $L_{mean}$ | 179.6 | 169.2 | 161.9 |

## A.3.2.3. Station AP38-2000

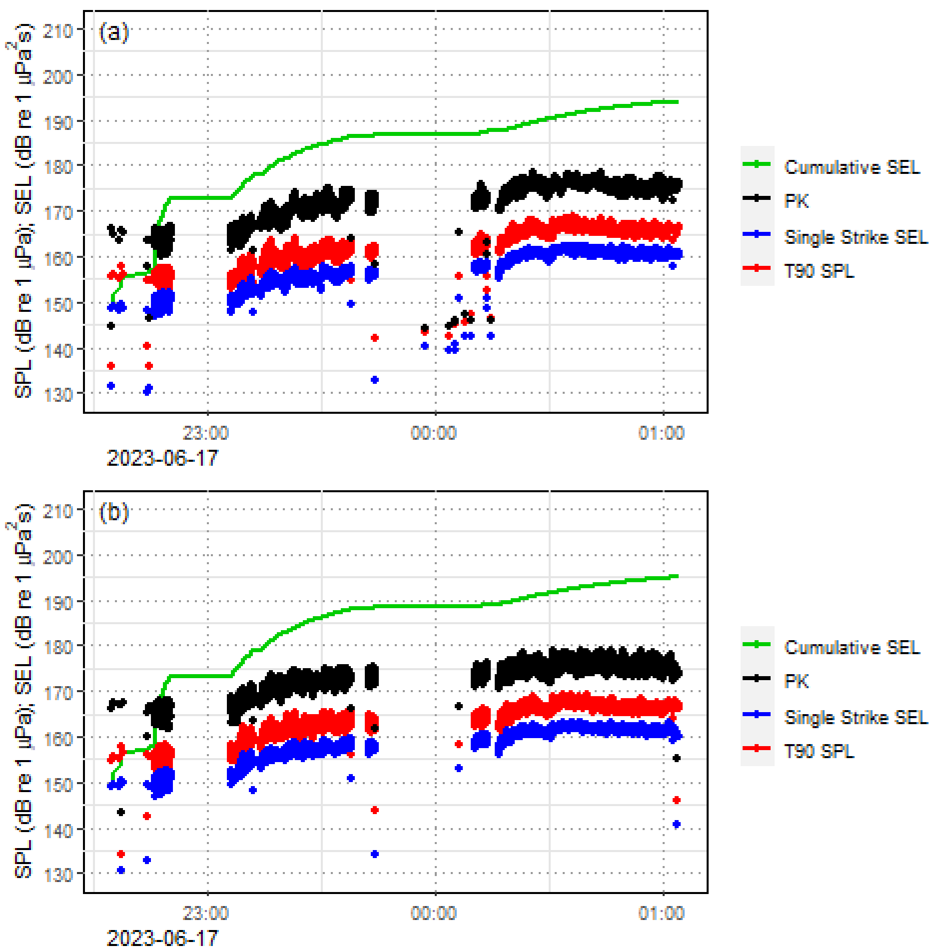


Figure A-29. Received levels for impact pile driving installation of AP-38 at monitoring station AP38-2000 for channel 1 (a) and channel 2 (b). Peak SPL (PK, black), rms SPL (T90 SPL, red), single strike SEL (blue) and cumulative SEL (green) versus time (UTC). For periods during which there was no pile driving the cSEL is necessarily displayed as a constant value over time.

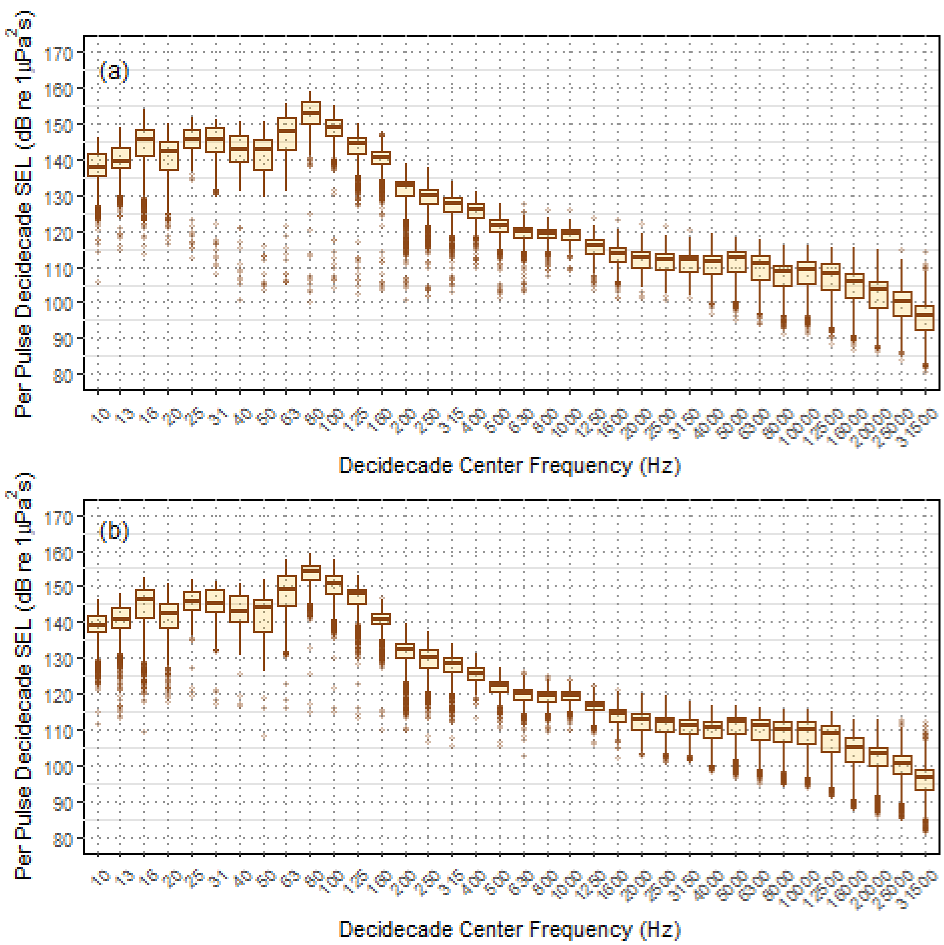


Figure A-30. Distribution of decidecade band level single strike SEL for pile driving installation of AP-38 at monitoring station AP38-2000 for channel 1 (a) and channel 2 (b). Beige bars indicate the first, second, and third quartiles (*25th*, *50th*, and *75th*) or as exceedances $L_{75}$, $L_{50}$, and $L_{25}$. Upper error bars indicate the maximum levels ($L_{max}$). Lower error bars indicate the 5th percentile or $L_{95}$.

Table A-22. Received level statistics for pile driving installation of AP-38 at monitoring station AP38-2000.

| Sound level statistic | PK (dB re 1 µPa) | rms SPL (dB re 1 µPa$^2$) | SELss (dB re 1 µPa$^2$·s) |
|---|---|---|---|
| **Channel 1 (bottom)** | | | |
| $L_{max}$ | 178.4 | 168.8 | 162.4 |
| $L_{5}$ | 176.8 | 167.0 | 161.6 |
| $L_{25}$ | 175.4 | 165.8 | 160.7 |
| $L_{50}$ | 173.1 | 162.7 | 157.6 |
| $L_{75}$ | 169.9 | 159.8 | 154.9 |
| $L_{95}$ | 164.0 | 155.3 | 150.4 |
| $L_{mean}$ | 173.5 | 163.7 | 158.6 |
| **Channel 2 (mid-water)** | | | |
| $L_{max}$ | 178.9 | 169.2 | 163.3 |
| $L_{5}$ | 177.1 | 167.7 | 162.3 |
| $L_{25}$ | 175.4 | 166.4 | 161.5 |
| $L_{50}$ | 173.6 | 164.2 | 159.1 |
| $L_{75}$ | 171.2 | 161.6 | 156.6 |
| $L_{95}$ | 165.6 | 156.0 | 151.2 |
| $L_{mean}$ | 173.9 | 164.7 | 159.6 |

## A.3.2.4. Station AP38-4000

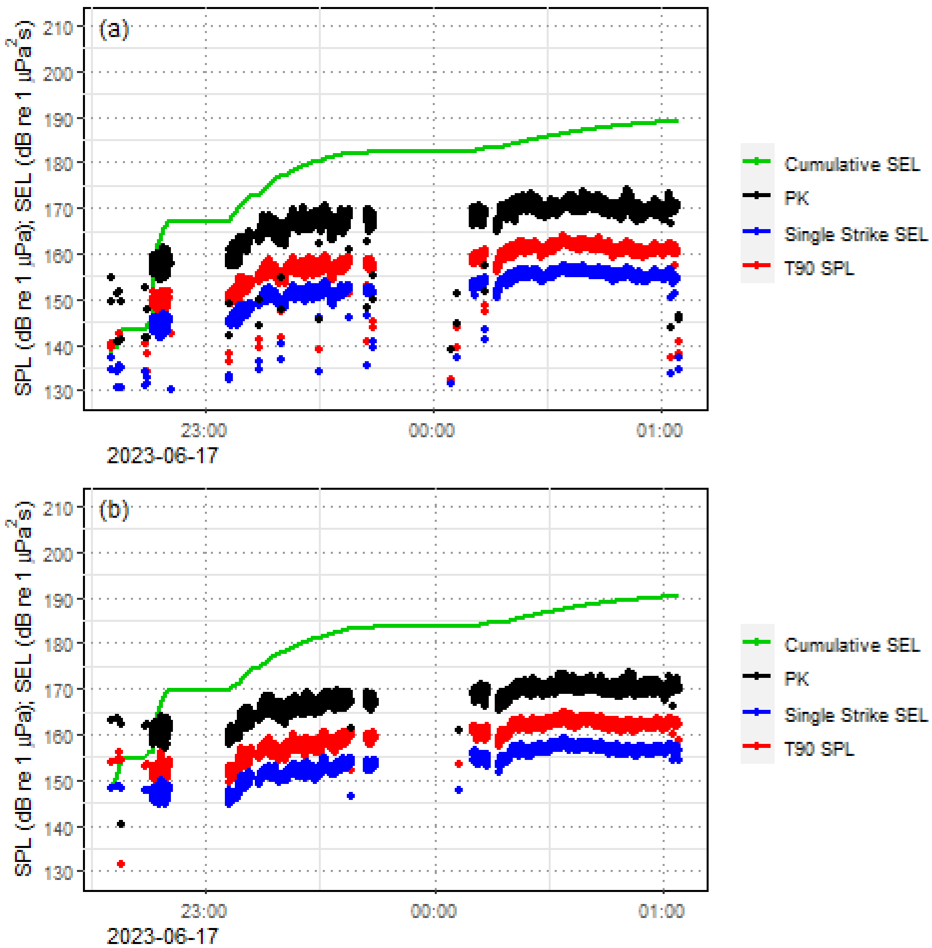


Figure A-31. Received levels for impact pile driving installation of AP-38 at monitoring station AP38-4000 for channel 1 (a) and channel 2 (b). Peak SPL (PK, black), rms SPL (T90 SPL, red), single strike SEL (blue) and cumulative SEL (green) versus time (UTC). For periods during which there is no pile driving the cSEL is necessarily displayed as a constant value over time.

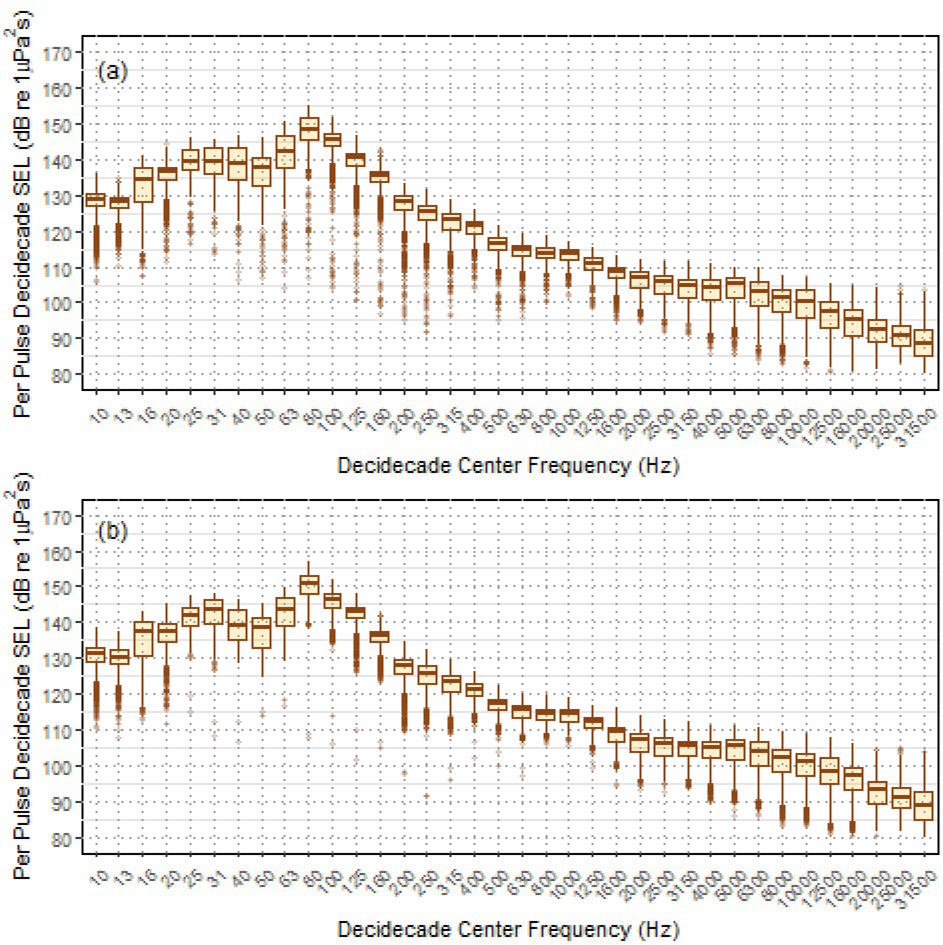


Figure A-32. Distribution of decidecade band level single strike SEL for pile driving installation of AP-38 at monitoring station AP38-4000 for channel 1 (a) and channel 2 (b). Beige bars indicate the first, second, and third quartiles (*25th*, *50th*, and *75th*) or as exceedances $L_{75}$, $L_{50}$, and $L_{25}$. Upper error bars indicate the maximum levels ($L_{max}$). Lower error bars indicate the 5th percentile or $L_{95}$.

Table A-23. Received level statistics for pile driving installation of AP-38 at monitoring station AP38-4000.

| Sound level statistic | PK (dB re 1 µPa) | rms SPL (dB re 1 µPa$^2$) | SELss (dB re 1 µPa$^2$·s) |
|---|---|---|---|
| **Channel 1 (bottom)** | | | |
| $L_{max}$ | 174.2 | 163.8 | 157.6 |
| $L_5$ | 171.7 | 162.3 | 156.4 |
| $L_{25}$ | 170.1 | 161.1 | 155.5 |
| $L_{50}$ | 168.4 | 158.8 | 153.0 |
| $L_{75}$ | 165.9 | 156.4 | 150.8 |
| $L_{95}$ | 158.5 | 150.3 | 144.9 |
| $L_{mean}$ | 168.5 | 159.3 | 153.6 |
| **Channel 2 (mid-water)** | | | |
| $L_{max}$ | 173.5 | 164.8 | 159.0 |
| $L_5$ | 171.5 | 163.2 | 157.7 |
| $L_{25}$ | 170.2 | 162.3 | 156.8 |
| $L_{50}$ | 168.6 | 160.1 | 154.5 |
| $L_{75}$ | 166.1 | 157.3 | 151.8 |
| $L_{95}$ | 160.9 | 152.4 | 147.4 |
| $L_{mean}$ | 168.7 | 160.5 | 155.0 |

## A.3.2.5. Station AP38-9000

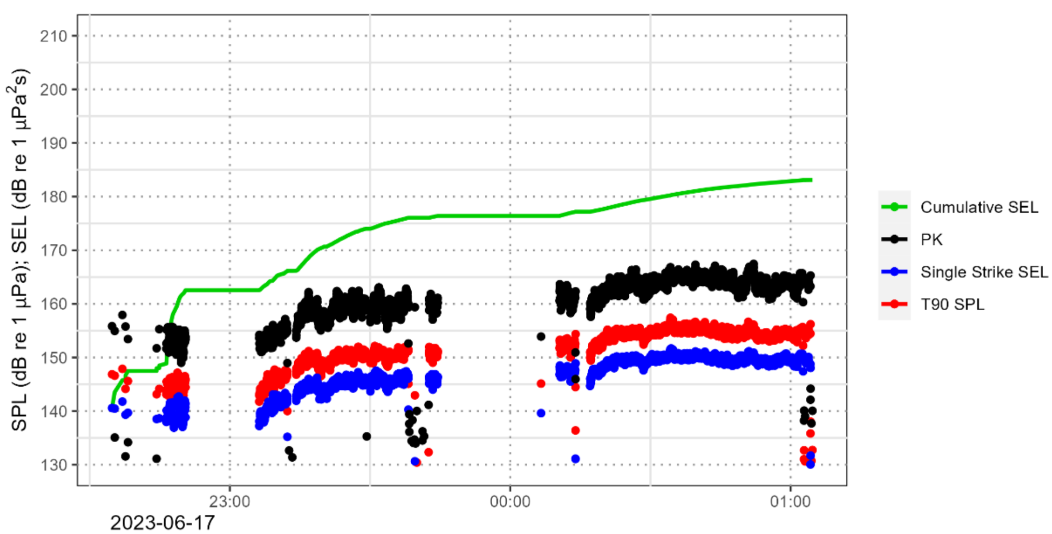


Figure A-33. Received levels for impact pile driving installation of AP-38 at monitoring station AP38-9000 for channel 2. Peak SPL (PK, black), rms SPL (T90 SPL, red), single strike SEL (blue) and cumulative SEL (green) versus time (UTC). For periods during which there is no pile driving the cSEL is necessarily displayed as a constant value over time.

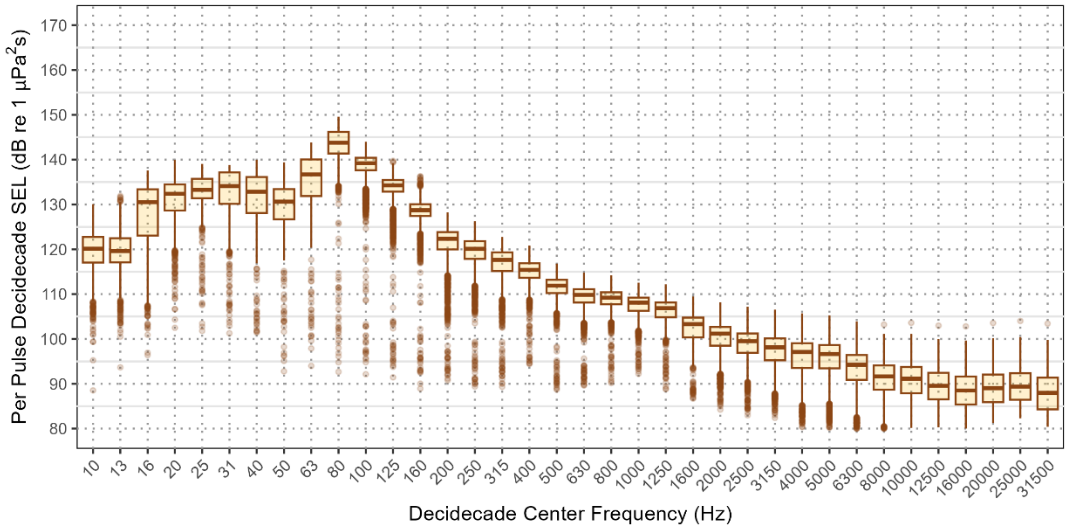


Figure A-34. Distribution of decidecade band level single strike SEL for pile driving installation of AP-38 at monitoring station AP38-9000 for channel 2. Beige bars indicate the first, second, and third quartiles (*25th*, *50th*, and *75th*) or as exceedances $L_{75}$, $L_{50}$, and $L_{25}$. Upper error bars indicate the maximum levels ($L_{max}$). Lower error bars indicate the 5th percentile or $L_{95}$.

Table A-24. Sound level statistics for the pile driving of AP-38 at monitoring station AP38-9000.

| Sound level statistic | PK (dB re 1 µPa) | rms SPL (dB re 1 µPa²) | SELss (dB re 1 µPa²·s) |
|---|---|---|---|
| **Channel 2 (mid-water)** | | | |
| $L_{max}$ | 167.5 | 157.4 | 151.7 |
| $L_5$ | 165.5 | 155.6 | 150.4 |
| $L_{25}$ | 163.9 | 154.5 | 149.6 |
| $L_{50}$ | 161.4 | 152.1 | 147.4 |
| $L_{75}$ | 158.8 | 150.0 | 145.2 |
| $L_{95}$ | 153.0 | 144.1 | 139.4 |
| $L_{mean}$ | 162.1 | 152.8 | 147.8 |

### A.3.3. Ranges to Acoustic Thresholds

Table A-25. Isopleth distances to NMFS physiological thresholds for impact driving installation of pile AP-38.

| Group | Injury: PK | | | | Injury: cSEL | | | |
|---|---|---|---|---|---|---|---|---|
| | Level (dB re 1µPa) | Predicted (m) | Measured (m) | Measured w/ attn. coeff. (m) | Level (dB re 1 $\mu Pa^2 \cdot s$) | Predicted (m) | Measured (m) | Measured w/ attn. coeff. (m) |
| LFC | 219 | 17 | 10 | 10 | 183 | 3,191 | 2500 | 3220 |
| MFC | 230 | 5 | 10 | 10 | 185 | 43 | 10 | 10 |
| HFC | 202 | 119 | 70 | 70 | 155 | 71 | 450 | 300 |
| PW | 218 | 19 | 10 | 10 | 185 | 153 | 90 | 10 |
| ST | 232 | 0 | 10 | 10 | 204 | 161 | 180 | 30 |
| AS | 206 | 78 | 40 | 40 | 187 | 6,894 | 5820 | 6250 |

Table A-26. Estimated isopleth distances for the NMFS behavioral thresholds for impact driving of pile AP-38.

| Group | Behavior: SPL | | | |
|---|---|---|---|---|
| | Level (dB re 1$\mu Pa^2$) | Predicted (m) | Measured (m) | Measured w/ attn. coeff. (m) |
| MM | 160 | 4,121 | 5,410 | 5,740 |
| ST | 175 | 1,400 | 620 | 550 |
| AS | 150 | 9,229 | 22,960 | 13,970 |

## A.3.4. Regression Analysis for Transmission Loss

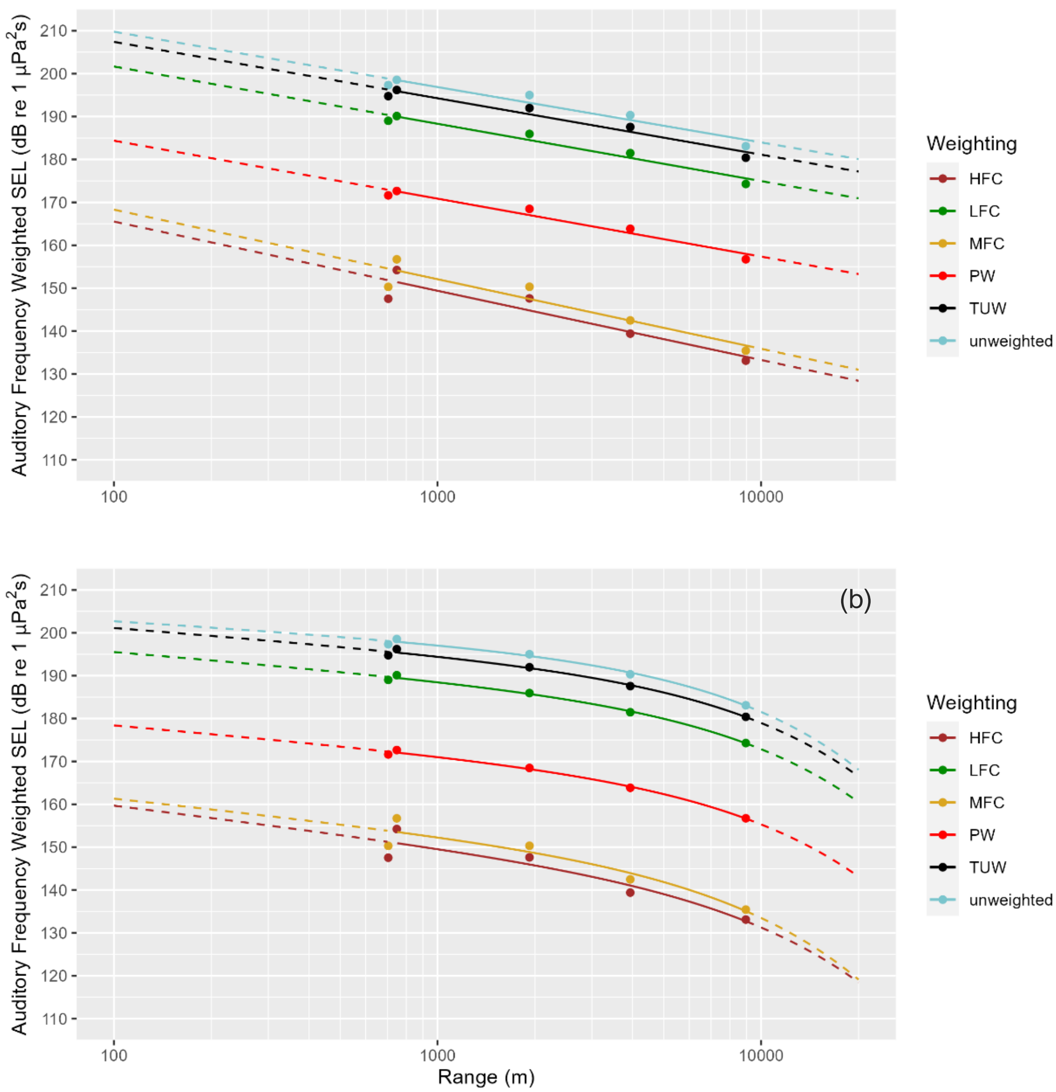


Figure A-35. Transmission loss determination based on regression analysis without (a) and with (b) intrinsic attenuation for the maximum received cumulative SEL (cSEL) at each recording station during installation of pile AP-38 on 17 Jun 2023.

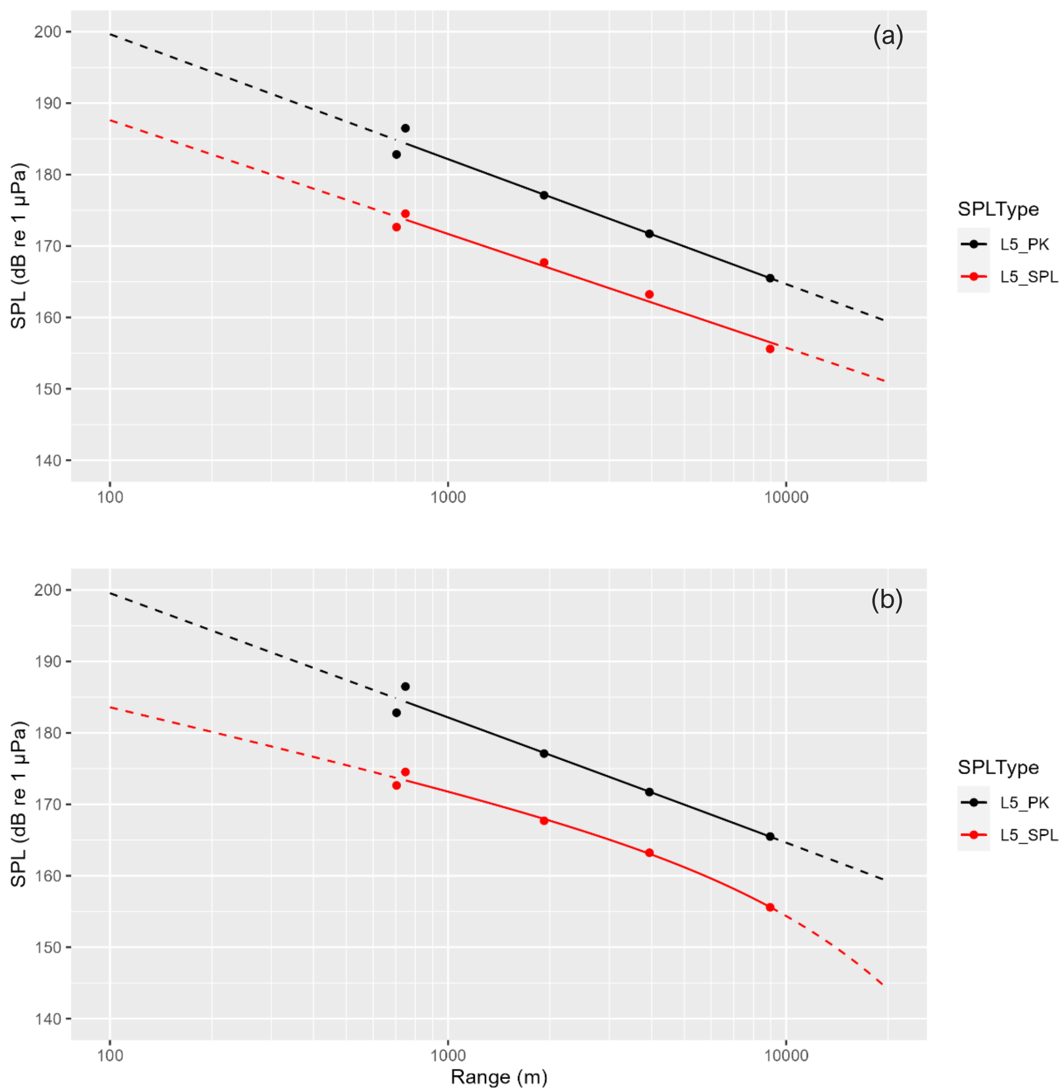


Figure A-36. Transmission loss determination based on regression analysis without (a) and with (b) intrinsic attenuation for $L_5$ PK and SPL maxima at each recording station during installation of pile AP-38 on 17 Jun 2023.

Table A-27. Regression analysis fitting coefficients for transmission loss with and without intrinsic attenuation for installation of pile AP-38 on 17 Jun 2023.

| Metric | A (dB/decade m) A*log(r) | A (dB/decade m) A*log(r) + αr/1000 | α (dB/ m) A*log(r) + αr/1000 |
|---|---|---|---|
| PK ($L_5$) (dB re 1 μPa) | -17.5 | -17.4 | -0.017 x $10^{-3}$ |
| rms SPL ($L_5$) (dB re 1 μPa$^2$) | -15.9 | -11.2 | -0.690 x $10^{-3}$ |
| cSEL (dB re 1 μPa$^2$·s) | -13.3 | -5.8 | -1.091 x $10^{-3}$ |
| cSEL, LF (dB re 1 μPa$^2$·s) | -14.0 | -7.4 | -0.960 x $10^{-3}$ |
| cSEL, MF (dB re 1 μPa$^2$·s) | -16.5 | -18.1 | 0.225 x $10^{-3}$ |
| cSEL, HF (dB re 1 μPa$^2$·s) | -16.6 | -19.6 | 0.438 x $10^{-3}$ |
| cSEL, PW (dB re 1 μPa$^2$·s) | -14.1 | -8.2 | -0.848 x $10^{-3}$ |
| cSEL, TU (dB re 1 μPa$^2$·s) | -13.7 | -6.9 | -0.989 x $10^{-3}$ |

## A.4. Foundation AV-39

Summary of measurements are shown in Table A-28.

### A.4.1. Summary of Measured Sound Levels

Table A-28. Summary of Autonomous Multichannel Acoustic Recorder (AMAR) locations and measured sound levels for pile AV-39. Computed PK and SPL levels are shown for the $L_{max}$.

| Location (nominal) | Recorder ID | Distance (m) | Water depth (m) | Channel | Impulses detected* (clipped) | PK (dB re 1 μPa) | SPL (dB re 1 μPa$^2$) | cSEL (dB re 1 μPa$^2$·s) |
|---|---|---|---|---|---|---|---|---|
| 750 | AMAR-863 | 761 | 45.0 | 1 | 3962 | 181.3 | 171.3 | 197.0 |
| | | | | 2 | 3968 | 182.8 | 171.8 | 197.8 |
| 750 @ 90° | AMAR-865 | 732 | 45.0 | 1 | 3973 | 184.3 | 173.7 | 198.7 |
| | | | | 2 | 3978 | 181.6 | 172.2 | 196.9 |
| 2000 | AMAR-855 | 1992 | 45.2 | 1 | 3275 | 176.3 | 165.3 | 191.6 |
| | | | | 2 | 2898 | 177.0 | 166.0 | 191.8 |
| 4000 | AMAR-860 | 3987 | 46.6 | 1 | 3645 | 170.4 | 160.2 | 185.9 |
| | | | | 2 | 3584 | 171.4 | 161.3 | 187.4 |
| 8000 | AMAR-603 | 8032 | 49.3 | 1 | 3916 | 164.7 | 154.9 | 181.3 |
| | | | | 2 | 3398 | 165.2 | 155.6 | 181.7 |

* Number of strikes produced (from hammer log): 4007

# A.4.2. Sound Levels per Station

## A.4.2.1. Station AV39-750

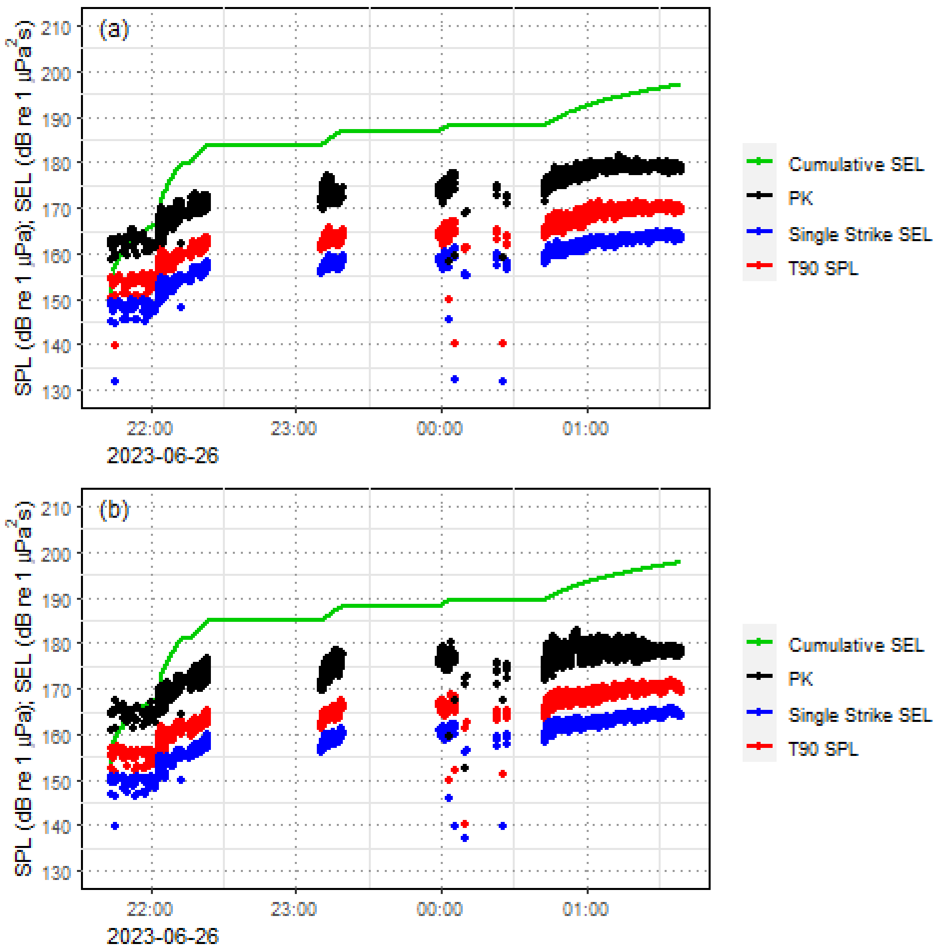


Figure A-37. Received levels for impact pile driving installation of AV-39 at monitoring station AV39-750 for channel 1 (a) and channel 2 (b). Peak SPL (PK, black), rms SPL (T90 SPL, red), single strike SEL (blue) and cumulative SEL (green) versus time (UTC). For periods during which there was no pile driving the cSEL is necessarily displayed as a constant value over time.

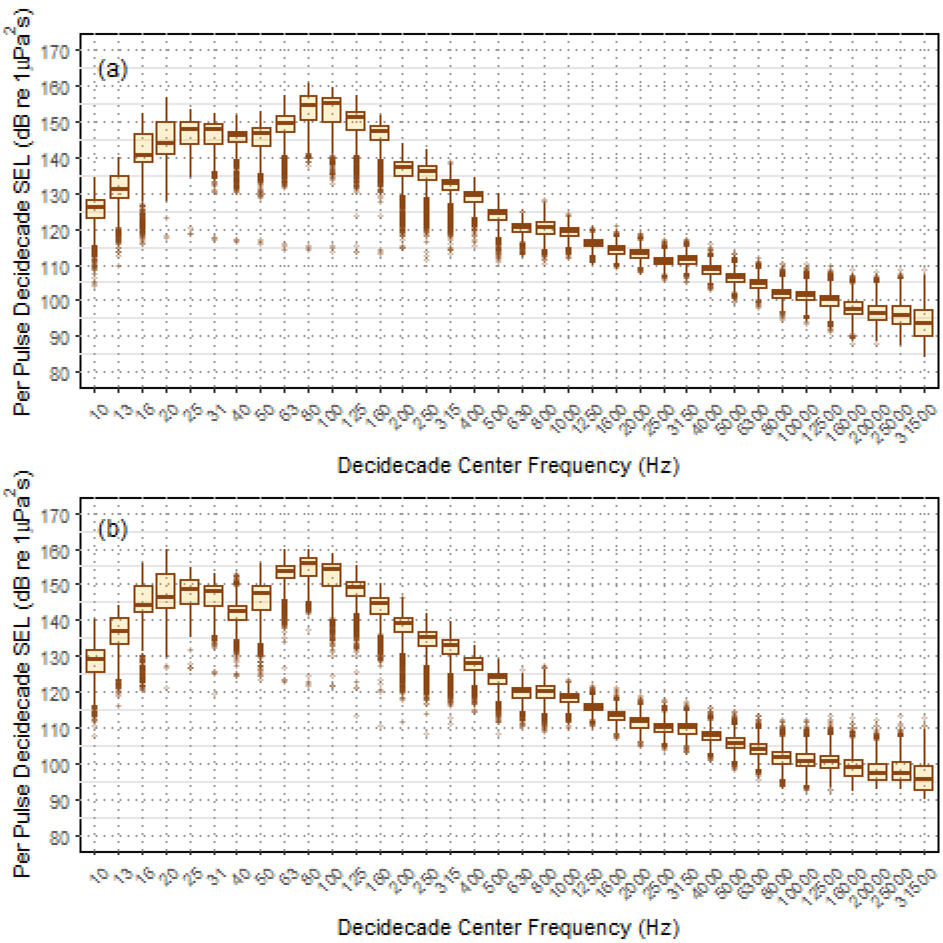


Figure A-38. Distribution of decidecade band level single strike SEL for pile driving installation of AV-39 at monitoring station AV39-750 for channel 1 (a) and channel 2 (b). Beige bars indicate the first, second, and third quartiles (*25th*, *50th*, and *75th*) or as exceedances $L_{75}$, $L_{50}$, and $L_{25}$. Upper error bars indicate the maximum levels ($L_{max}$). Lower error bars indicate the 5th percentile or $L_{95}$.

Table A-29. Received level statistics for pile driving installation of AV-39 at monitoring station AV39-750.

| Sound level statistic | PK (dB re 1 µPa) | rms SPL (dB re 1 µPa$^2$) | SELss (dB re 1 µPa$^2$·s) |
|---|---|---|---|
| **Channel 1 (bottom)** | | | |
| $L_{max}$ | 181.3 | 171.3 | 164.9 |
| $L_5$ | 179.4 | 170.3 | 163.9 |
| $L_{25}$ | 178.8 | 169.5 | 162.9 |
| $L_{50}$ | 176.6 | 166.8 | 161.0 |
| $L_{75}$ | 171.8 | 162.6 | 157.1 |
| $L_{95}$ | 166.9 | 157.7 | 152.5 |
| $L_{mean}$ | 176.6 | 167.3 | 161.1 |
| **Channel 2 (mid-water)** | | | |
| $L_{max}$ | 182.8 | 171.8 | 165.8 |
| $L_5$ | 180.3 | 170.6 | 164.8 |
| $L_{25}$ | 178.6 | 169.5 | 163.4 |
| $L_{50}$ | 177.5 | 167.7 | 161.9 |
| $L_{75}$ | 174.0 | 163.9 | 158.5 |
| $L_{95}$ | 168.5 | 159.3 | 153.7 |
| $L_{mean}$ | 177.2 | 167.6 | 161.8 |

## A.4.2.2. Station AV39-75090

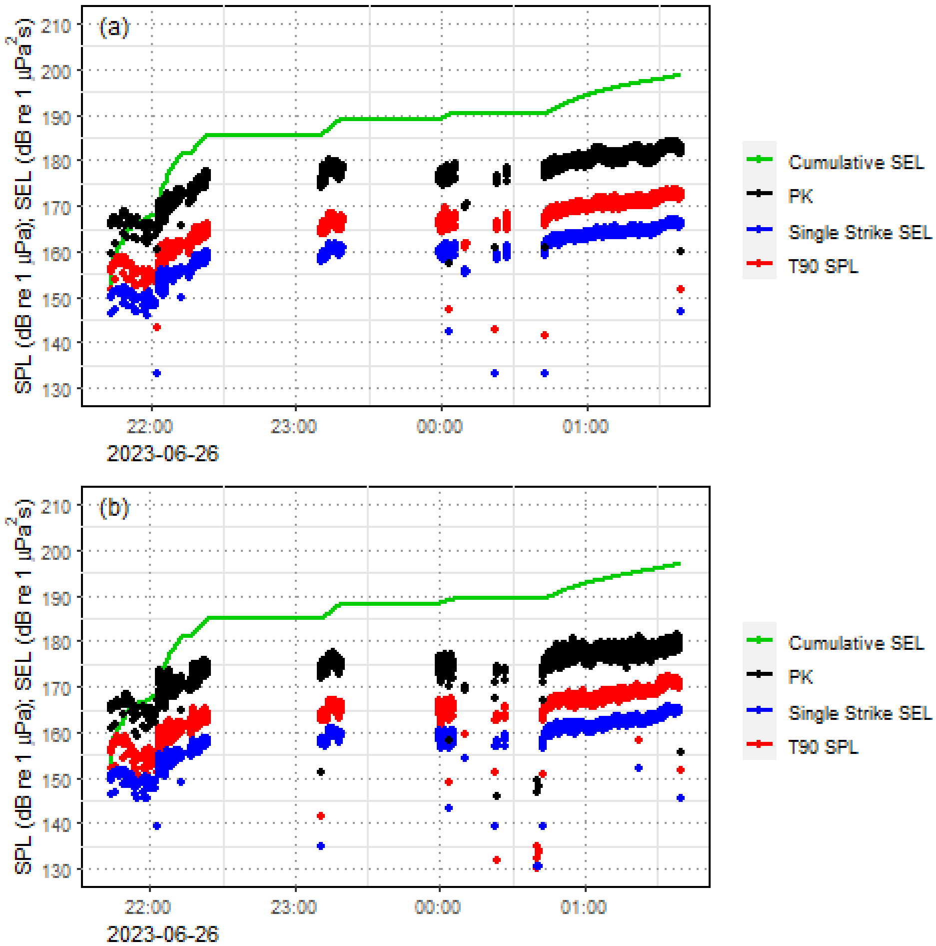


Figure A-39. Received levels for impact pile driving installation of AV-39 at monitoring station AV39-75090 for channel 1 (a) and channel 2 (b). Peak SPL (PK, black), rms SPL (T90 SPL, red), single strike SEL (blue) and cumulative SEL (green) versus time (UTC). For periods during which there was no pile driving the cSEL is necessarily displayed as a constant value over time.

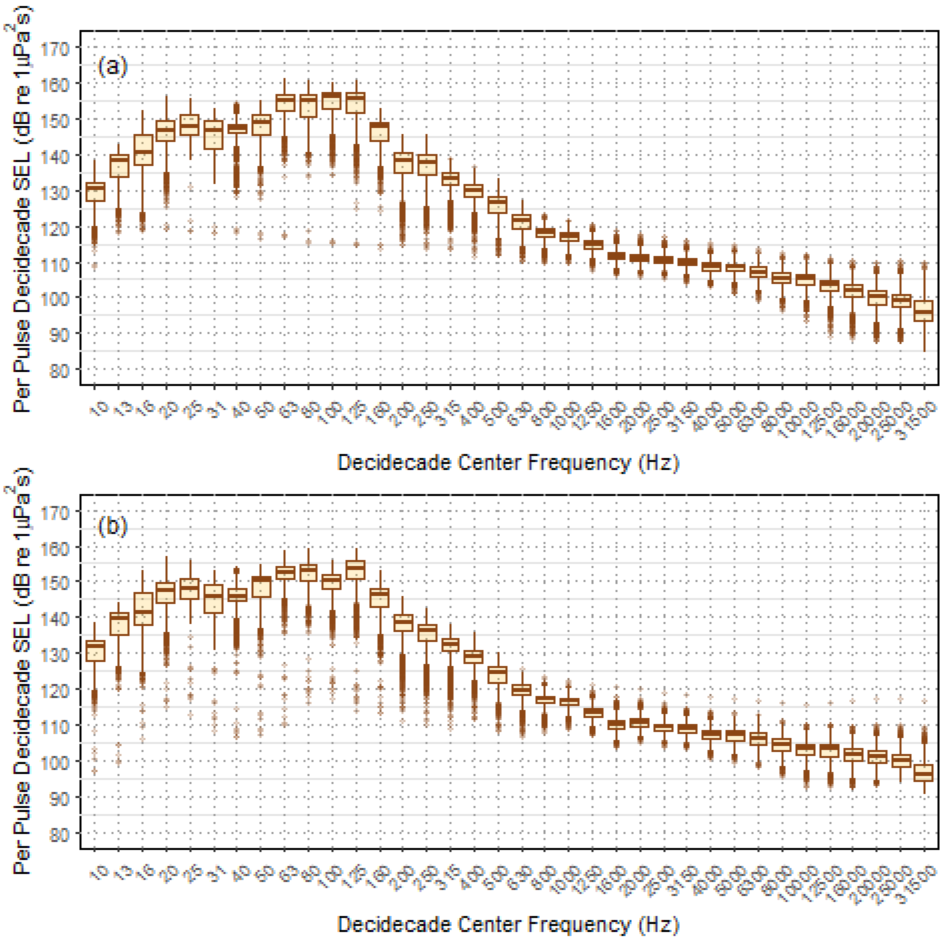


Figure A-40. Distribution of decidecade band level single strike SEL for pile driving installation of AP-38 at monitoring station AP38-75090 for channel 1 (a) and channel 2 (b). Beige bars indicate the first, second, and third quartiles (*25th*, *50th*, and *75th*) or as exceedances $L_{75}$, $L_{50}$, and $L_{25}$. Upper error bars indicate the maximum levels ($L_{max}$). Lower error bars indicate the 5th percentile or $L_{95}$.

Table A-30. Received level statistics for pile driving installation of AV-39 at monitoring station AV39-75090.

| Sound level statistic | PK (dB re 1 µPa) | rms SPL (dB re 1 µPa$^2$) | SELss (dB re 1 µPa$^2$·s) |
|---|---|---|---|
| **Channel 1 (bottom)** | | | |
| $L_{max}$ | 184.3 | 173.7 | 166.8 |
| $L_5$ | 182.8 | 172.4 | 165.9 |
| $L_{25}$ | 181.0 | 170.8 | 164.4 |
| $L_{50}$ | 179.5 | 169.3 | 162.9 |
| $L_{75}$ | 176.7 | 165.3 | 159.4 |
| $L_{95}$ | 169.9 | 159.7 | 154.2 |
| $L_{mean}$ | 179.6 | 169.1 | 162.7 |
| **Channel 2 (mid-water)** | | | |
| $L_{max}$ | 181.6 | 172.2 | 165.7 |
| $L_5$ | 179.4 | 170.7 | 164.5 |
| $L_{25}$ | 178.0 | 168.4 | 162.3 |
| $L_{50}$ | 176.4 | 166.7 | 160.7 |
| $L_{75}$ | 173.9 | 163.8 | 158.0 |
| $L_{95}$ | 169.0 | 159.0 | 153.3 |
| $L_{mean}$ | 176.5 | 167.0 | 160.9 |

### A.4.2.3. Station AV39-2000

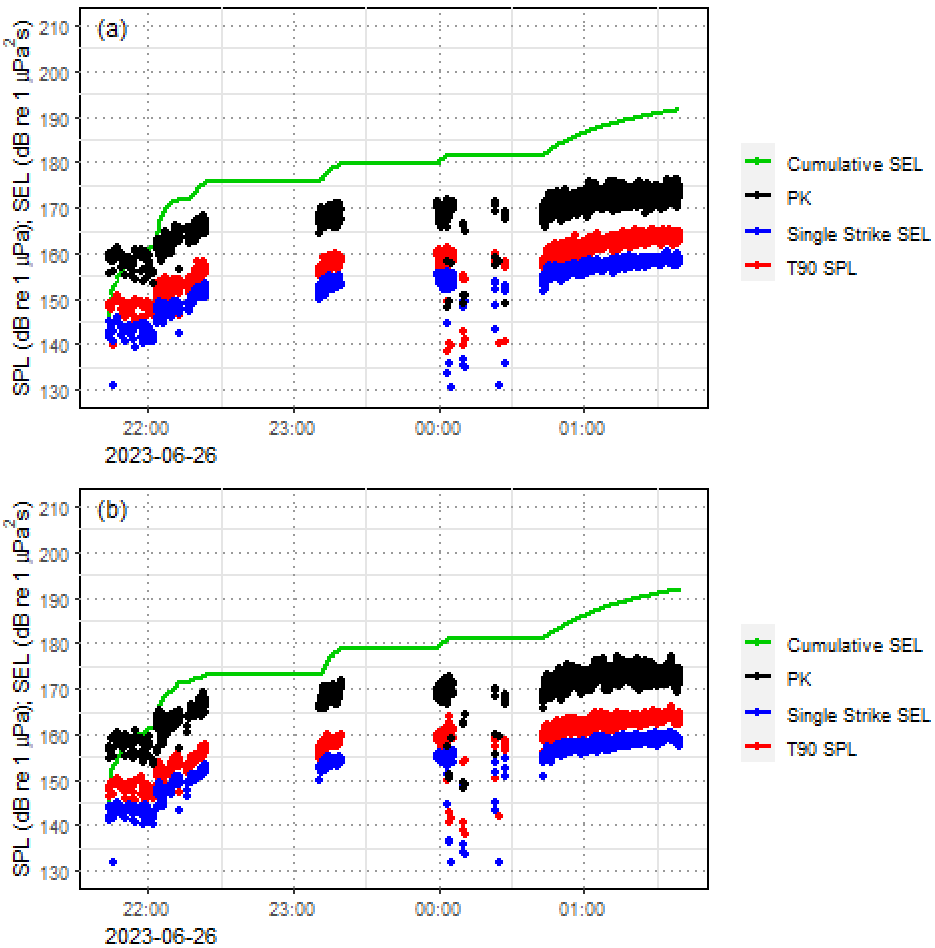


Figure A-41. Received levels for impact pile driving installation of AV-39 at monitoring station AV39-2000 for channel 1 (a) and channel 2 (b). Peak SPL (PK, black), rms SPL (T90 SPL, red), single strike SEL (blue) and cumulative SEL (green) versus time (UTC). For periods during which there was no pile driving the cSEL is necessarily displayed as a constant value over time.

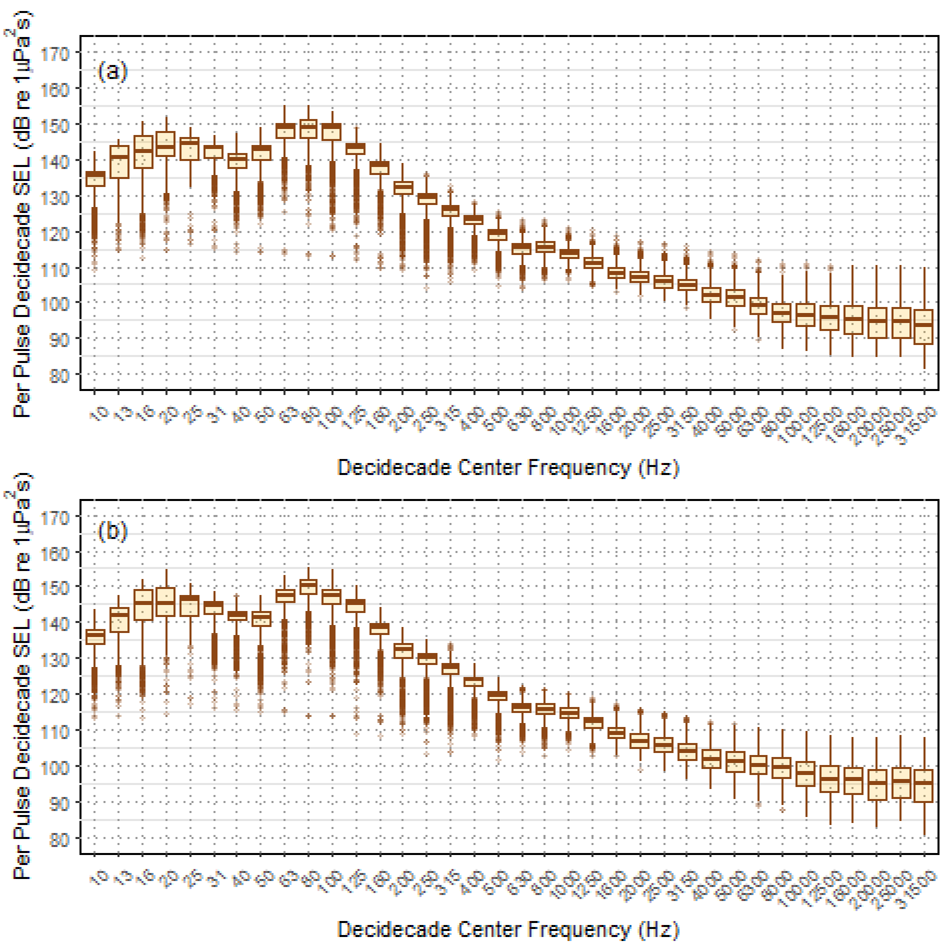


Figure A-42. Distribution of decidecade band level single strike SEL for pile driving installation of AV-39 at monitoring station AV39-2000 for channel 1 (a) and channel 2 (b). Beige bars indicate the first, second, and third quartiles (*25th*, *50th*, and *75th*) or as exceedances $L_{75}$, $L_{50}$, and $L_{25}$. Upper error bars indicate the maximum levels ($L_{max}$). Lower error bars indicate the 5th percentile or $L_{95}$.

Table A-31. Received level statistics for pile driving installation of AV-39 at monitoring station AV39-2000.

| Sound level statistic | PK (dB re 1 µPa) | rms SPL (dB re 1 µPa$^2$) | SELss (dB re 1 µPa$^2$·s) |
|---|---|---|---|
| **Channel 1 (bottom)** | | | |
| $L_{max}$ | 176.3 | 165.3 | 160.2 |
| $L_5$ | 174.3 | 164.0 | 158.8 |
| $L_{25}$ | 172.6 | 162.9 | 157.9 |
| $L_{50}$ | 171.2 | 161.2 | 156.7 |
| $L_{75}$ | 168.5 | 158.2 | 154.1 |
| $L_{95}$ | 161.2 | 151.8 | 147.4 |
| $L_{mean}$ | 171.2 | 161.2 | 156.4 |
| **Channel 2 (mid-water)** | | | |
| $L_{max}$ | 177.0 | 166.0 | 160.5 |
| $L_5$ | 175.0 | 164.2 | 159.5 |
| $L_{25}$ | 173.4 | 163.2 | 158.7 |
| $L_{50}$ | 172.0 | 162.0 | 157.4 |
| $L_{75}$ | 169.9 | 159.6 | 155.1 |
| $L_{95}$ | 161.4 | 151.5 | 147.4 |
| $L_{mean}$ | 172.0 | 161.8 | 157.2 |

## A.4.2.4. Station AV39-4000

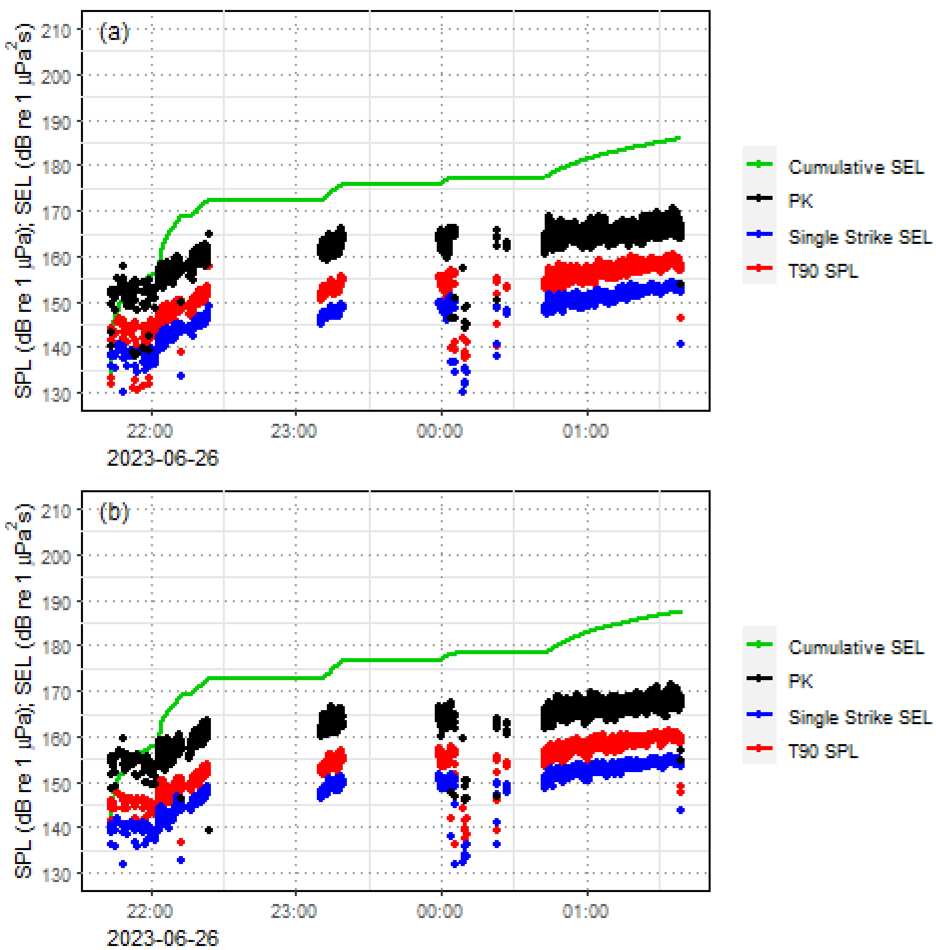


Figure A-43. Received levels for impact pile driving installation of AV-39 at monitoring station AV39-4000 for channel 1 (a) and channel 2 (b). Peak SPL (PK, black), rms SPL (T90 SPL, red), single strike SEL (blue) and cumulative SEL (green) versus time (UTC). For periods during which there is no pile driving the cSEL is necessarily displayed as a constant value over time.

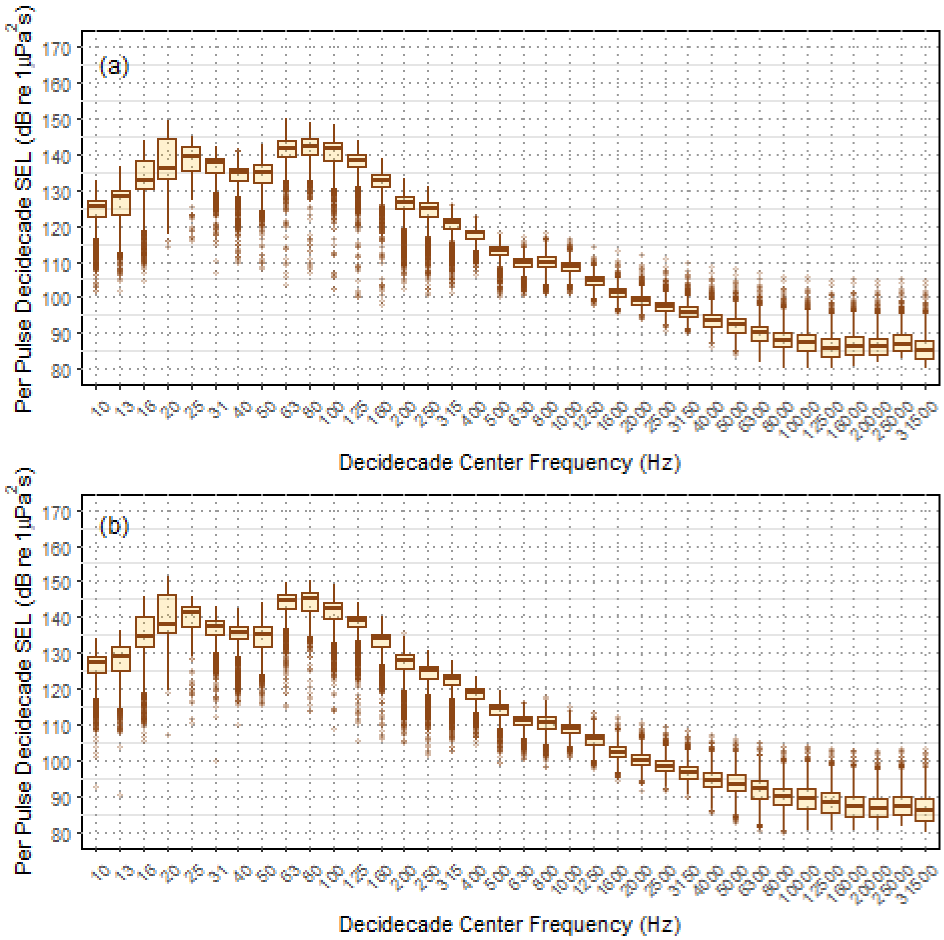


Figure A-44. Distribution of decidecade band level single strike SEL for pile driving installation of AV-39 at monitoring station AV39-4000 for channel 1 (a) and channel 2 (b). Beige bars indicate the first, second, and third quartiles (*25th*, *50th*, and *75th*) or as exceedances $L_{75}$, $L_{50}$, and $L_{25}$. Upper error bars indicate the maximum levels ($L_{max}$). Lower error bars indicate the 5th percentile or $L_{95}$.

Table A-32. Received level statistics for pile driving installation of AV-39 at monitoring station AV39-4000.

| Sound level statistic | PK (dB re 1 µPa) | rms SPL (dB re 1 µPa$^2$) | SELss (dB re 1 µPa$^2$·s) |
|---|---|---|---|
| **Channel 1 (bottom)** | | | |
| $L_{max}$ | 170.4 | 160.2 | 154.2 |
| $L_5$ | 167.8 | 158.9 | 153.3 |
| $L_{25}$ | 165.9 | 157.3 | 151.8 |
| $L_{50}$ | 164.4 | 155.8 | 150.3 |
| $L_{75}$ | 161.9 | 152.8 | 147.5 |
| $L_{95}$ | 155.6 | 146.9 | 142.0 |
| $L_{mean}$ | 164.5 | 155.8 | 150.3 |
| **Channel 2 (mid-water)** | | | |
| $L_{max}$ | 171.4 | 161.3 | 155.5 |
| $L_5$ | 168.6 | 160.1 | 154.6 |
| $L_{25}$ | 167.1 | 159.0 | 153.5 |
| $L_{50}$ | 165.9 | 157.3 | 152.1 |
| $L_{75}$ | 163.2 | 154.4 | 149.4 |
| $L_{95}$ | 155.8 | 147.3 | 142.6 |
| $L_{mean}$ | 165.7 | 157.3 | 151.9 |

### A.4.2.5. Station AV39-8000

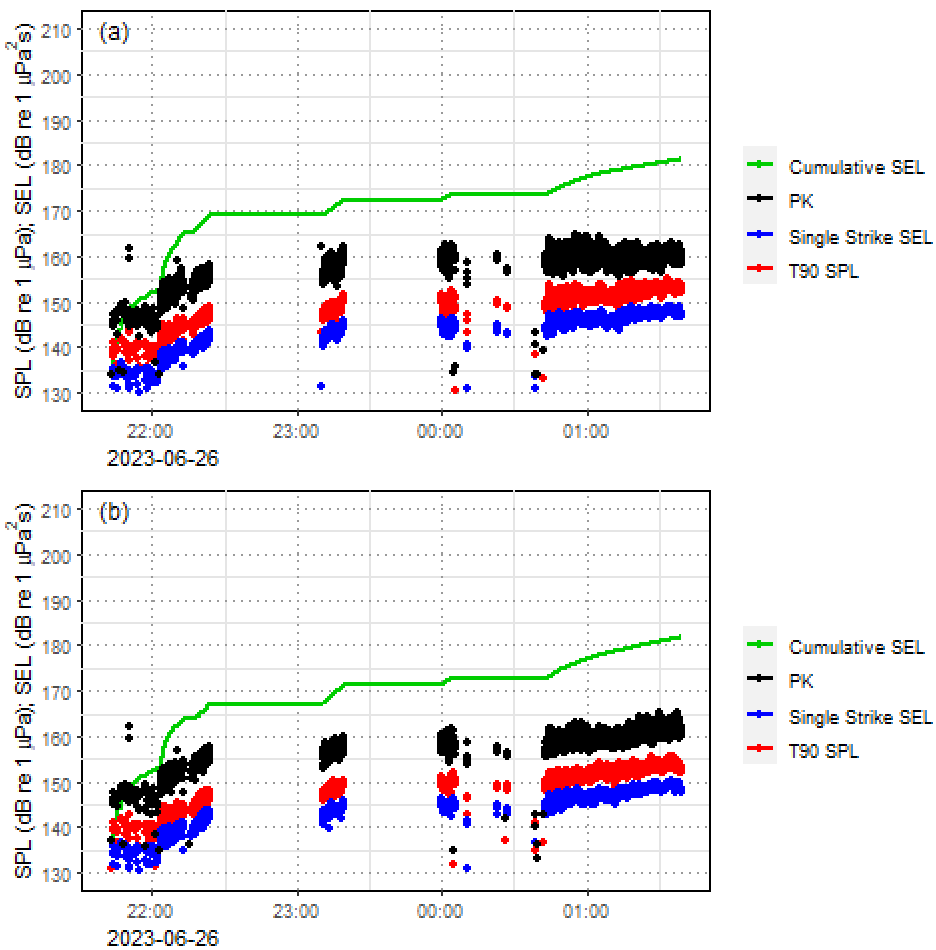


Figure A-45. Received levels for impact pile driving installation of AV-39 at monitoring station AV39-8000 for channel 1 (a) and channel 2 (b). Peak SPL (PK, black), rms SPL (T90 SPL, red), single strike SEL (blue) and cumulative SEL (green) versus time (UTC). For periods during which there is no pile driving the cSEL is necessarily displayed as a constant value over time.

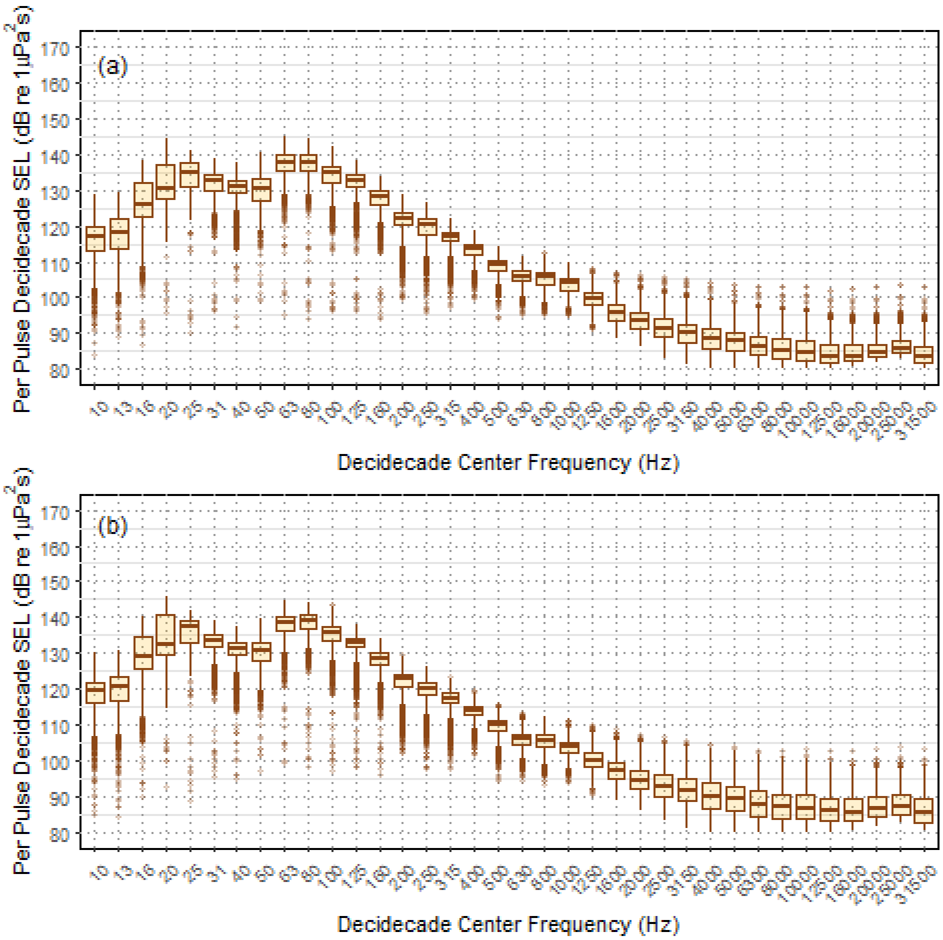


Figure A-46. Distribution of decidecade band level single strike SEL for pile driving installation of AV-39 at monitoring station AV39-8000 for channel 1 (a) and channel 2 (b). Beige bars indicate the first, second, and third quartiles (*25th*, *50th*, and *75th*) or as exceedances $L_{75}$, $L_{50}$, and $L_{25}$. Upper error bars indicate the maximum levels ($L_{max}$). Lower error bars indicate the 5th percentile or $L_{95}$.

Table A-33. Received level statistics for pile driving installation of AV-39 at monitoring station AV39-8000.

| Sound level statistic | PK (dB re 1 µPa) | rms SPL (dB re 1 µPa$^2$) | SELss (dB re 1 µPa$^2$·s) |
|---|---|---|---|
| **Channel 1 (bottom)** | | | |
| $L_{max}$ | 164.7 | 154.9 | 149.0 |
| $L_5$ | 162.2 | 153.4 | 148.1 |
| $L_{25}$ | 160.4 | 152.3 | 146.9 |
| $L_{50}$ | 159.1 | 150.9 | 145.6 |
| $L_{75}$ | 156.6 | 147.9 | 142.8 |
| $L_{95}$ | 151.2 | 142.9 | 137.9 |
| $L_{mean}$ | 159.1 | 150.7 | 145.4 |
| **Channel 2 (mid-water)** | | | |
| $L_{max}$ | 165.2 | 155.6 | 150.2 |
| $L_5$ | 162.5 | 154.2 | 149.2 |
| $L_{25}$ | 160.6 | 152.7 | 147.9 |
| $L_{50}$ | 159.1 | 151.4 | 146.5 |
| $L_{75}$ | 157.1 | 148.8 | 144.1 |
| $L_{95}$ | 150.5 | 142.3 | 138.1 |
| $L_{mean}$ | 159.3 | 151.3 | 146.4 |

## A.4.3. Ranges to Acoustic Thresholds

Table A-34. Isopleth distances to NMFS physiological thresholds for impact driving installation of pile AV-39.

| Group | Injury: PK | | | | Injury: cSEL | | | |
|---|---|---|---|---|---|---|---|---|
| | Level (dB re 1µPa) | Predicted (m) | Measured (m) | Measured w/ attn. coeff. (m) | Level (dB re 1 µPa$^2$·s) | Predicted (m) | Measured (m) | Measured w/ attn. coeff. (m) |
| LFC | 219 | 17 | 10 | 10 | 183 | 3,191 | 1,830 | 1,850 |
| MFC | 230 | 5 | 10 | 10 | 185 | 43 | 10 | 10 |
| HFC | 202 | 119 | 60 | 40 | 155 | 71 | 110 | 160 |
| PW | 218 | 19 | 10 | 10 | 185 | 153 | 140 | 140 |
| ST | 232 | 0 | 10 | 10 | 204 | 161 | 240 | 230 |
| AS | 206 | 78 | 40 | 20 | 187 | 6,894 | 3,950 | 4,130 |

Table A-35. Estimated isopleth distances for the NMFS behavioral thresholds for impact driving of pile AV-39.

| Group | Behavior: SPL | | | |
|---|---|---|---|---|
| | Level (dB re 1µPa$^2$) | Predicted (m) | Measured (m) | Measured w/ attn. coeff. (m) |
| MM | 160 | 4,121 | 3,710 | 3,790 |
| ST | 175 | 1,400 | 460 | 440 |
| AS | 150 | 9,229 | 14,950 | 13,410 |

## A.4.4. Regression Analysis for Transmission Loss

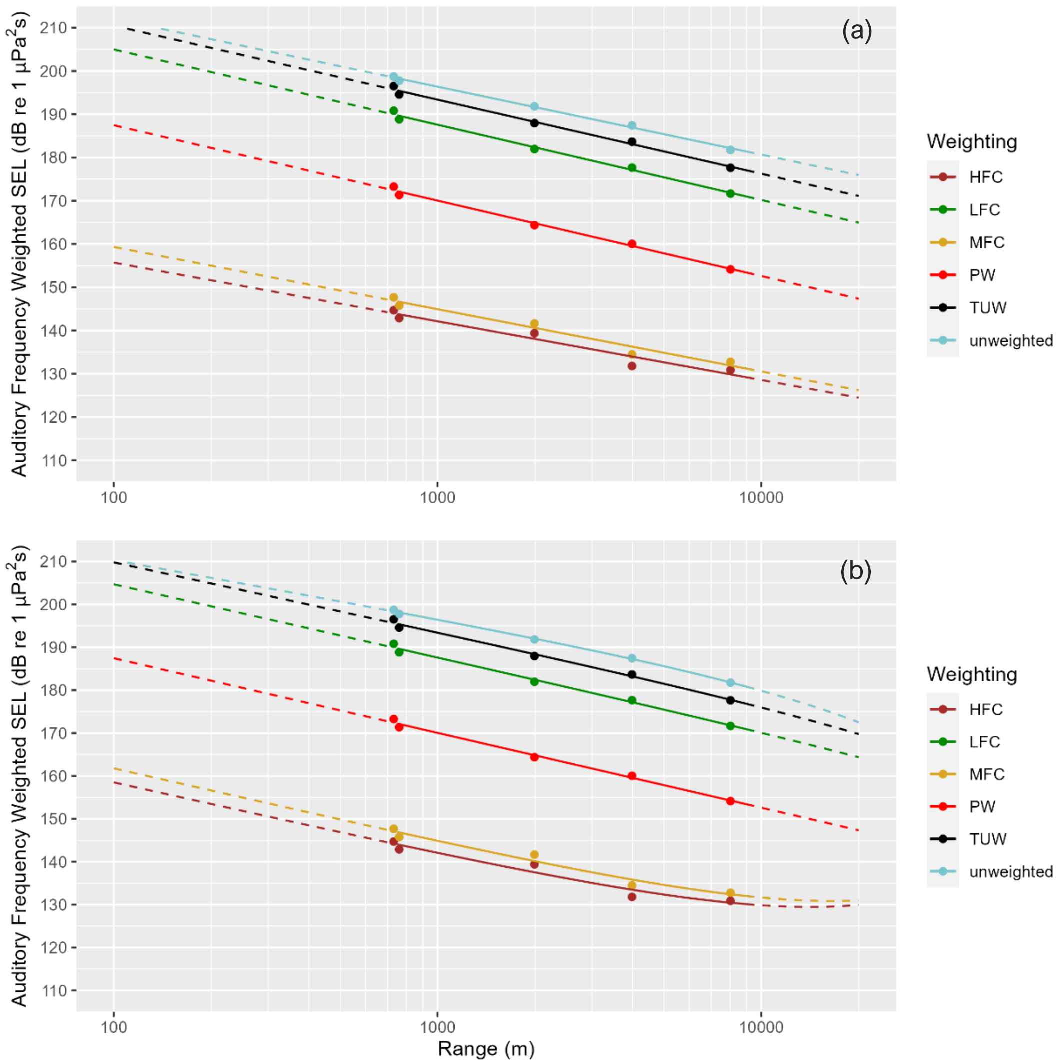


Figure A-47. Transmission loss determination based on regression analysis without (a) and with (b) intrinsic attenuation for the maximum received cumulative SEL (cSEL) at each recording station during installation of pile AV-39 on 26 Jun 2023.

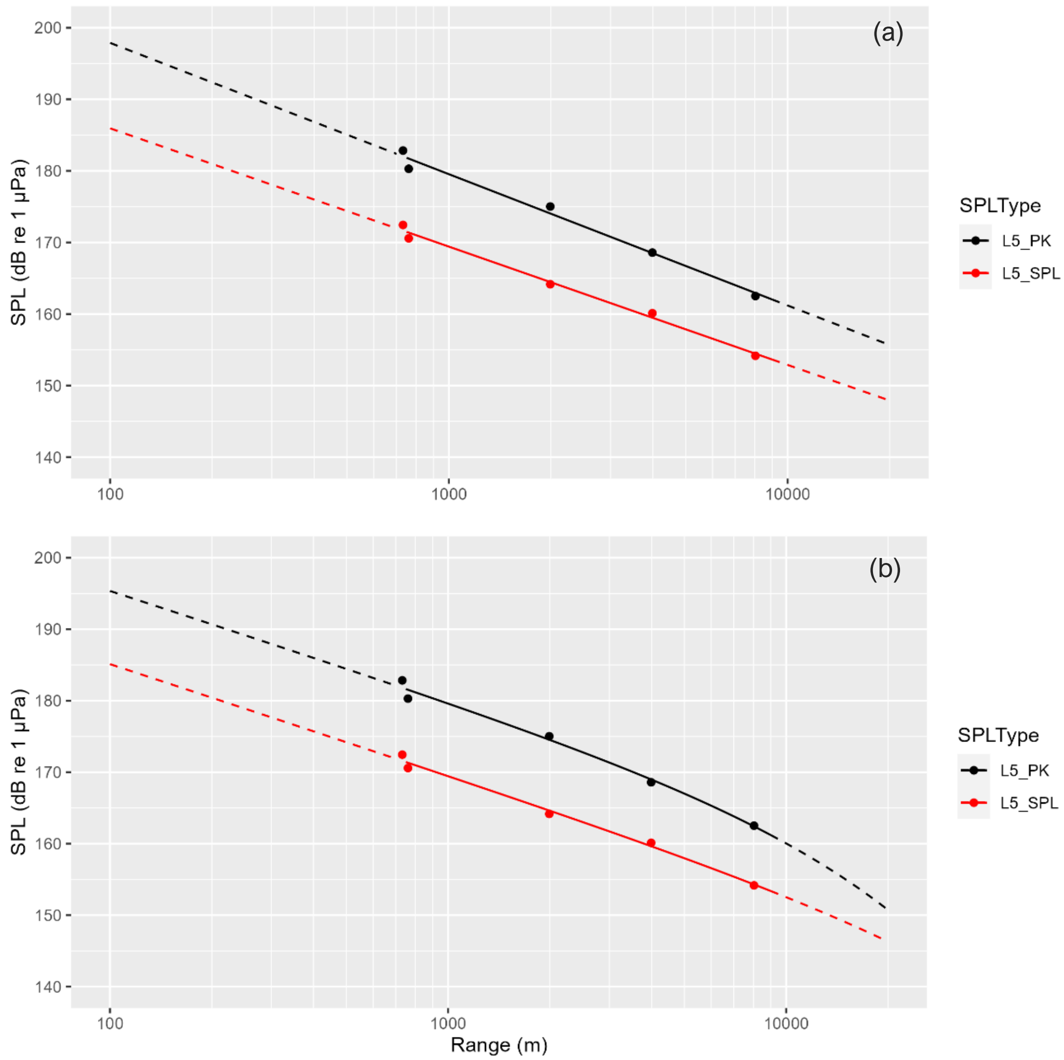


Figure A-48. Transmission loss determination based on regression analysis without (a) and with (b) intrinsic attenuation for $L_5$ PK and SPL maxima at each recording station during installation of pile AV-39 on 26 Jun 2023.

Table A-36. Regression analysis fitting coefficients for transmission loss with and without intrinsic attenuation for installation of pile AV-39 on 26 Jun 2023.

| Metric | A (dB/decade m) A*log(r) | A (dB/decade m) A*log(r) + αr/1000 | α (dB/ m) A*log(r) + αr/1000 |
|---|---|---|---|
| PK ($L_5$) (dB re 1 μPa) | -18.3 | -15.3 | $-0.469 \times 10^{-3}$ |
| rms SPL ($L_5$) (dB re 1 μPa$^2$) | -16.5 | -15.5 | $-0.154 \times 10^{-3}$ |
| cSEL (dB re 1 μPa$^2$·s) | -15.7 | -13.6 | $-0.326 \times 10^{-3}$ |
| cSEL, LF (dB re 1 μPa$^2$·s) | -17.4 | -17.0 | $-0.056 \times 10^{-3}$ |
| cSEL, MF (dB re 1 μPa$^2$·s) | -14.4 | -17.3 | $0.453 \times 10^{-3}$ [a] |
| cSEL, HF (dB re 1 μPa$^2$·s) | -13.6 | -16.9 | $0.519 \times 10^{-3}$ [a] |
| cSEL, PW (dB re 1 μPa$^2$·s) | -17.4 | -17.4 | $-0.004 \times 10^{-3}$ |
| cSEL, TU (dB re 1 μPa$^2$·s) | -17.1 | -16.3 | $-0.129 \times 10^{-3}$ |

[a] Positive attenuation coefficients could indicate ambient noise contamination and may not be valid.

## A.5. Foundation AR-39

Summary of measurements are shown in Table A-37. Channel 1 (bottom hydrophone) at station AR39-750 was not functioning properly and was excluded from the analysis. One of the base plates to which the AMARs were attached ( Appendix E.1) became unavailable prior to the pile driving of AR-39. Therefore, a station was placed at a nominal distance of 6000 m, between 4000 and 8000 m.

## A.5.1. Summary of Measured Sound Levels

Table A-37. Summary of Autonomous Multichannel Acoustic Recorder (AMAR) locations and measured sound levels for pile AR-39. Computed PK and SPL levels are shown for the $L_{max}$.

| Location (nominal) | Recorder ID | Distance (m) | Water depth (m) | Channel | Impulses Detected* (clipped) | PK (dB re 1 µPa) | SPL (dB re 1 µPa²) | cSEL (dB re 1 µPa²·s) |
|---|---|---|---|---|---|---|---|---|
| 750 | AMAR-863 | 752 | 43.9 | | | | | |
| | | | | 2 | 3908 | 183.8 | 173.4 | 197.5 |
| 750 @ 90° | AMAR-865 | 773 | 43.9 | 1 | 3909 | 182.4 | 172.0 | 196.4 |
| | | | | 2 | 3914 | 184.3 | 172.4 | 197.1 |
| 2000 | AMAR-855 | 1931 | 42.1 | 1 | 4139 | 176.7 | 165.4 | 191.7 |
| | | | | 2 | 4112 | 178.1 | 167.2 | 192.8 |
| 6000 | AMAR-864 | 5964 | 47.6 | 1 | 3900 | 168.0 | 159.3 | 184.0 |
| | | | | 2 | 3897 | 168.1 | 159.1 | 184.9 |

* Number of strikes produced (from hammer log): 3895

## A.5.2. Sound Levels per Station

### A.5.2.1. Station AR39-750

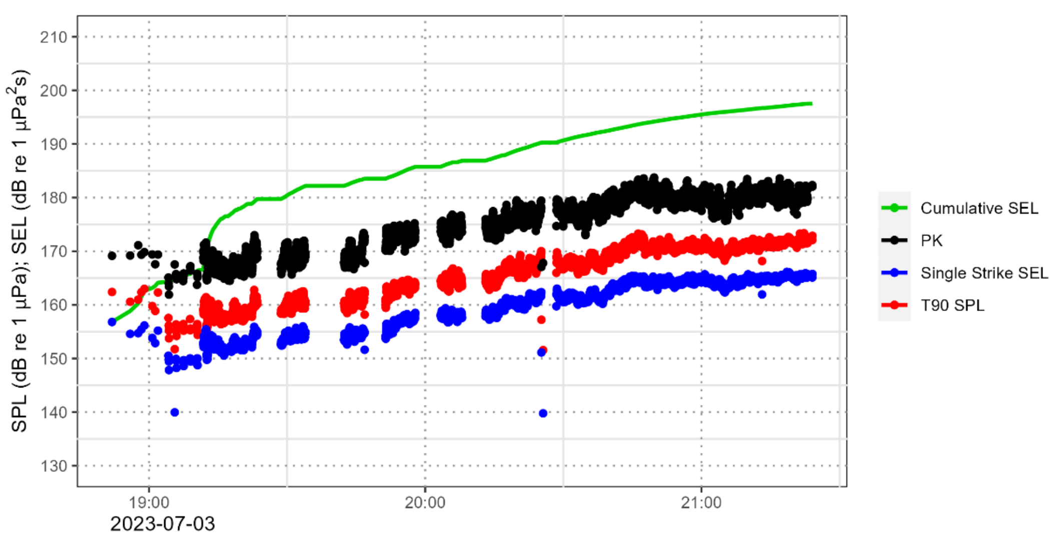


Figure A-49. Received levels for impact pile driving installation of AR-39 at monitoring station AR39-750 for channel 2. Peak SPL (PK, black), rms SPL (T90 SPL, red), single strike SEL (blue) and cumulative SEL (green) versus time (UTC). For periods during which there is no pile driving the cSEL is necessarily displayed as a constant value over time.

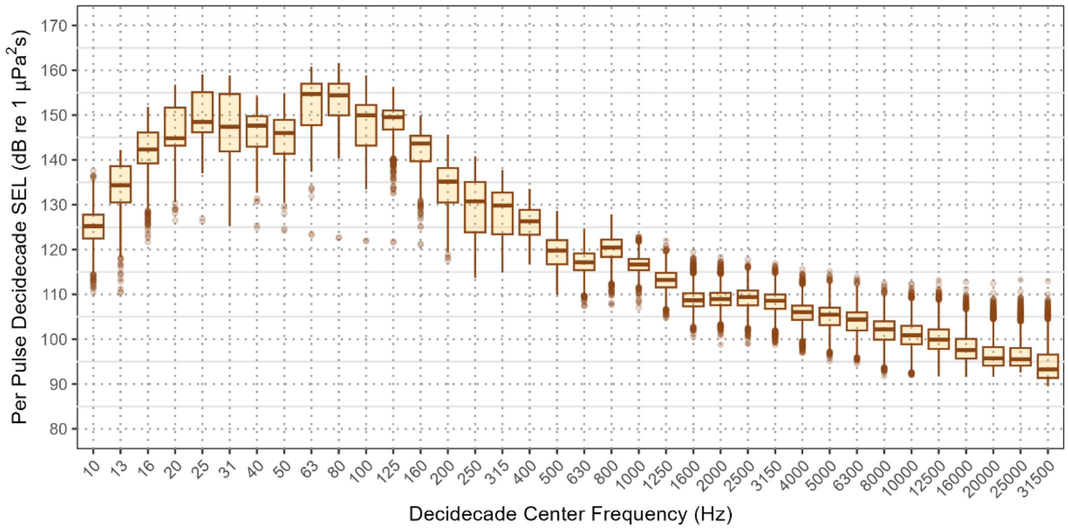


Figure A-50. Distribution of decidecade band level single strike SEL for pile driving installation of AR-39 at monitoring station AR39-750 for channel 2. Beige bars indicate the first, second, and third quartiles (*25th*, *50th*, and *75th*) or as exceedances $L_{75}$, $L_{50}$, and $L_{25}$. Upper error bars indicate the maximum levels ($L_{max}$). Lower error bars indicate the 5th percentile or $L_{95}$.

Table A-38. Received level statistics for pile driving installation of AR-39 at monitoring station AR39-750.

| Sound level statistic | PK (dB re 1 µPa) | rms SPL (dB re 1 µPa$^2$) | SELss (dB re 1 µPa$^2$·s) |
|---|---|---|---|
| **Channel 2 (mid-water)** | | | |
| $L_{max}$ | 183.8 | 173.4 | 166.2 |
| $L_5$ | 181.6 | 171.8 | 165.2 |
| $L_{25}$ | 179.5 | 170.5 | 164.1 |
| $L_{50}$ | 176.6 | 167.3 | 160.9 |
| $L_{75}$ | 171.6 | 161.9 | 155.4 |
| $L_{95}$ | 167.0 | 157.9 | 152.3 |
| $L_{mean}$ | 177.5 | 168.1 | 161.6 |

## A.5.2.2. Station AR39-75090

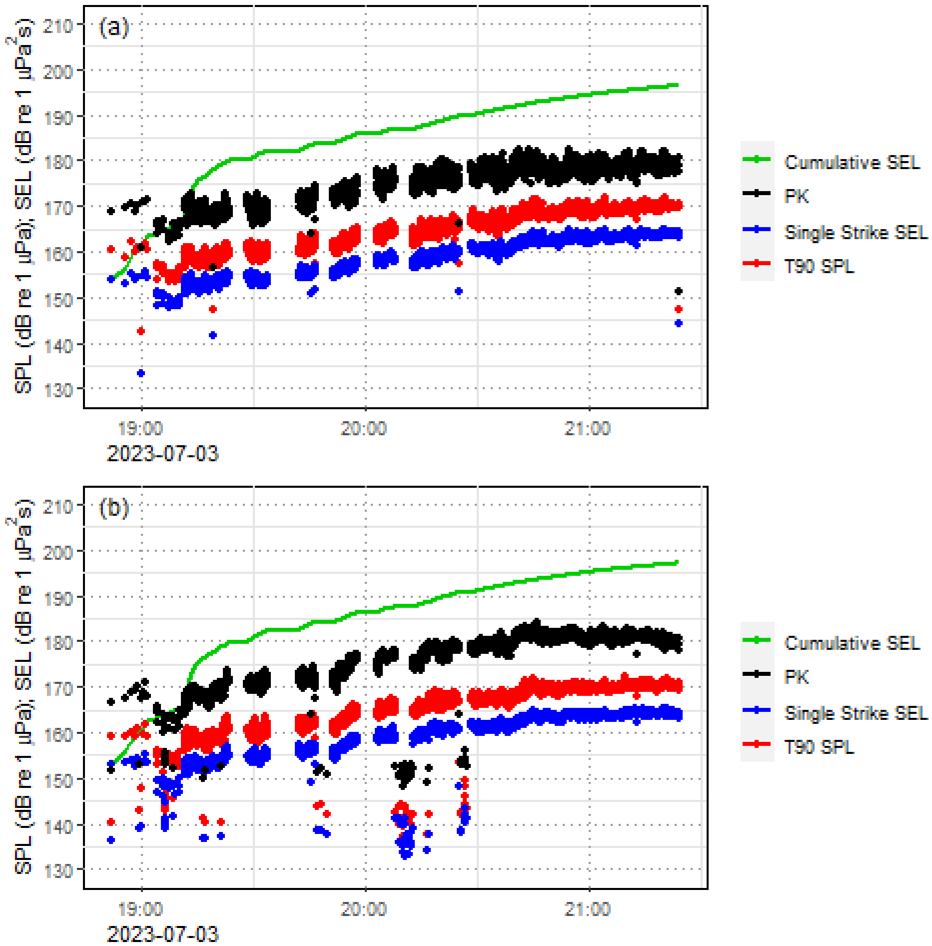


Figure A-51. Received levels for impact pile driving installation of AR-39 at monitoring station AR39-75090, for channel 1 (a) and channel 2 (b). Peak SPL (PK, black), rms SPL (T90 SPL, red), single strike SEL (blue) and cumulative SEL (green) versus time (UTC). For periods during which there is no pile driving the cSEL is necessarily displayed as a constant value over time.

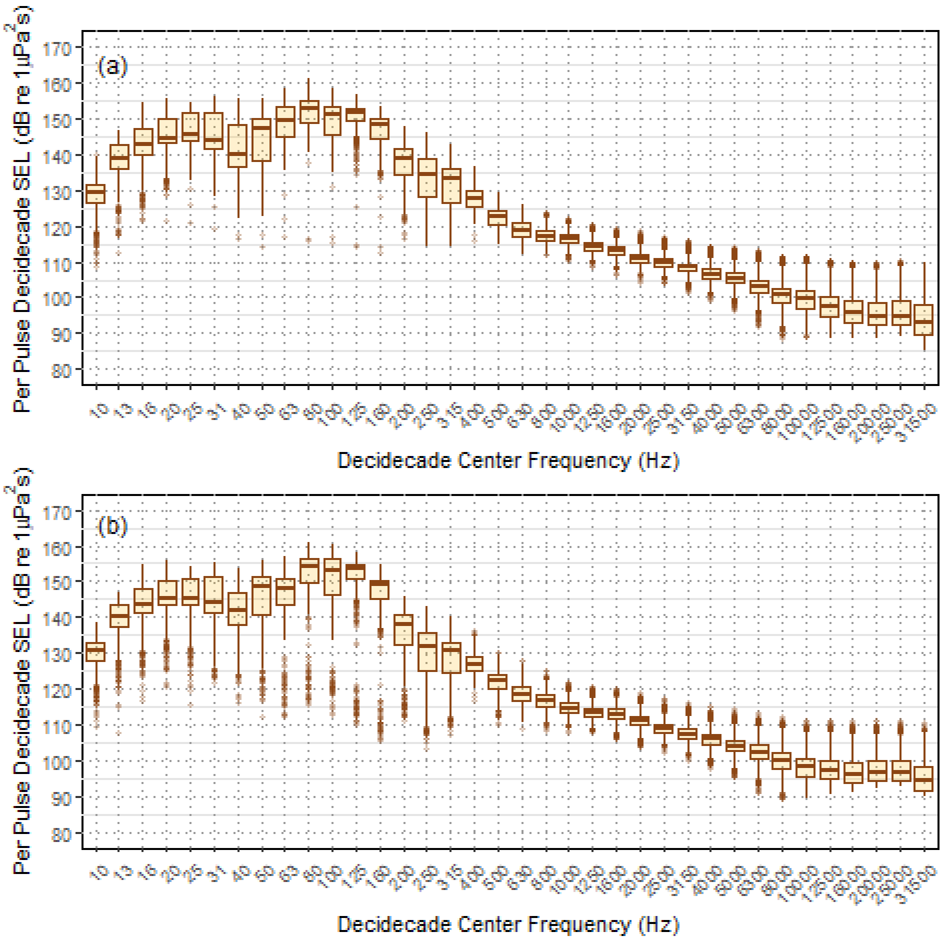


Figure A-52. Distribution of decidecade band level single strike SEL for pile driving installation of AR-39 at monitoring station AR39-75090 for channel 1 (a) and channel 2 (b). Beige bars indicate the first, second, and third quartiles (*25th*, *50th*, and *75th*) or as exceedances $L_{75}$, $L_{50}$, and $L_{25}$. Upper error bars indicate the maximum levels ($L_{max}$). Lower error bars indicate the 5th percentile or $L_{95}$.

Table A-39. Received level statistics for pile driving installation of AR-39 at monitoring station AR39-75090.

| Sound level statistic | PK (dB re 1 µPa) | rms SPL (dB re 1 µPa$^2$) | SELss (dB re 1 µPa$^2$·s) |
|---|---|---|---|
| **Channel 1 (bottom)** | | | |
| $L_{max}$ | 182.4 | 172.0 | 165.0 |
| $L_5$ | 180.2 | 170.1 | 163.9 |
| $L_{25}$ | 178.4 | 168.6 | 162.7 |
| $L_{50}$ | 176.7 | 165.6 | 159.7 |
| $L_{75}$ | 171.9 | 161.4 | 155.5 |
| $L_{95}$ | 167.9 | 158.2 | 152.7 |
| $L_{mean}$ | 176.7 | 166.5 | 160.5 |
| **Channel 2 (mid-water)** | | | |
| $L_{max}$ | 184.3 | 172.4 | 165.2 |
| $L_5$ | 182.0 | 170.5 | 164.4 |
| $L_{25}$ | 180.7 | 169.5 | 163.5 |
| $L_{50}$ | 178.6 | 167.0 | 160.8 |
| $L_{75}$ | 172.7 | 162.2 | 156.3 |
| $L_{95}$ | 167.8 | 158.2 | 152.7 |
| $L_{mean}$ | 178.6 | 167.3 | 161.2 |

### A.5.2.3. Station AR39-2000

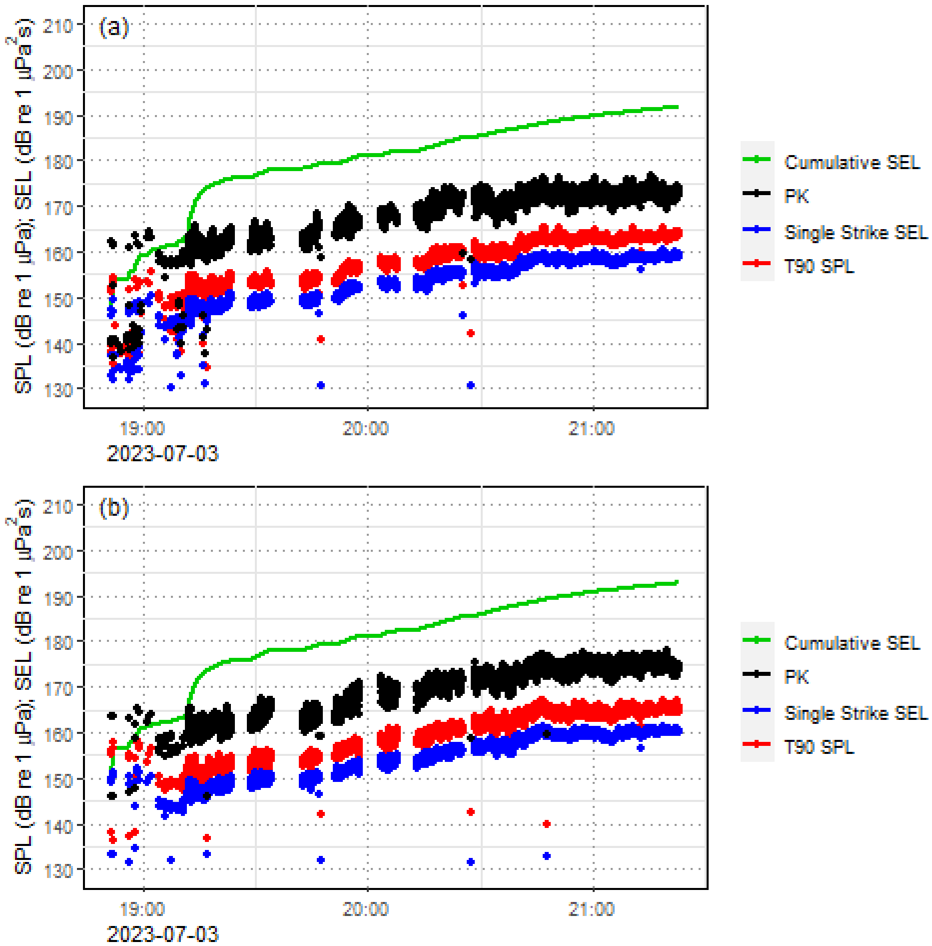


Figure A-53. Received levels for impact pile driving installation of AR-39 at monitoring station AR39-2000 for channel 1 (a) and channel 2 (b). Peak SPL (PK, black), rms SPL (T90 SPL, red), single strike SEL (blue) and cumulative SEL (green) versus time (UTC). For periods during which there was no pile driving the cSEL is necessarily displayed as a constant value over time.

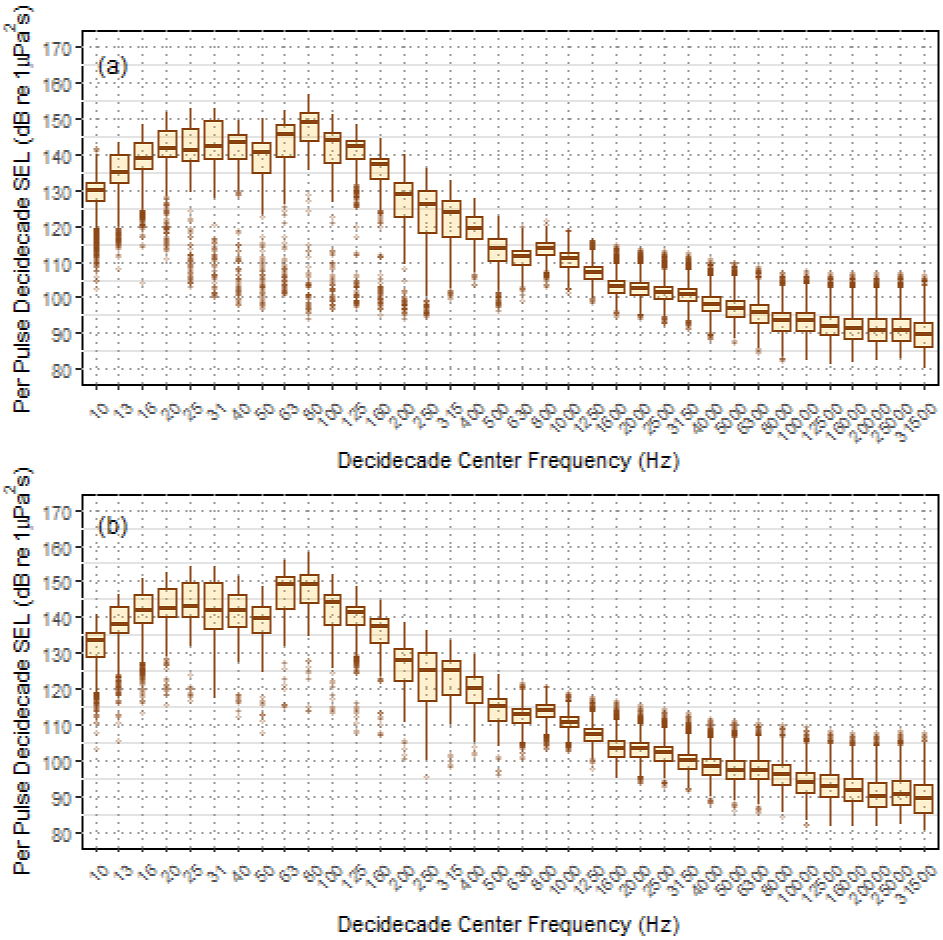


Figure A-54. Received levels for impact pile driving installation of AR-39 at monitoring station AR39-2000 for channel 1 (a) and channel 2 (b). Beige bars indicate the first, second, and third quartiles (*25th*, *50th*, and *75th*) or as exceedances $L_{75}$, $L_{50}$, and $L_{25}$. Upper error bars indicate the maximum levels ($L_{max}$). Lower error bars indicate the 5th percentile or $L_{95}$.

Table A-40. Received level statistics for pile driving installation of AR-39 at monitoring station AR39-2000.

| Sound level statistic | PK (dB re 1 µPa) | rms SPL (dB re 1 µPa$^2$) | SELss (dB re 1 µPa$^2$·s) |
|---|---|---|---|
| **Channel 1 (bottom)** | | | |
| $L_{max}$ | 176.7 | 165.4 | 160.4 |
| $L_5$ | 174.0 | 163.7 | 159.1 |
| $L_{25}$ | 172.2 | 162.4 | 158.0 |
| $L_{50}$ | 169.6 | 159.1 | 154.8 |
| $L_{75}$ | 163.9 | 153.9 | 149.7 |
| $L_{95}$ | 160.4 | 151.3 | 147.2 |
| $L_{mean}$ | 170.2 | 160.0 | 155.5 |
| **Channel 2 (mid-water)** | | | |
| $L_{max}$ | 178.1 | 167.2 | 161.3 |
| $L_5$ | 175.7 | 165.5 | 160.4 |
| $L_{25}$ | 173.7 | 164.0 | 159.3 |
| $L_{50}$ | 170.4 | 160.4 | 155.7 |
| $L_{75}$ | 164.3 | 154.6 | 150.1 |
| $L_{95}$ | 160.5 | 150.8 | 146.6 |
| $L_{mean}$ | 171.6 | 161.6 | 156.7 |

### A.5.2.4. Station AR39-6000

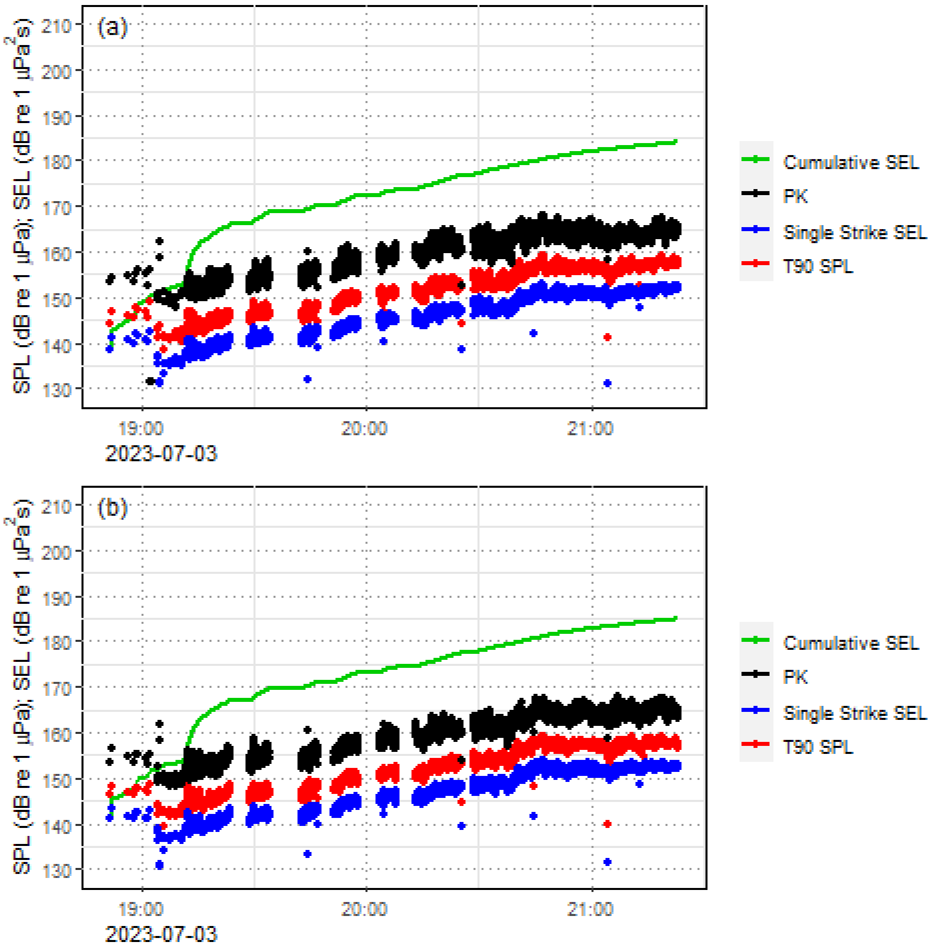


Figure A-55. Received levels for impact pile driving installation of AR-39 at monitoring station AR39-6000 for channel 1 (a) and channel 2 (b). Peak SPL (PK, black), rms SPL (T90 SPL, red), single strike SEL (blue) and cumulative SEL (green) versus time (UTC). For periods during which there is no pile driving the cSEL is necessarily displayed as a constant value over time.

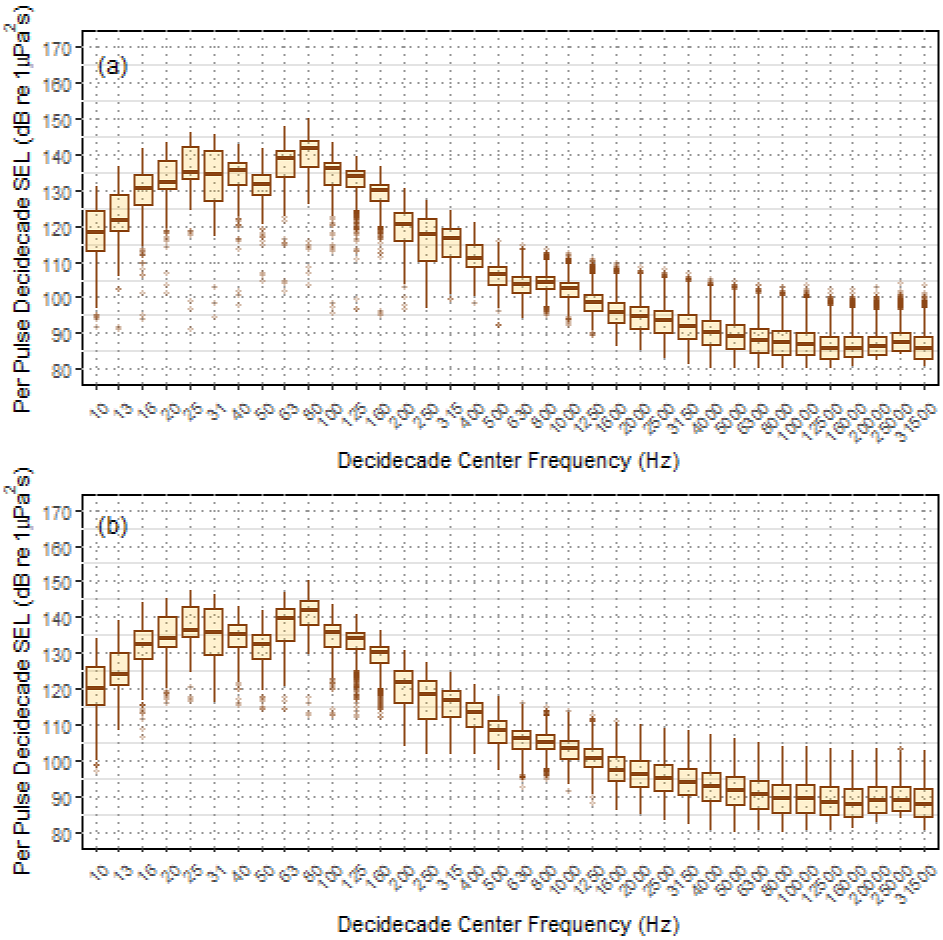


Figure A-56. Distribution of decidecade band level single strike SEL for pile driving installation of AR-39 at monitoring station AR39-6000 for channel 1 (a) and channel 2 (b). Beige bars indicate the first, second, and third quartiles (*25th*, *50th*, and *75th*) or as exceedances $L_{75}$, $L_{50}$, and $L_{25}$. Upper error bars indicate the maximum levels ($L_{max}$). Lower error bars indicate the 5th percentile or $L_{95}$.

Table A-41. Received level statistics for pile driving installation of AR-39 at monitoring station AR39-6000.

| Sound level statistic | PK (dB re 1 µPa) | rms SPL (dB re 1 µPa$^2$) | SELss (dB re 1 µPa$^2$·s) |
|---|---|---|---|
| **Channel 1 (bottom)** | | | |
| $L_{max}$ | 168.0 | 159.3 | 152.8 |
| $L_5$ | 165.5 | 157.5 | 151.8 |
| $L_{25}$ | 163.6 | 156.2 | 150.5 |
| $L_{50}$ | 161.3 | 152.9 | 147.1 |
| $L_{75}$ | 156.5 | 148.2 | 142.5 |
| $L_{95}$ | 152.2 | 144.2 | 138.7 |
| $L_{mean}$ | 161.8 | 153.8 | 148.1 |
| **Channel 2 (mid-water)** | | | |
| $L_{max}$ | 168.1 | 159.1 | 154.0 |
| $L_5$ | 165.6 | 157.9 | 152.7 |
| $L_{25}$ | 163.7 | 156.9 | 151.5 |
| $L_{50}$ | 160.8 | 153.1 | 147.8 |
| $L_{75}$ | 156.2 | 148.3 | 143.1 |
| $L_{95}$ | 152.5 | 145.0 | 139.8 |
| $L_{mean}$ | 161.7 | 154.3 | 149.0 |

## A.5.3. Ranges to Acoustic Thresholds

Table A-42. Isopleth distances to NMFS physiological thresholds for impact driving installation of pile AR-39.

| Group | Injury: PK | | | | Injury: cSEL | | | |
|---|---|---|---|---|---|---|---|---|
| | Level (dB re 1µPa) | Predicted (m) | Measured (m) | Measured w/ attn. coeff. (m) | Level (dB re 1 µPa$^2$·s) | Predicted (m) | Measured (m) | Measured w/ attn. coeff. (m) |
| LFC | 219 | 17 | 10 | 10 | 183 | 3,191 | 1,700 | 1,750 |
| MFC | 230 | 5 | 10 | 10 | 185 | 43 | 10 | 10 |
| HFC | 202 | 119 | 60 | 20 | 155 | 71 | 30 | <100 |
| PW | 218 | 19 | 10 | 10 | 185 | 153 | 100 | 90 |
| ST | 232 | 0 | 10 | 10 | 204 | 161 | 180 | 140 |
| AS | 206 | 78 | 40 | 10 | 187 | 6,894 | 4,460 | 4,670 |

Table A-43. Isopleth distances to NMFS behavioral thresholds for impact driving installation of pile AR-39.

| Group | Behavior: SPL | | | |
|---|---|---|---|---|
| | Level (dB re 1µPa$^2$) | Predicted (m) | Measured (m) | Measured w/ attn. coeff. (m) |
| MM | 160 | 4,121 | 4,390 | 4,450 |
| ST | 175 | 1,400 | 420 | 400 |
| AS | 150 | 9,229 | 20,850 | 15,760 |

## A.5.4. Regression Analysis for Transmission Loss

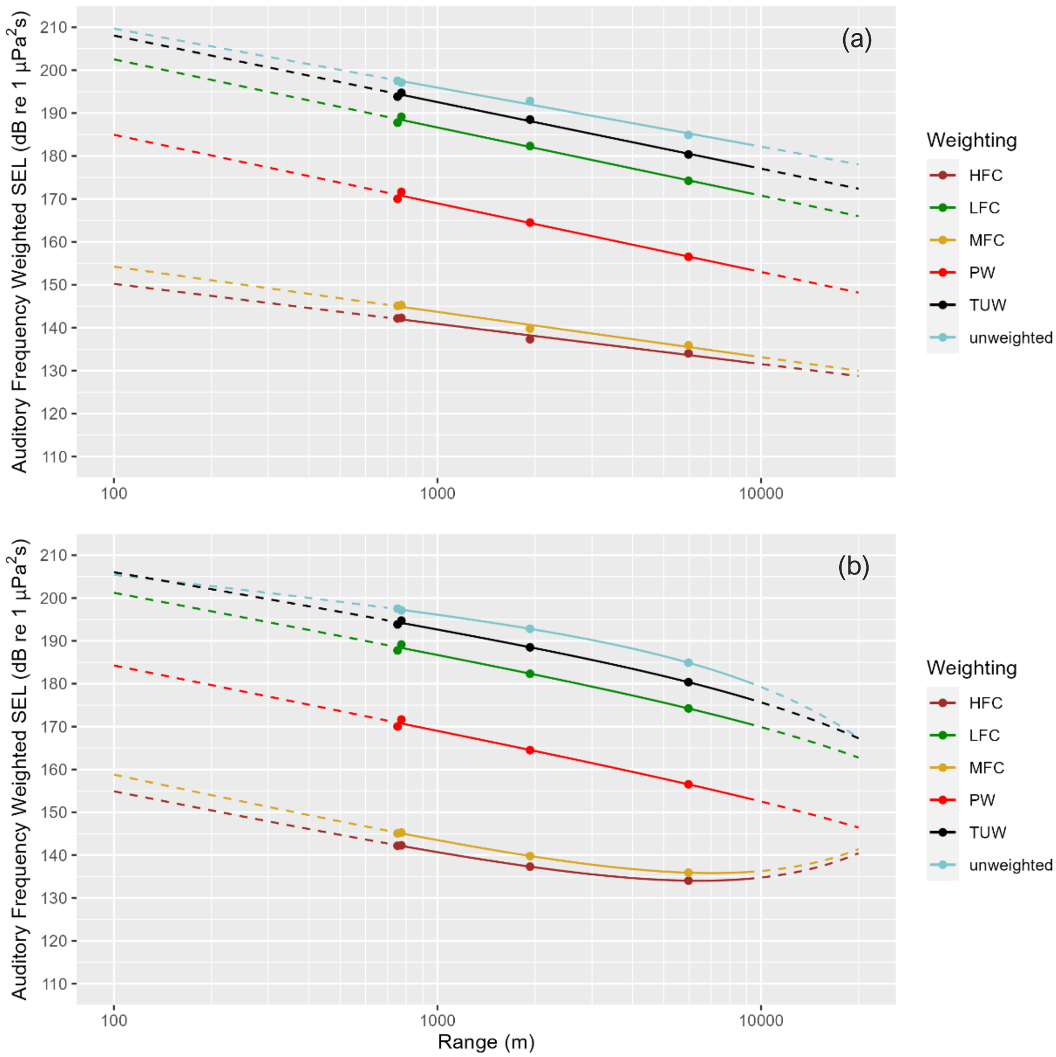


Figure A-57. Transmission loss determination based on regression analysis without (a) and with (b) intrinsic attenuation  for the maximum received cumulative SEL (cSEL) at each recording station during installation of pile AR-39 on 3 Jul 2023.

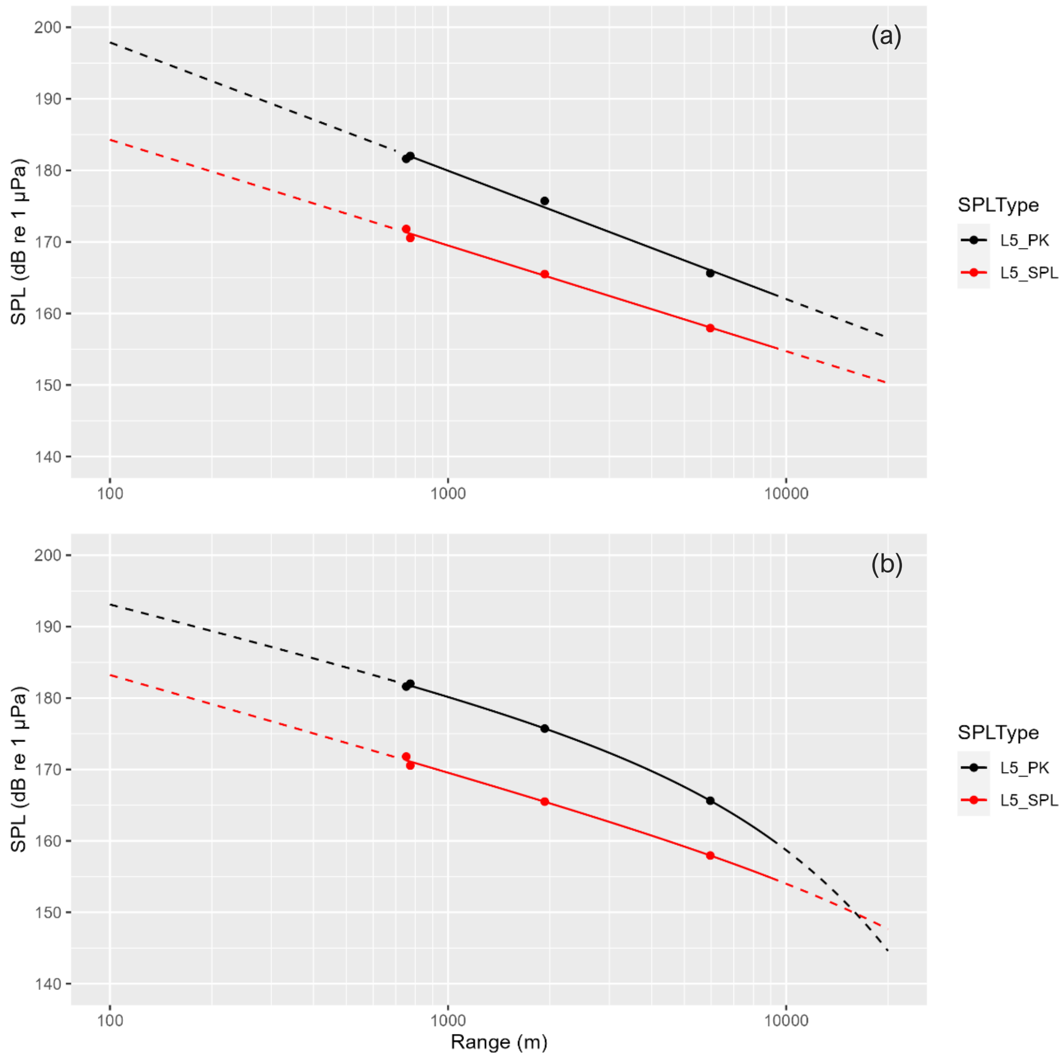


Figure A-58. Transmission loss determination based on regression analysis without (a) and with (b) intrinsic attenuation for $L_5$ PK and SPL maxima at each recording station during installation of pile AR-39 on 3 Jul 2023.

Table A-44. Regression analysis fitting coefficients for transmission loss with and without intrinsic attenuation for installation of pile AR-39 on 3 Jul 2023.

| Metric | A (dB/decade m) A*log(r) | A (dB/decade m) A*log(r) + αr/1000 | α (dB/ m) A*log(r) + αr/1000 |
|---|---|---|---|
| PK ($L_5$) (dB re 1 μPa) | -17.9 | -12.0 | -1.049 x $10^{-3}$ |
| rms SPL ($L_5$) (dB re 1 μPa$^2$) | -14.8 | -13.5 | -0.230 x $10^{-3}$ |
| cSEL (dB re 1 μPa$^2$·s) | -13.7 | -8.5 | -0.933 x $10^{-3}$ |
| cSEL, LF (dB re 1 μPa$^2$·s) | -15.9 | -14.3 | -0.283 x $10^{-3}$ |
| cSEL, MF (dB re 1 μPa$^2$·s) | -10.5 | -16.2 | 0.998 x $10^{-3}$ [a] |
| cSEL, HF (dB re 1 μPa$^2$·s) | -9.3 | -15.1 | 1.023 x $10^{-3}$ [a] |
| cSEL, PW (dB re 1 μPa$^2$·s) | -16.0 | -15.1 | -0.153 x $10^{-3}$ |
| cSEL, TU (dB re 1 μPa$^2$·s) | -15.5 | -13.0 | -0.448 x $10^{-3}$ |

[a] Positive attenuation coefficients could indicate ambient noise contamination and may not be valid.

## A.6. Foundation AW-38

Summary of measurements are shown in Table A-45. Channel 1 (bottom hydrophone) at station AW38-750 was not functioning properly and was excluded from the analysis.

### A.6.1. Summary of Measured Sound Levels

Table A-45. Summary of Autonomous Multichannel Acoustic Recorder (AMAR) locations and measured sound levels for pile AW-38. Computed PK and SPL levels are shown for the $L_{max}$.

| Location (nominal) | Recorder ID | Distance (m) | Water depth (m) | Channel | Impulses Detected* (clipped) | PK (dB re 1 μPa) | SPL (dB re 1 μPa$^2$) | cSEL (dB re 1 μPa$^2$·s) |
|---|---|---|---|---|---|---|---|---|
| 750 | AMAR-863 | 759 | 46 | | | | | |
| | | | | 2 | 3428 | 187.6 | 175.6 | 200.2 |
| 750 @ 90° | AMAR-865 | 762 | 46 | 1 | 3426 | 184.6 | 173.6 | 199.4 |
| | | | | 2 | 3429 | 186.8 | 175.0 | 199.6 |
| 2000 | AMAR-855 | 2001 | 47 | 1 | 3429 | 178.4 | 167.8 | 193.9 |
| | | | | 2 | 3408 | 179.3 | 169.2 | 194.8 |
| 4000 | AMAR-860 | 3941 | 47 | 1 | 3429 | 173.7 | 164.4 | 189.8 |
| | | | | 2 | 3431 | 173.9 | 164.6 | 190.4 |
| 8000 | AMAR-603 | 8007 | 51 | 1 | 3426 | 170.1 | 159.7 | 185.4 |
| | | | | 2 | 3427 | 168.3 | 158.3 | 184.8 |

* Number of strikes produced (from hammer log): 3419

# A.6.2. Sound Levels per Station

## A.6.2.1. Station AW38-750

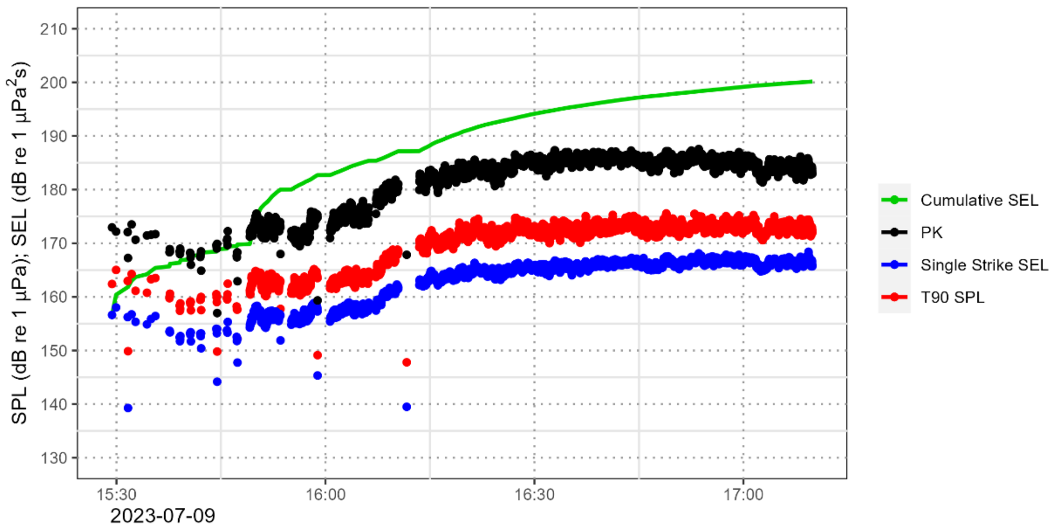


Figure A-59. Received levels for impact pile driving installation of AW-38 at monitoring station AW38-750 for channel 2. Peak SPL (PK, black), rms SPL (T90 SPL, red), single strike SEL (blue) and cumulative SEL (green) versus time (UTC). For periods during which there is no pile driving the cSEL is necessarily displayed as a constant value over time.

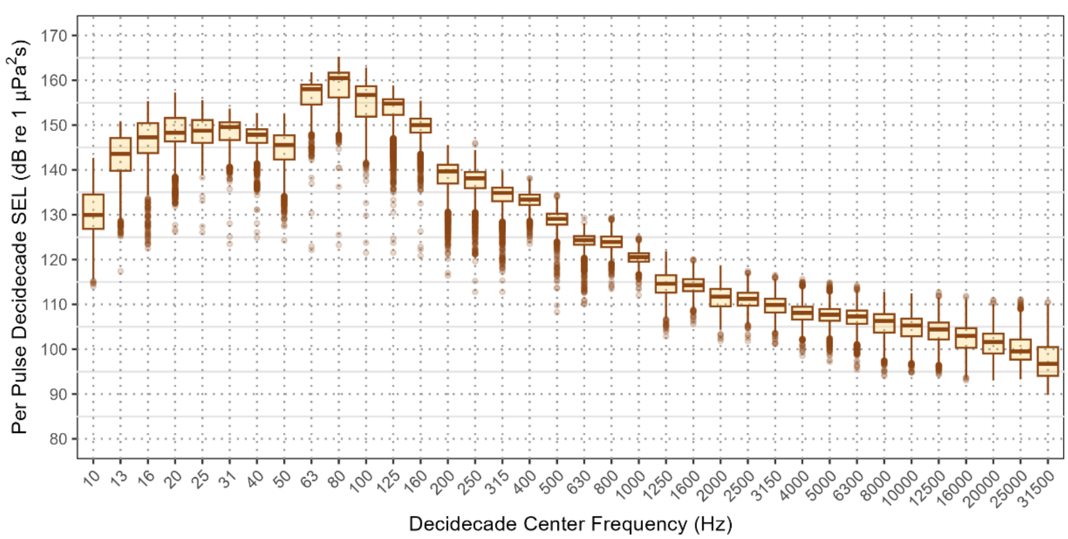


Figure A-60. Distribution of decidecade band level single strike SEL for pile driving installation of AW-38 at monitoring station AW38-750 for channel 2. Beige bars indicate the first, second, and third quartiles (*25th*, *50th*, and *75th*) or as exceedances $L_{75}$, $L_{50}$, and $L_{25}$. Upper error bars indicate the maximum levels ($L_{max}$). Lower error bars indicate the 5th percentile or $L_{95}$.

Table A-46. Received level statistics for pile driving installation of AW-38 at monitoring station AW38-750.

| Sound level statistic | PK (dB re 1 µPa) | rms SPL (dB re 1 µPa$^2$) | SELss (dB re 1 µPa$^2$·s) |
|---|---|---|---|
| **Channel 2 (mid-water)** | | | |
| $L_{max}$ | 187.6 | 175.6 | 168.4 |
| $L_5$ | 186.4 | 174.1 | 167.1 |
| $L_{25}$ | 185.4 | 173.1 | 166.3 |
| $L_{50}$ | 184.2 | 172.1 | 165.4 |
| $L_{75}$ | 180.7 | 168.3 | 161.7 |
| $L_{95}$ | 171.9 | 161.8 | 155.9 |
| $L_{mean}$ | 182.1 | 170.2 | 163.6 |

### A.6.2.2. Station AW38-75090

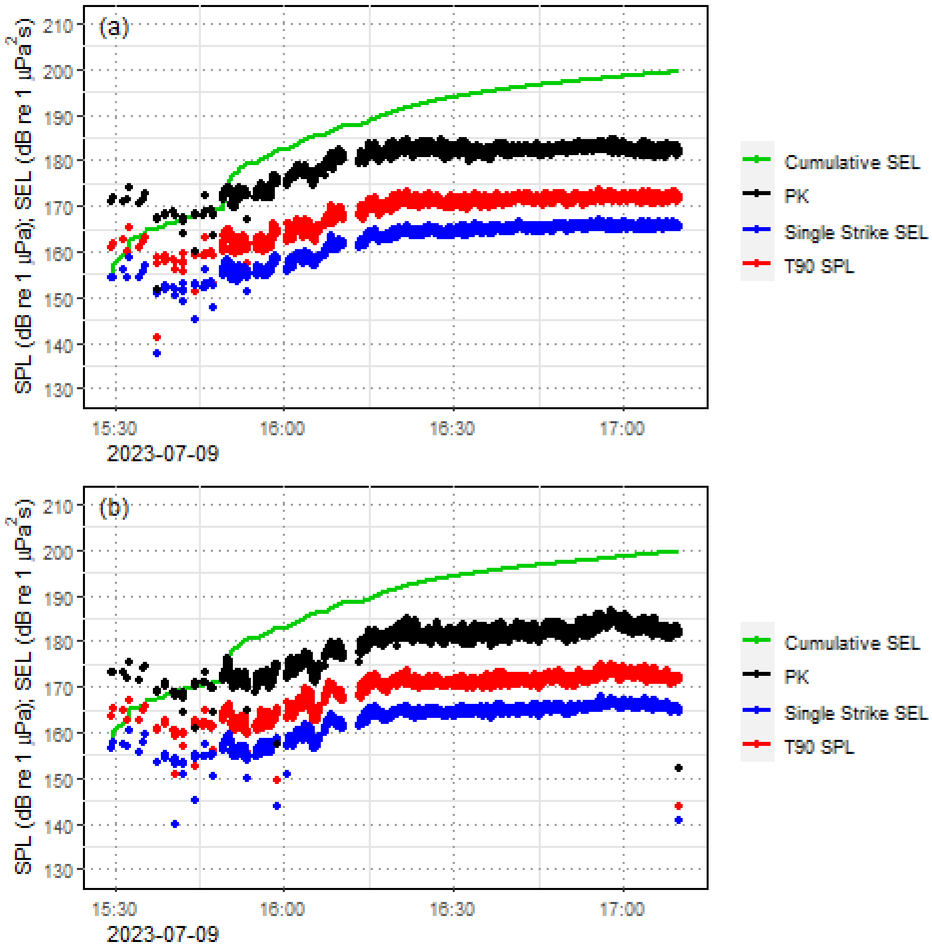


Figure A-61. Received levels for impact pile driving installation of AW-38 at monitoring station AW38-75090, for channel 1 (a) and channel 2 (b). Peak SPL (PK, black), rms SPL (T90 SPL, red), single strike SEL (blue) and cumulative SEL (green) versus time (UTC). For periods during which there is no pile driving the cSEL is necessarily displayed as a constant value over time.

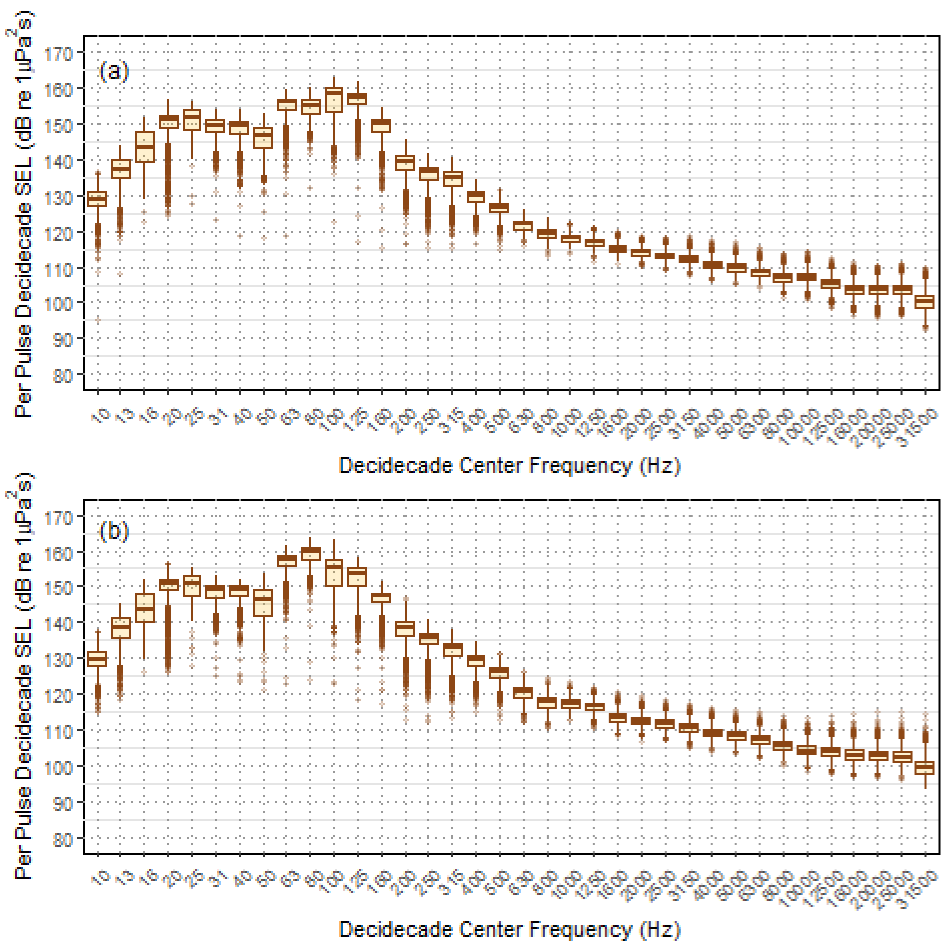


Figure A-62. Distribution of decidecade band level single strike SEL for pile driving installation of AW-38 at monitoring station AW38-75090 for channel 1 (a) and channel 2 (b). Beige bars indicate the first, second, and third quartiles (*25th*, *50th*, and *75th*) or as exceedances $L_{75}$, $L_{50}$, and $L_{25}$. Upper error bars indicate the maximum levels ($L_{max}$). Lower error bars indicate the 5th percentile or $L_{95}$.

Table A-47. Received level statistics for pile driving installation of AW-38 at monitoring station AW38-75090.

| Sound level statistic | PK (dB re 1 µPa) | rms SPL (dB re 1 µPa$^2$) | SELss (dB re 1 µPa$^2$·s) |
|---|---|---|---|
| **Channel 1 (bottom)** | | | |
| $L_{max}$ | 184.6 | 173.6 | 166.9 |
| $L_5$ | 183.6 | 172.4 | 166.1 |
| $L_{25}$ | 182.8 | 171.8 | 165.5 |
| $L_{50}$ | 182.1 | 171.1 | 164.7 |
| $L_{75}$ | 180.7 | 168.7 | 162.1 |
| $L_{95}$ | 172.7 | 161.5 | 155.5 |
| $L_{mean}$ | 180.7 | 169.5 | 163.1 |
| **Channel 2 (mid-water)** | | | |
| $L_{max}$ | 186.8 | 175.0 | 167.9 |
| $L_5$ | 184.6 | 173.3 | 166.5 |
| $L_{25}$ | 182.6 | 172.1 | 165.5 |
| $L_{50}$ | 181.5 | 171.2 | 164.7 |
| $L_{75}$ | 178.8 | 169.4 | 162.7 |
| $L_{95}$ | 171.6 | 162.2 | 156.1 |
| $L_{mean}$ | 180.1 | 169.9 | 163.4 |

### A.6.2.3. Station AW38-2000

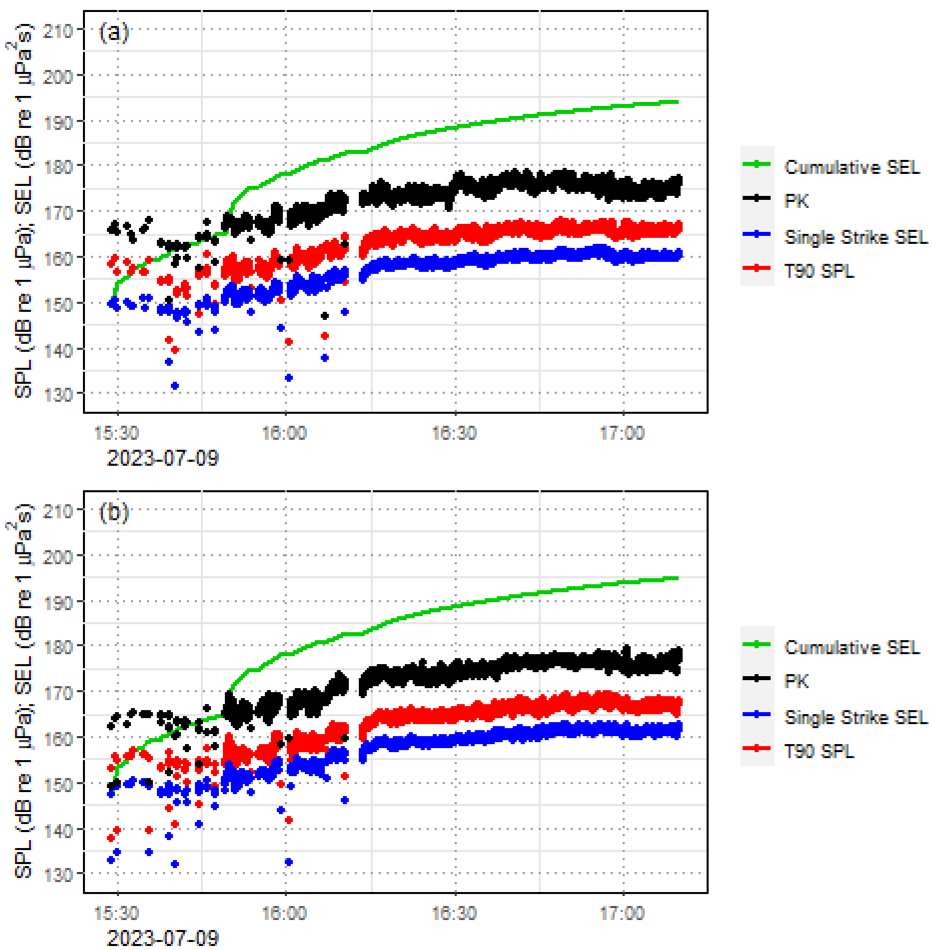


Figure A-63. Received levels for impact pile driving installation of AW-38 at monitoring station AW38-2000 for channel 1 (a) and channel 2 (b). Peak SPL (PK, black), rms SPL (T90 SPL, red), single strike SEL (blue) and cumulative SEL (green) versus time (UTC). For periods during which there was no pile driving the cSEL is necessarily displayed as a constant value over time.

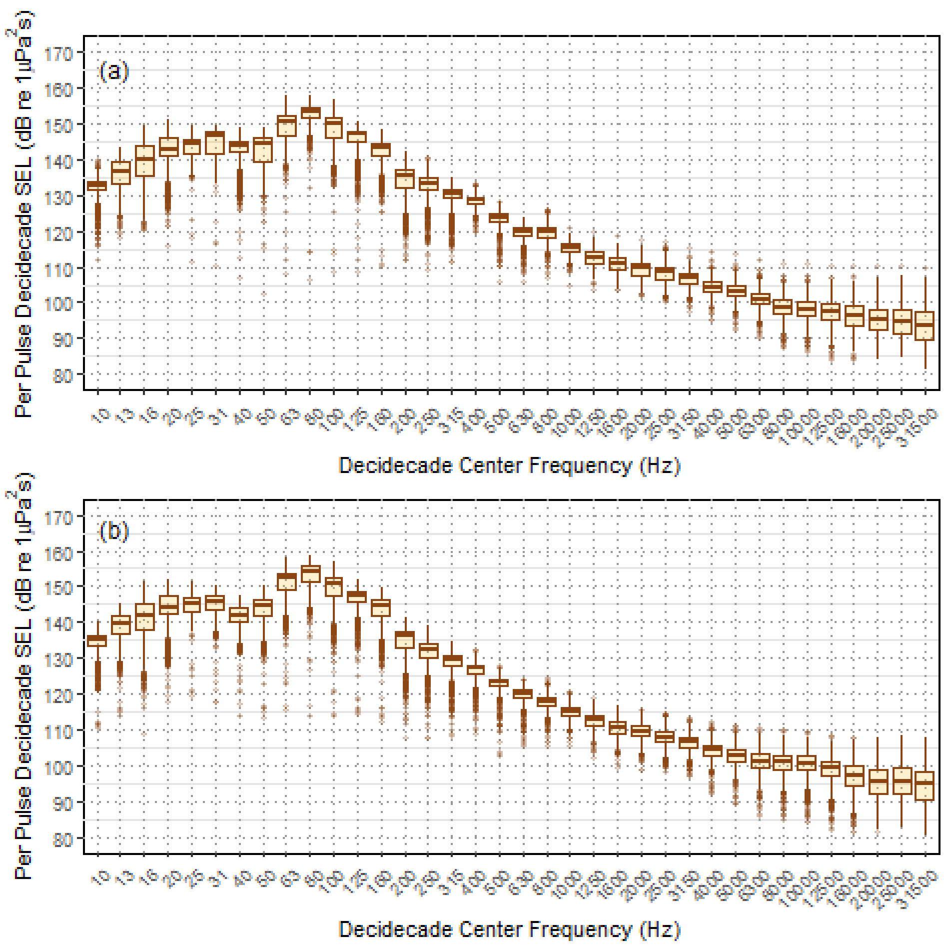


Figure A-64. Distribution of decidecade band level single strike SEL for pile driving installation of AW-38 at monitoring station AW38-2000 for channel 1 (a) and channel 2 (b). Beige bars indicate the first, second, and third quartiles (*25th*, *50th*, and *75th*) or as exceedances $L_{75}$, $L_{50}$, and $L_{25}$. Upper error bars indicate the maximum levels ($L_{max}$). Lower error bars indicate the 5th percentile or $L_{95}$.

Table A-48. Received level statistics for pile driving installation of AW-38 at monitoring station AW38-2000.

| Sound level statistic | PK (dB re 1 µPa) | rms SPL (dB re 1 µPa$^2$) | SELss (dB re 1 µPa$^2$·s) |
|---|---|---|---|
| **Channel 1 (bottom)** | | | |
| $L_{max}$ | 178.4 | 167.8 | 161.8 |
| $L_5$ | 177.2 | 166.6 | 160.7 |
| $L_{25}$ | 175.7 | 165.7 | 159.9 |
| $L_{50}$ | 174.2 | 164.8 | 158.9 |
| $L_{75}$ | 172.1 | 162.0 | 156.0 |
| $L_{95}$ | 166.8 | 157.2 | 151.4 |
| $L_{mean}$ | 173.3 | 163.5 | 157.7 |
| **Channel 2 (mid-water)** | | | |
| $L_{max}$ | 179.3 | 169.2 | 162.8 |
| $L_5$ | 177.2 | 167.9 | 161.9 |
| $L_{25}$ | 176.1 | 166.7 | 161.1 |
| $L_{50}$ | 174.5 | 165.2 | 159.5 |
| $L_{75}$ | 171.5 | 161.8 | 156.5 |
| $L_{95}$ | 165.1 | 156.0 | 151.3 |
| $L_{mean}$ | 173.1 | 163.8 | 158.3 |

### A.6.2.4. Station AW38-4000

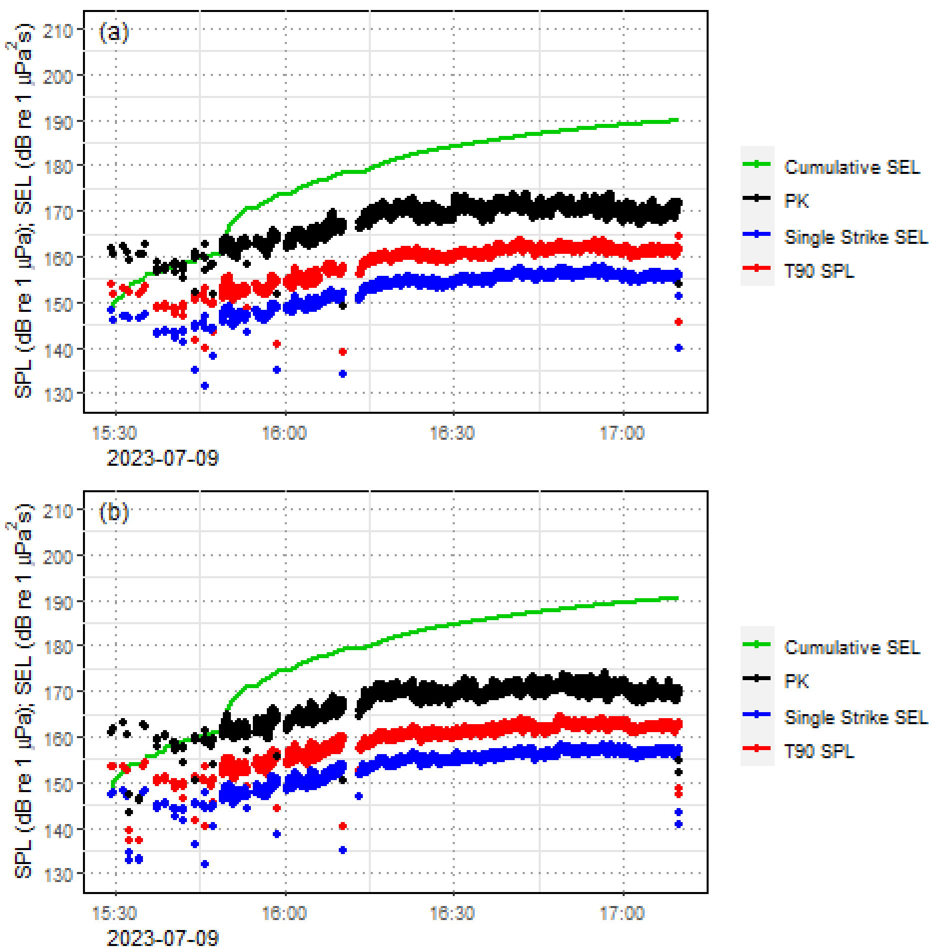


Figure A-65. Received levels for impact pile driving installation of AW-38 at monitoring station AW38-4000 for channel 1 (a) and channel 2 (b). Peak SPL (PK, black), rms SPL (T90 SPL, red), single strike SEL (blue) and cumulative SEL (green) versus time (UTC). For periods during which there is no pile driving the cSEL is necessarily displayed as a constant value over time.

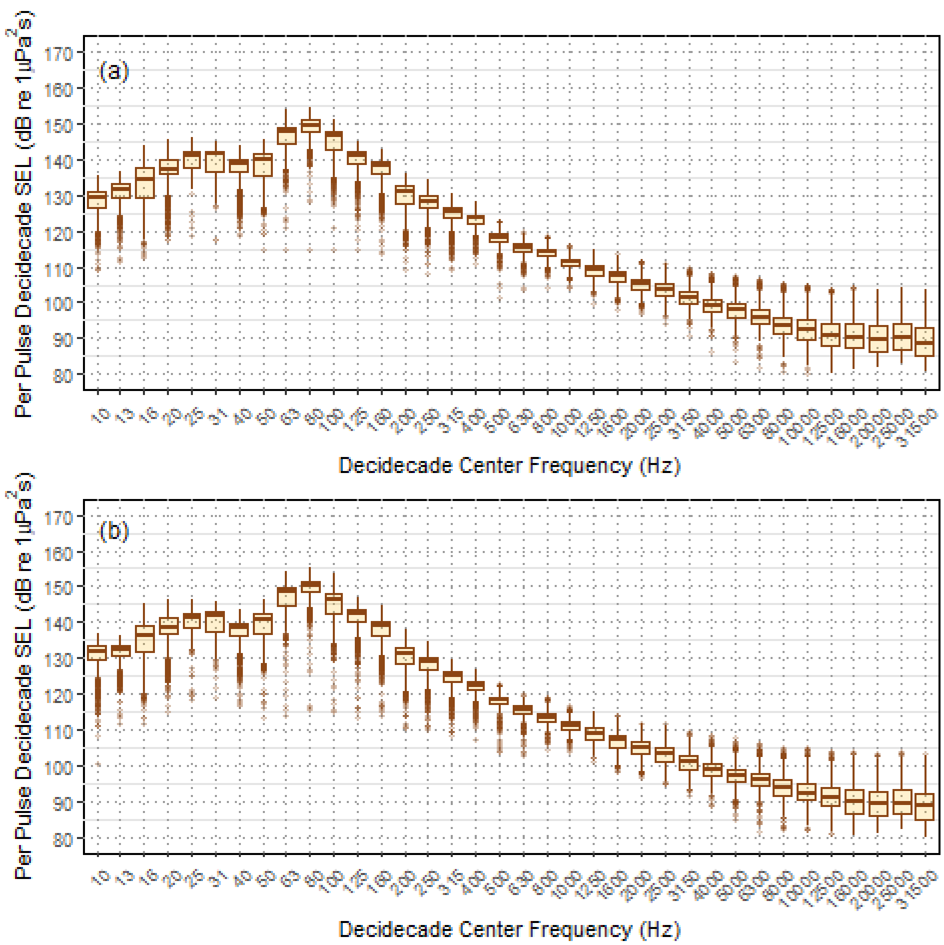


Figure A-66. Distribution of decidecade band level single strike SEL for pile driving installation of AW-38 at monitoring station AW38-4000 for channel 1 (a) and channel 2 (b). Beige bars indicate the first, second, and third quartiles (*25th*, *50th*, and *75th*) or as exceedances $L_{75}$, $L_{50}$, and $L_{25}$. Upper error bars indicate the maximum levels ($L_{max}$). Lower error bars indicate the 5th percentile or $L_{95}$.

Table A-49. Received level statistics for pile driving installation of AW-38 at monitoring station AW38-4000.

| Sound level statistic | PK (dB re 1 µPa) | rms SPL (dB re 1 µPa$^2$) | SELss (dB re 1 µPa$^2$·s) |
|---|---|---|---|
| **Channel 1 (bottom)** | | | |
| $L_{max}$ | 173.7 | 164.4 | 157.7 |
| $L_5$ | 172.2 | 162.3 | 156.6 |
| $L_{25}$ | 170.8 | 161.5 | 155.8 |
| $L_{50}$ | 169.7 | 160.5 | 154.8 |
| $L_{75}$ | 167.3 | 157.7 | 151.8 |
| $L_{95}$ | 162.2 | 152.4 | 146.7 |
| $L_{mean}$ | 168.6 | 159.2 | 153.5 |
| **Channel 2 (mid-water)** | | | |
| $L_{max}$ | 173.9 | 164.6 | 158.4 |
| $L_5$ | 171.9 | 163.1 | 157.3 |
| $L_{25}$ | 170.6 | 162.2 | 156.5 |
| $L_{50}$ | 169.6 | 161.0 | 155.4 |
| $L_{75}$ | 167.0 | 158.2 | 152.5 |
| $L_{95}$ | 161.4 | 153.2 | 147.6 |
| $L_{mean}$ | 168.4 | 159.8 | 154.1 |

## A.6.2.5. Station AW38-8000

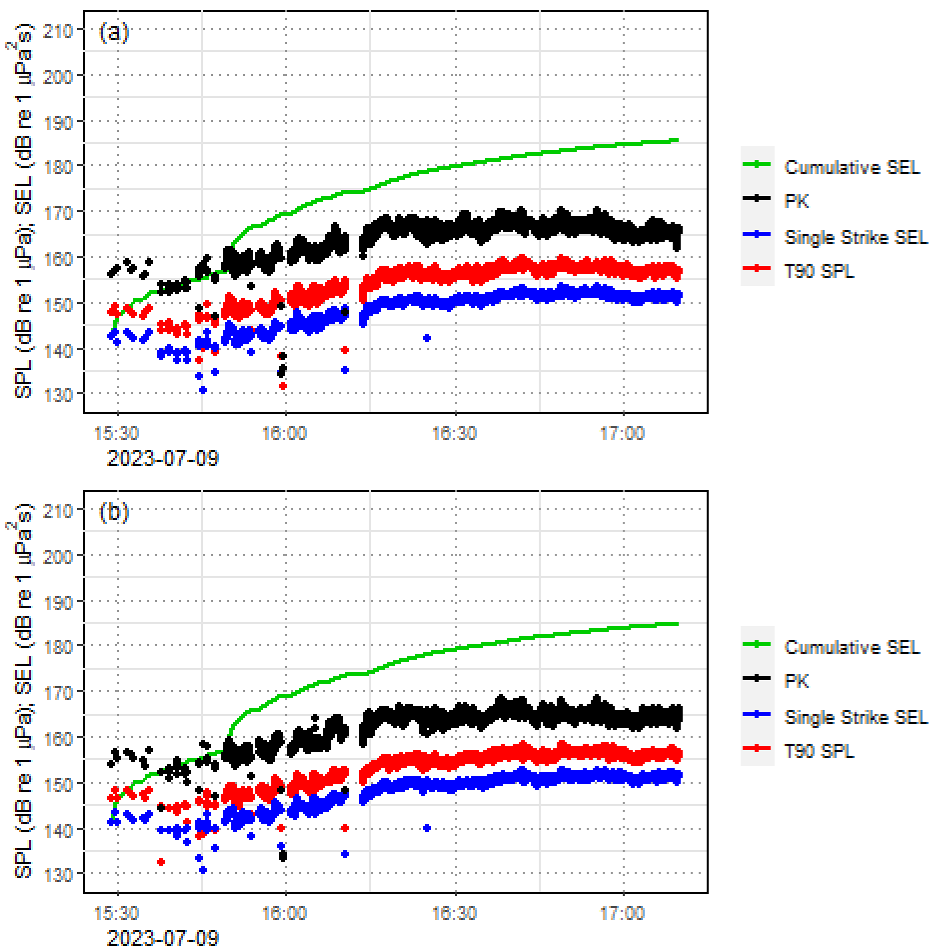


Figure A-67. Received levels for impact pile driving installation of AW-38 at monitoring station AW38-8000 for channel 1 (a) and channel 2 (b). Peak SPL (PK, black), rms SPL (T90 SPL, red), single strike SEL (blue) and cumulative SEL (green) versus time (UTC). For periods during which there is no pile driving the cSEL is necessarily displayed as a constant value over time.

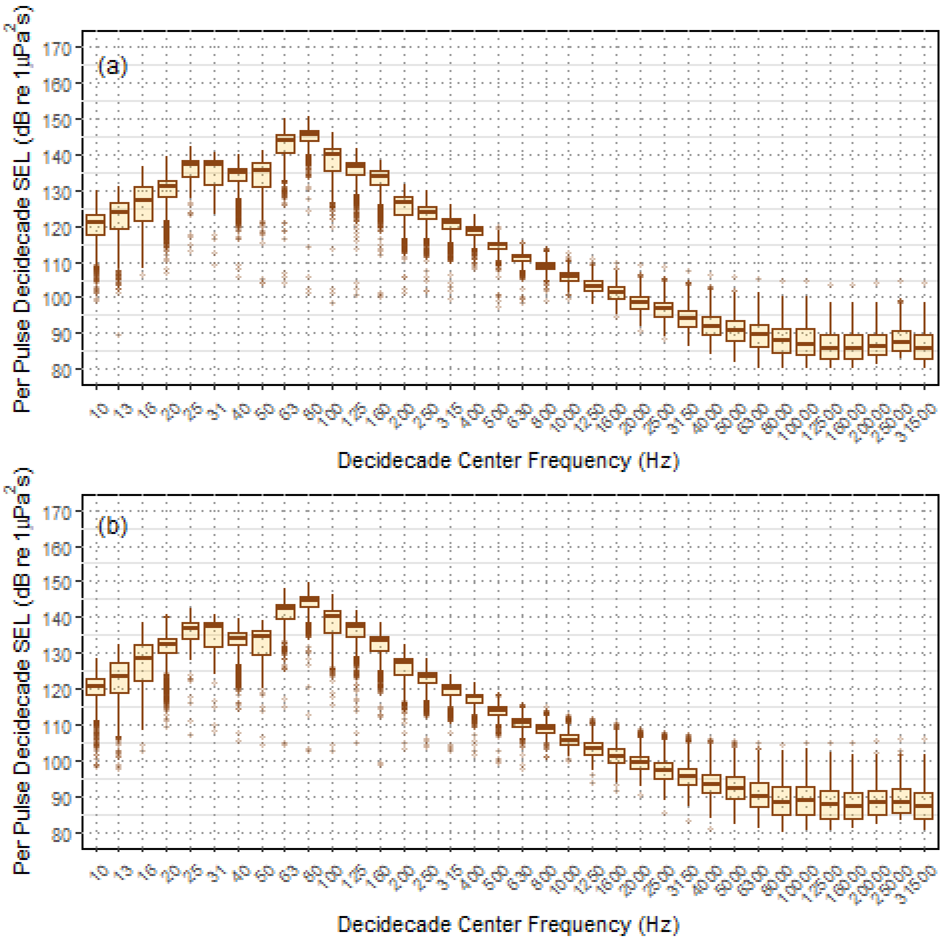


Figure A-68. Distribution of decidecade band level single strike SEL for pile driving installation of AW-38 at monitoring station AW38-8000 for channel 1 (a) and channel 2 (b). Beige bars indicate the first, second, and third quartiles (*25th*, *50th*, and *75th*) or as exceedances $L_{75}$, $L_{50}$, and $L_{25}$. Upper error bars indicate the maximum levels ($L_{max}$). Lower error bars indicate the 5th percentile or $L_{95}$.

Table A-50. Received level statistics for pile driving installation of AW-38 at monitoring station AW38-8000.

| Sound level statistic | PK (dB re 1 µPa) | rms SPL (dB re 1 µPa$^2$) | SELss (dB re 1 µPa$^2$·s) |
|---|---|---|---|
| **Channel 1 (bottom)** | | | |
| $L_{max}$ | 170.1 | 159.7 | 153.3 |
| $L_5$ | 168.2 | 158.3 | 152.3 |
| $L_{25}$ | 166.9 | 157.3 | 151.4 |
| $L_{50}$ | 165.7 | 156.4 | 150.5 |
| $L_{75}$ | 163.5 | 153.3 | 147.5 |
| $L_{95}$ | 158.5 | 148.1 | 142.5 |
| $L_{mean}$ | 164.7 | 155.0 | 149.2 |
| **Channel 2 (mid-water)** | | | |
| $L_{max}$ | 168.3 | 158.3 | 152.7 |
| $L_5$ | 166.1 | 156.9 | 151.6 |
| $L_{25}$ | 164.9 | 156.1 | 150.9 |
| $L_{50}$ | 163.9 | 155.0 | 149.8 |
| $L_{75}$ | 161.9 | 151.8 | 146.8 |
| $L_{95}$ | 156.2 | 147.1 | 142.1 |
| $L_{mean}$ | 162.8 | 153.7 | 148.6 |

## A.6.3. Ranges to Acoustic Thresholds

Table A-51. Isopleth distances to NMFS physiological thresholds for impact driving installation of pile AW-38.

| Group | Injury: PK | | | | Injury: cSEL | | | |
|---|---|---|---|---|---|---|---|---|
| | Level (dB re 1µPa) | Predicted (m) | Measured (m) | Measured w/ attn. coeff. (m) | Level (dB re 1 µPa²·s) | Predicted (m) | Measured (m) | Measured w/ attn. coeff. (m) |
| LFC | 219 | 17 | 10 | 20 | 183 | 3,191 | 3,050 | 3,190 |
| MFC | 230 | 5 | 10 | 10 | 185 | 43 | 10 | 10 |
| HFC | 202 | 119 | 80 | 130 | 155 | 71 | 150 | 190 |
| PW | 218 | 19 | 10 | 20 | 185 | 153 | 140 | 120 |
| ST | 232 | 0 | 10 | 10 | 204 | 161 | 280 | 240 |
| AS | 206 | 78 | 50 | 80 | 187 | 6,894 | 6,580 | 6,500 |

Table A-52. Isopleth distances to NMFS behavioral thresholds for impact driving installation of pile AW-38.

| Group | Behavior: SPL | | | |
|---|---|---|---|---|
| | Level (dB re 1µPa²) | Predicted (m) | Measured (m) | Measured w/ attn. coeff. (m) |
| MM | 160 | 4,121 | 6,300 | 6,290 |
| ST | 175 | 1,400 | 640 | 620 |
| AS | 150 | 9,229 | 29,120 | 20,720 |

### A.6.4. Regression Analysis for Transmission Loss

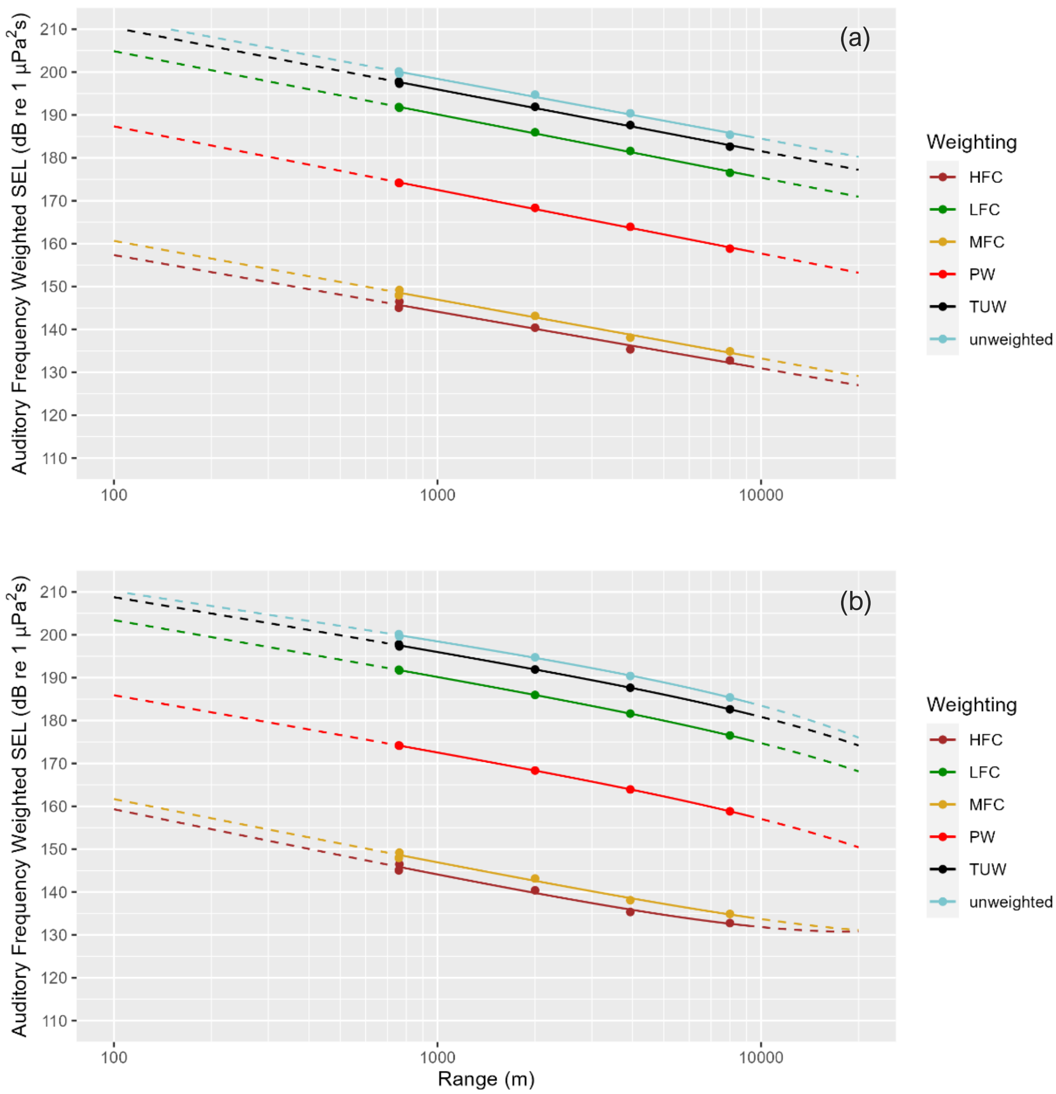


Figure A-69. Transmission loss determination based on regression analysis without (a) and with (b) intrinsic attenuation for the maximum received cumulative SEL (cSEL) at each recording station during installation of pile AW-38 on 9 Jul 2023.

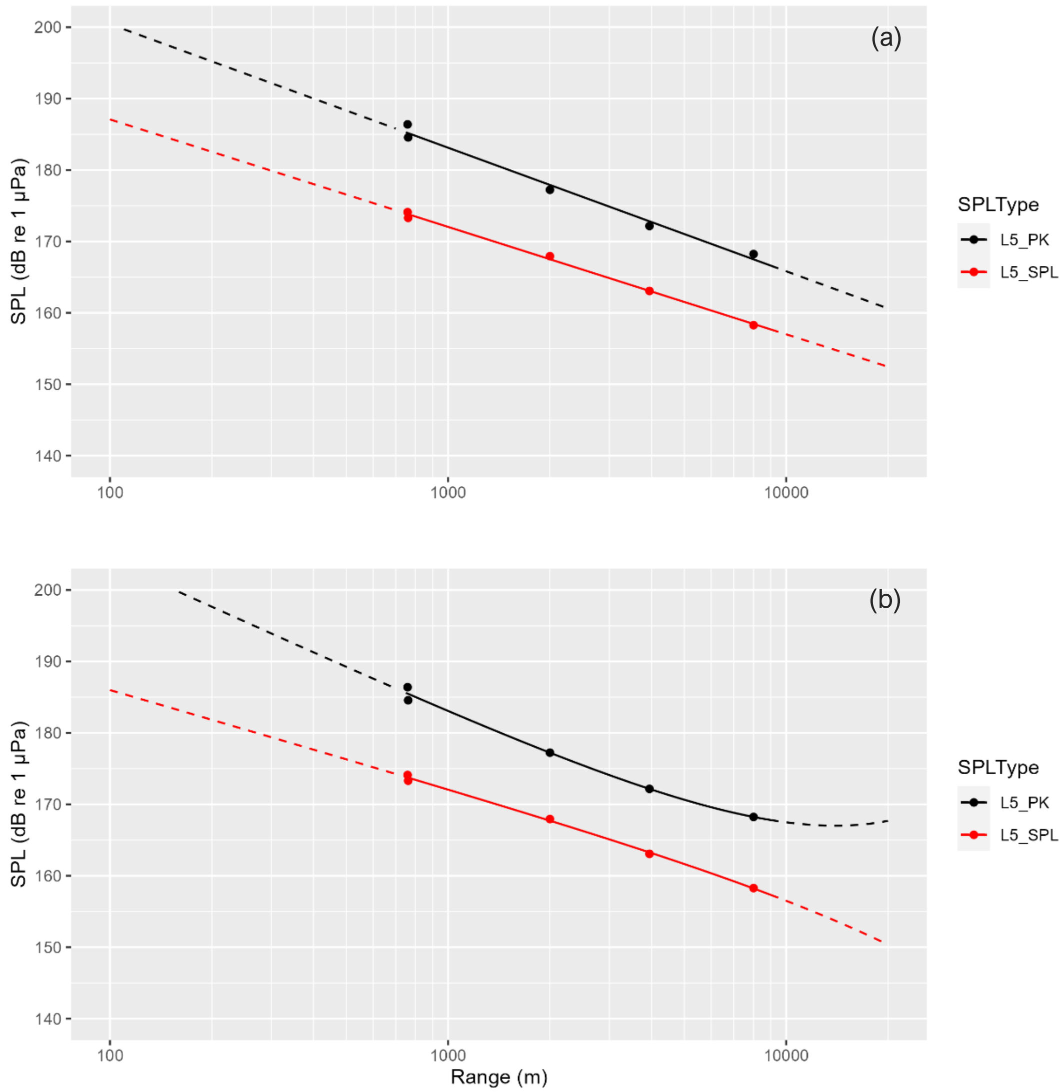


Figure A-70. Transmission loss determination based on regression analysis without (a) and with (b) intrinsic attenuation for $L_5$ PK and SPL maxima at each recording station during installation of pile AW-38 on 9 Jul 2023.

Table A-53. Regression analysis fitting coefficients for transmission loss with and without intrinsic attenuation for installation of pile AW-38 on 9 Jul 2023.

| Metric | A (dB/decade m) A*log(r) | A (dB/decade m) A*log(r) + αr/1000 | α (dB/ m) A*log(r) + αr/1000 |
|---|---|---|---|
| PK ($L_5$) (dB re 1 µPa) | -17.3 | -21.6 | 0.672 x $10^{-3}$ [a] |
| rms SPL ($L_5$) (dB re 1 µPa$^2$) | -15.0 | -13.8 | -0.020 x $10^{-3}$ |
| cSEL (dB re 1 µPa$^2$·s) | -14.0 | -11.4 | -0.403 x $10^{-3}$ |
| cSEL, LF (dB re 1 µPa$^2$·s) | -14.7 | -13.0 | -0.266 x $10^{-3}$ |
| cSEL, MF (dB re 1 µPa$^2$·s) | -13.7 | -14.9 | -0.189 x $10^{-3}$ |
| cSEL, HF (dB re 1 µPa$^2$·s) | -13.2 | -15.5 | -0.362 x $10^{-3}$ |
| cSEL, PW (dB re 1 µPa$^2$·s) | -14.8 | -13.1 | -0.266 x $10^{-3}$ |
| cSEL, TU (dB re 1 µPa$^2$·s) | -14.4 | -12.5 | -0.288 x $10^{-3}$ |

[a] Positive attenuation coefficients could indicate ambient noise contamination and may not be valid.

## A.7. Foundation AM-37

Summary of measurements are shown in Table A-54. Foundation AM-37 comprised the pile driving of 4 piles, namely leg A2, leg C4, leg C2 and leg A4, in order of installation. Channel 1 (bottom hydrophone) at station AM37-750 was not functioning properly and was excluded from the analysis.

### A.7.1. Summary of Measured Sound Levels

Table A-54. Summary of Autonomous Multichannel Acoustic Recorder (AMAR) locations and measured sound levels for pile AM-37. Computed PK and SPL levels are shown for the $L_{max}$.

| Location (nominal) | Recorder ID | Distance (m) | Water depth (m) | Channel | Impulses Detected* (clipped) | PK (dB re 1 µPa) | SPL (dB re 1 µPa$^2$) | cSEL (dB re 1 µPa$^2$·s) |
|---|---|---|---|---|---|---|---|---|
| 750 | AMAR-863 | 823 | 39 | | | | | |
| | | | | 2 | 28252 | 177.1 | 165.0 | 197.5 |
| 750 @ 90° | AMAR-865 | 810 | 49 | 1 | 28249 | 176.7 | 165.3 | 196.9 |
| | | | | 2 | 28396 | 179.9 | 168.1 | 197.5 |
| 2000 | AMAR-855 | 2062 | 40 | 1 | 19354 | 169.9 | 161.7 | 190.3 |
| | | | | 2 | 28177 | 170.3 | 160.3 | 192.4 |
| 4000 | AMAR-860 | 4070 | 41 | 1 | 22406 | 163.5 | 155.3 | 186.5 |
| | | | | 2 | 27309 | 164.5 | 153.7 | 187.4 |
| 8000 | AMAR-603 | 8020 | 42 | 1 | 24987 | 163.1 | 150.6 | 181.7 |
| | | | | 2 | 28396 | 163.2 | 148.6 | 181.6 |

* Number of strikes produced (from hammer log): (A2) 7572 (B4) 6774 (C2) 7198 (C4) 6782; Total 28,326

## A.7.2. Sound Levels per Station

### A.7.2.1. Station AM37-750

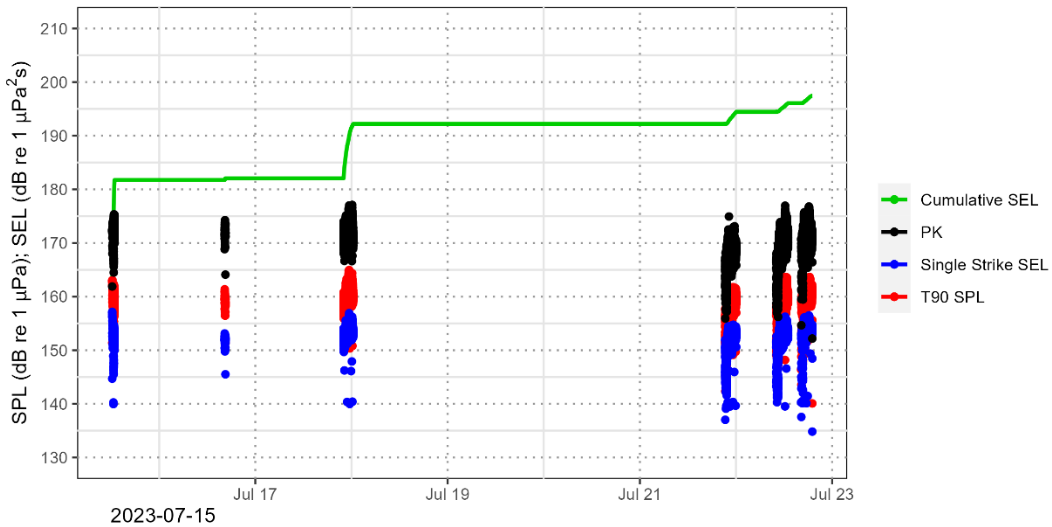


Figure A-71. Received levels for impact pile driving installation of AM-37 at monitoring station AM37-750 for channel 2. Peak SPL (PK, black), rms SPL (T90 SPL, red), single strike SEL (blue) and cumulative SEL (green) versus time (UTC). For periods during which there is no pile driving the cSEL is necessarily displayed as a constant value over time.

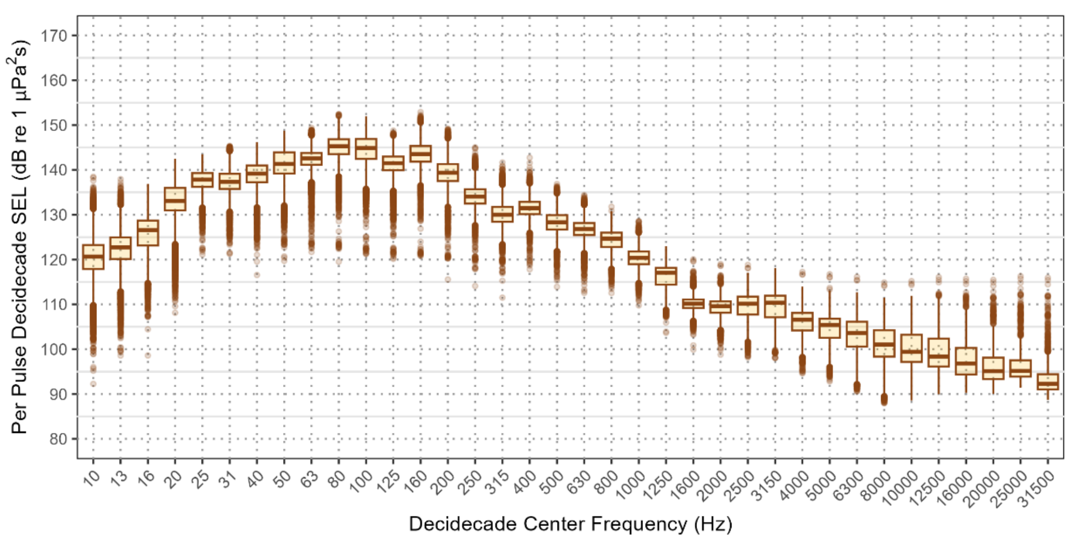


Figure A-72. Distribution of decidecade band level single strike SEL for pile driving installation of AM-37 at monitoring station AM37-750 for channel 2. Beige bars indicate the first, second, and third quartiles (*25th*, *50th*, and *75th*) or as exceedances $L_{75}$, $L_{50}$, and $L_{25}$. Upper error bars indicate the maximum levels ($L_{max}$). Lower error bars indicate the 5th percentile or $L_{95}$.

Table A-55. Received level statistics for pile driving installation of AM-37 at monitoring station AM37-750.

| Sound level statistic | PK (dB re 1 µPa) | rms SPL (dB re 1 µPa$^2$) | SELss (dB re 1 µPa$^2$·s) |
|---|---|---|---|
| **Channel 2 (mid-water)** | | | |
| $L_{max}$ | 177.1 | 165.0 | 157.2 |
| $L_5$ | 174.3 | 162.1 | 154.9 |
| $L_{25}$ | 172.3 | 160.6 | 153.7 |
| $L_{50}$ | 170.3 | 159.5 | 152.9 |
| $L_{75}$ | 168.3 | 158.3 | 152.0 |
| $L_{95}$ | 166.2 | 156.3 | 150.0 |
| $L_{mean}$ | 170.2 | 159.3 | 152.7 |

### A.7.2.2. Station AM37-75090

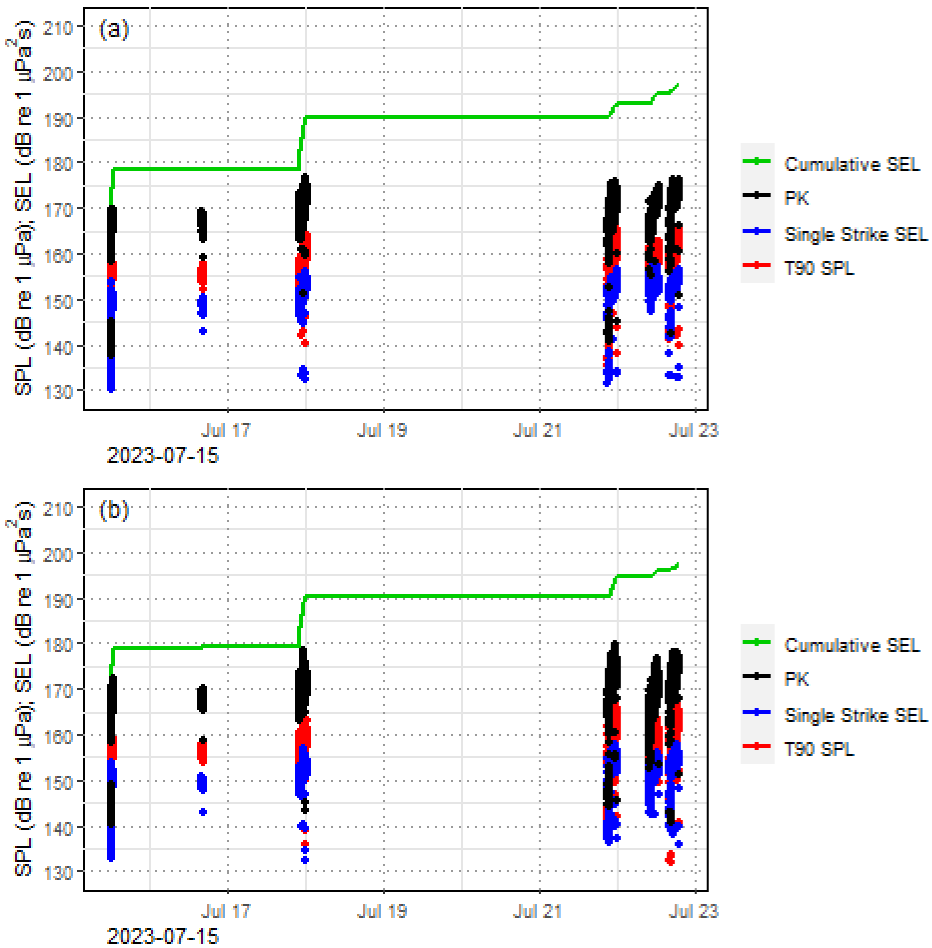


Figure A-73. Received levels for impact pile driving installation of AM-37 at monitoring station AM37-75090, for channel 1 (a) and channel 2 (b). Peak SPL (PK, black), rms SPL (T90 SPL, red), single strike SEL (blue) and cumulative SEL (green) versus time (UTC). For periods during which there is no pile driving the cSEL is necessarily displayed as a constant value over time.

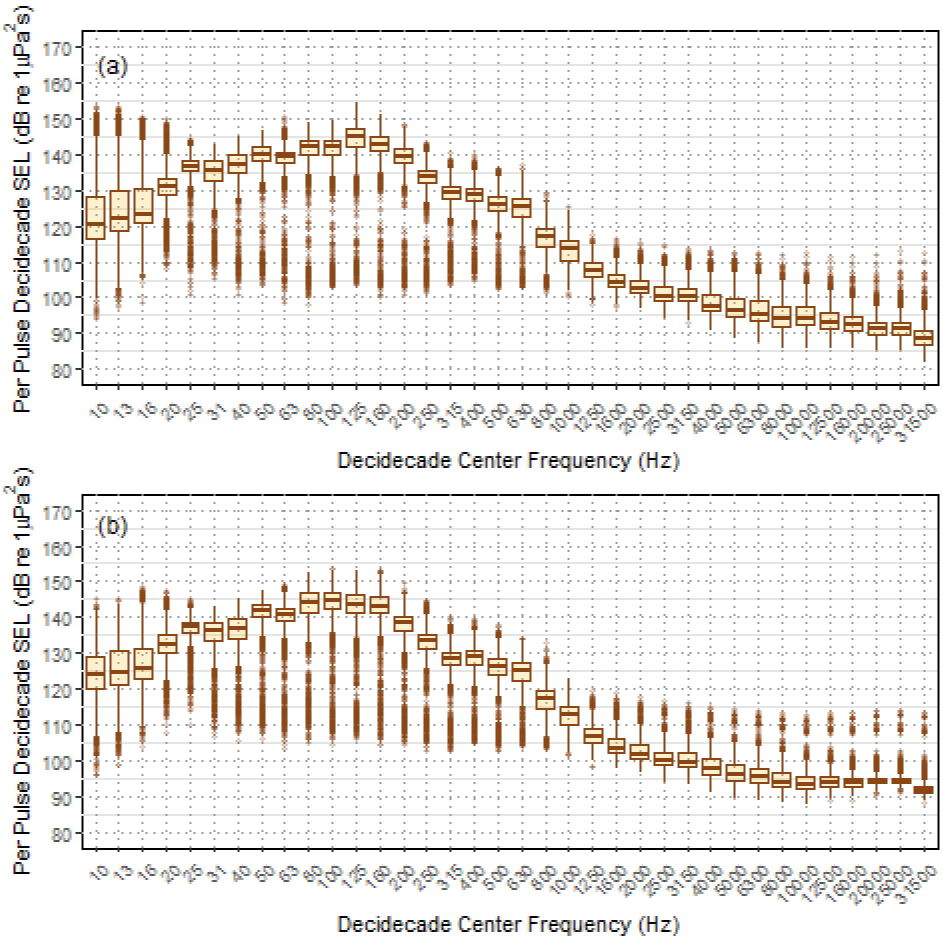


Figure A-74. Distribution of decidecade band level single strike SEL for pile driving installation of AM-37 at monitoring station AM37-75090 for channel 1 (a) and channel 2 (b). Beige bars indicate the first, second, and third quartiles (*25th*, *50th*, and *75th*) or as exceedances $L_{75}$, $L_{50}$, and $L_{25}$. Upper error bars indicate the maximum levels ($L_{max}$). Lower error bars indicate the 5th percentile or $L_{95}$.

Table A-56. Received level statistics for pile driving installation of AM-37 at monitoring station AM37-75090.

| Sound level statistic | PK (dB re 1 µPa) | rms SPL (dB re 1 µPa$^2$) | SELss (dB re 1 µPa$^2$·s) |
|---|---|---|---|
| **Channel 1 (bottom)** | | | |
| $L_{max}$ | 176.7 | 165.3 | 158.1 |
| $L_5$ | 173.9 | 162.0 | 154.5 |
| $L_{25}$ | 172.2 | 160.2 | 153.3 |
| $L_{50}$ | 170.5 | 158.8 | 152.3 |
| $L_{75}$ | 168.3 | 157.0 | 151.0 |
| $L_{95}$ | 165.8 | 154.9 | 148.9 |
| $L_{mean}$ | 170.1 | 158.5 | 152.0 |
| **Channel 2 (mid-water)** | | | |
| $L_{max}$ | 179.9 | 168.1 | 158.0 |
| $L_5$ | 175.9 | 163.8 | 155.4 |
| $L_{25}$ | 173.7 | 161.4 | 154.0 |
| $L_{50}$ | 171.7 | 159.6 | 152.8 |
| $L_{75}$ | 169.0 | 157.3 | 151.2 |
| $L_{95}$ | 166.0 | 155.4 | 149.5 |
| $L_{mean}$ | 171.2 | 159.4 | 152.5 |

### A.7.2.3. Station AM37-2000

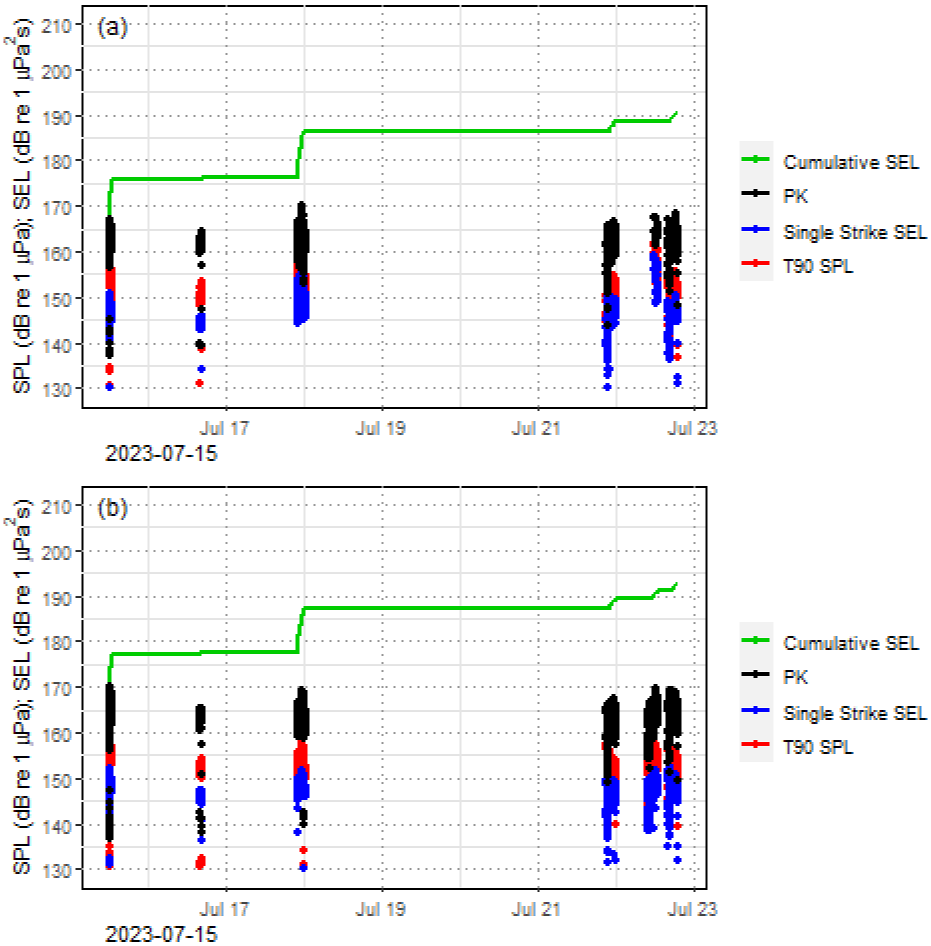


Figure A-75. Received levels for impact pile driving installation of AM-37 at monitoring station AM37-2000 for channel 1 (a) and channel 2 (b). Peak SPL (PK, black), rms SPL (T90 SPL, red), single strike SEL (blue) and cumulative SEL (green) versus time (UTC). For periods during which there was no pile driving the cSEL is necessarily displayed as a constant value over time.

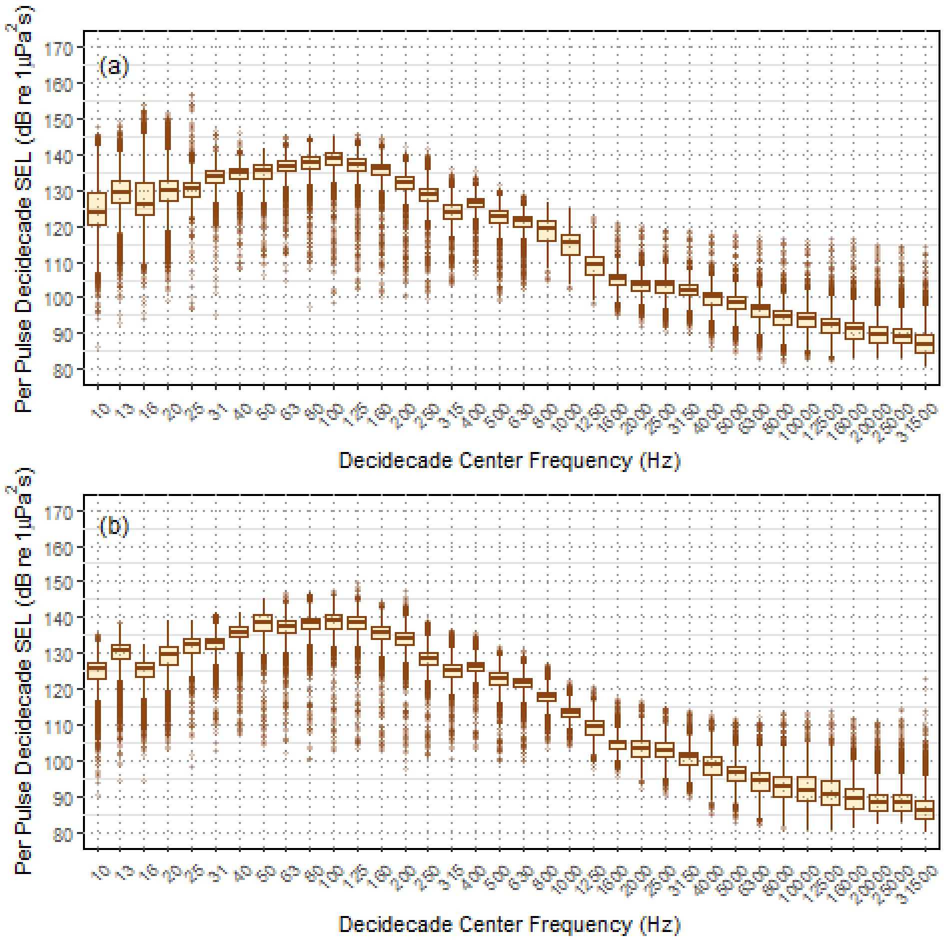


Figure A-76. Distribution of decidecade band level single strike SEL for pile driving installation of AM-37 at monitoring station AM37-2000 for channel 1 (a) and channel 2 (b). Beige bars indicate the first, second, and third quartiles (*25th*, *50th*, and *75th*) or as exceedances $L_{75}$, $L_{50}$, and $L_{25}$. Upper error bars indicate the maximum levels ($L_{max}$). Lower error bars indicate the 5th percentile or $L_{95}$.

Table A-57. Received level statistics for pile driving installation of AM-37 at monitoring station AM37-2000.

| Sound level statistic | PK (dB re 1 µPa) | rms SPL (dB re 1 µPa$^2$) | SELss (dB re 1 µPa$^2$·s) |
|---|---|---|---|
| **Channel 1 (bottom)** | | | |
| $L_{max}$ | 169.9 | 161.7 | 159.1 |
| $L_5$ | 165.1 | 154.4 | 149.8 |
| $L_{25}$ | 163.6 | 152.7 | 147.9 |
| $L_{50}$ | 162.6 | 151.9 | 147.1 |
| $L_{75}$ | 161.4 | 151.0 | 146.3 |
| $L_{95}$ | 159.6 | 149.3 | 145.0 |
| $L_{mean}$ | 162.4 | 151.8 | 147.1 |
| **Channel 2 (mid-water)** | | | |
| $L_{max}$ | 170.3 | 160.3 | 152.4 |
| $L_5$ | 166.8 | 155.6 | 149.9 |
| $L_{25}$ | 165.0 | 154.0 | 148.7 |
| $L_{50}$ | 163.5 | 152.8 | 147.8 |
| $L_{75}$ | 162.2 | 151.8 | 146.9 |
| $L_{95}$ | 160.3 | 150.3 | 145.4 |
| $L_{mean}$ | 163.5 | 152.8 | 147.7 |

### A.7.2.4. Station AM37-4000

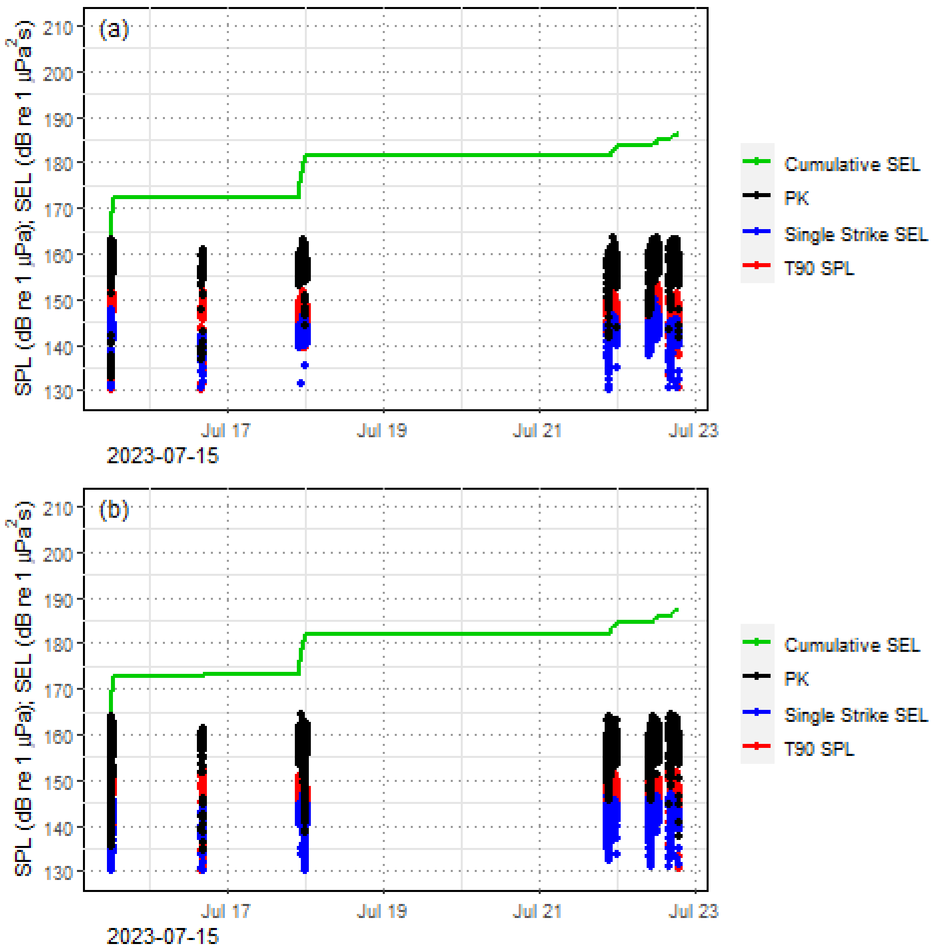


Figure A-77. Received levels for impact pile driving installation of AM-37 at monitoring station AM37-4000 for channel 1 (a) and channel 2 (b). Peak SPL (PK, black), rms SPL (T90 SPL, red), single strike SEL (blue) and cumulative SEL (green) versus time (UTC). For periods during which there is no pile driving the cSEL is necessarily displayed as a constant value over time.

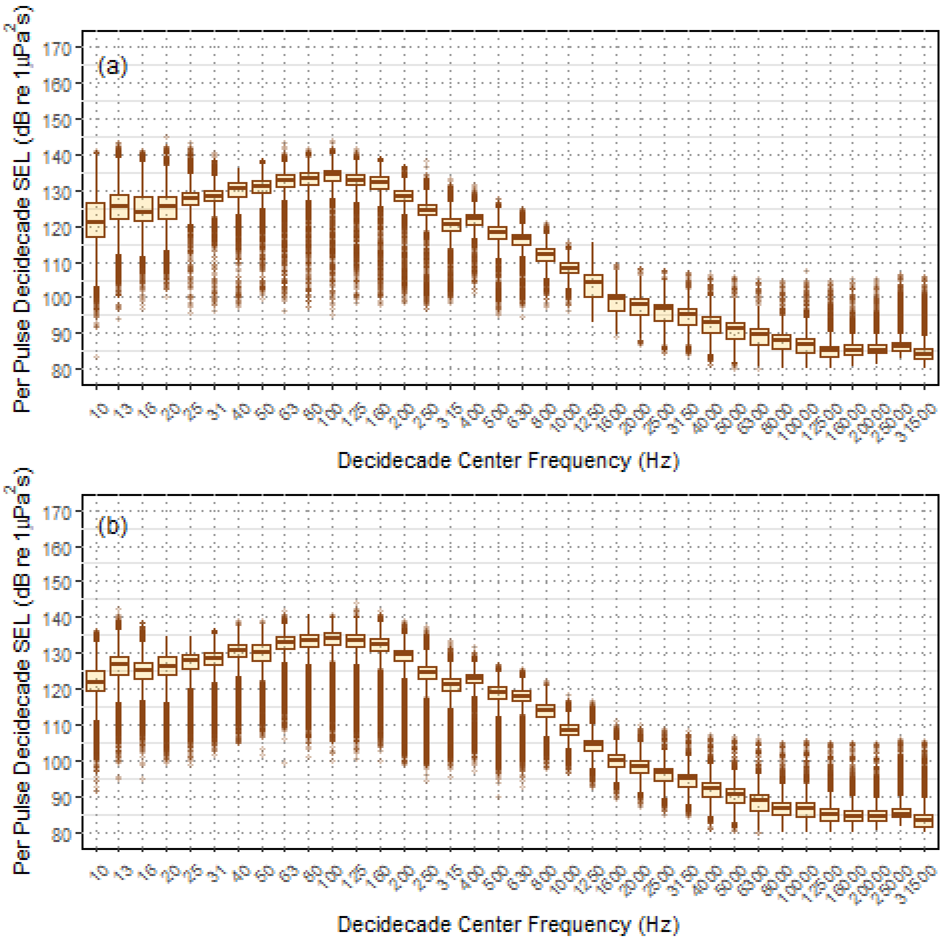


Figure A-78. Distribution of decidecade band level single strike SEL for pile driving installation of AM-37 at monitoring station AM37-4000 for channel 1 (a) and channel 2 (b). Beige bars indicate the first, second, and third quartiles (*25th*, *50th*, and *75th*) or as exceedances $L_{75}$, $L_{50}$, and $L_{25}$. Upper error bars indicate the maximum levels ($L_{max}$). Lower error bars indicate the 5th percentile or $L_{95}$.

Table A-58. Received level statistics for pile driving installation of AM-37 at monitoring station AM37-4000.

| Sound level statistic | PK (dB re 1 µPa) | rms SPL (dB re 1 µPa$^2$) | SELss (dB re 1 µPa$^2$·s) |
|---|---|---|---|
| **Channel 1 (bottom)** | | | |
| $L_{max}$ | 163.5 | 155.3 | 149.9 |
| $L_5$ | 160.6 | 150.3 | 144.9 |
| $L_{25}$ | 159.1 | 149.1 | 143.7 |
| $L_{50}$ | 158.0 | 148.2 | 142.8 |
| $L_{75}$ | 156.8 | 147.3 | 142.0 |
| $L_{95}$ | 155.0 | 145.8 | 140.7 |
| $L_{mean}$ | 157.9 | 148.1 | 142.8 |
| **Channel 2 (mid-water)** | | | |
| $L_{max}$ | 164.5 | 153.7 | 147.9 |
| $L_5$ | 160.6 | 150.2 | 144.7 |
| $L_{25}$ | 159.1 | 149.1 | 143.8 |
| $L_{50}$ | 158.1 | 148.3 | 143.1 |
| $L_{75}$ | 156.9 | 147.3 | 142.4 |
| $L_{95}$ | 154.6 | 144.7 | 140.4 |
| $L_{mean}$ | 157.7 | 147.8 | 142.7 |

## A.7.2.5. Station AM37-8000

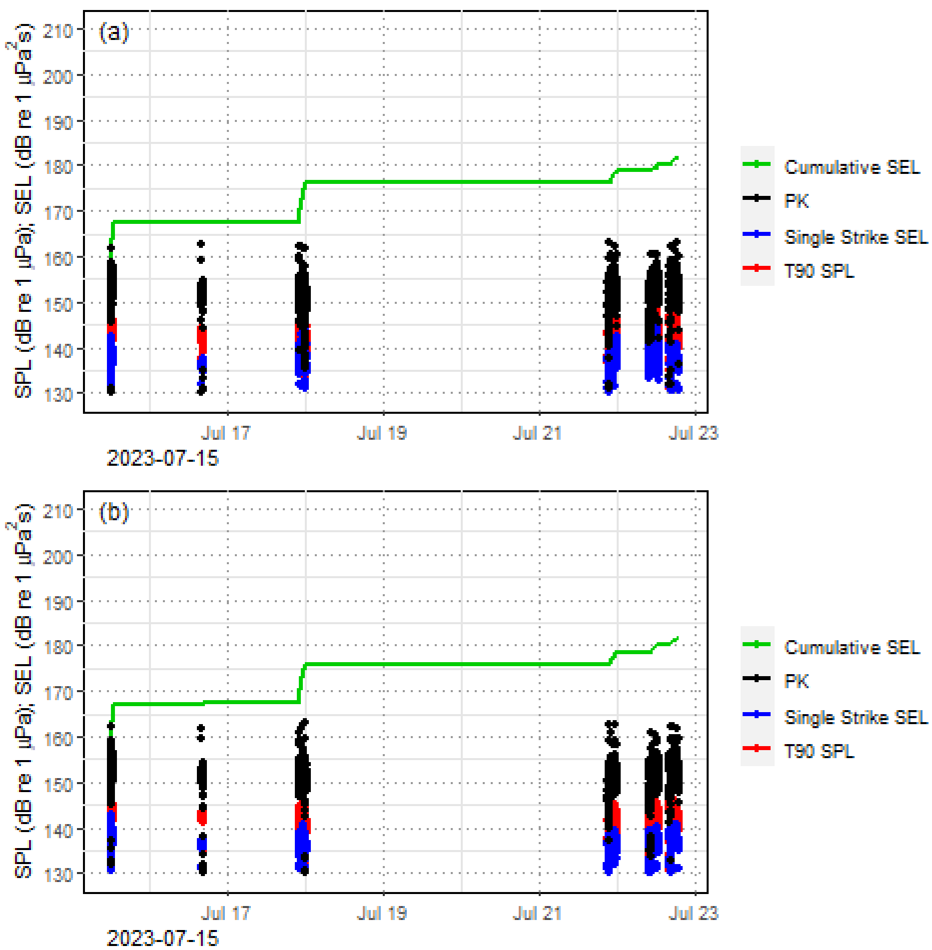


Figure A-79. Received levels for impact pile driving installation of AM-37 at monitoring station AM37-8000 for channel 1 (a) and channel 2 (b). Peak SPL (PK, black), rms SPL (T90 SPL, red), single strike SEL (blue) and cumulative SEL (green) versus time (UTC). For periods during which there is no pile driving the cSEL is necessarily displayed as a constant value over time.

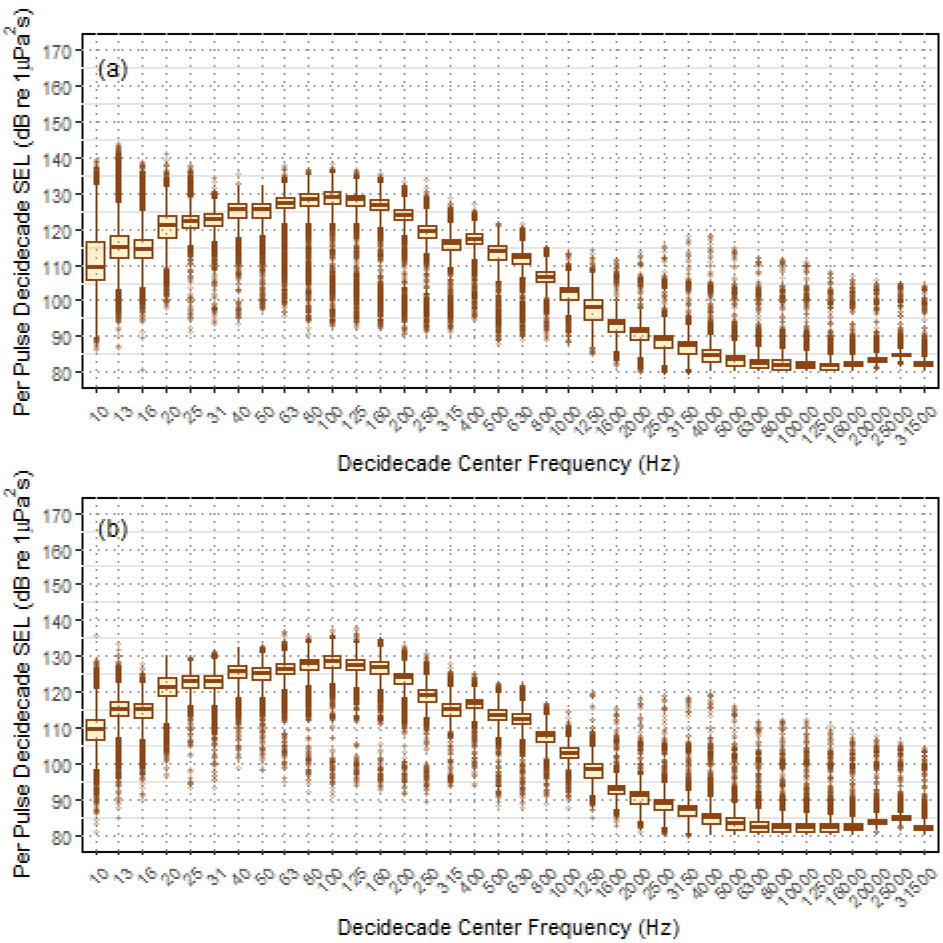


Figure A-80. Distribution of decidecade band level single strike SEL for pile driving installation of AM-37 at monitoring station AM37-8000 for channel 1 (a) and channel 2 (b). Beige bars indicate the first, second, and third quartiles (*25th*, *50th*, and *75th*) or as exceedances $L_{75}$, $L_{50}$, and $L_{25}$. Upper error bars indicate the maximum levels ($L_{max}$). Lower error bars indicate the 5th percentile or $L_{95}$.

Table A-59. Received level statistics for pile driving installation of AM-37 at monitoring station AM37-8000.

| Sound level statistic | PK (dB re 1 µPa) | rms SPL (dB re 1 µPa$^2$) | SELss (dB re 1 µPa$^2$·s) |
|---|---|---|---|
| **Channel 1 (bottom)** | | | |
| $L_{max}$ | 163.1 | 150.6 | 149.3 |
| $L_5$ | 155.4 | 145.0 | 139.7 |
| $L_{25}$ | 153.7 | 143.7 | 138.4 |
| $L_{50}$ | 152.5 | 142.9 | 137.6 |
| $L_{75}$ | 151.3 | 141.9 | 136.6 |
| $L_{95}$ | 149.5 | 140.5 | 135.2 |
| $L_{mean}$ | 152.4 | 142.8 | 137.5 |
| **Channel 2 (mid-water)** | | | |
| $L_{max}$ | 163.2 | 148.6 | 143.0 |
| $L_5$ | 154.3 | 144.2 | 138.8 |
| $L_{25}$ | 152.7 | 143.0 | 137.8 |
| $L_{50}$ | 151.6 | 142.3 | 137.1 |
| $L_{75}$ | 150.5 | 141.4 | 136.4 |
| $L_{95}$ | 148.9 | 139.9 | 134.9 |
| $L_{mean}$ | 151.6 | 142.1 | 137.0 |

## A.7.3. Ranges to Acoustic Thresholds

Table A-60. Isopleth distances to NMFS physiological thresholds for impact driving installation of pile AM-37.

| Group | Injury: PK | | | | Injury: cSEL | | | |
|---|---|---|---|---|---|---|---|---|
| | Level (dB re 1µPa) | Predicted (m) | Measured (m) | Measured w/ attn. coeff. (m) | Level (dB re 1 µPa$^2$·s) | Predicted (m) | Measured (m) | Measured w/ attn. coeff. (m) |
| LFC | 219 | 17 | 10 | 10 | 183 | 7,253 | 2,610 | 2,810 |
| MFC | 230 | 5 | 10 | 10 | 185 | 71 | 10 | 10 |
| HFC | 202 | 119 | 40 | 50 | 155 | 564 | 220 | 280 |
| PW | 218 | 19 | 10 | 10 | 185 | 977 | 180 | 120 |
| ST | 232 | 0 | 10 | 10 | 204 | 381 | 260 | 200 |
| AS | 206 | 78 | 20 | 30 | 187 | 7,803 | 4,060 | 4,410 |

Table A-61. Isopleth distances to NMFS behavioral thresholds for impact driving installation of pile AM-37.

| Group | Behavior: SPL | | | |
|---|---|---|---|---|
| | Level (dB re 1µPa$^2$) | Predicted (m) | Measured (m) | Measured w/ attn. coeff. (m) |
| MM | 160 | 3,330 | 1,180 | 1,180 |
| ST | 175 | 727 | 180 | 180 |
| AS | 150 | 7,355 | 4,220 | 4,200 |

## A.7.4. Regression Analysis for Transmission Loss

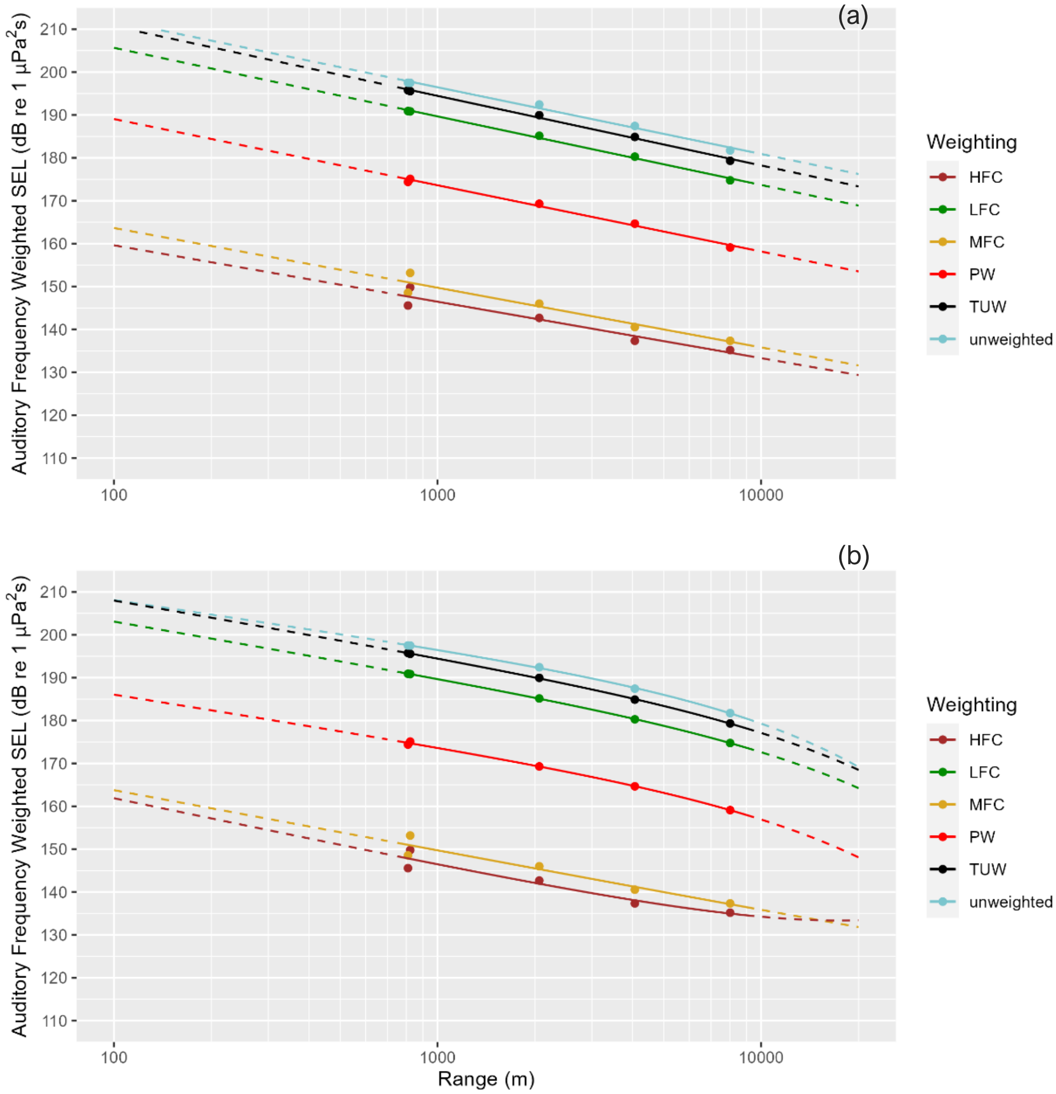


Figure A-81. Transmission loss determination based on regression analysis without (a) and with (b) intrinsic attenuation for the maximum received cumulative SEL (cSEL) at each recording station during installation of pile AM-37 on 15–22 Jul 2023.

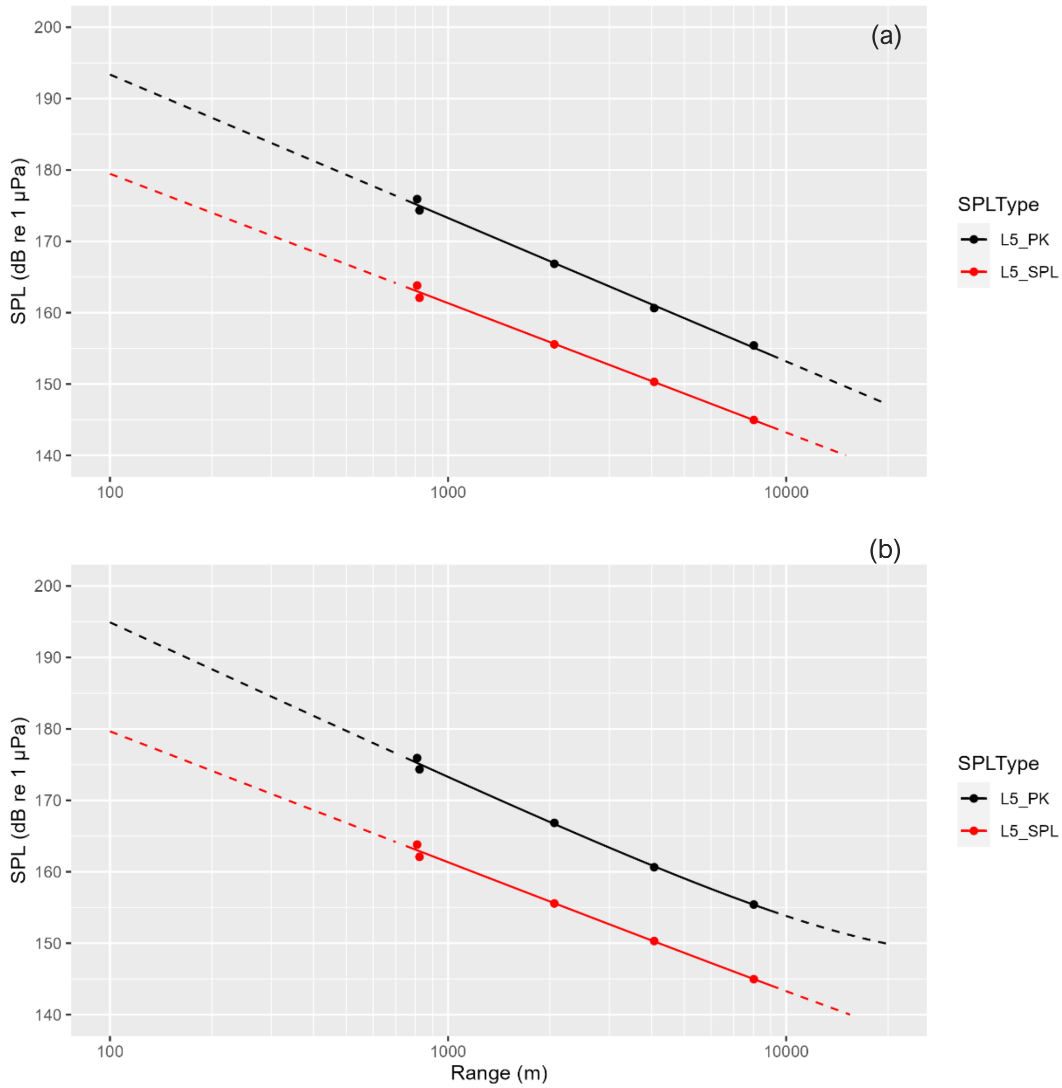


Figure A-82. Transmission loss determination based on regression analysis without (a) and with (b) intrinsic attenuation for $L_5$ PK and SPL maxima at each recording station during installation of pile AM-37 on 15–22 Jul 2023.

Table A-62. Regression analysis fitting coefficients for transmission loss with and without intrinsic attenuation for installation of pile AM-37 on 15–22 Jul 2023.

| Metric | A (dB/decade m) A*log(r) | A (dB/decade m) A*log(r) + αr/1000 | α (dB/ m) A*log(r) + αr/1000 |
|---|---|---|---|
| PK ($L_5$) (dB re 1 µPa) | -20.1 | -21.9 | 0.268 x $10^{-3}$ [a] |
| rms SPL ($L_5$) (dB re 1 µPa$^2$) | -18.1 | -18.4 | 0.034 x $10^{-3}$ [a] |
| cSEL (dB re 1 µPa$^2$·s) | -15.6 | -11.1 | -0.678 x $10^{-3}$ |
| cSEL, LF (dB re 1 µPa$^2$·s) | -16.0 | -13.0 | -0.447 x $10^{-3}$ |
| cSEL, MF (dB re 1 µPa$^2$·s) | -13.9 | -14.1 | -0.021 x $10^{-3}$ |
| cSEL, HF (dB re 1 µPa$^2$·s) | -13.2 | -15.8 | -0.392 x $10^{-3}$ |
| cSEL, PW (dB re 1 µPa$^2$·s) | -15.4 | -12.0 | -0.522 x $10^{-3}$ |
| cSEL, TU (dB re 1 µPa$^2$·s) | -16.2 | -13.1 | -0.468 x $10^{-3}$ |

[a] Positive attenuation coefficients could indicate ambient noise contamination and may not be valid.

## A.8. Foundation AQ-38

Summary of measurements are shown in Table A-63. Channel 1 (bottom hydrophone) at station AQ38-750 was not functioning properly and was excluded from the analysis.

### A.8.1. Summary of Measured Sound Levels

Table A-63. Summary of Autonomous Multichannel Acoustic Recorder (AMAR) locations and measured sound levels for pile AQ-38. Computed PK and SPL levels are shown for the $L_{max}$.

| Location (nominal) | Recorder ID | Distance (m) | Water depth (m) | Channel | Impulses Detected* (clipped) | PK (dB re 1 µPa) | SPL (dB re 1 µPa$^2$) | cSEL (dB re 1 µPa$^2$·s) |
|---|---|---|---|---|---|---|---|---|
| 750 | AMAR-863 | 767 | 43.2 | | | | | |
| | | | | 2 | 2867 | 180.2 | 170.5 | 194.3 |
| 750 @ 90° | AMAR-865 | 729 | 41.0 | 1 | 673 | 179.4 | 170.8 | 189.7 |
| | | | | 2 | 820 | 180.0 | 168.9 | 188.6 |
| 2000 | AMAR-855 | 1998 | 47.0 | 1 | 1694 | 176.0 | 165.3 | 188.8 |
| | | | | 2 | 2535 | 174.6 | 164.4 | 190.3 |
| 4000 | AMAR-860 | 4017 | 46.3 | 1 | 2673 | 168.4 | 160.1 | 183.9 |
| | | | | 2 | 2670 | 168.8 | 159.4 | 184.3 |
| 8000 | AMAR-603 | 8033 | 47.5 | 1 | 2423 | 164.8 | 155.2 | 179.4 |
| | | | | 2 | 2509 | 165.2 | 153.9 | 178.6 |

* Number of strikes produced (from hammer log): 3023

## A.8.2. Sound Levels per Station

### A.8.2.1. Station AQ38-750

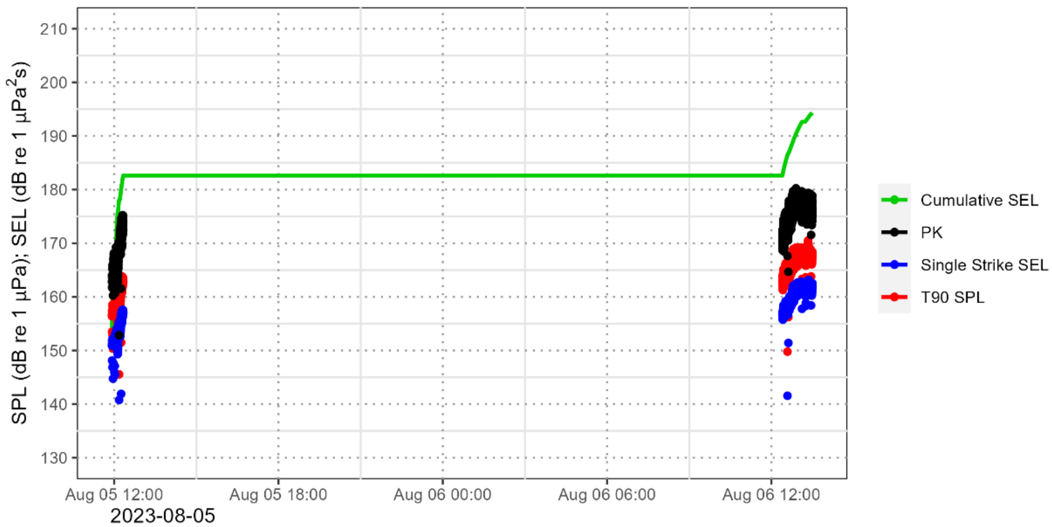


Figure A-83. Received levels for impact pile driving installation of AQ-38 at monitoring station AQ38-750 for channel 2. Peak SPL (PK, black), rms SPL (T90 SPL, red), single strike SEL (blue) and cumulative SEL (green) versus time (UTC). For periods during which there is no pile driving the cSEL is necessarily displayed as a constant value over time.

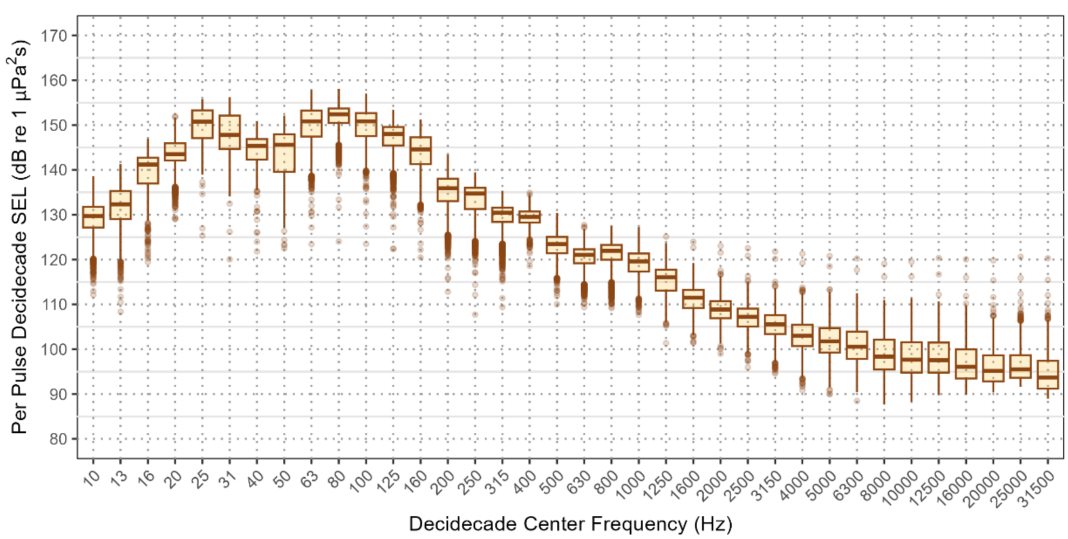


Figure A-84. Distribution of decidecade band level single strike SEL for pile driving installation of AQ-38 at monitoring station AQ38-750 for channel 2. Beige bars indicate the first, second, and third quartiles (*25th*, *50th*, and *75th*) or as exceedances $L_{75}$, $L_{50}$, and $L_{25}$. Upper error bars indicate the maximum levels ($L_{max}$). Lower error bars indicate the 5th percentile or $L_{95}$.

Table A-64. Received level statistics for pile driving installation of AQ-38 at monitoring station AQ38-750.

| Sound level statistic | PK (dB re 1 µPa) | rms SPL (dB re 1 µPa$^2$) | SELss (dB re 1 µPa$^2$·s) |
|---|---|---|---|
| **Channel 2 (mid-water)** | | | |
| $L_{max}$ | 180.2 | 170.5 | 163.2 |
| $L_5$ | 178.4 | 168.3 | 162.3 |
| $L_{25}$ | 177.1 | 167.4 | 161.5 |
| $L_{50}$ | 175.4 | 165.8 | 159.6 |
| $L_{75}$ | 172.0 | 162.9 | 156.9 |
| $L_{95}$ | 166.0 | 157.8 | 152.2 |
| $L_{mean}$ | 174.2 | 164.7 | 158.7 |

### A.8.2.2. Station AQ38-75090

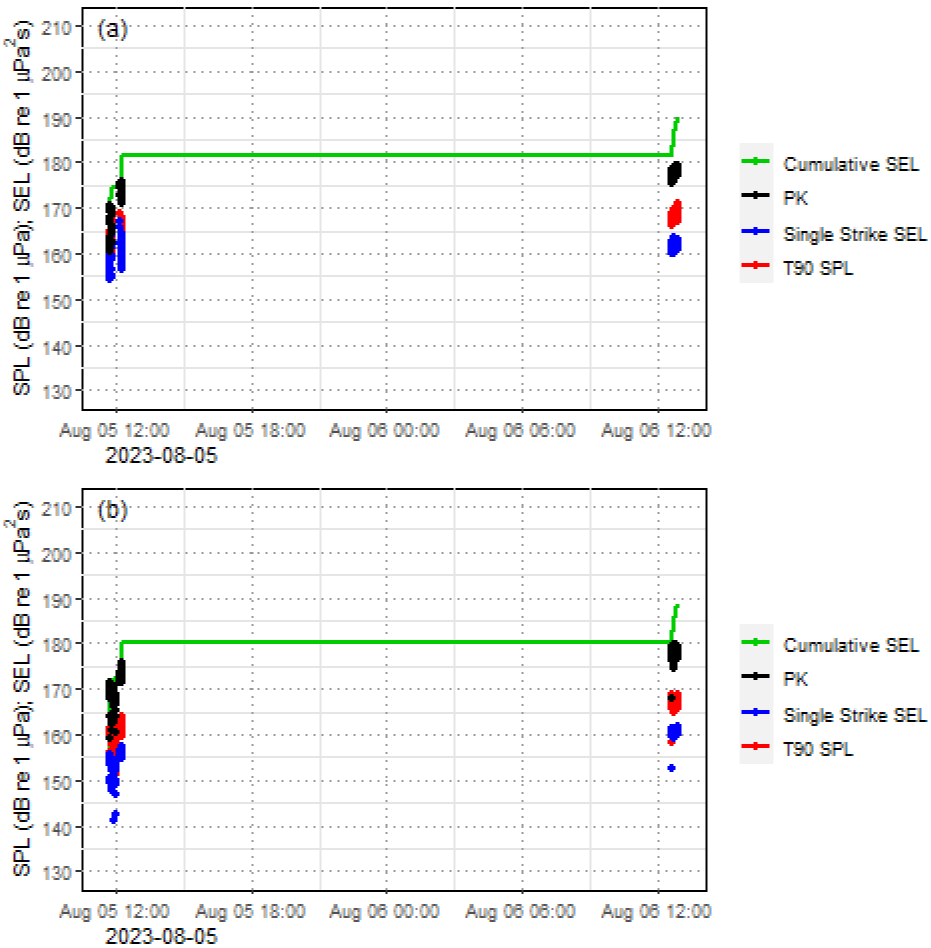


Figure A-85. Received levels for impact pile driving installation of AQ-38 at monitoring station AQ38-75090, for channel 1 (a) and channel 2 (b). Peak SPL (PK, black), rms SPL (T90 SPL, red), single strike SEL (blue) and cumulative SEL (green) versus time (UTC). For periods during which there is no pile driving the cSEL is necessarily displayed as a constant value over time.

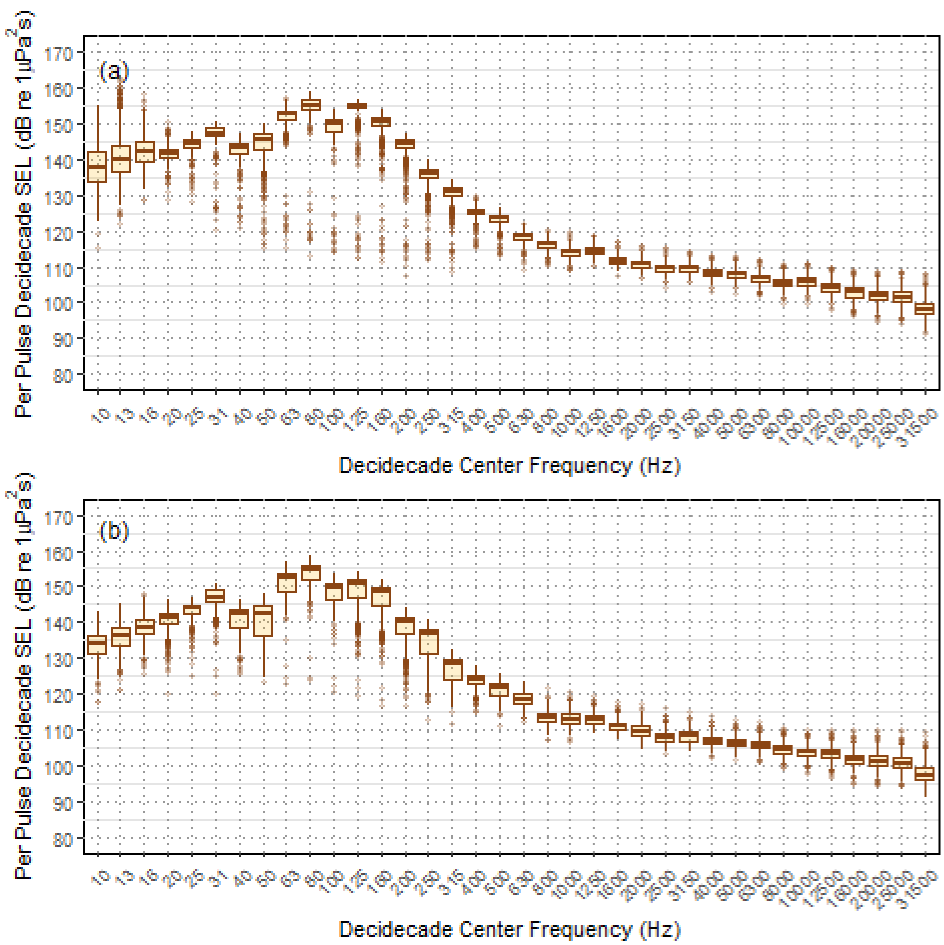


Figure A-86. Distribution of decidecade band level single strike SEL for pile driving installation of AQ-38 at monitoring station AQ38-75090 for channel 1 (a) and channel 2 (b). Beige bars indicate the first, second, and third quartiles (*25th*, *50th*, and *75th*) or as exceedances $L_{75}$, $L_{50}$, and $L_{25}$. Upper error bars indicate the maximum levels ($L_{max}$). Lower error bars indicate the 5th percentile or $L_{95}$.

Table A-65. Received level statistics for pile driving installation of AQ-38 at monitoring station AQ38-75090.

| Sound level statistic | PK (dB re 1 µPa) | rms SPL (dB re 1 µPa$^2$) | SELss (dB re 1 µPa$^2$·s) |
|---|---|---|---|
| **Channel 1 (bottom)** | | | |
| $L_{max}$ | 179.4 | 170.8 | 167.1 |
| $L_5$ | 178.8 | 169.5 | 162.6 |
| $L_{25}$ | 178.2 | 168.7 | 162.0 |
| $L_{50}$ | 177.5 | 168.1 | 161.6 |
| $L_{75}$ | 176.5 | 167.3 | 161.1 |
| $L_{95}$ | 170.4 | 162.9 | 158.0 |
| $L_{mean}$ | 176.6 | 167.5 | 161.2 |
| **Channel 2 (mid-water)** | | | |
| $L_{max}$ | 180.0 | 168.9 | 161.8 |
| $L_5$ | 179.1 | 167.8 | 161.2 |
| $L_{25}$ | 178.4 | 167.1 | 160.8 |
| $L_{50}$ | 177.7 | 166.5 | 160.3 |
| $L_{75}$ | 174.0 | 162.4 | 156.6 |
| $L_{95}$ | 168.0 | 158.7 | 153.0 |
| $L_{mean}$ | 175.9 | 164.9 | 158.7 |

### A.8.2.3. Station AQ38-2000

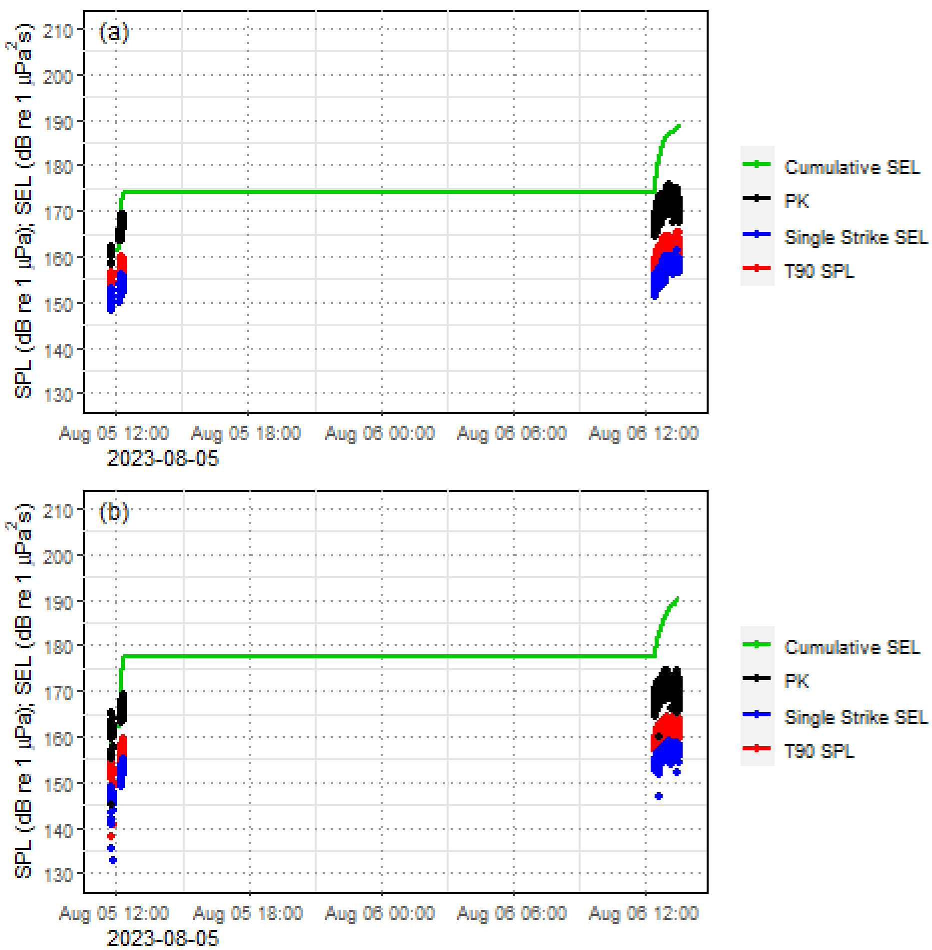


Figure A-87. Received levels for impact pile driving installation of AQ-38 at monitoring station AQ38-2000 for channel 1 (a) and channel 2 (b). Peak SPL (PK, black), rms SPL (T90 SPL, red), single strike SEL (blue) and cumulative SEL (green) versus time (UTC). For periods during which there was no pile driving the cSEL is necessarily displayed as a constant value over time.

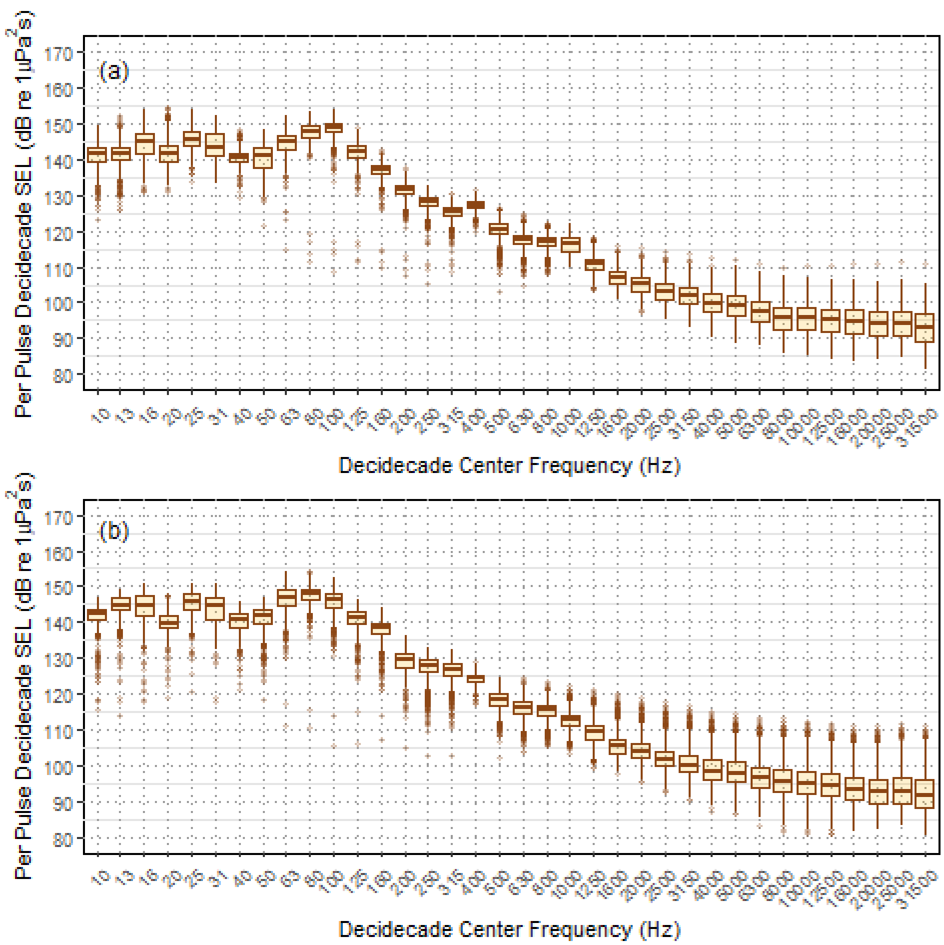


Figure A-88. Distribution of decidecade band level single strike SEL for pile driving installation of AQ-38 at monitoring station AQ38-2000 for channel 1 (a) and channel 2 (b). Beige bars indicate the first, second, and third quartiles (*25th*, *50th*, and *75th*) or as exceedances $L_{75}$, $L_{50}$, and $L_{25}$. Upper error bars indicate the maximum levels ($L_{max}$). Lower error bars indicate the 5th percentile or $L_{95}$.

Table A-66. Received level statistics for pile driving installation of AQ-38 at monitoring station AQ38-2000.

| Sound level statistic | PK (dB re 1 µPa) | rms SPL (dB re 1 µPa$^2$) | SELss (dB re 1 µPa$^2$·s) |
|---|---|---|---|
| **Channel 1 (bottom)** | | | |
| $L_{max}$ | 176.0 | 165.3 | 161.5 |
| $L_5$ | 173.8 | 163.5 | 158.7 |
| $L_{25}$ | 172.1 | 162.3 | 157.8 |
| $L_{50}$ | 170.7 | 161.0 | 156.1 |
| $L_{75}$ | 169.2 | 159.4 | 154.8 |
| $L_{95}$ | 166.3 | 157.4 | 153.0 |
| $L_{mean}$ | 170.5 | 160.7 | 156.1 |
| **Channel 2 (mid-water)** | | | |
| $L_{max}$ | 174.6 | 164.4 | 159.0 |
| $L_5$ | 172.4 | 162.9 | 158.2 |
| $L_{25}$ | 171.0 | 162.0 | 157.4 |
| $L_{50}$ | 169.9 | 161.1 | 156.4 |
| $L_{75}$ | 168.4 | 159.5 | 154.7 |
| $L_{95}$ | 165.0 | 156.6 | 152.0 |
| $L_{mean}$ | 169.4 | 160.5 | 155.8 |

## A.8.2.4. Station AQ38-4000

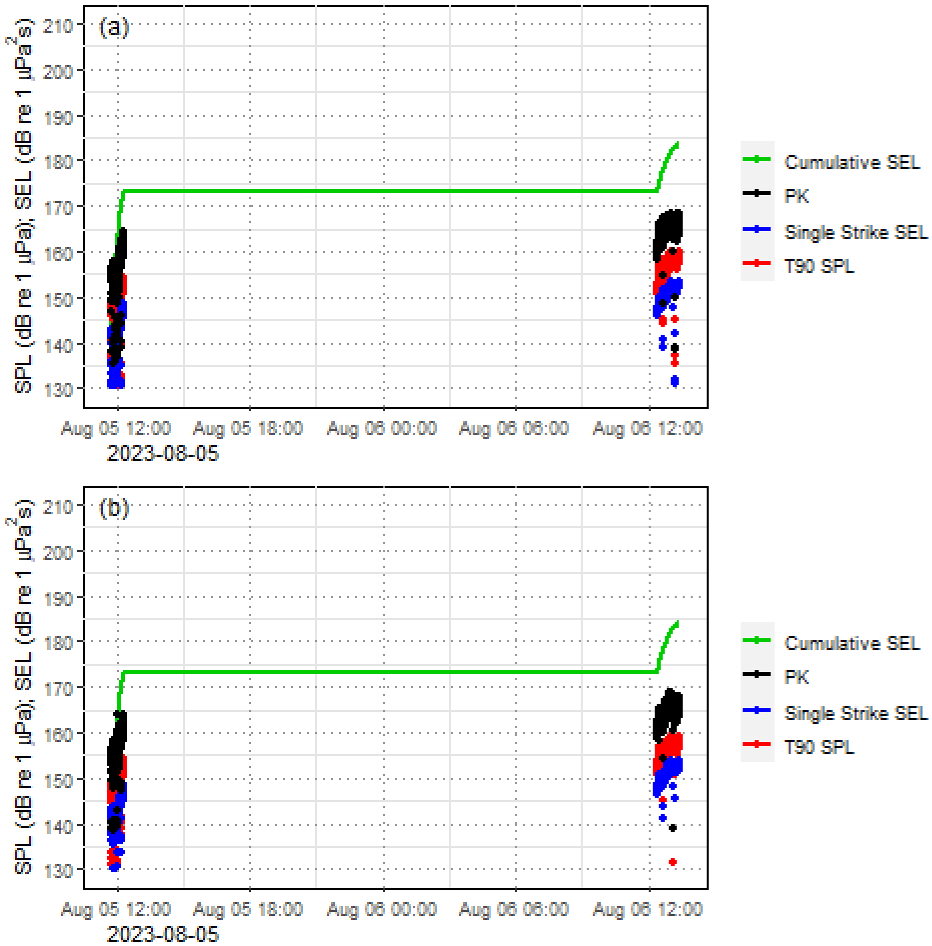


Figure A-89. Received levels for impact pile driving installation of AQ-38 at monitoring station AQ38-4000 for channel 1 (a) and channel 2 (b). Peak SPL (PK, black), rms SPL (T90 SPL, red), single strike SEL (blue) and cumulative SEL (green) versus time (UTC). For periods during which there is no pile driving the cSEL is necessarily displayed as a constant value over time.

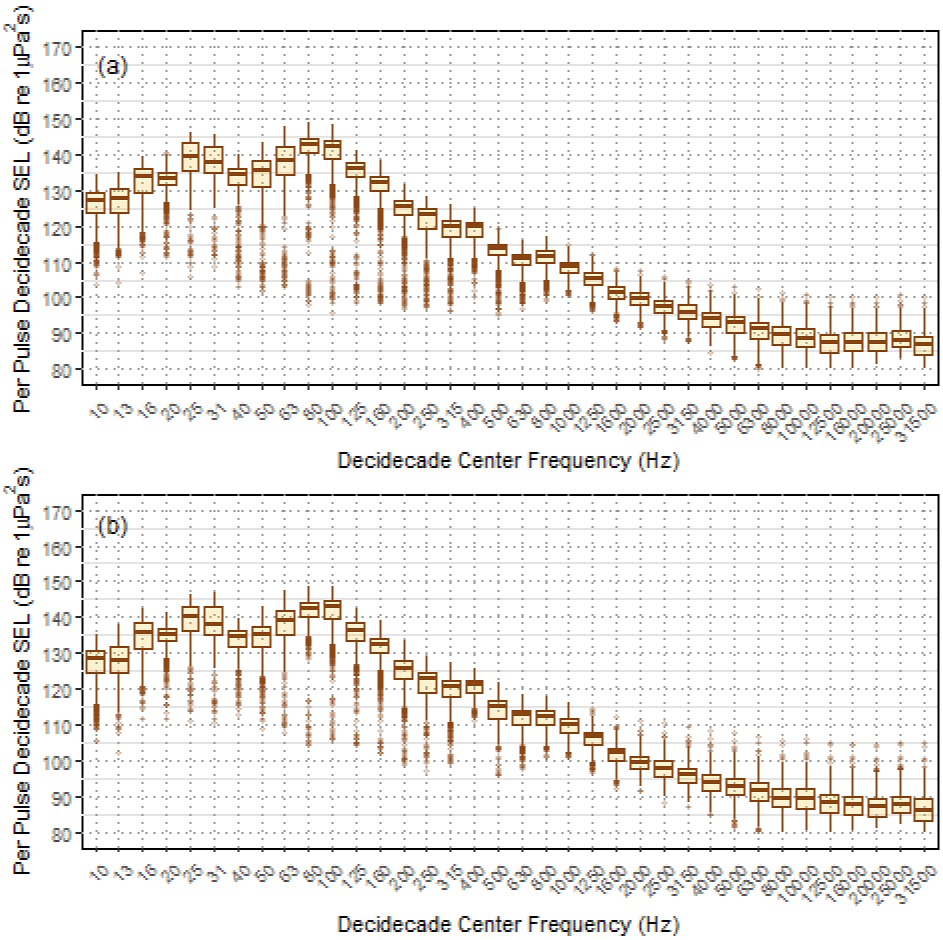


Figure A-90. Distribution of decidecade band level single strike SEL for pile driving installation of AQ-38 at monitoring station AQ38-4000 for channel 1 (a) and channel 2 (b). Beige bars indicate the first, second, and third quartiles (*25th*, *50th*, and *75th*) or as exceedances $L_{75}$, $L_{50}$, and $L_{25}$. Upper error bars indicate the maximum levels ($L_{max}$). Lower error bars indicate the 5th percentile or $L_{95}$.

Table A-67. Received level statistics for pile driving installation of AQ-38 at monitoring station AQ38-4000.

| Sound level statistic | PK (dB re 1 µPa) | rms SPL (dB re 1 µPa$^2$) | SELss (dB re 1 µPa$^2$·s) |
|---|---|---|---|
| **Channel 1 (bottom)** | | | |
| $L_{max}$ | 168.4 | 160.1 | 153.5 |
| $L_5$ | 166.6 | 158.4 | 152.5 |
| $L_{25}$ | 165.3 | 157.2 | 151.4 |
| $L_{50}$ | 164.2 | 155.3 | 149.6 |
| $L_{75}$ | 160.8 | 152.3 | 146.9 |
| $L_{95}$ | 154.7 | 147.0 | 141.6 |
| $L_{mean}$ | 162.5 | 154.1 | 148.5 |
| **Channel 2 (mid-water)** | | | |
| $L_{max}$ | 168.8 | 159.4 | 153.8 |
| $L_5$ | 166.7 | 158.0 | 152.6 |
| $L_{25}$ | 165.1 | 157.0 | 151.8 |
| $L_{50}$ | 163.5 | 155.4 | 150.0 |
| $L_{75}$ | 160.6 | 152.4 | 147.1 |
| $L_{95}$ | 155.0 | 147.2 | 142.2 |
| $L_{mean}$ | 162.4 | 154.1 | 148.9 |

### A.8.2.5. Station AQ38-8000

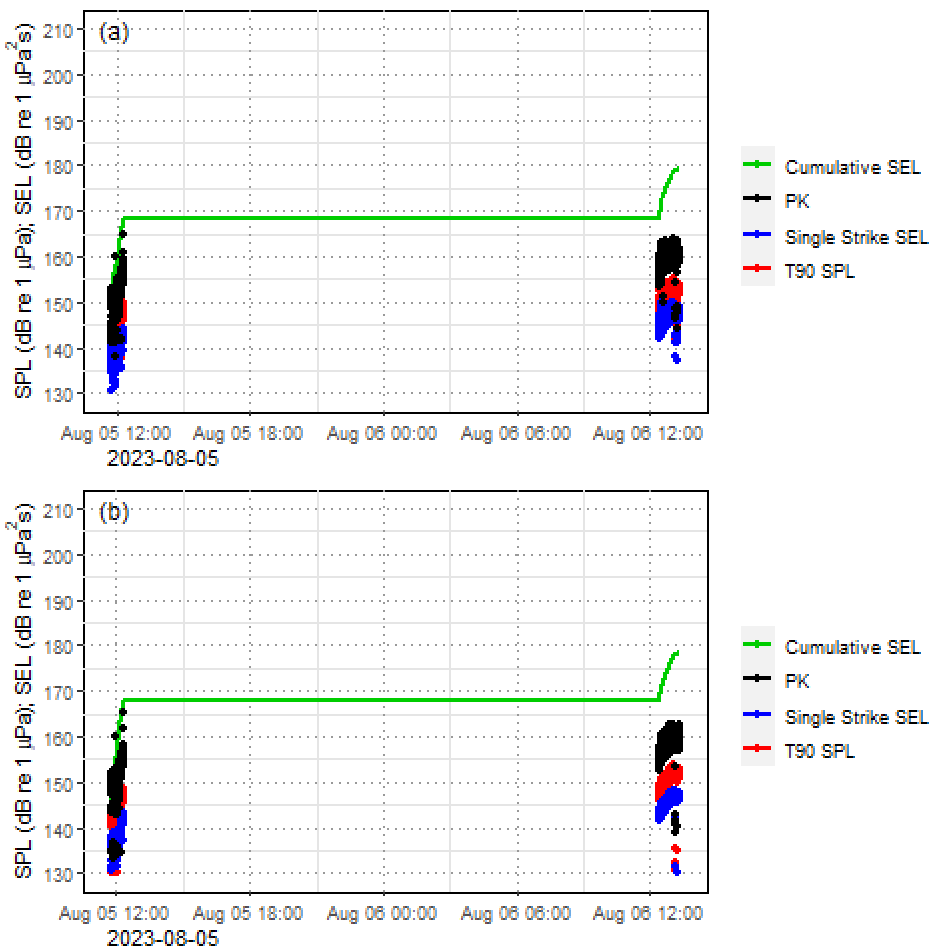


Figure A-91. Received levels for impact pile driving installation of AQ-38 at monitoring station AQ38-8000 for channel 1 (a) and channel 2 (b). Peak SPL (PK, black), rms SPL (T90 SPL, red), single strike SEL (blue) and cumulative SEL (green) versus time (UTC). For periods during which there is no pile driving the cSEL is necessarily displayed as a constant value over time.

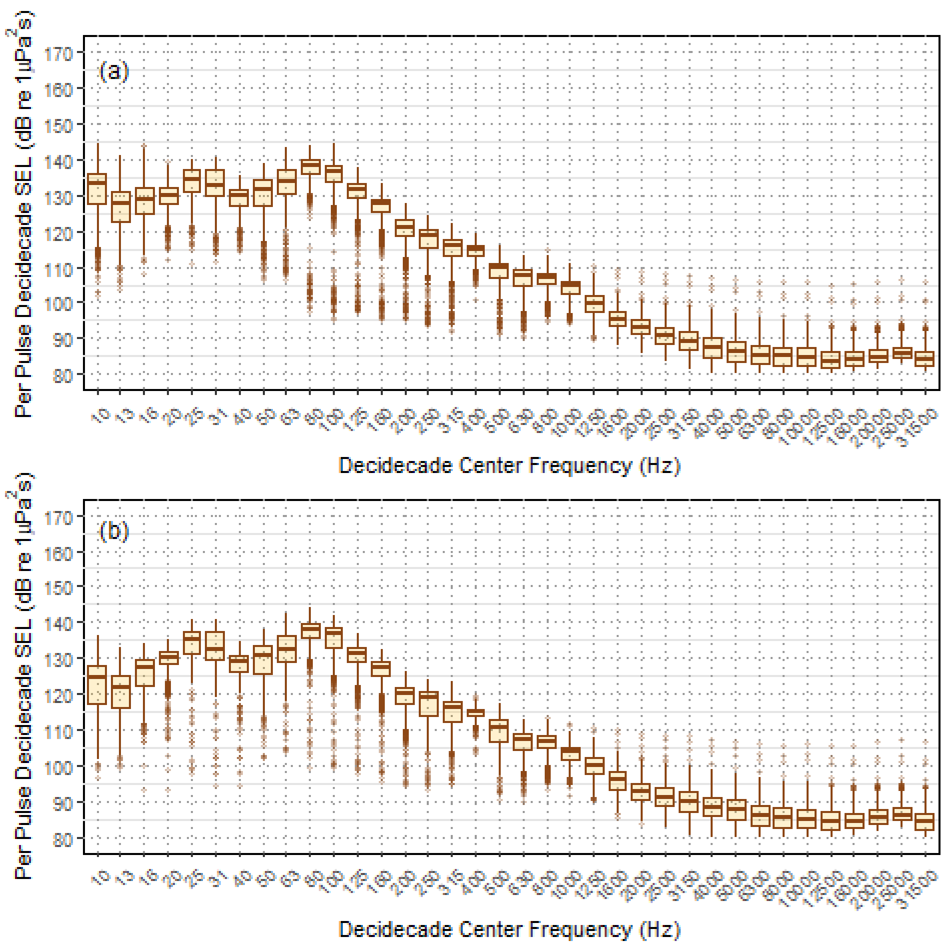


Figure A-92. Distribution of decidecade band level single strike SEL for pile driving installation of AQ-38 at monitoring station AQ38-8000 for channel 1 (a) and channel 2 (b). Beige bars indicate the first, second, and third quartiles (*25th*, *50th*, and *75th*) or as exceedances $L_{75}$, $L_{50}$, and $L_{25}$. Upper error bars indicate the maximum levels ($L_{max}$). Lower error bars indicate the 5th percentile or $L_{95}$.

Table A-68. Received level statistics for pile driving installation of AQ-38 at monitoring station AQ38-8000.

| Sound level statistic | PK (dB re 1 µPa) | rms SPL (dB re 1 µPa$^2$) | SELss (dB re 1 µPa$^2$·s) |
|---|---|---|---|
| **Channel 1 (bottom)** | | | |
| $L_{max}$ | 164.8 | 155.2 | 150.0 |
| $L_5$ | 161.9 | 153.3 | 148.0 |
| $L_{25}$ | 160.4 | 152.3 | 147.0 |
| $L_{50}$ | 159.1 | 151.1 | 145.9 |
| $L_{75}$ | 156.2 | 147.9 | 142.7 |
| $L_{95}$ | 149.7 | 142.6 | 138.0 |
| $L_{mean}$ | 159.0 | 150.8 | 145.6 |
| **Channel 2 (mid-water)** | | | |
| $L_{max}$ | 165.2 | 153.9 | 148.2 |
| $L_5$ | 160.6 | 152.5 | 147.2 |
| $L_{25}$ | 159.2 | 151.6 | 146.4 |
| $L_{50}$ | 157.8 | 149.8 | 144.7 |
| $L_{75}$ | 154.6 | 146.8 | 141.8 |
| $L_{95}$ | 149.5 | 141.5 | 136.9 |
| $L_{mean}$ | 157.7 | 149.8 | 144.6 |

## A.8.3. Ranges to Acoustic Thresholds

Table A-69. Isopleth distances to NMFS physiological thresholds for impact driving installation of pile AQ-38.

| Group | Injury: PK | | | | Injury: cSEL | | | |
|---|---|---|---|---|---|---|---|---|
| | Level (dB re 1µPa) | Predicted (m) | Measured (m) | Measured w/ attn. coeff. (m) | Level (dB re 1 µPa²·s) | Predicted (m) | Measured (m) | Measured w/ attn. coeff. (m) |
| LFC | 219 | 17 | 10 | 10 | 183 | 3,191 | 890 | 870 |
| MFC | 230 | 5 | 10 | 10 | 185 | 43 | 10 | 10 |
| HFC | 202 | 119 | 30 | 10 | 155 | 71 | 40 | 10 |
| PW | 218 | 19 | 10 | 10 | 185 | 153 | 30 | 10 |
| ST | 232 | 0 | 10 | 10 | 204 | 161 | 60 | 10 |
| AS | 206 | 78 | 20 | 10 | 187 | 6,894 | 2,300 | 3,140 |

Table A-70. Isopleth distances to NMFS behavioral thresholds for impact driving installation of pile AQ-38.

| Group | Behavior: SPL | | | |
|---|---|---|---|---|
| | Level (dB re 1µPa²) | Predicted (m) | Measured (m) | Measured w/ attn. coeff. (m) |
| MM | 160 | 4,121 | 3,060 | 3,290 |
| ST | 175 | 1,400 | 300 | 250 |
| AS | 150 | 9,229 | 14,280 | 11,440 |

## A.8.4. Regression Analysis for Transmission Loss

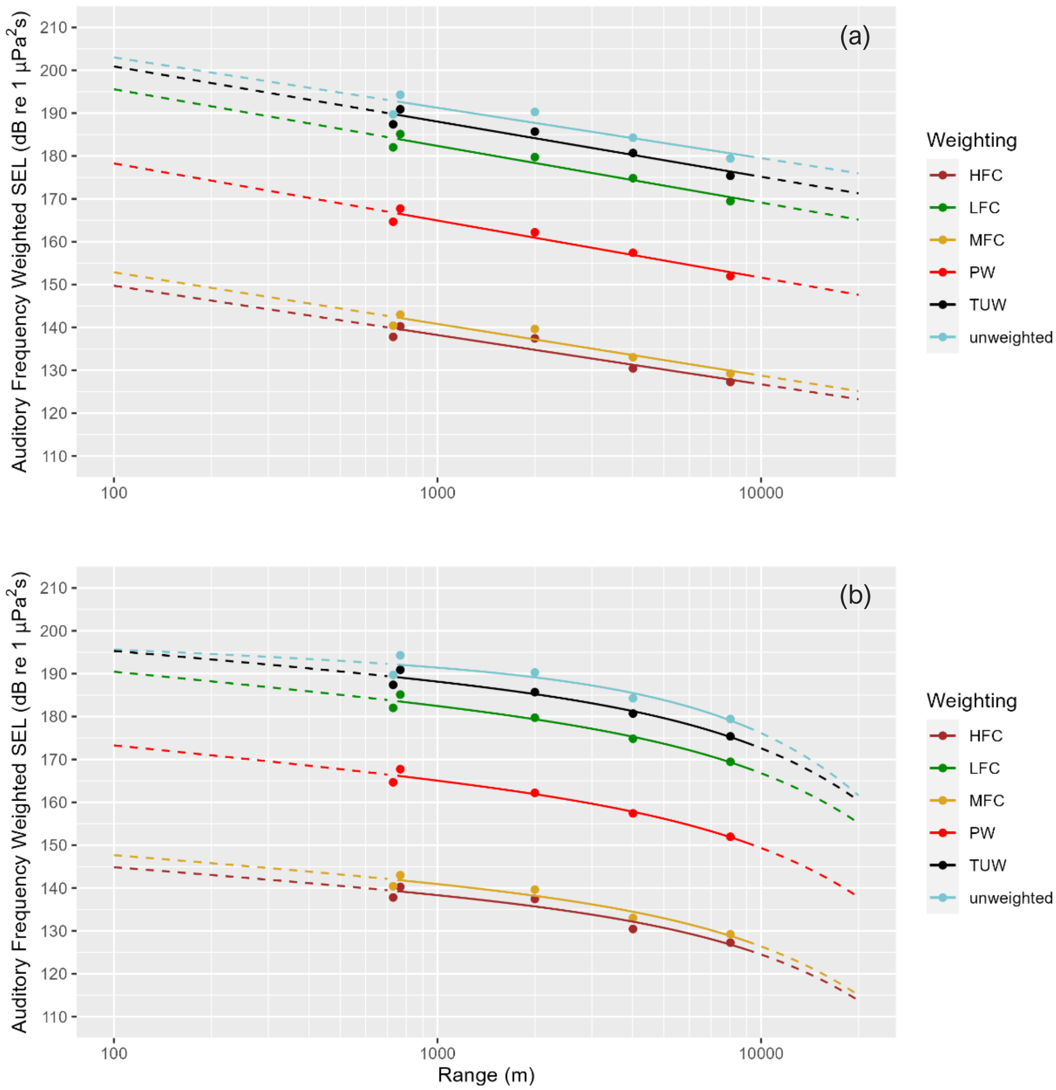


Figure A-93. Transmission loss determination based on regression analysis without (a) and with (b) intrinsic attenuation for the maximum received cumulative SEL (cSEL) at each recording station during installation of pile AQ-38 on 5–6 Aug 2023.

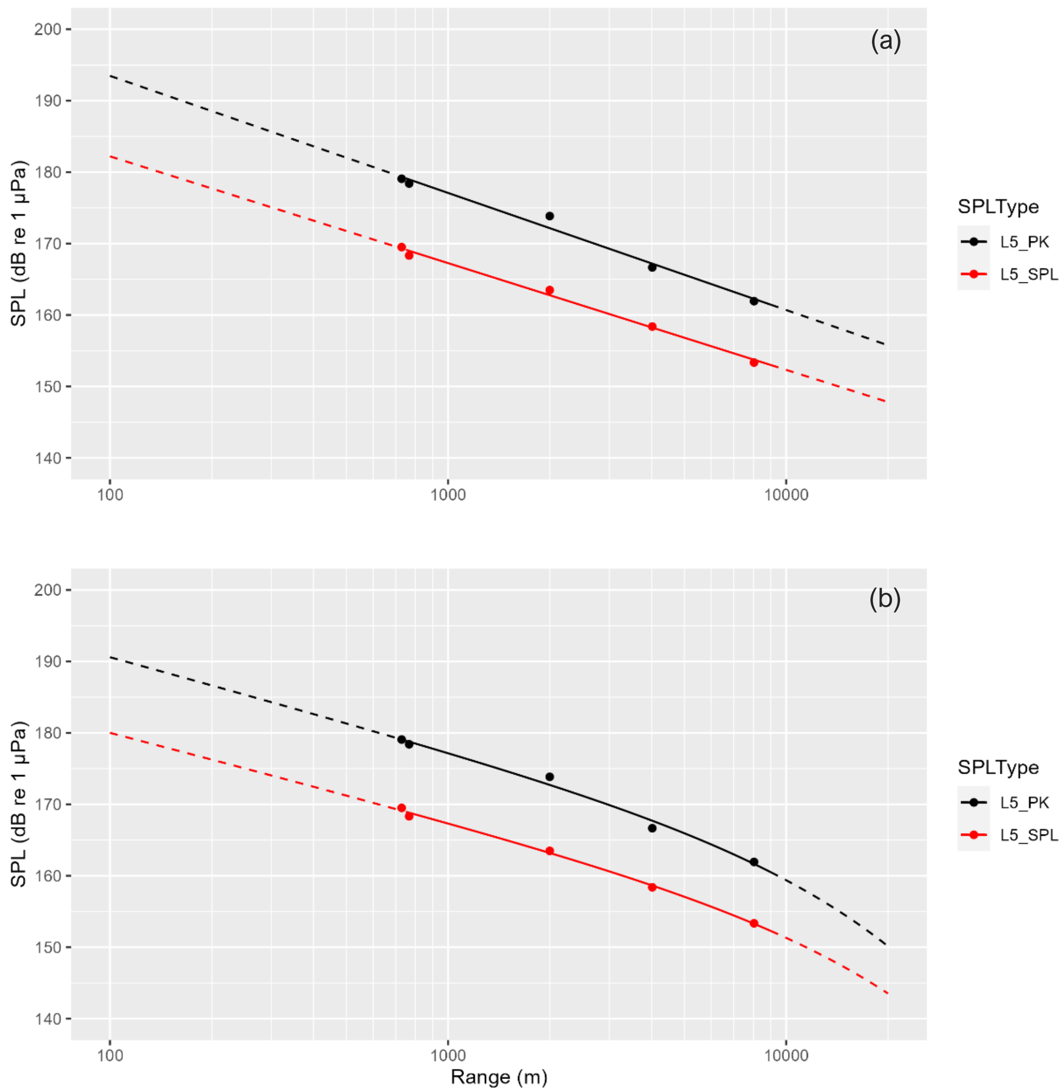


Figure A-94. Transmission loss determination based on regression analysis without (a) and with (b) intrinsic attenuation for $L_5$ PK and SPL maxima at each recording station during installation of pile AQ-38 on 5–6 Aug 2023.

Table A-71. Regression analysis fitting coefficients for transmission loss with and without intrinsic attenuation for installation of pile AQ-38 on 5–6 Aug 2023.

| Metric | A (dB/decade m) A*log(r) | A (dB/decade m) A*log(r) + αr/1000 | α (dB/ m) A*log(r) + αr/1000 |
|---|---|---|---|
| PK ($L_5$) (dB re 1 µPa) | -16.4 | -13.0 | $-0.534 \times 10^{-3}$ |
| rms SPL ($L_5$) (dB re 1 µPa$^2$) | -14.9 | -12.3 | $-0.407 \times 10^{-3}$ |
| cSEL (dB re 1 µPa$^2$·s) | -11.8 | -3.0 | $-1.365 \times 10^{-3}$ |
| cSEL, LF (dB re 1 µPa$^2$·s) | -13.2 | -6.2 | $-1.036 \times 10^{-3}$ |
| cSEL, MF (dB re 1 µPa$^2$·s) | -12.1 | -7.1 | $-0.948 \times 10^{-3}$ |
| cSEL, HF (dB re 1 µPa$^2$·s) | -11.5 | -5.9 | $-0.962 \times 10^{-3}$ |
| cSEL, PW (dB re 1 µPa$^2$·s) | -13.3 | -5.7 | $-0.902 \times 10^{-3}$ |
| cSEL, TU (dB re 1 µPa$^2$·s) | -12.9 | -7.4 | $-0.924 \times 10^{-3}$ |

# A.9. Foundation AT-39

Summary of measurements are shown in Table A-72. Channel 1 (bottom hydrophone) at stations AT39-750, AT39-4000, and AT39-8000 were not functioning properly and were excluded from the analysis. Station AT39-4000 was not included in the interim report as it was found to be very noisy. Further analysis recovered data from AT39-4000 channel 1 that is included in this report.

## A.9.1. Summary of Measured Sound Levels

Table A-72. Summary of Autonomous Multichannel Acoustic Recorder (AMAR) locations and measured sound levels for pile AT-39. Computed PK and SPL levels are shown for the $L_{max}$.

| Location (nominal) | Recorder ID | Distance (m) | Water depth (m) | Channel | Impulses Detected* (clipped) | PK (dB re 1 µPa) | SPL (dB re 1 µPa$^2$) | cSEL (dB re 1 µPa$^2$·s) |
|---|---|---|---|---|---|---|---|---|
| 750 | AMAR-863 | 770 | 42.6 | | | | | |
| | | | | 2 | 3165 | 183.6 | 173.1 | 197.2 |
| 750 @ 90° | AMAR-865 | 766 | 42.8 | 1 | 2554 | 184.7 | 174.2 | 197.9 |
| | | | | 2 | 2558 | 182.9 | 172.4 | 196.2 |
| 2000 | AMAR-855 | 2024 | 42.6 | 1 | 3085 | 177.1 | 166.4 | 192.0 |
| | | | | 2 | 3205 | 175.7 | 166.3 | 192.6 |
| 4000 | AMAR-860 | 4013 | 43.5 | | | | | |
| | | | | 2 | 3289 | 172.7 | 166.4 | 187.6 |
| 8000 | AMAR-864 | 8031 | 43.5 | | | | | |
| | | | | 2 | 3156 | 164.0 | 155.8 | 181.5 |

* Number of strikes produced (from hammer log): 3159

# A.9.2. Sound Levels per Station

## A.9.2.1. Station AT39-750

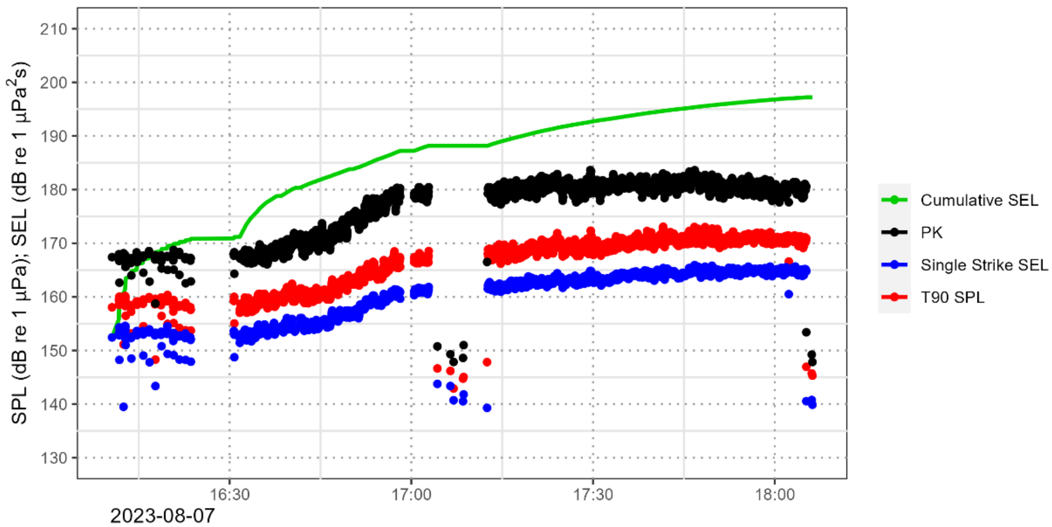


Figure A-95. Received levels for impact pile driving installation of AT-39 at monitoring station AT39-750 for channel 2. Peak SPL (PK, black), rms SPL (T90 SPL, red), single strike SEL (blue) and cumulative SEL (green) versus time (UTC). For periods during which there is no pile driving the cSEL is necessarily displayed as a constant value over time.

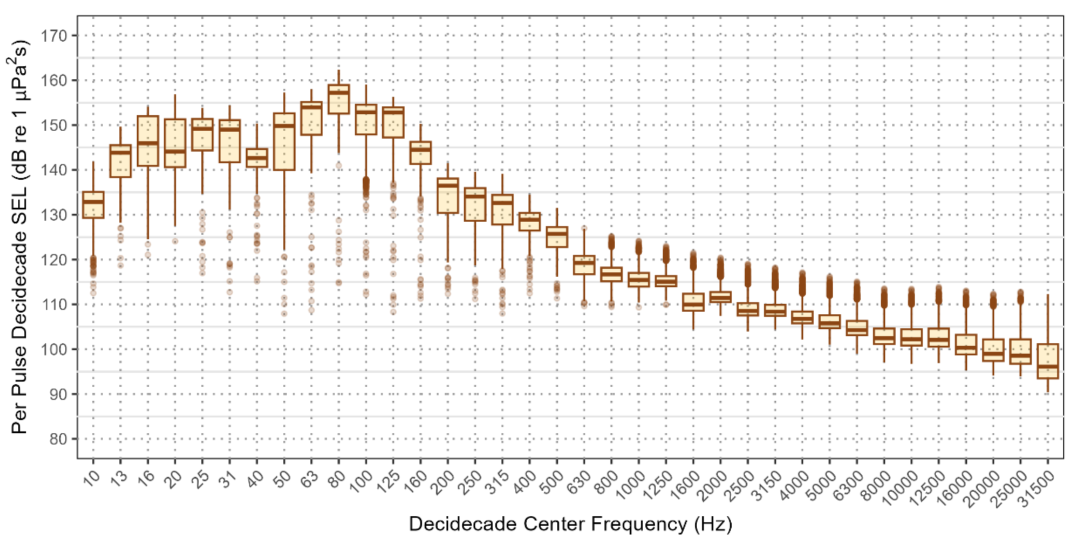


Figure A-96. Distribution of decidecade band level single strike SEL for pile driving installation of AT-39 at monitoring station AT39-750 for channel 2. Beige bars indicate the first, second, and third quartiles (*25th*, *50th*, and *75th*) or as exceedances $L_{75}$, $L_{50}$, and $L_{25}$. Upper error bars indicate the maximum levels ($L_{max}$). Lower error bars indicate the 5th percentile or $L_{95}$.

Table A-73. Received level statistics for pile driving installation of AT-39 at monitoring station AT39-750.

| Sound level statistic | PK (dB re 1 µPa) | rms SPL (dB re 1 µPa$^2$) | SELss (dB re 1 µPa$^2$·s) |
|---|---|---|---|
| **Channel 2 (mid-water)** | | | |
| $L_{max}$ | 183.6 | 173.1 | 165.9 |
| $L_5$ | 181.9 | 171.4 | 165.0 |
| $L_{25}$ | 180.9 | 170.3 | 164.2 |
| $L_{50}$ | 179.7 | 168.6 | 162.6 |
| $L_{75}$ | 172.8 | 162.3 | 156.6 |
| $L_{95}$ | 167.5 | 158.6 | 153.1 |
| $L_{mean}$ | 177.1 | 166.6 | 160.6 |

### A.9.2.2. Station AT39-75090

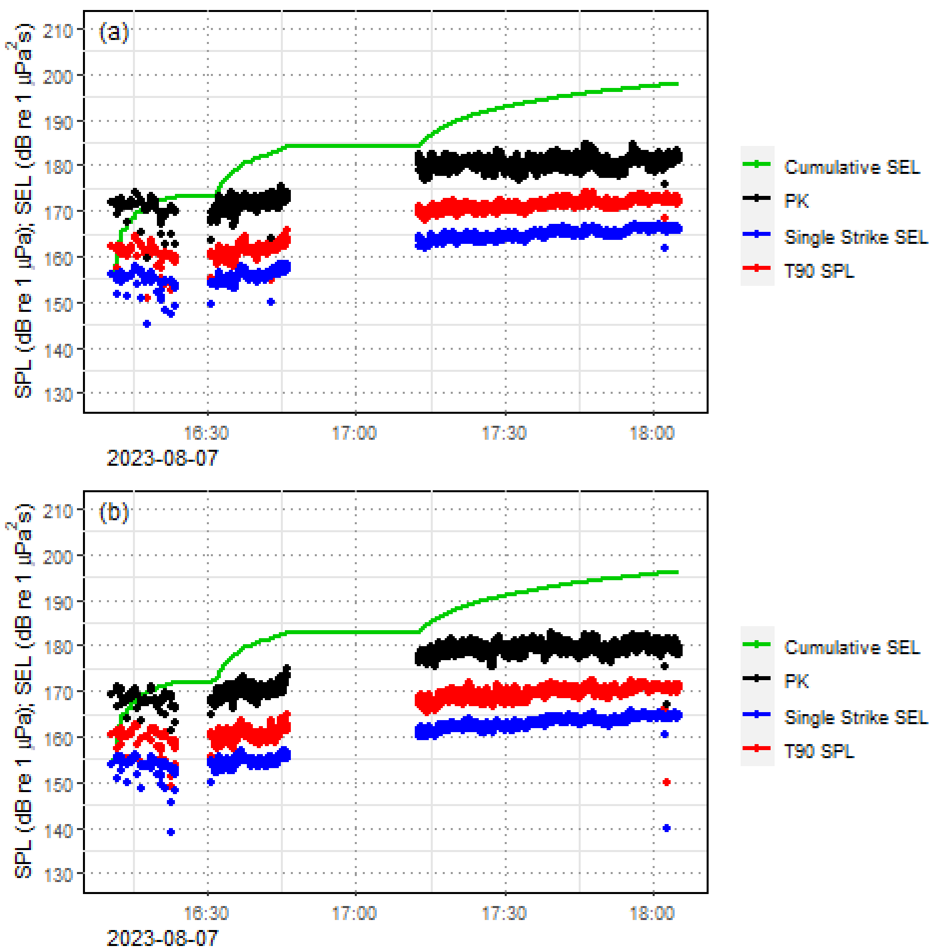


Figure A-97. Received levels for impact pile driving installation of AT-39 at monitoring station AT39-75090, for channel 1 (a) and channel 2 (b). Peak SPL (PK, black), rms SPL (T90 SPL, red), single strike SEL (blue) and cumulative SEL (green) versus time (UTC). For periods during which there is no pile driving the cSEL is necessarily displayed as a constant value over time.

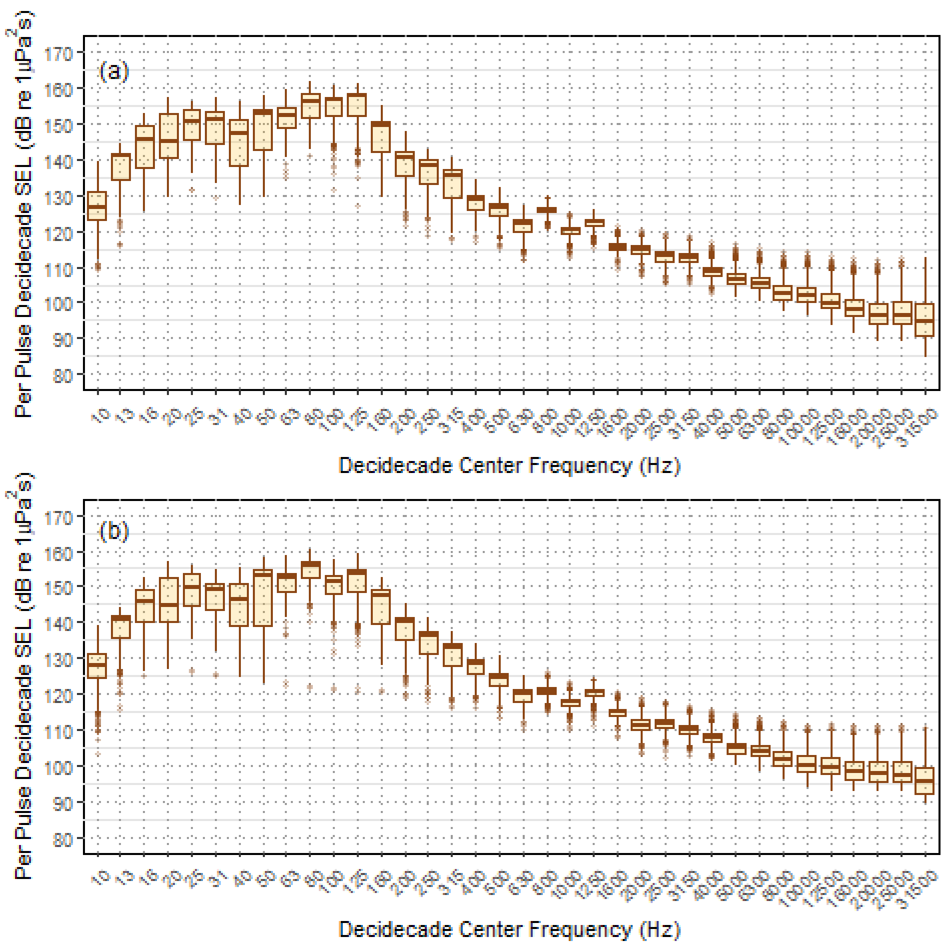


Figure A-98. Distribution of decidecade band level single strike SEL for pile driving installation of AT-39 at monitoring station AT39-75090 for channel 1 (a) and channel 2 (b). Beige bars indicate the first, second, and third quartiles (*25th*, *50th*, and *75th*) or as exceedances $L_{75}$, $L_{50}$, and $L_{25}$. Upper error bars indicate the maximum levels ($L_{max}$). Lower error bars indicate the 5th percentile or $L_{95}$.

Table A-74. Received level statistics for pile driving installation of AT-39 at monitoring station AT39-75090.

| Sound level statistic | PK (dB re 1 µPa) | rms SPL (dB re 1 µPa$^2$) | SELss (dB re 1 µPa$^2$·s) |
|---|---|---|---|
| **Channel 1 (bottom)** | | | |
| $L_{max}$ | 184.7 | 174.2 | 166.9 |
| $L_5$ | 182.6 | 172.8 | 166.3 |
| $L_{25}$ | 181.0 | 171.8 | 165.3 |
| $L_{50}$ | 179.9 | 170.9 | 164.3 |
| $L_{75}$ | 173.8 | 163.5 | 157.7 |
| $L_{95}$ | 170.4 | 160.1 | 154.5 |
| $L_{mean}$ | 178.1 | 168.7 | 162.4 |
| **Channel 2 (mid-water)** | | | |
| $L_{max}$ | 182.9 | 172.4 | 165.8 |
| $L_5$ | 181.3 | 171.2 | 164.7 |
| $L_{25}$ | 180.1 | 170.2 | 163.7 |
| $L_{50}$ | 179.0 | 169.0 | 162.4 |
| $L_{75}$ | 172.5 | 162.7 | 156.3 |
| $L_{95}$ | 168.8 | 159.3 | 153.6 |
| $L_{mean}$ | 177.0 | 167.1 | 160.8 |

### A.9.2.3. Station AT39-2000

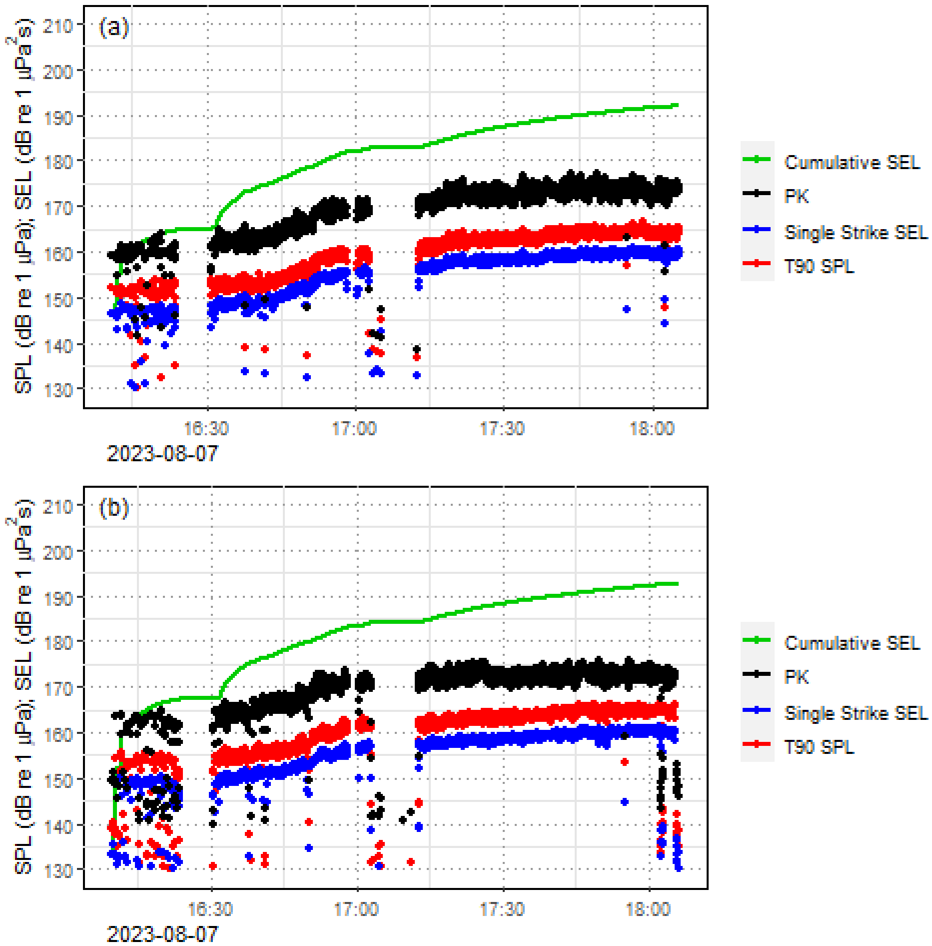


Figure A-99. Received levels for impact pile driving installation of AT-39 at monitoring station AT39-2000 for channel 1 (a) and channel 2 (b). Peak SPL (PK, black), rms SPL (T90 SPL, red), single strike SEL (blue) and cumulative SEL (green) versus time (UTC). For periods during which there was no pile driving the cSEL is necessarily displayed as a constant value over time.

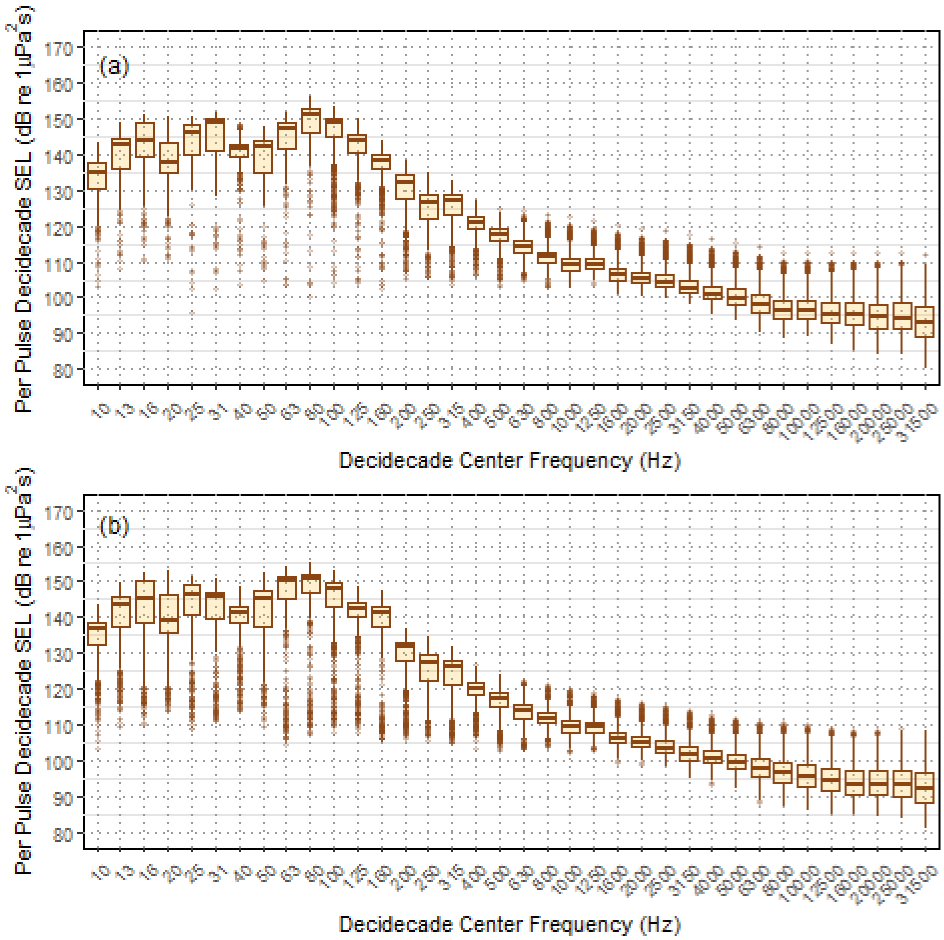


Figure A-100. Distribution of decidecade band level single strike SEL for pile driving installation of AT-39 at monitoring station AT39-2000 for channel 1 (a) and channel 2 (b). Beige bars indicate the first, second, and third quartiles (*25th*, *50th*, and *75th*) or as exceedances $L_{75}$, $L_{50}$, and $L_{25}$. Upper error bars indicate the maximum levels ($L_{max}$). Lower error bars indicate the 5th percentile or $L_{95}$.

Table A-75. Received level statistics for pile driving installation of AT-39 at monitoring station AT39-2000.

| Sound level statistic | PK (dB re 1 µPa) | rms SPL (dB re 1 µPa$^2$) | SELss (dB re 1 µPa$^2$·s) |
|---|---|---|---|
| **Channel 1 (bottom)** | | | |
| $L_{max}$ | 177.1 | 166.4 | 160.8 |
| $L_5$ | 174.8 | 164.8 | 159.9 |
| $L_{25}$ | 173.2 | 163.6 | 159.0 |
| $L_{50}$ | 171.5 | 162.0 | 157.6 |
| $L_{75}$ | 166.4 | 156.2 | 152.1 |
| $L_{95}$ | 161.4 | 152.2 | 148.1 |
| $L_{mean}$ | 169.7 | 160.0 | 155.5 |
| **Channel 2 (mid-water)** | | | |
| $L_{max}$ | 175.7 | 166.3 | 161.3 |
| $L_5$ | 173.9 | 165.2 | 160.4 |
| $L_{25}$ | 172.6 | 164.1 | 159.4 |
| $L_{50}$ | 171.5 | 162.5 | 157.9 |
| $L_{75}$ | 167.5 | 156.9 | 152.2 |
| $L_{95}$ | 162.9 | 153.7 | 149.2 |
| $L_{mean}$ | 169.8 | 160.5 | 155.8 |

## A.9.2.4. Station AT39-4000

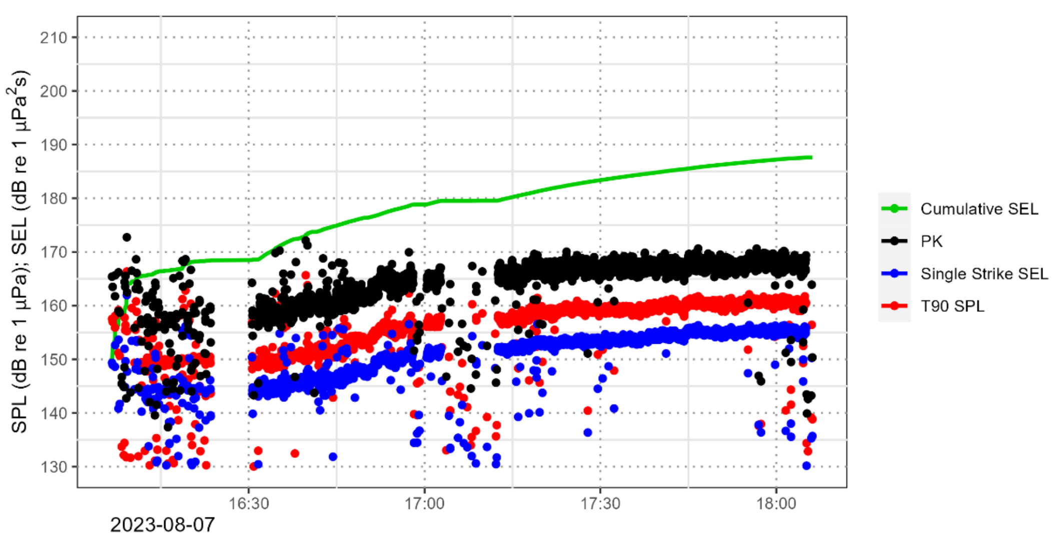


Figure A-101. Received levels for impact pile driving installation of AT-39 at monitoring station AT39-4000 for channel 2. Peak SPL (PK, black), rms SPL (T90 SPL, red), single strike SEL (blue) and cumulative SEL (green) versus time (UTC). For periods during which there is no pile driving the cSEL is necessarily displayed as a constant value over time.

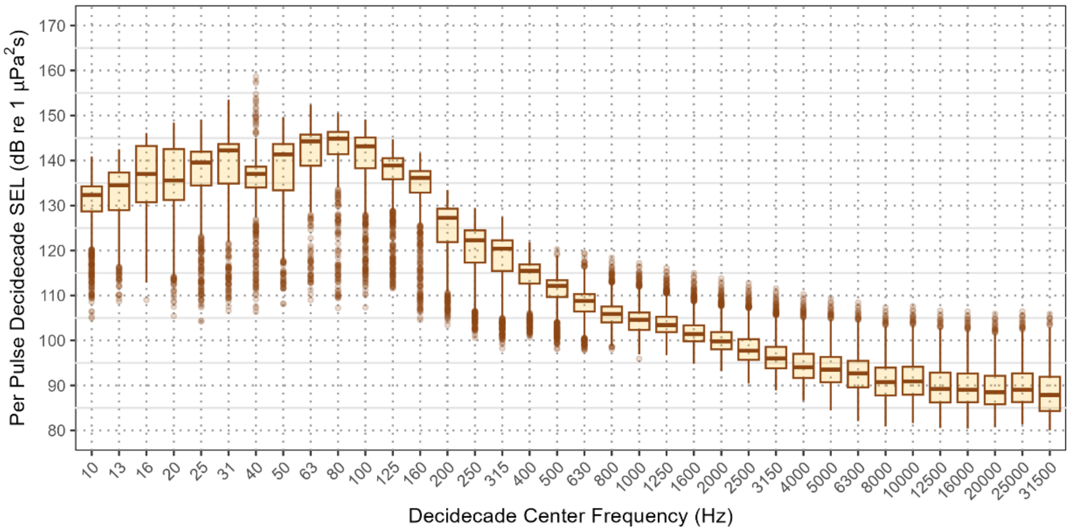


Figure A-102. Distribution of decidecade band level single strike SEL for pile driving installation of AT-39 at monitoring station AT39-4000 for channel 2. Beige bars indicate the first, second, and third quartiles (*25th*, *50th*, and *75th*) or as exceedances $L_{75}$, $L_{50}$, and $L_{25}$. Upper error bars indicate the maximum levels ($L_{max}$). Lower error bars indicate the 5th percentile or $L_{95}$.

Table A-76. Received level statistics for pile driving installation of AT-39 at monitoring station AT39-4000.

| Sound level statistic | PK (dB re 1 µPa) | rms SPL (dB re 1 µPa²) | SELss (dB re 1 µPa²·s) |
|---|---|---|---|
| Channel 2 (mid-water) | | | |
| $L_{max}$ | 172.7 | 166.4 | 161.9 |
| $L_5$ | 168.6 | 160.9 | 155.4 |
| $L_{25}$ | 167.4 | 159.8 | 154.3 |
| $L_{50}$ | 166.0 | 158.5 | 152.8 |
| $L_{75}$ | 161.8 | 153.1 | 147.5 |
| $L_{95}$ | 157.7 | 149.1 | 144.1 |
| $L_{mean}$ | 165.8 | 158.0 | 152.4 |

### A.9.2.5. Station AT39-8000

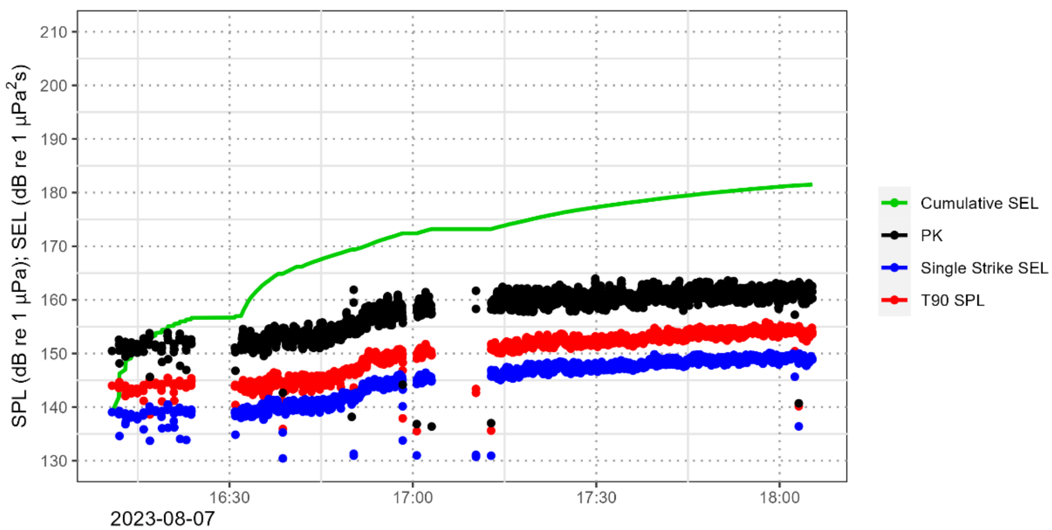


Figure A-103. Received levels for impact pile driving installation of AT-39 at monitoring station AT39-8000 for channel 2. Peak SPL (PK, black), rms SPL (T90 SPL, red), single strike SEL (blue) and cumulative SEL (green) versus time (UTC). For periods during which there is no pile driving the cSEL is necessarily displayed as a constant value over time.

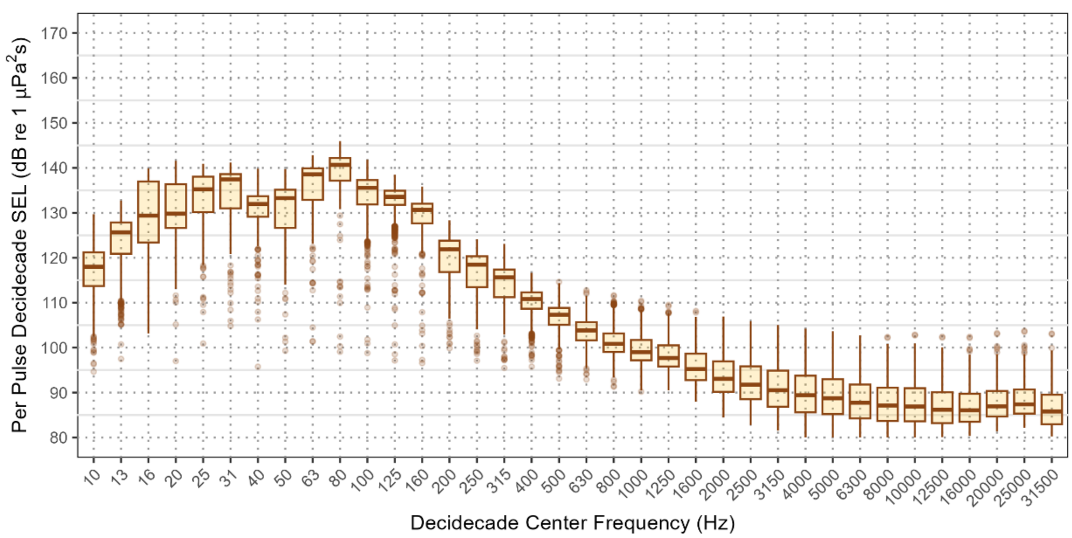


Figure A-104. Distribution of decidecade band level single strike SEL for pile driving installation of AT-39 at monitoring station AT39-8000 for channel 2. Beige bars indicate the first, second, and third quartiles (*25th*, *50th*, and *75th*) or as exceedances $L_{75}$, $L_{50}$, and $L_{25}$. Upper error bars indicate the maximum levels ($L_{max}$). Lower error bars indicate the 5th percentile or $L_{95}$.

Table A-77. Received level statistics for pile driving installation of AT-39 at monitoring station AT39-8000.

| Sound level statistic | PK (dB re 1 µPa) | rms SPL (dB re 1 µPa²) | SELss (dB re 1 µPa²·s) |
|---|---|---|---|
| Channel 2 (mid-water) | | | |
| $L_{max}$ | 164.0 | 155.8 | 150.1 |
| $L_{5}$ | 162.2 | 154.3 | 149.3 |
| $L_{25}$ | 160.9 | 153.2 | 148.3 |
| $L_{50}$ | 159.6 | 151.7 | 147.0 |
| $L_{75}$ | 154.8 | 146.5 | 141.8 |
| $L_{95}$ | 151.6 | 143.8 | 139.1 |
| $L_{mean}$ | 158.1 | 150.2 | 145.3 |

## A.9.3. Ranges to Acoustic Thresholds

Table A-78. Isopleth distances to NMFS physiological thresholds for impact driving installation of pile AT-39.

| Group | Injury: PK | | | | Injury: cSEL | | | |
|---|---|---|---|---|---|---|---|---|
| | Level (dB re 1µPa) | Predicted (m) | Measured (m) | Measured w/ attn. coeff. (m) | Level (dB re 1 µPa²·s) | Predicted (m) | Measured (m) | Measured w/ attn. coeff. (m) |
| LFC | 219 | 17 | 10 | 10 | 183 | 3,191 | 1,810 | 1,890 |
| MFC | 230 | 5 | 10 | 10 | 185 | 43 | 10 | 10 |
| HFC | 202 | 119 | 80 | 60 | 155 | 71 | 90 | 60 |
| PW | 218 | 19 | 10 | 10 | 185 | 153 | 120 | 100 |
| ST | 232 | 0 | 10 | 10 | 204 | 161 | 220 | 180 |
| AS | 206 | 78 | 50 | 30 | 187 | 6,894 | 4,000 | 4,430 |

Table A-79. Isopleth distances to NMFS behavioral thresholds for impact driving installation of pile AT-39.

| Group | Behavior: SPL | | | |
|---|---|---|---|---|
| | Level (dB re 1µPa²) | Predicted (m) | Measured (m) | Measured w/ attn. coeff. (m) |
| MM | 160 | 4,121 | 4,030 | 4,260 |
| ST | 175 | 1,400 | 530 | 480 |
| AS | 150 | 9,229 | 15,620 | 12,130 |

## A.9.4. Regression Analysis for Transmission Loss

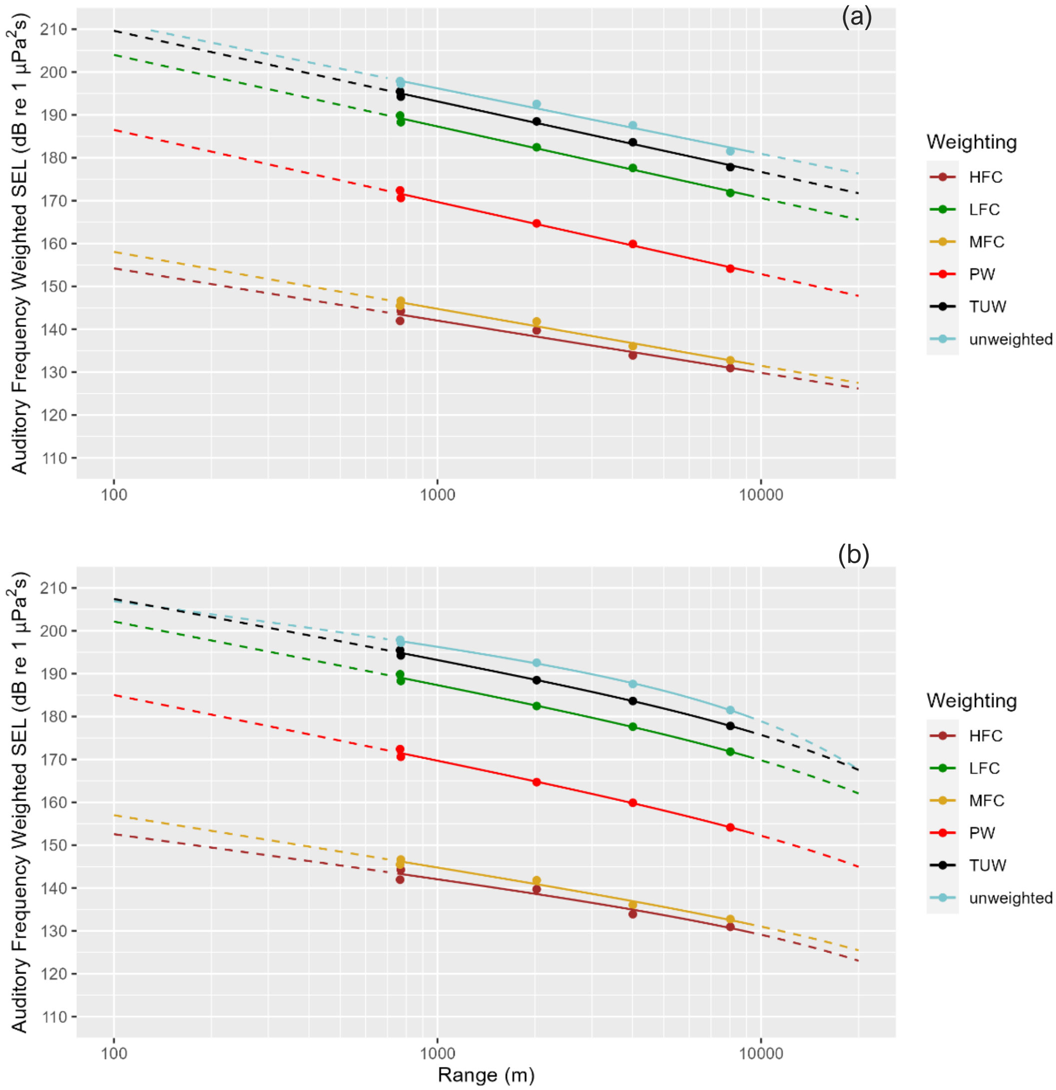


Figure A-105. Transmission loss determination based on regression analysis without (a) and with (b) intrinsic attenuation for the maximum received cumulative SEL (cSEL) at each recording station during installation of pile AT-39 on 7 Aug 2023.

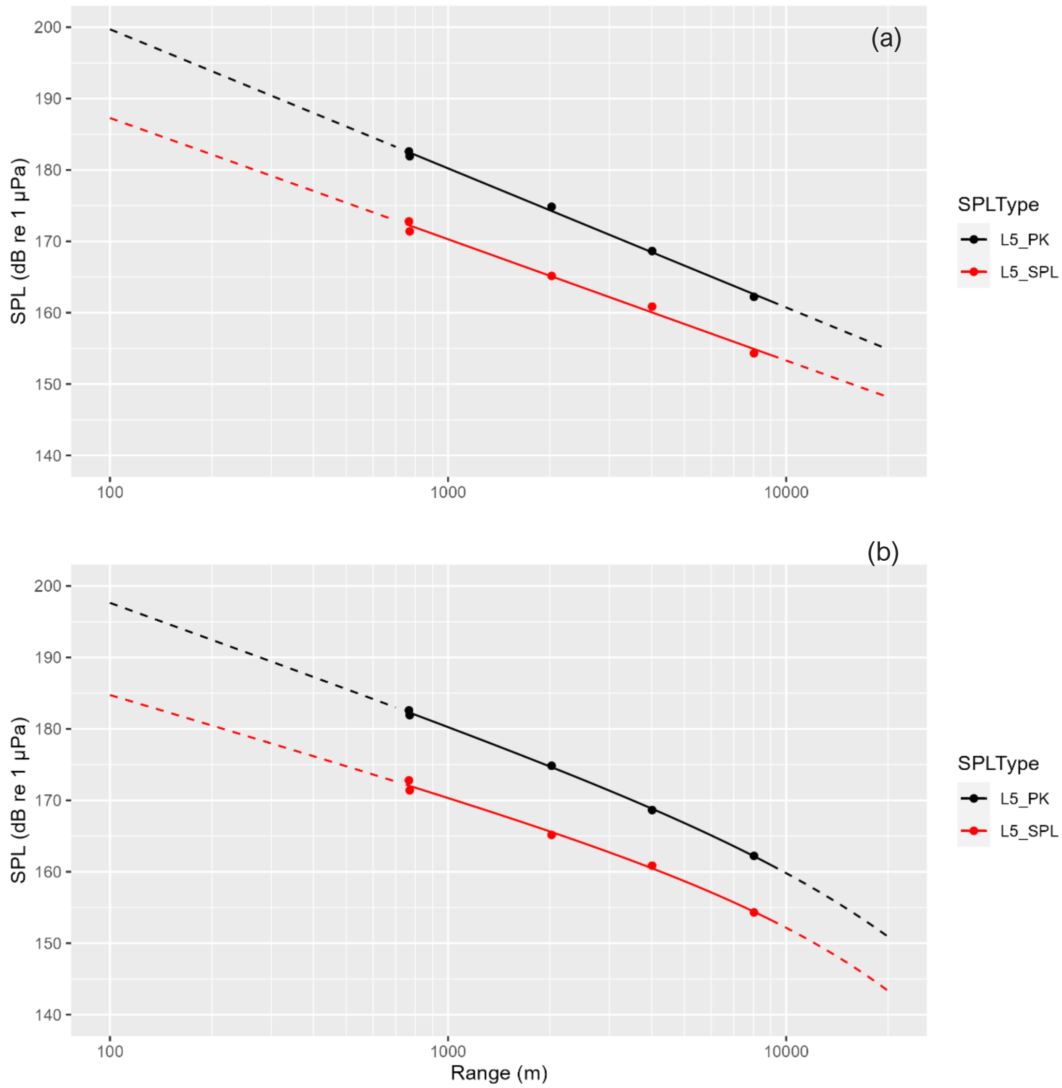


Figure A-106. Transmission loss determination based on regression analysis without (a) and with (b) intrinsic attenuation for $L_5$ PK and SPL maxima at each recording station during installation of pile AT-39 on 7 Aug 2023.

Table A-80. Regression analysis fitting coefficients for transmission loss with and without intrinsic attenuation for installation of pile AT-39 on 7 Aug 2023.

| Metric | A (dB/decade m) A*log(r) | A (dB/decade m) A*log(r) + αr/1000 | α (dB/ m) A*log(r) + αr/1000 |
|---|---|---|---|
| PK ($L_5$) (dB re 1 μPa) | -19.5 | -17.1 | -0.375 x $10^{-3}$ |
| rms SPL ($L_5$) (dB re 1 μPa²) | -17.0 | -14.0 | -0.460 x $10^{-3}$ |
| cSEL (dB re 1 μPa²·s) | -13.5 | -9.9 | -0.827 x $10^{-3}$ |
| cSEL, LF (dB re 1 μPa²·s) | -16.0 | -13.9 | -0.399 x $10^{-3}$ |
| cSEL, MF (dB re 1 μPa²·s) | -10.0 | -14.5 | -0.335 x $10^{-3}$ |
| cSEL, HF (dB re 1 μPa²·s) | -9.6 | -12.0 | -0.191 x $10^{-3}$ |
| cSEL, PW (dB re 1 μPa²·s) | -16.1 | -10.3 | -0.298 x $10^{-3}$ |
| cSEL, TU (dB re 1 μPa²·s) | -15.7 | -15.1 | -0.270 x $10^{-3}$ |

# A.10. Foundation AS-39

Summary of measurements are shown in Table A-81. Channel 1 (bottom hydrophone) at station AS39-750 and both channels at station AS39-8000 were not functioning properly and were excluded from the analysis.

## A.10.1. Summary of Measured Sound Levels

Table A-81. Summary of Autonomous Multichannel Acoustic Recorder (AMAR) locations and measured sound levels for pile AS-39. Computed PK and SPL levels are shown for the $L_{max}$.

| Location (nominal) | Recorder ID | Distance (m) | Water depth (m) | Channel | Impulses Detected* (clipped) | PK (dB re 1 μPa) | SPL (dB re 1 μPa²) | cSEL (dB re 1 μPa²·s) |
|---|---|---|---|---|---|---|---|---|
| 750 | AMAR-863 | 744 | 42.2 | | | | | |
| | | | | 2 | 2995 | 186.7 | 174.3 | 198.4 |
| 750 @ 90° | AMAR-865 | 751 | 43.0 | 1 | 2993 | 185.2 | 174.4 | 198.9 |
| | | | | 2 | 2994 | 184.1 | 173.6 | 198.2 |
| 2000 | AMAR-855 | 1991 | 43.7 | 1 | 3022 | 179.5 | 168.1 | 193.1 |
| | | | | 2 | 3009 | 178.2 | 168.0 | 193.6 |
| 4000 | AMAR-860 | 3925 | 43.9 | 1 | 3020 | 174.0 | 163.1 | 188.7 |
| | | | | 2 | 3016 | 173.1 | 163.7 | 189.2 |

* Number of strikes produced (from hammer log): 2995

## A.10.2. Sound Levels per Station

### A.10.2.1. Station AS39-750

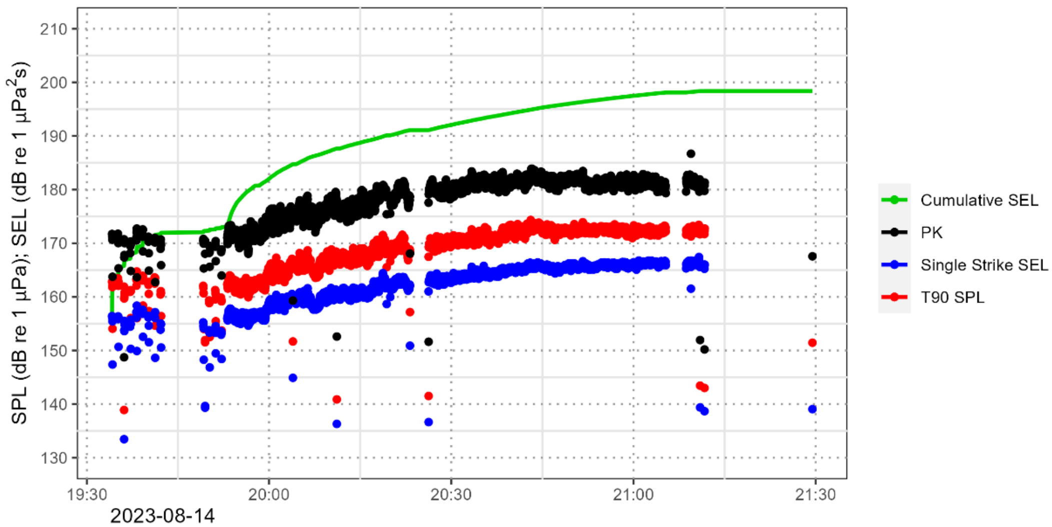


Figure A-107. Received levels for impact pile driving installation of AS-39 at monitoring station AS39-750 for channel 2. Peak SPL (PK, black), rms SPL (T90 SPL, red), single strike SEL (blue) and cumulative SEL (green) versus time (UTC). For periods during which there is no pile driving the cSEL is necessarily displayed as a constant value over time.

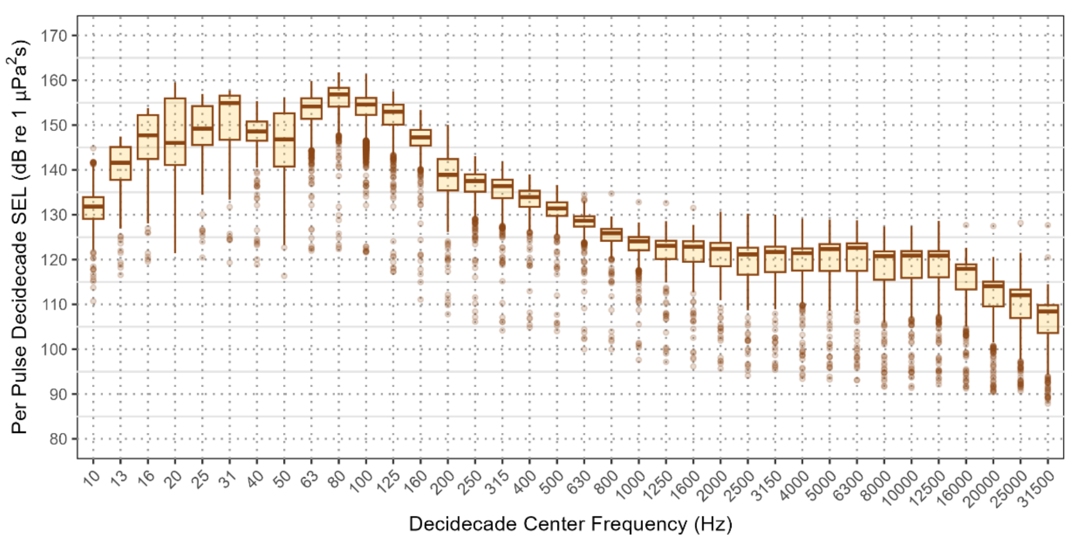


Figure A-108. Distribution of decidecade band level single strike SEL for pile driving installation of AS-39 at monitoring station AS39-750 for channel 2. Beige bars indicate the first, second, and third quartiles (*25th*, *50th*, and *75th*) or as exceedances $L_{75}$, $L_{50}$, and $L_{25}$. Upper error bars indicate the maximum levels ($L_{max}$). Lower error bars indicate the 5th percentile or $L_{95}$.

Table A-82. Received level statistics for pile driving installation of AS-39 at monitoring station AS39-750.

| Sound level statistic | PK (dB re 1 µPa) | rms SPL (dB re 1 µPa$^2$) | SELss (dB re 1 µPa$^2$·s) |
|---|---|---|---|
| Channel 2 (mid-water) | | | |
| $L_{max}$ | 186.7 | 174.3 | 167.4 |
| $L_5$ | 182.4 | 173.0 | 166.3 |
| $L_{25}$ | 181.4 | 172.3 | 165.6 |
| $L_{50}$ | 180.2 | 170.3 | 163.5 |
| $L_{75}$ | 175.7 | 166.4 | 159.9 |
| $L_{95}$ | 171.1 | 161.8 | 156.0 |
| $L_{mean}$ | 178.5 | 169.0 | 162.4 |

### A.10.2.2. Station AS39-75090

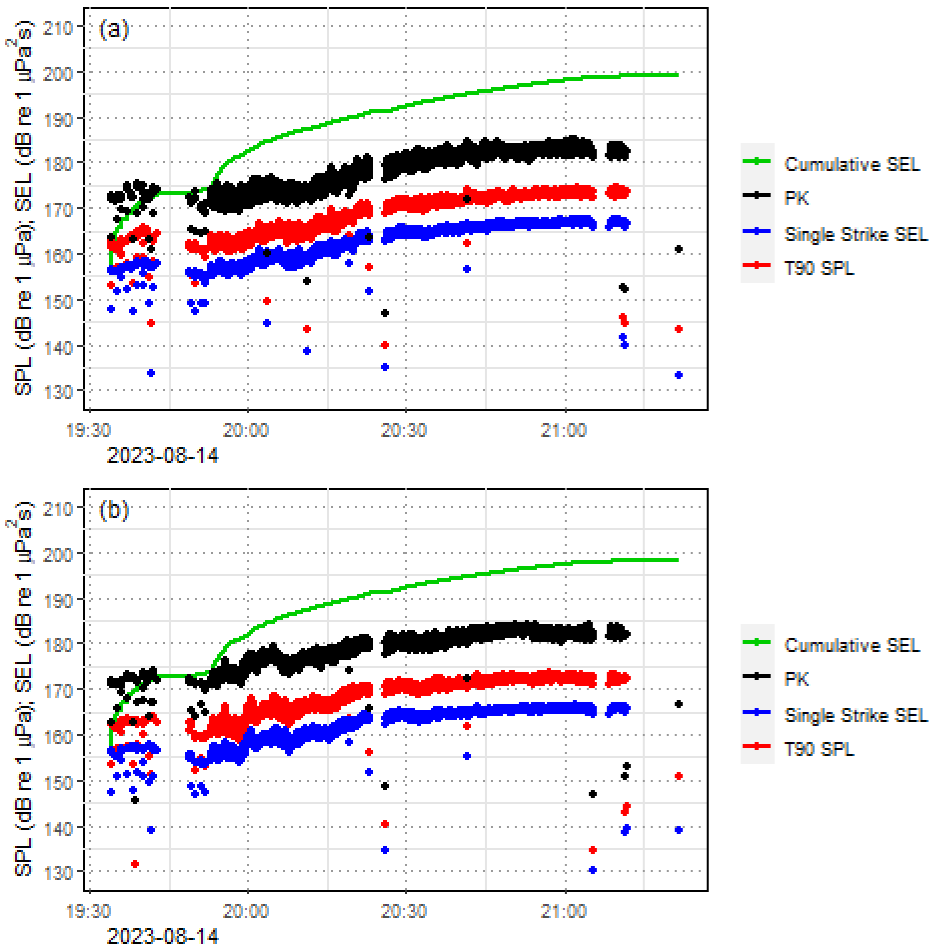


Figure A-109. Received levels for impact pile driving installation of AS-39 at monitoring station AS39-75090, for channel 1 (a) and channel 2 (b). Peak SPL (PK, black), rms SPL (T90 SPL, red), single strike SEL (blue) and cumulative SEL (green) versus time (UTC). For periods during which there is no pile driving the cSEL is necessarily displayed as a constant value over time.

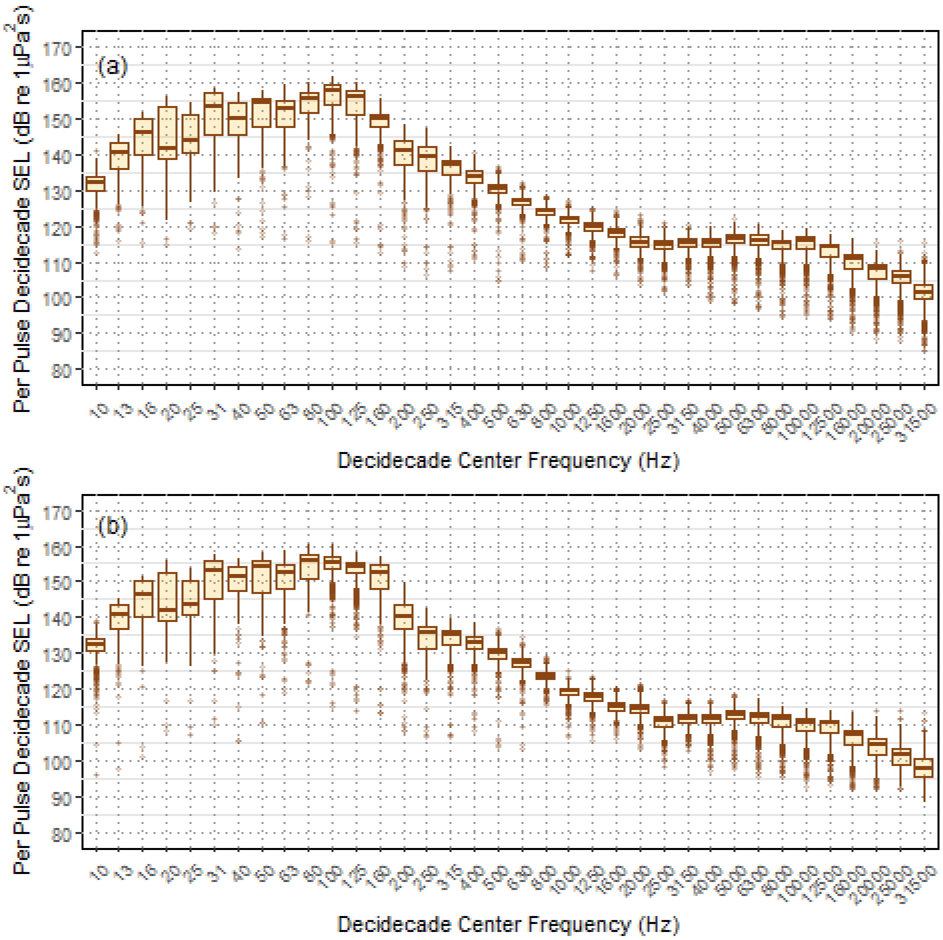


Figure A-110. Distribution of decidecade band level single strike SEL for pile driving installation of AS-39 at monitoring station AS39-75090 for channel 1 (a) and channel 2 (b). Beige bars indicate the first, second, and third quartiles (*25th*, *50th*, and *75th*) or as exceedances $L_{75}$, $L_{50}$, and $L_{25}$. Upper error bars indicate the maximum levels ($L_{max}$). Lower error bars indicate the 5th percentile or $L_{95}$.

Table A-83. Received level statistics for pile driving installation of AS-39 at monitoring station AS39-75090.

| Sound level statistic | PK (dB re 1 µPa) | rms SPL (dB re 1 µPa$^2$) | SELss (dB re 1 µPa$^2$·s) |
|---|---|---|---|
| **Channel 1 (bottom)** | | | |
| $L_{max}$ | 185.2 | 174.4 | 167.7 |
| $L_5$ | 183.5 | 173.6 | 167.0 |
| $L_{25}$ | 182.3 | 172.5 | 166.3 |
| $L_{50}$ | 179.9 | 170.7 | 164.4 |
| $L_{75}$ | 173.9 | 164.8 | 159.1 |
| $L_{95}$ | 171.6 | 161.8 | 156.3 |
| $L_{mean}$ | 178.3 | 168.9 | 162.8 |
| **Channel 2 (mid-water)** | | | |
| $L_{max}$ | 184.1 | 173.6 | 166.5 |
| $L_5$ | 183.1 | 172.6 | 165.9 |
| $L_{25}$ | 182.0 | 171.8 | 165.3 |
| $L_{50}$ | 180.2 | 170.3 | 164.0 |
| $L_{75}$ | 176.7 | 165.8 | 159.6 |
| $L_{95}$ | 172.5 | 161.6 | 155.7 |
| $L_{mean}$ | 179.1 | 168.6 | 162.3 |

### A.10.2.3. Station AS39-2000

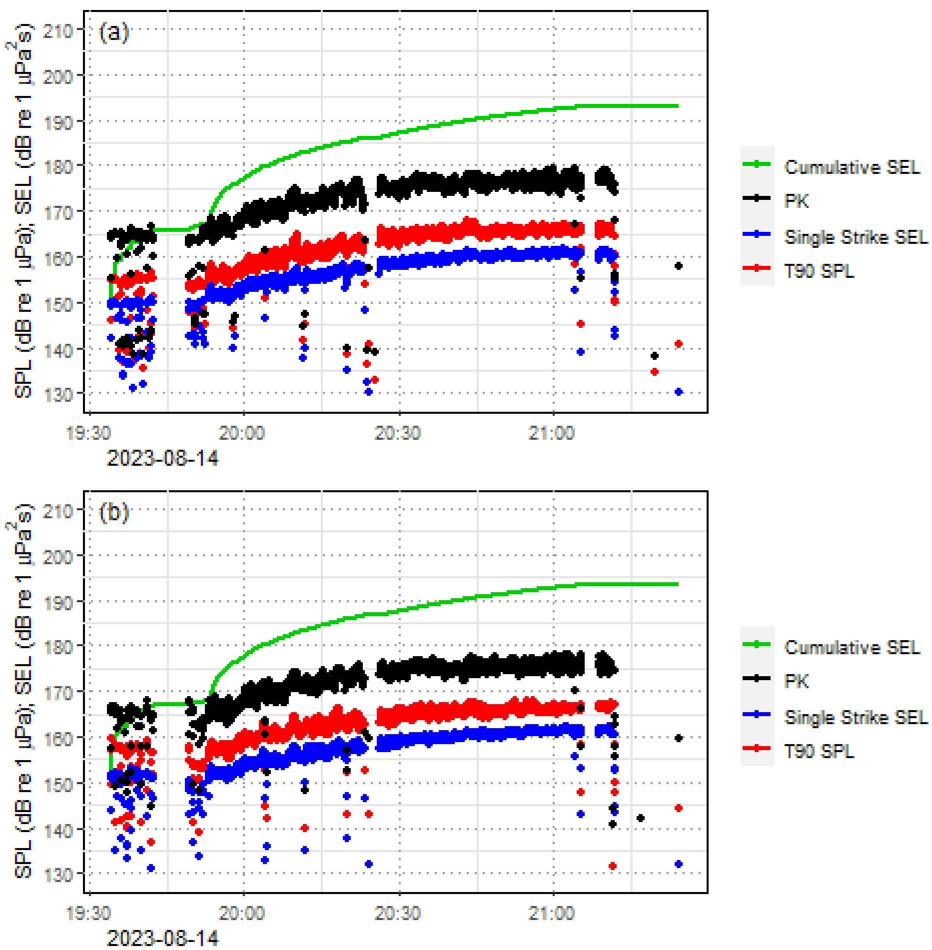


Figure A-111. Received levels for impact pile driving installation of AS-39 at monitoring station AS39-2000 for channel 1 (a) and channel 2 (b). Peak SPL (PK, black), rms SPL (T90 SPL, red), single strike SEL (blue) and cumulative SEL (green) versus time (UTC). For periods during which there was no pile driving the cSEL is necessarily displayed as a constant value over time.

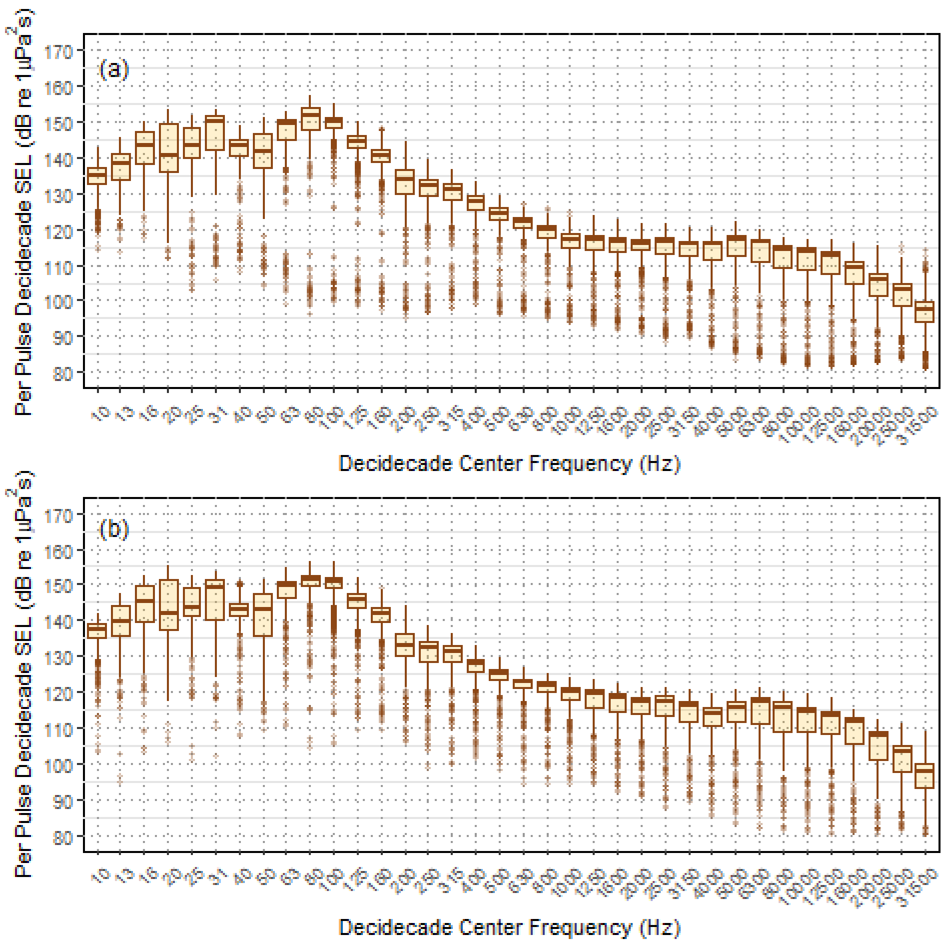


Figure A-112. Distribution of decidecade band level single strike SEL for pile driving installation of AS-39 at monitoring station AS39-2000 for channel 1 (a) and channel 2 (b). Beige bars indicate the first, second, and third quartiles (*25th*, *50th*, and *75th*) or as exceedances $L_{75}$, $L_{50}$, and $L_{25}$. Upper error bars indicate the maximum levels ($L_{max}$). Lower error bars indicate the 5th percentile or $L_{95}$.

Table A-84. Received level statistics for pile driving installation of AS-39 at monitoring station AS39-2000.

| Sound level statistic | PK (dB re 1 µPa) | rms SPL (dB re 1 µPa$^2$) | SELss (dB re 1 µPa$^2$·s) |
|---|---|---|---|
| **Channel 1 (bottom)** | | | |
| $L_{max}$ | 179.5 | 168.1 | 161.6 |
| $L_{5}$ | 177.5 | 166.3 | 161.0 |
| $L_{25}$ | 176.4 | 165.5 | 160.1 |
| $L_{50}$ | 175.1 | 164.0 | 158.5 |
| $L_{75}$ | 171.0 | 159.9 | 154.8 |
| $L_{95}$ | 165.5 | 155.2 | 151.0 |
| $L_{mean}$ | 173.2 | 162.3 | 157.1 |
| **Channel 2 (mid-water)** | | | |
| $L_{max}$ | 178.2 | 168.0 | 162.2 |
| $L_{5}$ | 176.4 | 166.6 | 161.5 |
| $L_{25}$ | 175.3 | 165.8 | 160.6 |
| $L_{50}$ | 174.2 | 164.5 | 158.9 |
| $L_{75}$ | 170.5 | 161.0 | 155.3 |
| $L_{95}$ | 165.4 | 157.1 | 151.7 |
| $L_{mean}$ | 172.6 | 163.1 | 157.7 |

### A.10.2.4. Station AS39-4000

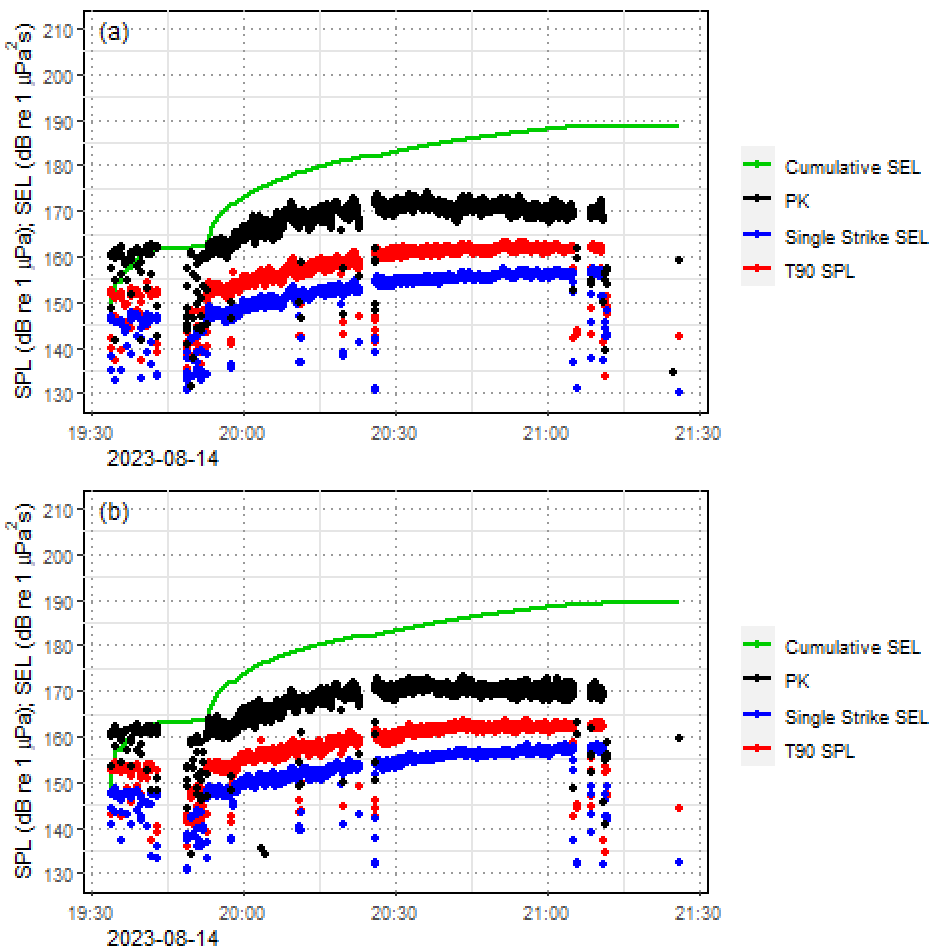


Figure A-113. Received levels for impact pile driving installation of AS-39 at monitoring station AS39-4000 for channel 1 (a) and channel 2 (b). Peak SPL (PK, black), rms SPL (T90 SPL, red), single strike SEL (blue) and cumulative SEL (green) versus time (UTC). For periods during which there is no pile driving the cSEL is necessarily displayed as a constant value over time.

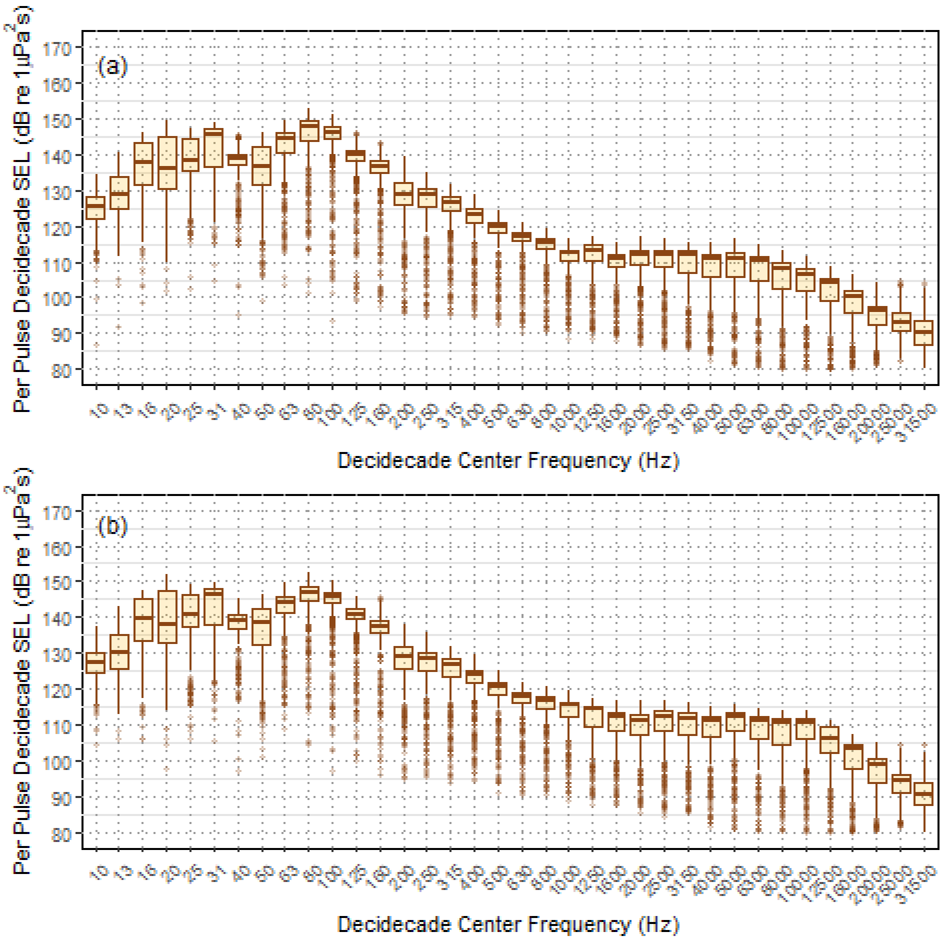


Figure A-114. Distribution of decidecade band level single strike SEL for pile driving installation of AS-39 at monitoring station AS39-4000 for channel 1 (a) and channel 2 (b). Beige bars indicate the first, second, and third quartiles (*25th*, *50th*, and *75th*) or as exceedances $L_{75}$, $L_{50}$, and $L_{25}$. Upper error bars indicate the maximum levels ($L_{max}$). Lower error bars indicate the 5th percentile or $L_{95}$.

Table A-85. Received level statistics for pile driving installation of AS-39 at monitoring station AS39-4000.

| Sound level statistic | PK (dB re 1 µPa) | rms SPL (dB re 1 µPa$^2$) | SELss (dB re 1 µPa$^2$·s) |
|---|---|---|---|
| **Channel 1 (bottom)** | | | |
| $L_{max}$ | 174.0 | 163.1 | 157.3 |
| $L_5$ | 172.3 | 162.3 | 156.5 |
| $L_{25}$ | 171.1 | 161.6 | 155.7 |
| $L_{50}$ | 169.9 | 160.5 | 154.4 |
| $L_{75}$ | 167.4 | 156.2 | 150.6 |
| $L_{95}$ | 161.4 | 152.0 | 146.7 |
| $L_{mean}$ | 168.5 | 158.5 | 152.7 |
| **Channel 2 (mid-water)** | | | |
| $L_{max}$ | 173.1 | 163.7 | 158.2 |
| $L_5$ | 171.6 | 162.6 | 157.2 |
| $L_{25}$ | 170.5 | 162.0 | 156.3 |
| $L_{50}$ | 169.5 | 160.1 | 154.3 |
| $L_{75}$ | 166.5 | 156.6 | 151.0 |
| $L_{95}$ | 161.0 | 152.9 | 147.5 |
| $L_{mean}$ | 168.0 | 158.9 | 153.3 |

## A.10.3. Ranges to Acoustic Thresholds

Table A-86. Isopleth distances to NMFS physiological thresholds for impact driving installation of pile AS-39.

| Group | Injury: PK | | | | Injury: cSEL | | | |
|---|---|---|---|---|---|---|---|---|
| | Level (dB re 1µPa) | Predicted (m) | Measured (m) | Measured w/ attn. coeff. (m) | Level (dB re 1 µPa$^2$·s) | Predicted (m) | Measured (m) | Measured w/ attn. coeff. (m) |
| LFC | 219 | 17 | 10 | 10 | 183 | 3,191 | 2,270 | 2,330 |
| MFC | 230 | 5 | 10 | 10 | 185 | 43 | 10 | 10 |
| HFC | 202 | 119 | 40 | 10 | 155 | 71 | 720 | 610 |
| PW | 218 | 19 | 10 | 10 | 185 | 153 | 110 | 70 |
| ST | 232 | 0 | 10 | 10 | 204 | 161 | 200 | 160 |
| AS | 206 | 78 | 20 | 10 | 187 | 6,894 | 6,080 | 5,250 |

Table A-87. Isopleth distances to NMFS behavioral thresholds for impact driving installation of pile AS-39.

| Group | Behavior: SPL | | | |
|---|---|---|---|---|
| | Level (dB re 1µPa$^2$) | Predicted (m) | Measured (m) | Measured w/ attn. coeff. (m) |
| MM | 160 | 4,121 | 5,740 | 6,870 |
| ST | 175 | 1,400 | 570 | 590 |
| AS | 150 | 9,229 | 26,830 | 14,030 |

## A.10.4. Regression Analysis for Transmission Loss

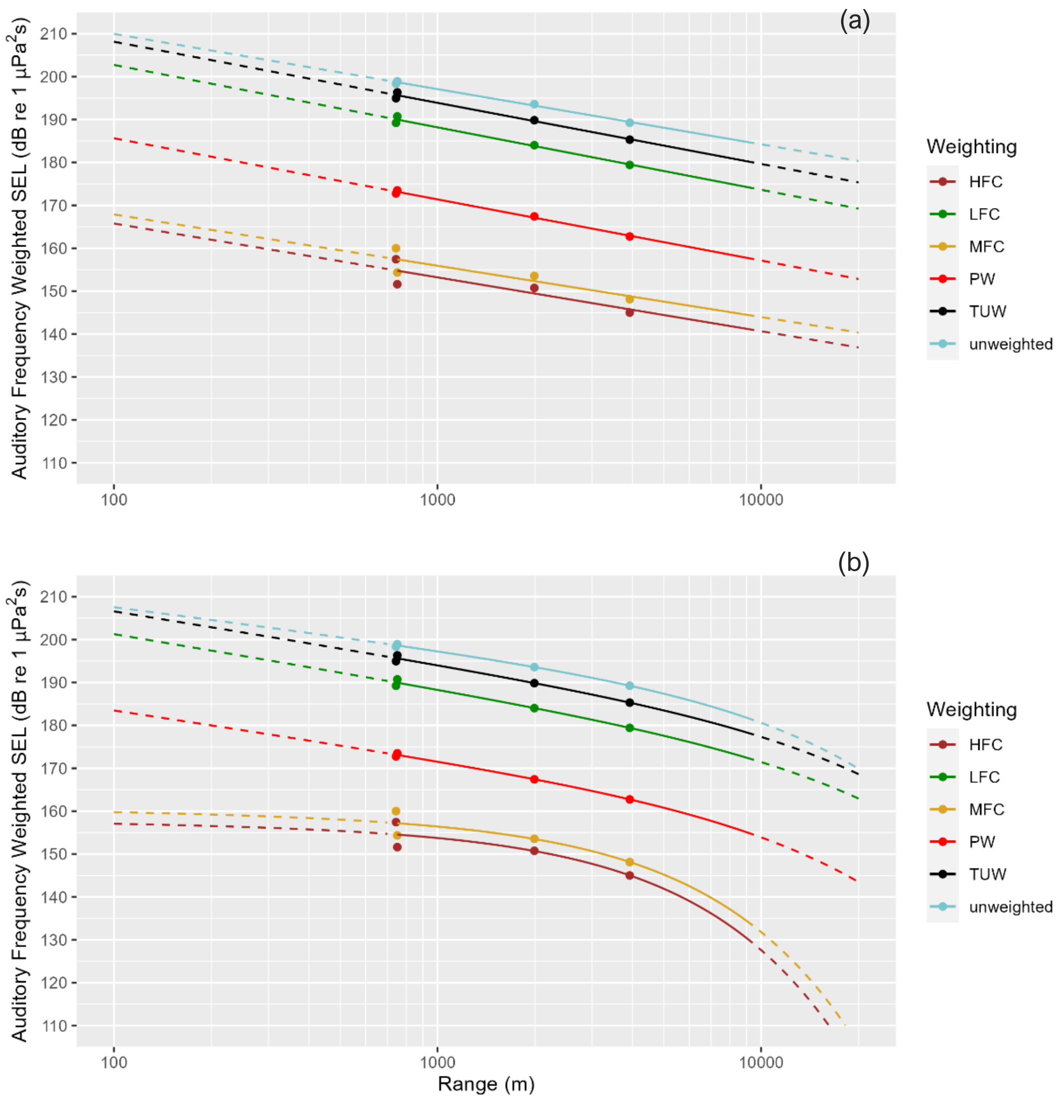


Figure A-115. Transmission loss determination based on regression analysis without (a) and with (b) intrinsic attenuation for the maximum received cumulative SEL (cSEL) at each recording station during installation of pile AS-39 on 14 Aug 2023.

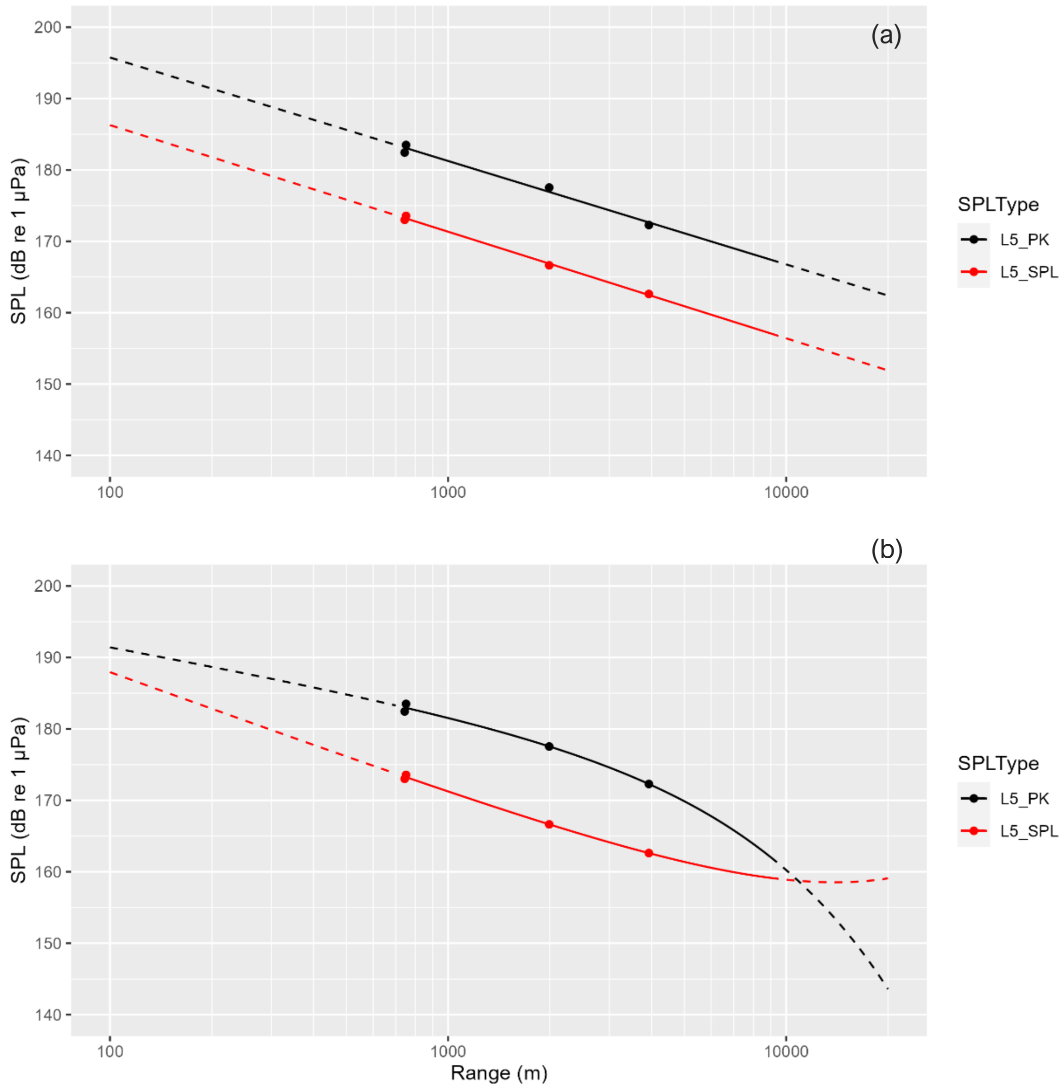


Figure A-116. Transmission loss determination based on regression analysis without (a) and with (b) intrinsic attenuation for $L_5$ PK and SPL maxima at each recording station during installation of pile AS-39 on 14 Aug 2023.

Table A-88. Regression analysis fitting coefficients for transmission loss with and without intrinsic attenuation for installation of pile AS-39 on 14 Aug 2023.

| Metric | A (dB/decade m) A*log(r) | A (dB/decade m) A*log(r) + αr/1000 | α (dB/ m) A*log(r) + αr/1000 |
|---|---|---|---|
| PK ($L_5$) (dB re 1 µPa) | -14.5 | -8.6 | -1.406 x $10^{-3}$ |
| rms SPL ($L_5$) (dB re 1 µPa$^2$) | -14.9 | -17.2 | -0.536 x $10^{-3}$ |
| cSEL (dB re 1 µPa$^2$·s) | -12.9 | -9.6 | -0.782 x $10^{-3}$ |
| cSEL, LF (dB re 1 µPa$^2$·s) | -14.6 | -12.6 | -0.471 x $10^{-3}$ |
| cSEL, MF (dB re 1 µPa$^2$·s) | -12.0 | -1.0 | -2.622 x $10^{-3}$ |
| cSEL, HF (dB re 1 µPa$^2$·s) | -12.6 | -0.8 | -2.815 x $10^{-3}$ |
| cSEL, PW (dB re 1 µPa$^2$·s) | -14.3 | -11.3 | -0.700 x $10^{-3}$ |
| cSEL, TU (dB re 1 µPa$^2$·s) | -14.2 | -12.1 | -0.503 x $10^{-3}$ |

## A.11. Foundation AV-38

Summary of measurements are shown in Table A-89. Channel 1 (bottom hydrophone) at stations AV38-750 and AV38-8000 were not functioning properly and were excluded from the analysis.

### A.11.1. Summary of Measured Sound Levels

Table A-89. Summary of Autonomous Multichannel Acoustic Recorder (AMAR) locations and measured sound levels for pile AV-38. Computed PK and SPL levels are shown for the $L_{max}$.

| Location (nominal) | Recorder ID | Distance (m) | Water depth (m) | Channel | Impulses Detected* (clipped) | PK (dB re 1 µPa) | SPL (dB re 1 µPa$^2$) | cSEL (dB re 1 µPa$^2$·s) |
|---|---|---|---|---|---|---|---|---|
| 750 | AMAR-863 | 801 | 46.1 | | | | | |
| | | | | 2 | 3363 | 182.6 | 171.9 | 197.0 |
| 750 @ 90° | AMAR-865 | 655 | 45 | 1 | 3364 | 187.0 | 175.9 | 199.7 |
| | | | | 2 | 3364 | 183.2 | 172.9 | 197.7 |
| 2000 | AMAR-855 | 2046 | 46.1 | 1 | 3366 | 175.8 | 166.3 | 191.6 |
| | | | | 2 | 3361 | 177.7 | 169.0 | 193.2 |
| 4000 | AMAR-860 | 4041 | 48.3 | 1 | 3281 | 172.0 | 162.2 | 187.2 |
| | | | | 2 | 3335 | 174.6 | 163.2 | 188.5 |
| 8000 | AMAR-603 | 8076 | 50.1 | | | | | |
| | | | | 2 | 3340 | 166.0 | 156.0 | 182.1 |

* Number of strikes produced (from hammer log): 3470

## A.11.2. Sound Levels per Station

### A.11.2.1. Station AV38-750

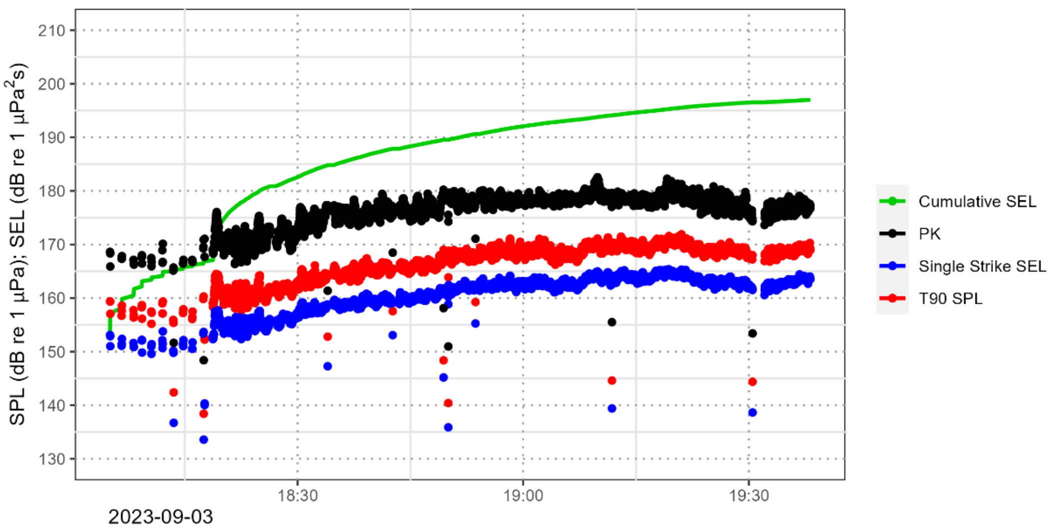


Figure A-117. Received levels for impact pile driving installation of AV-38 at monitoring station AV38-750 for channel 2. Peak SPL (PK, black), rms SPL (T90 SPL, red), single strike SEL (blue) and cumulative SEL (green) versus time (UTC). For periods during which there is no pile driving the cSEL is necessarily displayed as a constant value over time.

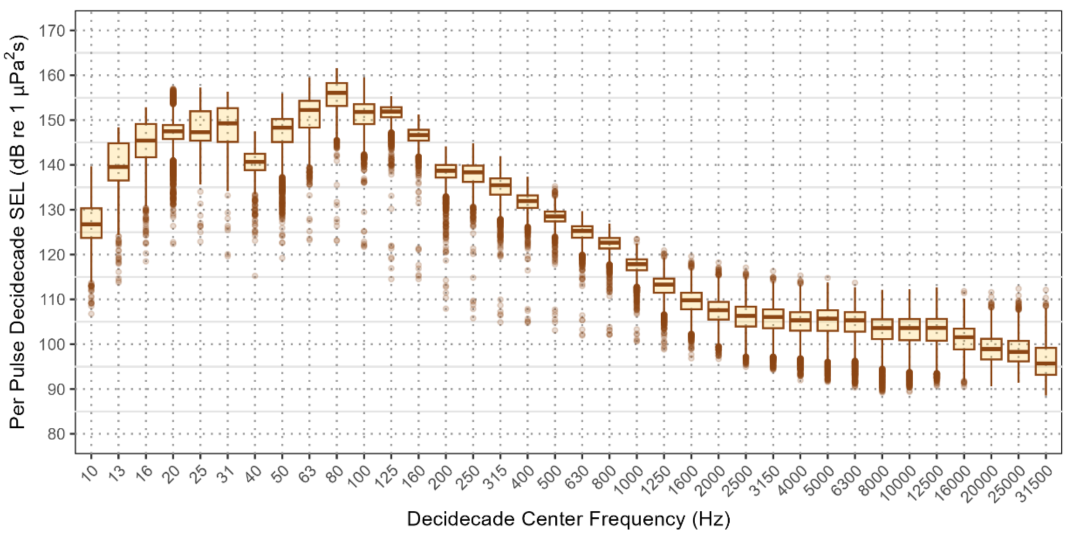


Figure A-118. Distribution of decidecade band level single strike SEL for pile driving installation of AV-38 at monitoring station AV38-750 for channel 2. Beige bars indicate the first, second, and third quartiles (*25th*, *50th*, and *75th*) or as exceedances $L_{75}$, $L_{50}$, and $L_{25}$. Upper error bars indicate the maximum levels ($L_{max}$). Lower error bars indicate the 5th percentile or $L_{95}$.

Table A-90. Received level statistics for pile driving installation of AV-38 at monitoring station AV38-750.

| Sound level statistic | PK (dB re 1 µPa) | rms SPL (dB re 1 µPa$^2$) | SELss (dB re 1 µPa$^2$·s) |
|---|---|---|---|
| **Channel 2 (mid-water)** | | | |
| $L_{max}$ | 182.6 | 171.9 | 165.4 |
| $L_5$ | 179.7 | 170.4 | 164.5 |
| $L_{25}$ | 178.4 | 169.1 | 163.2 |
| $L_{50}$ | 177.2 | 168.0 | 162.1 |
| $L_{75}$ | 175.3 | 164.5 | 158.8 |
| $L_{95}$ | 169.8 | 160.1 | 154.5 |
| $L_{mean}$ | 176.3 | 166.6 | 160.8 |

### A.11.2.2. Station AV38-75090

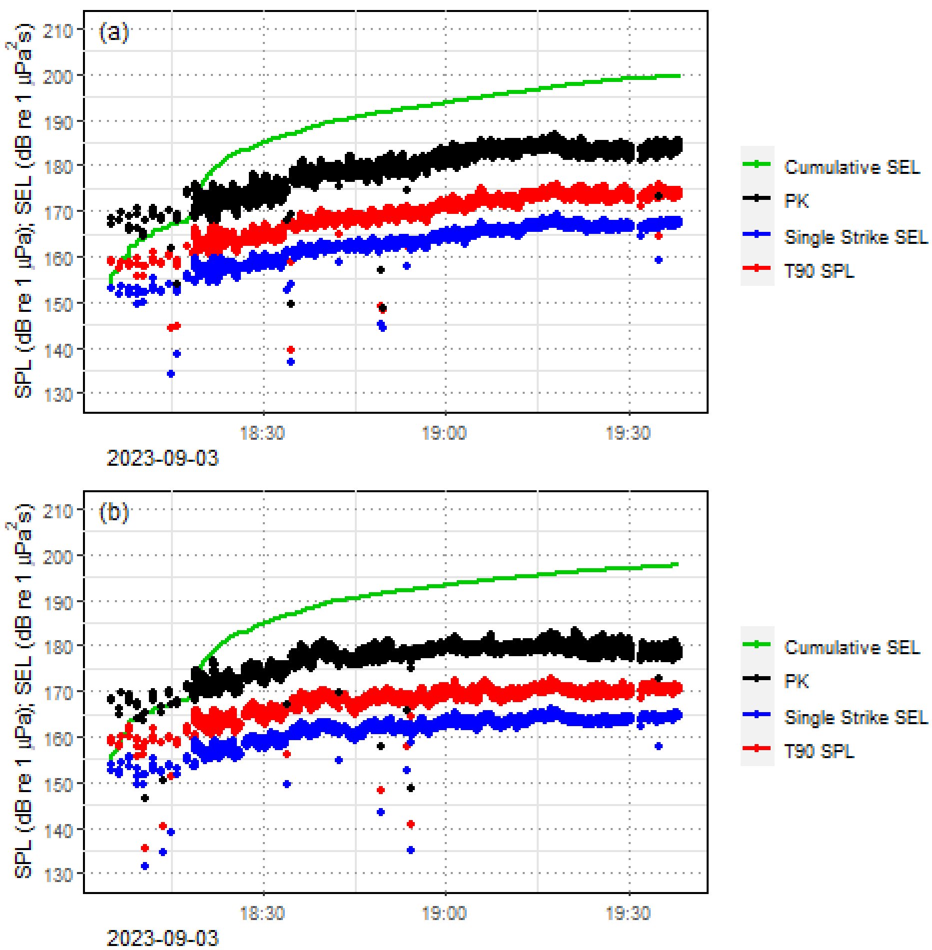


Figure A-119. Received levels for impact pile driving installation of AV-38 at monitoring station AV38-75090, for channel 1 (a) and channel 2 (b). Peak SPL (PK, black), rms SPL (T90 SPL, red), single strike SEL (blue) and cumulative SEL (green) versus time (UTC). For periods during which there is no pile driving the cSEL is necessarily displayed as a constant value over time.

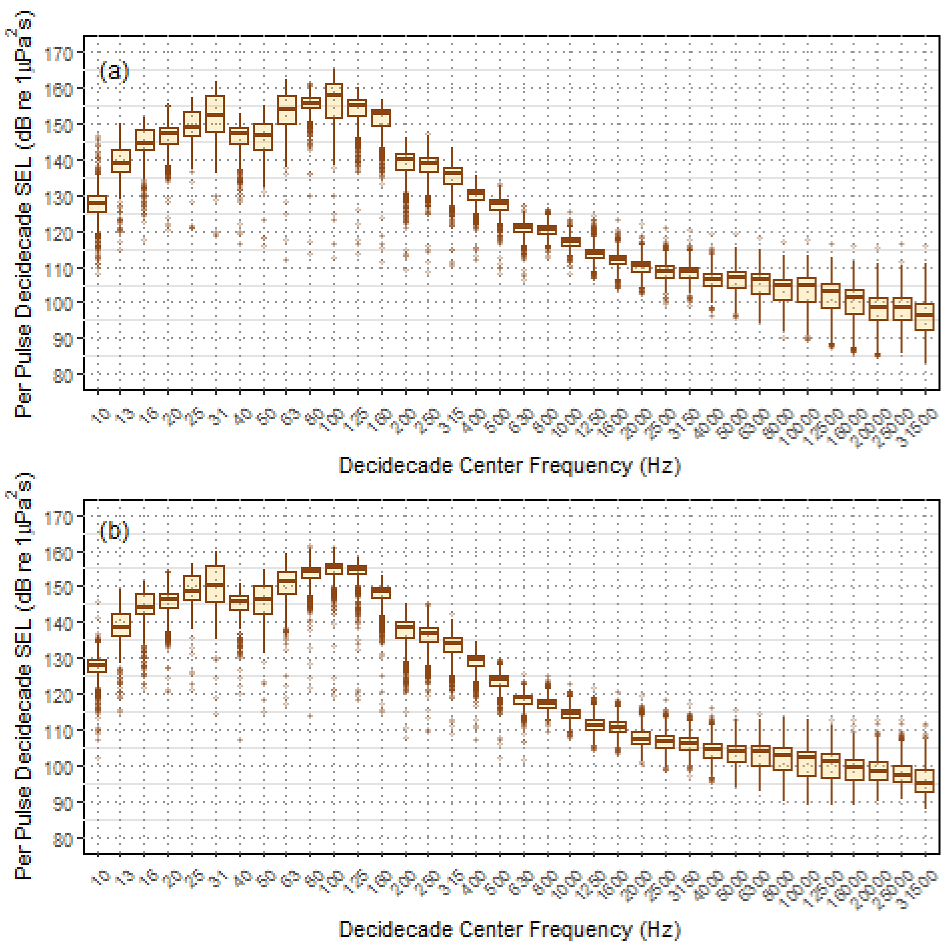


Figure A-120. Distribution of decidecade band level single strike SEL for pile driving installation of AV-38 at monitoring station AV38-75090 for channel 1 (a) and channel 2 (b). Beige bars indicate the first, second, and third quartiles (*25th*, *50th*, and *75th*) or as exceedances $L_{75}$, $L_{50}$, and $L_{25}$. Upper error bars indicate the maximum levels ($L_{max}$). Lower error bars indicate the 5th percentile or $L_{95}$.

Table A-91. Received level statistics for pile driving installation of AV-38 at monitoring station AV38-75090.

| Sound level statistic | PK (dB re 1 µPa) | rms SPL (dB re 1 µPa$^2$) | SELss (dB re 1 µPa$^2$·s) |
|---|---|---|---|
| **Channel 1 (bottom)** | | | |
| $L_{max}$ | 187.0 | 175.9 | 169.1 |
| $L_5$ | 184.6 | 174.2 | 167.4 |
| $L_{25}$ | 183.4 | 173.1 | 166.5 |
| $L_{50}$ | 181.1 | 170.2 | 163.7 |
| $L_{75}$ | 177.3 | 167.0 | 161.0 |
| $L_{95}$ | 171.4 | 162.7 | 156.8 |
| $L_{mean}$ | 179.8 | 169.6 | 163.2 |
| **Channel 2 (mid-water)** | | | |
| $L_{max}$ | 183.2 | 172.9 | 166.1 |
| $L_5$ | 180.6 | 170.9 | 164.6 |
| $L_{25}$ | 179.5 | 170.0 | 163.7 |
| $L_{50}$ | 178.6 | 168.9 | 162.6 |
| $L_{75}$ | 176.5 | 167.0 | 160.5 |
| $L_{95}$ | 171.2 | 162.8 | 156.6 |
| $L_{mean}$ | 177.5 | 168.1 | 161.8 |

### A.11.2.3. Station AV38-2000

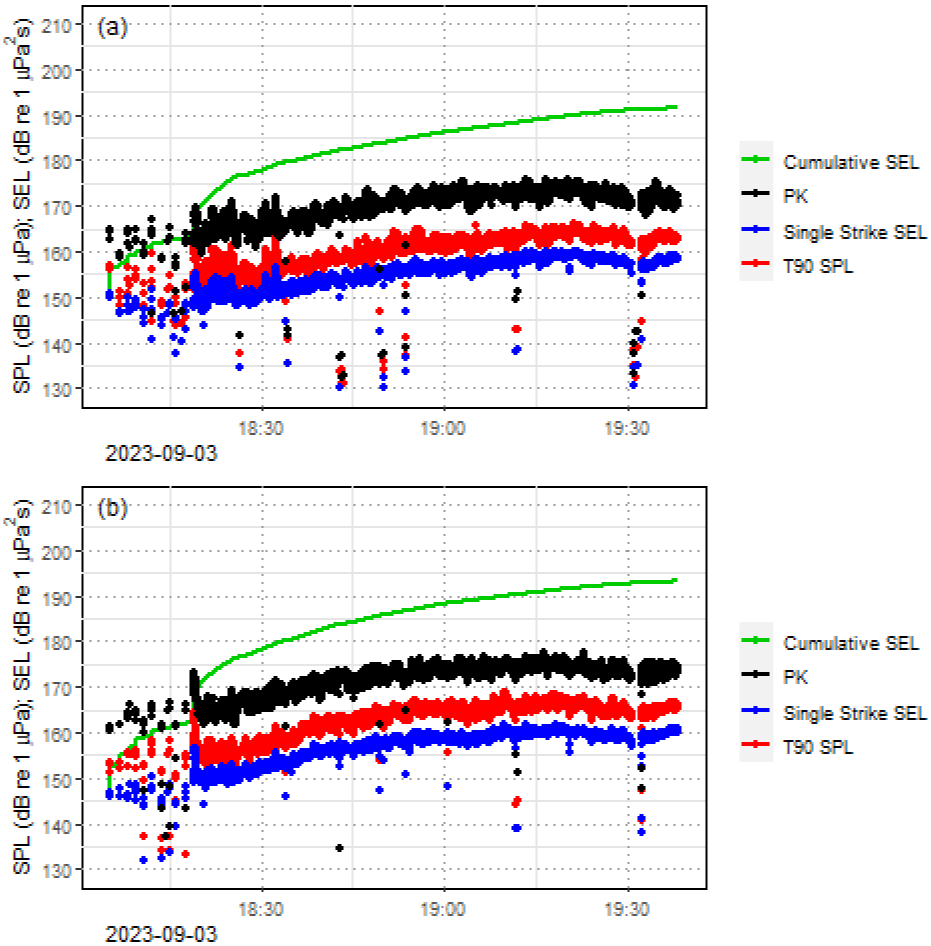


Figure A-121. Received levels for impact pile driving installation of AV-38 at monitoring station AV38-2000 for channel 1 (a) and channel 2 (b). Peak SPL (PK, black), rms SPL (T90 SPL, red), single strike SEL (blue) and cumulative SEL (green) versus time (UTC). For periods during which there was no pile driving the cSEL is necessarily displayed as a constant value over time.

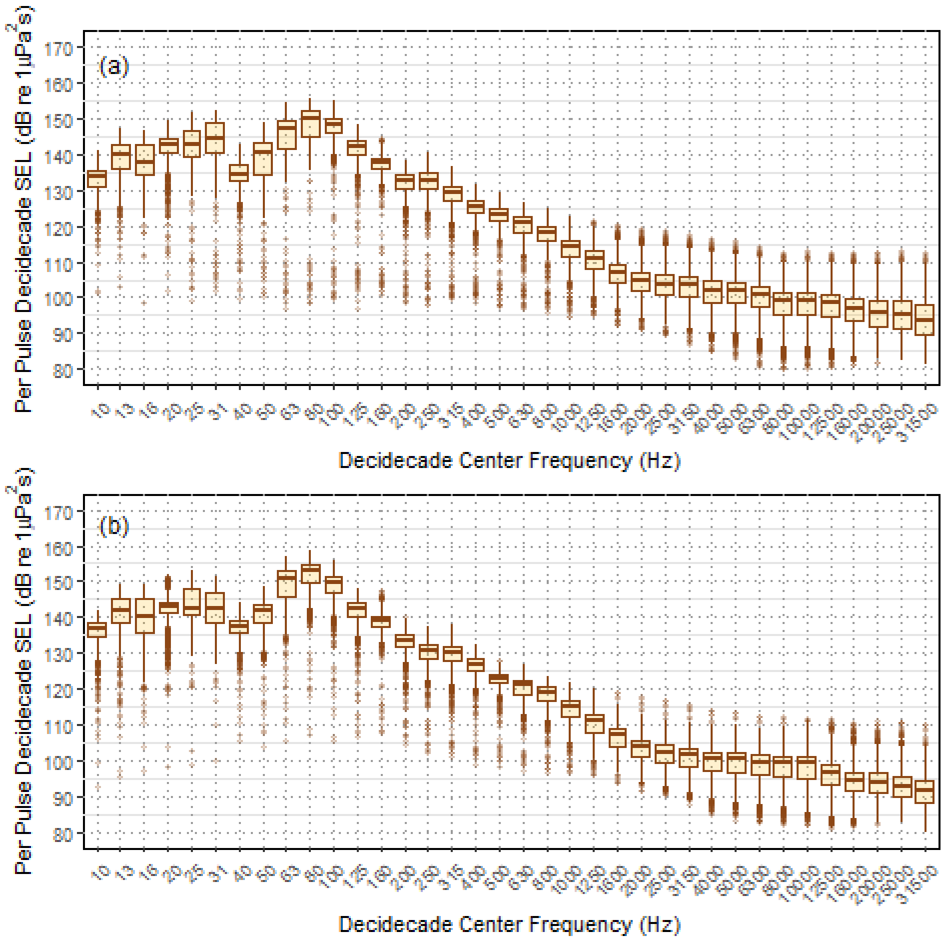


Figure A-122. Distribution of decidecade band level single strike SEL for pile driving installation of AV-38 at monitoring station AV38-2000 for channel 1 (a) and channel 2 (b). Beige bars indicate the first, second, and third quartiles (*25th*, *50th*, and *75th*) or as exceedances $L_{75}$, $L_{50}$, and $L_{25}$. Upper error bars indicate the maximum levels ($L_{max}$). Lower error bars indicate the 5th percentile or $L_{95}$.

Table A-92. Received level statistics for pile driving installation of AV-38 at monitoring station AV38-2000.

| Sound level statistic | PK (dB re 1 µPa) | rms SPL (dB re 1 µPa$^2$) | SELss (dB re 1 µPa$^2$·s) |
|---|---|---|---|
| **Channel 1 (bottom)** | | | |
| $L_{max}$ | 175.8 | 166.3 | 160.3 |
| $L_5$ | 174.2 | 164.4 | 159.3 |
| $L_{25}$ | 172.7 | 163.0 | 158.1 |
| $L_{50}$ | 171.1 | 161.3 | 156.3 |
| $L_{75}$ | 167.5 | 157.8 | 152.9 |
| $L_{95}$ | 163.4 | 153.7 | 149.3 |
| $L_{mean}$ | 169.9 | 160.1 | 155.2 |
| **Channel 2 (mid-water)** | | | |
| $L_{max}$ | 177.7 | 169.0 | 161.9 |
| $L_5$ | 175.5 | 166.8 | 160.6 |
| $L_{25}$ | 174.2 | 165.6 | 159.6 |
| $L_{50}$ | 172.9 | 164.2 | 158.4 |
| $L_{75}$ | 169.8 | 160.2 | 154.8 |
| $L_{95}$ | 164.3 | 155.1 | 150.1 |
| $L_{mean}$ | 171.6 | 162.6 | 156.9 |

### A.11.2.4. Station AV38-4000

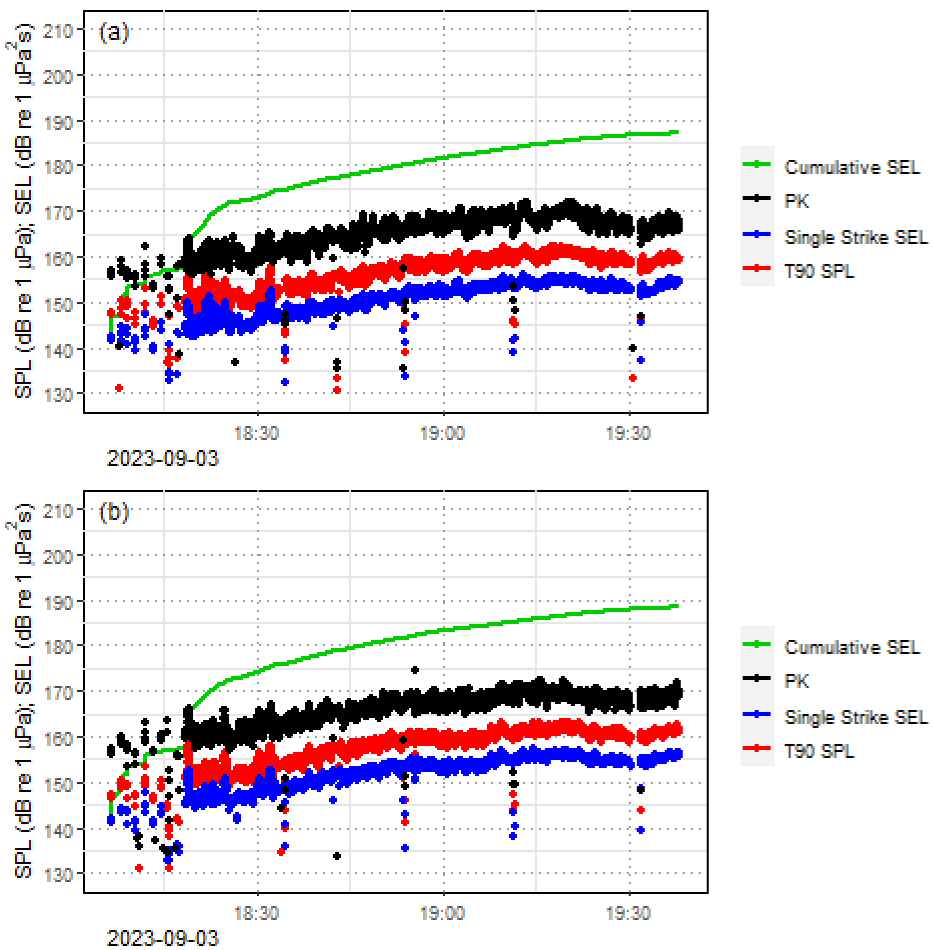


Figure A-123. Received levels for impact pile driving installation of AV-38 at monitoring station AV38-4000 for channel 1 (a) and channel 2 (b). Peak SPL (PK, black), rms SPL (T90 SPL, red), single strike SEL (blue) and cumulative SEL (green) versus time (UTC). For periods during which there is no pile driving the cSEL is necessarily displayed as a constant value over time.

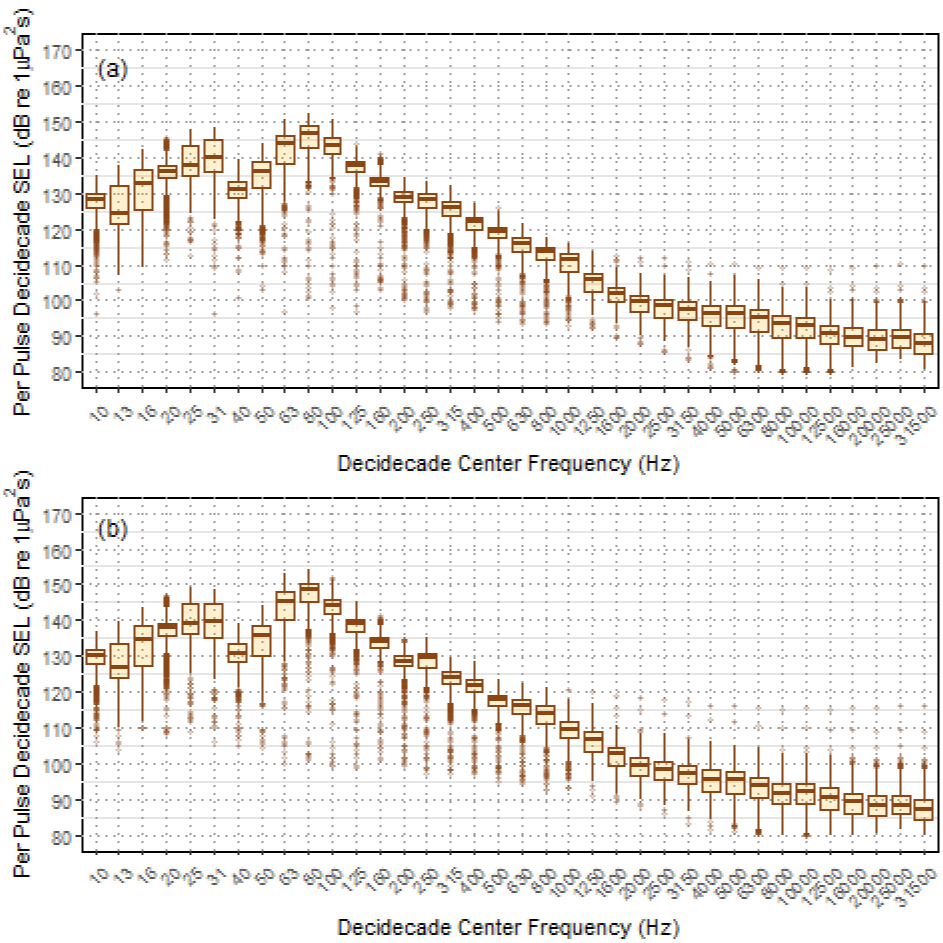


Figure A-124. Distribution of decidecade band level single strike SEL for pile driving installation of AV-38 at monitoring station AV38-4000 for channel 1 (a) and channel 2 (b). Beige bars indicate the first, second, and third quartiles (*25th*, *50th*, and *75th*) or as exceedances $L_{75}$, $L_{50}$, and $L_{25}$. Upper error bars indicate the maximum levels ($L_{max}$). Lower error bars indicate the 5th percentile or $L_{95}$.

Table A-93. Received level statistics for pile driving installation of AV-38 at monitoring station AV38-4000.

| Sound level statistic | PK (dB re 1 µPa) | rms SPL (dB re 1 µPa$^2$) | SELss (dB re 1 µPa$^2$·s) |
|---|---|---|---|
| **Channel 1 (bottom)** | | | |
| $L_{max}$ | 172.0 | 162.2 | 155.9 |
| $L_5$ | 170.1 | 161.0 | 154.9 |
| $L_{25}$ | 168.1 | 159.7 | 153.7 |
| $L_{50}$ | 166.3 | 158.0 | 152.1 |
| $L_{75}$ | 162.7 | 154.0 | 148.5 |
| $L_{95}$ | 158.5 | 149.9 | 144.6 |
| $L_{mean}$ | 165.3 | 156.7 | 150.9 |
| **Channel 2 (mid-water)** | | | |
| $L_{max}$ | 174.6 | 163.2 | 157.2 |
| $L_5$ | 170.2 | 162.0 | 156.1 |
| $L_{25}$ | 168.6 | 160.7 | 154.9 |
| $L_{50}$ | 167.0 | 159.1 | 153.4 |
| $L_{75}$ | 163.8 | 155.1 | 149.7 |
| $L_{95}$ | 159.7 | 151.0 | 145.9 |
| $L_{mean}$ | 166.0 | 157.7 | 152.1 |

## A.11.2.5. Station AV38-8000

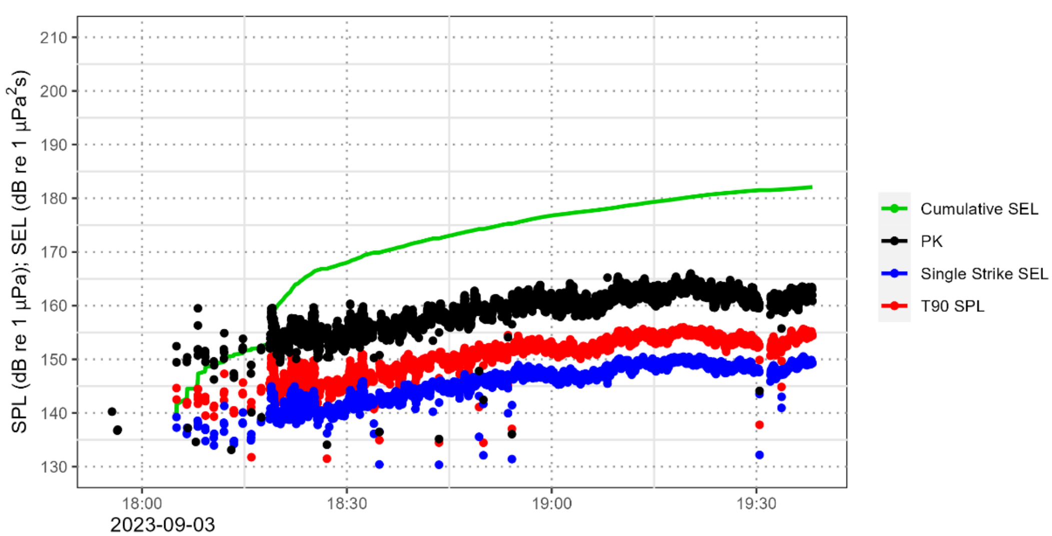


Figure A-125. Received levels for impact pile driving installation of AV-38 at monitoring station AV38-8000 for channel 2. Peak SPL (PK, black), rms SPL (T90 SPL, red), single strike SEL (blue) and cumulative SEL (green) versus time (UTC). For periods during which there is no pile driving the cSEL is necessarily displayed as a constant value over time.

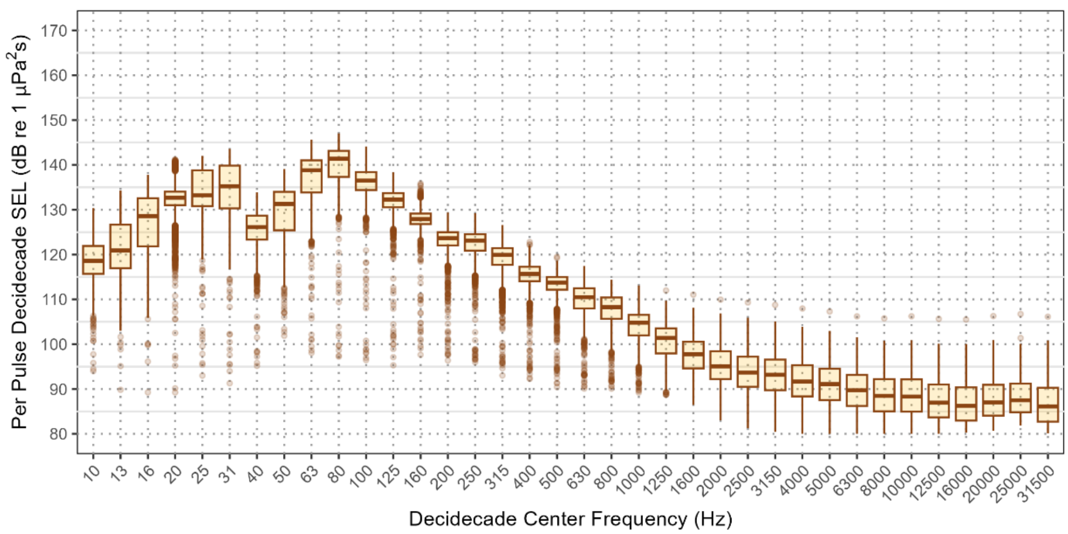


Figure A-126. Distribution of decidecade band level single strike SEL for pile driving installation of AV-38 at monitoring station AV38-8000 for channel 2. Beige bars indicate the first, second, and third quartiles (*25th*, *50th*, and *75th*) or as exceedances $L_{75}$, $L_{50}$, and $L_{25}$. Upper error bars indicate the maximum levels ($L_{max}$). Lower error bars indicate the 5th percentile or $L_{95}$.

Table A-94. Received level statistics for pile driving installation of AV-38 at monitoring station AV38-8000.

| Sound level statistic | PK (dB re 1 µPa) | rms SPL (dB re 1 µPa²) | SELss (dB re 1 µPa²·s) |
|---|---|---|---|
| **Channel 2 (mid-water)** | | | |
| $L_{max}$ | 166.0 | 156.0 | 150.5 |
| $L_5$ | 163.7 | 155.0 | 149.8 |
| $L_{25}$ | 161.9 | 153.6 | 148.6 |
| $L_{50}$ | 160.0 | 151.8 | 146.8 |
| $L_{75}$ | 156.6 | 148.3 | 143.3 |
| $L_{95}$ | 152.8 | 144.4 | 139.7 |
| $L_{mean}$ | 159.1 | 150.8 | 145.8 |

## A.11.3. Ranges to Acoustic Thresholds

Table A-95. Isopleth distances to NMFS physiological thresholds for impact driving installation of pile AV-38.

| Group | Injury: PK | | | | Injury: cSEL | | | |
|---|---|---|---|---|---|---|---|---|
| | Level (dB re 1µPa) | Predicted (m) | Measured (m) | Measured w/ attn. coeff. (m) | Level (dB re 1 µPa²·s) | Predicted (m) | Measured (m) | Measured w/ attn. coeff. (m) |
| LFC | 219 | 17 | 10 | 10 | 183 | 3,191 | 2,110 | 2,370 |
| MFC | 230 | 5 | 10 | 10 | 185 | 43 | 10 | 10 |
| HFC | 202 | 119 | 60 | 30 | 155 | 71 | 90 | 60 |
| PW | 218 | 19 | 10 | 10 | 185 | 153 | 130 | 80 |
| ST | 232 | 0 | 10 | 10 | 204 | 161 | 230 | 140 |
| AS | 206 | 78 | 30 | 20 | 187 | 6,894 | 4,460 | 4,860 |

Table A-96. Isopleth distances to NMFS behavioral thresholds for impact driving installation of pile AV-38.

| Group | Behavior: SPL | | | |
|---|---|---|---|---|
| | Level (dB re 1µPa²) | Predicted (m) | Measured (m) | Measured w/ attn. coeff. (m) |
| MM | 160 | 4,121 | 4,630 | 5,000 |
| ST | 175 | 1,400 | 530 | 440 |
| AS | 150 | 9,229 | 19,640 | 11,880 |

## A.11.4. Regression Analysis for Transmission Loss

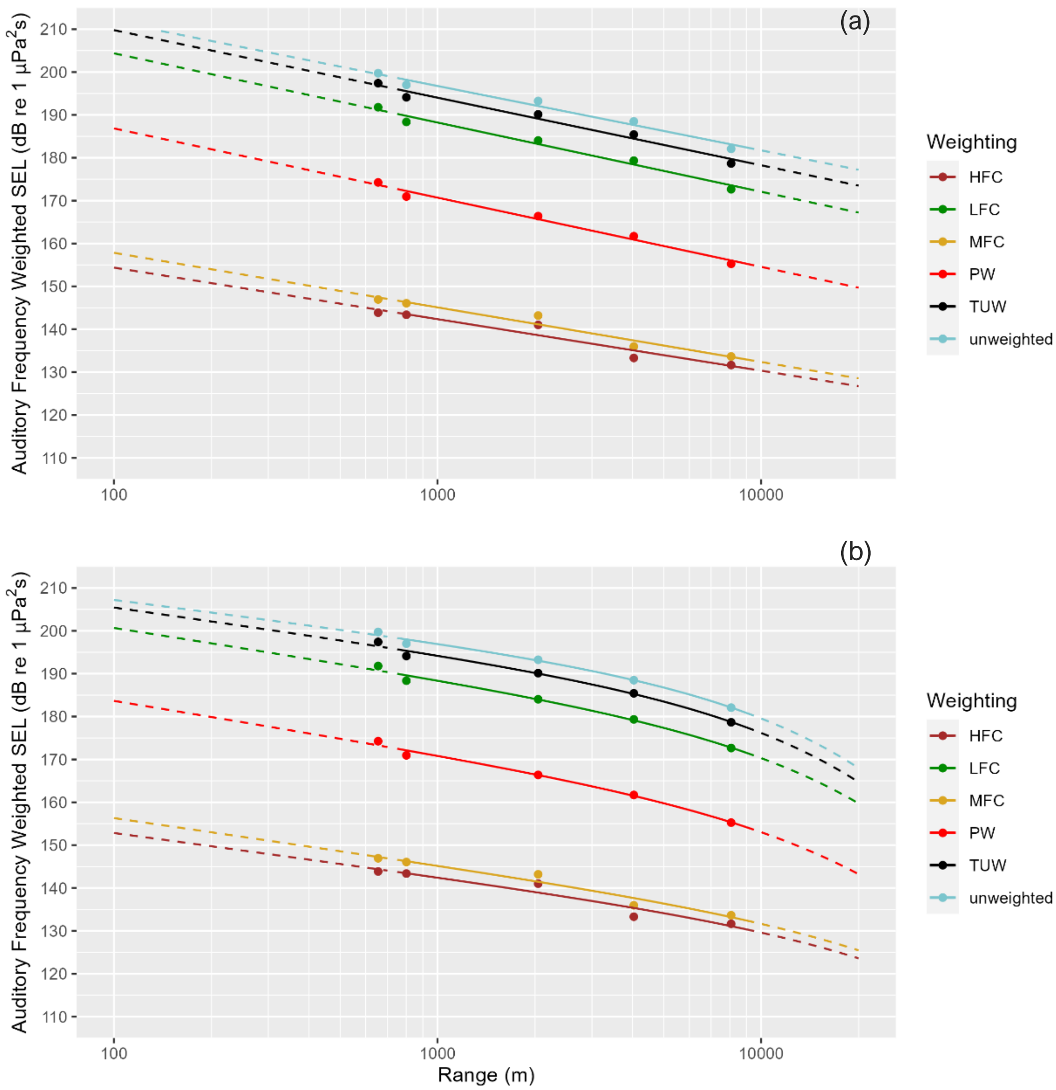


Figure A-127. Transmission loss determination based on regression analysis without (a) and with (b) intrinsic attenuation for the maximum received cumulative SEL (cSEL) at each recording station during installation of pile AV-38 on 3 Sep 2023.

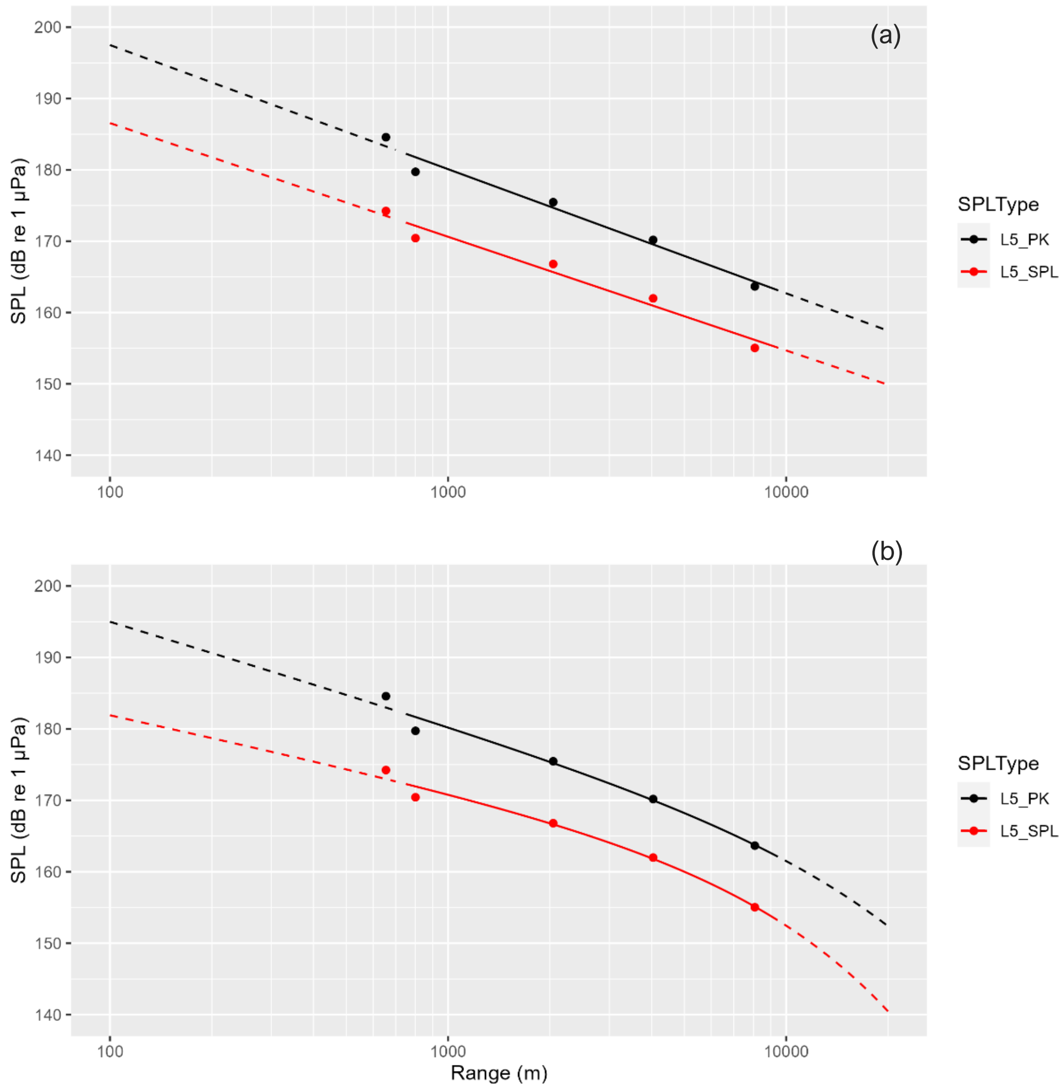


Figure A-128. Transmission loss determination based on regression analysis without (a) and with (b) intrinsic attenuation for $L_5$ PK and SPL maxima at each recording station during installation of pile AV-38 on 3 Sep 2023.

Table A-97. Regression analysis fitting coefficients for transmission loss with and without intrinsic attenuation for installation of pile AV-38 on 3 Sep 2023.

| Metric | A (dB/decade m) A*log(r) | A (dB/decade m) A*log(r) + αr/1000 | α (dB/ m) A*log(r) + αr/1000 |
|---|---|---|---|
| PK ($L_5$) (dB re 1 μPa) | -17.4 | -14.4 | -0.477 x $10^{-3}$ |
| rms SPL ($L_5$) (dB re 1 μPa$^2$) | -15.9 | -10.3 | -0.887 x $10^{-3}$ |
| cSEL (dB re 1 μPa$^2$·s) | -15.0 | -9.5 | -0.871 x $10^{-3}$ |
| cSEL, LF (dB re 1 μPa$^2$·s) | -16.1 | -11.7 | -0.705 x $10^{-3}$ |
| cSEL, MF (dB re 1 μPa$^2$·s) | -12.7 | -10.9 | -0.290 x $10^{-3}$ |
| cSEL, HF (dB re 1 μPa$^2$·s) | -12.0 | -10.2 | -0.294 x $10^{-3}$ |
| cSEL, PW (dB re 1 μPa$^2$·s) | -16.1 | -12.3 | -0.609 x $10^{-3}$ |
| cSEL, TU (dB re 1 μPa$^2$·s) | -15.8 | -10.5 | -0.830 x $10^{-3}$ |

## A.12. Foundation AN-37

Summary of measurements are shown in Table A-98. Channel 1 (bottom hydrophone) at stations AN37-750 and AN37-8000 were not functioning properly and were excluded from the analysis.

### A.12.1. Summary of Measured Sound Levels

Table A-98. Summary of Autonomous Multichannel Acoustic Recorder (AMAR) locations and measured sound levels for pile AN-37. Computed PK and SPL levels are shown for the $L_{max}$.

| Location (nominal) | Recorder ID | Distance (m) | Water depth (m) | Channel | Impulses Detected* (clipped) | PK (dB re 1 μPa) | SPL (dB re 1 μPa$^2$) | cSEL (dB re 1 μPa$^2$·s) |
|---|---|---|---|---|---|---|---|---|
| 750 | AMAR-863 | 769 | 42.9 | | | | | |
| | | | | 2 | 3552 | 182.0 | 172.0 | 196.3 |
| 750 @ 90° | AMAR-865 | 807 | 41 | 1 | 3519 | 178.9 | 169.7 | 195.6 |
| | | | | 2 | 3551 | 180.1 | 170.5 | 195.2 |
| 2000 | AMAR-855 | 2037 | 43.3 | 1 | 3563 | 174.5 | 163.9 | 190.9 |
| | | | | 2 | 4593 | 176.8 | 167.1 | 192.3 |
| 4000 | AMAR-860 | 4015 | 42.8 | 1 | 3612 | 169.5 | 159.8 | 185.3 |
| | | | | 2 | 3558 | 170.9 | 161.7 | 187.5 |
| 8000 | AMAR-603 | 8023 | 48.6 | | | | | |
| | | | | 2 | 3635 | 161.4 | 153.1 | 179.8 |

* Number of strikes produced (from hammer log): 3682

## A.12.2. Sound Levels per Station

### A.12.2.1. Station AN37-750

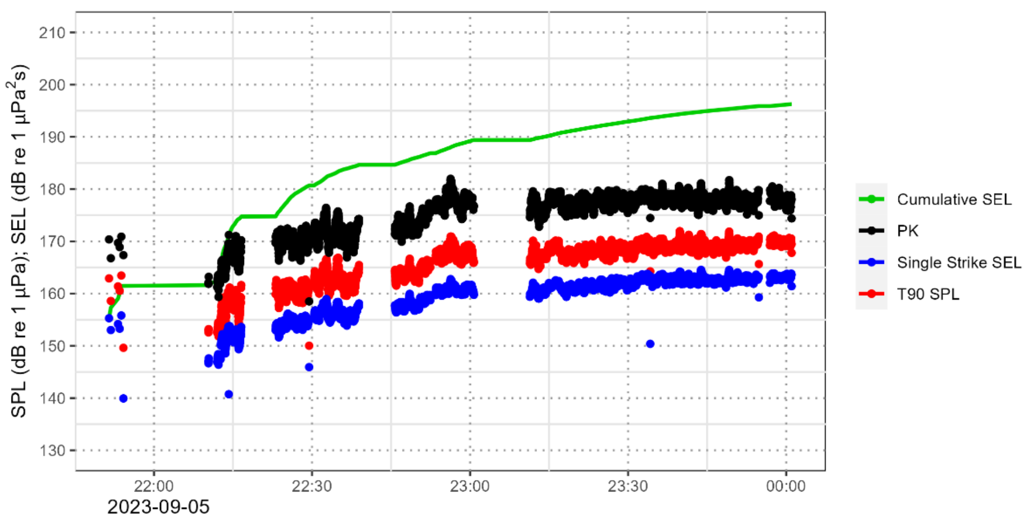


Figure A-129. Received levels for impact pile driving installation of AN-37 at monitoring station AN37-750 for channel channel 2. Peak SPL (PK, black), rms SPL (T90 SPL, red), single strike SEL (blue) and cumulative SEL (green) versus time (UTC). For periods during which there was no pile driving the cSEL is necessarily displayed as a constant value over time.

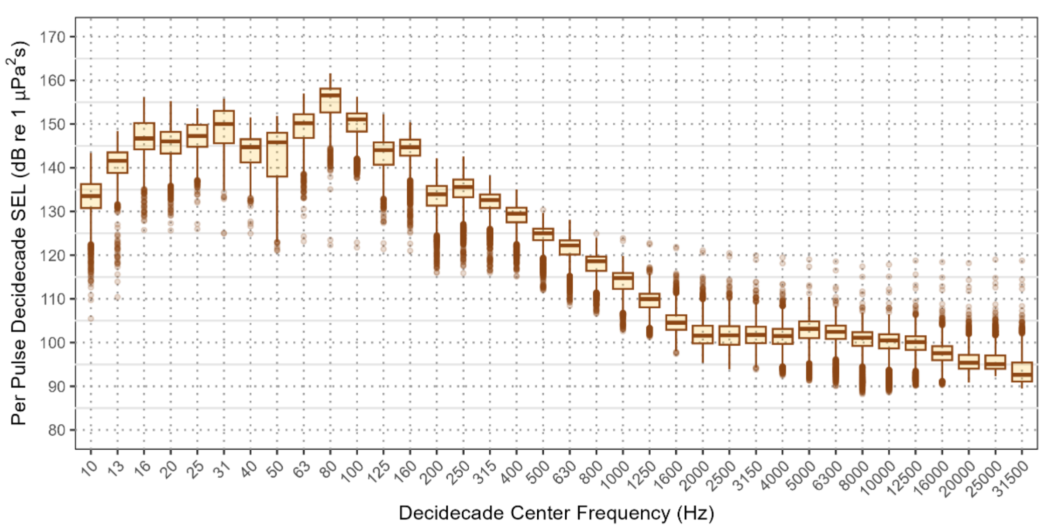


Figure A-130. Distribution of decidecade band level single strike SEL for pile driving installation of AN-37 at monitoring station AN37-750 for channel 2. Beige bars indicate the first, second, and third quartiles (*25th*, *50th*, and *75th*) or as exceedances $L_{75}$, $L_{50}$, and $L_{25}$. Upper error bars indicate the maximum levels ($L_{max}$). Lower error bars indicate the 5th percentile or $L_{95}$.

Table A-99. Received level statistics for pile driving installation of AN-37 at monitoring station AN37-750.

| Sound level statistic | PK (dB re 1 µPa) | rms SPL (dB re 1 µPa$^2$) | SELss (dB re 1 µPa$^2$·s) |
|---|---|---|---|
| **Channel 2 (mid-water)** | | | |
| $L_{max}$ | 182.0 | 172.0 | 164.5 |
| $L_5$ | 179.3 | 170.1 | 163.3 |
| $L_{25}$ | 178.2 | 169.0 | 162.4 |
| $L_{50}$ | 177.0 | 167.7 | 161.1 |
| $L_{75}$ | 172.4 | 163.4 | 157.2 |
| $L_{95}$ | 167.8 | 158.9 | 152.5 |
| $L_{mean}$ | 175.3 | 166.1 | 159.6 |

## A.12.2.2. Station AN37-75090

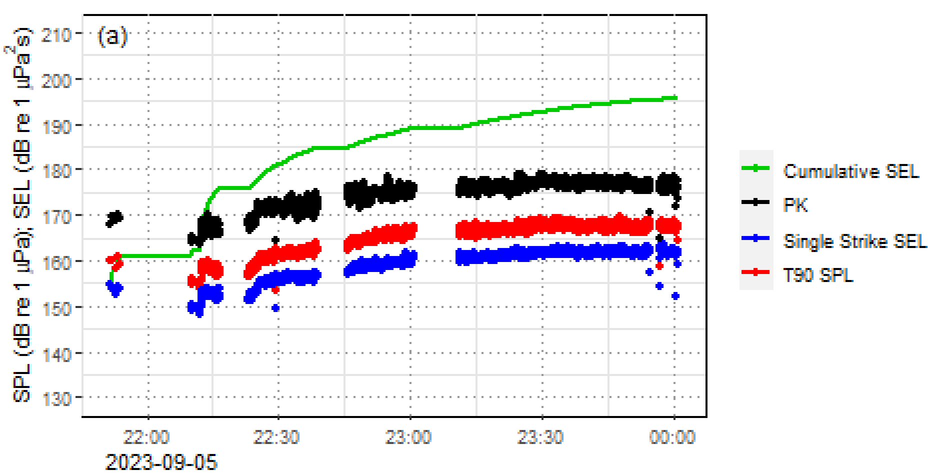


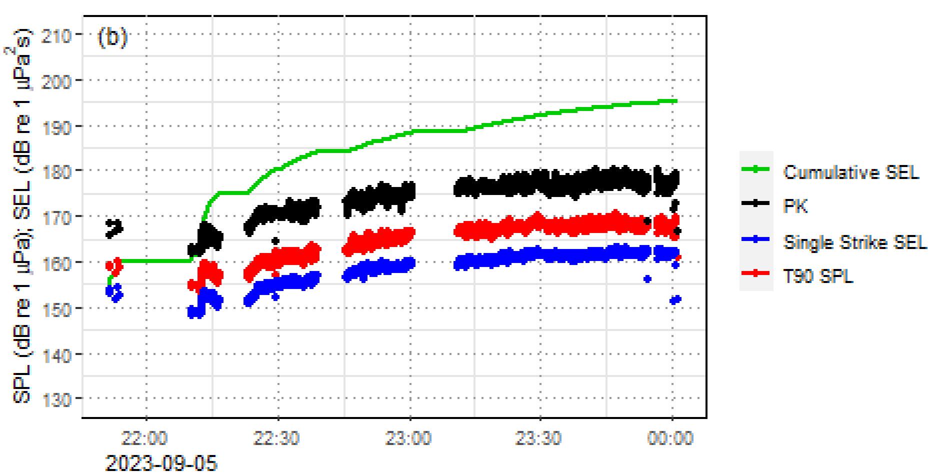


Figure A-131. Received levels for impact pile driving installation of AN-37 at monitoring station AN37-75090 for channel 1 (a) and channel 2 (b). Peak SPL (PK, black), rms SPL (T90 SPL, red), single strike SEL (blue) and cumulative SEL (green) versus time (UTC). For periods during which there was no pile driving the cSEL is necessarily displayed as a constant value over time.

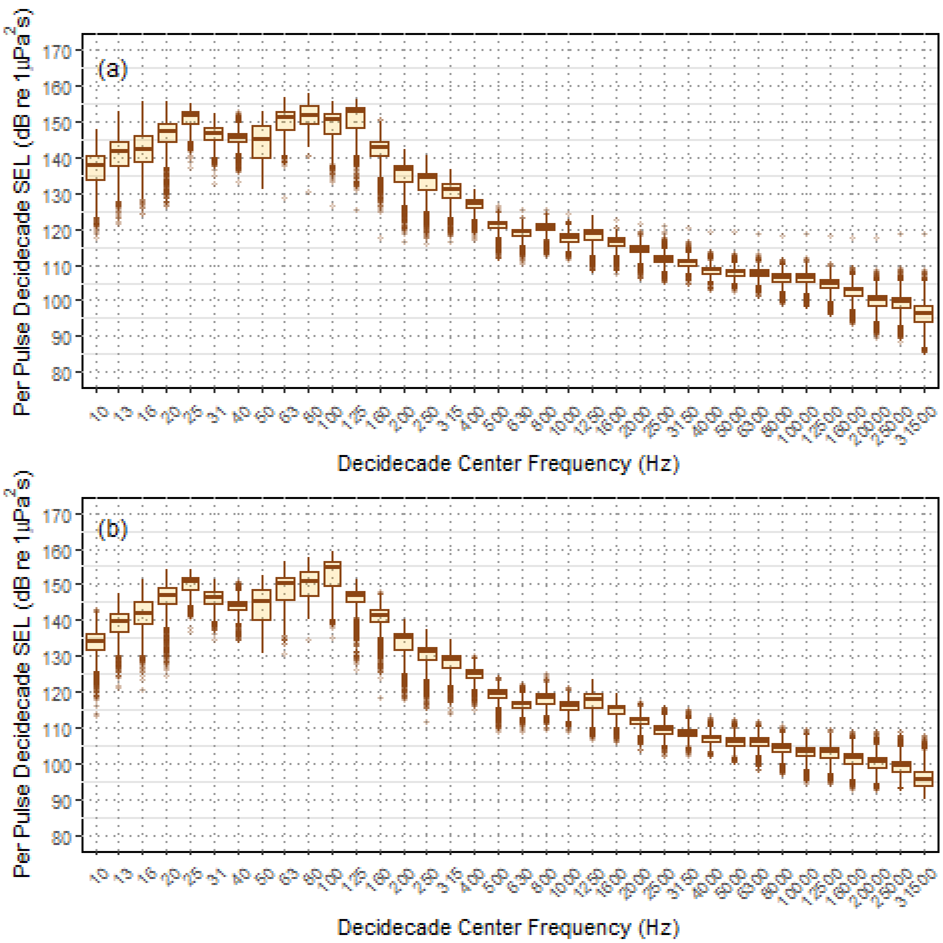


Figure A-132. Distribution of decidecade band level single strike SEL for pile driving installation of AN-37 at monitoring station AN37-75090 for channel 1 (a) and channel 2 (b). Beige bars indicate the first, second, and third quartiles (*25th*, *50th*, and *75th*) or as exceedances $L_{75}$, $L_{50}$, and $L_{25}$. Upper error bars indicate the maximum levels ($L_{max}$). Lower error bars indicate the 5th percentile or $L_{95}$.

Table A-100. Received level statistics for pile driving installation of AN-37 at monitoring station AN37-75090.

| Sound level statistic | PK (dB re 1 µPa) | rms SPL (dB re 1 µPa$^2$) | SELss (dB re 1 µPa$^2$·s) |
|---|---|---|---|
| **Channel 1 (bottom)** | | | |
| $L_{max}$ | 178.9 | 169.7 | 163.4 |
| $L_5$ | 177.7 | 168.2 | 162.4 |
| $L_{25}$ | 176.9 | 167.4 | 161.7 |
| $L_{50}$ | 175.9 | 166.5 | 160.7 |
| $L_{75}$ | 173.0 | 162.5 | 156.9 |
| $L_{95}$ | 168.1 | 158.2 | 152.7 |
| $L_{mean}$ | 174.7 | 165.0 | 159.3 |
| **Channel 2 (mid-water)** | | | |
| $L_{max}$ | 180.1 | 170.5 | 163.0 |
| $L_5$ | 178.6 | 168.7 | 162.2 |
| $L_{25}$ | 177.1 | 167.8 | 161.4 |
| $L_{50}$ | 175.8 | 166.6 | 160.1 |
| $L_{75}$ | 171.8 | 162.1 | 156.3 |
| $L_{95}$ | 166.3 | 157.9 | 152.1 |
| $L_{mean}$ | 174.4 | 165.0 | 158.8 |

### A.12.2.3. Station AN37-2000

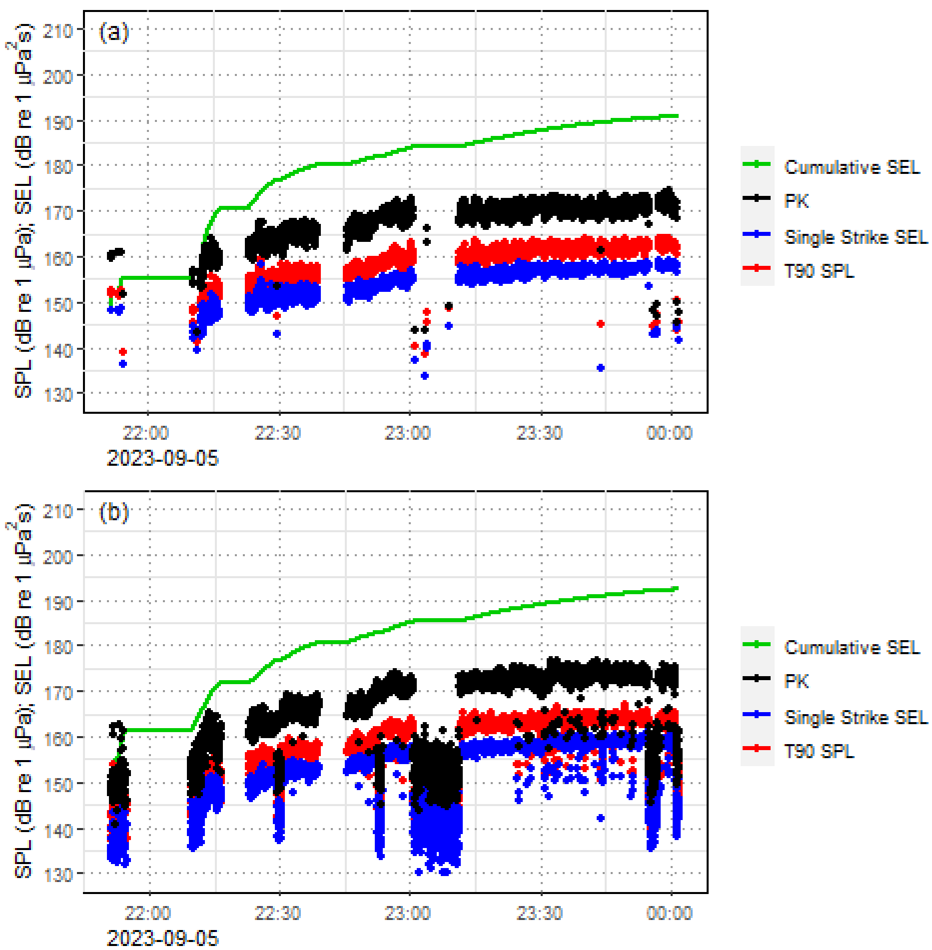


Figure A-133. Received levels for impact pile driving installation of AN-37 at monitoring station AN37-2000 for channel 1 (a) and channel 2 (b). Peak SPL (PK, black), rms SPL (T90 SPL, red), single strike SEL (blue) and cumulative SEL (green) versus time (UTC). For periods during which there was no pile driving the cSEL is necessarily displayed as a constant value over time.

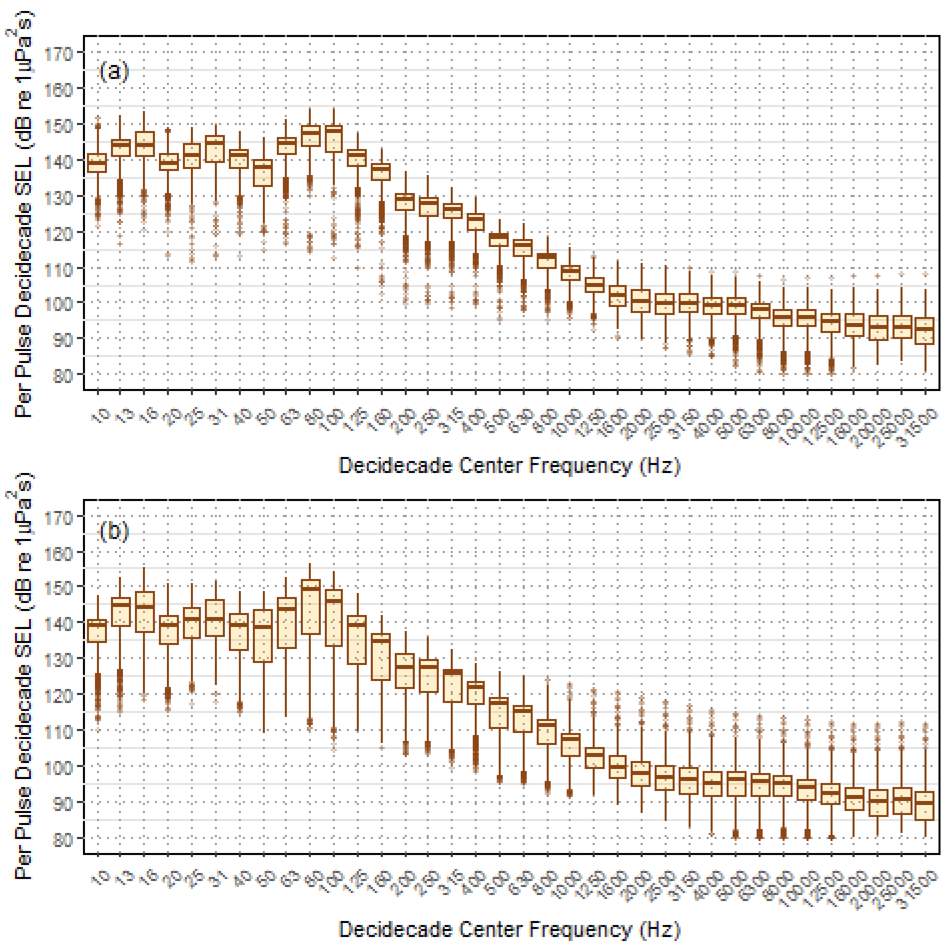


Figure A-134. Distribution of decidecade band level single strike SEL for pile driving installation of AN-37 at monitoring station AN37-2000 for channel 1 (a) and channel 2 (b). Beige bars indicate the first, second, and third quartiles (*25th*, *50th*, and *75th*) or as exceedances $L_{75}$, $L_{50}$, and $L_{25}$. Upper error bars indicate the maximum levels ($L_{max}$). Lower error bars indicate the 5th percentile or $L_{95}$.

Table A-101. Received level statistics for pile driving installation of AN-37 at monitoring station AN37-2000.

| Sound level statistic | PK (dB re 1 µPa) | rms SPL (dB re 1 µPa$^2$) | SELss (dB re 1 µPa$^2$·s) |
|---|---|---|---|
| **Channel 1 (bottom)** | | | |
| $L_{max}$ | 174.5 | 163.9 | 159.1 |
| $L_5$ | 172.2 | 162.7 | 157.9 |
| $L_{25}$ | 170.7 | 161.6 | 157.0 |
| $L_{50}$ | 169.3 | 160.3 | 155.7 |
| $L_{75}$ | 165.8 | 156.3 | 152.0 |
| $L_{95}$ | 160.6 | 152.2 | 148.0 |
| $L_{mean}$ | 168.0 | 158.9 | 154.4 |
| **Channel 2 (mid-water)** | | | |
| $L_{max}$ | 176.8 | 167.1 | 161.1 |
| $L_5$ | 174.6 | 164.4 | 159.3 |
| $L_{25}$ | 172.9 | 163.2 | 158.2 |
| $L_{50}$ | 169.0 | 159.9 | 155.3 |
| $L_{75}$ | 159.9 | 152.3 | 148.1 |
| $L_{95}$ | 150.1 | 142.8 | 138.7 |
| $L_{mean}$ | 165.8 | 157.1 | 152.4 |

## A.12.2.4. Station AN37-4000

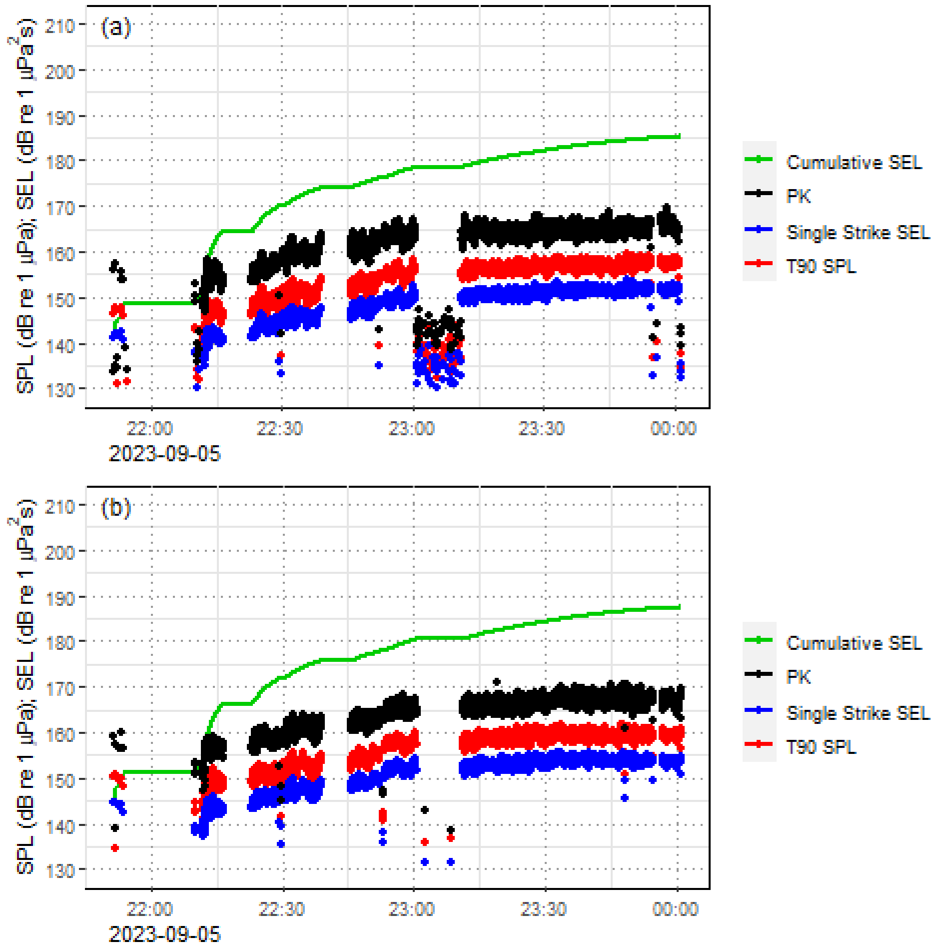


Figure A-135. Received levels for impact pile driving installation of AN-37 at monitoring station AN37-4000 for channel 1 (a) and channel 2 (b). Peak SPL (PK, black), rms SPL (T90 SPL, red), single strike SEL (blue) and cumulative SEL (green) versus time (UTC). For periods during which there is no pile driving the cSEL is necessarily displayed as a constant value over time.

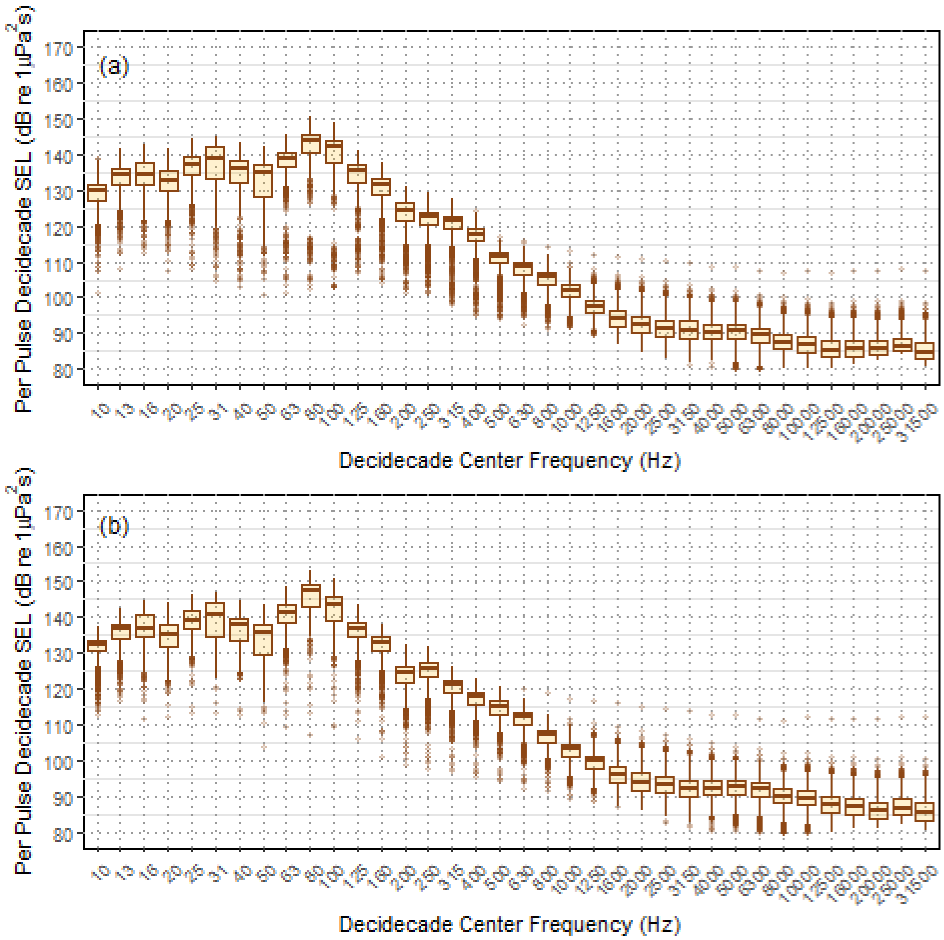


Figure A-136. Distribution of decidecade band level single strike SEL for pile driving installation of AN-37 at monitoring station AN37-4000 for channel 1 (a) and channel 2 (b). Beige bars indicate the first, second, and third quartiles (*25th*, *50th*, and *75th*) or as exceedances $L_{75}$, $L_{50}$, and $L_{25}$. Upper error bars indicate the maximum levels ($L_{max}$). Lower error bars indicate the 5th percentile or $L_{95}$.

Table A-102. Received level statistics for pile driving installation of AN-37 at monitoring station AN37-4000.

| Sound level statistic | PK (dB re 1 µPa) | rms SPL (dB re 1 µPa$^2$) | SELss (dB re 1 µPa$^2$·s) |
|---|---|---|---|
| **Channel 1 (bottom)** | | | |
| $L_{max}$ | 169.5 | 159.8 | 153.8 |
| $L_5$ | 166.4 | 158.0 | 152.2 |
| $L_{25}$ | 164.9 | 157.0 | 151.3 |
| $L_{50}$ | 163.6 | 155.9 | 150.2 |
| $L_{75}$ | 159.8 | 151.6 | 146.2 |
| $L_{95}$ | 154.1 | 146.7 | 141.1 |
| $L_{mean}$ | 162.0 | 154.0 | 148.5 |
| **Channel 2 (mid-water)** | | | |
| $L_{max}$ | 170.9 | 161.7 | 155.8 |
| $L_5$ | 168.7 | 160.4 | 154.6 |
| $L_{25}$ | 167.1 | 159.2 | 153.6 |
| $L_{50}$ | 165.6 | 158.1 | 152.5 |
| $L_{75}$ | 161.5 | 153.6 | 148.1 |
| $L_{95}$ | 156.9 | 149.2 | 143.6 |
| $L_{mean}$ | 164.2 | 156.4 | 150.8 |

## A.12.2.5. Station AN37-8000

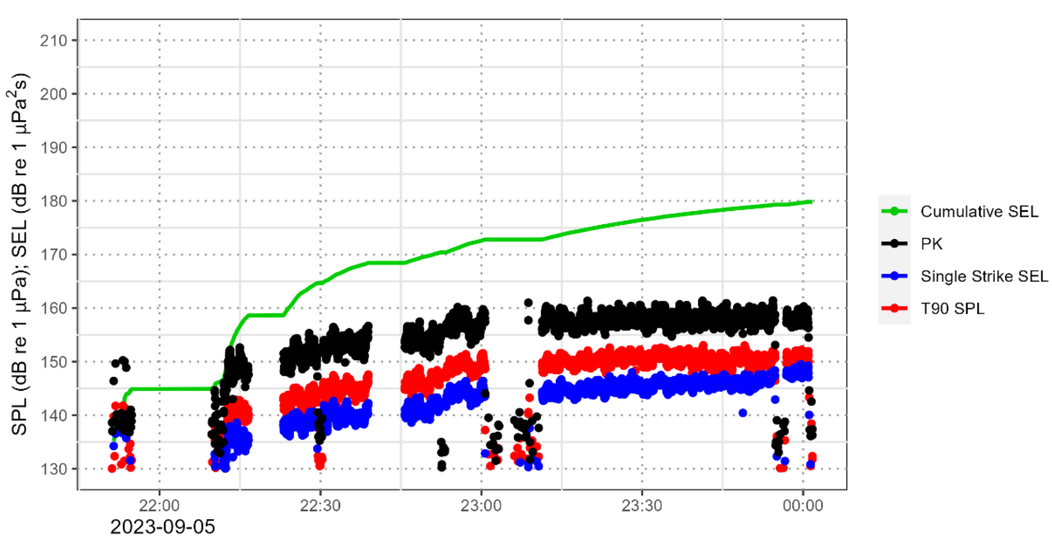


Figure A-137. Received levels for impact pile driving installation of AN-37 at monitoring station AN37-8000 for channel 2. Peak SPL (PK, black), rms SPL (T90 SPL, red), single strike SEL (blue) and cumulative SEL (green) versus time (UTC). For periods during which there is no pile driving the cSEL is necessarily displayed as a constant value over time.

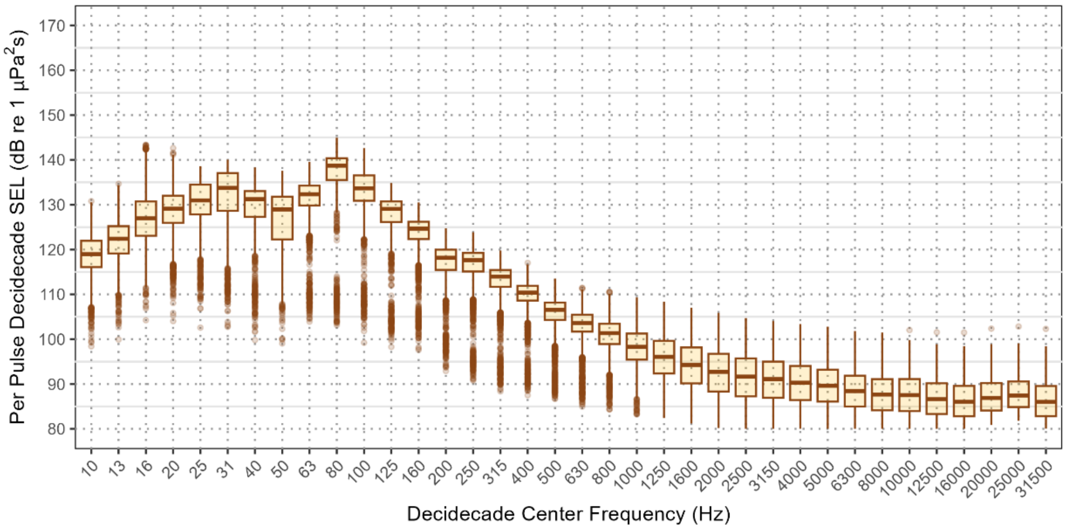


Figure A-138. Distribution of decidecade band level single strike SEL for pile driving installation of AN-37 at monitoring station AN37-8000 for channel 2. Beige bars indicate the first, second, and third quartiles (*25th*, *50th*, and *75th*) or as exceedances $L_{75}$, $L_{50}$, and $L_{25}$. Upper error bars indicate the maximum levels ($L_{max}$). Lower error bars indicate the 5th percentile or $L_{95}$.

Table A-103. Received level statistics for pile driving installation of AN-37 at monitoring station AN37-8000.

| Sound level statistic | PK (dB re 1 µPa) | rms SPL (dB re 1 µPa$^2$) | SELss (dB re 1 µPa$^2$·s) |
|---|---|---|---|
| **Channel 2 (mid-water)** | | | |
| $L_{max}$ | 161.4 | 153.1 | 149.5 |
| $L_5$ | 159.4 | 151.6 | 147.4 |
| $L_{25}$ | 158.1 | 150.6 | 145.8 |
| $L_{50}$ | 157.0 | 149.5 | 144.5 |
| $L_{75}$ | 153.5 | 145.3 | 140.2 |
| $L_{95}$ | 147.8 | 139.8 | 135.2 |
| $L_{mean}$ | 155.3 | 147.5 | 142.7 |

## A.12.3. Ranges to Acoustic Thresholds

Table A-104. Isopleth distances to NMFS physiological thresholds for impact driving installation of pile AN-37.

| Group | Injury: PK | | | | Injury: cSEL | | | |
|---|---|---|---|---|---|---|---|---|
| | Level (dB re 1µPa) | Predicted (m) | Measured (m) | Measured w/ attn. coeff. (m) | Level (dB re 1 µPa$^2$·s) | Predicted (m) | Measured (m) | Measured w/ attn. coeff. (m) |
| LFC | 219 | 17 | 10 | 10 | 183 | 3,191 | 1,500 | 1,820 |
| MFC | 230 | 5 | 10 | 10 | 185 | 43 | 10 | 10 |
| HFC | 202 | 119 | 50 | 10 | 155 | 71 | 80 | 200 |
| PW | 218 | 19 | 10 | 10 | 185 | 153 | 90 | 10 |
| ST | 232 | 0 | 10 | 10 | 204 | 161 | 160 | 10 |
| AS | 206 | 78 | 30 | 10 | 187 | 6,894 | 3,490 | 4,340 |

Table A-105. Isopleth distances to NMFS behavioral thresholds for impact driving installation of pile AN-37.

| Group | Behavior: SPL | | | |
|---|---|---|---|---|
| | Level (dB re 1µPa$^2$) | Predicted (m) | Measured (m) | Measured w/ attn. coeff. (m) |
| MM | 160 | 4,121 | 3,220 | 4,000 |
| ST | 175 | 1,400 | 390 | 130 |
| AS | 150 | 9,229 | 13,080 | 8,920 |

## A.12.4. Regression Analysis for Transmission Loss

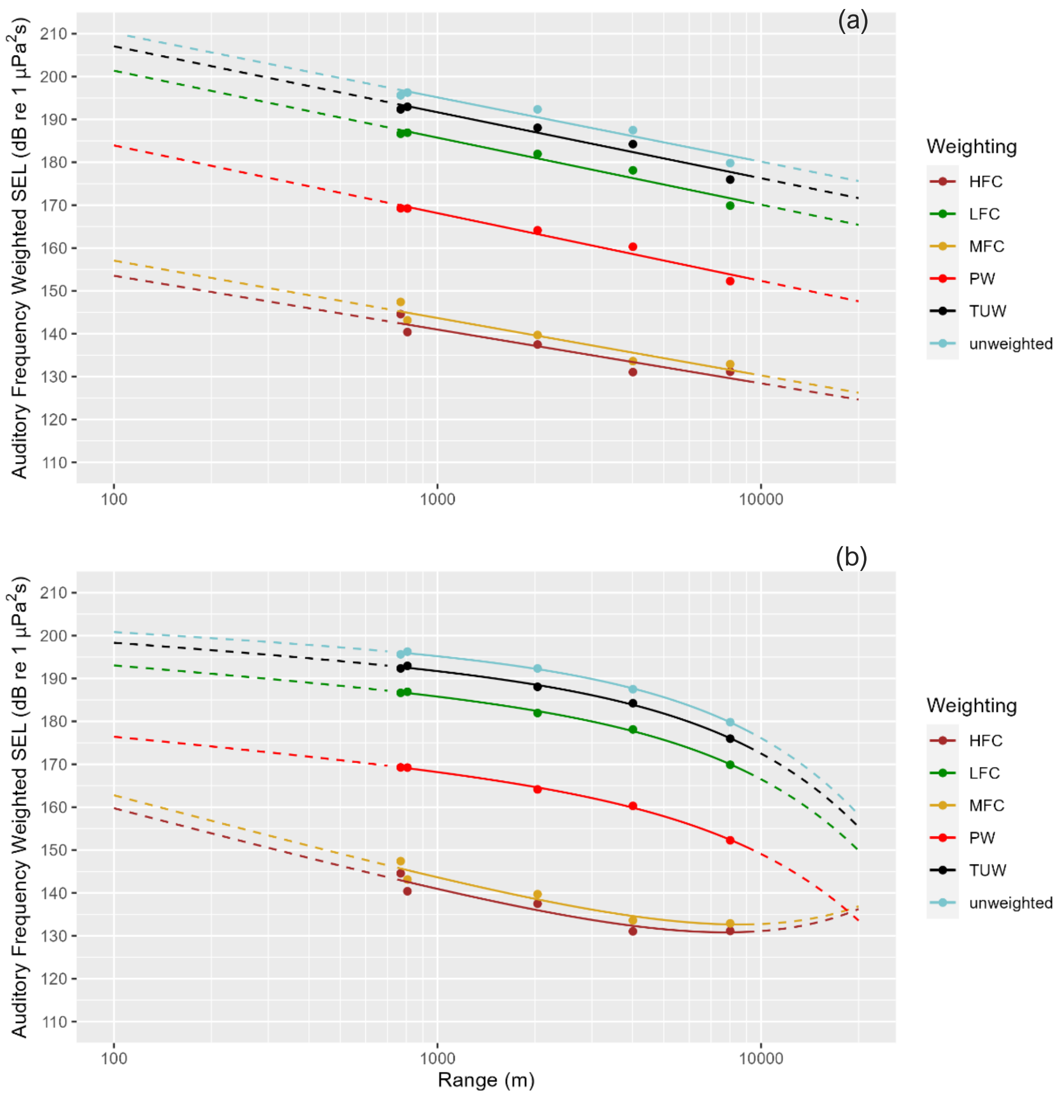


Figure A-139. Transmission loss determination based on regression analysis without (a) and with (b) intrinsic attenuation for the maximum received cumulative SEL (cSEL) at each recording station during installation of pile AN-37 on 5 Sep 2023.

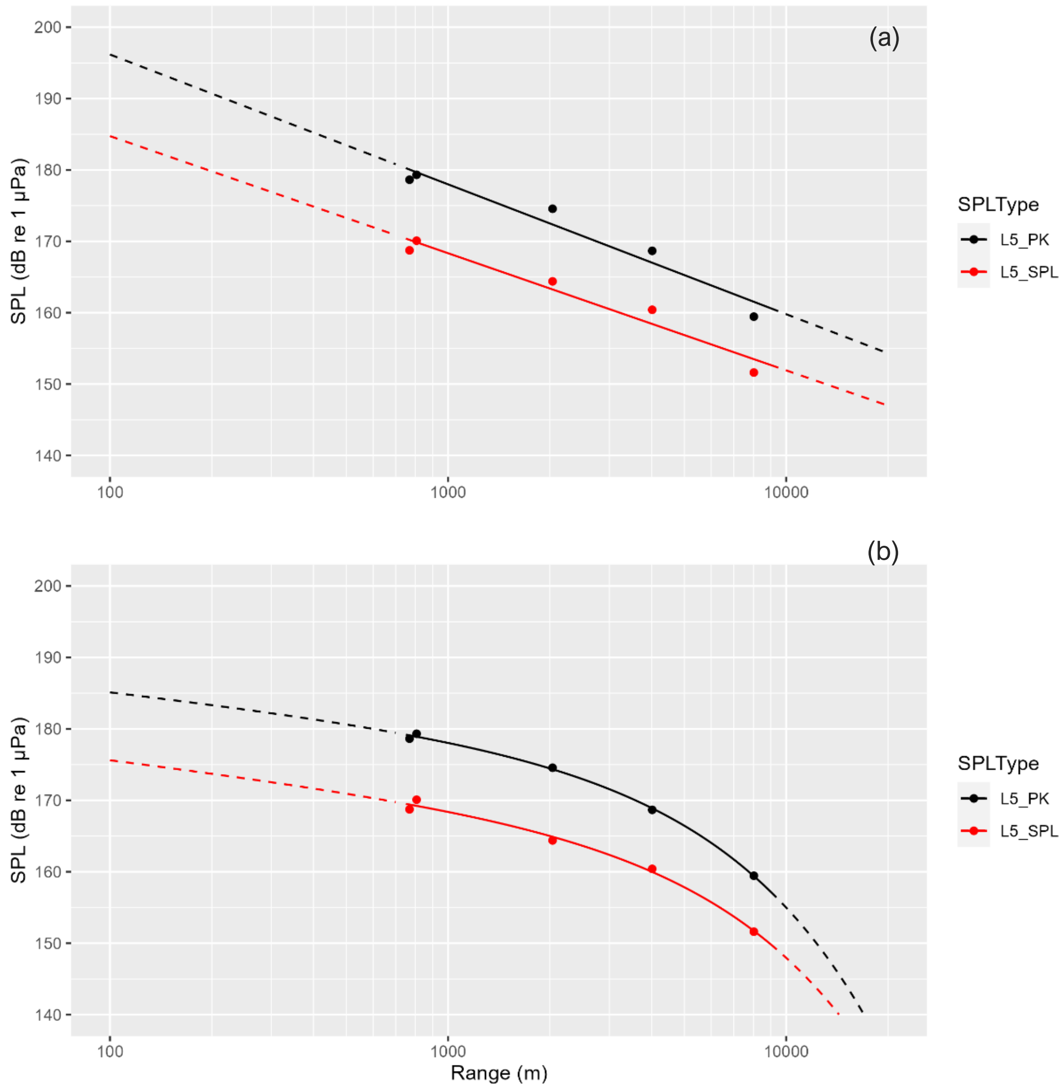


Figure A-140. Transmission loss determination based on regression analysis without (a) and with (b) intrinsic attenuation for $L_5$ PK and SPL maxima at each recording station during installation of pile AN-37 on 5 Sep 2023.

Table A-106. Regression analysis fitting coefficients for transmission loss with and without intrinsic attenuation for installation of pile AN-37 on 5 Sep 2023.

| Metric | A (dB/decade m) A*log(r) | A (dB/decade m) A*log(r) + αr/1000 | α (dB/ m) A*log(r) + αr/1000 |
|---|---|---|---|
| PK ($L_5$) (dB re 1 μPa) | -18.2 | -5.3 | -1.971 x $10^{-3}$ |
| rms SPL ($L_5$) (dB re 1 μPa$^2$) | -16.4 | -5.8 | -1.627 x $10^{-3}$ |
| cSEL (dB re 1 μPa$^2$·s) | -15.0 | -4.1 | -1.662 x $10^{-3}$ |
| cSEL, LF (dB re 1 μPa$^2$·s) | -15.6 | -5.9 | -1.482 x $10^{-3}$ |
| cSEL, MF (dB re 1 μPa$^2$·s) | -13.4 | -20.0 | 1.018 x $10^{-3}$ [a] |
| cSEL, HF (dB re 1 μPa$^2$·s) | -12.6 | -19.8 | 1.109 x $10^{-3}$ [a] |
| cSEL, PW (dB re 1 μPa$^2$·s) | -15.8 | -7.1 | -1.339 x $10^{-3}$ |
| cSEL, TU (dB re 1 μPa$^2$·s) | -15.4 | -5.2 | -1.554 x $10^{-3}$ |

[a] Positive attenuation coefficients could indicate ambient noise contamination and may not be valid.

# A.13. Foundation AU-38

Summary of measurements are shown in Table A-107. Channel 1 (bottom hydrophone) at stations AU38-750 and AU38-8000 were not functioning properly and were excluded from the analysis.

## A.13.1. Summary of Measured Sound Levels

Table A-107. Summary of Autonomous Multichannel Acoustic Recorder (AMAR) locations and measured sound levels for pile AU-38. Computed PK and SPL levels are shown for the $L_{max}$.

| Location (nominal) | Recorder ID | Distance (m) | Water depth (m) | Channel | Impulses Detected* (clipped) | PK (dB re 1 μPa) | SPL (dB re 1 μPa$^2$) | cSEL (dB re 1 μPa$^2$·s) |
|---|---|---|---|---|---|---|---|---|
| 750 | AMAR-863 | 737 | 44.8 | | | | | |
| | | | | 2 | 2802 | 183.2 | 174.3 | 197.1 |
| 750 @ 90° | AMAR-865 | 822 | 44.4 | 1 | 2307 | 183.3 | 173.3 | 196.6 |
| | | | | 2 | 2308 | 182.2 | 172.2 | 194.9 |
| 2000 | AMAR-855 | 2012 | 46.1 | 1 | 2808 | 177.2 | 167.7 | 191.5 |
| | | | | 2 | 2797 | 177.4 | 169.0 | 192.5 |
| 4000 | AMAR-860 | 4016 | 46.1 | 1 | 2880 | 171.2 | 163.1 | 186.7 |
| | | | | 2 | 2800 | 172.1 | 164.2 | 188.3 |
| 8000 | AMAR-603 | 8390 | 50.1 | | | | | |
| | | | | 2 | 2811 | 164.3 | 156.9 | 181.3 |

* Number of strikes produced (from hammer log): 2884

# A.13.2. Sound Levels per Station

## A.13.2.1. Station AU38-750

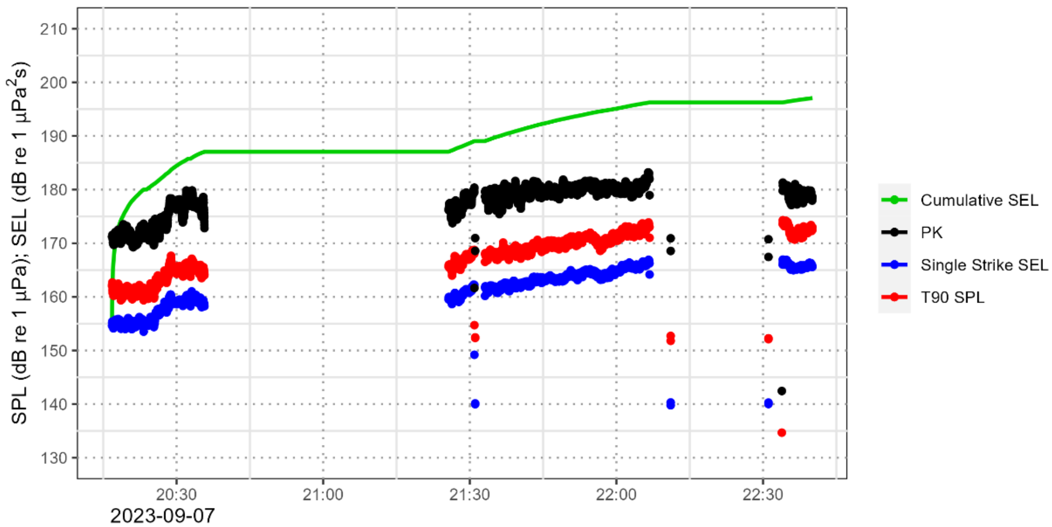


Figure A-141. Received levels for impact pile driving installation of AU-38 at monitoring station AU38-750 for channel channel 2. Peak SPL (PK, black), rms SPL (T90 SPL, red), single strike SEL (blue) and cumulative SEL (green) versus time (UTC). For periods during which there was no pile driving the cSEL is necessarily displayed as a constant value over time.

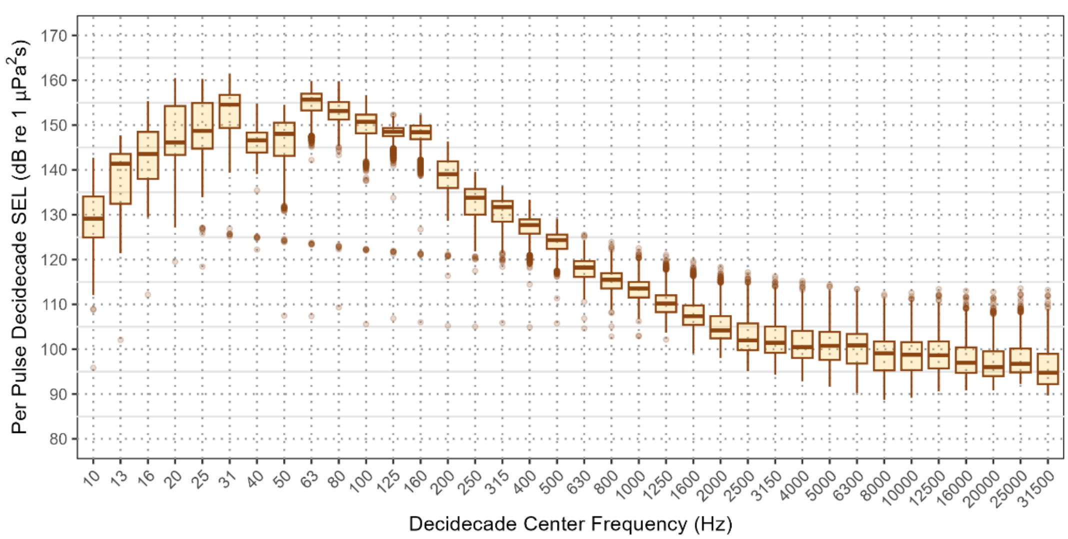


Figure A-142. Distribution of decidecade band level single strike SEL for pile driving installation of AU-38 at monitoring station AU38-750 for channel 2. Beige bars indicate the first, second, and third quartiles (*25th*, *50th*, and *75th*) or as exceedances $L_{75}$, $L_{50}$, and $L_{25}$. Upper error bars indicate the maximum levels ($L_{max}$). Lower error bars indicate the 5th percentile or $L_{95}$.

Table A-108. Received level statistics for pile driving installation of AU-38 at monitoring station AU38-750.

| Sound level statistic | PK (dB re 1 µPa) | rms SPL (dB re 1 µPa$^2$) | SELss (dB re 1 µPa$^2$·s) |
|---|---|---|---|
| **Channel 2 (mid-water)** | | | |
| $L_{max}$ | 183.2 | 174.3 | 167.0 |
| $L_5$ | 181.0 | 172.7 | 166.0 |
| $L_{25}$ | 180.0 | 170.7 | 164.2 |
| $L_{50}$ | 178.8 | 168.3 | 162.1 |
| $L_{75}$ | 176.4 | 165.2 | 159.2 |
| $L_{95}$ | 170.9 | 160.6 | 155.0 |
| $L_{mean}$ | 177.7 | 167.6 | 161.4 |

## A.13.2.2. Station AU38-75090

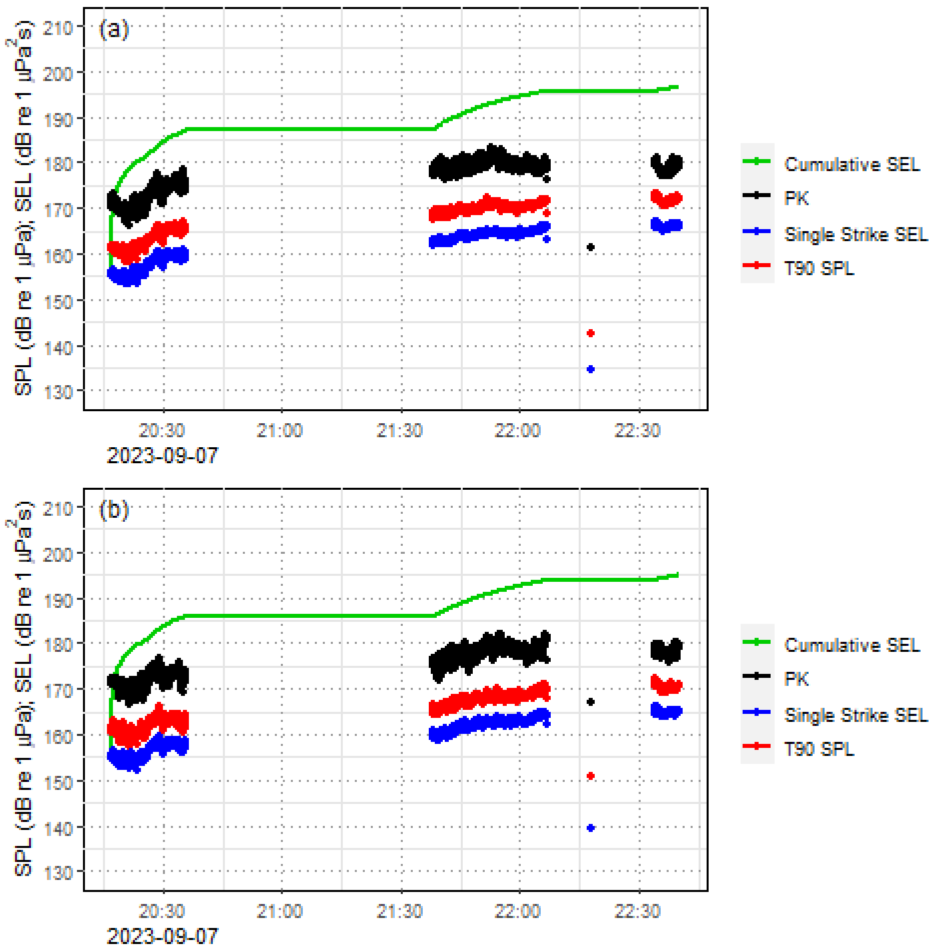


Figure A-143. Received levels for impact pile driving installation of AU-38 at monitoring station AU38-75090 for channel 1 (a) and channel 2 (b). Peak SPL (PK, black), rms SPL (T90 SPL, red), single strike SEL (blue) and cumulative SEL (green) versus time (UTC). For periods during which there was no pile driving the cSEL is necessarily displayed as a constant value over time.

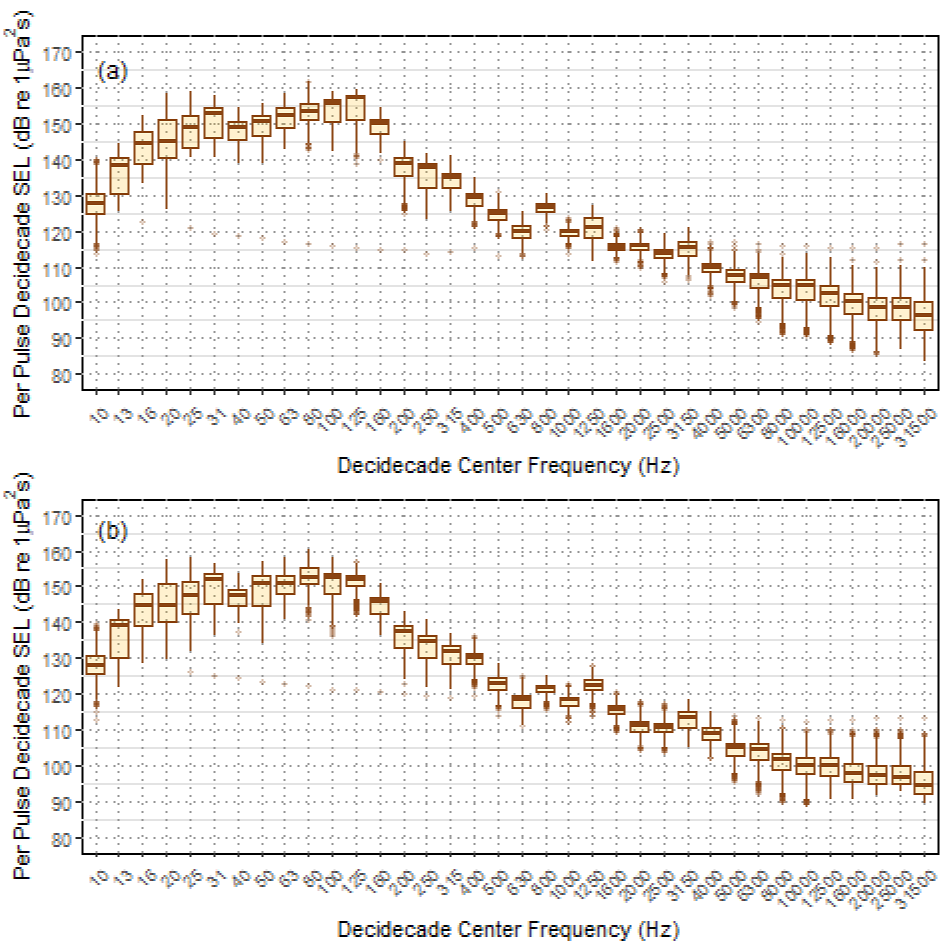


Figure A-144. Distribution of decidecade band level single strike SEL for pile driving installation of AU-38 at monitoring station AU38-75090 for channel 1 (a) and channel 2 (b). Beige bars indicate the first, second, and third quartiles (*25th*, *50th*, and *75th*) or as exceedances $L_{75}$, $L_{50}$, and $L_{25}$. Upper error bars indicate the maximum levels ($L_{max}$). Lower error bars indicate the 5th percentile or $L_{95}$.

Table A-109. Received level statistics for pile driving installation of AU-38 at monitoring station AU38-75090.

| Sound level statistic | PK (dB re 1 µPa) | rms SPL (dB re 1 µPa$^2$) | SELss (dB re 1 µPa$^2$·s) |
|---|---|---|---|
| **Channel 1 (bottom)** | | | |
| $L_{max}$ | 183.3 | 173.3 | 167.2 |
| $L_5$ | 181.2 | 171.8 | 166.0 |
| $L_{25}$ | 179.6 | 170.5 | 164.7 |
| $L_{50}$ | 178.2 | 169.4 | 163.4 |
| $L_{75}$ | 174.0 | 164.4 | 158.8 |
| $L_{95}$ | 169.3 | 160.5 | 155.0 |
| $L_{mean}$ | 176.7 | 167.5 | 161.7 |
| **Channel 2 (mid-water)** | | | |
| $L_{max}$ | 182.2 | 172.2 | 166.0 |
| $L_5$ | 180.1 | 170.3 | 164.7 |
| $L_{25}$ | 178.3 | 168.5 | 162.9 |
| $L_{50}$ | 176.7 | 166.7 | 161.1 |
| $L_{75}$ | 172.6 | 162.7 | 157.3 |
| $L_{95}$ | 169.4 | 159.7 | 154.2 |
| $L_{mean}$ | 175.5 | 165.7 | 160.1 |

### A.13.2.3. Station AU38-2000

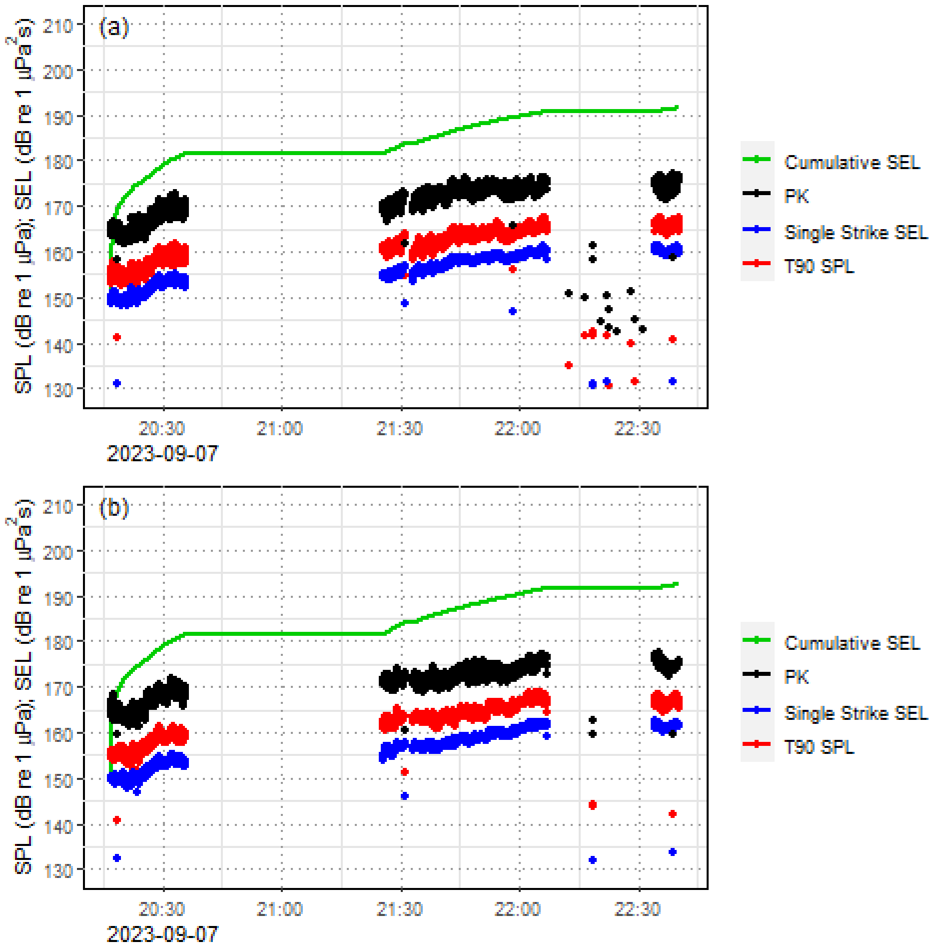


Figure A-145. Received levels for impact pile driving installation of AU-38 at monitoring station AU38-2000 for channel 1 (a) and channel 2 (b). Peak SPL (PK, black), rms SPL (T90 SPL, red), single strike SEL (blue) and cumulative SEL (green) versus time (UTC). For periods during which there was no pile driving the cSEL is necessarily displayed as a constant value over time.

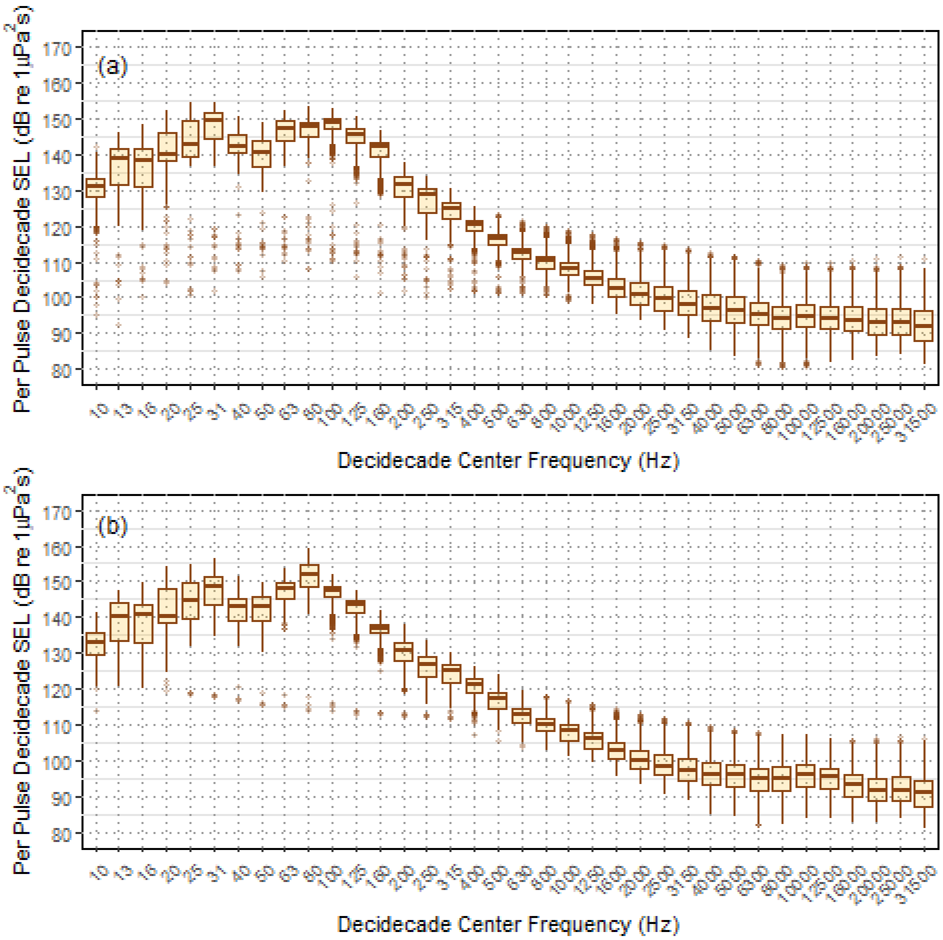


Figure A-146. Distribution of decidecade band level single strike SEL for pile driving installation of AU-38 at monitoring station AU38-2000 for channel 1 (a) and channel 2 (b). Beige bars indicate the first, second, and third quartiles (*25th*, *50th*, and *75th*) or as exceedances $L_{75}$, $L_{50}$, and $L_{25}$. Upper error bars indicate the maximum levels ($L_{max}$). Lower error bars indicate the 5th percentile or $L_{95}$.

Table A-110. Received level statistics for pile driving installation of AU-38 at monitoring station AU38-2000.

| Sound level statistic | PK (dB re 1 µPa) | rms SPL (dB re 1 µPa$^2$) | SELss (dB re 1 µPa$^2$·s) |
|---|---|---|---|
| **Channel 1 (bottom)** | | | |
| $L_{max}$ | 177.2 | 167.7 | 161.4 |
| $L_5$ | 175.2 | 166.0 | 160.2 |
| $L_{25}$ | 173.7 | 164.2 | 158.7 |
| $L_{50}$ | 172.1 | 162.0 | 156.5 |
| $L_{75}$ | 168.8 | 159.0 | 153.6 |
| $L_{95}$ | 163.9 | 154.8 | 149.4 |
| $L_{mean}$ | 170.9 | 161.3 | 155.8 |
| **Channel 2 (mid-water)** | | | |
| $L_{max}$ | 177.4 | 169.0 | 162.5 |
| $L_5$ | 175.5 | 167.7 | 161.7 |
| $L_{25}$ | 173.6 | 165.4 | 159.8 |
| $L_{50}$ | 171.7 | 163.4 | 157.2 |
| $L_{75}$ | 168.8 | 159.1 | 153.6 |
| $L_{95}$ | 163.8 | 154.9 | 149.5 |
| $L_{mean}$ | 170.9 | 162.4 | 156.6 |

### A.13.2.4. Station AU38-4000

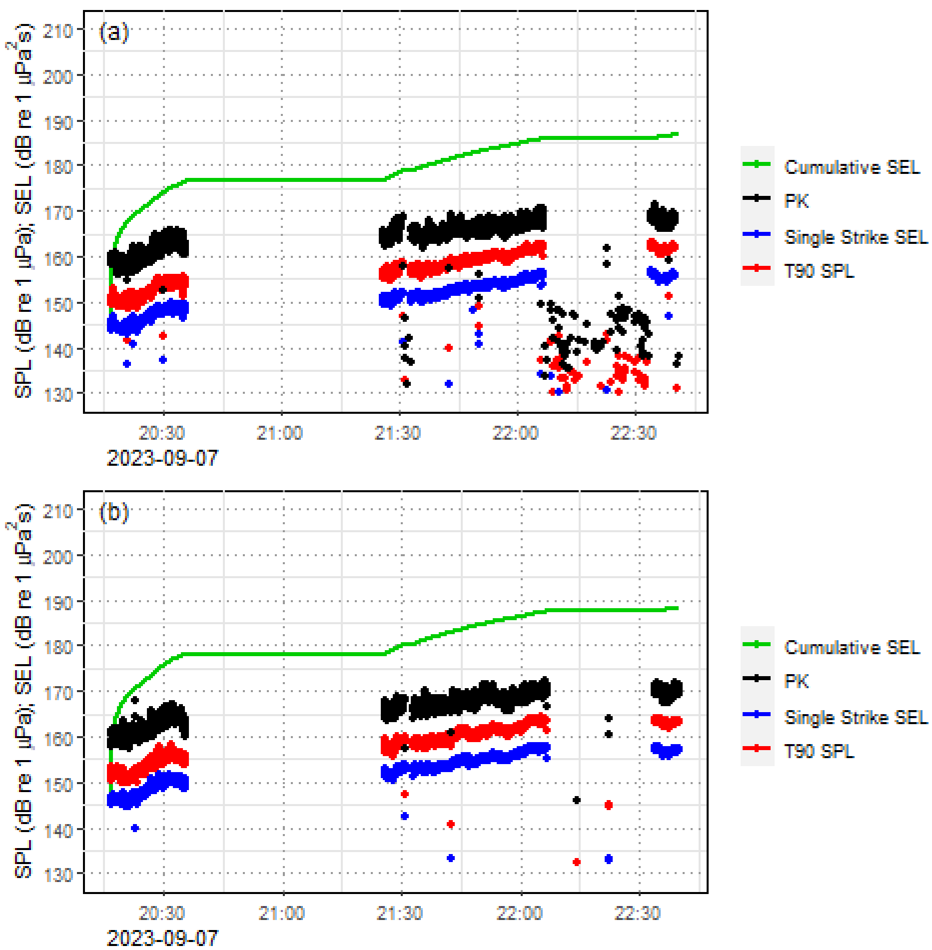


Figure A-147. Received levels for impact pile driving installation of AU-38 at monitoring station AU38-4000 for channel 1 (a) and channel 2 (b). Peak SPL (PK, black), rms SPL (T90 SPL, red), single strike SEL (blue) and cumulative SEL (green) versus time (UTC). For periods during which there is no pile driving the cSEL is necessarily displayed as a constant value over time.

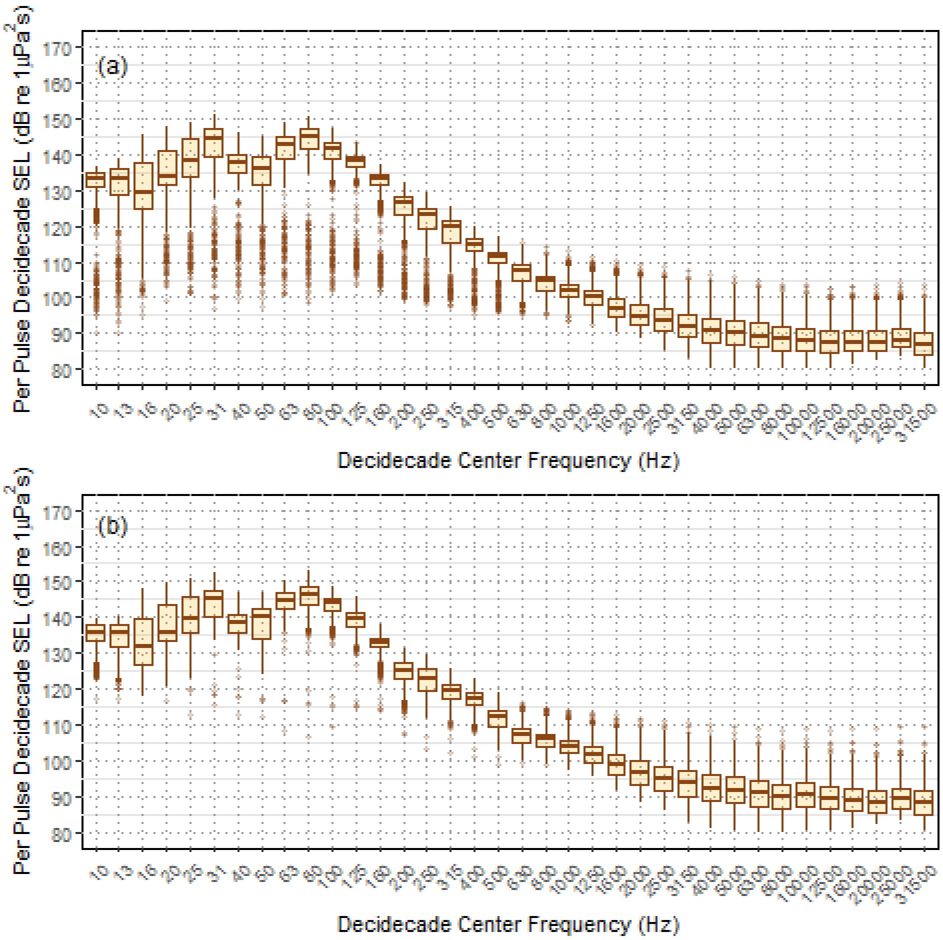


Figure A-148. Distribution of decidecade band level single strike SEL for pile driving installation of AU-38 at monitoring station AU38-4000 for channel 1 (a) and channel 2 (b). Beige bars indicate the first, second, and third quartiles (*25th*, *50th*, and *75th*) or as exceedances $L_{75}$, $L_{50}$, and $L_{25}$. Upper error bars indicate the maximum levels ($L_{max}$). Lower error bars indicate the 5th percentile or $L_{95}$.

Table A-111. Received level statistics for pile driving installation of AU-38 at monitoring station AU38-4000.

| Sound level statistic | PK (dB re 1 µPa) | rms SPL (dB re 1 µPa$^2$) | SELss (dB re 1 µPa$^2$·s) |
|---|---|---|---|
| **Channel 1 (bottom)** | | | |
| $L_{max}$ | 171.2 | 163.1 | 157.1 |
| $L_5$ | 168.6 | 161.9 | 155.7 |
| $L_{25}$ | 166.8 | 160.0 | 153.9 |
| $L_{50}$ | 165.3 | 157.6 | 151.6 |
| $L_{75}$ | 162.6 | 153.8 | 148.3 |
| $L_{95}$ | 157.3 | 149.7 | 144.2 |
| $L_{mean}$ | 164.0 | 156.2 | 150.3 |
| **Channel 2 (mid-water)** | | | |
| $L_{max}$ | 172.1 | 164.2 | 158.1 |
| $L_5$ | 170.5 | 163.4 | 157.3 |
| $L_{25}$ | 168.6 | 161.5 | 155.5 |
| $L_{50}$ | 166.8 | 159.1 | 153.3 |
| $L_{75}$ | 164.0 | 155.7 | 150.3 |
| $L_{95}$ | 159.9 | 151.5 | 146.0 |
| $L_{mean}$ | 166.1 | 158.4 | 152.6 |

### A.13.2.5. Station AU38-8000

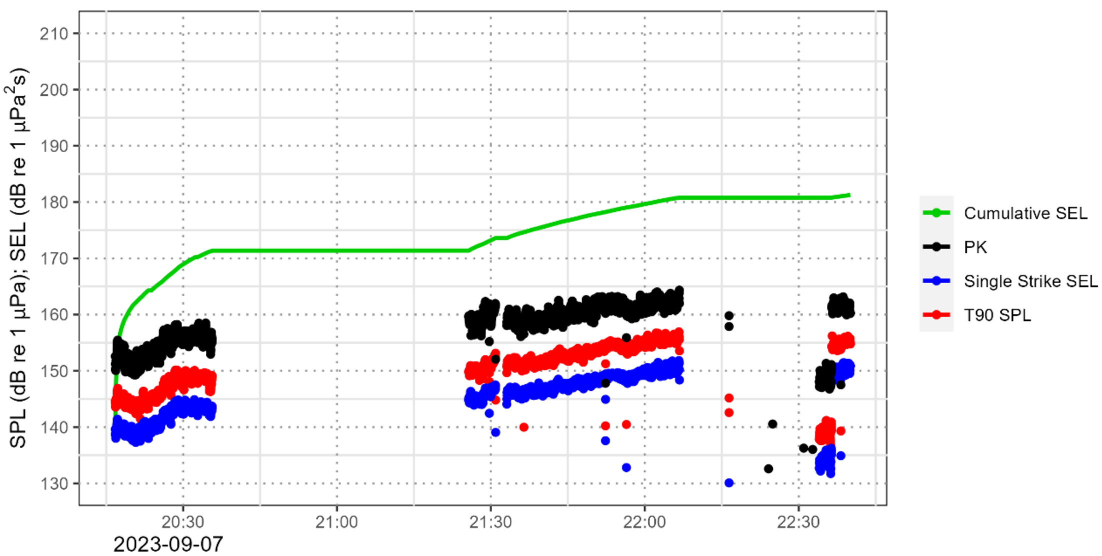


Figure A-149. Received levels for impact pile driving installation of AU-38 at monitoring station AU38-8000 for channel 2. Peak SPL (PK, black), rms SPL (T90 SPL, red), single strike SEL (blue) and cumulative SEL (green) versus time (UTC). For periods during which there is no pile driving the cSEL is necessarily displayed as a constant value over time.

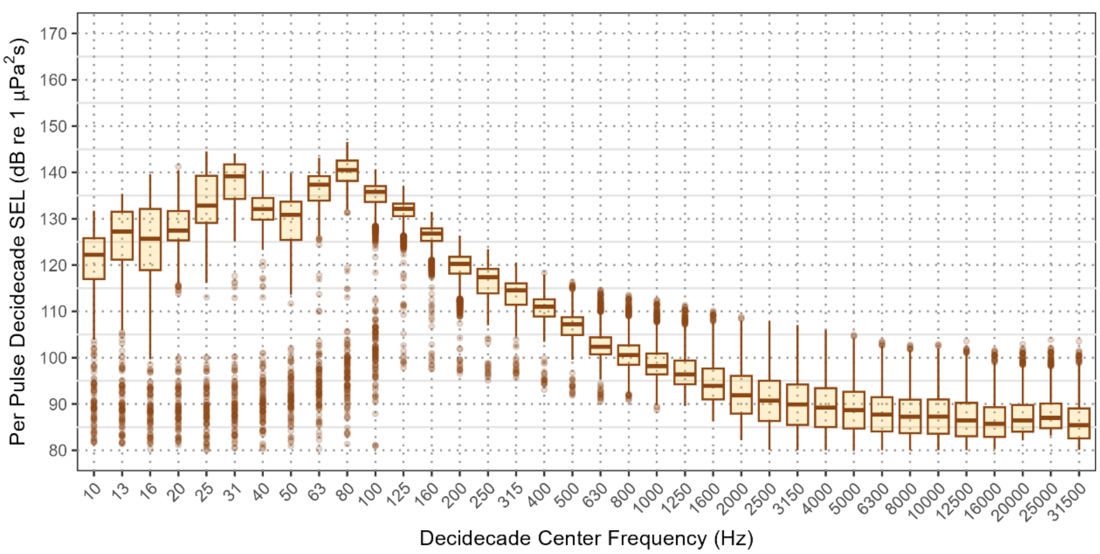


Figure A-150. Distribution of decidecade band level single strike SEL for pile driving installation of AU-38 at monitoring station AU38-8000 for channel 2. Beige bars indicate the first, second, and third quartiles (*25th*, *50th*, and *75th*) or as exceedances $L_{75}$, $L_{50}$, and $L_{25}$. Upper error bars indicate the maximum levels ($L_{max}$). Lower error bars indicate the 5th percentile or $L_{95}$.

Table A-112. Received level statistics for pile driving installation of AU-38 at monitoring station AU38-8000.

| Sound level statistic | PK (dB re 1 µPa) | rms SPL (dB re 1 µPa$^2$) | SELss (dB re 1 µPa$^2$·s) |
|---|---|---|---|
| Channel 2 (mid-water) | | | |
| $L_{max}$ | 164.3 | 156.9 | 151.8 |
| $L_5$ | 162.5 | 155.4 | 150.3 |
| $L_{25}$ | 161.0 | 153.9 | 148.6 |
| $L_{50}$ | 159.2 | 151.5 | 146.2 |
| $L_{75}$ | 155.5 | 148.1 | 143.1 |
| $L_{95}$ | 150.7 | 143.5 | 138.2 |
| $L_{mean}$ | 157.9 | 150.4 | 145.2 |

## A.13.3. Ranges to Acoustic Thresholds

Table A-113. Isopleth distances to NMFS physiological thresholds for impact driving installation of pile AU-38.

| Group | Injury: PK | | | | Injury: cSEL | | | |
|---|---|---|---|---|---|---|---|---|
| | Level (dB re 1µPa) | Predicted (m) | Measured (m) | Measured w/ attn. coeff. (m) | Level (dB re 1 µPa$^2$·s) | Predicted (m) | Measured (m) | Measured w/ attn. coeff. (m) |
| LFC | 219 | 17 | 10 | 10 | 183 | 3,191 | 1,630 | 1,860 |
| MFC | 230 | 5 | 10 | 10 | 185 | 43 | 10 | 10 |
| HFC | 202 | 119 | 50 | 10 | 155 | 71 | 50 | 70 |
| PW | 218 | 19 | 10 | 10 | 185 | 153 | 90 | 40 |
| ST | 232 | 0 | 10 | 10 | 204 | 161 | 160 | 50 |
| AS | 206 | 78 | 30 | 10 | 187 | 6,894 | 4,090 | 4,710 |

Table A-114. Isopleth distances to NMFS behavioral thresholds for impact driving installation of pile AU-38.

| Group | Behavior: SPL | | | |
|---|---|---|---|---|
| | Level (dB re 1µPa$^2$) | Predicted (m) | Measured (m) | Measured w/ attn. coeff. (m) |
| MM | 160 | 4,121 | 5,310 | 5,720 |
| ST | 175 | 1,400 | 560 | 370 |
| AS | 150 | 9,229 | 23,750 | 11,900 |

## A.13.4. Regression Analysis for Transmission Loss

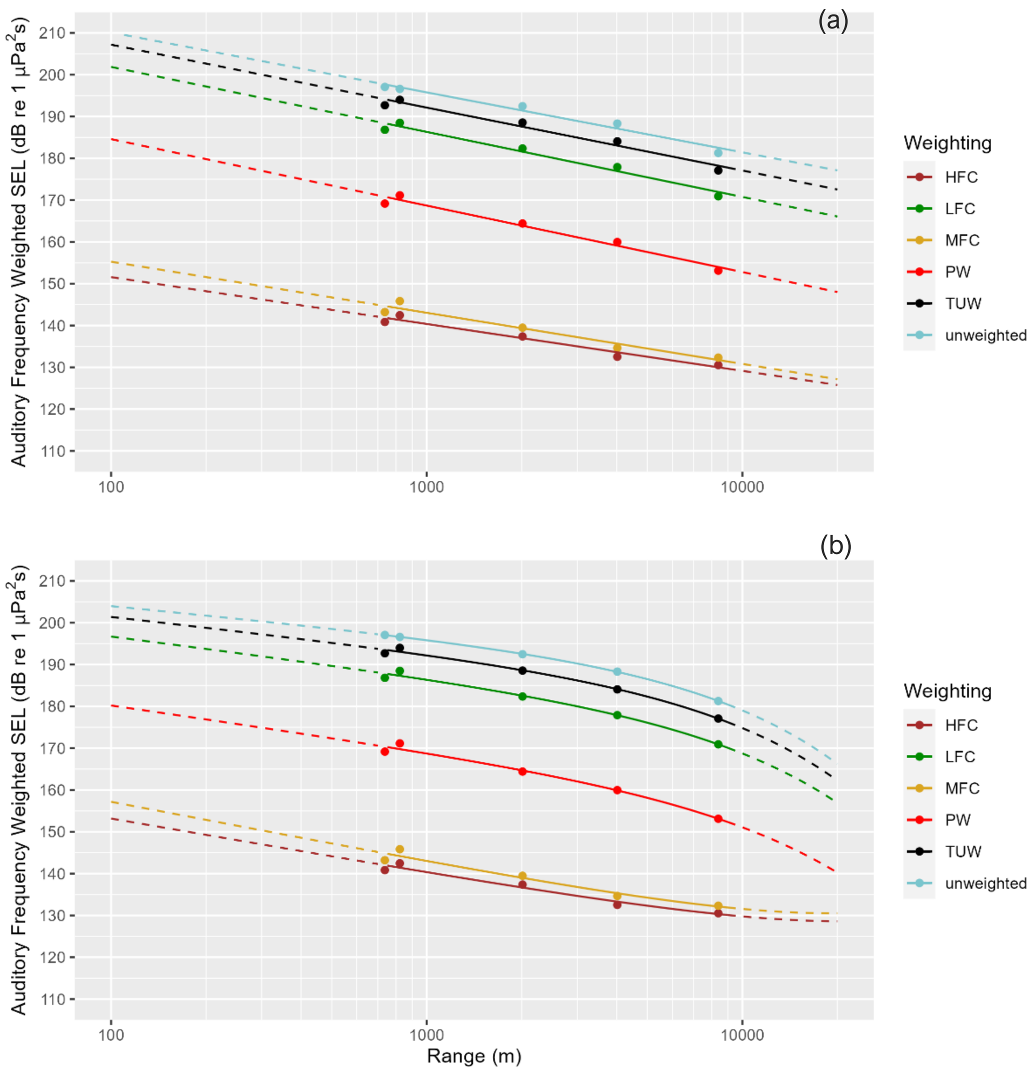


Figure A-151. Transmission loss determination based on regression analysis without (a) and with (b) intrinsic attenuation for the maximum received cumulative SEL (cSEL) at each recording station during installation of pile AU-38 on 7 Sep 2023.

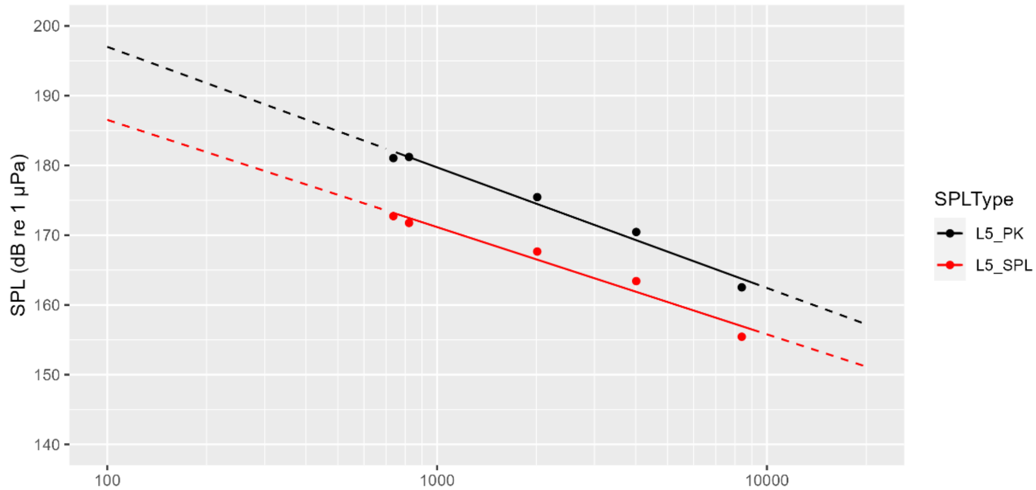


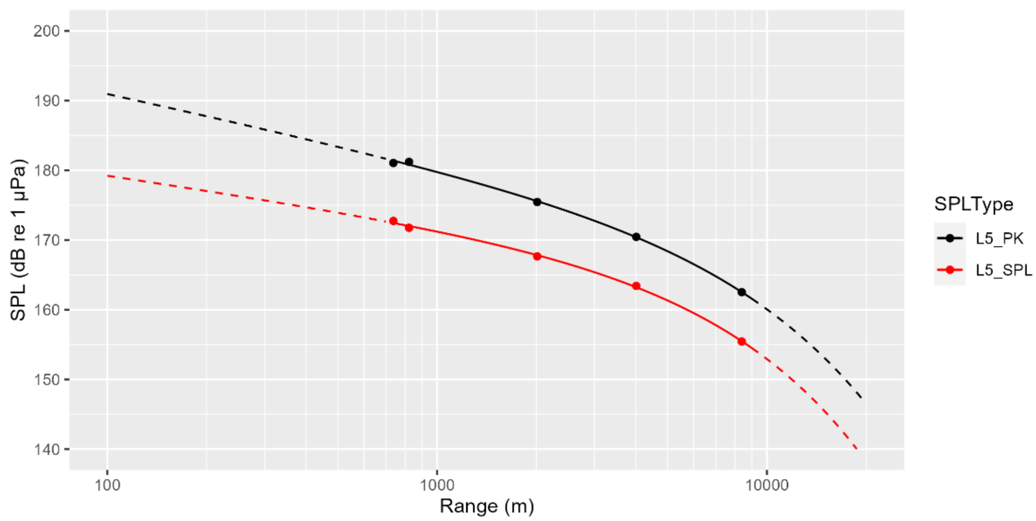


Figure A-152. Transmission loss determination based on regression analysis without (a) and with (b) intrinsic attenuation for $L_5$ PK and SPL maxima at each recording station during installation of pile AU-38 on 7 Sep 2023.

Table A-115. Regression analysis fitting coefficients for transmission loss with and without intrinsic attenuation for installation of pile AU-38 on 7 Sep 2023.

| Metric | A (dB/decade m) A*log(r) | A (dB/decade m) A*log(r) + αr/1000 | α (dB/ m) A*log(r) + αr/1000 |
|---|---|---|---|
| PK ($L_5$) (dB re 1 µPa) | -17.3 | -10.3 | $-1.048 \times 10^{-3}$ |
| rms SPL ($L_5$) (dB re 1 µPa$^2$) | -15.4 | -6.9 | $-1.265 \times 10^{-3}$ |
| cSEL (dB re 1 µPa$^2$·s) | -14.3 | -7.2 | $-1.062 \times 10^{-3}$ |
| cSEL, LF (dB re 1 µPa$^2$·s) | -15.6 | -9.5 | $-0.896 \times 10^{-3}$ |
| cSEL, MF (dB re 1 µPa$^2$·s) | -12.2 | -14.4 | $0.331 \times 10^{-3}$ [a] |
| cSEL, HF (dB re 1 µPa$^2$·s) | -11.2 | -13.1 | $0.276 \times 10^{-3}$ [a] |
| cSEL, PW (dB re 1 µPa$^2$·s) | -15.9 | -10.8 | $-0.759 \times 10^{-3}$ |
| cSEL, TU (dB re 1 µPa$^2$·s) | -15.1 | -8.3 | $-1.004 \times 10^{-3}$ |

[a] Positive attenuation coefficients could indicate ambient noise contamination and may not be valid.

# Appendix B. Signal Kurtosis and Pulse Duration Per Foundation

## B.1. Foundation AT-40

The kurtosis of the received signals was calculated at each of the recording locations for pile AT-40 (Figure B-1). The summary of the signal kurtosis statistics is presented in Table B-1. The pulse duration time of the received signals was calculated at each of the recording locations (Figure B-2).

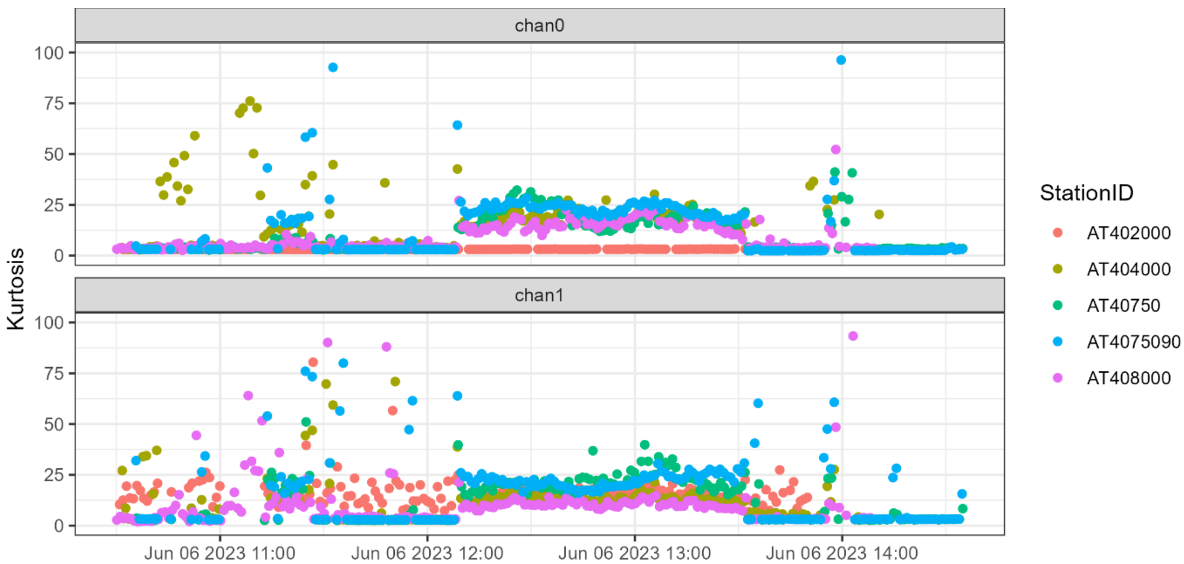


Figure B-1. Signal kurtosis for each strike for both channel 1 (top) and channel 2 (bottom) at each recording location for pile AT-40.

Table B-1. Signal kurtosis statistic summary for Pile AT-40.

| Kurtosis statistics | AT40-750 | AT40-75090 | AT40-2000 | AT40-4000 | AT40-8000 |
|---|---|---|---|---|---|
| **Channel 1 (bottom)** | | | | | |
| $L_{max}$ | 41.1 | 190.8 | - | 173.1 | - |
| $L_5$ | 27.4 | 27.7 | - | 62.4 | - |
| $L_{25}$ | 16.2 | 22.9 | - | 20.6 | - |
| $L_{50}$ | 4.0 | 7.6 | - | 14.7 | - |
| $L_{75}$ | 3.4 | 2.9 | - | 4.1 | - |
| $L_{95}$ | 3.0 | 2.4 | - | 3.1 | - |
| $L_{mean}$ | 9.9 | 15.2 | - | 19.1 | - |
| **Channel 2 (mid-water)** | | | | | |
| $L_{max}$ | 198.2 | 179.7 | 197.4 | 191.1 | 141.5 |
| $L_5$ | 150.3 | 50.4 | 135.8 | 148.9 | 30.3 |
| $L_{25}$ | 22.2 | 23.4 | 19.4 | 14.4 | 11.0 |
| $L_{50}$ | 15.4 | 17.6 | 16.5 | 11.9 | 8.8 |
| $L_{75}$ | 3.0 | 3.0 | 13.6 | 3.5 | 3.6 |
| $L_{95}$ | 2.6 | 2.9 | 9.2 | 2.9 | 2.8 |
| $L_{mean}$ | 23.8 | 17.0 | 29.0 | 22.6 | 11.4 |

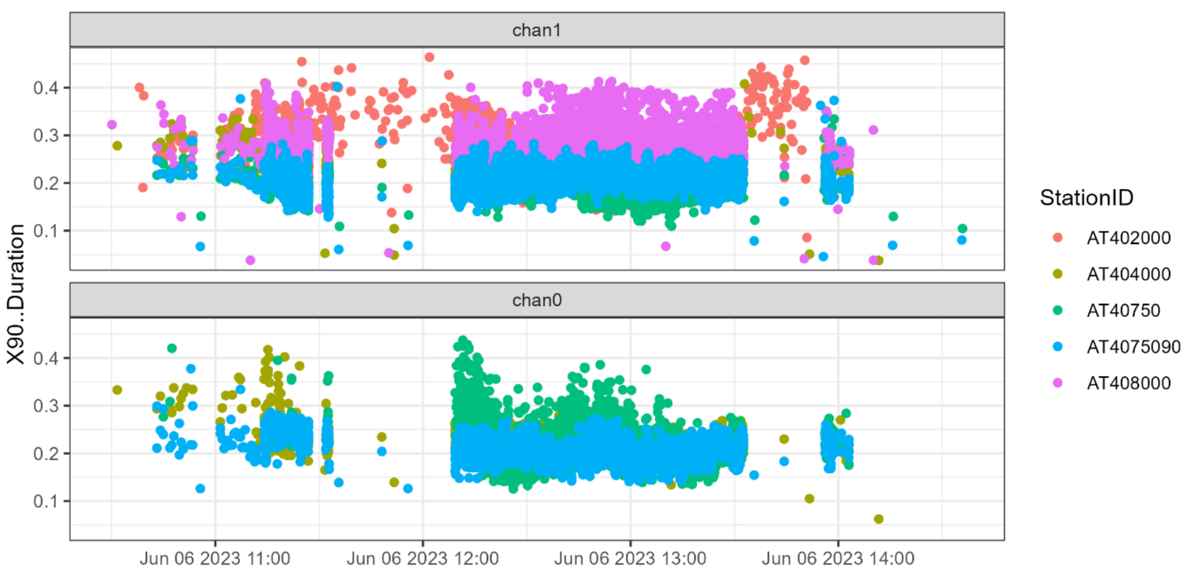


Figure B-2. Rise time as pulse duration in seconds (s) between 5% and 95% energy for each strike for both channel 1 (top) and channel 2 (bottom) at each recording location for pile AT-40.

## B.2. Foundation AU-39

The kurtosis of the received signals was calculated at each of the recording locations for pile AU-39 (Figure B-3). The summary of the signal kurtosis statistics is presented in Table B-2. The pulse duration time of the received signals was calculated at each of the recording locations (Figure B-4).

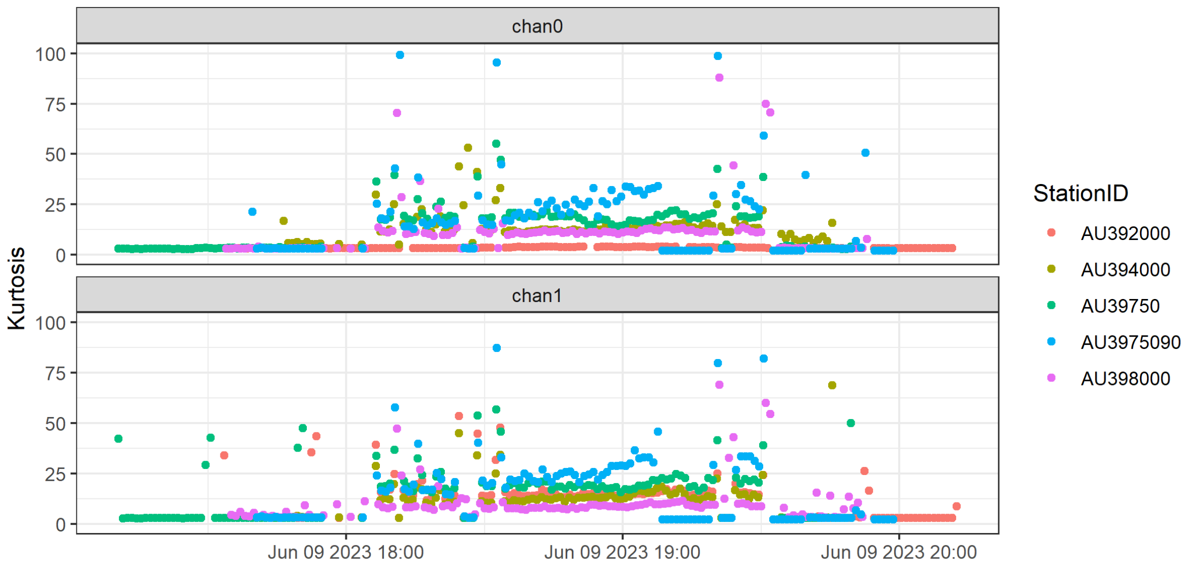


Figure B-3. Signal kurtosis for each strike for both channel 1 (top) and channel 2 (bottom) at each recording location for pile AU-39.

Table B-2. Signal kurtosis statistic summary for Pile AU-39.

| Kurtosis statistics | AU39-750 | AU39-75090 | AU39-2000 | AU39-4000 | AU39-8000 |
|---|---|---|---|---|---|
| **Channel 1 (bottom)** | | | | | |
| $L_{max}$ | 185.3 | 99.2 | - | 183.0 | - |
| $L_{5}$ | 119.3 | 41.8 | - | 42.4 | - |
| $L_{25}$ | 19.3 | 25.8 | - | 14.7 | - |
| $L_{50}$ | 16.7 | 15.1 | - | 12.5 | - |
| $L_{75}$ | 3.3 | 3.0 | - | 11.4 | - |
| $L_{95}$ | 2.9 | 2.1 | - | 5.4 | - |
| $L_{mean}$ | 21.1 | 16.9 | - | 19.6 | - |
| **Channel 2 (mid-water)** | | | | | |
| $L_{max}$ | 197.4 | 166.7 | 173.7 | 198.7 | 191.1 |
| $L_{5}$ | 42.7 | 44.7 | 33.2 | 58.1 | 130.5 |
| $L_{25}$ | 20.7 | 25.6 | 15.4 | 15.1 | 10.1 |
| $L_{50}$ | 17.4 | 16.7 | 13.9 | 12.6 | 8.4 |
| $L_{75}$ | 2.9 | 3.0 | 3.0 | 9.9 | 7.1 |
| $L_{95}$ | 2.8 | 2.1 | 3.0 | 3.0 | 3.4 |
| $L_{mean}$ | 16.5 | 18.5 | 12.7 | 18.7 | 20.4 |

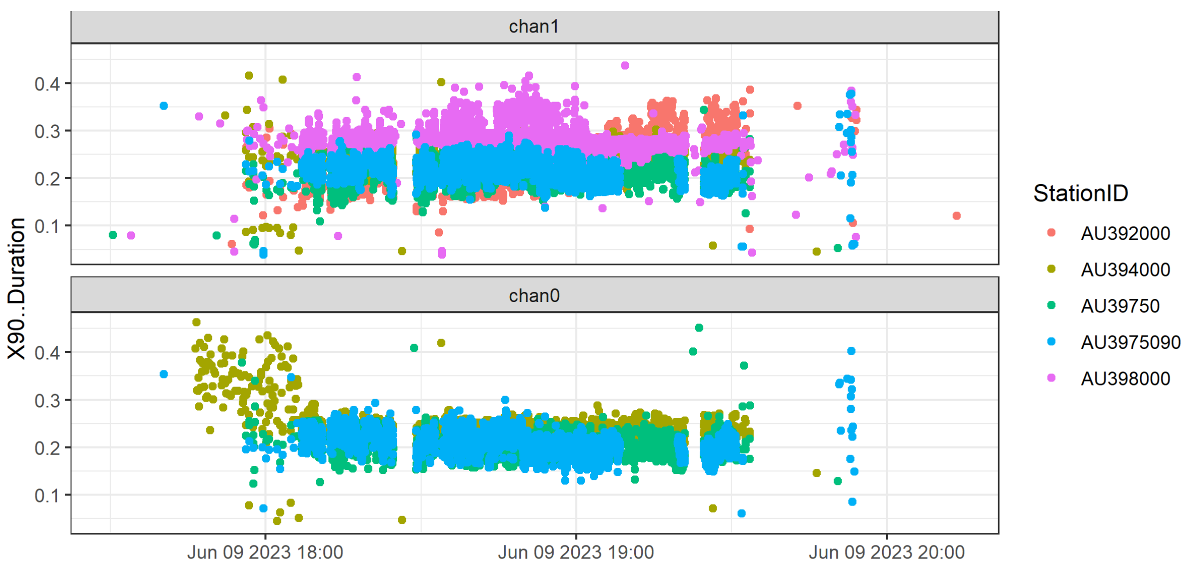


Figure B-4. Rise time as pulse duration in seconds (s) between 5% and 95% energy for each strike for both channel 1 (top) and channel 2 (bottom) at each recording location for pile AU-39.

## B.3. Foundation AP-38

The kurtosis of the received signals was calculated at each of the recording locations for pile AP-38 (Figure B-5). The summary of the signal kurtosis statistics is presented in Table B-3. The pulse duration time of the received signals was calculated at each of the recording locations (Figure B-6).

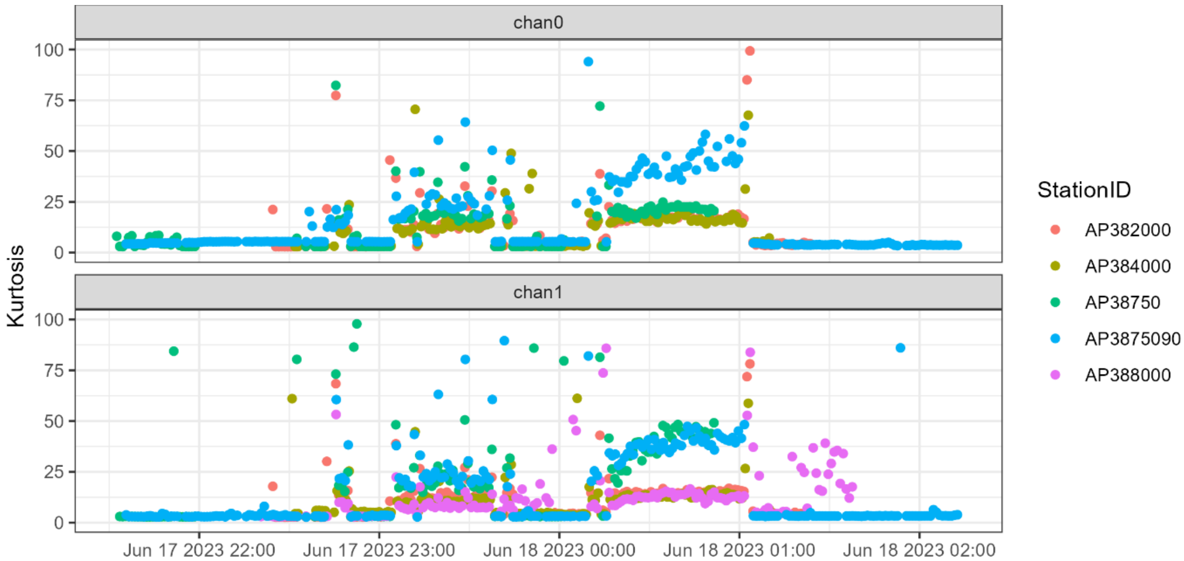


Figure B-5. Signal kurtosis for each strike for both channel 1 (top) and channel 2 (bottom) at each recording location for pile AP-38.

Table B-3. Signal kurtosis statistic summary for Pile AP-38.

| Kurtosis statistics | AP38-750 | AP38-75090 | AP38-2000 | AP38-4000 | AP38-8000 |
|---|---|---|---|---|---|
| **Channel 1 (bottom)** | | | | | |
| $L_{max}$ | 82.3 | - | 177.5 | 198.0 | - |
| $L_5$ | 31.7 | - | 29.9 | 59.2 | - |
| $L_{25}$ | 20.3 | - | 16.9 | 16.8 | - |
| $L_{50}$ | 16.5 | - | 11.7 | 13.6 | - |
| $L_{75}$ | 3.0 | - | 3.6 | 3.4 | - |
| $L_{95}$ | 3.0 | - | 2.9 | 3.2 | - |
| $L_{mean}$ | 13.9 | - | 13.4 | 18.3 | - |
| **Channel 2 (mid-water)** | | | | | |
| $L_{max}$ | 165.4 | 168.2 | 146.7 | 199.3 | 191.8 |
| $L_5$ | 83.5 | 46.9 | 26.8 | 72.8 | 126.1 |
| $L_{25}$ | 37.4 | 25.7 | 14.7 | 13.4 | 16.0 |
| $L_{50}$ | 18.4 | 3.4 | 12.3 | 11.1 | 9.4 |
| $L_{75}$ | 3.0 | 3.2 | 4.1 | 5.1 | 5.4 |
| $L_{95}$ | 2.9 | 2.9 | 2.8 | 3.9 | 3.0 |
| $L_{mean}$ | 25.1 | 17.0 | 12.7 | 17.1 | 22.2 |

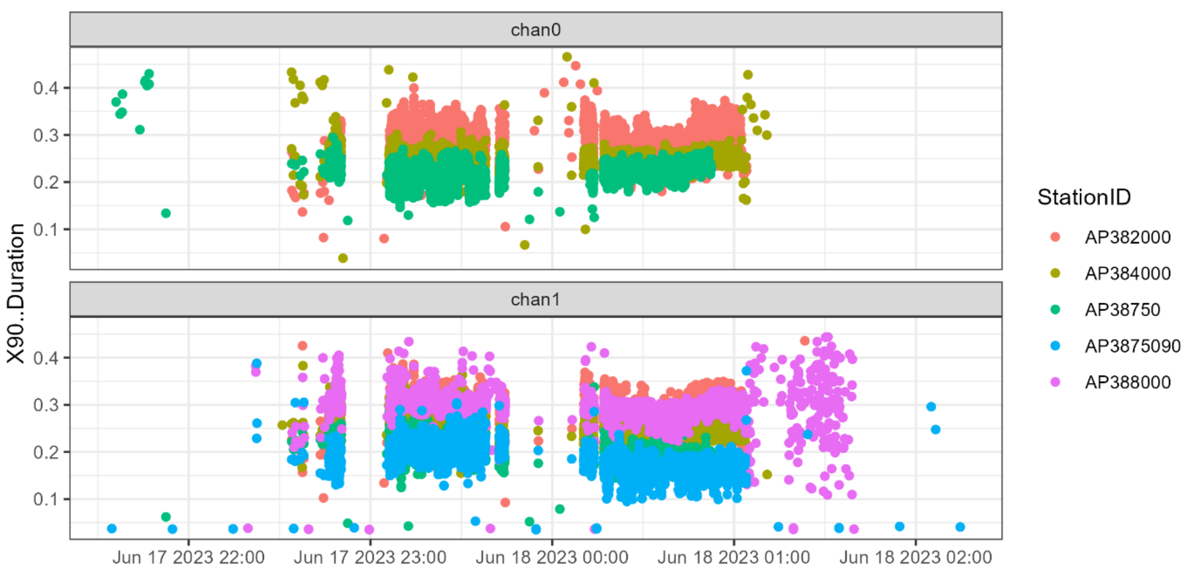


Figure B-6. Rise time as pulse duration in seconds (s) between 5% and 95% energy for each strike for both channel 1 (top) and channel 2 (bottom) at each recording location for pile AP-38.

## B.4. Foundation AV-39

The kurtosis of the received signals was calculated at each of the recording locations for pile AV-39 (Figure B-7). The summary of the signal kurtosis statistics is presented in Table B-4. The pulse duration time of the received signals was calculated at each of the recording locations (Figure B-8).

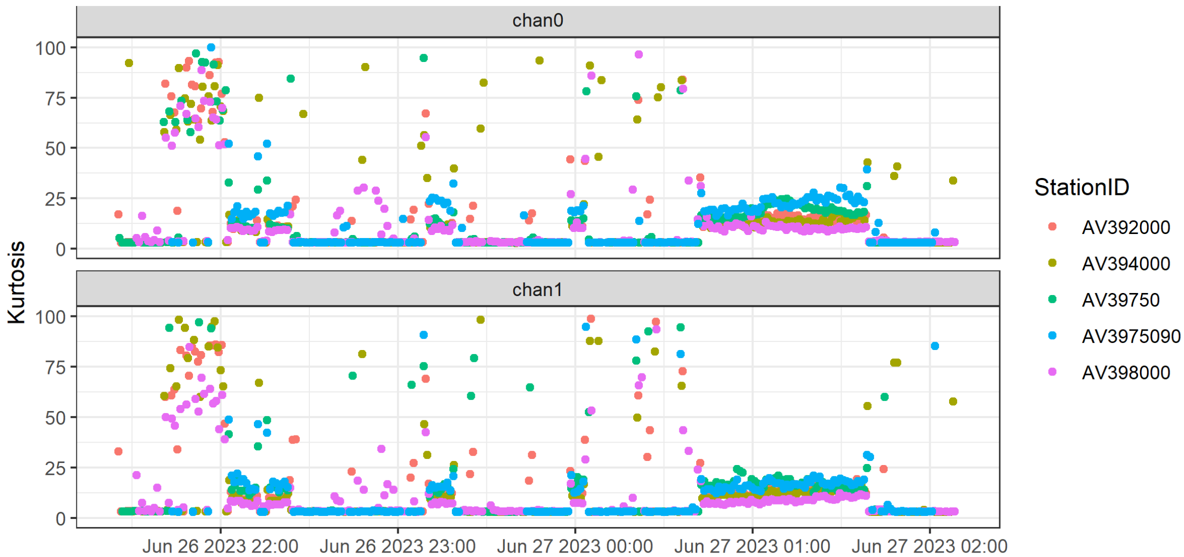


Figure B-7. Signal kurtosis for each strike for both channel 1 (top) and channel 2 (bottom) at each recording location for pile AV-39.

Table B-4. Signal kurtosis statistic summary for Pile AV-39.

| Kurtosis statistics | AV39-750 | AV39-75090 | AV39-2000 | AV39-4000 | AV39-8000 |
|---|---|---|---|---|---|
| **Channel 1 (bottom)** | | | | | |
| $L_{max}$ | 126.6 | 194.4 | 198.0 | 182.5 | 198.5 |
| $L_{5}$ | 78.6 | 148.1 | 84.9 | 89.8 | 73.9 |
| $L_{25}$ | 17.7 | 22.7 | 14.8 | 13.8 | 11.0 |
| $L_{50}$ | 4.5 | 11.2 | 9.8 | 3.3 | 8.5 |
| $L_{75}$ | 3.1 | 3.1 | 3.2 | 3.1 | 3.3 |
| $L_{95}$ | 3.0 | 3.0 | 3.1 | 3.0 | 3.1 |
| $L_{mean}$ | 16.5 | 24.4 | 17.6 | 19.6 | 16.7 |
| **Channel 2 (mid-water)** | | | | | |
| $L_{max}$ | 183.5 | 188.2 | 181.3 | 183.3 | 176.9 |
| $L_{5}$ | 116.8 | 147.1 | 82.9 | 100.7 | 69.3 |
| $L_{25}$ | 18.1 | 17.9 | 14.4 | 13.3 | 9.3 |
| $L_{50}$ | 11.9 | 13.3 | 9.2 | 3.5 | 6.7 |
| $L_{75}$ | 3.2 | 3.1 | 3.2 | 3.1 | 3.3 |
| $L_{95}$ | 3.1 | 3.0 | 3.1 | 3.0 | 3.1 |
| $L_{mean}$ | 24.2 | 26.1 | 17.5 | 20.5 | 15.8 |

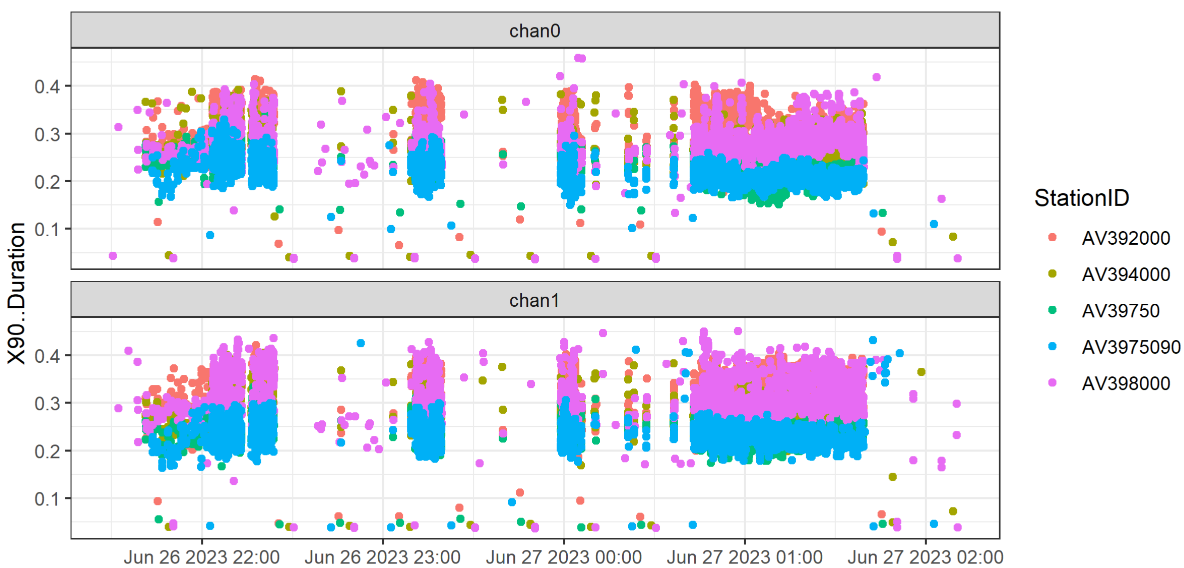


Figure B-8. Rise time as pulse duration in seconds (s) between 5% and 95% energy for each strike for both channel 1 (top) and channel 2 (bottom) at each recording location for pile AV-39.

## B.5. Foundation AR-39

The kurtosis of the received signals was calculated at each of the recording locations for pile AR-39 (Figure B-9). The summary of the signal kurtosis statistics is presented in Table B-5. The pulse duration time of the received signals was calculated at each of the recording locations (Figure B-10).

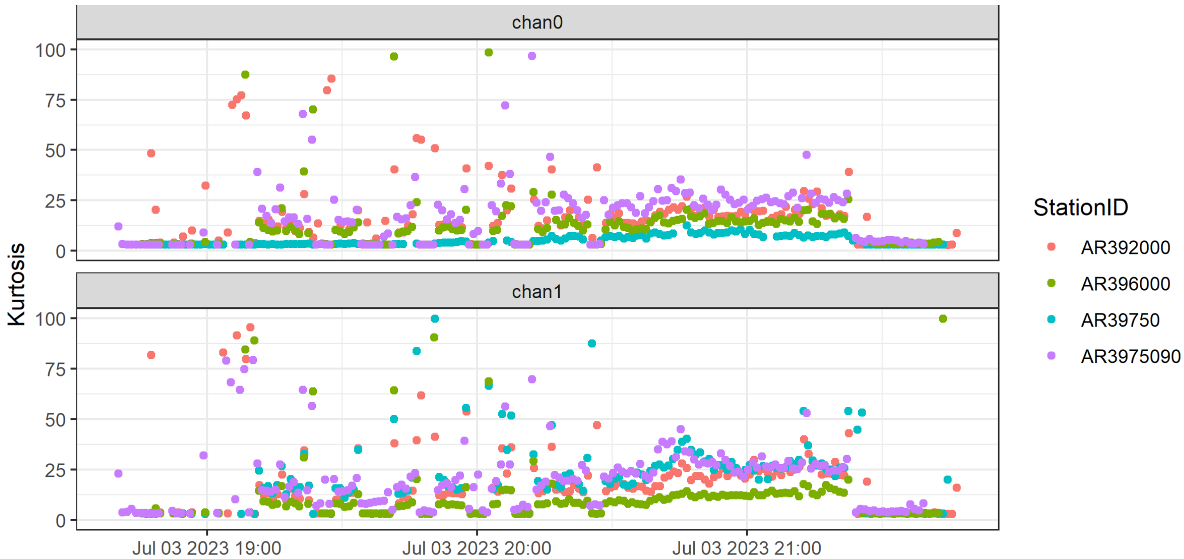


Figure B-9. Signal kurtosis for each strike for both channel 1 (top) and channel 2 (bottom) at each recording location for pile AR-39.

Table B-5. Signal kurtosis statistic summary for Pile AR-39.

| Kurtosis statistics | AR39-750 | AR39-75090 | AR39-2000 | AR39-6000 |
|---|---|---|---|---|
| **Channel 1 (bottom)** | | | | |
| $L_{max}$ | - | 187.0 | 159.7 | 184.2 |
| $L_{5}$ | - | 51.4 | 69.6 | 97.7 |
| $L_{25}$ | - | 25.1 | 20.3 | 15.7 |
| $L_{50}$ | - | 19.6 | 14.9 | 11.4 |
| $L_{75}$ | - | 3.8 | 6.9 | 3.8 |
| $L_{95}$ | - | 3.0 | 3.0 | 3.0 |
| $L_{mean}$ | - | 21.4 | 19.9 | 18.4 |
| **Channel 2 (mid-water)** | | | | |
| $L_{max}$ | 195.5 | 106.9 | 150.0 | 160.9 |
| $L_{5}$ | 77.8 | 56.3 | 74.9 | 87.1 |
| $L_{25}$ | 27.3 | 27.2 | 23.3 | 12.9 |
| $L_{50}$ | 18.6 | 19.6 | 15.1 | 8.4 |
| $L_{75}$ | 3.2 | 7.3 | 3.5 | 3.4 |
| $L_{95}$ | 3.0 | 3.5 | 3.1 | 3.1 |
| $L_{mean}$ | 24.6 | 20.8 | 20.5 | 15.7 |

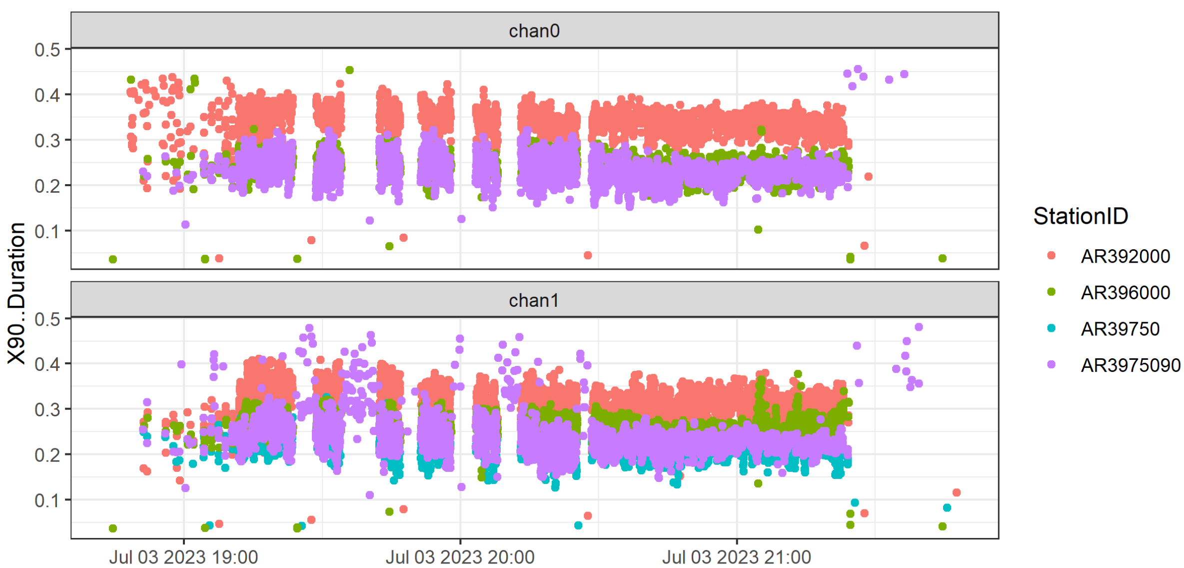


Figure B-10. Rise time as pulse duration in seconds (s) between 5% and 95% energy for each strike for both channel 1 (top) and channel 2 (bottom) at each recording location for pile AR-39.

## B.6. Foundation AW-38

The kurtosis of the received signals was calculated at each of the recording locations for pile AW-38 (Figure B-11). The summary of the signal kurtosis statistics is presented in Table B-6. The pulse duration time of the received signals was calculated at each of the recording locations (Figure B-12).

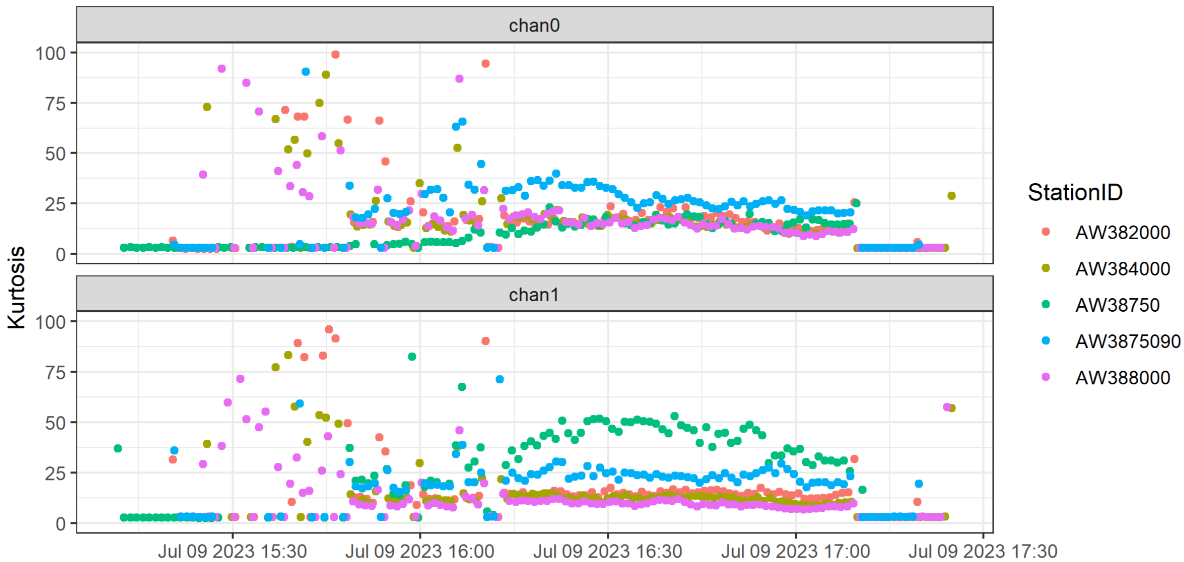


Figure B-11. Signal kurtosis for each strike for both channel 1 (top) and channel 2 (bottom) at each recording location for pile AW-38.

Table B-6. Signal kurtosis statistic summary for Pile AW-38.

| Kurtosis statistics | AW38-750 | AW38-75090 | AW38-2000 | AW38-4000 | AW38-8000 |
|---|---|---|---|---|---|
| **Channel 1 (bottom)** | | | | | |
| $L_{max}$ | - | 191.2 | 180.0 | 182.7 | 153.8 |
| $L_{5}$ | - | 117.3 | 117.3 | 76.9 | 87.2 |
| $L_{25}$ | - | 32.8 | 19.0 | 17.9 | 18.4 |
| $L_{50}$ | - | 25.2 | 15.6 | 14.3 | 14.5 |
| $L_{75}$ | - | 18.7 | 11.7 | 10.1 | 9.8 |
| $L_{95}$ | - | 3.0 | 2.7 | 2.9 | 3.0 |
| $L_{mean}$ | - | 31.2 | 26.9 | 22.4 | 21.1 |
| **Channel 2 (mid-water)** | | | | | |
| $L_{max}$ | 185.2 | 196.7 | 166.3 | 178.3 | 71.7 |
| $L_{5}$ | 116.5 | 124.9 | 106.2 | 78.3 | 46.1 |
| $L_{25}$ | 46.8 | 24.9 | 15.8 | 13.6 | 11.0 |
| $L_{50}$ | 36.7 | 22.3 | 14.1 | 11.9 | 9.2 |
| $L_{75}$ | 18.1 | 17.9 | 11.1 | 8.8 | 7.0 |
| $L_{95}$ | 2.6 | 3.0 | 2.9 | 3.0 | 3.0 |
| $L_{mean}$ | 38.9 | 28.9 | 24.1 | 19.8 | 12.5 |

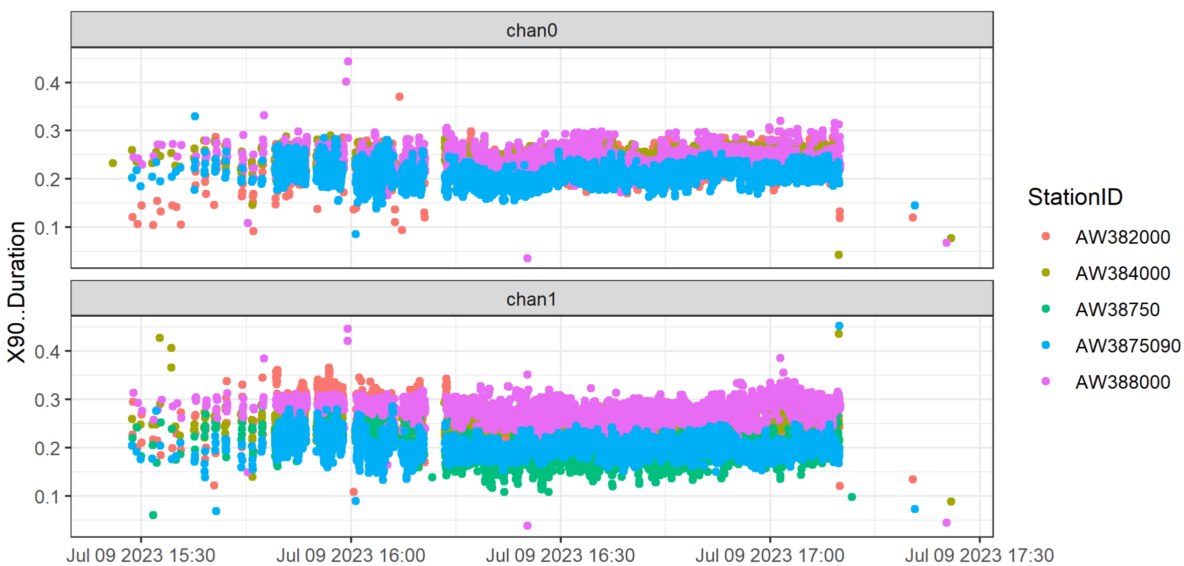


Figure B-12. Rise time as pulse duration in seconds (s) between 5% and 95% energy for each strike for both channel 1 (top) and channel 2 (bottom) at each recording location for pile AW-38.

## B.7. Foundation AM-37

The kurtosis of the received signals was calculated at each of the recording locations for pile AM-37 (Figure B-13). The summary of the signal kurtosis statistics is presented in Table B-7. The pulse duration time of the received signals was calculated at each of the recording locations (Figure B-14).

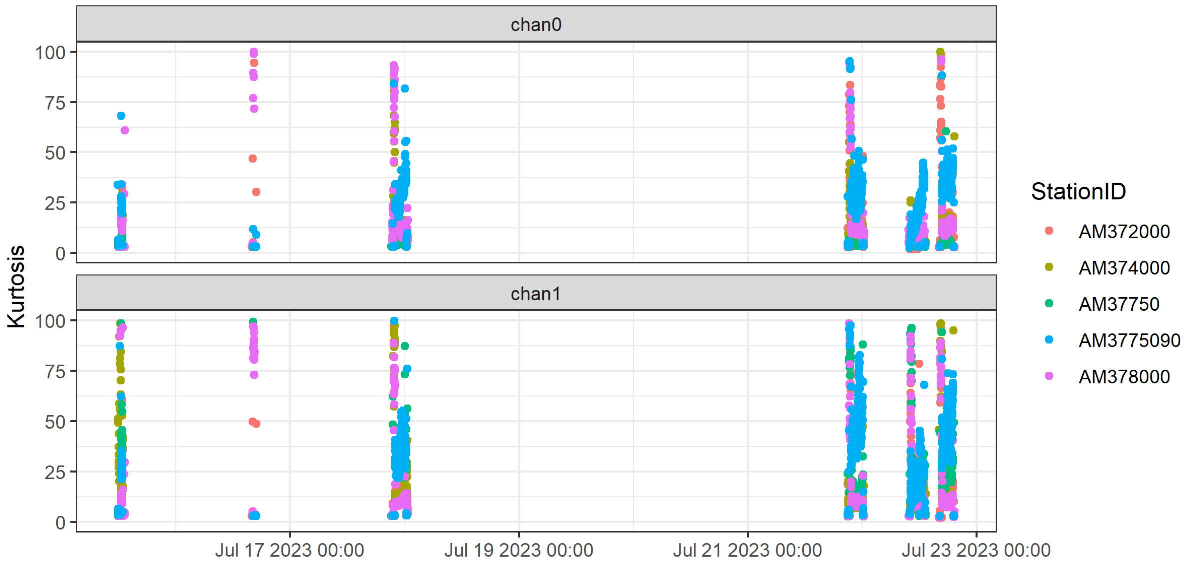


Figure B-13. Signal kurtosis for each strike for both channel 1 (top) and channel 2 (bottom) at each recording location for pile AM-37.

Table B-7. Signal kurtosis statistic summary for Pile AM-37.

| Kurtosis statistics | AM37-750 | AM37-75090 | AM37-2000 | AM37-4000 | AM37-8000 |
|---|---|---|---|---|---|
| **Channel 1 (bottom)** | | | | | |
| $L_{max}$ | - | 199.8 | 188.2 | 182.2 | 196.4 |
| $L_5$ | - | 139.5 | 77.0 | 105.1 | 103.4 |
| $L_{25}$ | - | 35.6 | 13.6 | 13.4 | 12.2 |
| $L_{50}$ | - | 27.0 | 9.8 | 10.9 | 10.4 |
| $L_{75}$ | - | 16.9 | 3.2 | 6.3 | 7.3 |
| $L_{95}$ | - | 3.1 | 2.1 | 3.0 | 3.0 |
| $L_{mean}$ | - | 34.3 | 16.1 | 18.3 | 18.9 |
| **Channel 2 (mid-water)** | | | | | |
| $L_{max}$ | 197.8 | 198.5 | 188.2 | 182.0 | 175.7 |
| $L_5$ | 90.3 | 116.8 | 111.6 | 89.8 | 86.5 |
| $L_{25}$ | 31.6 | 45.9 | 17.7 | 12.9 | 10.7 |
| $L_{50}$ | 22.3 | 34.1 | 14.4 | 11.3 | 9.4 |
| $L_{75}$ | 15.5 | 18.0 | 11.6 | 9.2 | 8.2 |
| $L_{95}$ | 2.9 | 3.3 | 3.0 | 3.0 | 3.0 |
| $L_{mean}$ | 28.8 | 38.5 | 24.1 | 19.2 | 17.7 |

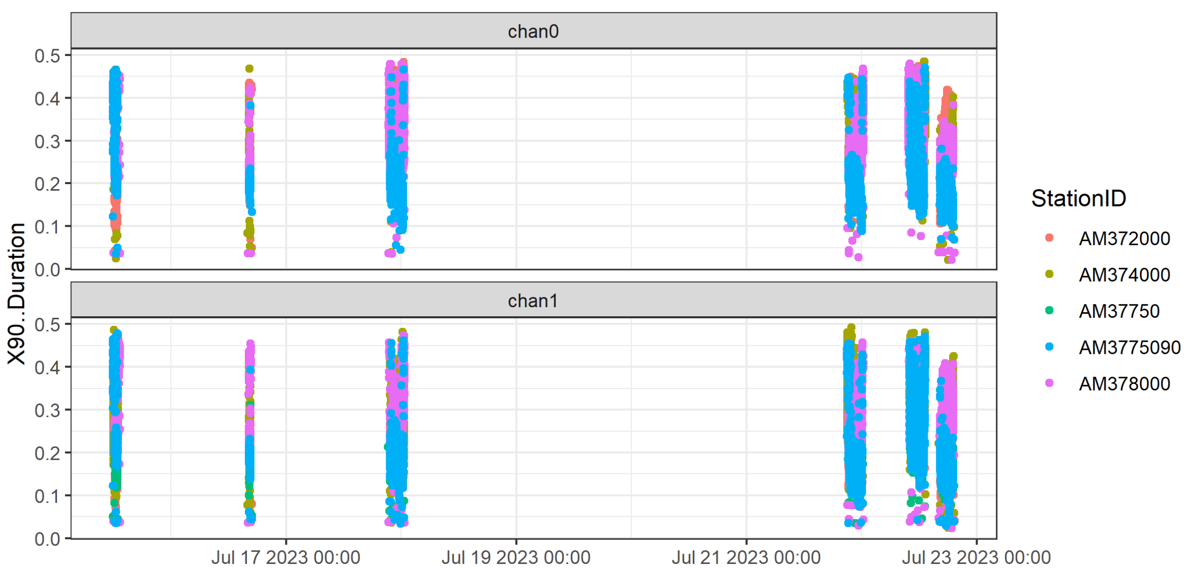


Figure B-14. Rise time as pulse duration in seconds (s) between 5% and 95% energy for each strike for both channel 1 (top) and channel 2 (bottom) at each recording location for pile AM-37.

## B.8. Foundation AQ-38

The kurtosis of the received signals was calculated at each of the recording locations for pile AQ-38 (Figure B-15). The summary of the signal kurtosis statistics is presented in Table B-8. The pulse duration time of the received signals was calculated at each of the recording locations (Figure B-16).

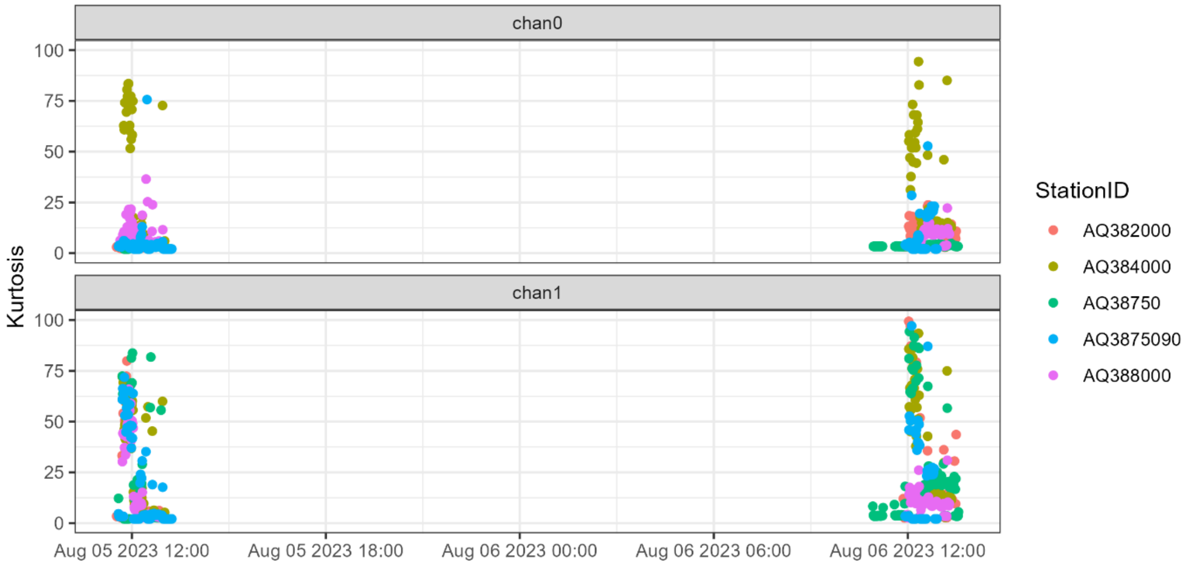


Figure B-15. Signal kurtosis for each strike for both channel 1 (top) and channel 2 (bottom) at each recording location for pile AQ-38.

Table B-8. Signal kurtosis statistic summary for Pile AQ-38.

| Kurtosis statistics | AQ38-750 | AQ38-75090 | AQ38-2000 | AQ38-4000 | AQ38-8000 |
|---|---|---|---|---|---|
| **Channel 1 (bottom)** | | | | | |
| $L_{max}$ | - | 75.6 | 23.8 | 160.9 | 36.5 |
| $L_5$ | - | 21.3 | 16.3 | 83.6 | 20.3 |
| $L_{25}$ | - | 4.6 | 11.5 | 51.6 | 11.4 |
| $L_{50}$ | - | 3.5 | 7.2 | 14.3 | 9.6 |
| $L_{75}$ | - | 2.1 | 3.4 | 4.9 | 5.5 |
| $L_{95}$ | - | 2.1 | 2.9 | 3.3 | 3.7 |
| $L_{mean}$ | - | 6.0 | 8.0 | 28.5 | 9.9 |
| **Channel 2 (mid-water)** | | | | | |
| $L_{max}$ | 115.4 | 97.1 | 184.5 | 122.3 | 175.4 |
| $L_5$ | 81.4 | 60.4 | 118.7 | 75.0 | 59.3 |
| $L_{25}$ | 21.9 | 26.5 | 21.2 | 44.6 | 19.0 |
| $L_{50}$ | 12.4 | 3.9 | 12.3 | 12.6 | 9.2 |
| $L_{75}$ | 3.5 | 2.1 | 3.7 | 6.1 | 4.2 |
| $L_{95}$ | 2.5 | 2.1 | 2.9 | 3.3 | 2.9 |
| $L_{mean}$ | 20.7 | 16.9 | 28.2 | 24.2 | 21.3 |

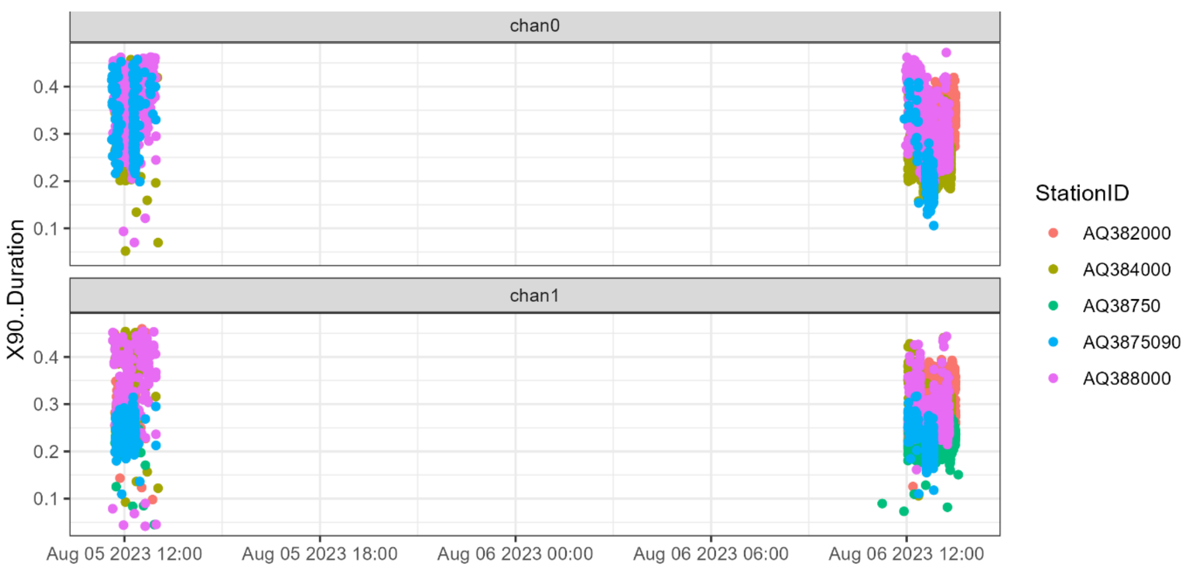


Figure B-16. Rise time as pulse duration in seconds (s) between 5% and 95% energy for each strike for both channel 1 (top) and channel 2 (bottom) at each recording location for pile AQ-38.

## B.9. Foundation AT-39

The kurtosis of the received signals was calculated at each of the recording locations for pile AT-39 (Figure B-17). The summary of the signal kurtosis statistics is presented in Table B-9. The pulse duration time of the received signals was calculated at each of the recording locations (Figure B-18).

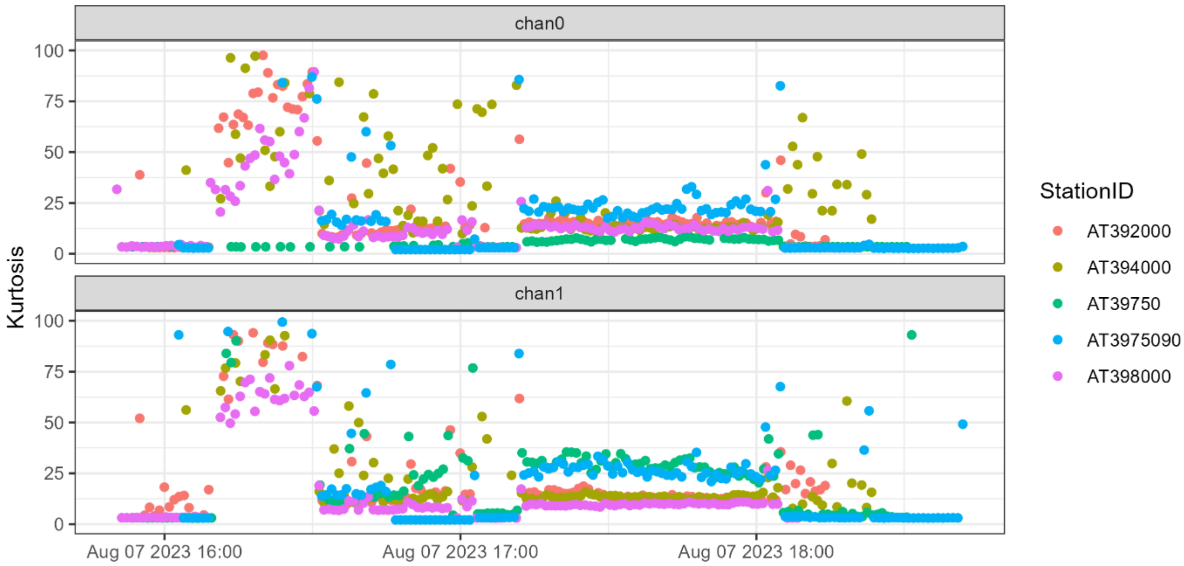


Figure B-17. Signal kurtosis for each strike for both channel 1 (top) and channel 2 (bottom) at each recording location for pile AT-39.

Table B-9. Signal kurtosis statistic summary for Pile AT-39.

| Kurtosis statistics | AT39-750 | AT39-75090 | AT39-2000 | AT39-4000 | AT39-8000 |
|---|---|---|---|---|---|
| **Channel 1 (bottom)** | | | | | |
| $L_{max}$ | - | 162.7 | 170.3 | - | - |
| $L_{5}$ | - | 131.7 | 79.8 | - | - |
| $L_{25}$ | - | 23.7 | 17.1 | - | - |
| $L_{50}$ | - | 17.6 | 14.3 | - | - |
| $L_{75}$ | - | 2.9 | 9.4 | - | - |
| $L_{95}$ | - | 2.1 | 3.1 | - | - |
| $L_{mean}$ | - | 28.6 | 23.3 | - | - |
| **Channel 2 (mid-water)** | | | | | |
| $L_{max}$ | 182.9 | 158.7 | 126.9 | 195.5 | 155.6 |
| $L_{5}$ | 126.3 | 125.9 | 105.5 | 165.5 | 70.1 |
| $L_{25}$ | 32.4 | 29.2 | 18.9 | 37.0 | 10.9 |
| $L_{50}$ | 24.8 | 22.5 | 14.1 | 14.1 | 9.6 |
| $L_{75}$ | 5.3 | 3.2 | 12.4 | 12.7 | 7.0 |
| $L_{95}$ | 3.1 | 2.1 | 3.4 | 10.3 | 3.1 |
| $L_{mean}$ | 32.6 | 30.7 | 27.5 | 38.7 | 19.8 |

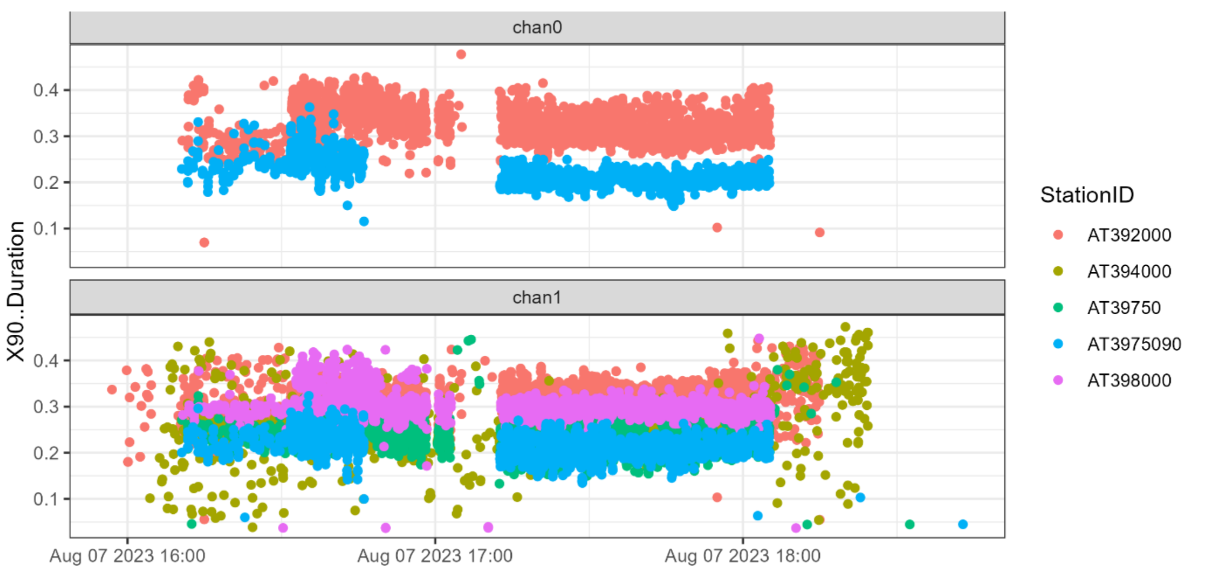


Figure B-18. Rise time as pulse duration in seconds (s) between 5% and 95% energy for each strike for both channel 1 (top) and channel 2 (bottom) at each recording location for pile AT-39.

## B.10. Foundation AS-39

The kurtosis of the received signals was calculated at each of the recording locations for pile AS-39 (Figure B-19). The summary of the signal kurtosis statistics is presented in Table B-10. The pulse duration time of the received signals was calculated at each of the recording locations (Figure B-20).

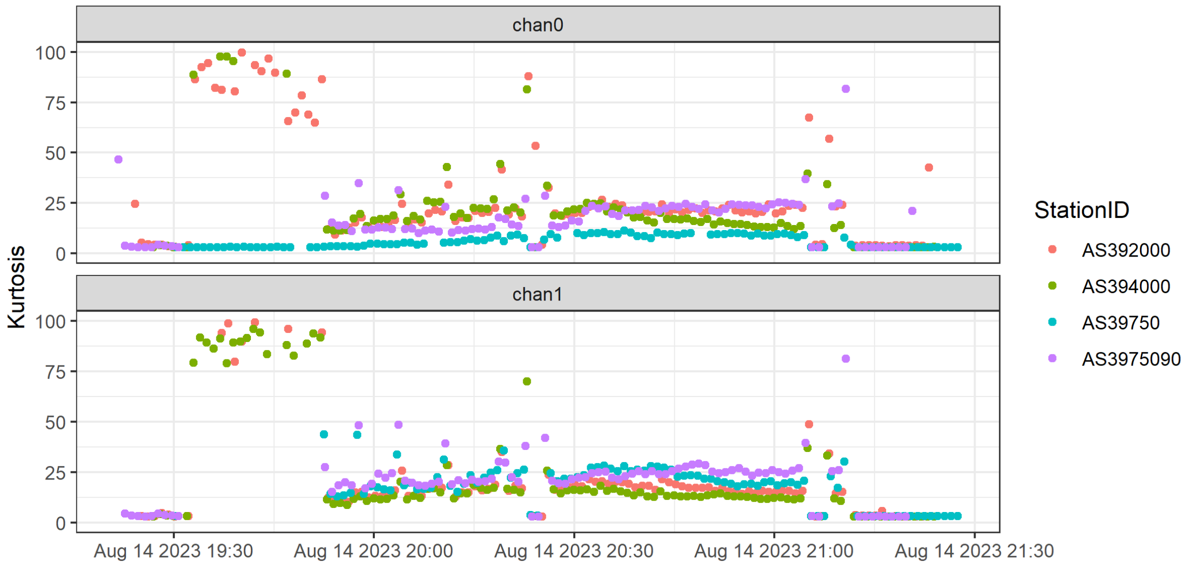


Figure B-19. Signal kurtosis for each strike for both channel 1 (top) and channel 2 (bottom) at each recording location for pile AS-39.

Table B-10. Signal kurtosis statistic summary for Pile AS-39.

| Kurtosis statistics | AS39-750 | AS39-75090 | AS39-2000 | AS39-4000 |
|---|---|---|---|---|
| **Channel 1 (bottom)** | | | | |
| $L_{max}$ | - | 198.3 | 124.1 | 151.1 |
| $L_5$ | - | 168.4 | 93.7 | 126.9 |
| $L_{25}$ | - | 25.2 | 24.6 | 27.5 |
| $L_{50}$ | - | 21.2 | 20.7 | 18.0 |
| $L_{75}$ | - | 11.7 | 15.3 | 13.2 |
| $L_{95}$ | - | 3.0 | 3.8 | 3.0 |
| $L_{mean}$ | - | 41.0 | 30.8 | 35.5 |
| **Channel 2 (mid-water)** | | | | |
| $L_{max}$ | 194.0 | 199.1 | 169.9 | 164.4 |
| $L_5$ | 153.4 | 178.1 | 112.9 | 94.0 |
| $L_{25}$ | 28.1 | 28.1 | 21.0 | 18.5 |
| $L_{50}$ | 21.7 | 24.0 | 16.7 | 13.5 |
| $L_{75}$ | 16.5 | 19.1 | 13.1 | 11.5 |
| $L_{95}$ | 3.1 | 3.0 | 3.1 | 3.0 |
| $L_{mean}$ | 41.4 | 40.9 | 31.7 | 28.1 |


Figure B-20. Rise time as pulse duration in seconds (s) between 5% and 95% energy for each strike for both channel 1 (top) and channel 2 (bottom) at each recording location for pile AS-39.

## B.11. Foundation AV-38

The kurtosis of the received signals was calculated at each of the recording locations for pile AV-38 (Figure B-21). The summary of the signal kurtosis statistics is presented in Table B-11. The pulse duration time of the received signals was calculated at each of the recording locations (Figure B-22).

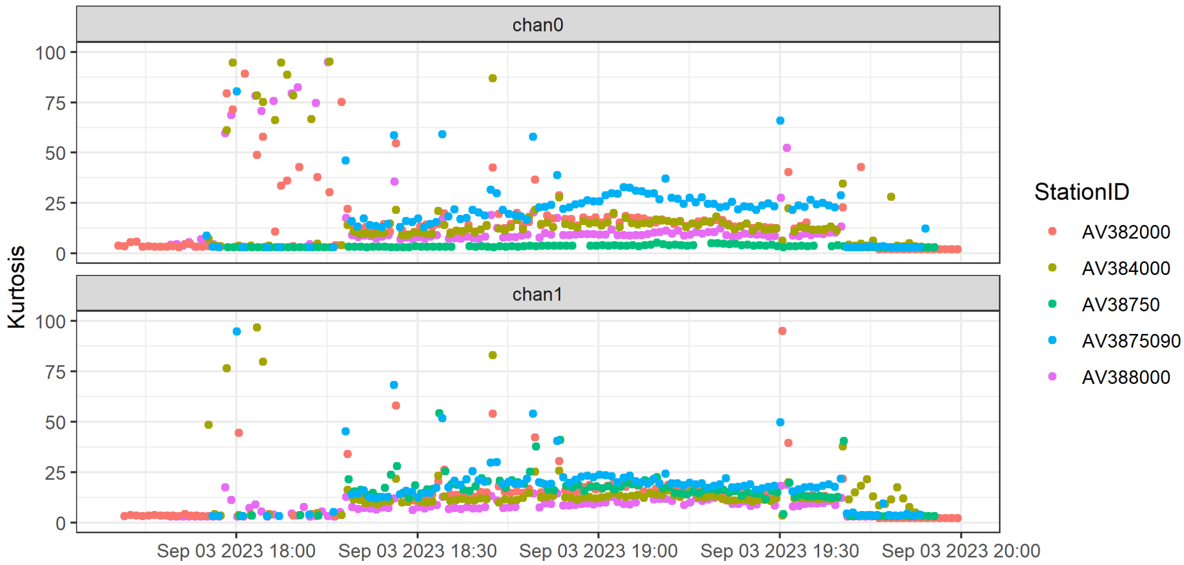


Figure B-21. Signal kurtosis for each strike for both channel 1 (top) and channel 2 (bottom) at each recording location for pile AV-38.

Table B-11. Signal kurtosis statistic summary for Pile AV-38.

| Kurtosis statistics | AV38-750 | AV38-75090 | AV38-2000 | AV38-4000 | AV38-8000 |
|---|---|---|---|---|---|
| **Channel 1 (bottom)** | | | | | |
| $L_{max}$ | - | 192.3 | 135.5 | 145.4 | 163.0 |
| $L_{5}$ | - | 154.5 | 59.3 | 94.8 | 85.0 |
| $L_{25}$ | - | 28.8 | 17.1 | 16.1 | 10.7 |
| $L_{50}$ | - | 23.1 | 13.4 | 13.2 | 9.1 |
| $L_{75}$ | - | 14.5 | 3.7 | 10.1 | 7.7 |
| $L_{95}$ | - | 3.1 | 2.1 | 3.8 | 3.2 |
| $L_{mean}$ | - | 32.8 | 17.8 | 23.5 | 19.8 |
| **Channel 2 (mid-water)** | | | | | |
| $L_{max}$ | 175.5 | 181.4 | 198.0 | 192.0 | - |
| $L_{5}$ | 144.6 | 155.8 | 142.0 | 124.0 | - |
| $L_{25}$ | 19.5 | 23.0 | 17.4 | 14.7 | - |
| $L_{50}$ | 16.1 | 19.0 | 14.1 | 12.2 | - |
| $L_{75}$ | 13.0 | 14.8 | 3.6 | 10.9 | - |
| $L_{95}$ | 3.2 | 3.3 | 2.1 | 3.9 | - |
| $L_{mean}$ | 25.7 | 33.7 | 25.2 | 25.6 | - |

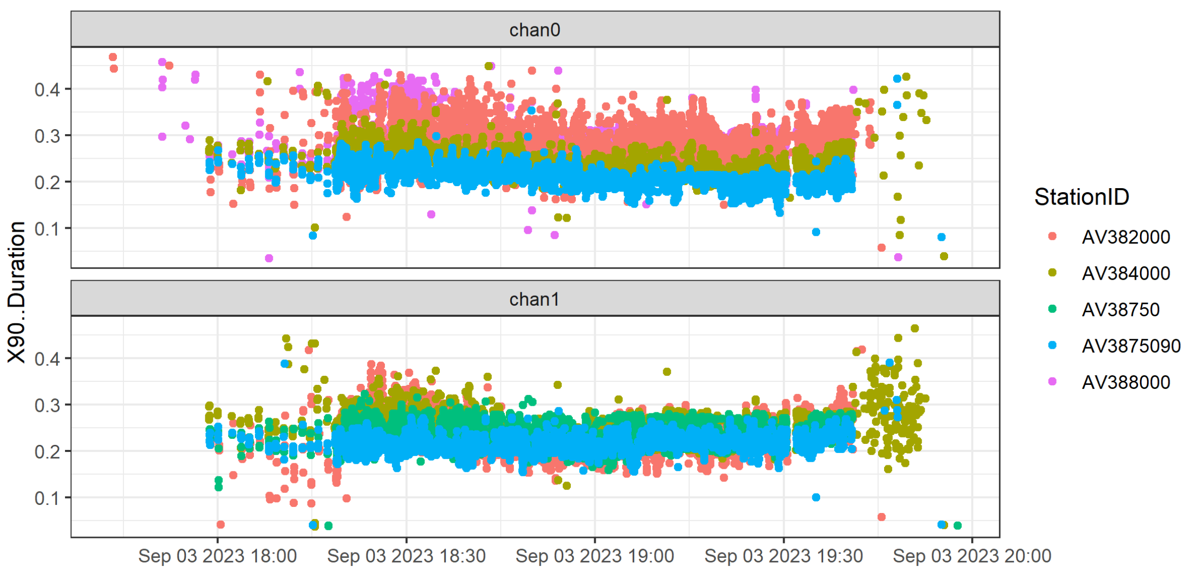


Figure B-22. Rise time as pulse duration in seconds (s) between 5% and 95% energy for each strike for both channel 1 (top) and channel 2 (bottom) at each recording location for pile AV-38.

## B.12. Foundation AN-37

The kurtosis of the received signals was calculated at each of the recording locations for pile AN-37 (Figure B-23). The summary of the signal kurtosis statistics is presented in Table B-12. The pulse duration time of the received signals was calculated at each of the recording locations (Figure B-24).

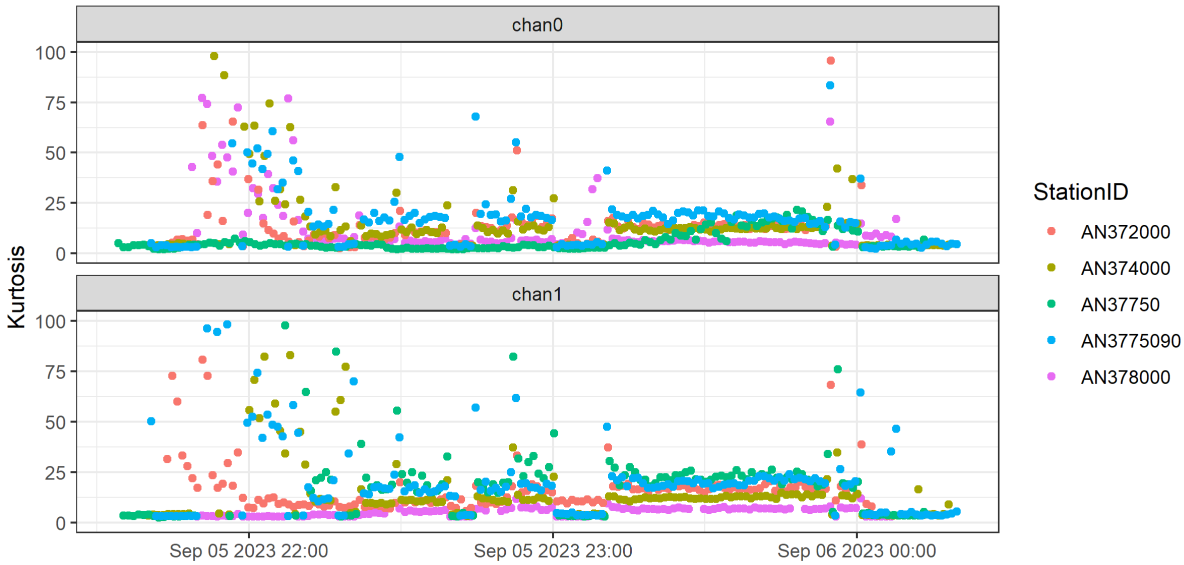


Figure B-23. Signal kurtosis for each strike for both channel 1 (top) and channel 2 (bottom) at each recording location for pile AN-37.

Table B-12. Signal kurtosis statistic summary for Pile AN-37.

| Kurtosis statistics | AN37-750 | AN37-75090 | AN37-2000 | AN37-4000 | AN37-8000 |
|---|---|---|---|---|---|
| **Channel 1 (bottom)** | | | | | |
| $L_{max}$ | - | 177.2 | 199.3 | 142.1 | 77.1 |
| $L_5$ | - | 85.0 | 51.8 | 62.6 | 48.6 |
| $L_{25}$ | - | 20.0 | 14.5 | 13.2 | 9.6 |
| $L_{50}$ | - | 17.1 | 12.4 | 11.7 | 6.2 |
| $L_{75}$ | - | 4.6 | 7.4 | 4.4 | 5.5 |
| $L_{95}$ | - | 3.2 | 3.4 | 3.9 | 4.7 |
| $L_{mean}$ | - | 23.5 | 16.9 | 16.2 | 12.7 |
| **Channel 2 (mid-water)** | | | | | |
| $L_{max}$ | 191.1 | 158.1 | 80.9 | 190.8 | - |
| $L_5$ | 93.2 | 96.3 | 34.9 | 78.5 | - |
| $L_{25}$ | 23.6 | 22.2 | 17.9 | 13.2 | - |
| $L_{50}$ | 19.6 | 18.0 | 15.3 | 11.7 | - |
| $L_{75}$ | 3.8 | 4.9 | 9.9 | 4.2 | - |
| $L_{95}$ | 3.1 | 3.2 | 7.4 | 3.6 | - |
| $L_{mean}$ | 24.5 | 25.0 | 16.6 | 19.4 | - |


Figure B-24. Rise time as pulse duration in seconds (s) between 5% and 95% energy for each strike for both channel 1 (top) and channel 2 (bottom) at each recording location for pile AN-37.

## B.13. Foundation AU-38

The kurtosis of the received signals was calculated at each of the recording locations for pile AU-38 (Figure B-25). The summary of the signal kurtosis statistics is presented in Table B-13. The pulse duration time of the received signals was calculated at each of the recording locations (Figure B-26).

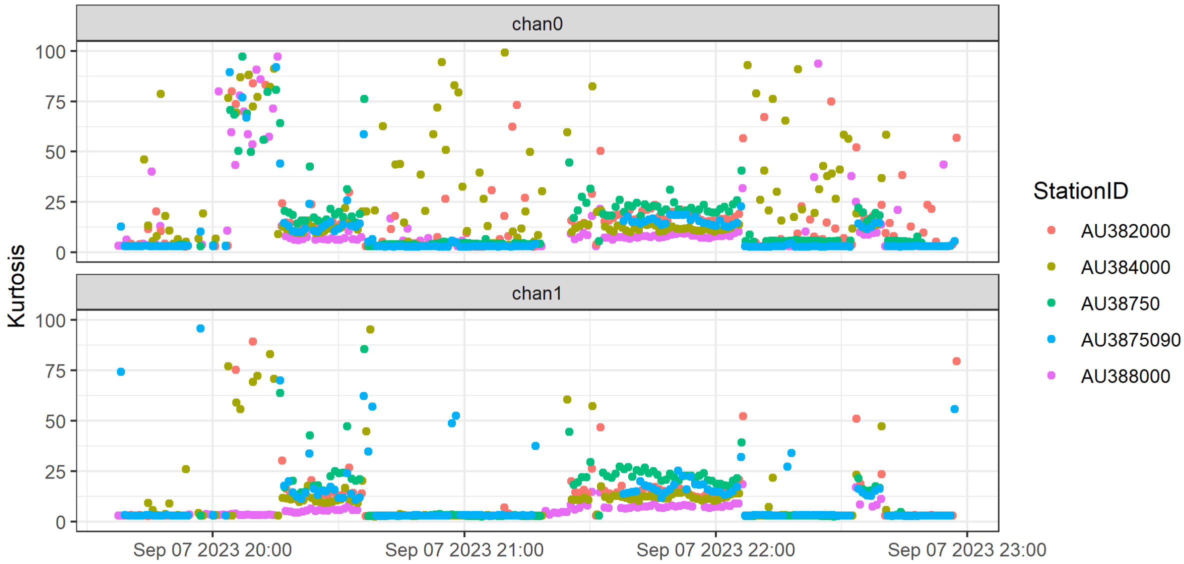


Figure B-25. Signal kurtosis for each strike for both channel 1 (top) and channel 2 (bottom) at each recording location for pile AU-38.

Table B-13. Signal kurtosis statistic summary for Pile AU-38.

| Kurtosis statistics | AU38-750 | AU38-75090 | AU38-2000 | AU38-4000 | AU38-8000 |
|---|---|---|---|---|---|
| **Channel 1 (bottom)** | | | | | |
| $L_{max}$ | - | 197.3 | 175.2 | 186.3 | 191.5 |
| $L_5$ | - | 115.8 | 118.8 | 111.9 | 85.1 |
| $L_{25}$ | - | 14.4 | 20.7 | 43.7 | 9.3 |
| $L_{50}$ | - | 3.1 | 14.5 | 13.9 | 6.4 |
| $L_{75}$ | - | 3.0 | 4.1 | 11.0 | 3.3 |
| $L_{95}$ | - | 2.8 | 3.0 | 5.3 | 3.0 |
| $L_{mean}$ | - | 18.7 | 24.6 | 33.8 | 16.6 |
| **Channel 2 (mid-water)** | | | | | |
| $L_{max}$ | 186.0 | 192.6 | 186.8 | 187.6 | - |
| $L_5$ | 98.8 | 88.3 | 103.2 | 126.1 | - |
| $L_{25}$ | 22.1 | 15.9 | 15.0 | 13.3 | - |
| $L_{50}$ | 4.6 | 3.1 | 3.2 | 10.1 | - |
| $L_{75}$ | 2.9 | 3.0 | 3.0 | 3.0 | - |
| $L_{95}$ | 2.7 | 2.9 | 2.7 | 2.9 | - |
| $L_{mean}$ | 20.1 | 18.3 | 17.7 | 21.3 | - |

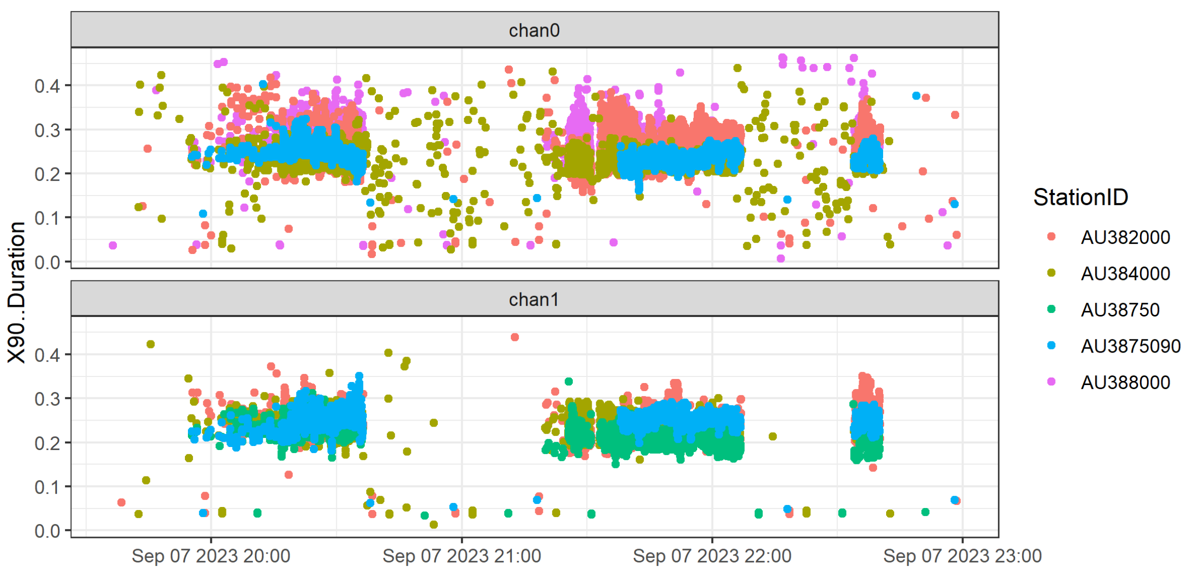


Figure B-26. Rise time as pulse duration in seconds (s) between 5% and 95% energy for each strike for both channel 1 (top) and channel 2 (bottom) at each recording location for pile AU-38.

# Appendix C. Impact Hammering Log Plots

Hammer energies achieved during the installation of each of the SFV monitored piles as a function of time were provided by DEME. They were plotted and are shown in this Appendix.

## C.1. Hammering schedule AT-40

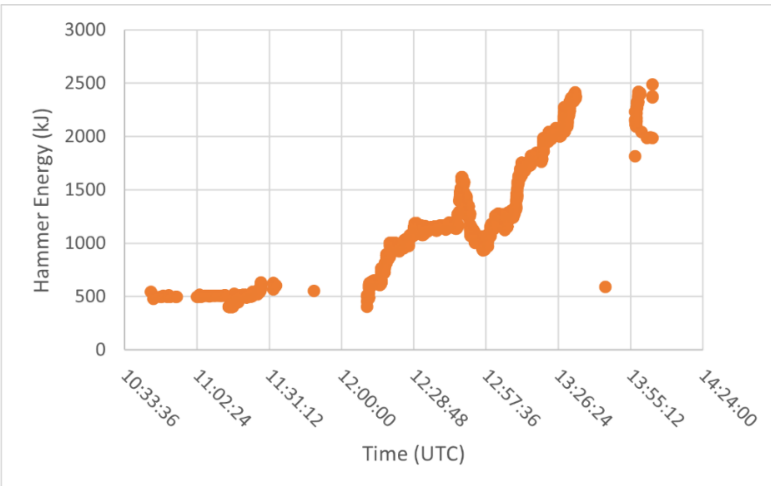


Figure C-1. Hammer energy over time for impact pile driving of pile AT-40 on 6 Jun 2023.

## C.2. Hammering schedule AU-39

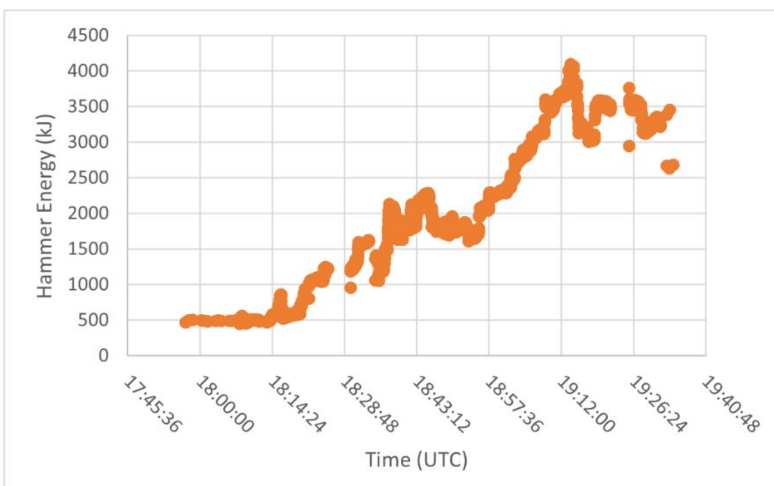


Figure C-2. Hammer energy over time for impact pile driving of pile AU-39 on 9 Jun 2023.

## C.3. Hammering schedule AP-38

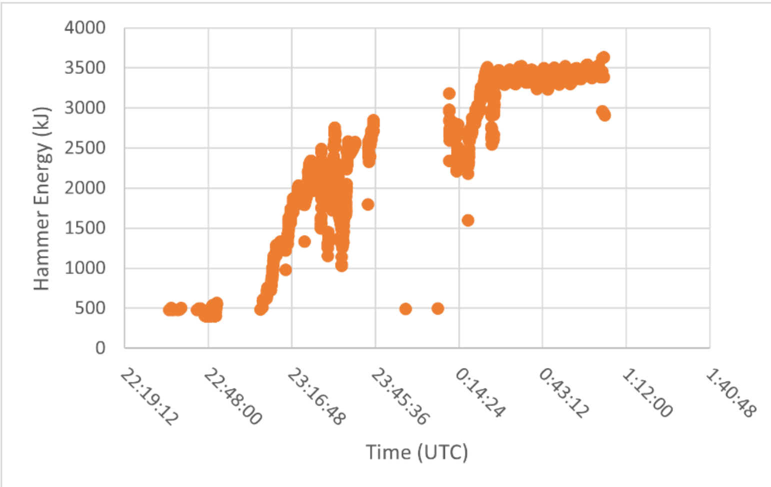


Figure C-3. Hammer energy over time for impact pile driving of pile AP-38 on 17 Jun 2023.

## C.4. Hammering schedule AV-39

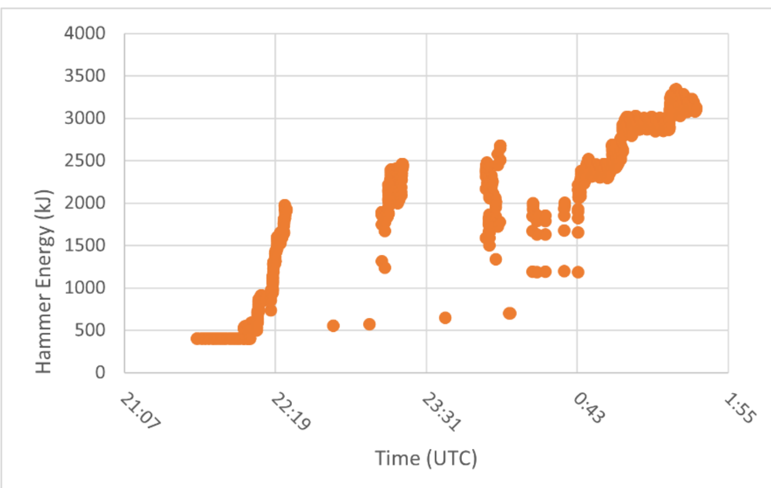


Figure C-4. Hammer energy over time for impact pile driving of pile AV-39 on 26 Jun 2023.

## C.5. Hammering schedule AR-39

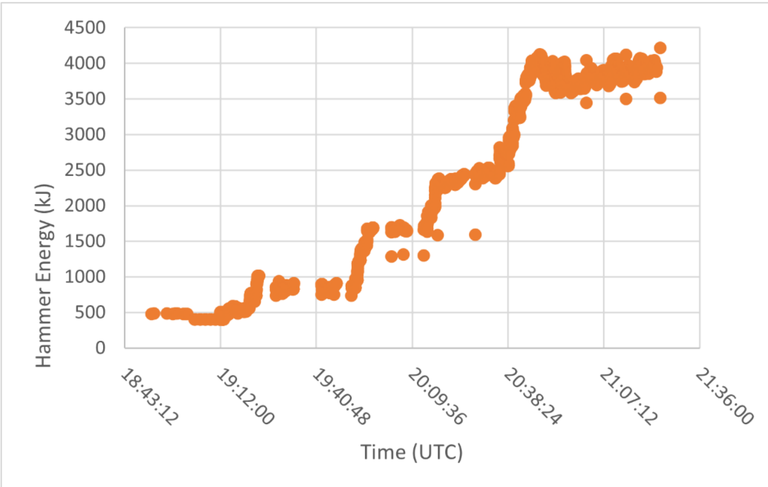


Figure C-5. Hammer energy over time for impact pile driving of pile AR-39 on 3 Jul 2023.

## C.6. Hammering schedule AW-38

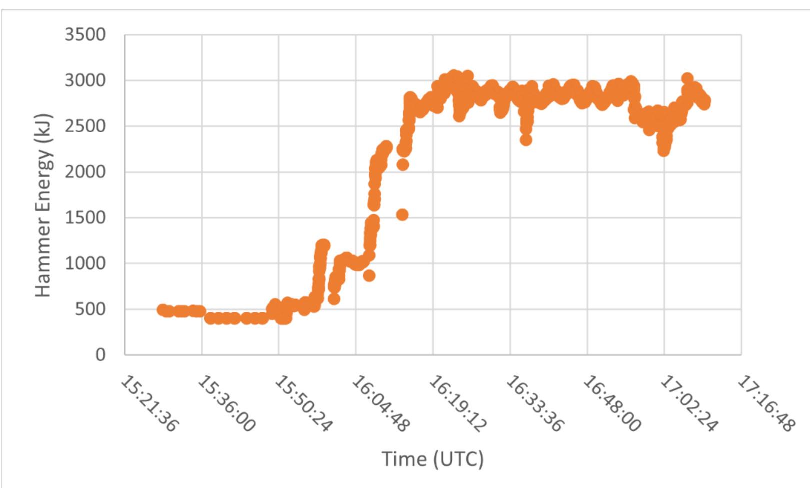


Figure C-6. Hammer energy over time for impact pile driving of pile AW-38 on 9 Jul 2023.

## C.7. Hammering schedule AM-37

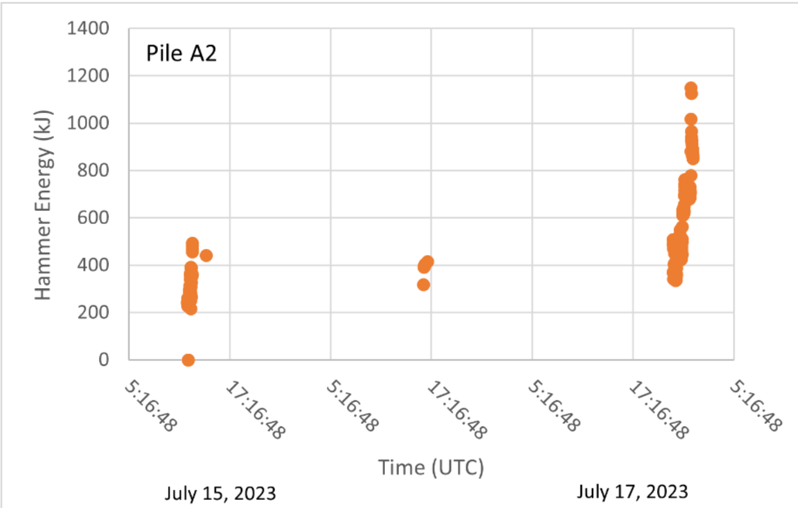


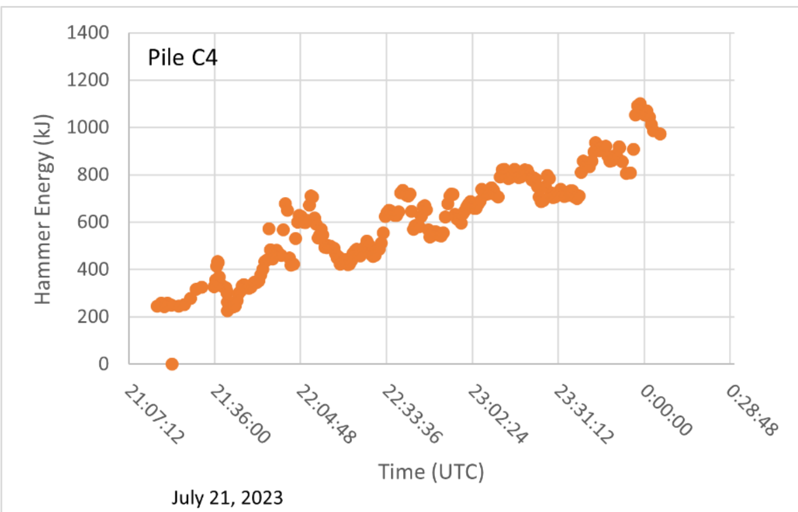


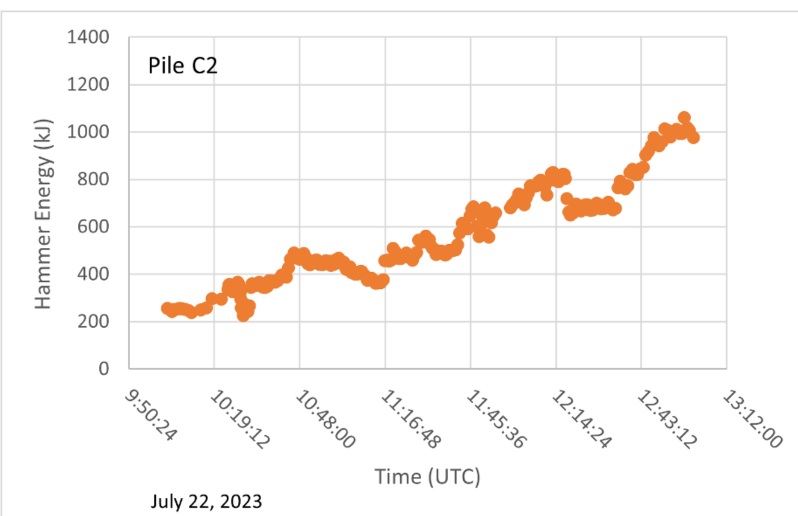

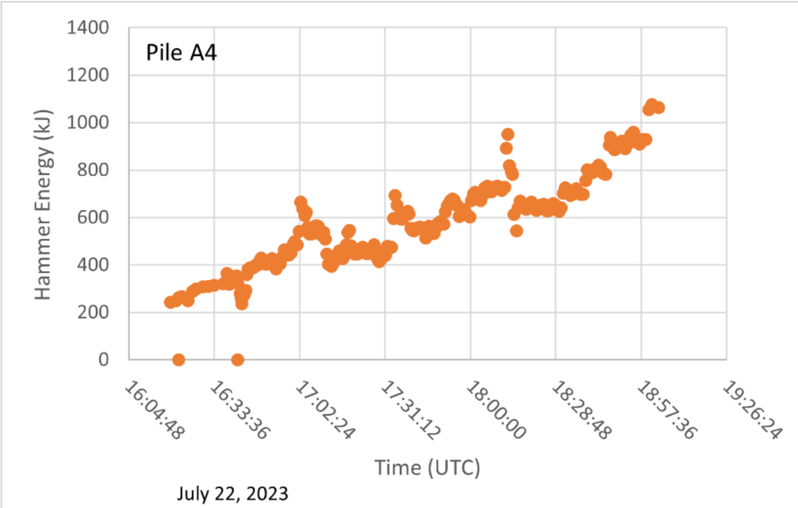


Figure C-7. Hammer energy over time for impact pile driving of each of the jacket foundation piles (A2, C4, C2, and A4) from 15 through 22 Jul 2023.

## C.8. Hammering schedule AQ-38

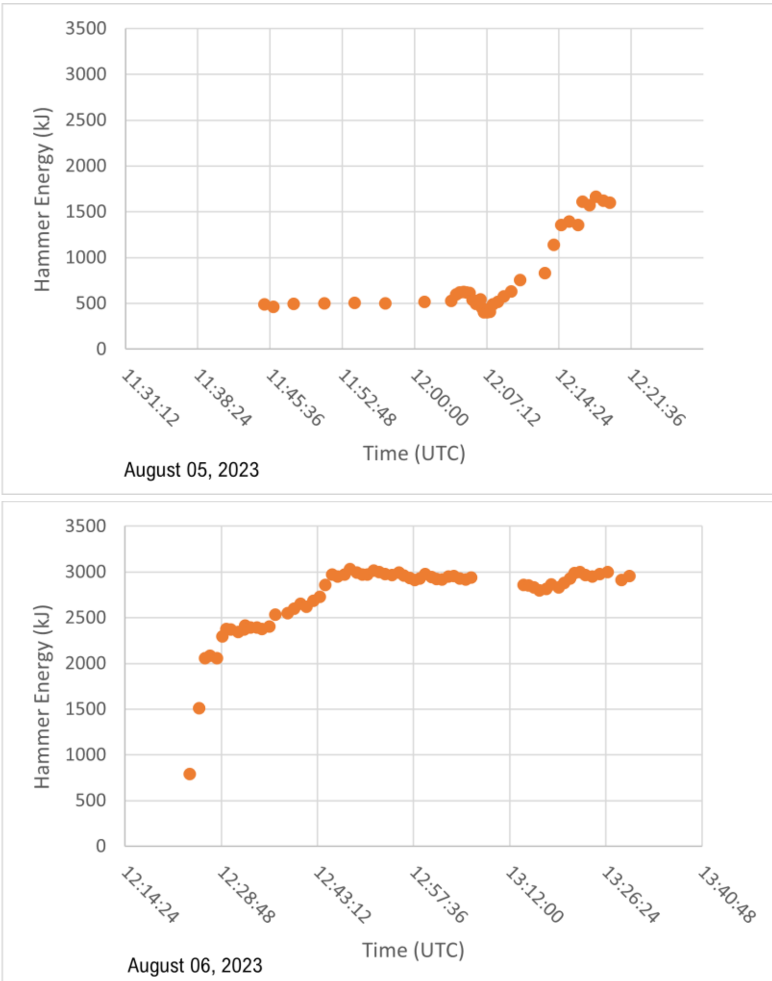


Figure C-8. Hammer energy over time for impact pile driving of pile AQ-38 on 5 Aug (top) and 6 Aug (bottom) 2023.

## C.9. Hammering schedule AT-39

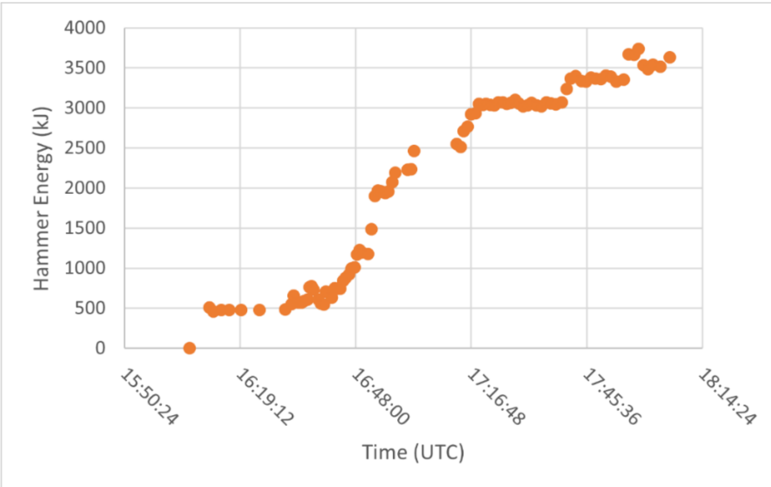


Figure C-9. Hammer energy over time for impact pile driving of pile AT-39 on 8 Aug 2023.

## C.10. Hammering schedule AS-39

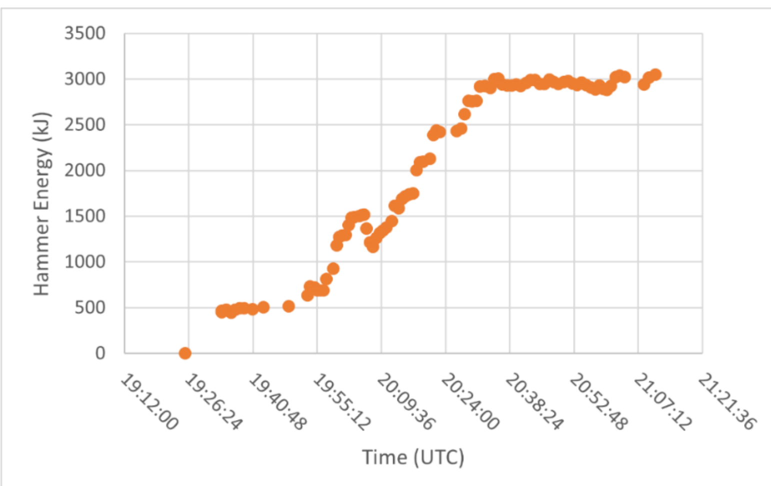


Figure C-10. Hammer energy over time for impact pile driving of pile AS-39 on 15 Aug 2023.

## C.11. Hammering schedule AV-38

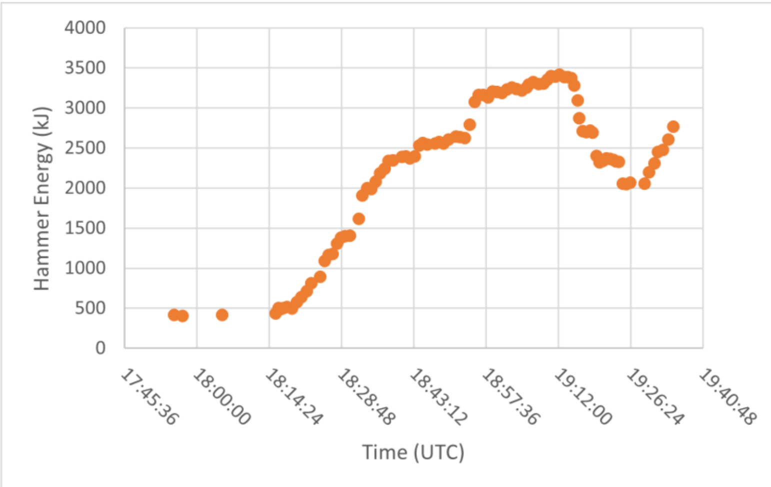


Figure C-11. Hammer energy over time for impact pile driving of pile AV-38 on 3 Sep 2023.

## C.12. Hammering schedule AN-37

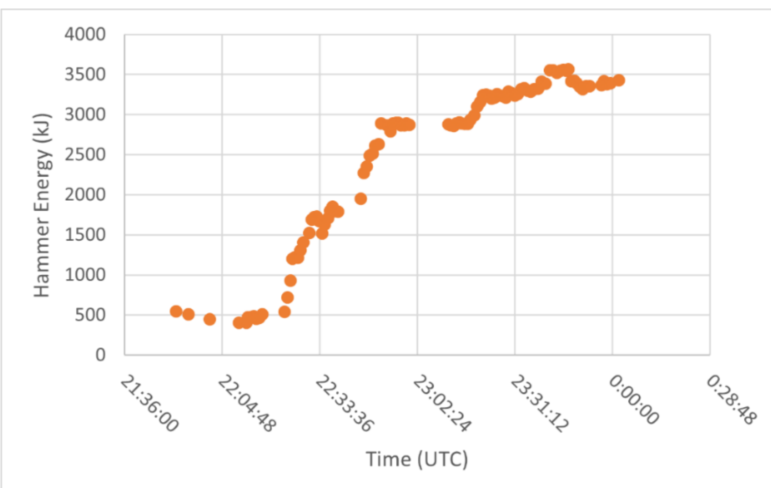


Figure C-12. Hammer energy over time for impact pile driving of pile AN-37 on 5 Sep 2023.

## C.13. Hammering schedule AU-38

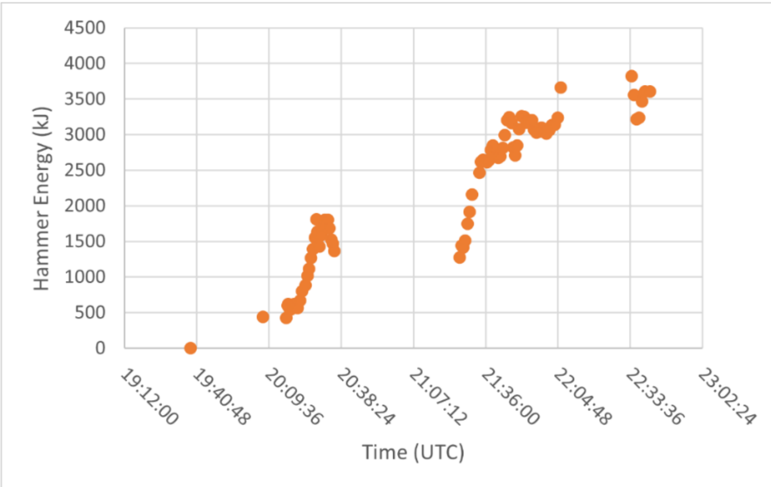


Figure C-13. Hammer energy over time for impact pile driving of pile AU-38 on 7 Sep 2023.

# Appendix D. Ambient Sound Levels Per Foundation

Figures D-1 through D-13 show the spectra of the ambient sound prior to pile driving for each monitored pile and at each station for which enough data was available for this analysis.

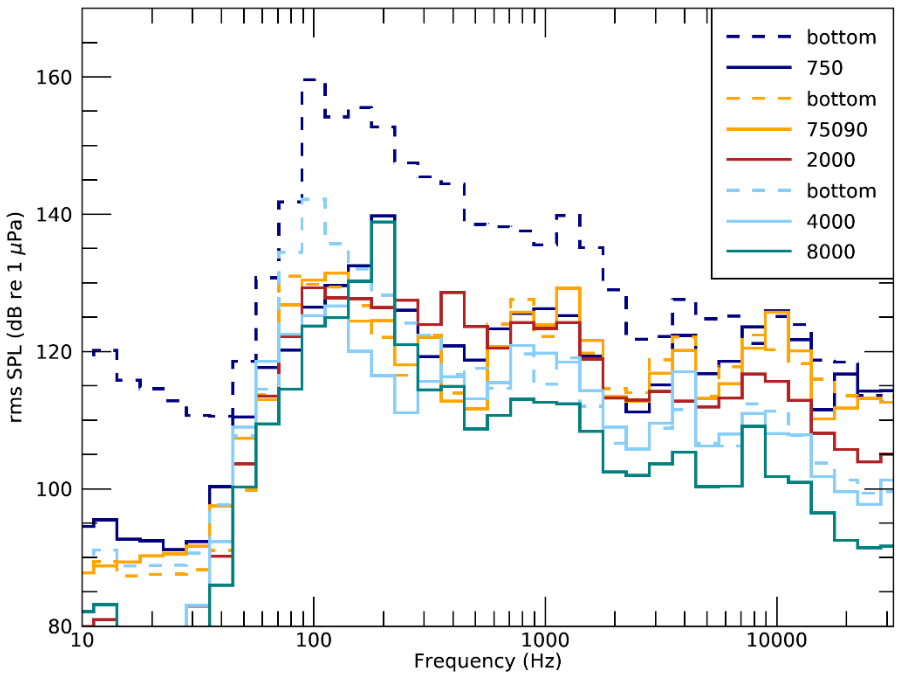


Figure D-1. Decidecade band levels of ambient noise (rms SPL) at approximately 10 minutes before the start of pile driving installation of AT-40, at all stations. Dashed lines correspond to channel 1 (bottom) and solid lines correspond to channel 2 (mid-water).

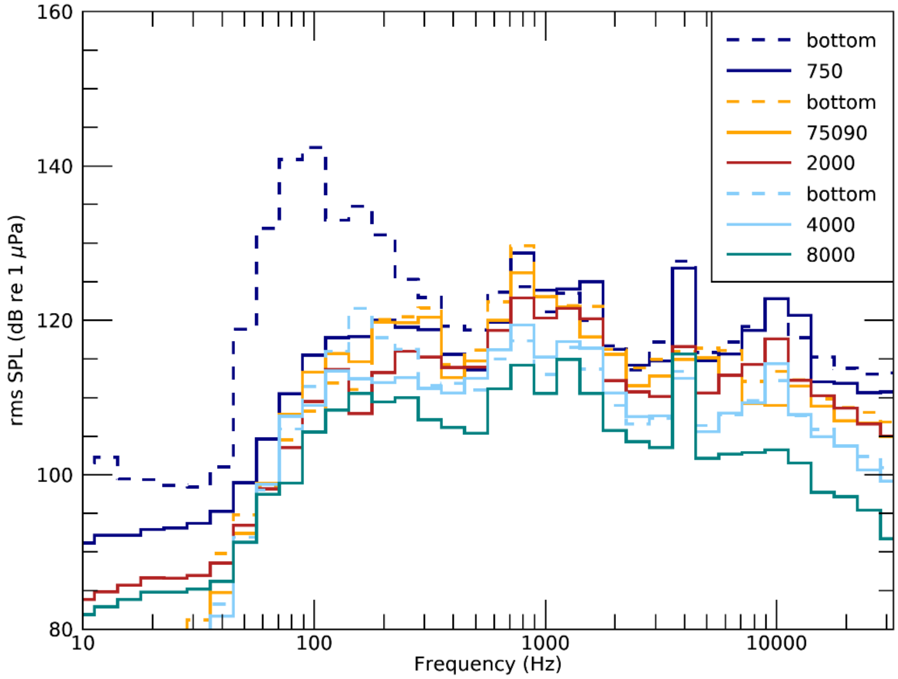


Figure D-2. Decidecade band levels of ambient noise (rms SPL) at approximately 10 minutes before the start of pile driving installation of AU-39, at all stations. Dashed lines correspond to channel 1 (bottom) and solid lines correspond to channel 2 (mid-water).

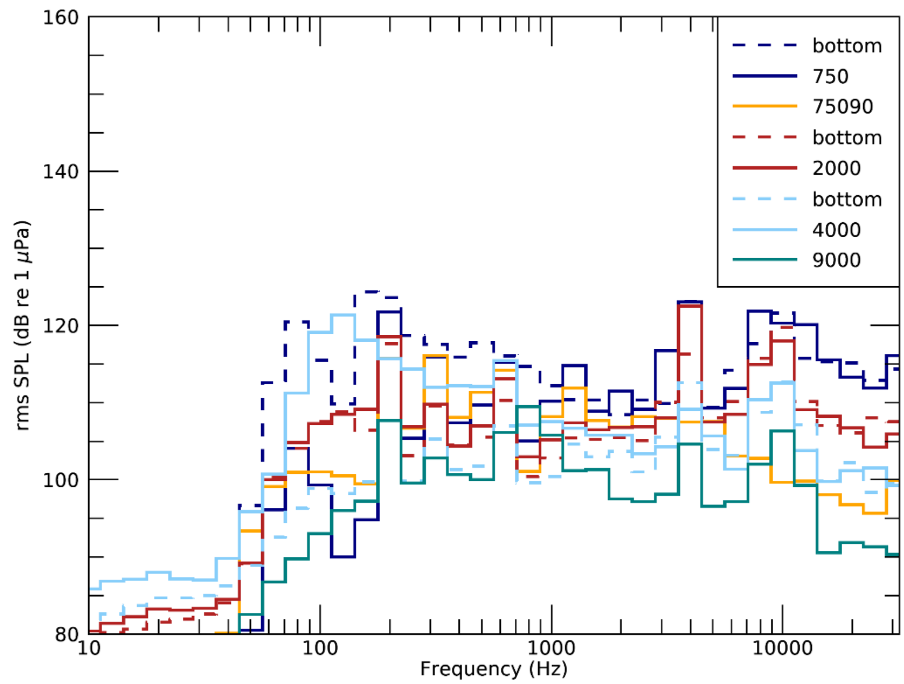


Figure D-3. Decidecade band levels of ambient noise (rms SPL) at approximately 10 minutes before the start of pile driving installation of AP-38, at all stations. Dashed lines correspond to channel 1 (bottom) and solid lines correspond to channel 2 (mid-water).

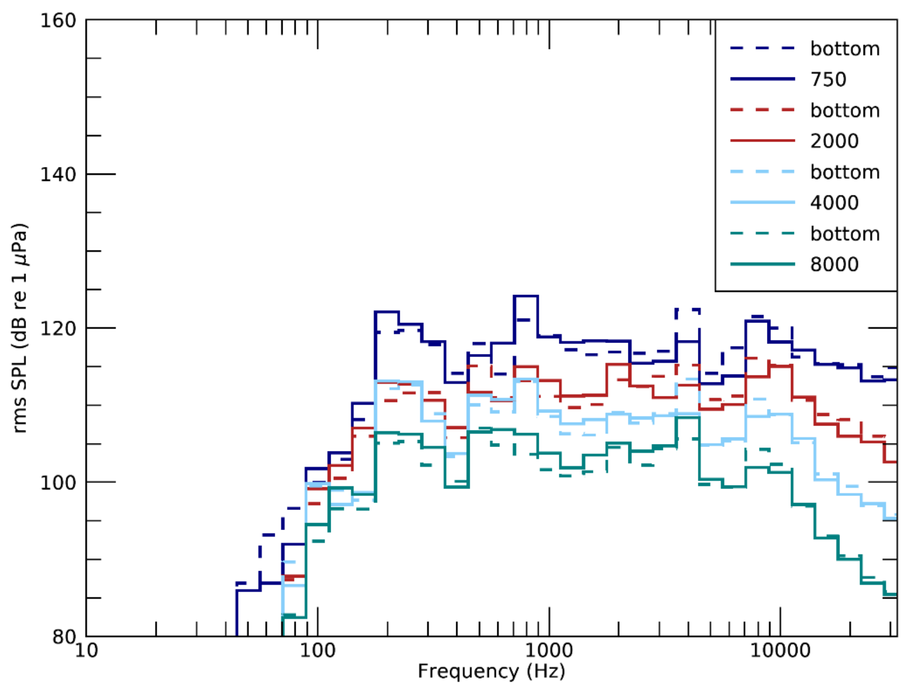


Figure D-4. Decidecade band levels of ambient noise (rms SPL) at approximately 10 minutes before the start of pile driving installation of AV-39, at all stations. Dashed lines correspond to channel 1 (bottom) and solid lines correspond to channel 2 (mid-water).

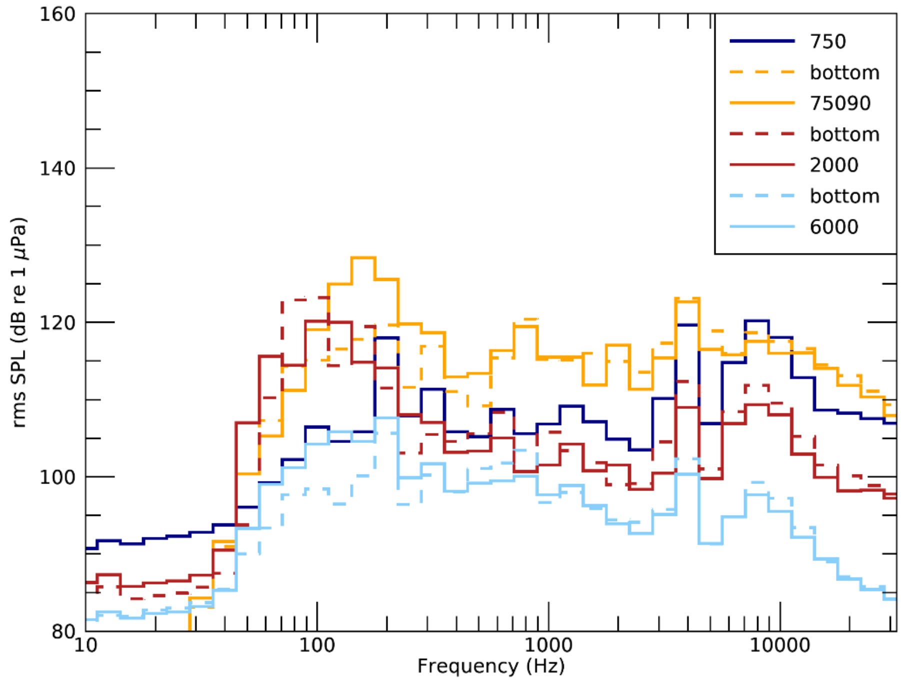


Figure D-5. Decidecade band levels of ambient noise (rms SPL) at approximately 10 minutes before the start of pile driving installation of AR-39, at all stations. Dashed lines correspond to channel 1 (bottom) and solid lines correspond to channel 2 (mid-water).

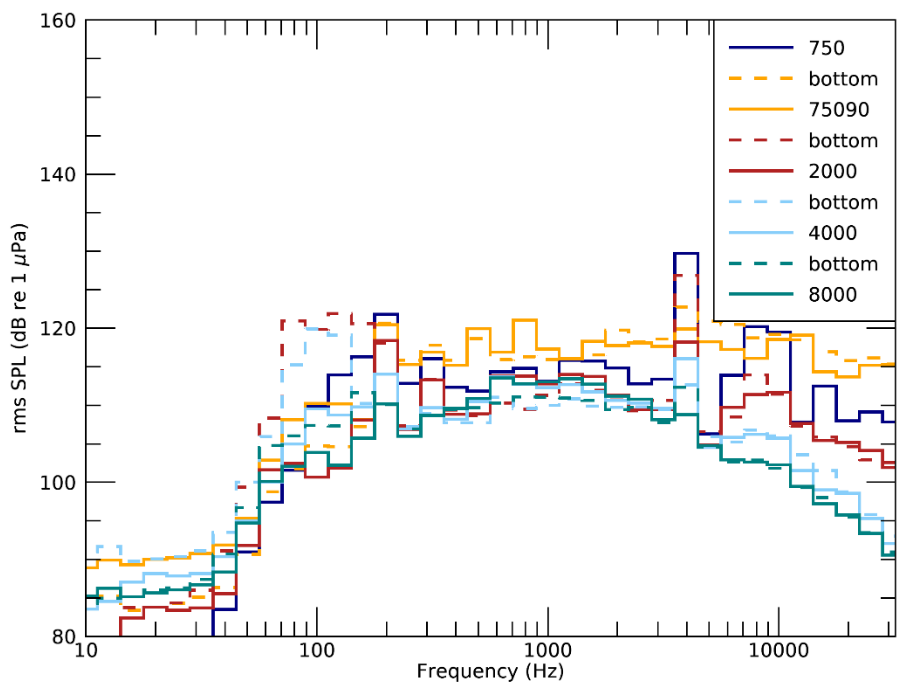


Figure D-6. Decidecade band levels of ambient noise (rms SPL) at approximately 10 minutes before the start of pile driving installation of AW-38, at all stations. Dashed lines correspond to channel 1 (bottom) and solid lines correspond to channel 2 (mid-water).

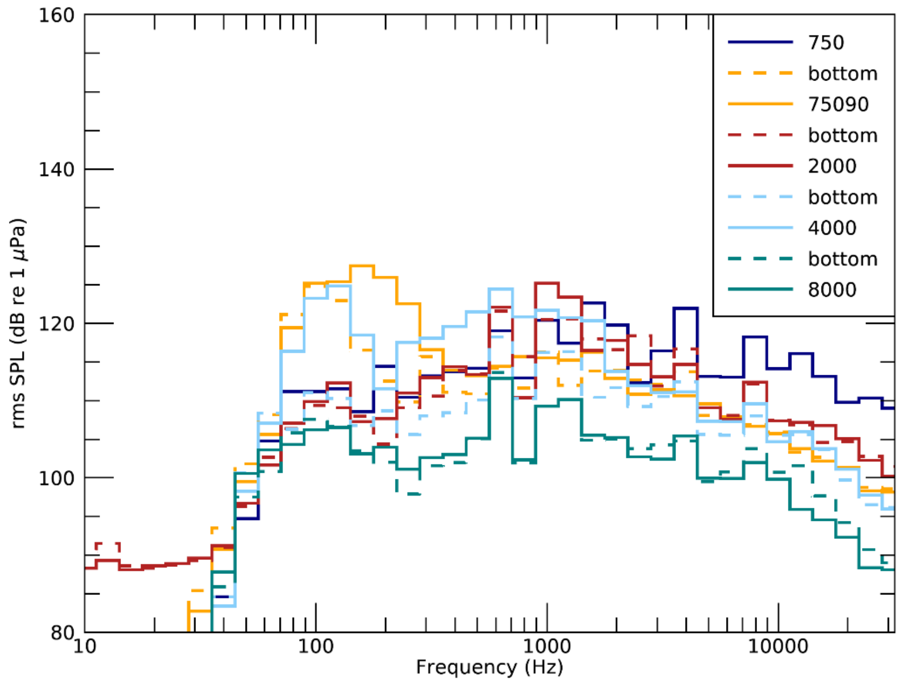


Figure D-7. Decidecade band levels of ambient noise (rms SPL) at approximately 10 minutes before the start of pile driving installation of AM-37, at all stations. Dashed lines correspond to channel 1 (bottom) and solid lines correspond to channel 2 (mid-water).

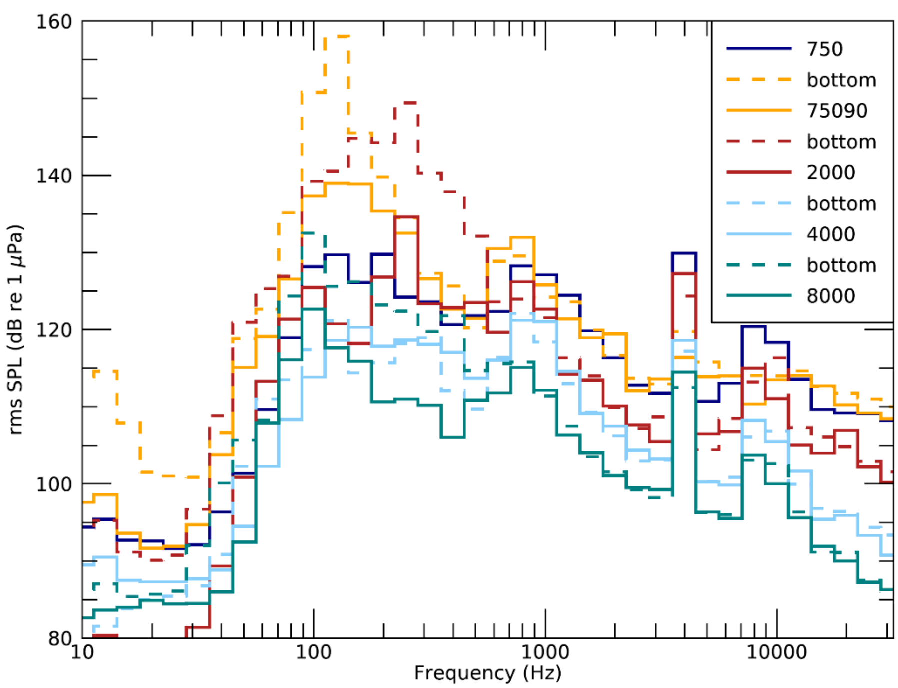


Figure D-8. Decidecade band levels of ambient noise (rms SPL) at approximately 10 minutes before the start of pile driving installation of AQ-38, at all stations. Dashed lines correspond to channel 1 (bottom) and solid lines correspond to channel 2 (mid-water).

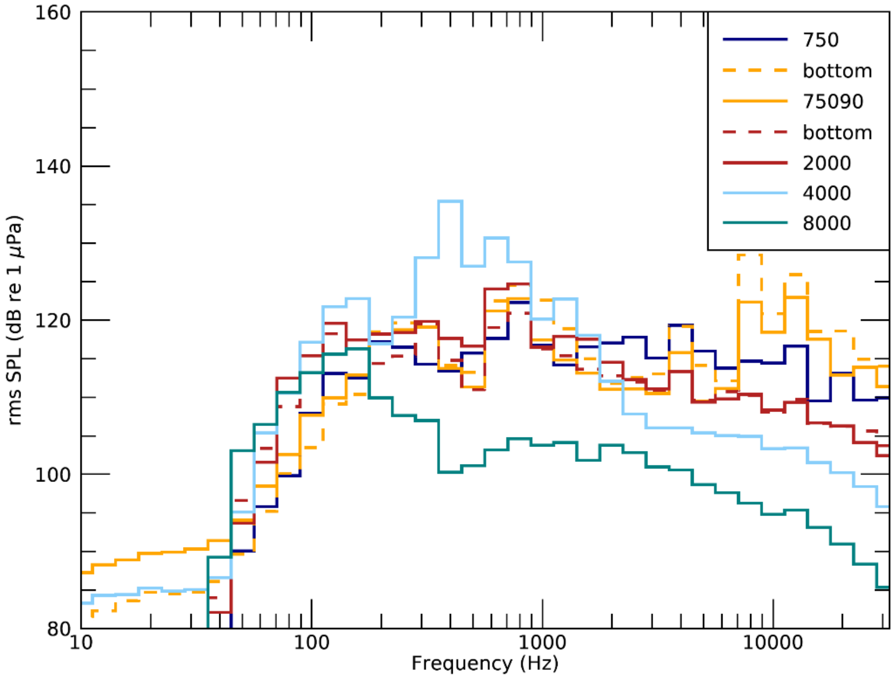


Figure D-9. Decidecade band levels of ambient noise (rms SPL) at approximately 10 minutes before the start of pile driving installation of AT-39, at all stations. Dashed lines correspond to channel 1 (bottom) and solid lines correspond to channel 2 (mid-water).

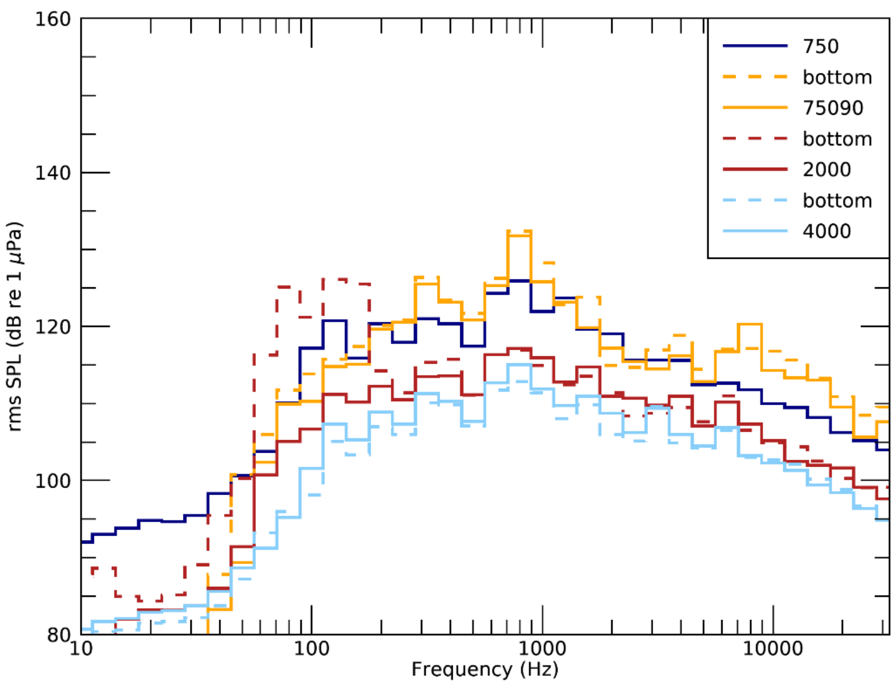


Figure D-10. Decidecade band levels of ambient noise (rms SPL) at approximately 10 minutes before the start of pile driving installation of AS-39, at all stations. Dashed lines correspond to channel 1 (bottom) and solid lines correspond to channel 2 (mid-water).

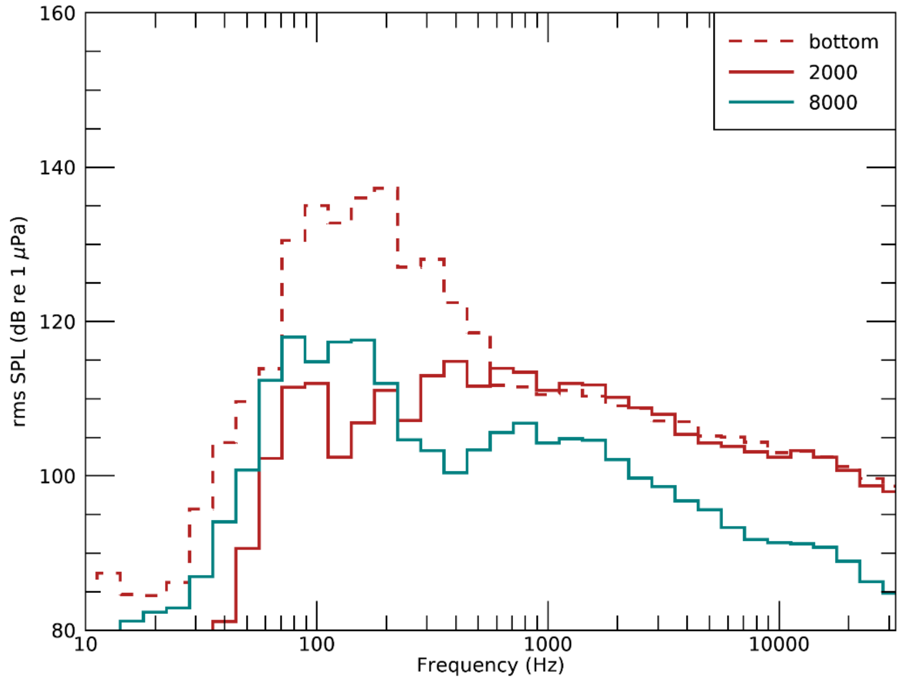


Figure D-11. Decidecade band levels of ambient noise (rms SPL) at approximately 10 minutes before the start of pile driving installation of AV-38, at all stations. Dashed lines correspond to channel 1 (bottom) and solid lines correspond to channel 2 (mid-water).

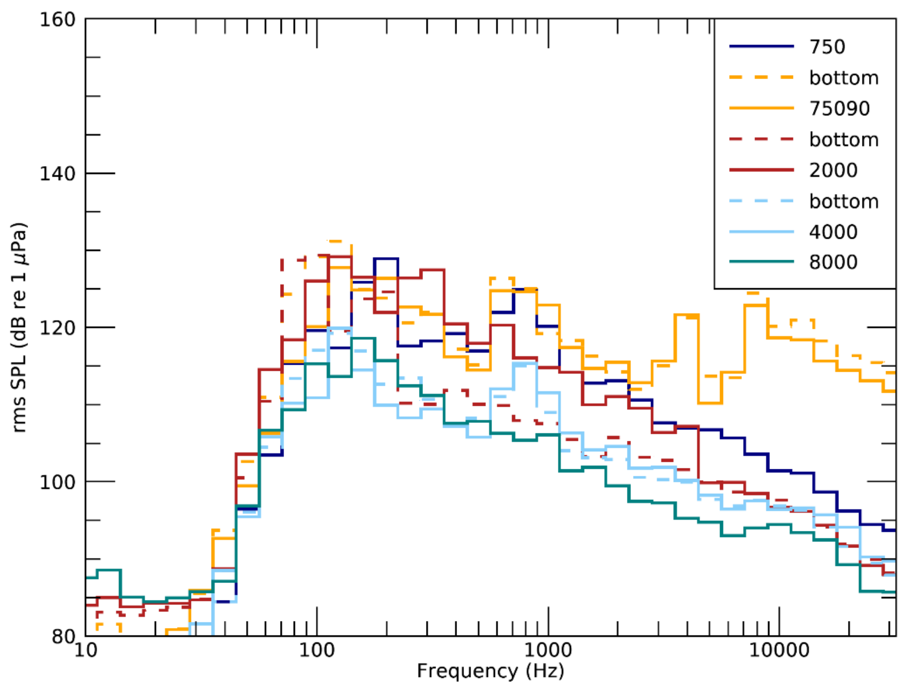


Figure D-12. Decidecade band levels of ambient noise (rms SPL) at approximately 10 minutes before the start of pile driving installation of AN-37, at all stations. Dashed lines correspond to channel 1 (bottom) and solid lines correspond to channel 2 (mid-water).

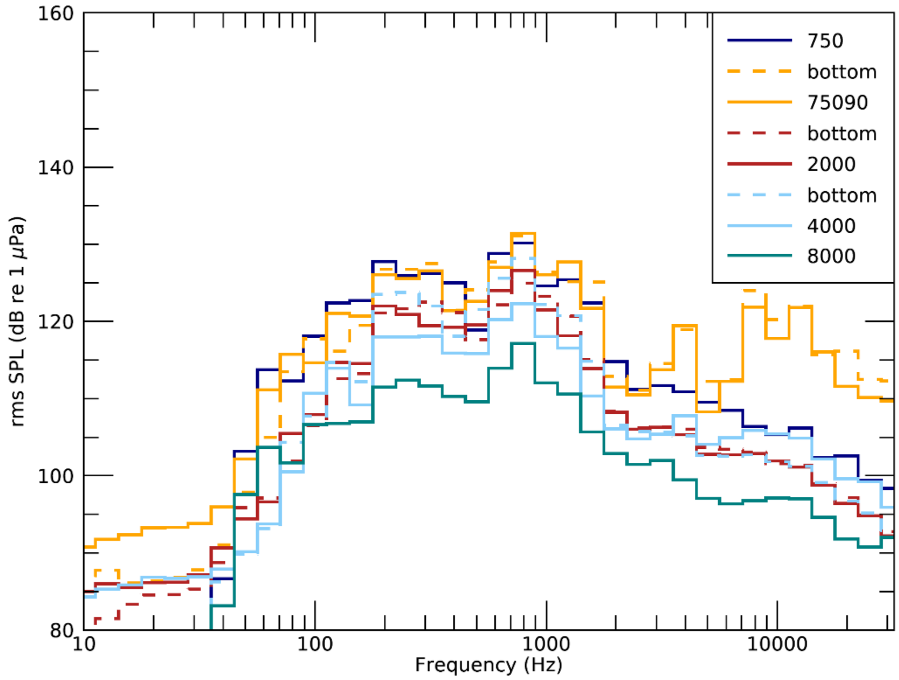


Figure D-13. Decidecade band levels of ambient noise (rms SPL) at approximately 10 minutes before the start of pile driving installation of AU-38, at all stations. Dashed lines correspond to channel 1 (bottom) and solid lines correspond to channel 2 (mid-water).

# Appendix E. Mooring Design and Recording Systems

## E.1. Recorder Mooring Design

At each monitoring location, a JASCO Autonomous Multichannel Acoustic Recorder Generation 4 (AMAR G4) was installed on a bottom plate mooring (Figure E-1). Each AMAR was fitted with two GeoSpectrum M36 hydrophones configured to sample at 64 ksps (10 Hz to 32 kHz recording bandwidth) with 24-bit resolution. The hydrophones were placed at 3 m from the bottom and at 20 m from the bottom. During deployment, the baseplate moorings were lowered to the bottom and the groundline was payed out. Once the end of the groundline was reached, a clump weight, including a surface line and float, was released from the vessel. During retrieval, the surface float was recovered, and a winch was used to retrieve the surface float line and groundline. Once the baseplate was at the surface, the vessel's crane was used to lift the baseplate aboard.

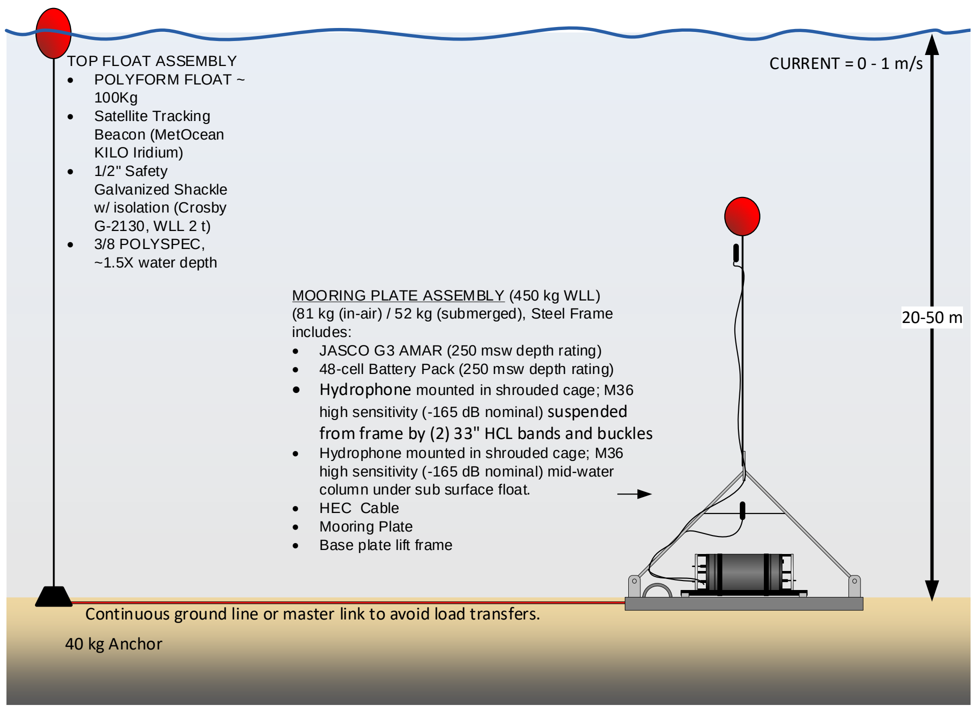


Figure E-1. Mooring design with one Acetyl-housing Autonomous Multichannel Acoustic Recorder Generation 4 (AMAR G4 ACE) attached to a bottom plate with a groundline and surface float.

Figure E-2. SFV base plates on the deck of the FV Beth Anne.

## E.1.1. Hydrophone Sensitivity

Three different sensitivity GTI hydrophones (-210, -200, and -165 dB re 1V/µPa) were used on the moorings for the SFV. The closest two stations had the least sensitive hydrophones, -210 dB re 1V/µPa, to avoid saturation during pile driving events. The middle stations used -200 dB re 1V/µPa hydrophones, and the farthest station will have one -200 dB re 1V/µPa along with one highly sensitive hydrophone, -165 dB re 1V/µPa (that was replaced with a -200 dB re 1V/µPa). Hydrophone sensitivity as a function of frequency is shown in Figures Figure E-3 - Figure E-5.

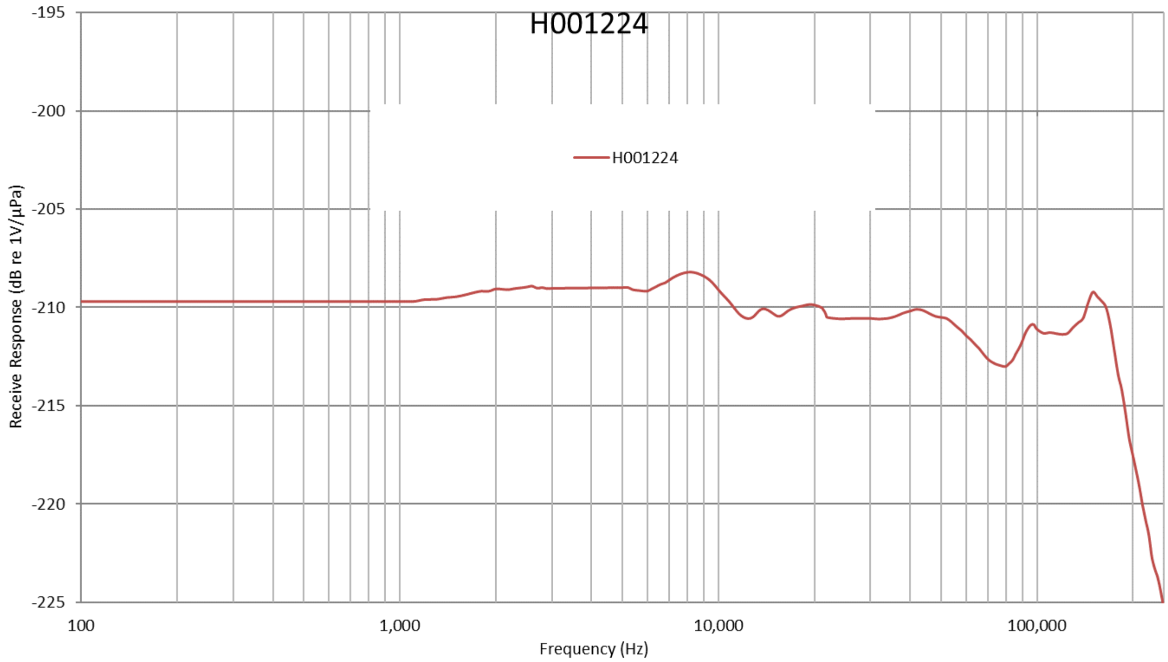


Figure E-3. Spectral response of -210 dB re 1V/µPa GTI M36-V00-902 hydrophones

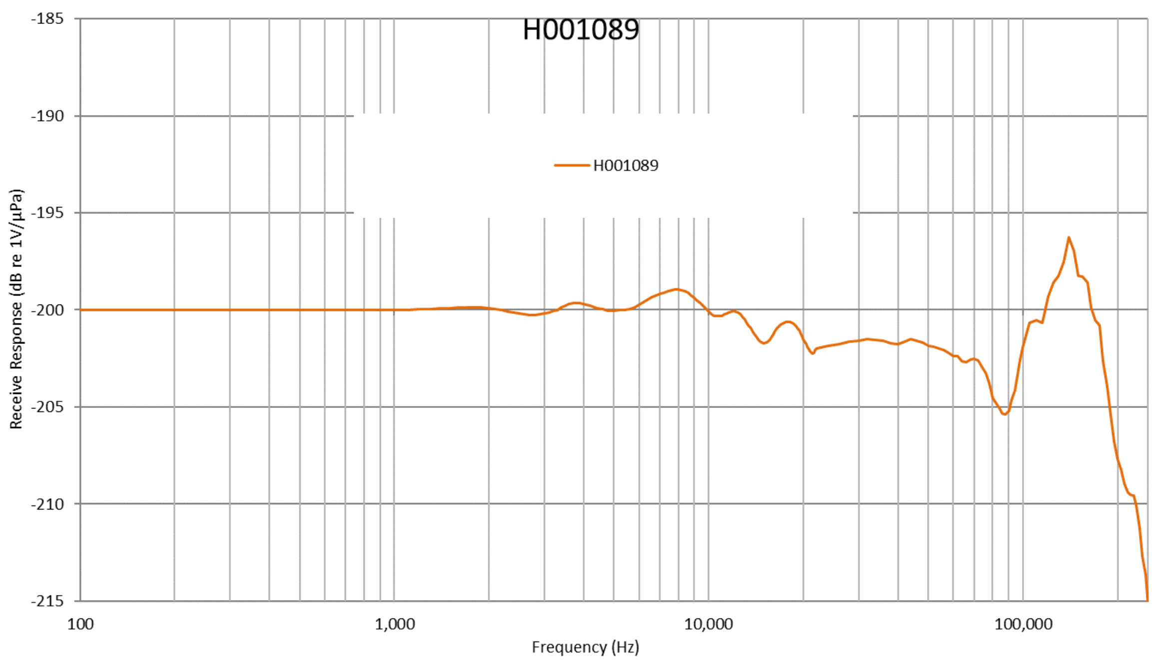


Figure E-4. Spectral response of -200 dB re 1V/µPa GTI M36-900 hydrophones

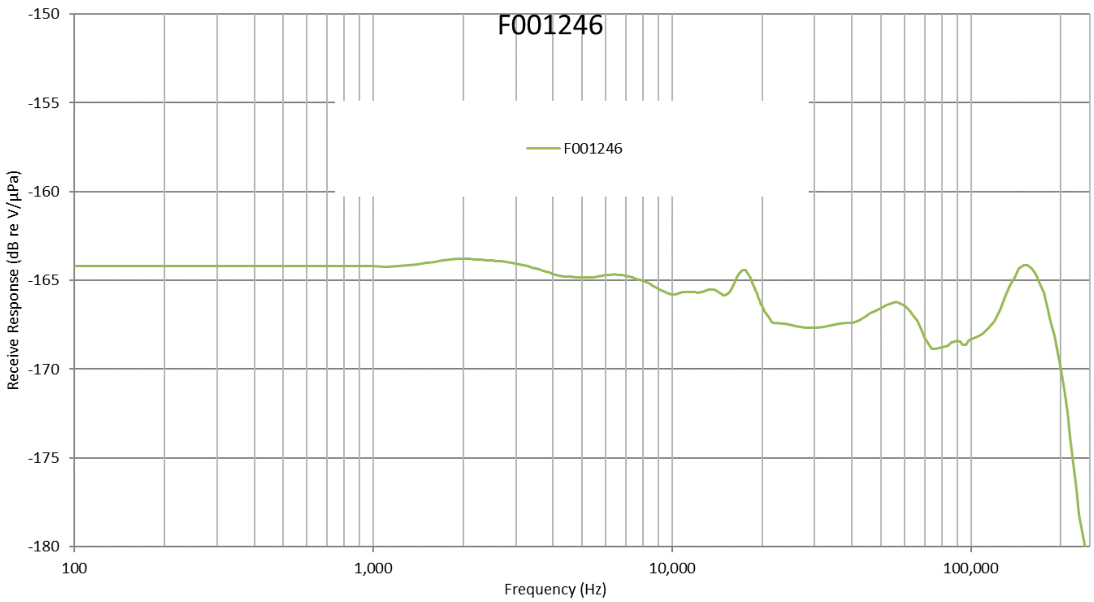


Figure E-5. Spectral response of -165 dB re 1V/μPa GTI M36-V35-900 hydrophone

## E.2. System Calibrations

Each recording system (AMAR +hydrophones) were calibrated at the warehouse before shipping (Table E-1) and then before deployment and upon retrieval with a pistonphone type 42AC precision sound source (G.R.A.S. Sound & Vibration A/S; Figure E-6). The pistonphone calibrator produces a constant tone at 250 Hz at a fixed distance from the hydrophone sensor in an airtight space of known volume. The recorded level of the reference tone on the AMAR yields the system gain for the AMAR and hydrophone. To determine absolute sound pressure levels, this gain was applied during data analysis. Only field calibrations within 0.7 dB absolute pressure of the warehouse calibration were used for analysis in this project.

Figure E-6. Split view of a G.R.A.S. 42AC pistonphone calibrator with an M36 hydrophone.

Table E-2. Warehouse system calibrations.

| Calibration Date | AMAR S/N | Channel | Hydrophone Model | Hydrophone S/N | System Gain @250 Hz (dB re FS/µPa) | H-phone Sens @250 Hz (dB re 1 V/µPa) |
|---|---|---|---|---|---|---|
| 2023-03-28 | 855 | 1 | M36-V0-900 | H001089 | -199.40 | -200.32 |
| 2023-03-28 | 855 | 2 | M36-V0-900 | H001098 | -199.50 | -200.42 |
| 2023-03-28 | 860 | 1 | M36-V0-900 | H001090 | -198.90 | -199.82 |
| 2023-03-28 | 860 | 2 | M36-V0-900 | H001097 | -199.20 | -200.12 |
| 2023-03-28 | 863 | 1 | M36-V0-900 | H001091 | -199.50 | -200.42 |
| 2023-03-28 | 863 | 2 | M36-V0-902 | H001224 | -208.80 | -209.72 |
| 2023-03-28 | 865 | 1 | M36-V0-900 | H001093 | -199.30 | -200.22 |
| 2023-03-28 | 865 | 2 | M36-V0-902 | H001226 | -208.50 | -209.42 |
| 2023-03-28 | 864 | 1 | M36-V35-900 | F001246 | -163.40 | -164.32 |
| 2023-03-28 | 864 | 2 | M36-V0-900 | H001092 | -199.30 | -200.22 |
| 2023-06-30 | 603 | 1 | M36-V0-900 | D000760 | -199.80 | -200.72 |
| 2023-06-30 | 603 | 2 | M36-V0-900 | H001096 | -199.20 | -200.12 |

# Appendix F. Acoustic Data Analysis

## F.1. Acoustic Metrics

### F.1.1. Sound pressure

Sound pressure, usually measured in Pascals (Pa), is the amount of force per unit area. Often in acoustics, sound pressure is expressed in decibels (dB) which is a logarithmic unit. Decibels are used to describe noise relative to a reference pressure; underwater, this is in reference to 1μPa.

### F.1.2. Exceedance Levels

The Nth percent exceedance level, or exceedance percentile, is defined as the "time-weighted and frequency-weighted sound pressure level that is exceeded for N% of the time interval considered" ([ISO] International Organization for Standardization 1996). The 50% exceedance level is the median, and the 90% exceedance level is close to the highest level of noise (Dekeling et al. 2014). The exceedance levels are defined using the following notation:

$L_{max}$: Maximum over all values,

$L_P$: $P$ = 100–$N$ ; N% exceedance level

$L_{mean}$: *Linear mean of all values.*

For example, the exceedance level at which 95% of the data is exceeded is denoted $L_5$.

### F.1.3. Sound Pressure Level (SPL)

In underwater acoustics, sound pressure is expressed as a sound pressure level (SPL). This may be calculated by:

$$SPL = 20\log_{10}\left(\frac{P}{P_0}\right)$$

Where $P$ is a measured sound pressure and $P_0$ is a reference pressure of 1 μPa. This results in SPL being expressed in dB re 1 μPa. The most common convention in underwater acoustics for expressing SPL is for it be expressed as a root mean square (RMS) value, which is a time averaged pressure value. This is calculated using the equation:

$$SPL_{RMS} = 20\log_{10}\left(\sqrt{\frac{1}{T}\int_T P(t)^2 dt}\right)$$

where $T$ is the window length of the selected sound.

### F.1.4. 0-to-Peak SPL

The maximum absolute sound pressure during a stated time interval (such as a pulse) is referred to as the zero-to-peak SPL ($SPL_{ZP}$). A peak sound pressure may arise from a positive or negative sound pressure.

In a symmetrical waveform, the zero-to-peak amplitude will be half the value of the peak-to-peak amplitude. The $SPL_{ZP}$ is calculated using:

$$SPL_{ZP} = 20\log\left(\frac{P_{ZP}}{P_0}\right)$$

Where $P_{ZP}$ is the zero-to-peak pressure (the maximum absolute sound pressure) and $P_0$ is a reference pressure of 1 μPa$^2$.

## F.1.5. Sound Exposure Level (SEL)

Sound exposure level (SEL) is a measure of the energy within a sound pulse. The SEL for a single strike (SELss) is calculated by integrating the square of the pressure waveform over the duration of the pulse. The duration of the pulse is defined as the region of the waveform containing the central 90% of the energy of the pulse. This is because it can be difficult to determine the exact start and end of a pulse when the waveform contains noise. This is given by the equation:

$$E_{90} = \int_{t_5}^{t_{95}} P^2(t)dt$$

Where $P^2$ is the square of the pressure waveform. This value is expressed in dB re 1 μPa$^2$·s. This value is then used against a reference to calculate SELss.

$$SEL_{ss} = 10\log\left(\frac{E_{90}}{E_0}\right)$$

Where $E_0$ is the reference value of 1 μPa$^2$·s. The SEL for each impulsive noise event ($SEL_{SS}$) can be aggregated by summation to calculate the cumulative SEL (SELcum). This has been completed per pile using the equation:

$$SEL_{cum} = 10\log_{10}\sum_i 10^{\frac{SEL_i}{10}}$$

where $SEL_i$ is the SELss for the $i^{th}$ strike in the exposure period. Cumulative SEL is expressed in dB re 1 μPa$^2$·s.

## F.1.6. Power Spectral Density (PSD)

Power spectral density (PSD) is a measure of a signal power intensity in the frequency domain and describes how the power of a signal is distributed with frequency. This is reported in dB re 1 μPa$^2$Hz$^{-1}$. This is estimated using the equation:

$$\gamma(f) = |P(f)|^2$$

where $P(f)$ is the Fourier transform at frequency $f$.

# F.2. 1/3 Octave Band Analysis

One third octave bands (TOB) were defined for noise characterisation as a frequency band whose upper band limit frequency is the lower band limit multiplied by the cube root of two.

# F.3. Marine Mammal Auditory Frequency Weighting

## F.3.1. Frequency Weighting Functions – Technical Guidance (NMFS 2018)

In 2015, a US Navy technical report by Finneran (2015) recommended new auditory weighting functions. The overall shape of the auditory weighting functions is similar to human A-weighting functions, which follows the sensitivity of the human ear at low sound levels. This frequency-weighting function is expressed as:

$$G(f) = K + 10\log_{10}\left[\left(\frac{(f/f_{lo})^{2a}}{[1+(f/f_{lo})^2]^a[1+(f/f_{hi})^2]^b}\right)\right]. \quad .(\text{F-1})$$

Finneran (2015) proposed five functional hearing groups for marine mammals in water: low-, mid-, and high-frequency cetaceans, phocid pinnipeds, and otariid pinnipeds. The parameters for these frequency-weighting functions were further modified the following year (Finneran 2016) and were adopted in NOAA's technical guidance that assesses noise impacts on marine mammals (NMFS, 2018). Table F-1 lists the frequency-weighting parameters for each hearing group; Figure B-1 shows the resulting frequency-weighting curves.

Table F-1. Parameters for the auditory weighting functions recommended by NMFS (2018).

| Hearing group | a | b | $f_{lo}$ (Hz) | $f_{hi}$ (Hz) | $K$ (dB) |
|---|---|---|---|---|---|
| Low-frequency cetaceans | 1.0 | 2 | 200 | 19,000 | 0.13 |
| Mid-frequency cetaceans | 1.6 | 2 | 8,800 | 110,000 | 1.20 |
| High-frequency cetaceans | 1.8 | 2 | 12,000 | 140,000 | 1.36 |
| Phocid pinnipeds in water | 1.0 | 2 | 1,900 | 30,000 | 0.75 |
| Otariid pinnipeds in water | 2.0 | 2 | 940 | 25,000 | 0.64 |
| Sea turtles | 1.4 | 2 | 77 | 440 | 2.35 |

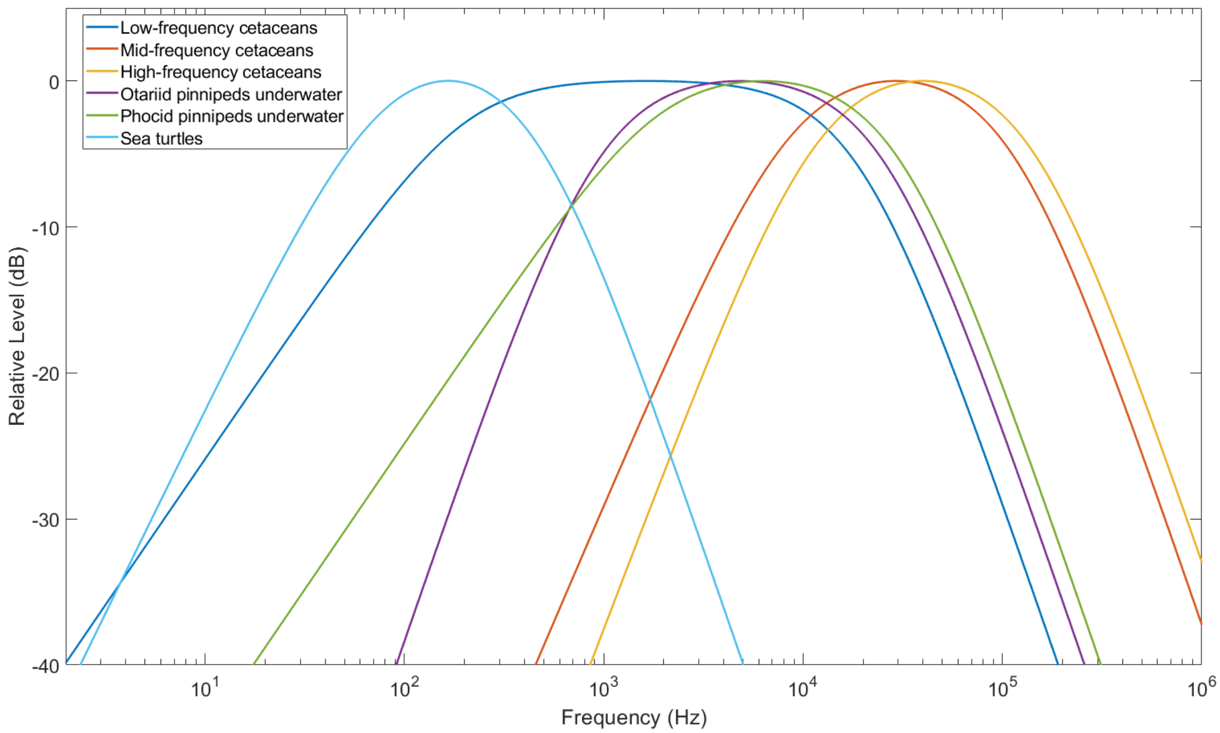


Figure F-1. Auditory weighting functions for the functional marine mammal hearing groups as recommended by NMFS (2018).

# F.4. Kurtosis and Rise Time Calculation Method

## F.4.1. Kurtosis

Kurtosis is a measure of the symmetry of a probability distribution that quantifies the extremity of outliers away from the mean for a given set of data. In acoustic timeseries data, kurtosis can be used to estimate the extent to which data is non-Gaussian, or impulsive, over a period of time (Martin and Barclay 2019).

The kurtosis is defined for a pressure timeseries $p_w$ over a window of time *T* as the ratio of the fourth $(\mu_4)$ and second $(\mu_2)$ moment (Martin et al. 2020):

$$\beta = \frac{\mu_4}{\mu_2};\ T = t_2 - t_1$$

$$\mu_2 = \frac{1}{T}\int_{t_1}^{t_2} [p_w(t) - \overline{p_w}\,]^2 dt$$

$$\mu_4 \frac{1}{T}\int_{t_1}^{t_2} [p_w(t) - \overline{p_w}\,]^4 dt$$

where $\bar{x}$ is the mean of the real-valued variable *x*.

For the Vineyard Wind 1 installation, the kurtosis was calculated for each window length of *T*=60 seconds across the duration of the pile installation for Piles Z01, A12, A08, A10, and A03. The start and end of the piling period were determined from the construction piling logs, with 10 seconds added after piling to ensure acoustic reflections were included. The pressure timeseries was sampled by the hydrophone sensors at 48 kHz, and the discrete approximation was used to estimate $\mu_2$ and $\mu_4$.

$$\mu_2 = \frac{1}{N}\sum_{i=1}^{N}[p_w[i] - \overline{p_w}]^2; \qquad \mu_4 = \frac{1}{N}\sum_{i=1}^{N}[p_w[i] - \overline{p_w}]^4.$$

To estimate the maximum, mean, and exceedance levels of kurtosis, the kurtosis values for all 60 windows across the entire pile driving period were included.

## F.4.2. Rise Time

The rise time was calculated here as the time duration in seconds of each detected impact pile driving strike. For each impulse, the rise time is defined here as the duration of the center 90% of the energy in the impulse (see Section 2.2.1 for details of impulse detection). It is noted that the true definition of rise time is the elapsed time between when 5% of the pulse energy has been reached and when the peak pulse energy is reached. Rise time quantifies the rate of onset of an impulse, and it is an indicator of the spread of a pulse from impact pile driving.

# Appendix G. CTD Data Measurements

Figures G-1 and G-2 show the collection of all CTD measurements taken during three months of SFV monitoring, from June through August. CTD measurements down to 40 m deep, which is close to the bottom in most stations monitored. While Figure G-1 shows a 3D plot with temporal variation of the profiles, Figure G-2 compares the magnitude of the sound speeds measured. Color code is by pile, when CTD casts were taken. For comparison, xxx shows the sound speed profile used as input to the propagation model to obtain the predicted ranges to thresholds.

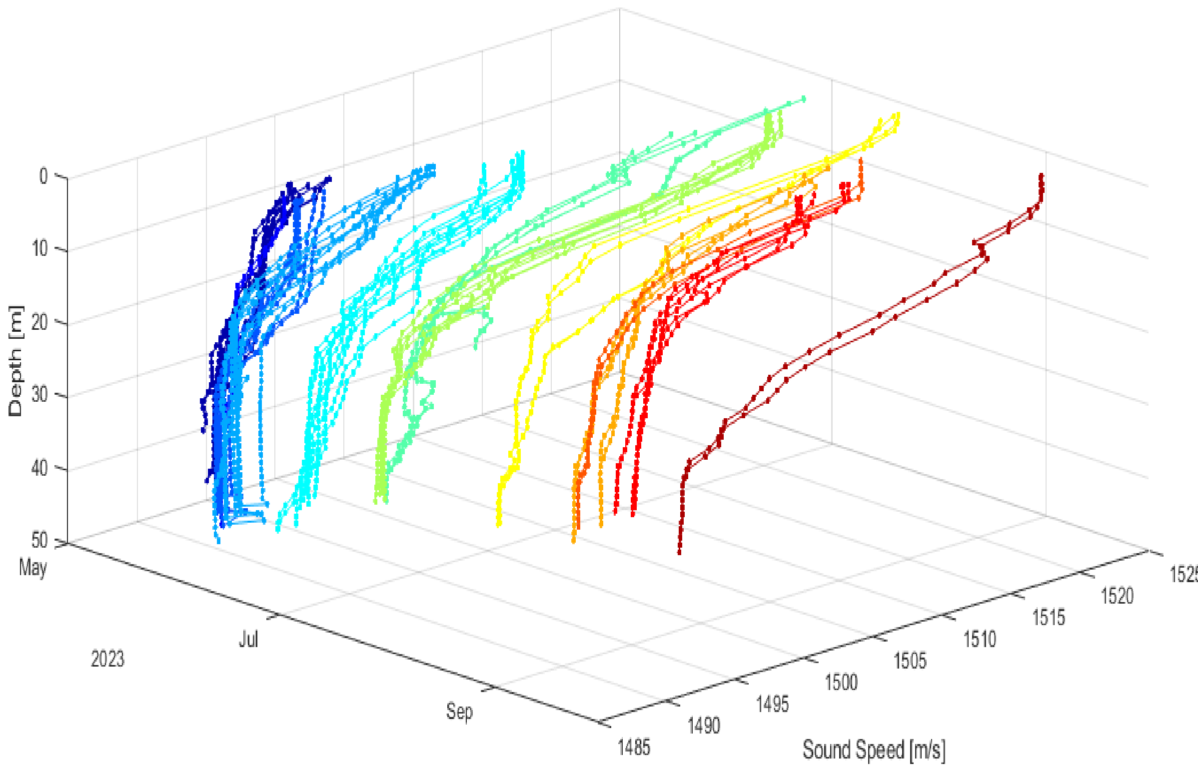


Figure G-1. Temporal variation of sound speed profiles collected from June (dark blue) through August (dark red).

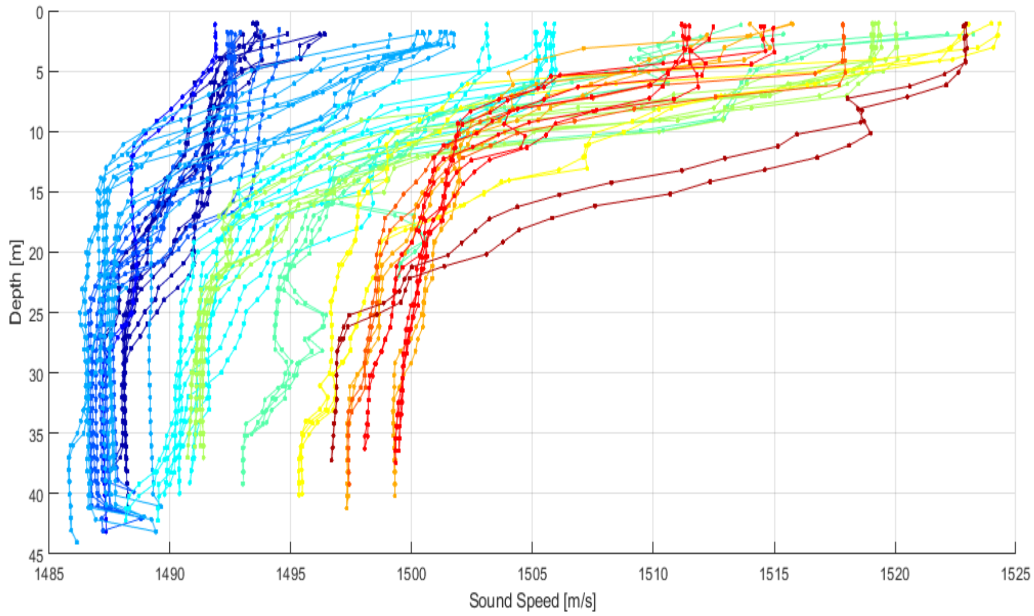


Figure G-2. Variation in magnitude of measured sound speed profiles throughout the SFV project from the beginning of June (blue colors) through August (red colors).

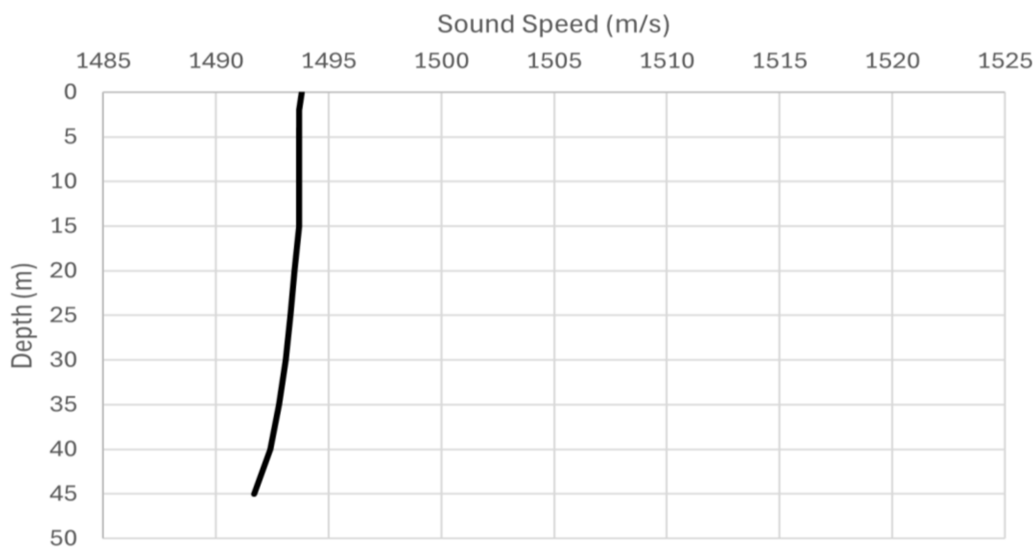


Figure G-3. GDEM seasonal Fall sound speed profile used in the modeling to obtain predicted ranges to threshold.